TN
269
G4

GEOPHYSICAL PROSPECTING

Official Journal of the
European Association of Exploration Geophysicists

CONTENTS
OF
VOLUME III
1955

MARCH

Number 1

page

J. W. de Bruyn:
Isogam Maps of Europe and North Africa 1
W. Domzalski:
Three Dimensional Gravity Survey 15
G. Muratori:
Drilling Methods in Sand and Gravel Formation 56
F. W. Hales and T. E. Edwards:
Some Theoretical Considerations on the Use of Multiple Geophones arranged Linearly along the Line of Traverse 65
Book Review 74
E.A.E.G. Abstract Service 77

Supplement
page

J. Goguel:
Tidal Gravity Corrections for 1955 1
C. Morelli:
Tidal Gravity Corrections for 1955 30

JUNE

Number 2

page

H. Flathe:
Possibilities and Limitations in applying Geoelectrical Methods to Hydrogeological Problems in the Coastal Areas of North West Germany 95
A. Volker et J. Dijkstra:
Détermination des salinités des eaux dans le sous-sol du Zuiderzee par prospection géophysique 111
J. Baumgarte:
Konstruktive Darstellung von seismischen Horizonten unter Berücksichtigung der Strahlenbrechung im Raum. 126
A. Selem and E. Merlini:
Electrical Hazards in Seismic Prospecting 163
W. M. Jones and A. T. Dennison:
A Low-frequency Refraction Geophone 168
H. Richard et M. Rimbaut:
Mesure du bruit et sismos multiples 177
Book Review 195
E.A.E.G. Abstract Service 196

Supplement
page

J. Goguel:
Tidal Gravity Corrections for 1955 1

SEPTEMBER Number 3

page
J. GOGUEL:
De quelques sujétions de la géophysique minière. 205
W. DOMZALSKI:
Relative Determination of the Density of Surface Rocks and the Mean Density of the Earth from Vertical Gravity Measurements . 212
R. BOLLO et J. GOGUEL:
Un intégrateur pour le calcul des corrections topographiques . . 228
J. SCHOEFFLER et E. DIEMER:
Rapporteur pour la construction rapide du rayon refracte . . . 234
Y. D'ERCEVILLE:
Etude théorique de la vitesse des ondes de compression dans les vases 240
A. M. SELEM:
Reflection Survey in Rough Topography. 246
O. KOEFOED:
Resistivity Curves for a Conducting Layer of Finite Thickness Embedded in an Otherwise Homogeneous and Less Conducting Earth 258
H. FLATHE:
A Practical Method of Calculating Geoelectrical Model Graphs for Horizontally Stratified Media 268
Book Review 295
E.A.E.G. Abstract Service 296

Supplement
page
La Compagnie Générale de Géophysique:
Abaques de sondage électrique 1

DECEMBER Number 4

page
J. G. HAGEDOORN:
Templates for fitting Smooth Velocity Functions to Seismic Refraction and Reflection Data 325
B. FAVRE:
Détermination de la position dans l'espace d'un miroir situé sous un réfracteur séparant deux milieux de vitesses différentes, à partir des données d'un tir en croix isolé 339
F. MUIR and F. W. HALES:
A Rational Approach to the Design of Electrical Filters and of Shot-hole and Geophone Patterns in Seismic Reflection Prospecting . 350
A. KORSCHUNOW:
On Surface-waves on Loose Materials of the Soil 359

O. Koefoed:
On the Effect of Poisson's Ratios of Rock Strata on the Reflection Coefficients of Plane Waves 381
E. W. Carpenter:
Some Notes concerning the Wenner Configuration 388
G. C. Colley:
Gravity Variations in Surveys across Geological Boundaries . . 403
E.A.E.G. Abstract Service 425

Supplement
page

Service Hydrographique de la Marine and Compagnie Générale de Géophysique:
Tidal Gravity Corrections for 1956 1

INDEX BY AUTHOR

	No.	Page
Baumgarte, J. Konstruktive Darstellung von seismischen Horizonten unter Berücksichtigung der Strahlenbrechung im Raum	2	126
Bollo, R. Un intégrateur pour le calcul des corrections topographiques. . .	3	228
Bruyn, J. W. de. Isogam Maps of Europe and North Africa	1	1
Carpenter, E. W. Some Notes concerning the Wenner Configuration . . .	4	388
Colley, G. C. Gravity Variations in Surveys across Geological Boundaries .	4	403
Compagnie Générale de Géophysique, La. Abaques de sondage électrique .	suppl.	1
——. Tidal Gravity Corrections for 1956	suppl.	1
Dennison, A. T. A Low-frequency Refraction Geophone	2	168
Diemer, E. Rapporteur pour la construction rapide du rayon refracte . . .	3	234
Dijkstra, J. Détermination des salinités des eaux dans le sous-sol du Zuiderzee par prospection géophysique	2	111
Domzalski, W. Three Dimensional Gravity Survey	1	15
——. Relative Determination of the Density of Surface Rocks and the Mean Density of the Earth from Vertical Gravity Measurements	3	212
Edwards, T. E. Some Theoretical Considerations on the Use of Multiple Geophones arranged Linearly along the Line of Traverse	1	65
Erceville. Y. d'. Etude théorique de la vitesse des ondes de compression dans les vases	3	240
Favre, B. Détermination de la position dans l'espace d'un miroir situé sous un réfracteur séparant deux milieux de vitesses différentes, à partir des données d'un tir en croix isolé	4	339
Flathe, H. Possibilities and Limitations in applying Geoelectrical Methods to Hydrogeological Problems in the Coastal Areas of North West Germany	2	95
——. A Practical Method of Calculating Geoelectrical Model Graphs for Horizontally Stratified Media	3	268
Goguel, J. Tidal Gravity Corrections for 1955	suppl.	1
——. Tidal Gravity Corrections for 1955	suppl.	1
——. De quelques sujétions de la géophysique minière.	3	205
——. Un intégrateur pour le calcul des corrections topographiques.	3	228
Hagedoorn, J. G. Templates for fitting Smooth Velocity Functions to Seismic Refraction and Reflection data	4	325
Hales, F. W. Some Theoretical Considerations on the Use of Multiple Geophones arranged Linearly along the Line of Traverse.	1	65
——. A Rational Approach to the Design of Electrical Filters and of Shothole and Geophone Patterns in Seismic Reflection Prospecting . . .	4	350
Jones, W. M. A Low-frequency Refraction Geophone	2	168

Koefoed, O. Resistivity Curves for a Conducting Layer of Finite Thickness Embedded in an Otherwise Homogeneous and Less Conducting Earth 3 258
——. On the Effect of Poisson's Ratios of Rock Strata on the Reflection Coefficients of Plane Waves 4 381
Korschunov, A. On Surface-waves on Loose Materials of the Soil 4 359
Merlini, E. Electrical Hazards in Seismic Prospecting 2 163
Morelli, C. Tidal Gravity Corrections for 1955 . . . . suppl. 30
Muir, F. A Rational Approach to the Design of Electrical Filters and of Shot-hole and Geophone Patterns in Seismic Reflection Prospecting . 4 350
Muratori, G. Drilling Methods in Sand and Gravel Formation. 1 56
Richard, H. Mesure du bruit et sismos multiples 2 177
Rimbaut, M. Mesure du bruit et sismos multiples. 2 177
Schoeffler, J. Rapporteur pour la construction rapide de rayon refracte , 3 234
Selem, A. Electrical Hazards in Seismic Prospecting 2 163
——. Reflection Survey in Rough Topography 3 246
Service Hydrografique de la Marine. Tidal Gravity Corrections for 1956 suppl. 1
Volker, A. Détermination des salinités des eaux dans le sous-sol du Zuiderzee par prospection géophysique 2 111

ISOGAM MAPS OF EUROPE AND NORTH AFRICA *

BY

J. W. DE BRUYN **

The Bouguer and Isostatic isogam maps of "Europe and North Africa" were compiled from published data and from B.P.M. and affiliated companies' gravity surveys. Both are on the scale of 1 : 5.000.000 and with an isogam interval of 25 mgl with 5 mgl contours shown in parts.

These composite maps in their present form serve two purposes, firstly they provide a regional map of the gravity field in Europe and, secondly, stimulate others to contribute data for an improved edition of this map.

The map was virtually completed when many new data were received during and after the Rome meeting of the U.G.G.I. These data could not be incorporated in the present issue, but we hope to use them for the preparation of a later edition. For this purpose we request everybody to submit to the central office of the E.A.E.G. any relevant data or additions they have to-day and further information whenever it becomes available.

A few details of how these maps were made are given in the following paragraph. A full account is given in the Appendix for the interested specialists.

The maps are primarily based on published data. These are usually either Bouguer isogam maps (e.g. France, England, Poland, Sweden, Northern Italy, Morocco, etc.) or lists of pendulum stations (e.g. Mediterranean, Switzerland, Spain). The latter lists usually give not only the Bouguer anomalies but also various isostatic anomalies.

B.P.M. and affiliated companies have contributed surveys in the Netherlands and Roumania.

The data from these various sources were brought to Potsdam level, using the international ties made by Woollard, Morelli, Martin and others. The Cassinis International Formula was used for the latitude correction. The Bouguer correction was nearly everywhere computed or recomputed with a density of 2.67 because this is the standard figure used by B.P.M. It is, of course, too high for the observations in the sedimentary basins, but since the difference between say 2.2 and 2.67 in the Bouguer correction formula only amounts to 2 mgl/100 m and the station elevations in these plains are rather low, it does not make much difference there, whereas 2.67 for the observations in the mountainous areas, where the Bouguer corrections become large, usually represents a fair approximation.

---

* Presented at the Seventh Meeting of the European Association of Exploration Geophysicists, held at The Hague, 8-10 December 1954.

** N.V. De Bataafsche Petroleum Maatschappij, The Hague. (Royal Dutch Shell Group).

For the isostatic correction the Airy-Heiskanen method, $R = O, T = 30$ km, was used, implying local compensation and a crustal thickness of 30 km.

To enable the reader to judge the accuracy of the isogams, an index map is given showing on which data the isogams are based.

In the areas covered by detail and regional gravimeter surveys (e.g. the Netherlands; Morocco) and those covered by a dense network of good pendulum stations (e.g. Switzerland), the isogams are drawn with a 5 mgl interval where this was possible without blurring the picture. No individual pendulum stations are shown in these areas.

In the areas covered by a widely spaced number of pendulum stations (e.g. Spain, Mediterranean) the isogams are drawn in full with an interval of 25 mgls.

Wherever the isogams are based on widely spaced stations of limited accuracy (e.g. Czecho-Slovakia) the 25 mgl isogams are drawn with a dashed line.

All these areas are coloured. Areas without observations are left blank with an occasional 25 mgl inferred isogam line, dashed, to show the general trends of the isogams.

The colour scheme is analogous to that of a topographical map: yellow to red denote high (= positive) areas, green to dark blue low to deep (= negative) areas.

The *Bouguer* isogam map shows the principle of isostasy clearly: the great mountain chains and high plateaus are supported by light roots and the sea water is compensated by heavy antiroots. Strong local deviations of these general rules are visible.

The *Isostatic* isogam map shows predominantly positive anomalies, with an average value of +13 mgl.

Vening Meinez' remark that strong negative anomalies tend to appear in long narrow strips and positive anomalies in large fields seems also to be generally true for Europe. Apparent exceptions can be noticed, but they are either much smaller in areal extent or in gravity intensity.

The basins are usually roundish negative areas. Sometimes however, they are only relative minima with respect to their surroundings and they never show the pronounced negative anomalies of Vening Meinesz' zones.

The young graben are expressed in the gravity field as long narrow minima with sharp flanks.

Near Crete and Cyprus we observe very pronounced arcuate maxima and minima. The first-mentioned area shows two arcuate troughs in the sea floor separated by an island arc and active volcanoes on the inner side of the arc. Both areas show great seismic unrest.

The Alps and Betic Mts-Riff-arc are arcuate minima with strong positive anomalies on the inner side and negative foredeeps on the outer side.

They represent folded mountain systems with light roots.

The Apennines with their foredeeps are covered by arcuate parallel maxima and minima, the axis of the former lying on the inner side of the mountains and the axis of the latter following the outer foothills. On incomplete evidence it seems as if the Carpathians show a similar picture.

The Carpathians and Apennines and their foredeeps seem to be up- and downwarps of the crust, the latter being filled with light sediments.

The old Palaeozoic massifs are usually isostatically adjusted and very pronounced anomalies like those over the younger tectonical elements are not observed. They often consist of large basement blocks, representing the core of the older uplifts, frequently bounded by faults. In that case they seem to be expressed in the gravity field as local maxima of gravity, the sediments surrounding them being lighter. Others consist of a greater variety of rocks in their outcrops and then the gravity picture is likewise more complicated. Usually the granite areas then show up as local negative anomalies.

ACKNOWLEDGEMENTS

Large composite maps are, of course, usually the result of the co-operation of several men, and in this case Messrs. J. Gonlag and B. J. Hofman should be mentioned as having contributed large shares in the work. The drawing of the maps was very ably done by Mr. D. Keetelaar.

Thanks are due to the Bataafsche Petroleum Maatschappij and its affiliated companies for permission to publish the maps containing parts of their gravity surveys. The Iraq Petroleum Company gave permission to use their gravity surveys on Cyprus. The Geological Survey of Great Britain provided data about gravity surveys as yet unpublished. Professor C. Morelli provided isogam maps of NE Italy and the Adriatic Sea as yet unpublished.

APPENDIX

1. *Algeria.* The isogams are based upon some hundreds of Holweck pendulum stations made by Lagrula (1951).

The calibration of the pendulums is based upon the gravity difference of 1024 mgls between Paris and Bouzareah, the Algerian base station. Harrison connected Bouzareah with Maison Blanche—Algiers Airport and found a gravity difference of 5.39 mgls (private communication). Woollard's (1952) value at Algiers Airport is 979,905.5, which makes Bouzareah 979 910.9. Taking Paris as 980,943, this gives us a gravity difference of 1032 mgls between Paris and Bouzareah as against 1024 mgls used by Lagrula.

The value of Algiers Airport, Maison Blanche, is confirmed by the measurements of Duclaux and Martin (1952). Their values in Africa are systematically higher than Woollard's values by an average of 1.4 mgl. Subtracting this amount from his value of 979,907.55 at Maison Blanche gives us 979,906.1, which agrees quite well with Woollard's value. This difference of 8 mgls means a difference of 0.8 % in the calibration, and Lagrula's values were therefore lowered by 8 mgls and by 0.8 mgl per 100 mgl difference between Bouzareah and the relevant stations.

Lagrula's (1952) modern gravimeter stations between Ain Sefra and Colomb Béchar in the SW part of Algeria were lowered by 8 mgls.

The Bouguer isogam map shows only the individual Holweck stations south of the —25 mgl isogam, the area north of this line being too crowded with stations.

2. *Austria* is covered by the well known publications of Tanni (1942) and Holopainen (1947). Both use various figures for the Bouguer correction factor; the old measurements by Von Sterneck and his collaborators, as published by Borass (1911), those near the Tauerntunnel (Schütte, 1930) and the modern ones published by Weiken (1950) were therefore recomputed with $d = 2.67$ and the Cassinis formula.

A detail isogam map of the Vienna basins was published by Barsch (1943). B.P.M. files contain detail maps of the Graz basin and of the Molasse basin of Lower Austria. The level of these maps was lowered by 12 mgls to allow for the difference between the Helmert and Cassinis latitude formula.

An isogam map of the area NE of Salzburg, published by Bürgl (1949) had to be lowered by 20 mgls to allow for this same difference and for a serious mistake in the computation of the terrain effect.

Nothing is known about the Bouguer correction factor of the above-mentioned detail maps.

On the isostatic isogam map Tanni's and Holopainen's figures were used.

3. *Baltic Sea.* Haalck (1935) made some observations of limited accuracy with a gravimeter on board a ship in the North and Baltic Seas. Only those S of Sweden and N of the Elbe were plotted, after having been corrected for the difference Helmert-Cassinis and adjusted to the modern value of Copenhagen: 981,558.

The islands of Bornholm and Gothland are dealt with under Denmark and Sweden.

4. *Belgium.* A modern regional gravimeter survey covers Belgium. The results were published by Jones (1948, 1951). In the hilly part of the country, south of the rivers Sambre and Meuse, 2.65 was used in the Bouguer correction factor; in the other part 2.1.

5. *Czecho-Slovakia.* The only parts of the country covered by detail surveys are a part of the Vienna basin and an area E of Bratislava (Behounek, 1952). Otherwise only pendulum stations are available, most of them made by Von Sterneck et al. (Borass, 1911). The only modern ones are those published by

Weiken (1950) and Mrkos (Travaux de la Section de Géodésie et Géophysique de l'U.G.G.I., tome 16).

Picha (1950) made a series of observations with a gravimeter. All observations were corrected using 2.67 in the Bouguer correction formula.

On the isostatic map Tanni's (1942) values were used for the old stations.

6. *Cyprus.* Mace (1939) made a dozen pendulum stations on the island and I.P.C. a gravimeter survey in the plains around Nicosia and Famagusta. A density of 1.8 was used in the Bouguer formula.

7. *Denmark.* The gravity data consist of pendulum stations and gravimeter surveys. Using Andersen's (1947) measurements as a base, it was found necessary to lower the pendulum stations from Borass (1911) by 18 mgls and those from the Travaux, tomes 2 and 6, by 2 mgls. The observations from the Travaux, tome 8 were discarded. The gravimeter surveys published by Nörgaard (1936, 1939a, 1939b) were taken over unaltered. The Bouguer anomaly map is then based upon Copenhagen-Buddinge 951,558, which, according to Saxov (1952), is correct.

Saxov (1945) made a modern detail gravimeter survey on the island of Bornholm.

8. *Egypt.* There are some 10 pendulum stations in Northern Egypt, all on or near the delta, based on Helwan (Cole, 1944). Cole mentions as the best value for Helwan $g = 979{,}288$, but the anomalies are based upon the original value of 979,295 because this figure gives a better agreement with Woollard's (1952) values.

Von Triulzi made some observations along the coasts of the Gulf of Suez, Gulf of Akaba and Red Sea (Borass, 1911). They are based upon Pola, $g = 980{,}926$, which, according to Tanni's list in Publ. No. 18 of the Isostatic Institute "On the continental undulations of the geoid as determined from the present gravity material", has to be lowered by 5 mgls.

Woollard (1952) measured several stations in Egypt. His value at Alexandria Harbor is the same as Vening Meinesz' (1948) value; at Helwan Observatory his value is 979,295 which is the same as Cole's first value. At Suez he found 979,308. Vening Meinesz' value at Suez is out by some 30 mgls. At Port Said Cole's original and Woollard's values are both 979,448.

9. *France.* The Bouguer isogam map is a copy of the "Carte gravimétrique de France" (Lejay Goudey, Goron, 1949, 1951). Corsica was copied from Lejay's (1953) isogam map.

10. *Germany.* The isogams of Germany, as given here, are based on detail isogam maps from B.P.M. files which were constructed using the "Geophysikalische Karte von Nordwestdeutschland" (Reich, 1948) and other data by Reich (1949) and Siemens (1953). Weiken (1950) published the results of the modern German pendulum measurements, part of which are in France, Austria, Poland and Russia. These were recomputed using 2.67 for the Bouguer correction and the Cassinis formula. Using these anomalies it was possible to

convert the above-mentioned detail isogam maps into this same system.

The remaining blank areas were filled in with pendulum stations, taken from Schütte's (1930) compilation, recomputed in the same manner.

11. *Great Britain*. The pendulum measurements up to 1936 were compiled by Bullard and Jolly (1936). Later additions and check measurements were published by Cook (1950) and Bullerwell (1952). Although it seems certain that the base station, Cambridge, is too low by 3 mgls, the present value of $g = 981{,}265$ was maintained.

Results of gravimeter surveys are given by Cook and Thirlaway (1948, 1952), White (1949), Falcon and Tarrant (1951), Cook, Hospers and Parasnis (1952), Bott and Masson Smith (1953), Hospers and Wilmore (1953) and Cook (1953). These Bouguer isogam maps, computed with various Bouguer correction factors, were simply copied. This does not matter much because elevations are rather low.

The Geological Survey kindly provided us with advance information about surveys not yet published and these data are included also.

The results of the submarine gravity surveys in the waters around the British Isles were published by Browne and Cooper (1950, 1952). These publications give "modified Bouguer anomalies". The infinite plate formula was used to compute Bouguer anomalies.

12. *Hungary*. Very many observations were made in the course of years in the Hungarian Plains and surrounding areas: pendulum observations by Von Sterneck and his collaborators (Borass, 1911), newer pendulum observations by Oltay and his collaborators (Travaux, tomes 8, 12 and 14), torsion balance stations by Baron Eötvös and still later gravimeter surveys.

Only a small part of those measurements is incorporated in our map, which is made up mainly from large published isogam compilation maps.

The following discussion is not limited to Hungary proper, but covers the Hungarian plains, of which parts now belong to Yugo-Slavia and Roumania.

Vajk (1952) published an isogam map of the plains W. of the Danube and N. of the Drava-Mura rivers. The isogam lines join those of neighbouring Austria (par. 2) quite smoothly. An isogam map of the area between the rivers Drava and Sava and of the Banat was published by Mayer-Gürr (1953). A large area east and north of the Danube is covered by an isogam map published by Szurovy (1948). These maps partly overlap each other, and by lowering the level of the latter by 15 mgls a fair agreement between all three maps and the pendulum observations of Oltay (Travaux, tomes 8, 12 and 14) was reached.

Nothing is known about the densities used in the Bouguer correction factor.

The area around the Balaton lake is covered by an article of Facsinay (1948). Some of the pendulum stations were remeasured with a modern gravimeter and these values are plotted on our map.

The other pendulum stations are those of Tanni (1942) recomputed with $d = 2.67$ for the Bouguer isogam map.

Facsinay's values, however, were used for the line of stations NE of Debrecen, crossing the Carpathians in this same direction, because some of these old pendulum measurements there apparently are wrong.

13. *Ireland.* The gravity data of Ireland consist of 4 pendulum stations (Cook, 1950) and three regional gravimeter surveys (Thirlaway, 1951; Murphy, 1952; Cook and Murphy, 1952). Most of the observations were corrected with 2.67 in the Bouguer formula.

14. *Italy.* The gravity map of Italy is largely based upon the work of Morelli, who collected the pendulum data and adjusted them (Morelli, 1948). A new network of base stations measured with a Worden gravimeter, was established in 1952 (Morelli 1952). Morelli's values in Rome and Naples are about 1 mgl lower than Woollard's (1952) values and his new value in Rome (Fac. Ing.) is 3 mgls lower than the one from his catalogue. Most stations in Central Italy are based on Rome F.I. and Vienna and have a rather limited accuracy. Morelli's Bouguer anomalies were therefore taken over unaltered. These anomalies are computed with various densities but with high figures for the mountain stations. In NE Italy two regional gravimeter surveys were made (Morelli 1951, 1954), the last one in the Adriatic Sea. Morelli kindly provided us with isogam maps of these two areas giving more data than those published. Another survey covers the island of Sicily (Morelli, Medi 1952). Cunietti (1952) made a regional gravimeter survey in NW Italy. Both Morelli's and Cunietti's Bouguer anomalies were taken over unaltered because in the mountainous areas various but high values were used in the Bouguer correction. Sicily was, however, recomputed with 2.67.

Solaini (1951) published an isogam map of the foothills of the Apennines, based on extensive torsion balance surveys. Since it is partly overlapped by the surveys of Morelli and Cunietti, it could be easily adjusted.

Two regional loops and a series of stations along the 40° parallel were observed by Boaga, Tribalto and Zaccara (1950a, 1950b) and Boaga (1953) with a modern gravimeter. They were recomputed with 2.67, lowered 5 mgls and are then based on Woollard's Rome F.I. value.

A small detail survey, SE of Rome, is reported by Tribalto, Zaccara and Beneo (1952). The level was lowered 5 mgls. A detail map of an area SW of Bari was made with Thyssen gravimeters. A few of Boaga's gravimeter stations enabled us to adjust this survey.

15. *Levant.* The Levant was covered by Lejay (1938) with a widely spaced network of Holweck pendulum stations.

The anomalies were recomputed, using the topographical data from Bourgoin's (1948) publication and $d = 2.67$ in the Bouguer formula.

A small survey in Turkey, SE of Alexandrette, in the Hatay-Asnik plain (Yüngül, 1951) could be adjusted with Lejay's station at Antioch.

16. *Libya.* Woollard's (1952) stations at Benghazi and Tripoli are shown.

17. *Luxemburg* is covered by a modern gravimeter survey as described by Gloden, Cagniard and Lucius (1950) and Gloden (1951).

18. *Mediterranean.* The gravity surveys in the Mediterranean were made in French, Italian, Dutch and British Submarines. The figures from Coster's (1945) publication were used for the "Vettor Pisani", "Fresnel" and "Espoir" stations, whereas Cooper, Harrison and Willmore's (1952) values were used for the "Des Geneys" and "Talent" stations. No harbour stations are shown, the observations on land usually being more accurate.

Comparisons of the Italian and French submarine observations with land stations and with the more accurate British stations in the C. and E. Mediterranean make it probable that the Fresnel and Espoir values in the W. and C. Mediterranean are about 5 mgls too high, whereas the Vettor Pisani and des Geneys values in the C. and E. Mediterranean seem to be too high by some 10 or 15 mgls Definite conclusions are, however, difficult to make, and for that reason Coster's and Cooper's values were left unaltered. Des Geneys (Cassinis, 1941) st. No. 38, S of Crete, was rejected.

The pendulum observations made by Carnera on the islands in the Aegean Sea (Travaux, tome 2) were recomputed with $d = 2.67$ and a value for Genoa of 978,557. The observation at Rhodos was rejected.

19. *Morocco.* A Bouguer isogam map, $d = 2.67$, on scale 1 : 1,500,000, isogam interval 10 mgls, has been published by the Geological Service of Morocco-Rabat. This map shows the stations but no values. The level was lowered by 8 mgls, just as Lagrula's values in SW Algeria (see para 1). The Woollard (1952) stations in Casablanca and Port Lyautey then show a fair agreement with the isogams.

20. *The Netherlands.* B.P.M. and the State Collieries (De Sitter, 1949) covered the country with a dense network of Holweck pendulum, torsion balance and gravimeter observations, based on De Bilt. A Bouguer isogam map with an interval of 5 mgls was published by Mulder (1950).

A few of Vening Meinesz' (1948) submarine observations fall within the limits of our map. "Normal" Bouguer anomalies and isostatic anomalies without the indirect effect were plotted.

21. *Norway.* The pendulum stations in Norway were taken from Heiskanen's (1939) Catalogue (table XIII). The anomalies were corrected with + 1 mgl because Jelstrup and Trovaag (1950) report a value for Oslo of 981,928, which is 1 mgl higher than Heiskanen's value.

22. *Poland.* Olczak (1951) published a Bouguer isogam map of the present territory of Poland on scale 1 : 2,000,000, isogam interval 5 mgls. The level was lowered by 10 mgls, being an approximation to the difference Helmert-Cassinis. The NE part of this map was augmented by the data given in Wieladek's (1951) article.

23. *Roumania.* B.P.M. covered the plains between Donau and Carpathians with a detail gravimeter survey. Two pendulum stations, one at Bucarest and one at Tiglina (Tanni, 1942), enabled us to convert the arbitrary level in the absolute one.

Both pendulum stations, however, were already observed in the first years of this century and are of limited accuracy. It is therefore quite possible that the chosen level is wrong by some 5 or 10 mgls. The observations in Transsylvania and the Banat were already discussed in para. 12.

24. *Spain.* The pendulum stations in Spain, Portugal, the Baleares and Spanish Morocco were established by Sans Huelin. They are reported in the Travaux, tomes 2, 6, 8, 12 and 14 and in Sans Huelin, 1944. The anomalies were recomputed using 2.67 in the Bouguer correction factor and 979,982 for Madrid. A few Holweck stations are mentioned by Lagrula (1935).

Modern gravimeter surveys cover the provinces of Huelva, Avila and Segovia (Sans Huelin, Lozano Calvo, 1947; Lozano Calvo 1950; Espinoza de los Monteros, Lozano Calvo 1950). They were tied to pendulum stations with which there is good agreement. The Bouguer anomalies were recomputed with $d = 2.67$.

25. *Sweden.* The gravity data in Sweden consist of a score of pendulum stations to which regional modern gravimeter surveys were added (Wideland 1942, 1946). His isogam map was copied, the Bouguer correction being computed with $d = 2.65$ or higher.

26. *Switzerland.* The gravity data of Switzerland consist of more than 200 pendulum stations of great accuracy. We took the figures from Heiskanen's (1939) Catalogue (Table XI), but recomputed the Bouguer anomalies with $d = 2.67$ using the formula given by Schütte (1930) on p. 3 of his publication.

27. *Tunisia.* The Holweck observations were published by Lagrula (1951).

28. *Turkey* is discussed in paragraph 15.

29. *U.S.S.R.* The pendulum stations in Lithuania were taken from Heiskanen's (1939) Catalogue.

The cluster of pendulum stations at 50° N, near the Polish border, are originally Polish measurements, reported in the Travaux, tome 16. The anomalies were recomputed with $d = 2.67$.

30. *Yugo-Slavia.* The observations in the N part of the country were already discussed in para. 12. The rest of the Balkan countries is devoid of gravity observations, except a few stations reported by Kossmat (1921), and some stations along the Dalmation Coast, measured by Von Triulzi (Borass, 1911).

The anomalies were recomputed using $d = 2.67$ and Cassinis' formula. Von Triulzi's measurements were lowered by 5 mgls, because the base-station Pola was too high by that amount (see para. 8). In Bulgaria there are two stations, reported by Tanni (1942). Istanbul was also taken from Tanni's publication.

Literature

Andersen, E., 1947. Gravity measurements in Sjaelland, Moen, Falster, and Lolland by means of the Askania-Gravimeter. Geod. Inst. Skrifter, 3 Raekke, Bind X, København.

Barsch, O., 1943. Aufgaben der angewandten Geophysik in Grossdeutschland und in östlichen Europäischen Raum. Jahrbuch Reichsamt für Bodenforschung, Band 63, Abb. 10.

Behounek, R., 1952. The gravity isonomals of the small Danubian lowland and adjoining regions. Sbornik du Service géologique de Tchéchoslovaqui, XIX.

Boaga, G., 1953. Profilo gravimetrico fra il Tirreno e lo Jonio lungo il parallelo 40°. Academia Nazionale dei Lincei, anno CCCL, Classe di Scienze fis., mat. e nat., Vol. XIV 1° sem., Fasc. 2.

——, Tribalto, G. and Zaccara, G., 1950a. Contributo alla construzione della carta gravimetrica d'Italia — le circuito. Servizio Geol. Italia, Boll. 1950, le Fasc., pp. 163/184.

——, Tribalto, G. and Zaccara, G., 1950b. Contributo alla construzione della carta gravimetrica d'Italia — circuito 2. Servizio Geol. Italia, Boll. vol. 72, fasc. 2, pp. 77/93.

Borass, E., 1911. Spezial Bericht über die relativen Schweremessungen. C. R. de la 16e Conférence générale de l'Ass. Géod. Intern., Vol. III.

Bott, M. H. P., Masson Smith, D., 1953. Gravity measurements over the Northern Pennines. Geol. Mag., vol. XC, No. 2, pp. 127/130.

Bourgoin, A., 1948. Sur les anomalies de la pesanteur en Syrie et en Libanon. Etudes géol. et géogr. sur le Liban, la Syrie et le Moyen-Orient, Tome IV, p. 59.

Browne, B. C., Cooper, R. I. B., 1950. The British Submarine gravity surveys of 1938 and 1946. Royal Society London, Philos. Trans. Series A Math. and Phys. Sciences No. 847, vol. 242, pp. 243/310.

——, Cooper, R. I. B., 1952. Gravity measurements in the English Channel. Royal Soc. London Proc., A, vol. 139.

Bullard, E. C., Jolly, H. L. P., 1936. Gravity measurements in Great Britain. R.A.S.-Monthly Notices. Geoph. Suppl., vol. 3, pp. 443/477.

Bullerwell, W., 1952. Gravimeter observations comparing pendulum stations at Cambridge, York, Newcastle upon Tyne, Edinburgh and Aberdeen. R.A.S. Monthly Notices. Geoph. Suppl., vol. 6, No. 5, pp. 303/315.

Bürgl, H., 1949. Der Untergrund der Molasse im bayrisch-österreichischen Grenzgebiet. Jahrbuch der Geologischen Bundesanstalt, Jahrgang 1948, XCIII Band.

Cassinis, G., 1941. La crociera gravimetrica del R. Sommergibile „Des Geneys", Anno 1935. Reale Acc. d'Italia, Fasc. 12, Ser. VII, Vol. II, Fasc. 12.

Cole, J. H., 1944. Geodesy in Egypt. Survey Dept., Min. of Finance, Chapter X.

Cook, A. H., 1950. Measurements of Gravity in Ireland. Pendulum observations at Dublin, Sligo, Galway and Cork. Dublin Institute for Advanced studies. Geophys. Mem. No. 2, part 1.

——, 1950. Values of gravity stations in Southern Britain. R.A.S. Monthly Notices Geoph. Suppl., vol. 6, No. 1, p. 9.

——, 1953. Adjustment of the principal gravity observations in Great Britain. R.A.S. Monthly Notices, Geoph. Suppl., vol. 6, No. 8.

——, Thirlaway, H. I. S., 1948. Recent observations of gravity in Wales and the Borders. Intern. Geol. Congress. Report of the 18th Session, Gr. Britain, 1948, Part V.

——, Thirlaway, H. I. S., 1952. A gravimeter survey in the Bristol and Somerset Coal fields. Geol. Soc. London, Quart. Journ., Vol. CVII, part 3, pp. 255/286.

——, Murphy, Th., 1952. Measurements of Gravity in Ireland. Gravity survey of Ireland north of the line Sligo-Dundalk. Dublin Institute for Advanced studies. Geoph. Mem. No. 2, part 4.

——, Hospers, J. G. and Parasnis, D. S., 1952. The results of a gravity survey in the country between the Clee Hills and Nuneaton. Geol. Soc. London, Quart. Journ. Vol. CVII, part 3, pp. 287/306.

Cooper, R. I. B., Harrison, J. C. and Willmore, P. L., 1952. Gravity measurements in the Eastern Mediterranean. Royal Soc. London Philos. Trans. Series A, Vol. 244.

Coster, H. P., 1945. The Gravity Field of the Western and Central Mediterranean. Dissertation, Utrecht.

Cunietti, M., 1952. Le anomalie della gravitò nell' Italia nord-occidentale. Ist. Geogr. Mil. Firenze. Boll. di Geodesia e sci. affini, VII, 3, pp. 279/336.

Duclaux, Mme F., Martin, M. J., 1952. Résultats de la première campagne gravimétrique, effectuée en Afrique de mars à juin 1951. Office de la recherche scientifique Outremer-Paris.

Espinoza de los Monteros, I. M., Lozano Calvo, L., 1950. Red de Observaciones con gravimetro en la provincia de Huelva. Inst. geogr. y catastral Sección la. Servicia de Geod.

Facsinay, L., 1948. Isostatic anomalies of Transdanubia — Hungary, according to the gravity meter measurements. Geofis. Pura e Applicata. V 13, Nos. 1-2, pp. 28/42.

Falcon, N. L., Tarrant, H. M., 1951. The gravitational and magnetic exploration of parts of the Mesozoic-covered areas of south-central England. Geological Society London. Quart. Journ. V 106, pp. 141/167.

Gloden, A., 1951. Détermination des anomalies de la pesanteur au Grand-Duché de Luxembourg. Soc. des Naturalistes Luxembourgeois Nouv. Série 45e année No. LVI des Publ. de la Soc. Botanique.

——, Gagniard, L. and Lucius, M., 1950. Déterminations expérimentales de la pesanteur du Grand-Duché de Luxembourg. Inst. Grand Ducal de Luxembourg, Archives, Nouvelle Série, Années 1948/49, tome XVIII.

Haalck, H., 1935. Verzeichnis der im Jahre 1934 mit dem Statischen Schweremesser auf der Nord- und Ostsee und in Nord-Deutschland gemessenen Schwerewerte. Zeitschr. f. Geophys., Jahrg. 11, H. 3.

Heiskanen, W., 1939. Catalogue of isostatically reduced gravity stations. Isostatic. Inst. Publ. No. 5.

Hofman, B. J., 1952. The gravity field of the West-Mediterranean Area. Geologie en Mijnbouw Nieuwe serie No. 8, 14e jaargang, pp. 297/306.

Holopainen, P. E., 1947. On the Gravity Field and the Isostatic Structure of the Earth's Crust in the East Alps. Isostatic. Inst. Publ. No. 16.

Hospers, J., Willmore, P. L., 1953. Gravity Measurements in Durham and Northumberland. Geol. Mag. Vol. XC No. 2, pp. 117/126.

Jelstrup, G., Trovaag, O., 1950. Gravity comparisons, Oslo-Teddington, Stockholm, Copenhagen. Norske grådmaling kommisjon og norges geografiske oppmåling.

Jones, L., 1948. La levée gravimétrique de la Belgique (1947-1948). Inst. Géogr. Mil.

——, 1951. Les anomalies isostatiques en Belgique. Inst. Géogr. Mil. Appendix: Répertoire des anomalies.

Kossmat, F., 1921. Die Mediterranen Kettengebirge in ihrer Beziehung zum Gleichgewichtszustande der Erdrinde. Abh. d. Math.-phys. Kl. d. Sächs. Akad. d. Wiss., B. 38, No. 2.

Lagrula, J., 1935. Sur l'intensité de la pesanteur en Algérie, dans le Midi de la France et dans l'île de Majorque. Ac. Sc. Paris C. R. tome 201, p. 1095.

——, 1951. Etude gravimétrique de l'Algérie-Tunisie. Bull. du Service de la Carte Géol. de l'Algérie, 4e Série Géoph., No. 2.

——, 1952. Sur la prolongation du réseau gravimétrique Nord-Africain aux Sahara-français. Travaux de l'Inst. de Recherche Saharienne, tome VIII.

Lejay, P., 1938. Exploration gravimétrique des Etats du Levant sous mandat français. Comité nat. français Géod. Géoph.

——, 1953. Etude gravimétrique de la Corse. Ac. Sc. Paris C. R. Vol. 237, No. 7, pp. 447/450.

Lozano Calvo, L., 1950. Red de observaciones con gravimetro en la Provincia de Avila. Inst. geogr. y catastral.

Mace, C., 1939. Gravity Measurements in Cyprus. R.A.S. Monthly Notices, Geophys. Suppl., Vol. 4, No. 7.

Mayer-Gürr, A., 1953. Yugoslavia. The Science of Petroleum, Vol. VI, part 1. The World's Oilfields. The Eastern Hemisphere, p. 60.

Morelli, C., 1948. La rete geofisica e geodetica in Italia etc. Osservatorio Geof., Trieste, Pubbl. No. 222.

——, 1951. Rilièvo gravimetrico e reduzione isostatica nell'Italia Nord-Orientale. Osservatorio Geof., Trieste, Nuòva Serie, Pubbl. No. 20.

——, 1952. Primo contributo per una rete gravimetrica fondamentale in Italia. Annali Geofisica, No. V, No. 1.

——, 1954. Rilièvo gravimetrico dell'alto Adriatico. Technica Italiana. Rev. d'ing. e scienze, Nuòva Serie, anno IX, numero 1.

——, Medi, E., 1952. Rilièvo gravimetrico della Sicilia. Annali Geofisica, Vol. 5, No. 2, pp. 209/245.

Mulder, A. J., 1950. Oil in the Netherlands and Emsland. Journ. Inst. Petroleum, Vol. 36, No. 315, pp. 124/136.

Murphy, Th., 1952. Measurements of gravity in Ireland. Gravity survey of Central Ireland. Dublin Inst. of Advanced Studies. Geoph. Mem. No. 2, part 3.

Nørgaard, G., 1936. Statische Schweremessungen auf See. Verh. d. 8. Tag d. Balt. Geod. Komm. Helsinki.

——, 1939a. Ein statischer Quarschweremesser und Schweremessungen. Geod. Inst. København, Meddelelse No. 10.

——, 1939b. Einige Schwereverhältnisse in Dänemark. Geod. Inst. København, Meddelelse No. 12.

Olczak, T., 1951. Mapa grawimetryczna Polski. Panstwowy Inst. Geol. Buil. 64, seria geofizyczna, No. 5.

Picha, J., 1950. Gravity values on some pendulum stations in Czechoslovakia measured by the Nörgaard gravimeter. Inst. Géoph. National,, Praha, Publ., Travaux spéciaux, No. 4.

Reich, H., 1949. Geophysikalische Probleme im bayrisch-schwäbischen Donau-Raum. Erdöl u. Kohle, 2e Jahrgang.

Sans Huelin, G., 1944. Determinaciones relativas de la intensidad de la gravidad. 1933/42. Inst. Geogr. y Catastral, tomo XVII, II.

——, Lozano Calvo, L., 1947. Red. de observaciones con gravimetro en la Provincia de Segovia. Inst. Geogr. y Catastral. Servicio de Geodesia.

Saxov, S. E., 1945. Some gravity measurements on the Island of Bornholm. Geod. Inst. København. Meddelelse No. 19.

——, 1952. The Danish gravity reference stations. Geod. Inst. København. Meddelelse No. 25.

Schütte, K., 1930. Karte der Schwereabweichungen von Süddeutschland. Veröff. d. Bayerische Komm. f. d. Intern. Erdmessungen, München.

Siemens, G., 1953. Die Schwerekarte der D.D.R. Freiberger Forschungshefte, Reihe C, Angew. Naturwissenschaften, Heft 7.

Sitter, de, L. H., 1949. Eindverslag van het geophysisch onderzoek in ZO-Nederland. Geol. Stichting. Mededelingen, Serie C, I, 3, No. 1.

Solaini, E., 1951. Principal characteristics and results of the gravimetric surveys made in Italy for oil and gas exploration. Proc. 3rd. World Petr. Congress, Section 1, p. 240.

Szurovy, G., 1948. Geological structure of the southern part of the Great Hungarian Plain. Annales Historico-Naturales Musei Nationalis Hungarici, vol. XLI, No. 1, pp. 1/24.

Tanni, L., 1942. On the Isostatic Structure of the Earth's Crust in the Carpathian Countries and the related Phenomena. Isostatic. Inst., Publ. No. 11.

Thirlaway, H. C. S., 1951. Measurements of Gravity in Ireland. Gravimeter observations between Dublin, Sligo, Galway and Cork. Dublin Institute for Advanced Studies. Geoph. Mem. No. 2, part 2.

Tribalto, G., Zaccara, G. and Beneo, E., 1952. Misure gravimetriche nella valle Latina (Lazio) con deduzioni geoliche. Servizio geologico d'Italia, Boll., V 73, fasc. 2, pp. 357/370.

Vajk, R., 1952. Geophysical Exploration of south-west Hungary. Geophysics, vol.. XVII, No. 2, pp. 278/310.

Vecchia, O., 1952. Sui principali carratteri strutturali dell' Italia settentrionale dalle misure gravimetriche. Riv. Geofisica Appl. anno XIII, No. 1.

Vening Meinesz, F. A. 1948. Gravity expeditions at Sea. Vol. IV. Publ. Netherlands Geod. Comm.

Weiken, K., 1950. Ergebnisse der Pendelmessungen der Jahre 1934 bis 1943. Geod. Inst. Potsdam Veröff. No. 3.

White, P. H. N., 1949. Gravity data obtained in Great Britain by the Anglo-American Oil Company Limited. Geol. Soc. London Quart. Journ., 104, pp. 339/364.

Wideland, B., 1942. Relative Schwerebestimmungen in Schweden im Jahre 1941. Die Tätigkeit der Balt. Komm. 1938-1941, Helsinki.

——, 1946. Relative Schweremessungen in Süd- und Mittelschweden in den Jahren 1943-44. Rikets Allm. Kartverk., Meddelande Nr. 6, Stockholm.

Wieladek, R., 1951. Podstawowe pomiary gravimetryczne W. Polnocno Wschodniej Polsce. Panstwowy Inst. Geol. seria geofiziczna No. 7.

Woollard, G. P., 1952. World wide gravity measurements conducted during the period June 1949-January 1952. Woods Hole Oceanographic Institute.

Yüngül, S., 1951. Rift Valleys, and some tectonic results of the Hatay Gravity Survey. Geological Society of Turkey Bull. vol. III, No. 7.

Discussion

Mr. Baranov: Mr. de Bruyn a-t-il les données gravimétriques pour la région de la Mer Rouge.

En 1939 j'ai trouvé dans cette région de très fortes anomalies positives. Du point de vue de la théorie de Wegener la question me paraît intéressante.

Ne pourrait-on pas demander aux compagnies qui ont fait des mesures gravimétriques dans cette région de publier une partie des résultats.

Mr. de Bruyn: Von Triulzi observed 47 stations in 1897 in the Red Sea area. Vening Meinesz made observations in a submarine in the Red Sea.

B.P.M. did not make any observations here.

Mr. Morelli: Since the maps of Mr. de Bruyn represent a basic, fundamental work, all efforts should be made to improve and complete them. At the present state of research, it is of general interest that the general lines of the gravimetric field over great areas be known.

More stations could be obtained from private prospecting compagnies, and members of E.A.E.G. in each country should make efforts in this direction. A compensated reference net for Europe is now ready.

Mr. Domzalski: How was the value of density used for the reduction of the gravity data arrived at?

It seems to me that perhaps more suitable values could be obtained by determining the densities from gravity measurements in the shafts located in representative areas throughout the whole area covered by the gravity observations.

Mr. de Bruyn: Using variable figures for the density in the Bouguer correction factor is only possible for a Bouguer isogam map. When one wants to correct a Bouguer isogam map for isostasy, a uniform density of 2.67, however, is necessary because in the isostatic computations a density of 2.67 for all topographic features is assumed.

Mr. Schleusener: Regarding density maps of Europe I want to mention that I introduced on all the German regional gravity maps 1 : 200,000 lines of equal densities used for Bouguer corrections in the form of density provinces. This has not been difficult as these maps refer to a datum level. Going down to sea-level the densities would become more uncertain as we had to assume a geology down to sea-level which we of course do not know exactly. But it still seems to me better to use the best assumed density than a uniform value which is already known to be wrong at many places. In addition, we have already fixed by our method the main density provinces.

THREE DIMENSIONAL GRAVITY SURVEY *

BY

W. DOMZALSKI **

Abstract

The paper describes and discusses the results of an experimental gravity survey which was carried out underground on different levels of a mine, in the mine shafts, and on the surface above the mine workings.

The paper is composed of three complementing sections. The part dealing with gravity measurements in the shafts gives also attention to the particular problem of the terrain corrections underground, due to the surface topography. The interval densities from gravity measurements in the shafts are computed and adjusted in accordance with known geology and compared with the stratigraphical columns of the shafts. The effect of the ore body on the stations in the shaft is derived theoretically and compared with the observed one.

The gravity contours are constructed on different levels in the mine workings and discussed in relation to the known extent of the ore body. The gravity profile across a fault underground is presented and discussed. Another gravity profile was run underground in the same plan position as a surface traverse 1000 feet above it. The line of boreholes along this traverse gives good account of geology which includes step-faulting. This known geology is compared with the deductions based on the gravity results. This is also done in the case of another gravity profile run over a known geological section. A number of gravity measurements were also taken in the same plan position, separated by the vertical distance of 800-1,100 feet. These points were placed by the boreholes previously drilled in the area. Attempt in correlation of these and gravity results is made.

The densities computed from the gravity measurements are compared with the laboratory determinations of the densities, carried out on samples from different parts of the mine.

The contours on the top of the base formation are constructed from the information obtained from the boreholes, and are compared with the gravity contours on the surface above.

A simple method of computation of the effects of slabs and blocks is presented as applied to the calculation of the corrections for underground drifts and faults. A table is appended for use with this method.

Introduction

The application of gravity methods to large scale structural investigations such as oil exploration has not been paralleled in investigations carried out on a smaller scale. Admittedly the problems confronting a geophysicist engaged on a gravity survey which aims at the location of an ore body, or a small fault, are more difficult. This is so because the order of the expected anomaly approaches dangerously the accuracy of the observations and is often less than the effects of the disturbing factors such as the topography or changes in the overburden thickness. Nevertheless gravity measurements carried out not on a regional but on a local scale, apart from the interesting results which they offer, can be of real assistance in the determination of the small local structures. If it is possible to extend these measurements underground, they can assist in a variety of problems. The purpose of this paper is to present the results of such a three dimensional gravity survey and to correlate these results with known geology and conditions, indicating at the same time the unorthodox techniques which had to be used.

---

* Presented at the sixth meeting of the European Association of Exploration Geophysicists, held in Copenhagen, May 19/21, 1954.

** Mining & Geophysical Services Ltd., London.

Gravity measurements were carried out in Florence Mines. The observations were taken in two mine shafts, on different levels in the mine workings, in the drifts connecting the shafts and on the surface, in the same plan position, whenever possible, as the stations underground.

The densities of samples collected in the mine were determined in the laboratory and compared with the determinations from gravity measurements. Geological sections based on borehole information were constructed for comparison with the surface and underground gravity profiles. A simple method for the computation of the attraction of semi-infinite slabs and blocks is presented in the appendix and an indication is given of how it was applied to the calculation of the effect of underground roadways.

Gravity measurements in the same plan position on the surface and underground furnish data which are interesting from the geodetic point of view, such as derivation of the mean earth density, which is however beyond the scope of this paper.

Relevant Information about the Site

Florence Mines are situated close to Egremont in Cumberland, England. The mining operations are conducted about 850 feet under the surface on a deposit of hematite ore in limestone. The mining has been going on for some considerable time and there are large local areas of subsidence on the surface above the mine workings. The mineralisation in the area provided scope for several mining enterprises, some of which have joined up in their operations. Florence and Ullcoats workings are connected by an underground haulage drift which runs in an approximate ESE direction from Florence shafts for a distance of about 3,150 feet (c. 960 metres) and then turns practically due north to reach the Ullcoats No. 7 shaft distant about 1,750 feet (c. 530 metres) (Fig. 1).

The information from about forty boreholes in the area helped in the appreciation of the geology. The cover of the Glacial Drift rests on Sandstone beds underlain in turn by Conglomerate, Limestone and Ordovician Slate, which is the deepest formation penetrated by the boreholes. Sandstone is of Triassic, Conglomerate of Permian and Limestone of Carboniferous age. The relative thicknesses of the formations vary and the whole area is crossed by

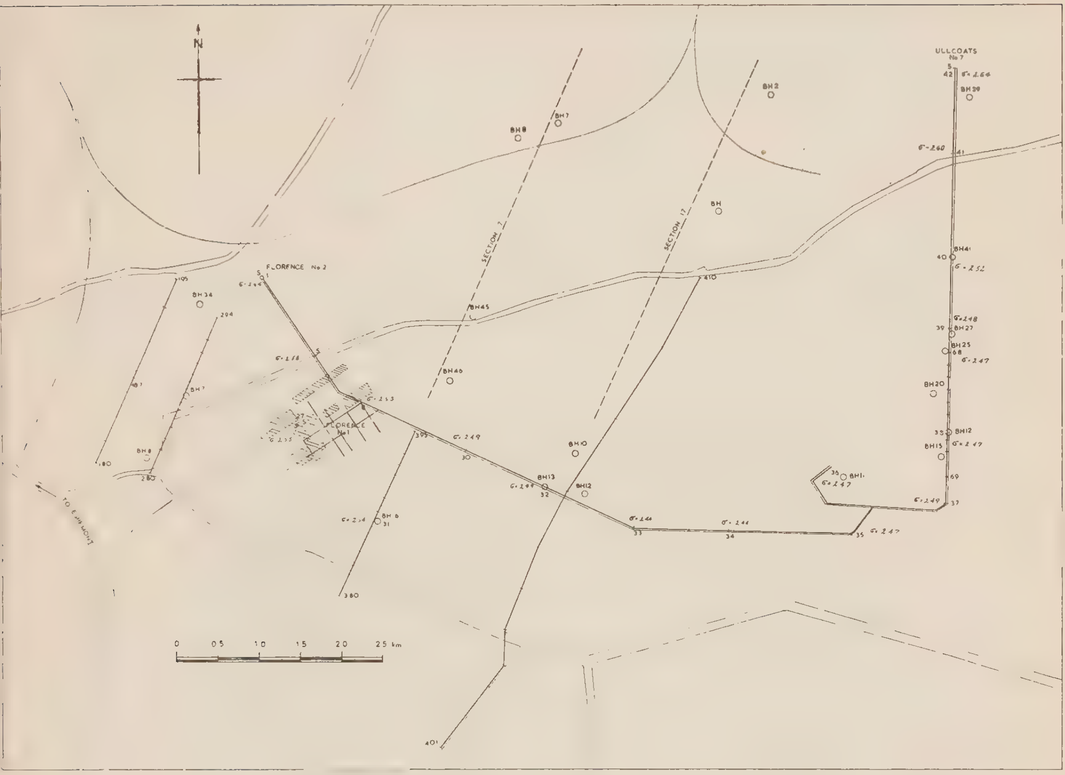

Fig. 1. Plan of general disposition of surface and underground gravity stations.

a number of faults running in an approximately NW-SE direction. The topography is accentuated by the subsidence and the range of surface elevations over the area concerned is 240 feet.

General Description of the Work carried out

Surface stations were located vertically above previously established underground stations. Apart from these the observations were made on four additional traverses on the surface. The layout of the surface and underground stations is illustrated on Fig. 1, which also shows the positions of some of the boreholes.

In the mine workings the observations were made on four different levels referred to later as level 313-330, level 370, level 385 and level 400. The actual elevations of the stations occupied on these levels remained within a few feet of the level reference elevation. The location of the stations underground was limited to the accessible places and governed by the existing cross-cuts and drifts. The general scheme was to have the stations on different levels, as well as those on the surface above the workings, in the same plan position.

The other factor taken into consideration when choosing the positions of the stations in the main haulage drift was to locate them as close as possible to the positions of the boreholes. Whenever possible the existing mine plans were used.

Accuracy and Corrections

Gravity measurements were carried out with a Worden gravity meter. The estimated accuracy of the single observation was ± 0.03 milligal.

All the relative gravity values are referred to the base station No. 27 at the top of the Florence No. 1 shaft for which the assumed uncorrected value was 200.00 milligals. Thus all the surface and underground stations are tied to a common base. The error of closure of the vertical loop was + 0.10 milligal. This loop ran from the top of the Florence No. 1 Shaft to Ullcoats No. 7 shaft (station 42) down this shaft and along the main haulage drift back to Florence No. 1 shaft and up this shaft to Station 27 on the top. On the whole some 90 stations are involved in a distance of 11,700 feet (3566 metres). Considering that measurements in the shafts under difficult conditions are included this can be considered a good closure.

All the gravity values observed on the surface and underground stations had to be corrected for a variety of effects. Most of these corrections are standard, however additional corrections had to be applied for the underground and shaft stations. The amount of computations and labour involved in the determination of all these corrections was very considerable, but as they are not of main interest in this discussion the prominence given to them is out of proportion to the work involved. The latitude correction was applied to all surface and underground stations, using the latitude of Ullcoats No. 7 shaft as the base latitude. Terrain corrections for the surface stations were calculated using Hammer's Tables up to the zone J (radius 21,826 feet or 6,652 metres). For the shaft and underground stations these corrections were computed from first principles, using however the same radius and size of the compartments. Further mention is made of the terrain corrections for the shaft stations in the paragraph dealing with the measurements in the shafts. To reduce the amount of work involved in the calculation of the terrain corrections, a certain amount of interpolation was carried out between primary stations. The distances between the primary stations were decreased when less distant topography was considered. Checks were made to ascertain that this method does not affect the accuracy.

The elevation corrections were applied very carefully using different densities for reduction, according to the area and the range of elevations. The general scheme was to carry out separate reductions for individual profiles to the lowest point on the given profile with the density of the underlying material. The further reduction to one common datum was then undertaken with appropriate densities (Domzalski 1954b). The datum for the elevation corrections of the underground stations was chosen in each instance to pass through the reference elevation of the given level. Consequently the corrected values of the observed gravity cannot be compared directly between different levels without further reduction, which is not however necessary for the purpose of this discussion. The additional correction was applied in the case of the underground stations to compensate for the effect due to the excavation of roadways (Appendix).

GRAVITY MEASUREMENTS IN THE SHAFTS

Gravity measurements in the vertical shafts became possible with the advent of small and easily portable gravity meters and are an early development of a technique leading to the construction and use of a commercial borehole gravity meter. A full discussion of a gravity survey in a vertical shaft has been offered previously (Hammer 1950, Smith 1950, Rogers 1952, Domzalski 1954a) and only essentials will be considered here.

Fig. 2. Gravity observations in a shaft.

The measurements were carried out in two shafts, namely — Florence No. 1 and Ullcoats No. 7 to a depth of 921.5 feet (281 m) and 980 feet (299 m) respectively. Both shafts have circular cross-sections: of 18 feet (5.5 m) and 20 feet (6.1 m) radius. The observations were also made at the top and bottom of the third shaft Florence No. 2. Of these three shafts Florence No. 1 passes through the deposit of hematite between the depths of 820-880 feet below the surface (250-268 m). The stratigraphy of two shafts where gravity stations were established is illustrated on Fig. 5 and will be discussed together with the interval density values.

The number of set-ups in F. No. 1 was fourteen and in U. No. 7 twelve. Their positions were planned so as to be on, or closest possible to the boundaries between the different formations. Ultimately however this depended on the disposition of the transverse wooden buntings, supporting the pipes and cables in the shaft. The observations were taken from the top of the cage (Fig. 2) with the gravity meter placed on the little platform, nailed to the bunting (Fig. 3). The attempts to take the observations with the gravity meter on the cage failed, because such a set-up was not steady enough.

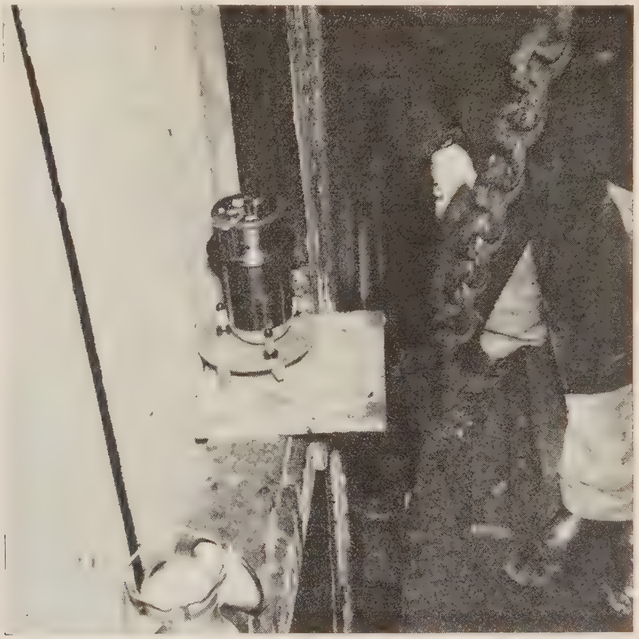

Fig. 3. A set-up for gravity meter in a shaft.

The results of the measurements in the two shafts are shown in Table 1 and Table 2. The "uncorrected gravity" in column 3 of these tables is the observed gravity adjusted for drift, closure and averaged if more than one observation was taken at any position. The correction datum is passing through the shaft collar.

TABLE 1

GRAVITY OBSERVATIONS IN FLORENCE NO. 1 SHAFT

All Gravity Values in Milligals
Depth in Feet

1 Station	2 Depth Below Shaft Collar	3 Uncorrected Gravity	4 Free Air Correction	5 Terrain Correction Due to Surface Topography	6 Correction For Shaft Effect	7 Correction For Underground Excavation	8 Corrected Gravity
a	+ 1.0	200.00	+ 0.09	+0.27	+0.13	+0.03	200.52
b	— 24.0	201.10	— 2.26	+0.27	+0.08	+0.03	199.22
c	—255.5	209.07	—24.03	+0.31	+0.03	+0.03	185.41
d	—466.5	215.27	—43.88	+0.42	+0.03	+0.03	171.87
e	—487.0	215.81	—45.81	+0.43	+0.03	+0.03	170.49
f	—607.5	219.07	—57.14	+0.49	+0.03	+0.02	162.47
g	—658.0	220.34	—61.89	+0.52	+0.03	+0.02	159.02
h	—718.0	221.99	—67.54	+0.54	+0.03	+0.02	155.04
j	—758.5	223.06	—71.34	+0.56	+0.04	+0.01	152.33
k	—798.5	224.19	—75.11	+0.57	+0.04	+0.01	149.70
l	—829.0	224.80	—77.98	+0.58	+0.04	+0.01	147.45
m	—859.0	224.85	—80.80	+0.58	+0.02	0	144.65
n	—889.0	225.21	—83.62	+0.58	—0.03	0	142.14
o	—921.5	226.29	—86.68	+0.58	—0.01	—0.01	139.98*

* including —0.19 correction for roadway.

TABLE 2

GRAVITY OBSERVATIONS IN ULLCOATS NO. 7 SHAFT

All Gravity Values in Milligals
Depth in Feet

1 Station	2 Depth Below Shaft Collar	3 Uncorrected Gravity	4 Free Air Correction	5 Terrain Correction Due to Surface Topography	6 Correction For Shaft Effect	7 Corrected Gravity
a	+ 2.0	197.99	+ 0.19	+0.23	+0.12	198.53
b	— 60.0	200.40	— 5.64	+0.48	+0.06	195.30
c	— 98.0	201.61	— 9.22	+0.55	+0.05	192.99
d	—212.5	204.57	—19.99	+0.69	+0.02	185.29
e	—327.0	207.46	—30.76	+0.74	+0.01	177.45
f	—403.5	209.35	—37.95	+0.77	+0.01	172.18
g	—479.5	211.24	—45.10	+0.79	0	166.93
h	—518.0	212.30	—48.72	+0.80	0	164.38
j	—559.0	213.15	—52.30	+0.81	0	161.66
k	—671.0	215.94	—62.88	+0.85	0	153.91
l	—825.0	219.78	—77.41	+0.89	0	143.26
m	—980.0	223.77	—92.18	+0.94	—0.01	132.40*

* including —0.12 correction for roadway.

TABLE 3

ORE BODY EFFECT AND INTERVAL DENSITIES IN FLORENCE SHAFT NO. 1

Gravity Values in Milligals
Elevations in Feet

1 Station	2 Corrected Gravity	3 Correction for Ore Body Effect	4 Final Gravity Value	5 Difference of Gravity	6 Difference of Elevation	7 Interval Density
a	200.52	−0.02	200.50			
				1.30	24.0	2.12
b	199.22	−0.02	199.20			
				13.84	231.5	2.34
c	185.41	−0.05	185.36			
				13.57	211.0	2.52
d	171.87	−0.08	171.79			
				1.40	20.5	2.67
e	170.49	−0.10	170.39			
				8.05	120.5	2.62
f	162.47	−0.14	162.34			
				3.49	50.5	2.71
g	159.02	−0.17	158.85			
				4.11	60.0	2.62
h	155.04	−0.27	154.77			
				2.82	40.5	2.73
j	152.33	−0.38	151.95			
				2.85	40.0	2.79
k	149.70	−0.60	149.10			
				—	—	—
l	—	−0.57	—			
				—	—	—
m	—	+0.18	—			
				—	—	—
n	142.14	+0.69	142.83			
				2.36	32.5	2.85
o	139.98	+0.49	140.47			

The correction for the effect of the ore body in F. No. 1 shaft is introduced in Table 3 and 3 A. The effect of the cavities due to mine workings in case of the stations in the Ullcoats shaft is negligible, and therefore not considered. Correction for the effect of the shaft was computed on the basis of formulae for the vertical cylinder. The corrections applied to the observations in the shaft and due to the surface topography are of interest, because they can attain a considerable value. This depends not only on the elevation of the surface feature above the datum through the top of the shaft and the distance of the topographical feature from the shaft, but also on the relative position of the shaft station in respect to the feature. Thus the correction may gradually increase to a maximum and then decrease. Its sign will depend on whether there is an excess or deficiency of mass in reference to datum (Domzalski 1954 a).

TABLE 3A

SPECIAL CORRECTION AND INTERVAL DENSITIES FOR STATIONS IN THE ORE IN FLORENCE SHAFT NO. 1

1 Station	2 Corrected Gravity	3 Special Correction	4 Final Gravity Value	5 Difference of Gravity	6 Difference of Elevation	7 Interval Densities
k	149.70	—0.51	149.19			
				2.43	30.5	3.12
l	147.45	—0.69	146.76			
l	147.45	—0.11	147.34			
				2.95	30.0	3.85
m	144.65	—0.26	144.39			
m	144.65	+0.53	145.18			
				2.67	30.0	3.49
n	142.14	+0.37	142.51			

The interval densities computed from the observed and corrected gravity values are affected most by the terrain corrections at the positions where the rate of change of this correction is highest. This will vary in each instance, but some idea of the possible effect is given by the following example. In Ullcoats shaft the interval density between stations c and d is calculated as 2.64 gr/cm^3. If the terrain correction was not applied this value would become 2.68 gr/cm^3. It is possible to quote examples where this error attained 10 %. This brief discussion of terrain corrections has to be brought to an end. It will only be added that the density used for their calculation was based on the first approximation from the measurements in the shafts and varied between 2.00 gr/cm^3 and 2.40 gr/cm^3 according to the range of elevations.

Before the discussion of interval densities is undertaken it will be necessary to say a few words about the shape of the ore body and the method of the evaluation of its effect. Fig. 4 shows the approximate shape of the ore body in plan and side elevation although the complexity of real shape is not thus revealed. The south-eastern boundaries are imposed by the advance of the mining operations. The approximate geometrical shapes chosen were a disc and a segment. The disc of 100 feet (c. 30 m) radius and the height of 62 feet (c. 19 m) fits reasonably well into the actual shape. The dimensions of the segment were calculated on the basis of the equivalent volume and are as follows: segment angle 52°, radius 600 feet (c. 183 m) and height 48 feet (c. 15 m). The calculated effect of this geometrical shape is shown in Table 3, column 3, and plotted on Fig. 7.

The interval densities were calculated from the observed corrected gravity values, using the expression $\Delta g = [\Delta F - 4\pi G\sigma] \,.\, \Delta h$, where Δg and ΔF are the observed gravity difference and the free air correction difference respect-

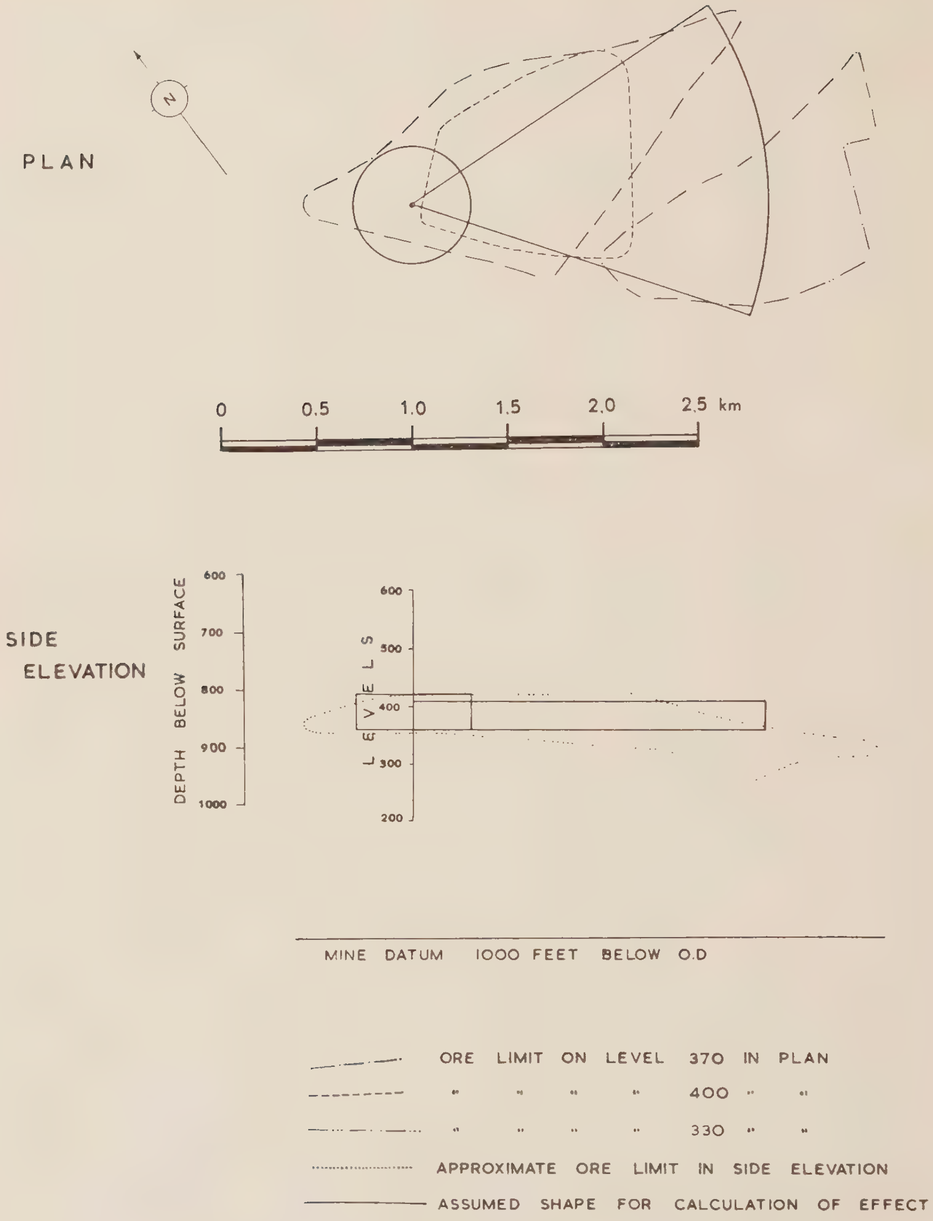
PLAN
N
0
0.5
1.0
1.5
2.0
2.5 km
SIDE ELEVATION
DEPTH BELOW SURFACE
600
700
800
900
1000
LEVELS
600
500
400
300
200
MINE DATUM 1000 FEET BELOW O.D
ORE LIMIT ON LEVEL 370 IN PLAN
" " " " 400 " "
" " " " 330 " "
APPROXIMATE ORE LIMIT IN SIDE ELEVATION
ASSUMED SHAPE FOR CALCULATION OF EFFECT

Fig. 4. Real and assumed shape of ore body.

ively for the vertical distance Δh between the two stations. G is the universal gravitational constant and σ the density. The Bouguer attraction is represented by the term $4\pi G\sigma\Delta h$ because the upward and downward attractions of the layer are combined. In the application of this formula certain assumptions have been made which however in practice are only approximated. These are: the infinite lateral extent of the layer Δh, its homogeneity and horizontality. The full discussion of these problems is offered elsewhere (Domzalski 1954 a). It will be enough to say here that the condition of the infinite lateral extent is sufficiently approximated if the ratio of this extent to the thickness of the layer Δh is greater than six; the effect of the layer is then 95 % of the effect of the infinite layer (Table 6 in the appendix).

The interval densities for Florence and Ullcoats shafts are presented in Tables 3, 3A and 4.

TABLE 4

INTERVAL DENSITIES IN ULLCOATS NO. 7 SHAFT

Gravity Values in Milligals
Elevations in Feet

1 Station	2 Corrected Gravity	3 Difference of Gravity	4 Difference of Elevation	5 Interval Densities
a	198.53			
		3.23	60.0	2.11
b	195.30			
		2.31	38.0	2.38
c	192.99			
		7.70	114.5	2.64
d	185.29			
		7.84	114.5	2.68
e	177.45			
		5.27	76.5	2.70
f	172.18			
		5.25	76.0	2.71
g	166.93			
		2.55	38.5	2.60
h	164.38			
		2.72	41.0	2.60
j	161.66			
		7.75	112.0	2.71
k	153.91			
		10.65	154.0	2.71
l	143.26			
		10.86	155.0	2.75
m	132.40			

The method of correction for the ore body effect as shown in Tables 3 and 3A requires some additional explanation. For the stations beyond the upper and lower limits of the ore, application of the correction is straightforward and based directly on the effect as computed from the assumed geometrical shape

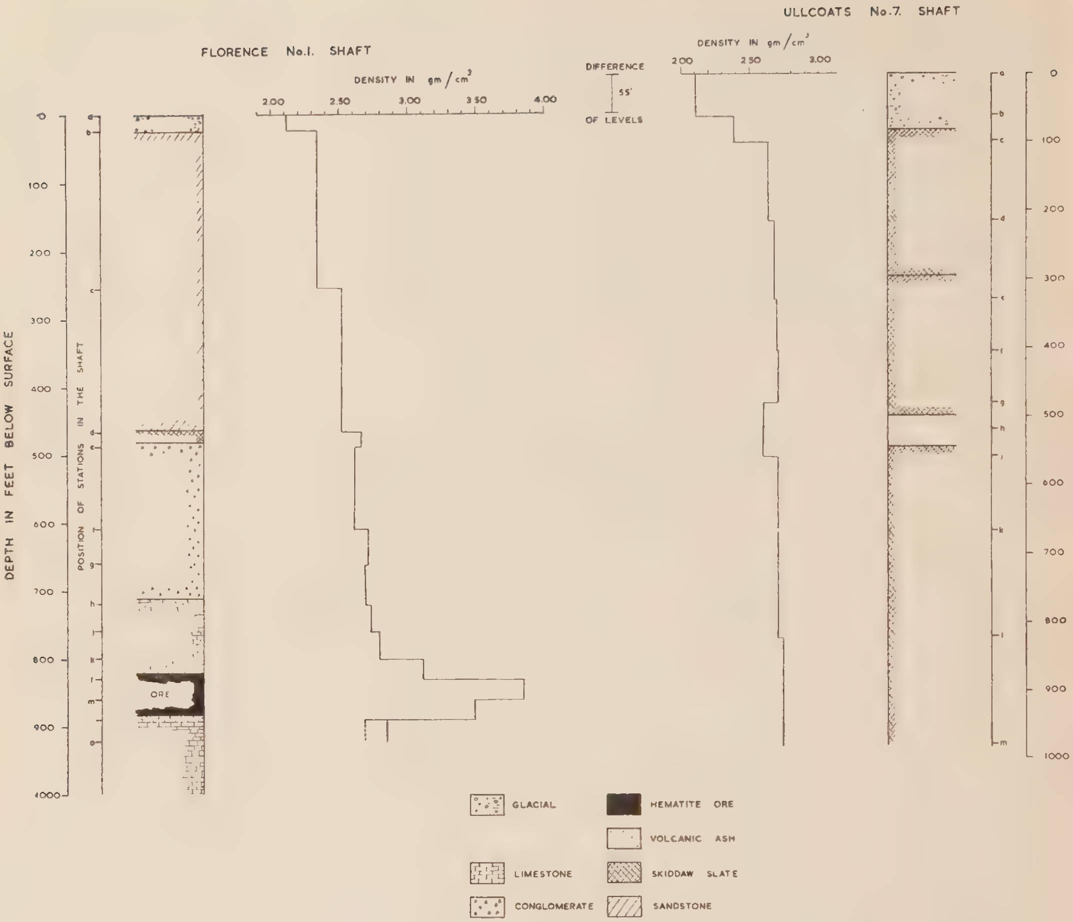

Fig. 5. Correlation of interval densities and stratigraphy for Florence and Ullcoats shafts (correction for ore body effect applied).

of the ore body. To calculate the interval density between the stations which are entirely within the ore it is necessary as the initial approximation to make an assumption that the layer of ore between the stations is infinite. Secondly the corrections for the effects of the ore above the upper station and below the lower station have to be applied. This involves what might be termed a partial correction for the ore body effect. The ore between the stations is considered as the cause of the gravity changes between these stations, after the effect of ore above and below had been removed. The effect of each portion of ore on each station has to be considered, and according to which pair of stations is under consideration the correction will change even for the same station. This explains the grouping of pairs of observations in Table 3A.

The interval densities are plotted in relation to the stratigraphical columns of Florence and Ullcoat shafts on Fig. 5. The changes in the stratigraphy are well illustrated by the variations of density.

Referring to the results for Florence shaft (Fig. 5) the most pronounced changes in density reflect the presence of the ore body. The changes of a lesser magnitude are observed near boundaries between the formations. The increase in density approximately half way down through Sandstone denotes probably the change in the lithology of the rock. The thin band of slate stands out between the Sandstone and the Conglomerate. Proceeding down towards the ore the density increases as could be logically expected due to the partial mineralisation of the region adjacent to the main ore body. This is not so well observed when the correction due to ore body effect is not considered. The greatest discrepancy between the corrected and uncorrected densities takes place for stations within the ore body, attaining 0.2 gr/cm³, which is over 5 % of the correct value. Another interesting effect is illustrated by the dashed line for the bottom interval on Fig. 5. This represents the density computed without correcting the gravity on the lowest station for the effect of the roadway. The error due to this is also 5 % of the correct value.

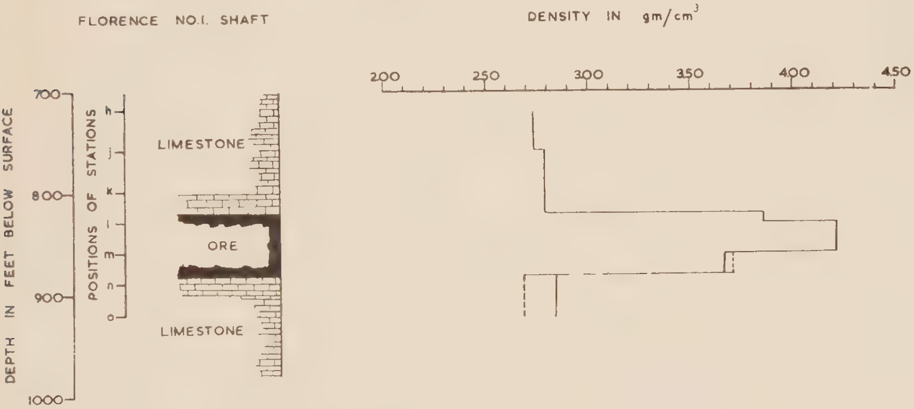

Fig. 6. Correlation of interval densities and ore boundaries.

The positions of the stations were chosen as close to the inter-formation boundaries as it was possible. It must be remembered however, that the distribution of the densities would be somewhat different if the stations were exactly on the boundaries. This would be most noticeable where the density contrast is largest. An attempt was therefore made to reconstruct the density distribution in such a case, considering at the same time the previously neglected fact that the horizontal dimensions of the ore are finite. This was done at first for the interval l-m. The calculation required a series of approximations and was carried out in two steps, the first of which dealt with the NE-SW section of the ore, and the second with the NW-SE section. The result of these corrections was to raise the calculated density of the ore to 4.22 gr/cm³. Next, the intervals

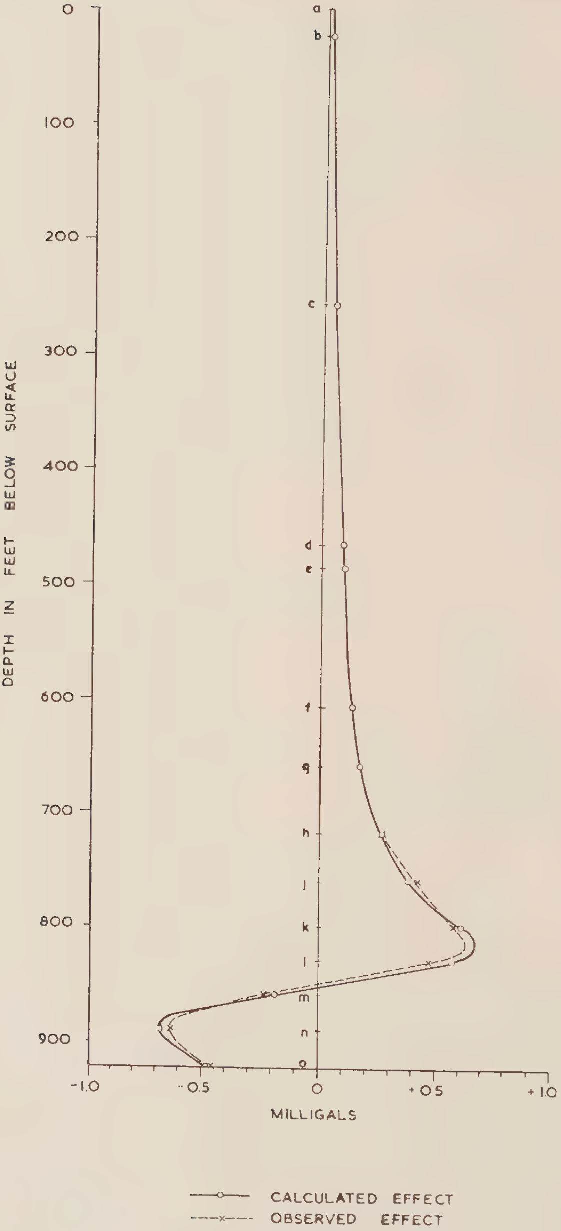

Fig. 7. Calculated and observed effects of the ore body in Florence No. 1 shaft.

k-l and m-n were considered and the resultant densities were respectively 3.86 gr/cm³ and 3.67 gr/cm³. The difference between these and the density of 4.22 gr/cm³ can be explained by the changes in the horizontal extent of the ore between stations k-l, m-n and l-m. This new distribution of the interval densities for stations in the vicinity of the ore is shown on Fig. 6 where the dashed line denotes, as before, the result of calculations uncorrected for the effect of the roadway on gravity of the bottom station.

The evaluation of the ore body effect at different depths in the shaft had been based, as previously described, on an approximated regular shape. This effect is compared with the observed effect on Fig. 7. The observed values of gravity were reduced according to standard procedure (although the Bouguer term of the correction is $4\pi G\sigma\Delta h$) using the average density of the medium in which the anomalous mass is contained. This comparison could not be made all the way down the Florence shaft, because of the effect of various formations having densities which differ from the density of Limestone in which the ore is contained. Consequently, for the purpose of comparison the reduction of observed gravity was carried out only from station h downwards, that is within the Limestone limits. The agreement is good and confirms that the approximated shape was sufficiently accurate. The elevation correction was calculated using the density of 2.75 gr/cm³, while for the theoretical calculations of the ore body effect the density contrast assumed was 1.25 gr/cm³. This suggests the average ore density of 4.00 gr/cm³, which falls between 3.85 gr/cm³ (Table 3A) and 4.22 gr/cm³, the interval densities values calculated without and with correction for finite ore extent, respectively.

The interval densities for the Ullcoats shaft (Table 4) also correlate satisfactorily with the stratigraphy (Fig. 5). The figures obtained for the density of Glacial Deposits for Florence and Ullcoats are 2.12 gr/cm³ and 2.11 gr/cm³ which would point to the uniformity of the overburden. With the exception of a layer of Volcanic Ash, the density distribution in Ullcoats shaft is almost uniform which is explained by the uniformity of the stratigraphical column.

There are two possible ways of approach in the interpretation of the shaft gravity observations. One which has been followed here is to convert the corrected observations into interval densities. It has the advantage of being easily comparable with the geology as demonstrated on the accompanying figures. The other is to assume what might be called a normal or average density, reduce all the corrected observations with this density and make the deductions from this vertical gravity profile. This is shown for two shafts on Fig. 8 where the average assumed density was $\sigma_a = 2.60$ gr/cm³. The reduction was carried out, using the formula $g_r = g_o - Fh + 4\pi G\sigma_a h$. The variations of gravity δg remaining after reduction are caused by the difference between the assumed average density σ_a and the true density σ_t of a given stratum. Consequently the difference between σ_a and σ_t can be expressed as $\delta\sigma = -(1/4\pi G)(\delta g/\Delta h)$ or substituting the numerical values $\delta\sigma = -39.18\,\delta g/\Delta h$, which indicates the functional relationship between the density and slope

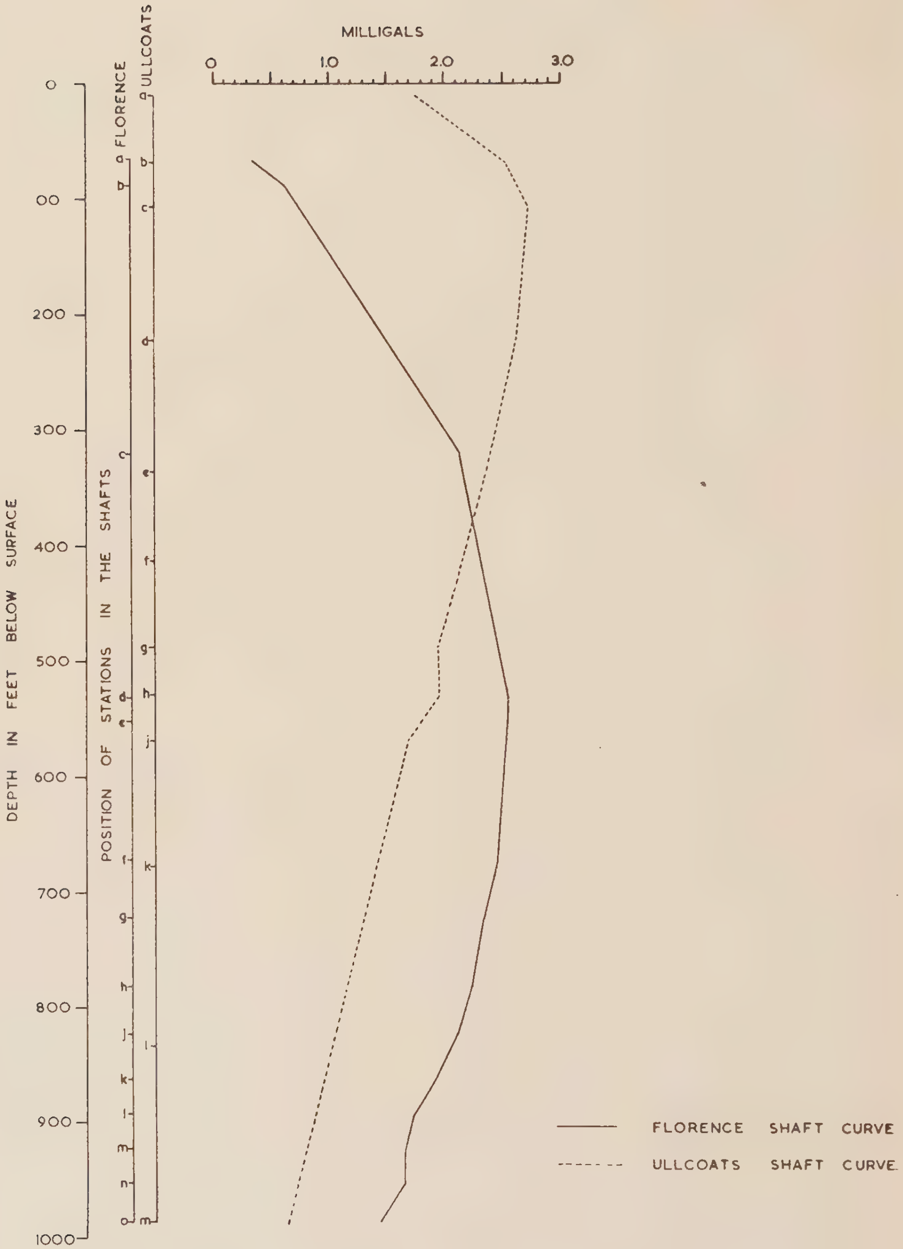

REDUCTION WITH AVERAGE DENSITY $\sigma_a = 2.60$ gr/cm^3

Fig. 8. Change of observed corrected gravity in Florence and Ullcoats shafts.

$\delta g/\Delta h$. Thus the changes in the slope reflect the variations of the actual densities of the formations traversed in respect to the assumed average density. Slope to the right indicates a density lower than average density, and vice versa.

Conclusions

It has been demonstrated in the preceding paragraph that good agreement between the density distribution as calculated from gravity measurements and the stratigraphy can be achieved. Satisfactory approximation to the natural conditions can be obtained from the assumption of simple geometrical form for the ore body. The attenuation of its effect is rapid. By applying certain reasonable approximations it may be possible to arrive at the general conclusions concerning the lateral extent of the ore body. Special attention has to be paid to the terrain corrections, corrections for the ore body effect and the effect of roadways.

In the presented discussion the accuracy of the elevation data was ± 1 foot. This would result in an accuracy of ± 0.03 gr/cm^3 in the computed density for the minimum encountered distance interval. For intervals larger than 120 feet the error is small and could be not considered. The accuracy of ± 0.03 milligal in gravity observations corresponds to ± 0.04 gr/cm^3 accuracy in computed density for the minimum interval of 30 feet. For the interval of 120 feet, the possible error in the computed density is reduced to ± 0.01 gr/cm^3.

Measurements on different levels in the Mine. (Figs. 9 and 10)

Gravity observations were made on different levels of the mine workings in the same plan position. Not all the stations could be occupied on different levels, as the degree to which the levels were developed differed. The elevation corrections were applied using different densities in different parts of the workings, according to whether the observations were taken in the ore, in the rock, or in the transition zones mineralized to a different degree. The densities used were 4.00 gr/cm^3 to 4.30 gr/cm^3 for different zones of mineralisation and 2.70-2.75 gr/cm^3 for the rock.

The gravity contours for different levels are presented on Figs. 11-13. The lowest contour value on each level has been assumed as zero value. Ore boundaries for all levels in plan are superimposed on the gravity contours in each instance. The relation between the gravity contours and the ore boundaries becomes more evident when the disposition of the ore below and above the given level is taken into account. The thickness of the ore above the 400 level (Fig. 11) is small, the bulk of it being concentrated below. Consequently the highest values of gravity are located near the south-east side of the shaft. This is the area where ore thickness underneath is probably greatest. If the position of ore in the shaft is taken as an index there should be about 15 feet of ore above and 50 feet of ore below the 400 level near the shaft. The trend of the contours would indicate the thinning of ore away from the shaft. The changes in the gravity values are more abrupt in the south than in the north-east which

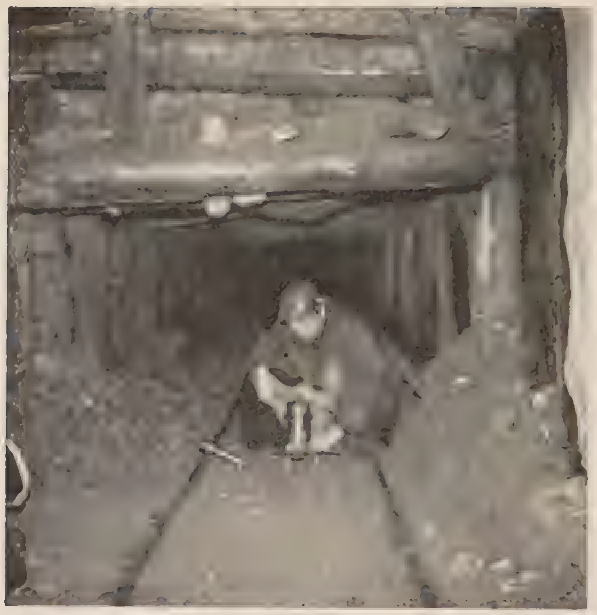

Fig. 9. Gravity observations in an underground roadway.

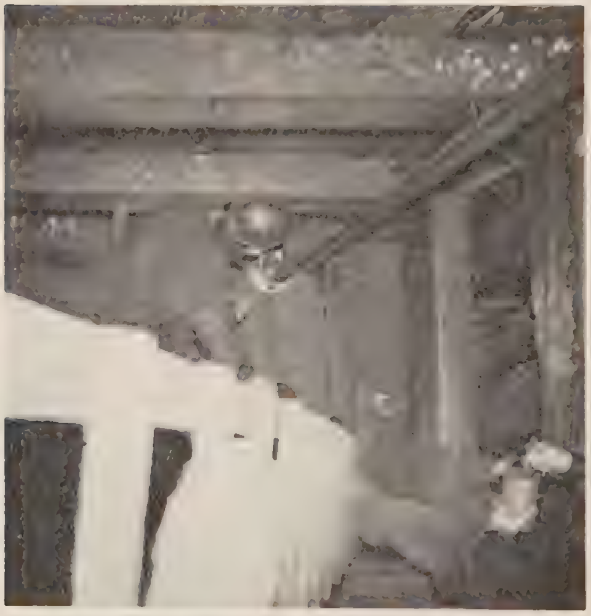

Fig. 10. Gravity observations in a rise between two mine levels.

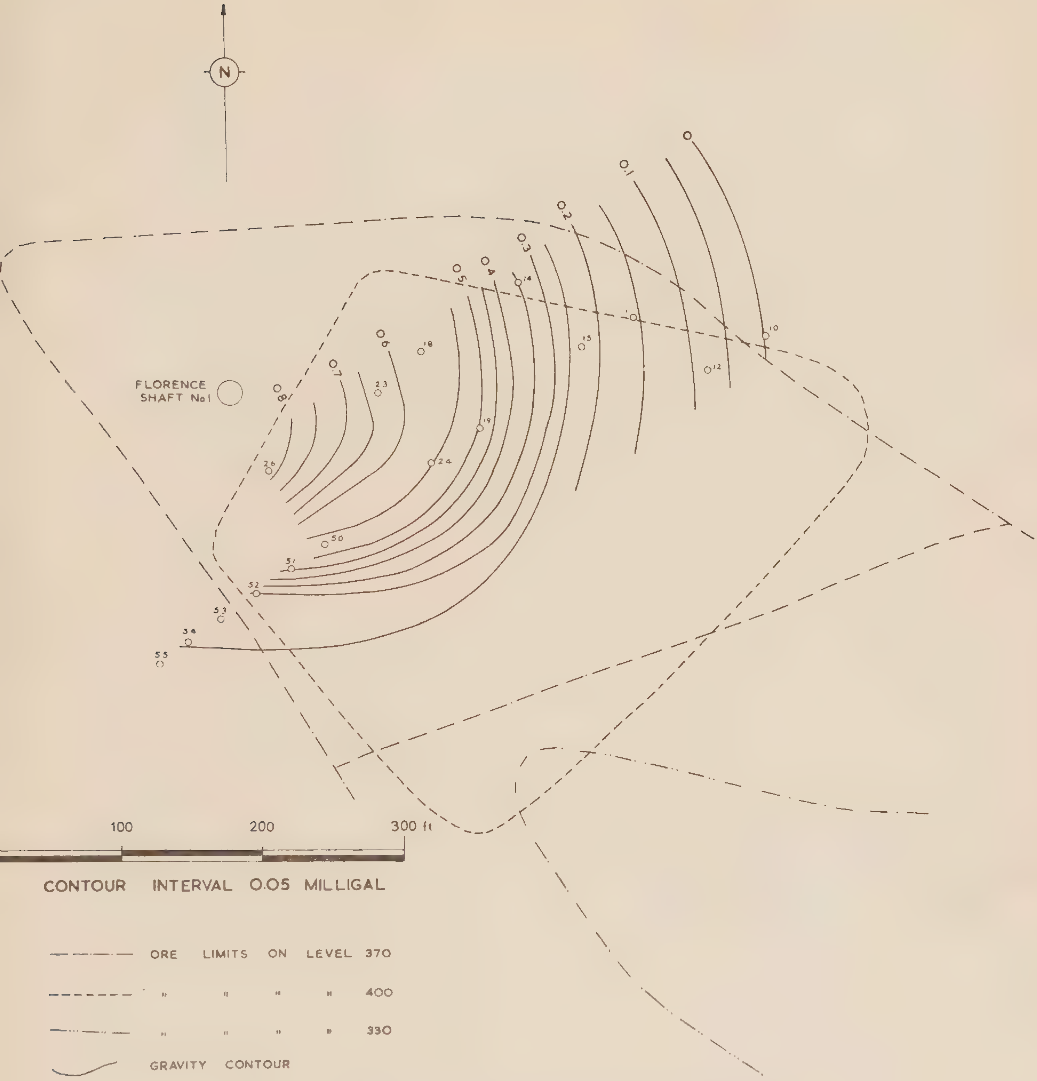

Fig. 11. Gravity contours on level 400, Florence Mine.

is explained by the fact that the southern extent of ore is terminated by a fault. On level 370 (Fig. 12) gravity increases proceeding away from the rock and into the ore. At the same time this increase takes place in the same general direction from north-east to south-west, as previously on level 400. The shape of gravity contours is however different in each case. It might be proper to emphasize here that the shown ore limits are based on the information available from existing drifts and headings. In some cases, the evidence of the boundaries

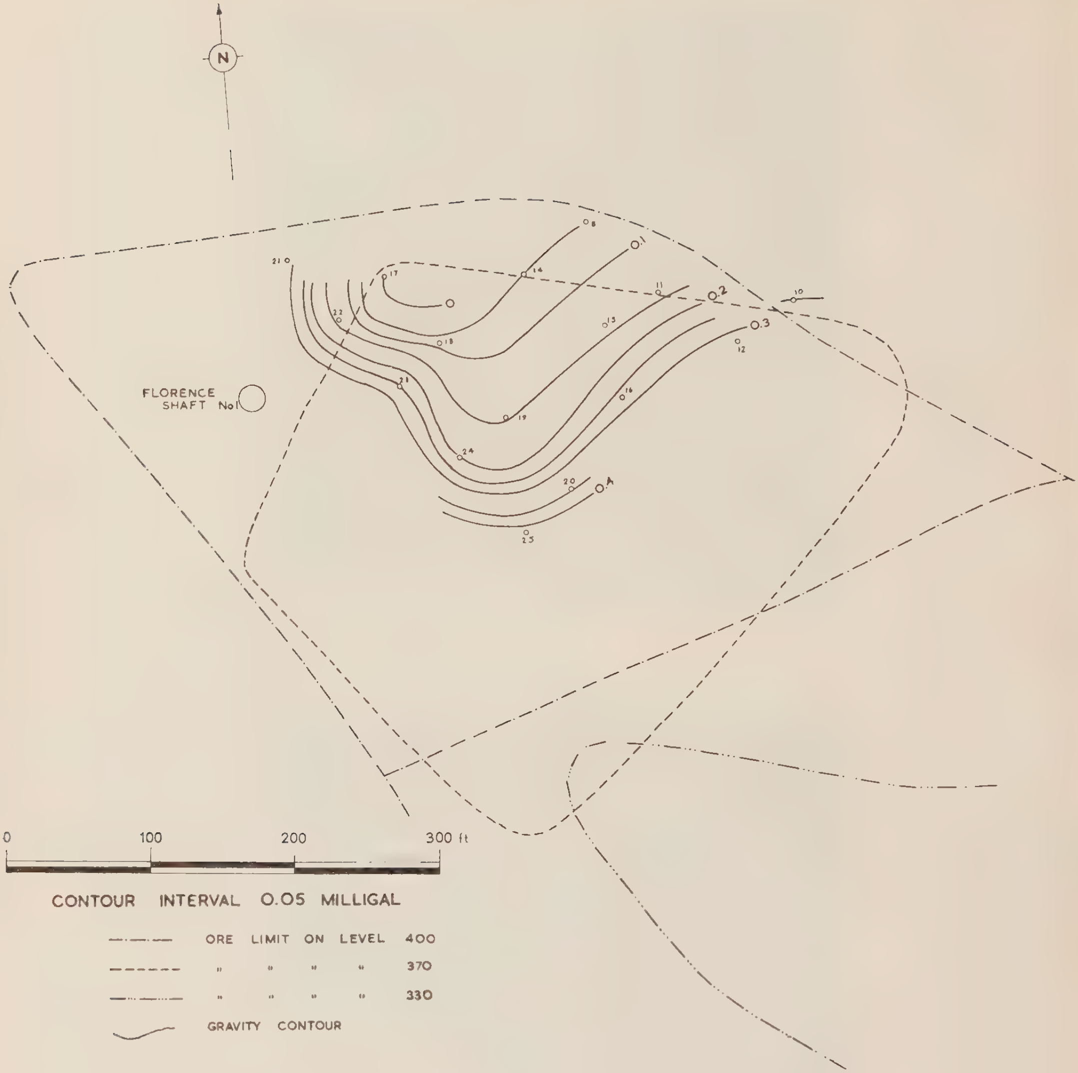

Fig. 12. Gravity contours on level 370, Florence Mine (corrections for effect of drifts and winzes applied).

is positive, such as the fault in the south west. In others there is some uncertainty as to what the shape of the ore is like. The gravity values on level 370 are resultant of the downward and upward attraction due to the ore. The existing trend shows that downward attraction becomes relatively stronger. This can be due either to the increase of the attracting mass below, or decrease of this mass above. The increase of the mass below is unlikely judging by the contours on level 400. The other alternative therefore has to be assumed. The

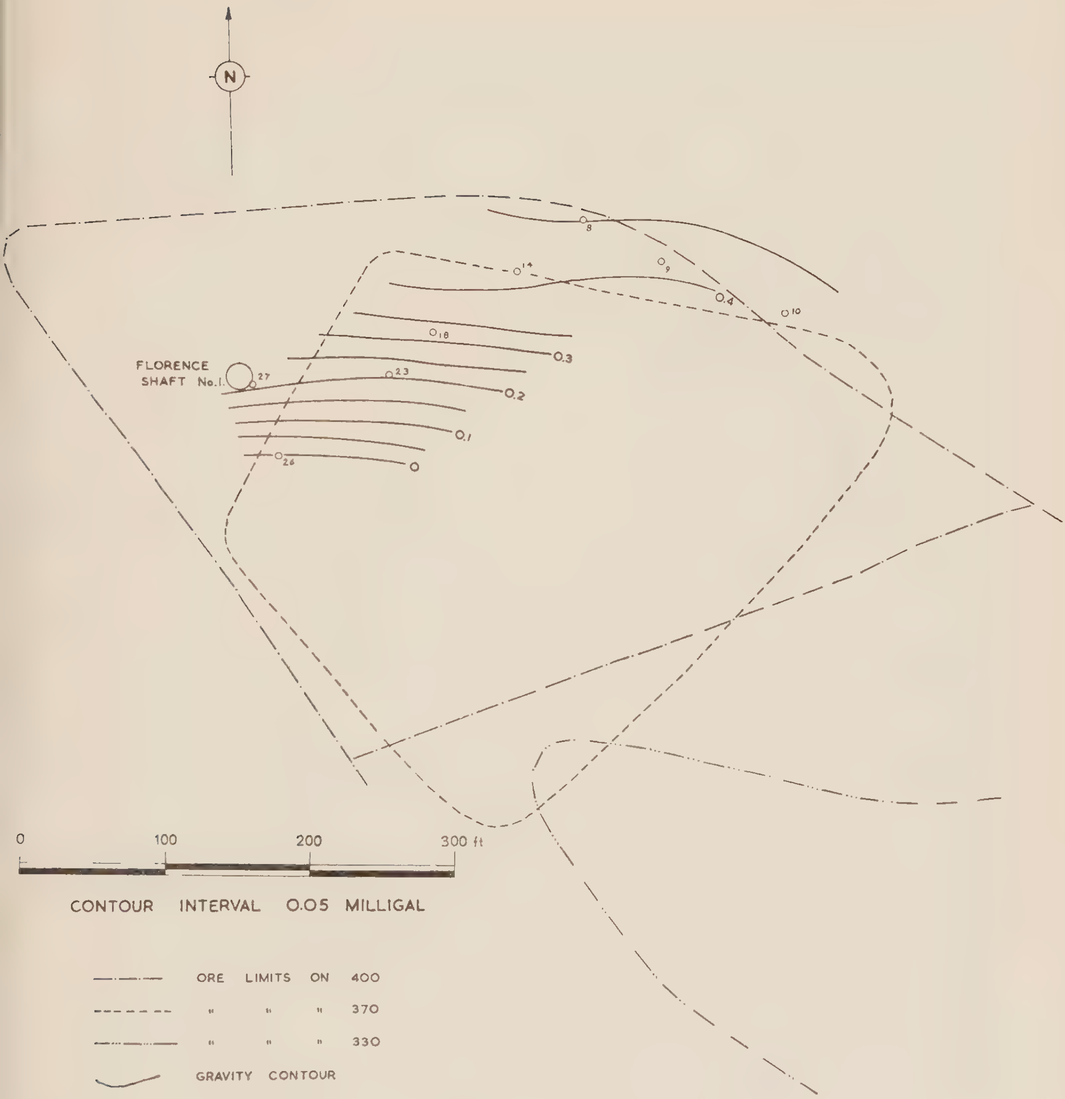

Fig. 13. Gravity contours on level 310, Florence Mine.

rate of change of gravity towards south-east on level 370 is less than towards south-west, which would mean more gradual thinning of the ore above 370 level in former direction, and possible thickening below as the shaft is approached.

The gravity contours on the lowest level 310 (Fig. 13) are very incomplete. It is possible however to see that the direction of trend is completely reversed,

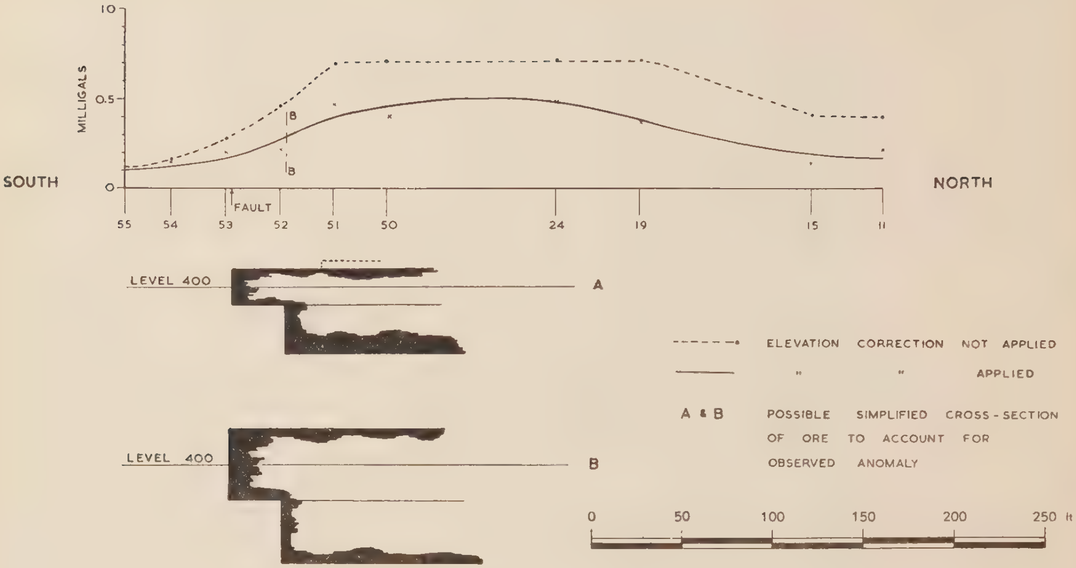

Fig. 14. Underground profile across the fault, level 400, Florence Mine.

as compared with the gravity maps on other levels. This level is below the ore, and the gravity increases as the upwards attraction decreases, i.e. proceeding towards ore limits (in plan).

Special attention has been given to the gravity traverse across the fault on level 400 (Fig. 14). The haulage road along which the observations were taken, is driven through the fault plane. The hematite ore is faulted against limestone. The problem of elevation corrections and corrections for the effect of the roadway is here particularly involved because of the sudden density contrast of 1.25 gr/cm^3. The reductions were carried out using the principle of apportioned densities (Domzalski 1954b) i.e. calculating the partial effects of blocks and slabs with their proper densities for each point of observations. The effect of the corrections can be assessed from Fig. 14 where the uncorrected and corrected profiles are shown. The decrease in gravity values towards north and south from the central maximum is not symmetrical. This is due to the fact that in the south the high density region (ore) terminates abruptly due to the fault. The transition in the density values in the north is more gradual. The position of the fault is known accurately and is marked on the profile. Proceeding north from station 55 the medium of high density is entered. The distribution of gravity will depend on relative disposition of the excess mass below and above the level of the drift. As the gravity values increase it is evident that the downward attraction is prevalent. A closer examination of the profile in the vicinity of the fault reveals however that the change is not symmetrical in relation to the plane of fault. It must be concluded that there is more ore below the level of the drift and that the excess mass is shifted north in relation to the fault plane. An attempt has been made to reconstruct the mass distribution in a way which would account for the observed gravity and this is shown by two sketches below the profile on Fig. 14. The interpretation is based on the known position of fault in the roadway and on the deduction concerning the excess mass below. Equal thickness of the ore above and below the roadway would not cause any change in the observed gravity. The observed effect therefore is entirely due to the lower slab displaced to the north. Line B-B on the profile shows the position of the front face of this assumed slab and has been chosen so that the change of gravity in respect to it is symmetrical. It is impossible to determine the depth and the thickness of this slab uniquely from the available gravity information alone. Identical effects can be obtained by varying this depth and thickness. The drawings A & B show two such possible solutions. The thickness of the compensated slab is 10 feet and the thickness of the lower slab is 28 feet in case A. These thicknesses are 20 feet and 35 feet respectively in case B. The uncertainty as to which is the correct answer, can however be eliminated if other information is available, because of the condition of equal thickness above and below the level for the compensated slab. The ore is known to extend in this area for about 15 feet above the level. This calls for the compensating thickness of 15 feet below the level and the corresponding thickness of the lower slab is 30 feet. Accordingly the extent of the ore below level 400 in this section would be 45 feet, which is of the known order.

All the stations on level 400 are in the same plan position as the stations on level 370. It is possible therefore to derive the densities of the material between the vertical pairs of stations, from the gravity measurements. This has been done following the same procedure, as the one explained in the section dealing with the measurements in the shaft. The gravity values used for the density computations were corrected for the effects of the roadways and the effect of the surface topography. They were not however corrected for the effect of the ore above the upper station and below the lower station for each vertical pair. The uncertainty of the actual ore disposition did not justify the calculation of this correction. It will be remembered that in the case of the shaft stations the error due to the omission of this correction amounted to 5 %. The contours of the densities thus computed are shown in Fig. 15. The density increases from 2.60 gr/cm^3 to 3.60 gr/cm^3 towards the centre of the area, enclosed by the marked ore boundaries. This is an expected result for obvious reasons. The highest value of 3.60 gr/cm^3 is somewhat lower than it might be expected. If the possible error of 5 % due to the effect of the ore is taken into account this value is raised to 3.78 gr/cm^3 which compares with 3.85 gr/cm^3 obtained from shaft measurements between the corresponding levels. This value for ore density in the shaft was raised further to 4.22 gr/cm^3 by considering the finite dimensions of the ore. The value of 3.78 gr/cm^3 could be probably also

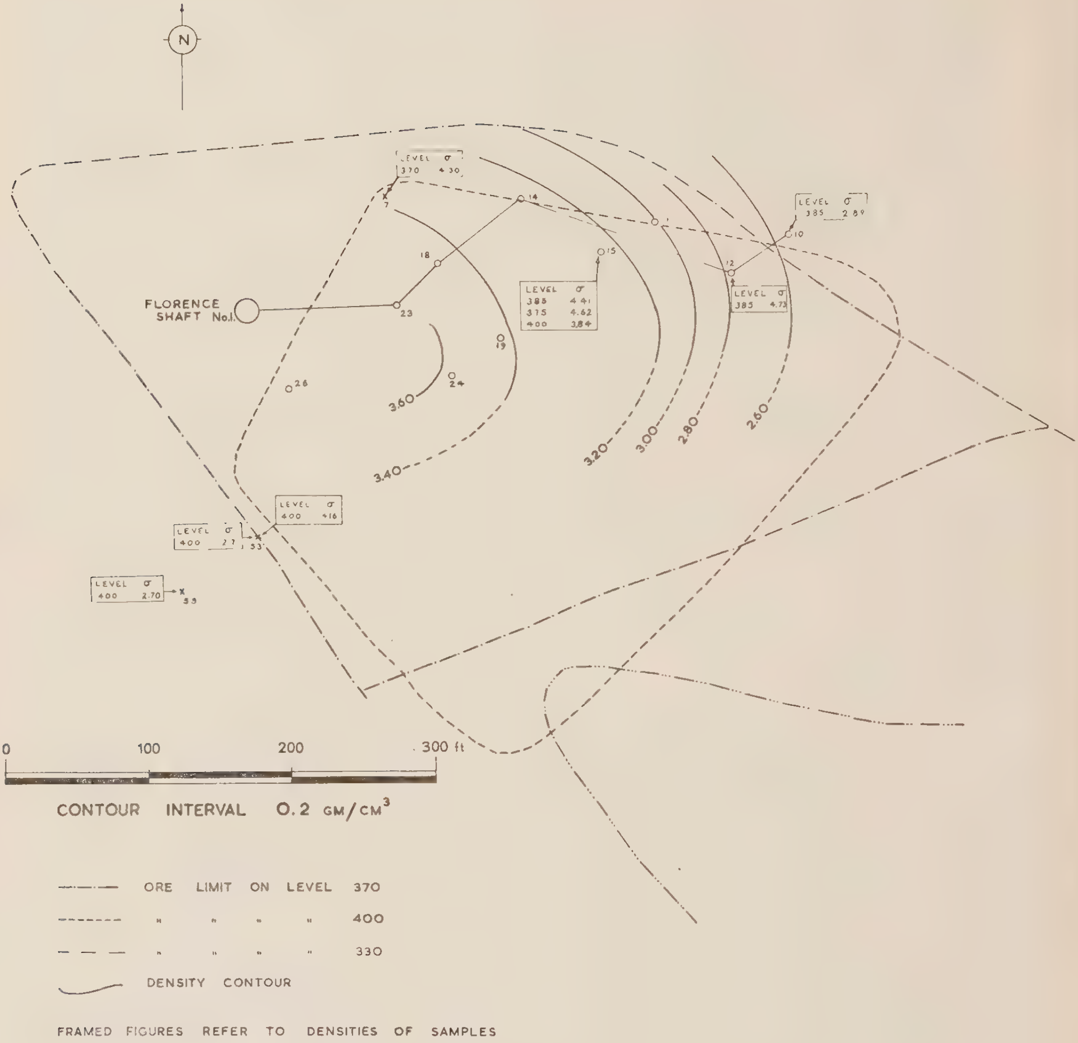

Fig. 15. Density contours between levels 370-400.

raised, although the increment might be less, because the ore extends laterally further in this area than it does near the shaft. It must be concluded therefore that the space between 370 and 400 levels is filled with ore of varying quality and that layers of non-ore material are present, resulting in the lower average density. The densities determined in the laboratory from the samples collected at different stations are shown against these stations on Fig. 15.

The densities of samples are higher than the densities determined from the gravity observations, on stations 10, 12, 15, and 17. The discrepancy is explained however by the fact that the samples were collected, with the exception of station 10, from ore while the densities computed from gravity measurements are influenced by the ore and the rock alike and represent an average density over a certain area. This, incidentally, is very useful as a way of predicting the possible extent of ore. If the densities of ore samples are much higher than the densities determined from gravity observations, it means that the ore cannot extend far beyond the limits known from the existing workings.

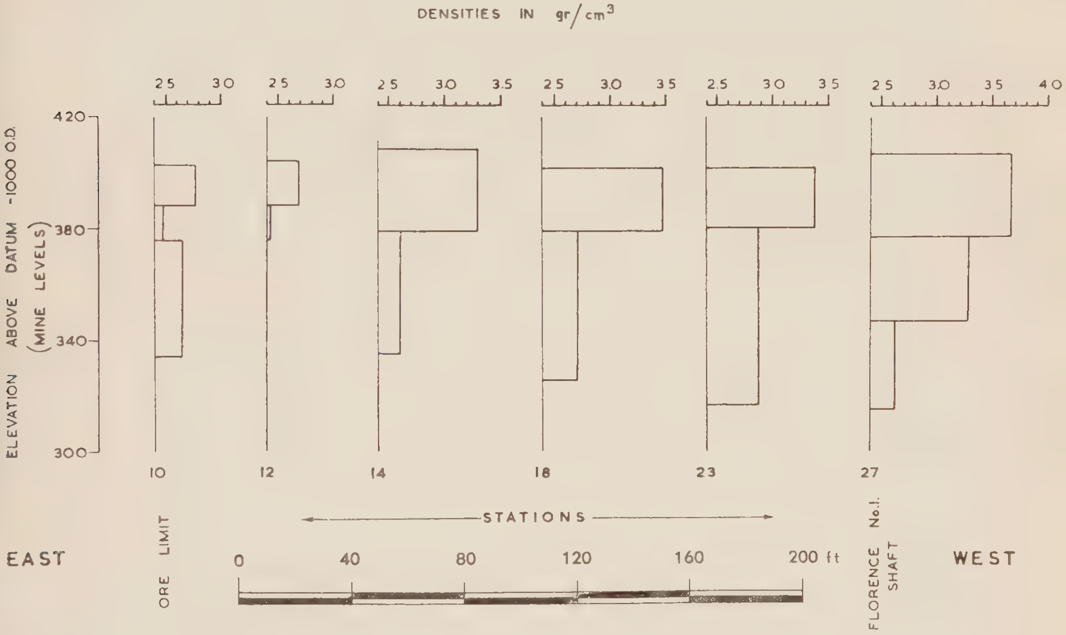

Fig. 16. Inter-level densities across the ore body from gravity measurements.

An attempt to illustrate the vertical changes in the densities, computed from gravity measurements, showing at the same time their horizontal pattern is presented on Fig. 16. The stations chosen for this illustration were occupied at least on three different levels. They are not located on a straight line, although they follow the general westerly direction from the boundary into the ore. There is a well marked increase in the density of the material between the two top levels and the middle levels. This illustration is thought to give a good general idea of the distribution of the ore values within the surveyed block. All the reservations concerning the actual values of densities, made in the preceding paragraphs, apply here. For the present purpose however it is of equal importance to know the relative density distribution.

CONCLUSIONS

The gravity contours constructed from the observations on different levels of the mine gave evidence as to the horizontal extent and variations in the thickness of the ore. They were compared with the known ore boundaries and supplemented the existing information. The attempted interpretation of the gravity profile across a fault led to the conclusions concerning the distribution of the ore above and below the considered level.

It was shown that the combined information based on the laboratory determined densities of samples and densities computed from the gravity measurements can give positive information concerning the extent of the high density material beyond the area penetrated by the mine workings.

ATTEMPT IN CORRELATION OF GRAVITY MEASUREMENTS WITH GENERAL GEOLOGY

General account of the geology of the area was given in one of the early paragraphs. This information was derived from the 6 inch map of the Geological

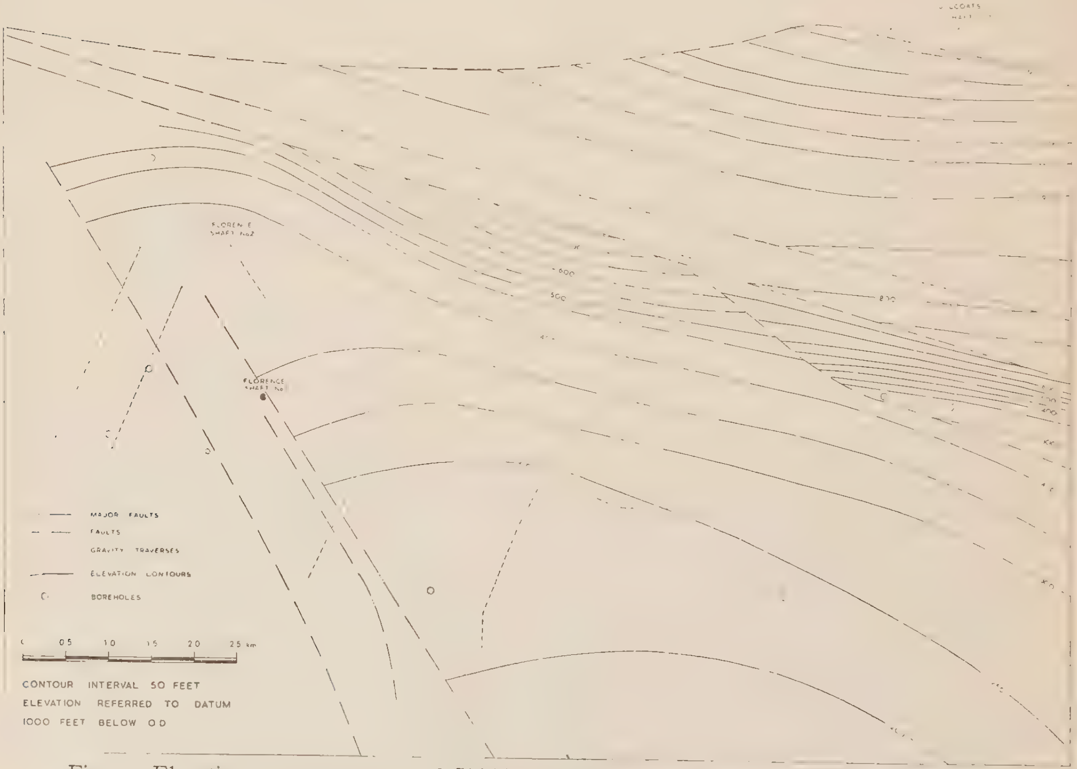

Fig. 17. Elevation contours on top of Skiddaw Slate between Florence and Ullcoats shafts.

Survey of England and Wales (Cumberland, Sheet 72 N.E.) and the data obtained from mining operations and boreholes which have been drilled in the area. By far the most data were provided by the borehole logs and they are the basis of the contour map, showing the variation in the elevation of the top of Slate (Fig. 17). The general trend of the contours is east-west with the elevation increasing towards the north. Two major faults run in approximately the same direction as the trend of the contours. A few minor faults are also present as shown on the contour map. A better picture of the geology can be obtained by reference to the two sections shown on Figs. 20 and 21.

The results of gravity observations are shown in the corresponding contour map and profiles accompanying the geological sections. The gravity contour map based on all surface stations is shown on Fig. 18. The comparison of the two contour maps can be resolved into four main points which are discussed in turn. Firstly the general trend of the contours is similar on both maps. The

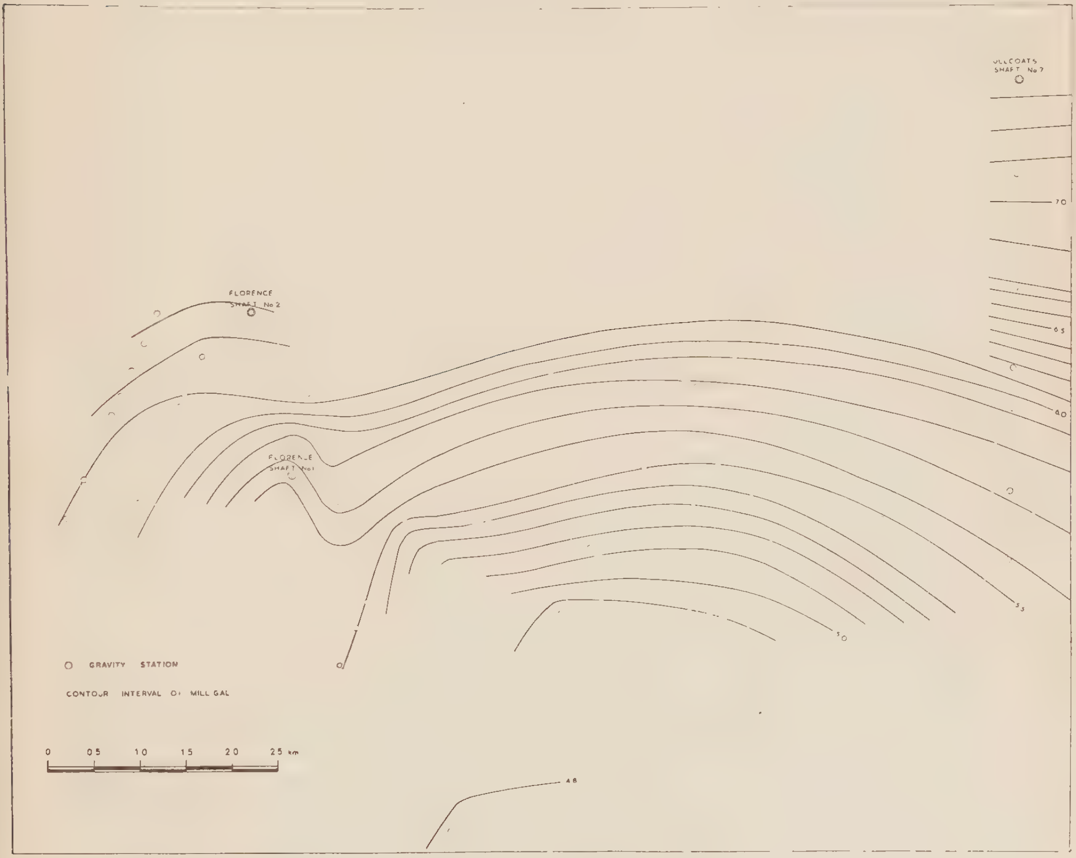

Fig. 18. Gravity Contours on the surface between Florence and Ullcoats shafts.

northerly increase in gravity corresponds t the increasing elevation of the top of the Skiddaw Slate. The rate of change of gravity which is gauged by the density of the contours is less in the southern portion of the area and increases towards the north. This also finds the counterpart in the behaviour of the elevation contours. Thirdly the changes in the density of gravity contours along the north-south line passing through Ullcoats shaft matches the existence of the faulted zone shown on the elevation contour map. Finally the disturbed gravity contours south-east from the Florence No. 1 shaft correspond to the position of faults running NW to SE in the vicinity of this shaft. With all due caution necessary when comparing the structural and gravitational contours it can be concluded that the general gravity picture reflects the subsurface structural conditions. The gravity contour map of the area adjacent to Florence No. 1 shaft on the surface (Fig. 19) is shown on a larger scale to conform to the previously discussed gravity contour maps on different levels underground. The similarity of shape between this and the 370 level map is misleading as can be readily checked by inspection of the direction in which the gravity values change and which is reversed. This anomaly on the surface is due to the combined effect of ore and faulting, the effect of ore however being of a much lesser magnitude and probably not detectable on its own.

Further interpretation of the observed gravity distribution in terms of the subsurface geology is continued in connection with the sections and profiles.

The observed gravity variations are a function of the density contrasts between the encountered formations. The determinations of density from measurements in the shaft provide the ranges of density values as follows: Sandstone 2.35 gr/cm^3 to 2.52 gr/cm^3, Conglomerate 2.60 gr/cm^3 to 2.70 gr/cm^3, Limestone 2.73 gr/cm^3 to 2.79 gr/cm^3 and Skiddaw Slates 2.70 gr/cm^3 to 2.75 gr/cm^3. From these ranges, the mean density values are chosen and they are used for the subsequent interpretation. The quoted values for Limestone and Skiddaw Slate are very similar and overlap so closely that these two formations are treated as one in the interpretation. The densities used in the computation of the gravitational effects were: Sandstone 2.45 gr/cm^3, Conglomerate 2.65 gr/cm^3, Limestone and Skiddaw Slates 2.75 gr/cm^3. Assuming Sandstone as the basic medium, the density contrasts are 0.20 gr/cm^3 and 0.30 gr/cm^3. The magnitude of these contrasts may appear small but the respective mass excesses are large and consequently the observed effect is well pronounced. Due to the fact that small contrasts and large masses are involved, the error in estimation of the mass i.e. in the construction of the section, will affect the calculated result less, than the error in assumed density contrast. The latter is likely to occur because of the small difference between the ranges of densities. The discrepancies therefore between the observed and the calculated values of gravity should be ascribed to the fact that the actual densities may differ slightly from the mean densities used in the calculations.

The geological sections have been based on the information from boreholes

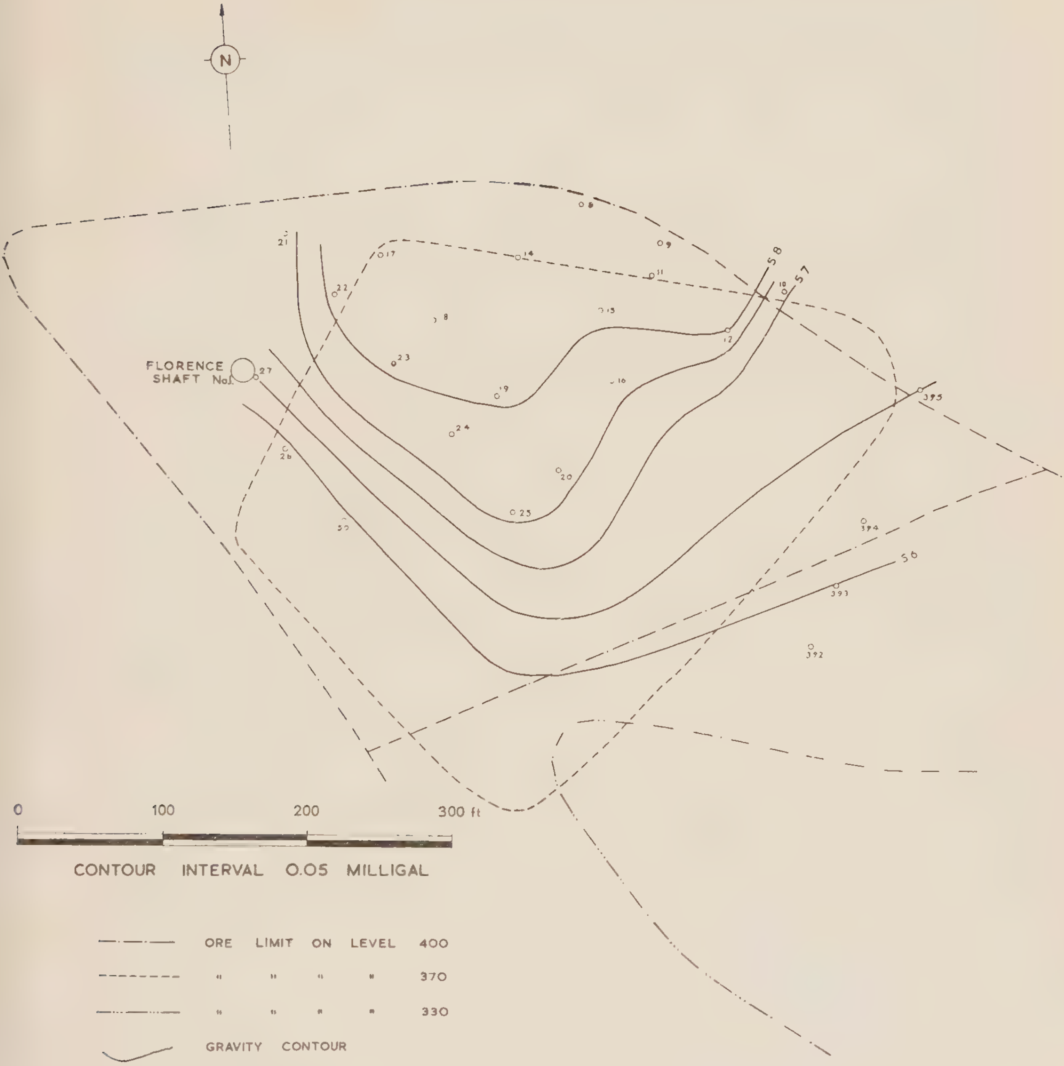

Fig. 19. Gravity contours on the surface, Florence Mine.

the position of which is shown on the sections. The boreholes were projected on to the planes of the sections from various distances not exceeding 200 feet.

The section along the Ullcoats haulage drift is shown with the accompanying surface and underground gravity profiles on Fig. 20. To account for the variation of gravity along the surface profile, the calculated effect was built up from the following component effects:

1. Contrast between Sandstone and Conglomerate above level 1000 using the density difference of 0.20 gr/cm³.
2. Contrast between Sandstone on one hand and the Limestone and Skiddaw Slate on the other, between levels 700 and 1000, using the density difference of 0.30 gr/cm³.

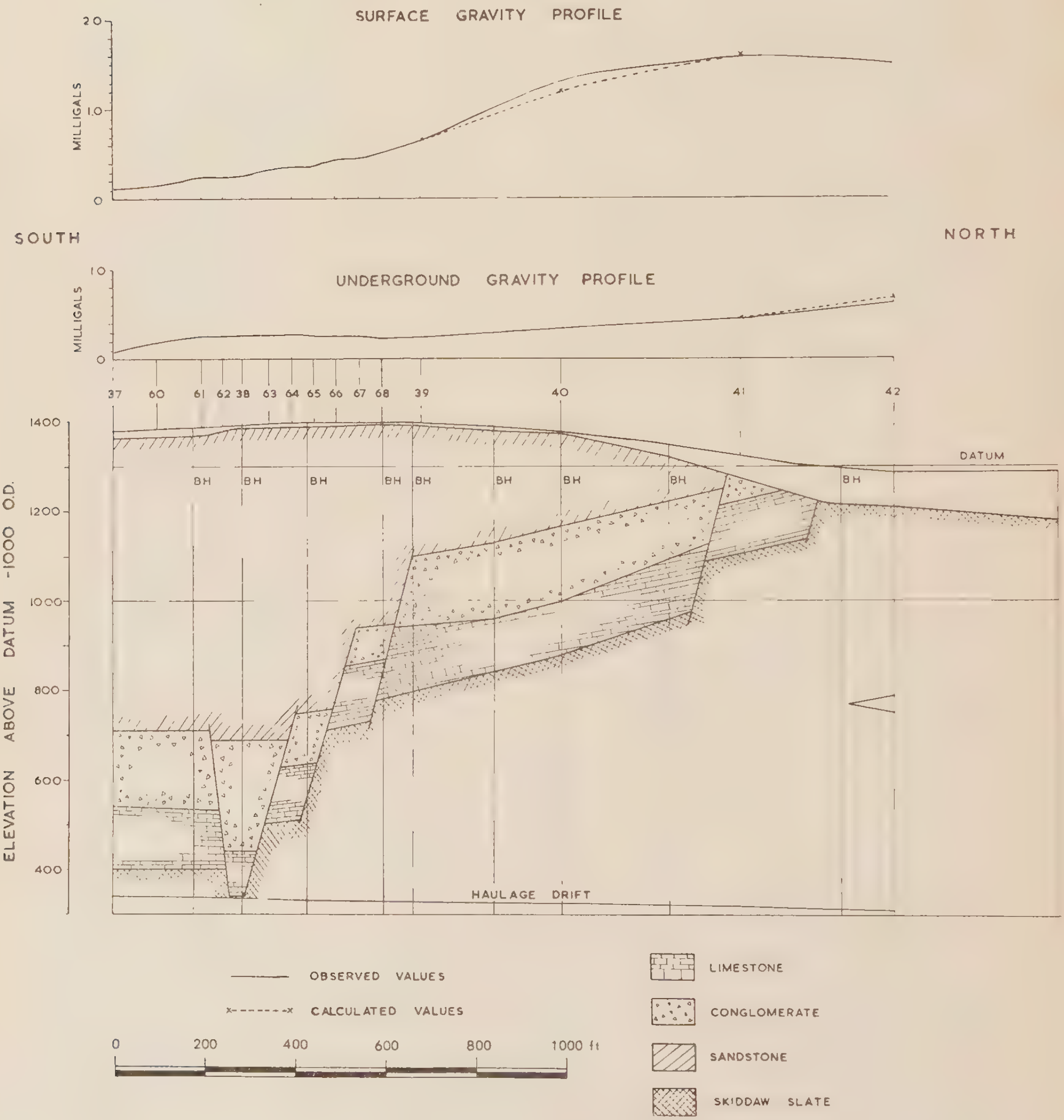

Fig. 20. Correlation of surface and underground gravity profiles with geological section along Ullcoats haulage drift.

3. Contrast between Conglomerate and Skiddaw Slates, between levels 550 and 700, with the density difference of 0.10 gr/cm^3.
4. Contrast between the rock (Sandstone and Conglomerate) and the overburden just below the datum, north of station 40, using the density difference of 0.40 gr/cm^3.

Magnitude of these effects varies, the effects listed as 1 and 2 being the greatest. The discrepancy between the dashed and the continuous line Fig. 20 is the measure of the difference between the observed and the calculated values. Same refers to the underground gravity profile. It must be remembered that in this case the effects due to the discussed geological section are reversed. As the underground gravity profile can be approximated on the basis of the shown geology it must be concluded that there are no major changes in geology and structure of the zone below the level of this profile for some reasonable depth.

The gravity profile observed along the traverse 401-410 is interesting because of the suggested effect of the subsidence on gravity observations. The effect computed from structural conditions shown on the geological section assuming the adopted density contrasts is shown by the dashed line on Fig. 21. The procedure adopted in these calculations was similar to the one, outlined when discussing the section shown on Fig. 20. It is evident that taking only these effects into consideration, the total increase in gravity can not be accounted for. It is known however that the area around station 407 has been subjected to subsidence, the magnitude of which can be assessed from the fact that the surface level was lowered by 30 to 40 feet. Such a subsidence must have caused a considerable amount of crushing and loosening of the rock material. If this assumption is made, the change in the calculated gravity is approaching closely the observed gravity values as shown by dash and dot line on Fig. 21. The density difference between the material affected by crushing, due to the subsidence and the unaffected one, was taken as 0.07 gr/cm^3.

The surface stations, as has been previously explained, were occupied whenever possible in the same plan position as the underground stations. It was possible therefore to calculate the average densities of the layer of ground between these pairs of stations in a manner and with the reservations already described. The distribution of the densities thus derived should to a certain extent reflect the lithological changes within the ground layer for which they were computed. The comparison will be of course worth while only among the widely spaced stations. This areal change of density is shown on Fig. 1. A better appreciation of the connection between the areal change of density and changes in the thickness of the geological formations is obtained by reference to Fig. 22. In this figure the densities computed from the observations on pairs of stations are shown together with the stratigraphical columns of the adjoining boreholes. (The boreholes are not in one straight line). Table 5 gives the comparison of

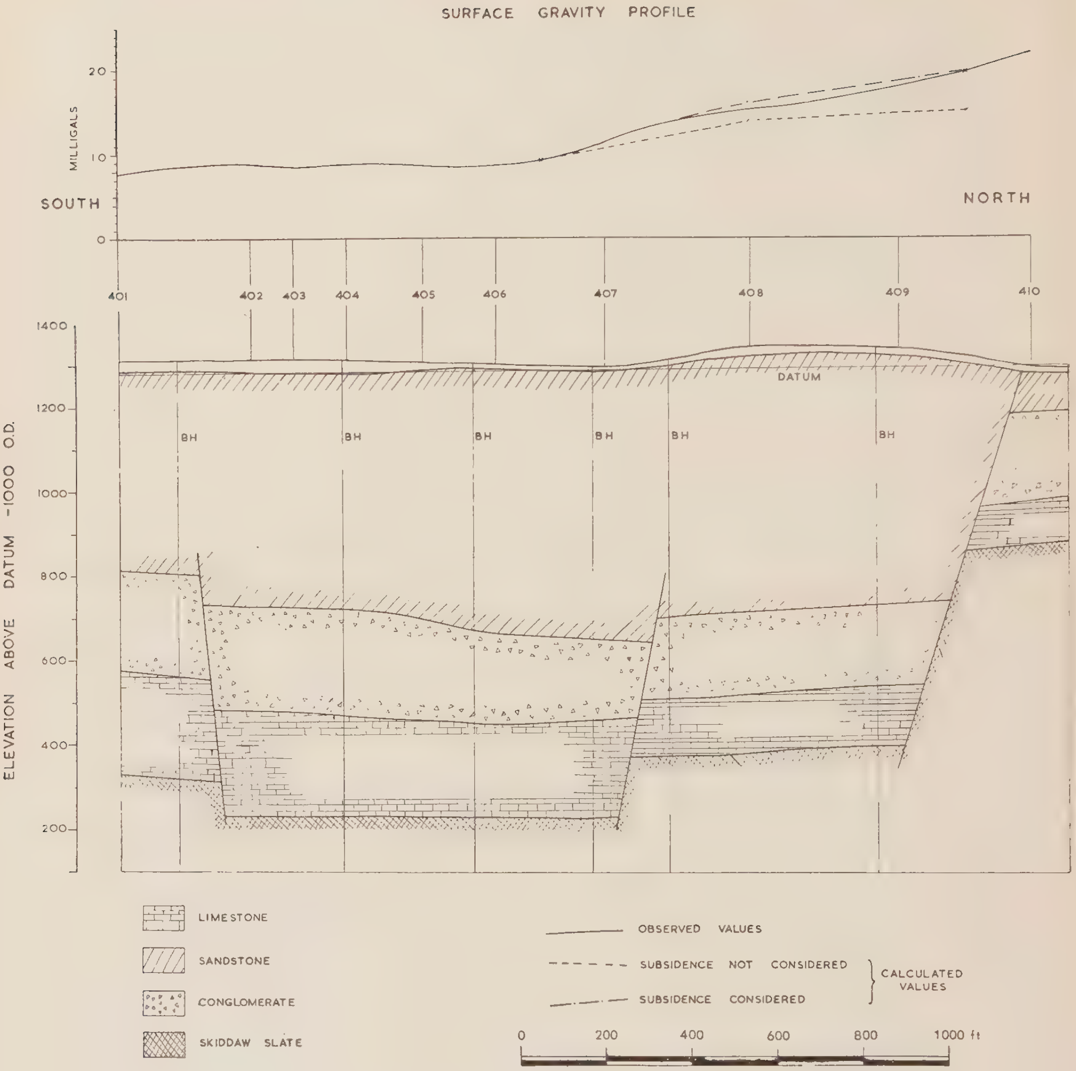

Fig. 21. Correlation of surface gravity profile with geological section along traverse 400-410.

densities which were obtained from gravity measurements, and the densities which were computed by assuming the average density to be the weighted resultant of the component densities of the formations which compose the borehole columns. The differences between the individual values derived in different ways are explained bv the fact that using the constant density for a given formation does not take into account the possible areal changes in the lithology.

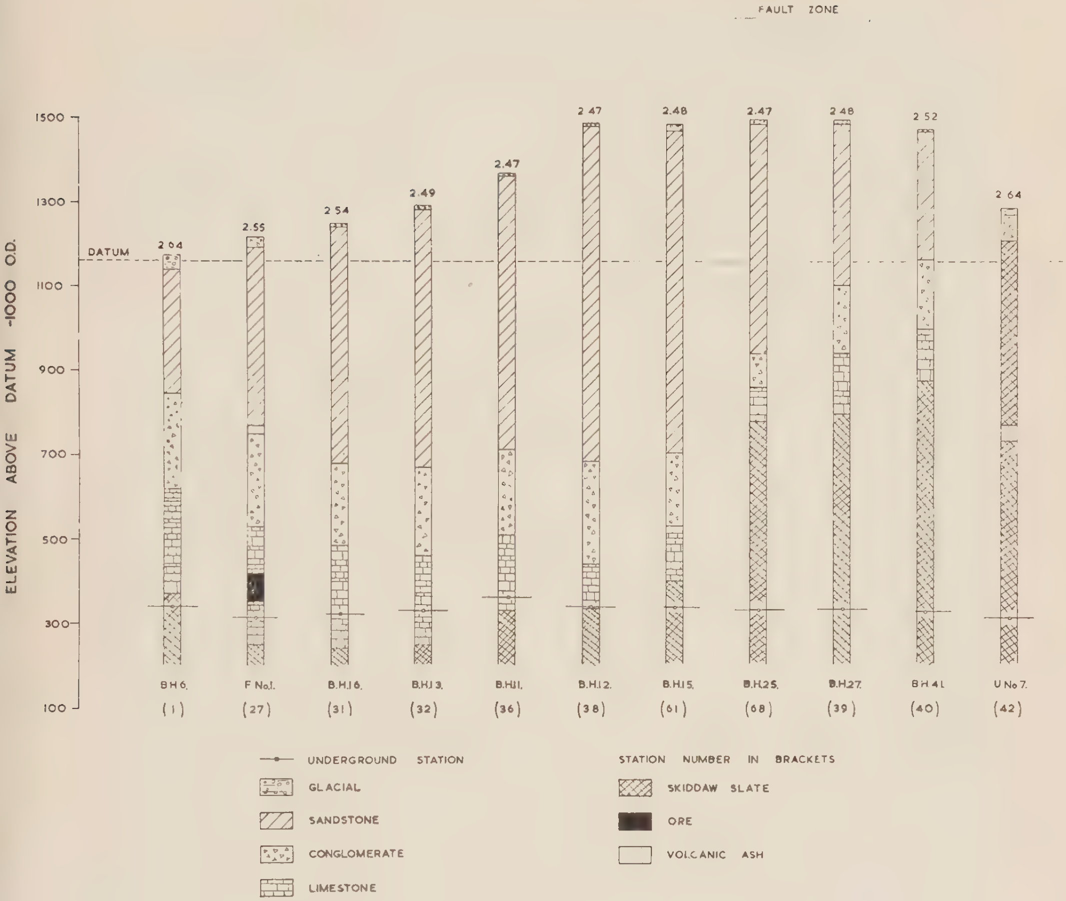

Fig. 22. Areal variations of overall density and thickness of geological formations.

TABLE 5

Station	Density in gr/cm^3 from gravity measurements	Weighted Density in gr/cm^3 from stratigraphy
1	2.64	2.56
27	2.55	2.54
31	2.54	2.50
32	2.49	2.49
36	2.47	2.49
38	2.47	2.47
61	2.48	2.48
68	2.47	2.56
39	2.48	2.57
40	2.52	2.58
42	2.64	2.65

The large differences on stations 68 and 39 are due to the fact that these stations are in the fault zone. Weighting the component densities by the thickness exhibited in the borehole column does not take into consideration the lateral changes which are most pronounced in the faulted zone. The numerical agreement has not been expected therefore and more importance should be attached to the fact, that in general the relaive increase in the thickness of the sandstone lowers the observed density. The density computed from gravity observations at station 1 has a value higher, than could be expected from the component densities assumed for the formations in the borehole. However, if these are raised by 0.02 gr/cm^3 the average weighted density is raised to 2.63 gr/cm^3 which is in agreement with the density obtained from gravity measurements.

The presented results show how much caution should be exercised when an attempt is made to explain the density changes in terms of the changes in the thickness of different layers. The two factors which may lead to errors are: horizontal discontinuity of the considered layers and the areal changes in the lithology of the given type of formation. In the quoted example of the calculations involving the data pertaining to station 1, it has been computed that the thickness of the sandstone layer is 190 feet. This computation has been based on the previously assumed densities for Sandstone and Conglomerate (Conglomerate and Limestone being treated as one) and the overall density obtained from the gravity measurements. The actual thickness of sandstone is of the order of 300 feet. The incurred error of over 30 % in the calculated thickness was caused by approximately ¾ % variation in each of the used densities.

CONCLUSIONS

Gravity measurements could be satisfactorily carried out in mine shafts, as routine surveys complementing wherever possible the areal surface surveys. In virgin areas it is of course impossible to envisage a convenient spacing of mine shafts, however there is a lot of gravity work carried out in the territories where gravity measurements in the shafts are possible. The densities of the various formations thus obtained could be used for elevation corrections, terrain corrections and the structural interpretation of gravity anomalies.

The observations of the gravitational field at different levels of a mine can be interpreted in a twofold way. The gravity contour maps can be constructed and the trend of the contours and their disposition taken as an indication of the heavy mass distribution laterally and in depth. It is also possible to compute the densities from gravity measurements taken on the station at different depths, but in the same plan position. The density contour map will indicate the lateral changes of the investigated mass distribution. The density derived in such a way can be compared with the density determined from samples and conclusions reached as to the extent of say, an ore body. Any additional gravity profiling such as a traverse across an underground fault can, in connection with geological information and/or certain assumptions, help in the attempts to reproduce the boundaries of materials of contrasting densities.

The surface and underground gravity profiles located vertically above each other can furnish information which would permit completion of the geological section if only a few borehole data were available.

The determination of the thickness of different strata from the gravity observations has to be done with the utmost care, because small variations in the density will cause large errors in the computed thickness.

Remarks

Throughout this discussion the importance of the density determinations has been emerging in almost all the phases. The necessity of possessing reasonably reliable density values or density contrasts is equally important in detail surveys of small extent as it is in regional surveys over large areas, be it in oil exploration, or in the investigations of purely geological nature. The author would like therefore to take this opportunity to advocate a campaign aiming at a systematic collection of data obtained from gravity measurements in the shafts, from different widely spaced localities all over the world. The tabulation of such data would permit to assign the density values to individual formations of specified age. These could be compared with known densities determined from samples. The data thus obtained could be available for use in the interpretation of gravity measurements. Even in the areas where there are no shafts, there is always a certain amount of information from geological reconnaissance or wild-cat drilling about the underlying formations, and the densities provided by the proposed tables would be better than pure guesswork or a few unrepresentative samples.

It is hoped that the presented discussion, in spite of all its failings, may stimulate further investigations in the field which has been considered here.

Appendix

The computations of the gravitational effects of geometrical forms become usually more involved as the geometry of the form develops. Certain simplifications however are justified when the practical accuracy is not significantly affected. Such is among others the assumption of the 'two-dimensional' bodies. The formulae derived for the effect of an infinite and semi-infinite slab are well established and it is sufficient to quote them without further justification. The effect of the semi-infinite slab [BCN] (nearest approach to the structural conception of a fault) at point B is $g_B = \pi G \sigma h$ ......(1). This effect at any other point at distance x from the edge of the slab, such as A, is $g_A = 2 G \sigma [h\alpha - x \log_e (r/x)]$ ... (2), where the symbols represent the quantities illustrated on Fig. 23, σ is the density and G the universal gravitational constant. Expression (2) becomes inconvenient when quick routine calculations have to

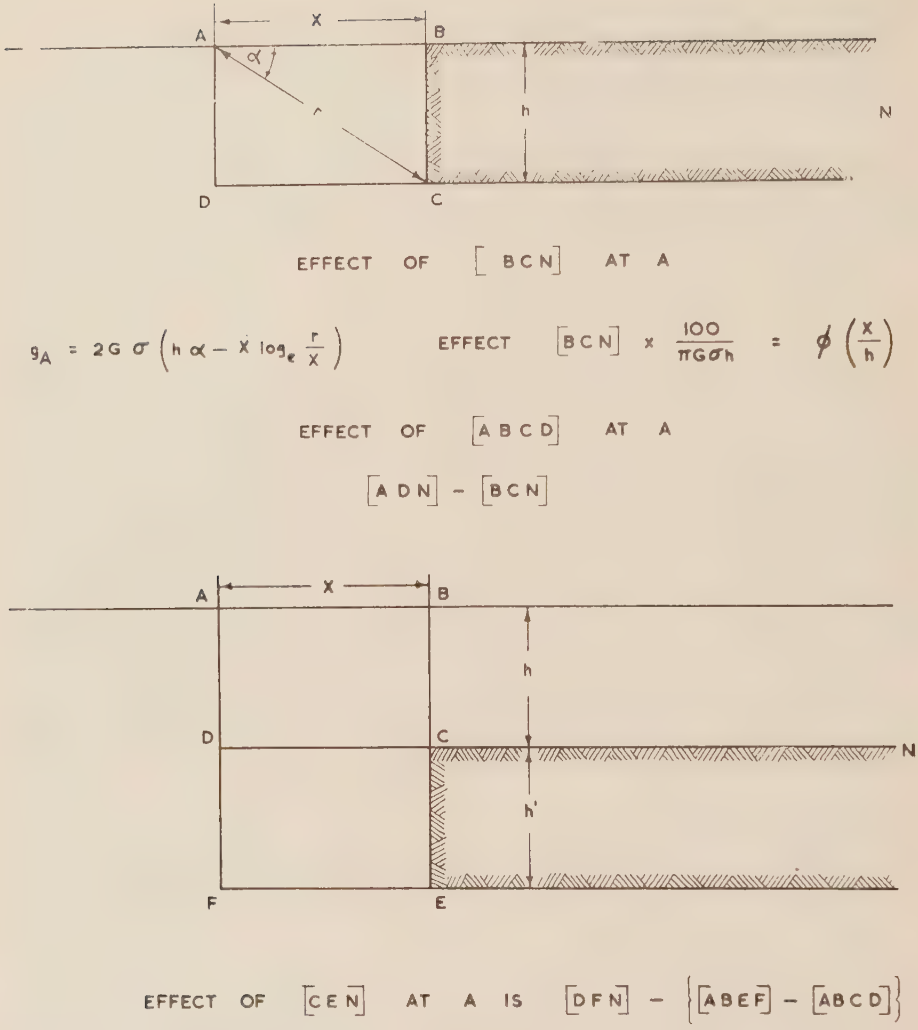
A
X
B
α
r
h
N
D
C
EFFECT OF [BCN] AT A
$g_A = 2G\sigma\left(h\alpha - X\log_e \frac{r}{X}\right)$
EFFECT [BCN] × $\frac{100}{\pi G\sigma h}$ = $\phi\left(\frac{X}{h}\right)$
EFFECT OF [ABCD] AT A
[ADN] − [BCN]
A
X
B
h
D
C
N
h'
F
E
EFFECT OF [CEN] AT A IS [DFN] − {[ABEF] − [ABCD]}

Fig. 23. A method of computation of the gravitational effect of two dimensional semi-infinite and finite blocks.

be performed. This expression however can be presented in a different form. Referring to Fig. 23 $r = (x^2 + h^2)^{1/2}$ and the term

$$\log_e (r/x) = \log_e \{ h\sqrt{(x/h)^2 + 1}/x \} = \log_e \{ (h/x)\sqrt{(x/h)^2 + 1} \} \quad . \quad . \quad (3)$$

bearing in mind that $\cot \alpha = x/h$, expression (2) becomes

$$g_A = 2G\sigma h \{ \cot^{-1}(x/h) - (x/h) \log_e [(h/x)\sqrt{(x/h)^2 + 1}] \} \quad . \quad . \quad (4)$$

If the effect at B, given by expression (1) is called the edge effect and assumed

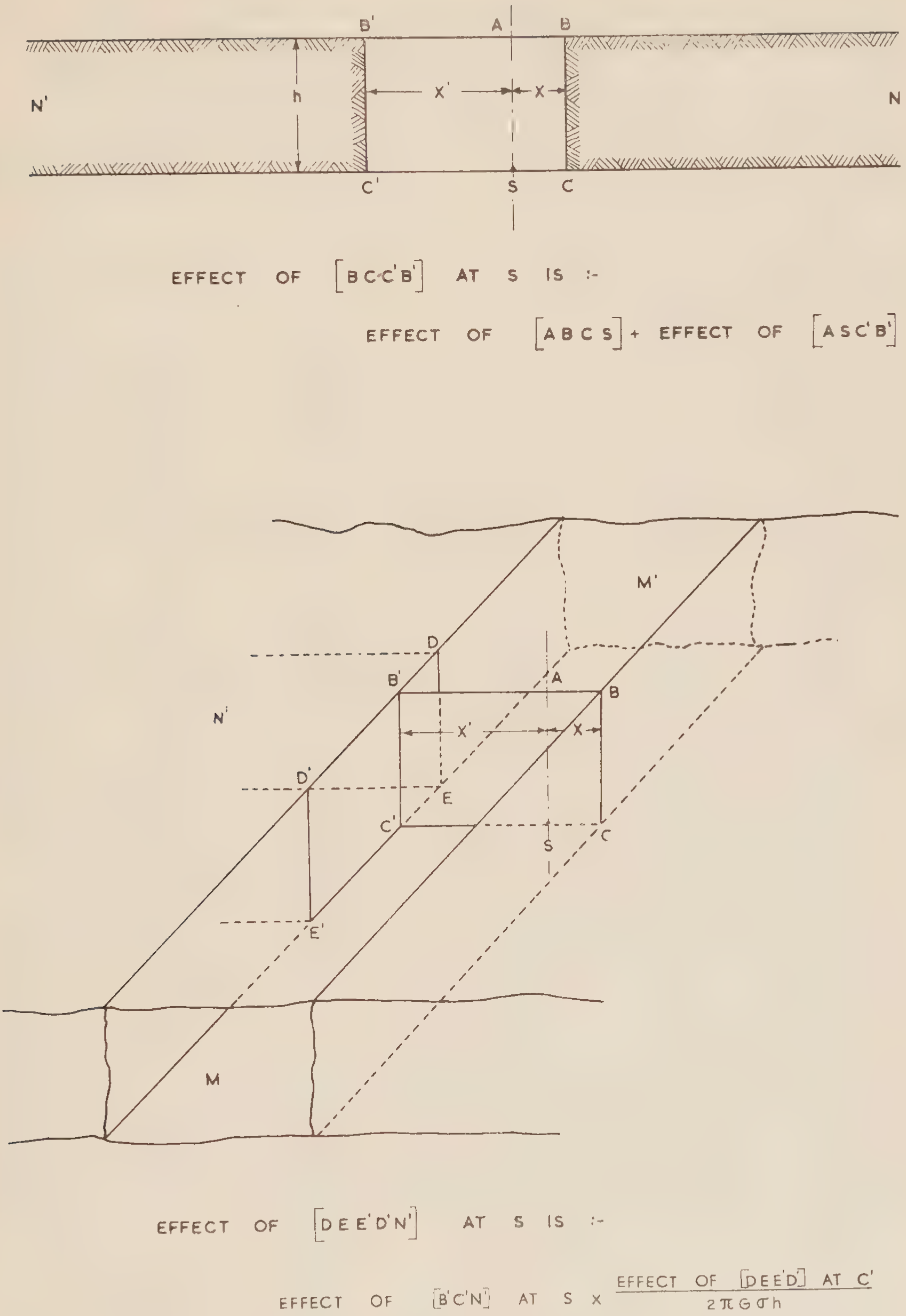

EFFECT OF [BCC'B'] AT S IS :-

EFFECT OF [ABCS] + EFFECT OF [ASC'B']

EFFECT OF [DEE'D'N'] AT S IS :-

EFFECT OF [B'C'N'] AT S × $\frac{\text{EFFECT OF [DEE'D'] AT C'}}{2\pi G\sigma h}$

Fig. 24. A method of computation of the gravitational effect of underground headings.

as reference for a given slab, then the effect of this slab at any other point can be expressed as the percentage of the edge effect thus

$$(g_A/g_B)\cdot 100 = (2/\pi)\left\{\cot^{-1}(x/h) - x/h \log_e\left[(h/x)\sqrt{(x/h)^2+1}\right]\right\}\cdot 100 \quad . \quad (5)$$

or

$$(g_A/g_B)\cdot 100 = \varphi(x/h) \quad . \; . \; . \; . \; . \; . \; . \; . \quad (6)$$

It is obvious from expressions (5) and (6) that the ratio x/h decides the magnitude of the effect.

The attached tables (Table 6) give the percentage of the edge effect as function of x/h. The two columns have been included: one gives the percent effect for the semi-infinite block [BCN] at a distance x from the point of observation, the other the effect of the finite block [ABCD]. Each value of the second column is of course a difference between 100 and the corresponding value of the first column. Thus the whole computation is reduced to one calculation of the edge effect from expression (1), which is simple enough, and thereafter the multiplication of this quantity by the percentage corresponding to ratio x/h.

This simplified method of calculation is probably even more apparent in reference to the blocks, the upper surface of which is below the plane of observation. The effect of a semi-infinite slab [CEN] (lower part of Fig. 23) at A is simply the difference between the effect of [BEN] and [BCN] computed as explained above.

This way of calculation can be applied to structural features, which approach in shape the semi-infinite or finite slabs. It was also applied in this paper for the computation of the correction due to underground roadways (Fig. 24).

Station S is located at a distance x from the wall BC. The effect of [BCB′C′] at S is the sum of the effects due to [ABCS] and [AB′C′S] which are easily found as the function of the ratios x/h, and x'/h. The lower part of the Fig. 24 shows the case when the station is located at a road junction. The effect due to the roadway MM′ at S (Section BB′CC′) is found as before.

The effect of [DD′E′EN′] at S can be determined in two steps. First the effect of [B′C′N′] at S is calculated on the assumption that it is a semi-infinite block, using the ratio x/h. This result has to be modified, due to the fact that the extent of the slab along direction MM′ is limited by DE and D′E′. This is done by assuming the proportioned effect and multiplying the previous result by the ratio: effect of [DEE′D′] at C′ to $2\pi G\sigma h$. Effect of [DEE′D′] at C′ is found using the "x/h" ratios as before.

TABLE 6

The effects of slabs and blocks at different distances from point "S", Expressed in % of ($\pi G\sigma h$) for different Ratios of Horizontal Distance to thickness (x/h)

Ratio	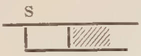	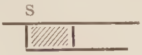
x/h	Percent of $\pi G\sigma h$	Percent of $\pi G\sigma h$
0.01	96.4	3.6
0.02	93.7	6.3
0.03	91.4	8.6
0.04	89.2	10.8
0.05	87.3	12.7
0.06	85.4	14.6
0.07	83.7	16.3
0.08	82.0	18.0
0.09	80.4	19.6
0.10	79.0	21.0
0.11	77.5	22.5
0.12	76.1	23.9
0.13	74.8	25.2
0.14	73.5	26.5
0.15	72.3	27.7
0.16	71.1	28.9
0.17	70.0	30.0
0.18	68.8	31.2
0.19	67.7	32.3
0.20	66.8	33.2
0.21	65.7	34.3
0.22	64.7	35.3
0.23	63.7	36.3
0.24	62.8	37.2
0.25	61.8	38.2
0.26	61.0	39.0
0.27	60.1	39.9
0.28	59.3	40.7
0.29	58.4	41.6
0.30	57.6	42.4
0.32	56.1	43.9
0.34	54.6	45.4
0.36	53.2	46.8
0.38	51.8	48.2
0.40	50.6	49.4
0.42	49.3	50.7
0.44	48.1	51.9
0.46	47.0	53.0
0.48	45.9	54.1
0.50	44.9	55.1
Ratio	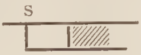	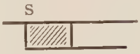
x/h	Percent of $\pi G\sigma h$	Percent of $\pi G\sigma h$
0.52	43.9	56.1
0.54	42.9	57.1
0.56	41.9	58.1
0.58	41.1	58.9
0.60	40.2	59.8
0.62	39.3	60.7
0.64	38.6	61.4
0.66	37.8	62.2
0.68	37.1	62.9
0.70	36.3	63.7
0.72	35.7	64.3
0.74	35.0	65.0
0.76	34.3	65.7
0.78	33.7	66.3
0.80	33.1	66.9
0.82	32.5	67.5
0.84	31.9	68.1
0.86	31.4	68.6
0.88	30.8	69.2
0.90	30.3	69.7
0.92	29.8	70.2
0.94	29.3	70.7
0.96	28.8	71.2
0.98	28.4	71.6
1.00	27.9	72.1
1.1	25.9	74.1
1.2	24.0	76.0
1.3	22.5	77.5
1.4	21.1	78.9
1.5	19.9	80.1
1.6	18.8	81.2
1.7	17.8	82.2
1.8	16.7	83.3
1.9	16.1	83.9
2.0	15.3	84.7
2.2	13.9	86.1
2.4	12.9	87.1

Ratio *x/h*	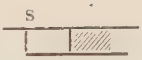 Percent of $\pi G\sigma h$	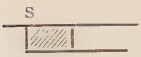 Percent of $\pi G\sigma h$	Ratio *x/h*	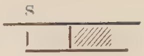 Percent of $\pi G\sigma h$	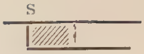 Percent of $\pi G\sigma h$
2.6	11.8	88.2	8.0	4.0	96.0
2.8	11.1	88.9	9.0	3.6	96.4
3.0	10.5	89.5	10.0	3.2	96.8
			15.0	2.5	97.5
3.5	9.0	91.0	20.0	1.9	98.1
4.0	7.5	92.5	30.0	0.9	99.1
4.5	7.2	92.8	50.0	0.7	99.3
5.0	6.3	93.7	80.0	0.4	99.6
6.0	5.3	94.7	100.0	0.3	99.7
7.0	4.6	95.4			

ACKNOWLEDGEMENTS

These results are published with the permission of the Directors of Mining and Geophysical Services Ltd., whose generosity and encouragement made the work possible.

The field observations were carried out with the kind permission of the Management of Florence Mines on their property underground and on the surface. The assistance offered by the Management and Staff was most valuable and included the provision of the elevations of surface and underground stations.

The author wishes to express his gratitude to Prof. J. Mc. G. Bruckshaw of the Imperial College, discussions with whom stimulated the investigations.

The drawings in their final form were executed by Mr. S. Denyer of the M.G.S. staff. The determinations of densities of the samples were carried out in the laboratories of Soil Mechanics Limited, an Associated Company.

REFERENCES

Domzalski, W., 1954a: Gravity Measurements in a Vertical Shaft, Transactions of the Institution of Mining and Metallurgy, Vol. 63, part 9, 429-445.

——, 1954b: Gravity Profile over the Hogs Back Fault. The Mining Magazine, Vol. XCI, N° 2; August 1954.

Hammer, S., 1950: Density Determinations by Underground Gravity Measurements. Geophysics, Vol. XV, pag. 637-652.

Rogers, George R., 1952: Subsurface Gravity Measurements. Geophysics, Vol. XVII, pag. 365-377.

Smith, Neal J., 1950: The Case for Gravity Data from Boreholes. Geophysics, Vol. XV, pag. 605-636.

DISCUSSIONS

Mr. A. SCHLEUSENER: Collection of density values is important, and I support the proposal of co-ordination of this work. A difficulty in determining the density from measurements in boreholes or shafts is the uncertainty about the vertical gravity gradient, and consequently there should always be made gravity measurements on the surface as a supplement to the determinations in the galleries.

Mr. W. DOMZALSKI: I agree with this.

DRILLING METHODS IN SAND AND GRAVEL FORMATIONS *

BY

G. MURATORI **

Abstract

In the development of seismic drilling methods in Northern Italy the most important considerations have been those of ease in transport and quickness of operation. Different drilling systems are described that are adapted to the different types of near surface formation that are encountered in the area. In soft sands a high pressure water jet is used, a rotary table not being required in a great many cases. In medium consistency sand and small gravel, the drill rods are rotated by a special roller wrench equipment instead of the more usual kelly. In coarse formations, gravel and boulders, casing is driven by special pile driving equipment with collapsible mast for easy transport.

Introduction

Special problems were encountered when drilling seismic shot holes in Northern Italy. Conventional drills, both of the rotary and churn type, have been used extensively and special drills and equipment have been experimented with and are discussed here.

Hole depths not exceeding thirty meters were usually found to be sufficient in various formations that may be classified as follows:

1) Soft sand, sometimes with peat layers. Marshy ground.
2) Medium grade and lighter sand and small gravel, sometimes with shale bands.
3) Coarse formations. Gravel and boulders, sometimes cemented.
4) Clay.

Since drilling in clay was done by ordinary rotary methods this aspect will not be discussed here.

Shallow drilling to 30 meters imposes particular requirements on the drilling equipment. Ability to attain a given depth is now less important than ease in transport and speed of operation. The time required per shot hole is usually small (½ to 1½ hour) and preliminary operations, such as digging mud tanks, circulating the mud, and if necessary the adding of bentonite, can be performed in quite a short time.

Mud tanks were small and a fluid capable of durably cementing the walls of the hole was seldom obtained; caving in was often experienced and the hole became useless before shooting or after the first shot. To prevent this occurrence, casing of holes is advisable and becomes essential when shooting below a critical depth. Lifting the line for adding a new rod is perhaps the most frequent cause of caving and a method was developed for simultaneous casing and drilling, both with rotary and percussion machines.

---

* Presented at the Fifth Meeting of the European Association of Exploration Geophysicists held in Milan, 2/4 December 1953.

** Azienda Generale Italiana Petroli, Milan.

The following methods were tried and are now in practical use:

1a) High pressure water jet.
2a) Special roller wrench equipment for rotary table.
3a) Diesel hammers.

Each methods is suited for a particular ground. Methods 1a) 2a) 3a) were found useful in formations 1) 2) 3) respectively as classified before.

High Pressure Water Jet Drilling

High pressure water jet drilling may prove practical and economical in operation only in very soft formations or marshy grounds with a large and easy water supply. In the simplest cases no rotary table is required. An injection swivel is screwed on the casing head and the tubes are slightly rotated around their axis while forcing them into the ground, the water jet doing practically all the penetration work. A clamping yoke is provided, as shown in fig. 1.

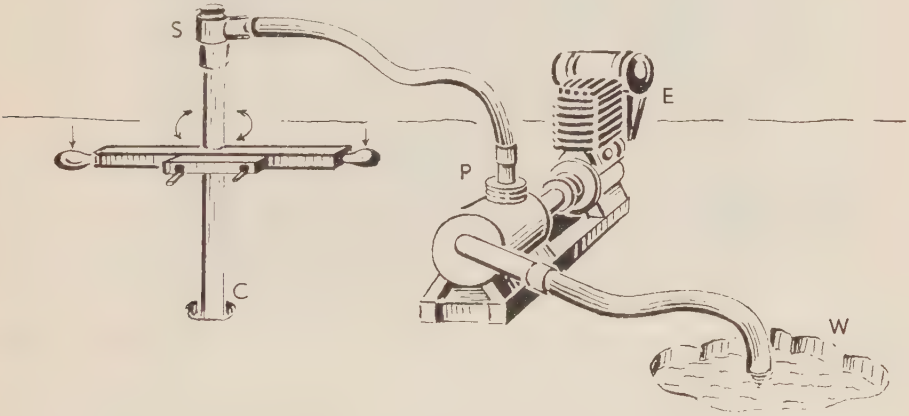

Fig. 1. Diagram of high pressure water jet drilling.

The pump may be a reciprocating duplex pump, a liquid ring SIHI type pump, or a centrifugal multi-stage pump. Delivery should be from 100 to 200 gallons per minute when using a 3½″ casing and a pressure of 5 to 15 atms.

Liquid ring pumps are about 60 % lighter than other types and, although more subject to abrasive action of sand, they may be successfully used if ease of transport is the principal requirement.

A somewhat more elaborate drill involves the use of a small rotary table and demountable mast. However, in loose formations the method is not advisable due to the increased danger of caving of the holes. A special fitting for the rotary table has been developed and is described in the following section.

Roller Wrench for Drilling with Casing Tubes

If holes could be drilled without lifting the line for adding a new rod, practically the only effect of the caving of holes would be an increased friction on the rotating tubes. An experimental roller wrench was constructed for rotating tubes or rods directly without using the kelly. Each tube is added in turn from above and takes the place of the kelly; the torque is transmitted by friction while the tube itself is left free to run axially through the wrench.

The experimental roller wrench is shown in fig. 2. It is used together with a bushing for rotary tabe as shown in fig. 3. The bushing carries three rubber covered vertical rods stiffened by a ring.

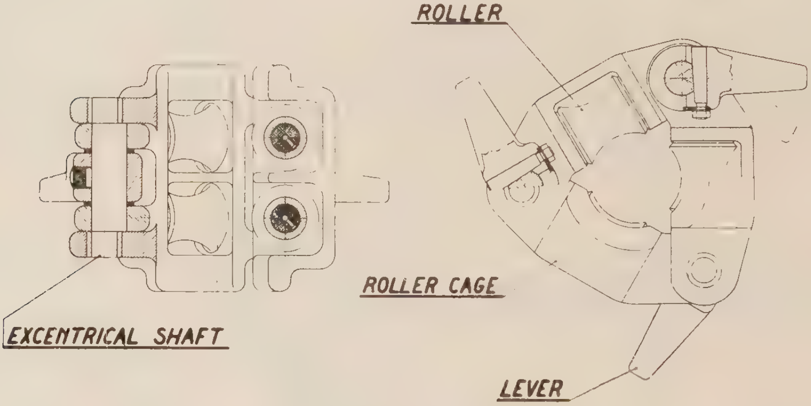

Fig. 2. Diagram of roller wrench.

When the rotary table rotates, these rods contact the levers that are fixed to the vertical eccentric shafts which are thereby rotated. Since the terminal off-center portions of each shaft are carried by one of the roller cages while the central portion is carried by the next roller cage, the polygon of the roller cages and eccentric shafts changes from ABCDEF to A′B′C′D′E′F′ (fig. 4). As a result the rollers come nearer to the centre of the wrench and are pushed against the tube with a force proportional to that applied to the levers. This force, in turn, is proportional to the torque transmitted by the rotary table. If the torque increases the forces applied to the levers also increase and the pressure between the rollers and the tube is proportionally increased.

The non-slipping condition for the rollers has been found to be

$$\frac{L}{l} \geq \frac{\sqrt{3}}{2} \cdot \frac{1}{\eta f} \cdot \frac{B}{d}$$

where *L*, *l*, *B*, *d* are shown in Fig. 5.

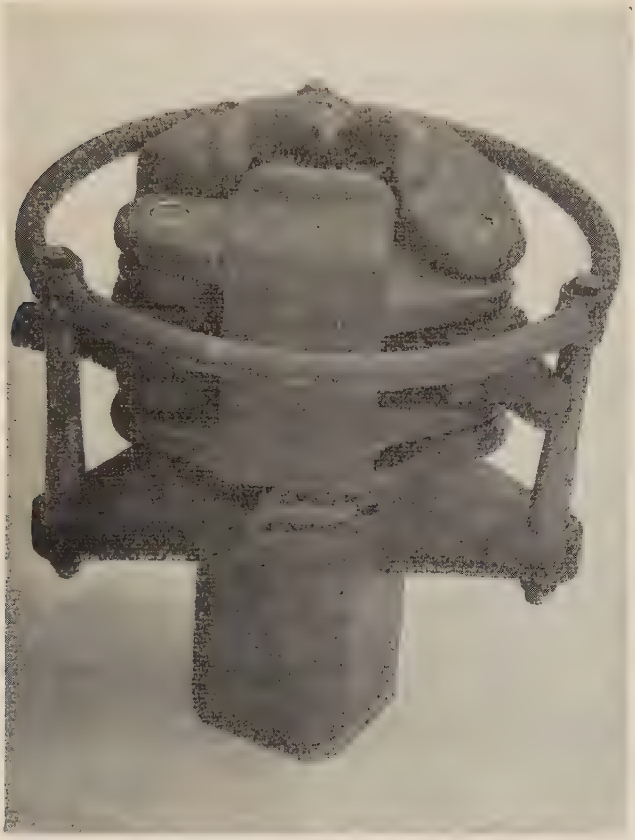

Fig. 3. Wroller wrench and bushing or rotary table.

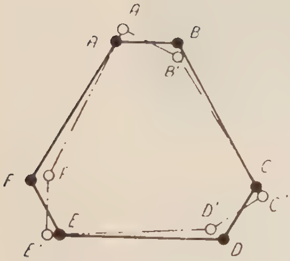

Fig. 4. Diagram illustrating the change in position of the roller cages.

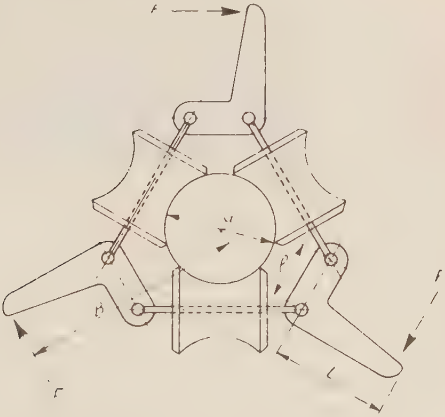

Fig. 5. Diagram illustrating notation.

η is the mechanical efficiency (about 0.9)
f is the friction coefficient (about 0.2 for steel rollers on steel tube).

If the above condition is fulfilled the rollers are prevented from slipping and the torque transmitted is limited only by mechanical failure of wrench, tubes or transmissions.

This special wrench has been tested extensively in sand and small or medium gravel.

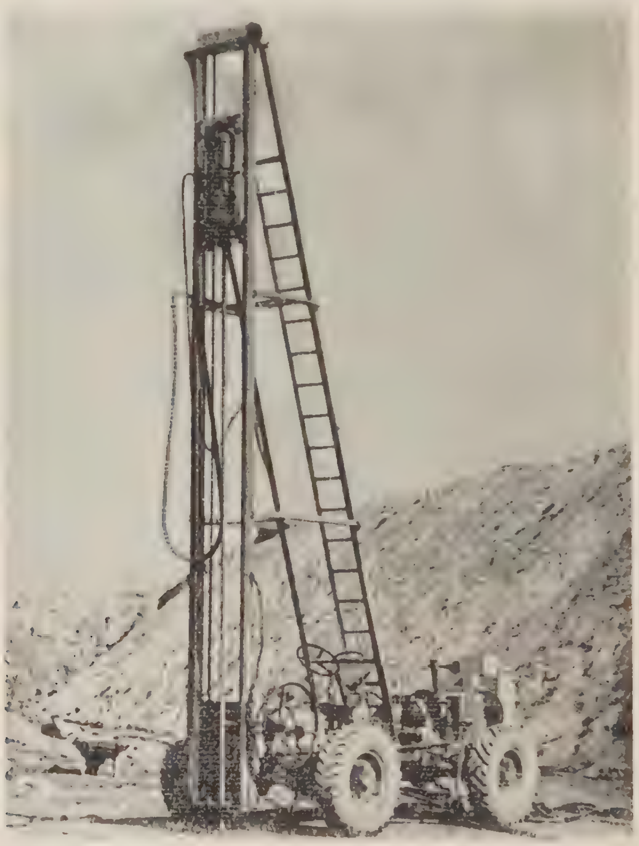

Fig. 6. Mandrel drill.

Full engine power (about 80 HP at 180 r.p.m., corresponding to a maximum torque of about 300 Kg m) was transmitted by the wrench without any slipping of the rollers even when the experimental tubes of 3½″ diameter and ¼″ thickness were badly forced at the connecting nipples and expanded about ⅛″ in diameter.

Before starting these experiments the possibility of drilling and casing holes with a mandrel drill, driven by a gasoline or electric motor such as that shown in fig. 6, had been considered. However, owing to the high cost and the complex problems arising in the construction of the swivel and mast, this solution was discarded. It was found preferable to add an extra fitting to an ordinary rotary table, together with a small platform in the upper part of the mast for a man to manoeuvre a breakout wrench.

In drilling with casing, ordinary fishtail bits are usually lost when firing the first shot in the hole. Core bits should be used whenever possible because they may be recovered by lifting the casing when lowering the explosive charge into the hole.

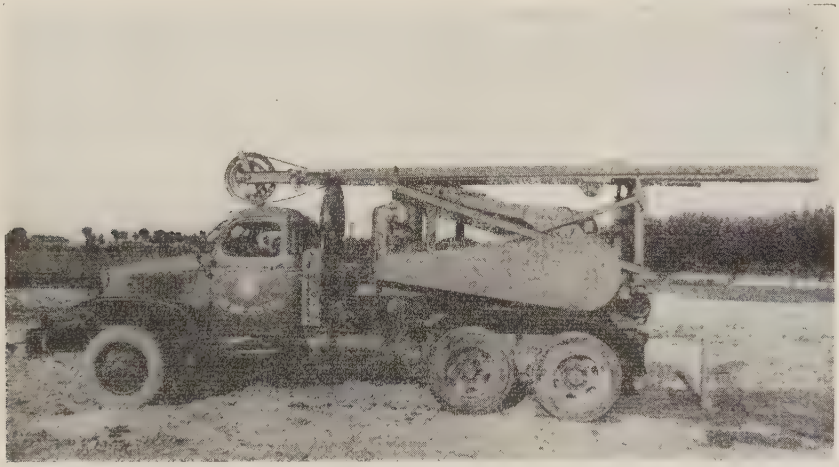

Fig. 7. Percussion drill, older type.

Diesel Hammer Method

When working in coarse formations, such as coarse gravel and boulders, rotary drilling may not prove to be the best method. A powerful and yet very light type of percussion drill was considered with the view of replacing the older percussion drills which had been used for many years in Northern Italy. One of those drills is shown in fig. 7. It is adopted from a conventional churn drill to act like a hammer, striking heavy blows with a 3½ tons mass on the head of 3½″ diameter tubes with a wall thickness of ⅜″. At the lower end these tubes carry a wrought iron, cone shaped penetrating point. The newer type of drill is shown in fig. 8. It carries a collapsible tubular tower, a Diesel pilehammer, winches, hydraulic pump and elevator for lifting the tower.

A collapsible tower was required by the small overall dimensions of the truck. The lower part of the tower is raised directly by the elevator. The axis, around which the upper part of the tower rotates with respect to its lower part, carries a pulley that is rigidly connected to the upper part. This pulley is connected by a steel rope to another pulley which is mounted on the axis of rotation of the lower part of the tower with respect to the chassis of the drill truck, and rigidly connected to the latter. The transmission ratio between the lower and the upper pulley is 2: 1. This movement link between tower and chassis provides for the simultaneous raising of the whole tower as shown in figs. 9, 10 and 11 in successive positions.

Fig. 12 shows the hydraulic elevator, the double winch for manoeuvering the Diesel Hammer, the lower pulley and rope on the left, and the hydraulic pump on the right.

Fig .13 is a close view of the hydraulic controls for the winches. The hammer works as follows: the hammer is lifted and set on the casing head using one of the two winches. The motor is started by raising the piston with the second winch; the piston is automatically released as it reaches the upper part of the cylinder and falls, activating the fuel injection pump and highly compressing the air in the combustion chamber until the ignition temperature for the sprayed fuel is reached. Combustion occurs, sending up the piston and at the same time delivering a blow on the casing head.

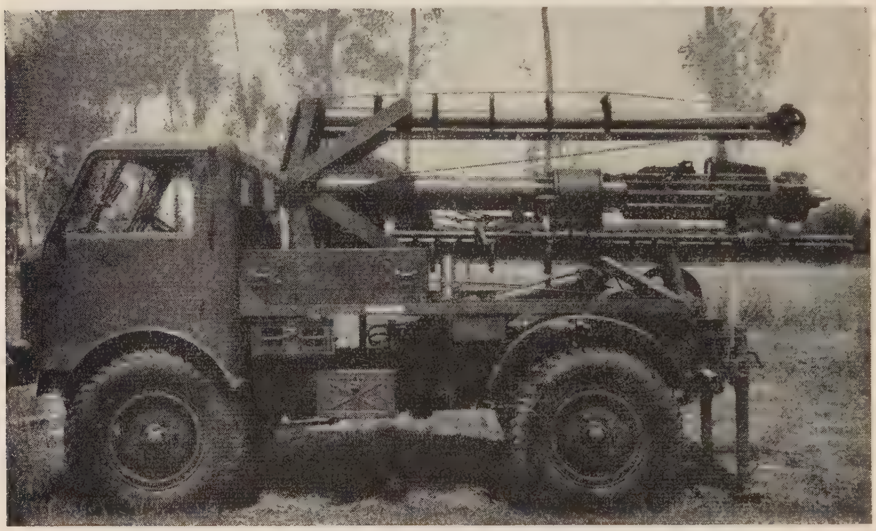

Fig. 8. New type percussion drill.

During the upward stroke ports are opened for exhaust and scavenging. The piston expends all its kinetic energy and then falls again, thus performing a two stroke diesel cycle.

The frequency is about 60 blows p.m., average power on the casing head 30 HP, total weight 2,1 tons, fuel consumption per day about 2 gallons of gasoil. Corresponding figures for the old type hammer are: 65 blows p.m.,

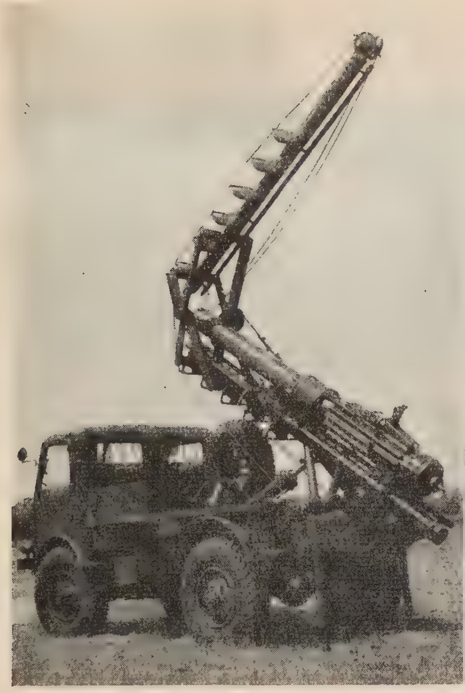

Fig. 9. Raising the collapsible tower, first position.

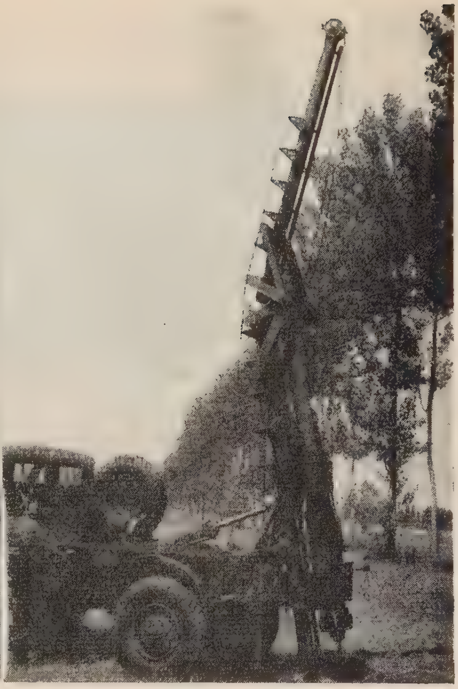

Fig. 10. Raising the collapsible tower, second position.

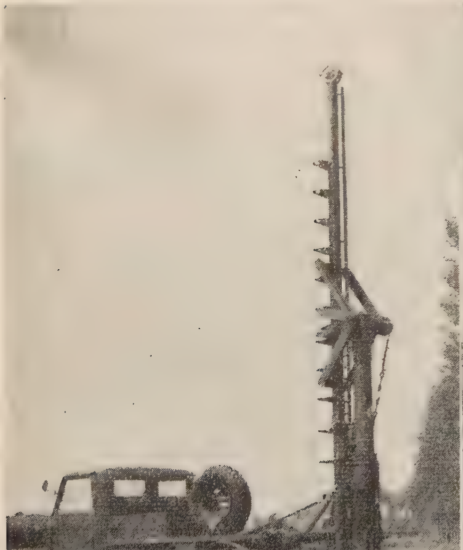

Fig. 11. Raising the collapsible tower, third position.

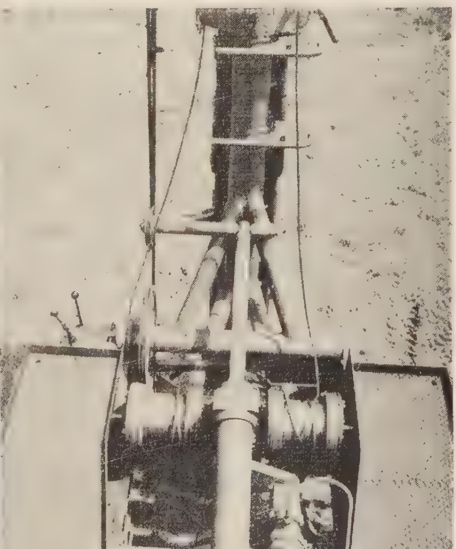

Fig. 12. Hydraulic elevator, and double winch for manoeuvering Diesel hammer.

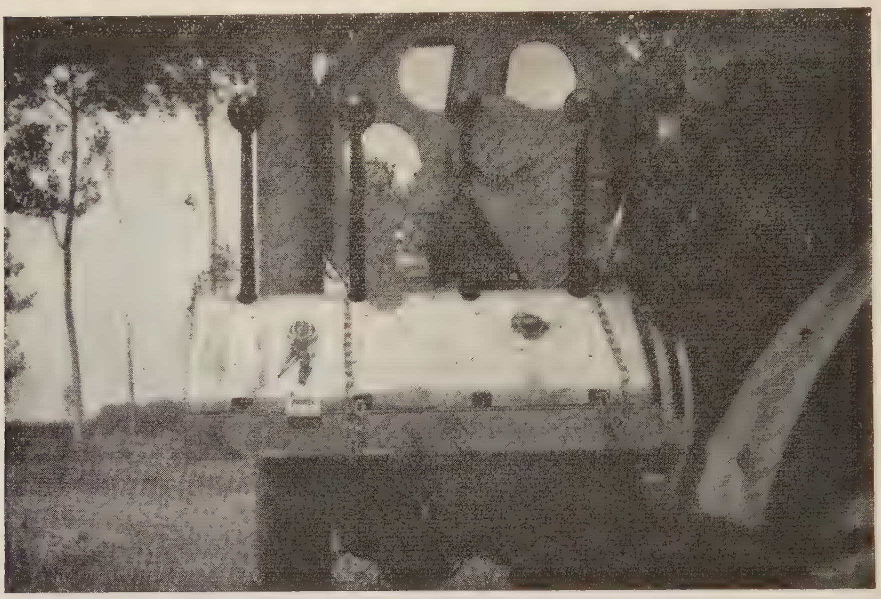

Fig. 13. Hydraulic controls for the winches.

10 HP on casing head, total weight 6.5 tons, fuel consumption 10 gallons of gasoline per day.

Thus the newer drill compares quite favourably with the older one particularly in the weight to power ratio.

During experimental and routine work the power was found to be even larger than was necessary and tubes were sometimes bent.

A harder material having a higher tensile strength (a carbon steel 65-70 kg/mm² breaking stress) was then used for casing and this was sufficient to avoid bending, without any serious increase in cost of tubes.

SOME THEORETICAL CONSIDERATIONS ON THE USE OF MULTIPLE GEOPHONES ARRANGED LINEARLY ALONG THE LINE OF TRAVERSE *

BY

F. W. HALES ** AND T. E. EDWARDS **

ABSTRACT

An analytical treatment is given of the response of linear arrays of multiple geophones, as a function of the direction of incidence of the wave and of the wave frequency. The relation between the response and the direction of incidence may be quite complicated, the response being zero in several directions. As a function of wave frequency, the response may also have several zero values within the frequency band in which reflections are expectable. This would result in a serious modification of the filter characteristics of the amplifier. It is shown, however, how such a modification of the filter characteristics may be avoided by a judicious choice of the number and the spacing of the geophones in a multiple group.

The following is intended to illustrate some of the operational difficulties which may be encountered through injudicious use of large numbers of multiple geophones placed in line along the line of traverse. The use of large numbers of multiples is being widely advocated as a means of bringing out reflection alignments in difficult areas, but the authors wish to emphasize that this procedure is not a panacea to be applied indiscriminately, but is one which calls for careful consideration in order that the observed results may really mean what they appear to mean.

ASSUMPTIONS

It is assumed that:

(a) The time increment (Δt) from geophone to geophone for any event will be constant along the particular group of multiples under consideration.

(b) The geophones are all equally and uniformly "planted".

(c) The impedance matching (and, therefore, damping) is correct so that geophone resonances are not operative.

(d) The output of the multiple group is the vector sum of the outputs of the individual geophones.

(e) Deductions valid for frequency components of a complex waveform are valid for the whole wave.

---

* Presented at the Sixth Meeting of the European Association of Exploration Geophysicists, held in Copenhagen, May 19/21, 1954.

** Seismograph Service Limited, London.

THEORETICAL

Directional Sensitivity.

It may be shown that if a wave $A \sin wt$ traverse a line of m equally spaced multiple geophones, the resultant output of the group will be expressed by

$$\Sigma = A\,[\sin(m\,w\,\Delta t/2)\;/\;\sin(w\,\Delta t/2)]\,\sin(w\,t) \quad . \quad . \quad . \quad . \quad . \quad (1)$$

where Δt is the time increment at each successive detector. In other words, the original amplitude A is modified by the term in brackets, and it is from the behaviour of this modifying factor that important criteria as to the use of linear multiple groups are seen to derive.

If we let

$$k = \sin(m\,w\,\Delta t/2)\;/\;\sin(w\,\Delta t/2) \quad . \quad . \quad . \quad . \quad . \quad . \quad . \quad . \quad (2)$$

it will be seen that k is dependent on the number of geophones (m), the frequency of the received disturbance ($f = w/2\pi$) and the stepout time (Δt) which, in turn, may be expressed more usefully in terms of geophone spacing (Δx).

For a wave-front arriving at a multiple group at an angle φ with the horizontal:

$$\Delta t = \Delta x \cos\varphi/V$$

where V is the velocity involved (Fig. 1).

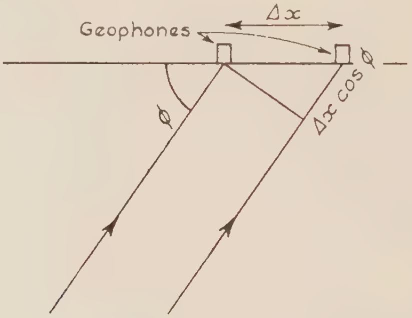

Fig. 1. Diagram illustrating the relation between Δt and Δx.

Equation (2) now reduces to:

$$k = \frac{\sin(\pi\,m\,f\,\Delta x\cos\varphi/V)}{\sin(\pi\,f\,\Delta x\cos\varphi/V)} \quad . \quad . \quad . \quad . \quad . \quad . \quad . \quad . \quad (3)$$

which may be more conveniently expressed as:

$$k = \frac{\sin(\pi\,mD\cos\varphi)}{\sin(\pi\,D\cos\varphi)} \quad . \quad . \quad . \quad . \quad . \quad . \quad . \quad . \quad . \quad (4)$$

where $D = f\,\Delta x/V = f\,L\;/\;(m-1)\,V$, L being the coverage of the group.

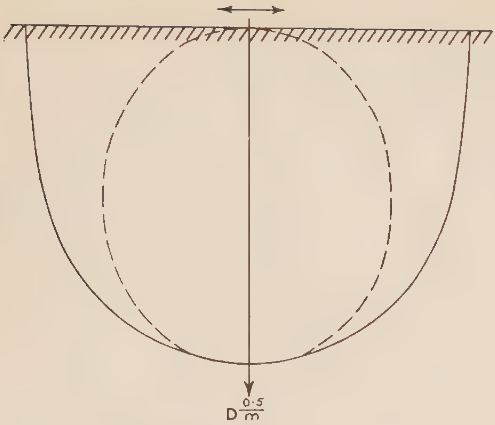

A. NO DIRECTION OF ZERO RESPONSE

B. ZERO RESPONSE WHEN $\phi = 0°$

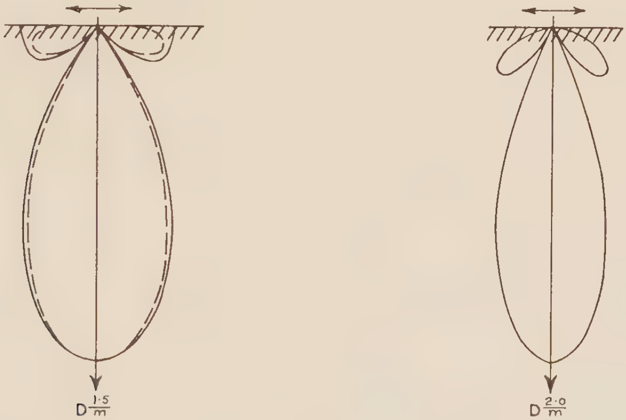

C. ZERO RESPONSE WHEN $\phi = 48{\cdot}2°$

D. ZERO RESPONSE WHEN $\phi = 0°$ & $60°$

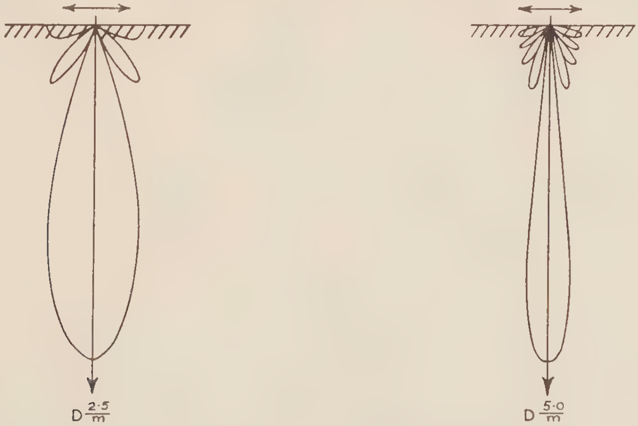

E. ZERO RESPONSE WHEN $\phi = 36{\cdot}9°$ & $66{\cdot}4°$

F. ZERO RESPONSE WHEN $\phi = 0°, 36{\cdot}9°, 53{\cdot}1°, 66{\cdot}4°$ & $78{\cdot}5°$

Fig. 2. Directional sensitivities of linear arrays of multiples.

Examination of Equation 4 shows that for values of φ given by:

$$\cos \varphi = n/mD \ (n \neq 0)$$

the response k will be equal to zero and in the special case where $n = 0$ it will attain limiting values of $\pm m$. For intermediate values of φ, k will oscillate with values always between $+m$ and $-m$, and its phase will change rapidly from positive to negative or vice versa, as zero values are passed through.

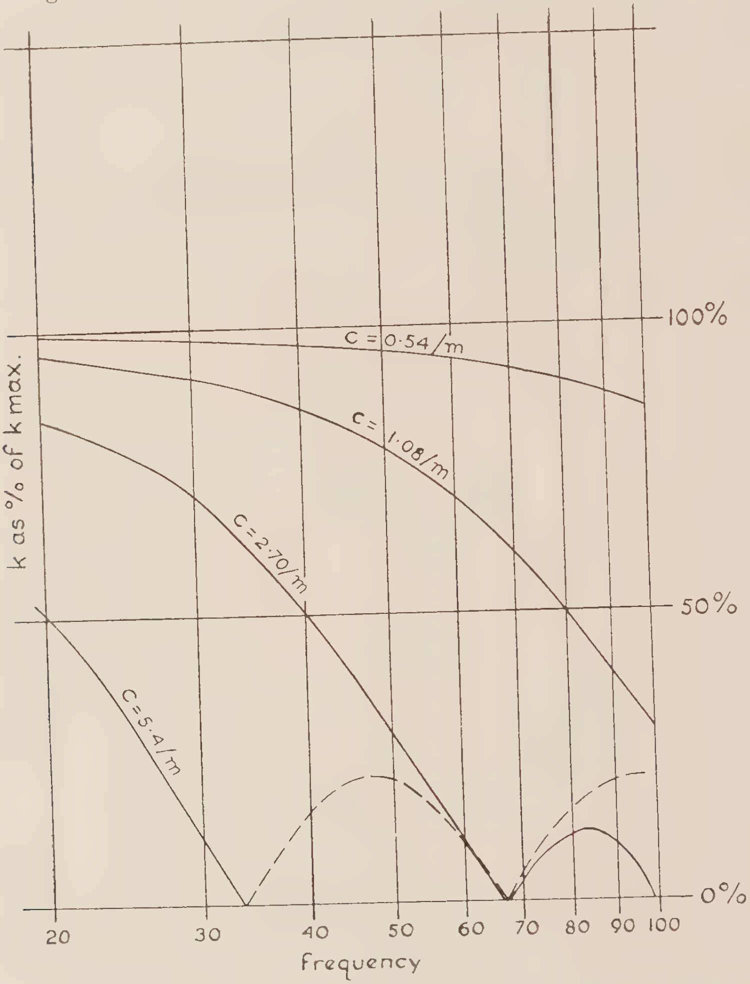

Fig. 3. Frequency response curves of linear arrays of multiple geophones.

For any particular values of m and D, Equation 4 is best demonstrated as a polar diagram similar to that derived for a multiple-antenna array for radio waves. A series of such diagrams is shown in Fig. 2, where directional sensitivities of linear multiple groups have been computed for various values of D between $0.5/m$ and $5.0/m$. It will be seen that:

(a) when $D = 0$ (i.e., $\Delta x = 0$) the polar liagram will be a semicircle with a radius of m units.
(b) when D increases to a value of $1/m$, the ideal single lobe with zero response in a horizontal direction is obtained
(c) For values of $D > 1/m$, side-lobes with phase reversals begin to appear.
(d) There is zero response in a horizontal direction when $D = n/m$, n being an integer not equal to zero.

The broken line curves in Fig. 2 are obtained by considering only the vertical component of a longitudinal wave which will apply in the case of reflections arriving at an angle with the vertical, the geophones being assumed to possess a single degree of freedom in a vertical direction.

Frequency Selectivity.

If we wish to examine the response of the multiple group to disturbances of different frequencies, Equation 4 may be re-written as:

$$k = \sin (m\, C\, f) \,/\, \sin (C\, f) \quad . \; . \; . \; . \; . \; . \; . \; . \; . \quad (5)$$

where $C = \pi\, \Delta x \cos \varphi / V$ and is considered a constant for disturbances arriving from a particular direction φ.

Plotting k against f (using a rectangular coordinate system), we obtain a family of frequency response curves for different values of C: that shown in Fig. 3 is for values between $C = 0.54/m$, when frequence discrimination is negligible, and $C = 5.4/m$, when it is serious.

In Fig. 4 is shown how the frequency response of the multiple group may modify the nominal characteristics of the amplifier filters to yield a resultant behaviour which is quite different from that expected by the observer. The multiple group with a C value of $2.70/m$ ($m = 30$, $\Delta x = 10$ ft., $V = 5000$ ft/sec, $\varphi = 75.5°$), fed into an amplifier system designed to peak at 50 c/s, will cause resultant behaviour which peaks near 40 c/s and cuts out completely at 66 c/s, higher frequencies suffering a phase reversal.

Noise Synthesis.

The transit of an undesired disturbance along the line of multiple geophones will generate frequencies which may well lie within the pass-band of the subsequent amplifiers.

Equation 1 may be re-written in the form:

$$\Sigma = \frac{A}{2 \sin (w\, \Delta t/2)} \left[\cos w\, (t - m\, \Delta t/2) - \cos w\, (t + m\, \Delta t/2)\right] \quad . \quad (6)$$

and becomes more readily recognized as involving a system of stationary waves. It is evident, therefore, that the behaviour of the multiple group will be similar to that of a single geophone in a stationary-wave field and, in the case of

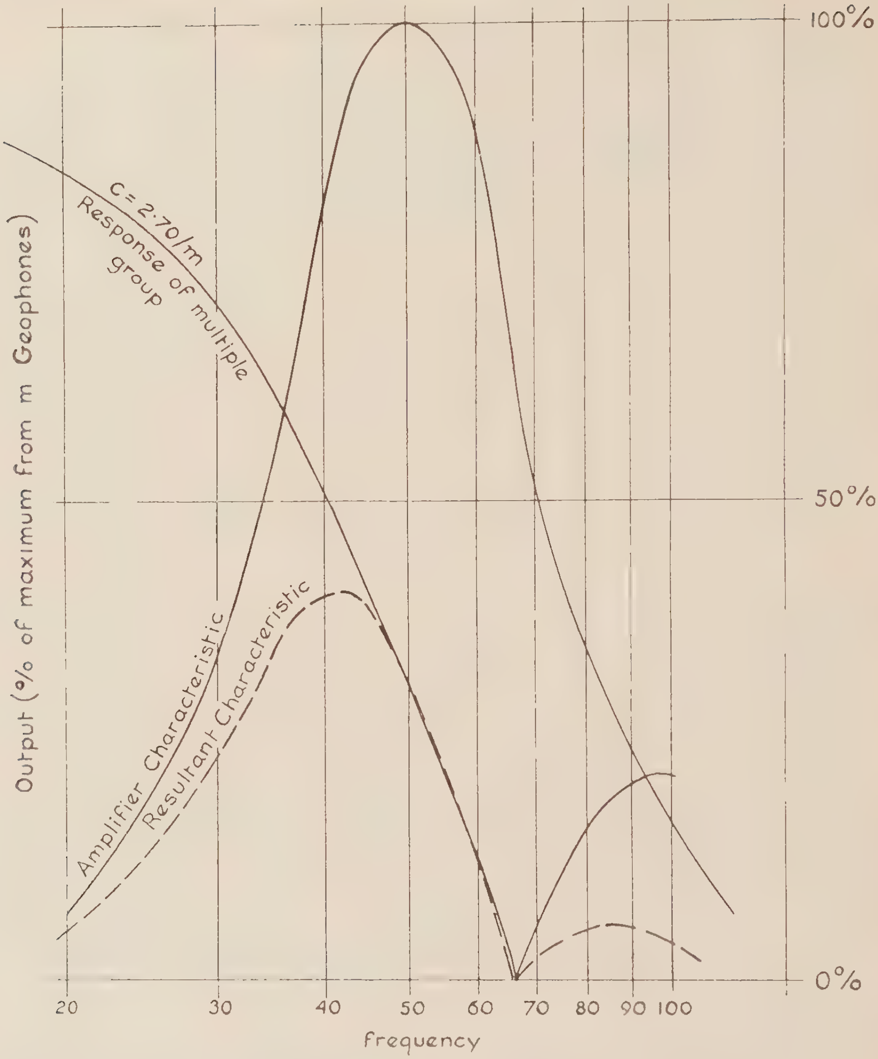

Fig. 4. Combined effect of the frequency response of a multiple group and the filter characteristic of an amplifier.

transients, frequencies may be present in the output signal which may well lie within the passband of the amplifiers and which may have dangerously large amplitudes through multiple reinforcements.

Practical Considerations

The use of groups of multiple geophones is normally resorted to in order to improve the ratio of desired seismic signal strength to undesired shot and random noise. Originally, the operational approach was to space the multiples so as to cut out shot noise in general and the ground roll in particular: the increase in desired signal amplitude was largely incidental. The present tendency appears to be the reverse of this and leads to field experimentation yielding data, the significance of which is not always appreciated and which may be quite dubious.

When the dimensions of a linear array are chosen, the first criterion should be the elimination of ground roll and shot noise. The frequencies and velocities involved are usually known from the initial experimental records, and it is a simple matter to compute the optimum conditions when $mD = 1, 2, 3 \ldots$ etc., (Equation 4), when the horizontal response of the group will be zero.

As a practical example, consider a case where the predominating interference is due to ground roll with a velocity of 750 ft/sec and a frequency of 15 c/s. If 30 geophones are to be used, we deduce a value for Δx equal to $1.\dot{6}$ ft. (When the length of traverse covered by the group is of the order of one wavelength), and its multiples, $3.\dot{3}$ ft., 5 ft., etc.

The next procedure should be to compute new values of D for the desired reflections, using the Δx values obtained above, so that the directional sensitivity pattern (Fig. 2) for reflections may be seen and approved. Thus, if the reflection frequency is 50 c/s and the sub-weathering velocity 5000 ft/sec., the series of possible Δx values will give values for D of $0.5/m$, $1.0/m$, $1.5/m \ldots$ etc., from which it is evident that spacings of $1.\dot{6}$ or $3.\dot{3}$ ft will give a useful single-lobe directional response while larger spacing will introduce zones of zero response and phase change.

It is of interest to consider what would happen if the commonly-advocated spacing of 10 ft were adopted in the above case; certainly the ground roll would be eliminated ($mD = 6.0$), but for reflection frequencies and velocities, D would be equal to $3.0/m$ and a response pattern intermediate between those of Figs 2(e) and (f) would be operative. The resultant seismic spread behaviour is illustrated in Fig. 5 where it is shown that from fairly shallow reflecting beds, the reflected energy would seem to disappear in a down-dip direction and would then reappear having suffered a phase reversal.

After the most satisfactory value for Δx has been determined, a value for C should be computed (Equation 5) using the smallest value for φ likely to be encountered. A check on any possible modification of amplifier response is thus obtained. Continuing with the example already chosen, it may be shown that for $\Delta x = 1.\dot{6}$ ft and $\varphi = 75°$, C will have a value equal to $0.47/m$ and frequency discrimination will be negligible (Fig. 3). If, on the other hand, we had chosen $\Delta x = 10$ ft, C would have equalled $2.8\,m$ and the behaviour of the amplifier filter settings would have been quite unpredictable.

Although it has not been stressed, the foregoing treatment can be applied to all types of multiple geophone grouping. The linear array has been chosen because it is the only economically practical one where m and/or Δt may be so

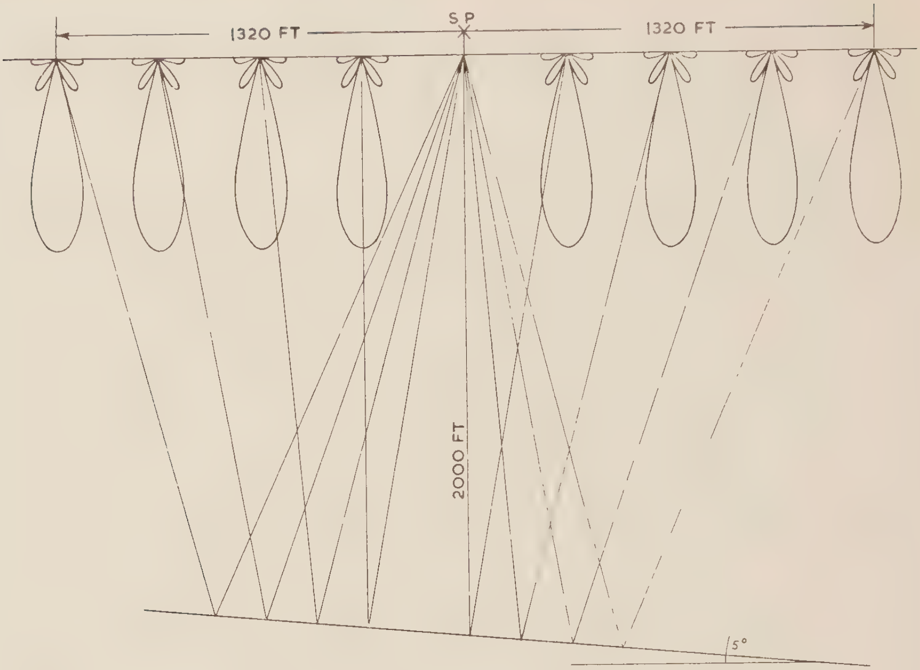

Fig. 5. Diagram illustrating disappearance and phase reversal of reflection event across a typical spread.

large as to lead to the dangers described. The use of clusters or broadside arrays of geophones has the added advantage of sampling a larger area of the reflector and in this way may lead to reflection improvement irrespective of any selective group behaviour.

It is possible to enlarge considerably on this treatment of the use and misuse of linear arrays of multiple geophones, particularly on the section which deals with the synthesis of noise. The authors hope, however, that sufficient has been suggested to initiate careful consideration of any problems where such use is advocated.

Acknowledgments

The authors wish to thank the directors of Seismograph Service, Limited, for their permission to publish this paper. In particular, they wish to acknowledge the advice and co-operation of Mr. E. J. P. van der Linden at whose instigation it was prepared.

Discussion

Mr. H. L. Brewer: I do not agree with the criticism of the multiple geophones; in my opinion important results have been obtained by their application.

Mr. F. W. Hales: The purpose of the investigation has been to show how undesired noise may be reduced, and is not a criticism of the use of multiple geophones.

Mr. G. Tait: The theory has been developed by assuming the continuous wave condition. In practice we have to deal with transients and a frequency spectrum which may vary from one shot to another even when these are from the one hole. The conditions are more difficult than those which have been assumed. I therefore feel that further investigation into this aspect of the problem is required.

Mr. F. W. Hales: It is my intention to include the effect of transients in my studies of the use of multiple geophones but they are not ready yet for publication.

Mr. G. Tait: I am very glad to hear of this intention and I should be very interested to see the experimental seismic records obtained during that investigation.

Mr. C. H. Johnson: To those who, like Mr. Tait, would like to see the transient solution of Mr. Hales' problem, I suggest looking in Geophysics, 1936 and 1937, for papers describing the Rieber Sonograph. The Sonograph provided a reproducible record of each of several unmixed traces. In the play-back of these records, all or several (generally all) of the traces were combined into a single summation. This summation could be done with various time differences introduced linearly between the traces. This seems to be the equivalent of Mr. Hales' simple summation of traces with variable move-out. If we accept this equivalence the Rieber illustrations show experimentally the extension of Mr. Hales' steady-state solutions to the transient case, since most of Rieber's illustrations were of actual transient reflections obtained in routine field work.

Mr. F. W. Hales: We were not aware of this previous communication, and thank Mr. Johnson for drawing our attention to it.

BOOK REVIEW

L. W. Sorokin. — Lehrbuch der Geophysikalischen Methoden zur Erkundung von Erdölvorkommen.

579 pp., 210 figs. VEB Verlag Technik — Berlin, 1953.

This book is a translation into German of a Russian text book on geophysical methods of oil exploration, which was first published in 1950. According to the preface, the book is intended primarily for college students.

The general approach to the subject is rather different from that of Western books of this nature. The physical principles that underly the geophysical methods are treated extremely briefly, and the emphasis is placed entirely on prescriptions for interpretation methods and for field operations. These prescriptions even cover such subjects as the number of labourers required and the time allotted to the preparation of a survey. With regard to interpretation methods, however, the book contains some pleasant surprises.

The first part of the book (115 pp.) deals with the gravimetric method. It contains rather extensive sections on the pendulum and on the torsion balance. Two Russian types of gravimeter and the Nörgaard gravimeter are described. The discussion of the interpretation of gravity data is brief and does not bring any new points of view.

The second part of the book (44 pp.) treats the magnetic method. Apart from the description of the Russian airborne magnetometer, this part does not contain anything new to Western readers.

The third part of the book deals with the geo-electrical methods. It contains 99 pages, of which 66 are devoted to the resistivity method. This part of the book gives particularly strongly the impression that it aims to give a description of standardized procedures, rather than to give to the student and understanding of the principles of the method. For instance, only one electrode configuration (that of Schlumberger) is described, and the possibility of setting up the electrodes in a different manner is not even hinted at. At the same time it is a pleasure to find such an extensive description of the Schlumberger procedure which, in the American text books, does not receive the attention which it deserves.

The section on the interpretation of resistivity observations is one of the pleasant surprises of the book. It is definitely more up to date than the corresponding sections in the American text books, and it contains some procedures, new in the published literature, which seem to be extremely useful. Of particular importance is the substitution of new (empiric) formulae for Hummel's formula for the replacement of two resistivity layers by a single one.

Some of the other geo-electrical methods are treated more briefly, others are omitted altogether. Resistivity profiling is described in 10 pages, galvanic electro-magnetic methods in 5 pages, telluric and spontaneous polarisation methods together in 9 pages. No mention is made of inductive methods nor of equipotential line methods.

The fourth part of the book (190 pp.) treats the seismic method. First, in a rather elementary manner the underlying physical principles are discussed. Then follows a chapter on seismic instruments and a chapter on seismic field procedure. The next chapter is entitled "Travel Time Curves of Seismic Waves". The interesting and original aspect of this chapter is that, from the very start, the propagation of seismic waves is described as a three dimensional phenomenon, and that travel time planes in x, y, t co-ordinates are used.

In the section on seismic interpretation certain methods which are well known in the West and have proved extremely useful there, are lacking entirely. Thus, no mention is made of the properties of linear velocity functions or of other continuous velocity functions. The interpretation appears to be based entirely on the concept of average velocity. At the same time procedures are described which have not been published in the West and which, to say the very least, give food for thought. Over 10 pages are devoted to the determination of the velocity distribution from reflection data and, in this, the dip of the reflecting boundary is taken into consideration, not as a correction afterwards, but from the very beginning. Although some of the procedures that are described do not seem to be very practical, this section contains many illuminating points of view. Another interesting method is an interpretation procedure of refraction data that is based on extending the wave fronts backwards from the known times of arrival at the recording stations.

The fifth part of the book (100 pp.) is entitled "Geological Interpretation of Geophysical Observations". It deals with the geophysical expression of different types of structure, and also contains a number of case histories.

Summarizing, most of the contents of Sorokin's book are not new to Western readers. This is not a criticism, since the book was not written for the benefit of Western readers but for Russian students. At the same time, the book contains several new ideas and procedures, which make it well deserve a place on a Western book shelf.

As a concluding remark, I wish to express regret that Sorokin, and Russian authors in general, do not follow the international nomenclature for fundamental geophysical concepts. Thus, the term "time field" is used for "wave front", and the expression "second derivative of gravity" for "gravity gradient" and "curvature".

O. K.

M. R. J. Wyllie. — The fundamentals of electric log interpretation. Academic Press Inc. — New York, Sept. 1954. Price $ 3.60.

In a small-size (5″ × 8″) booklet of 99 pages, with 9 figures in the text and 8 diagrams appended, the author has succeeded in giving a clear survey of electric logging theory and its quantitative application, i.e. the translation of log quantities into information on the texture of rocks penetrated in a borehole and on their fluid contents.

In the first part (24 pp.) the way in which rock texture and pore contents affect both potential and resistivity diagrams is discussed in plain language. Standard parameters, such as resistivity, formation factor and resistivity index, are clearly defined and basic formulae explained.

The second part (75 pp.) elaborates in more detail on methods and formulae as used under varied conditions of oilfield practice.

A rather large section (30 pp.) of this chapter is devoted to the spontaneous potential log. The reason for this as stated by the author, should be sought in the fact that, whilst good manuals already are available for resistivity log interpretation, the potential log cannot yet be considered to be adequately covered in this manner. The author's own predilection, however, for the latter subject, as evidenced by his well-known pioneering work and publications on SP phenomena, also might have played a part here.

In the remainder of the second part of the book the interpretation of standard resistivity logs is briefly reviewed, whereafter more extensive space is allotted to an appropriate and instructive survey of the newer resistivity methods, more particularly the "focussed current" (Laterolog type) and "contact logging" (micrdisplay type) devices, whilst also the induction log is dealt with in a clear and rather extensive manner.

Special attention is finally devoted to methods applicable in the determination of formation resistivity factors from various types of electric logs. In this connection the possibility of using information from neutron or scattered gamma ray logs is also briefly discussed.

Evidently—and as confirmed by the author in his preface— this booklet was not primarily written to be used by experts, but rather for the benefit of the allround petroleum engineer in the field. Under prevailing conditions of rapidly developing petrophysical routine it would appear to meet a long felt want. No similar manuel previously existed and one can but say that it made its appearance at a late, rather than too early a date.

A few minor inaccuracies such as the use of S_w for percentage water saturation in diagrams 4 and 5, and for fractional saturation in the text, do not substract from the usefulness of the book and may be corrected in a second issue.

The bibliography represents a small but representative selection from the great quantity of existing papers on the subject of electric log interpretation.

J. H. M. A. T.

E.A.E.G. ABSTRACT SERVICE

EXPLORATION — GENERAL

1. *Application of Geophysical Methods in Prospecting for Ground Water* (In Spanish).
J. Cantos, Inst. Geol. Min. Espana, Notas y Coms., No. 29, pp. 3-31, 1952.

A description of the exploratory work of the Institute of Geology and Minerals, especially of its geophysical section. This section started in 1930, using chiefly gravity, seismic-refraction, and electrical-resistivity methods. Twenty-two examples of surveys in which geophysical methods were used, and the results, are discussed. (From Geophysical Abstracts 153, U.S. Geol. Survey).

2. *Twenty Years of Advancements in Geophysical Techniques.*
H. Hoover, Jr., J. Petr. Technology, Vol. 5, No. 9, pp. 77-80, Sept., 1953.

A review of the advancements in technique and instrumentation in all branches of geophysics during the past 20 years. The economics of geophysics are discussed and future developments in the industry are speculated on.

3. *Accessibility Surveys Cut Costs.*
P. H. Blanchet, B. Kavanagh & F. E. Prebble, World Oil, Vol. 137, No. 7, pp. 93-8, December, 1953.

In Western Canada, accessibility is a costly problem. Surveys consisting basically of the stereoscopic analysis of aerial photographs help to indicate nature of the terrain, topography, and ground conditions. In comparison, ground surveys take much longer and are more expensive.

4. *Geophysical Prospecting for Oil.*
D. T. Germain-Jones, Trans. Soc. Instr. Tech., Vol. 5, No. 2, pp. 38-51, June, 1953.

Owing to the increasing difficulty of finding new oilfields, the oil industry will have to rely more and more on geophysical methods of prospecting. At the present time only those methods by which the shape of the rock strata can be determined have widespread application, though it is possible that direct oil finding techniques will be developed as the result of further research.

The basic techniques of the three principle methods now in use (magnetic, gravimetric and seismic), and the types of instruments employed, are described. The seismic method is capable of a much higher degree of resolution than the other two, and the latter are usually employed only for reconnaissance purposes.

5. *How to Plan an Exploration Campaign* (Part 1).
E. B. Noble, World Oil, Vol. 138, No. 1, pp. 84-92, January, 1954.

Important points in planning a geophysical survey are:

(1) Sizing up the area. All available literature and maps should be studied; local people should be contacted for advice on food, clothing, health matters, etc.; geology and geography of the area should be studied from the air.

(2) Choice of methods. Regional studies may suggest the best method of prospecting to use. Generally, however, for a large new area it is usual to consider use of the airborne magnetometer, gravimeter, and seismograph, in that order.

6. *Mining Geophysics* (In Mexican).

J. Melchiori, Mineria, Ano 1, No. 3, pp. 37-46, 1953.

A review of geophysical methods useful in mining, particularly those which are practical for smaller scale operations. The electrical, magnetic, and radioactive methods of prospecting for ore bodies are considered.

(From Geophysical Abstracts 154, U.S. Geol. Survey).

7. *The Relation of the Physical Properties of Reefs to Geophysical Exploration.*

G. R. Pickett, Mines Mag., Vol. 43, No. 7, pp. 23-29, 1953.

There are four types of modern reefs, composed principally of corals and calcareous algae. Presumably ancient reefs are similar to modern ones, although the conditions of deposition may have been quite different. Ancient reefs of economic importance occur in the Silurian, Devonian, and Permian periods. Reefs typically have blocky, irregular, almost vertical lateral boundaries and relatively flat tops. The density of reef material is variable, but may be less than that of pure limestone, but is often greater than that of the surrounding rock material.

Magnetic methods will not be useful in the direct location of reefs but may help to determine the relationships of reefs with basement uplifts. Extremely detailed gravity survey may occasionally locate reefs but are not generally applicable. Seismic-reflection surveys remain the most reliable geophysical method of locating reefs. Discoveries may result from direct structural mapping of the reef surface, evidence of compaction in the surrounding materials, or velocity anomalies in reef areas. Great detail is required for success.

(From Geophysical Abstracts 154, U.S. Geol. Survey).

8. *European Association of Exploration Geophysicists — Milan Meeting.*

T. C. Richards, Nature, Vol. 173, No. 4397, pp. 246-7, Feb. 6, 1954.

At the 5th meeting of the E.A.E.G. held in Milan during December 2nd-5th, twenty-two papers were read.

R. Cassinis and E. Carabelli (Italy) gave an account of a seismic survey for thickness determination over a glacier in the Italian Alps.

T. F. Gaskell (G.B.) described seismic refraction surveys in the Atlantic, Pacific and Indian Oceans.

F. Haarstick (Germany), J. G. Hagedoorn (Holland), J. Cholet and H. Richard (France) read three separate papers on seismic velocities.

M. Matschinski (France) proposed a method of dealing with elastic hysteresis in the propagation of seismic waves.

T. Krey (Germany) presented three-dimensional formulae for correcting reflections distorted by refractions.

G. Muratori (Italy) discussed practical aspects and design details of shot-hole drilling equipment.

V. Colledan & A. M. Selem (Italy) presented experimental data on the mechanism of explosions in seismic shooting.

E. Merlini and A. M. Selem (Italy) talked on safety in seismic surveys.

L. Solaini and G. Uglietti (Italy) described an electronic blaster which transmits a shot-instant signal unimpaired by 'noise'.

A. Marussi (Italy) discussed the second differential parameter in gravity interpretation.

V. Baranov and J. Tassencourt (France) gave a mathematical exposition of approximations in calculating the vertical gradient.

O. Rosenbach (Germany) demonstrated an application of vertical gradient and second derivative methods.

C. Morelli (Italy) described gravity measurements at sea using a tele-controlled Western gravimeter.

C. Morelli also reported an extension of his diurnal investigations into the tidal variations of gravity.

M. Cunietti and G. Inghilleri (Italy) provided a general analysis of the accuracy of tidal gravity curves.

R. Tomaschek (G.B.) discussed solutions to tidal gravity problems that could be applied in the field.

J. Goguel (France) reported the conclusions of the Tidal Committee who recommend that two kinds of tidal corrections for 1954 be published in 'Geophysical Prospecting.'

C. Morelli and L. Sogaro (Italy) described results of a magnetic survey of volcanic outcrops near the Adriatic Sea.

J. J. Breusse and G. Huot (France) illustrated the results of an electrical survey for water in Sicily.

J. Chastenet de Gery and G. Kunetz (France) presented an analysis method for electrical prospecting.

J. L. Mathieu (France) described a method of recording formation resistivity in boreholes.

O. Vecchia (Italy) discussed the application of electrical and seismic refraction methods in the building of a dam.

SEISMIC — GENERAL

9. *The Application of Modern Electronic Measuring Methods in Mining.*
W. Rentsch, Nachrichtentechnik, Vol. 3, pp. 218-221, May, 1953.

Information as to rock pressure may be obtained by measuring the velocity of propagation of longitudinal elastic waves in the rock. Two bore holes are made, a few metres apart, and in each a seismometer detects the wave due to the explosion of a small charge. The first seismometer signal triggers an oscilloscope while the signal from the second causes a vertical deflection of the trace. Timing pulses from an oscillator provide black markers on the trace so that the time of travel of the disturbance is easily measured. Another method uses an electronic counter, triggered by the signals, to count the timing pulses and give a direct reading of the time interval. Measurements on samples of rock subjected to varying pressure enable the velocity measurements to be converted into pressure data. The difficulties and limitations of the method are discussed.

10. *Seismic Refraction Experiments in the Indian Ocean and in the Mediterranean Sea.*
T. F. Gaskell & J. C. Swallow, Nature, Vol. 172, No. 4377, pp. 535-537, Sept. 19, 1953.

Five stations in the Indian Ocean and nine stations in various parts of the Mediterranean Sea were occupied between 1950 and 1952. The results are summarized.

11. *Limitations of Reflection Seismograph.*
L. E. Nugent, Jr., Bull. Am. Assoc. Petr. Geol., Vol. 37, No. 11, pp. 2513-29, November, 1953.

Factors determining the precision of data procured by the reflection seismograph are discussed under three main headings: (1) under instrumentation, errors caused by various components are considered; (2) under computation, errors introduced by uphole and primary wave computational procedures are discussed as well as those attendant with various plotting methods; and (3) under velocity, numerous vagaries and their potential errors are analyzed. It is concluded that surveys which involve only errors of the first two categories may be accurate to ± 50 feet, while those under the third may vitiate the results. The geologist, whose knowledge of stratigraphy may anticipate such velocity variables, can contribute significantly to the precision of the method by a thorough understanding of the ramifications.

12. *Seismic Prospecting in the deep Oceans.*

T. F. Gaskell, Petroleum Times, Vol. 57, No. 1470, pp. 1227-30, December 11, 1953.

Data from deep water refraction measurements may be of use geologically or in offshore experiments.

In 1946, Dr. M. N. Hill, in England, and Prof. M. Ewing, in the U.S., developed techniques using hydrophones to detect refractions from deep ocean beds. Ewing used two ships and a single hydrophone for each shot. Hill used one ship and a string of hydrophones suspended from sono-radio buoys, thus effecting an economy in charges and obtaining a time-distance line for each shot instead of a single point.

The hydrophone is a piezo-electric pressure-recording instrument. Its signal is amplified at the buoy and transmitted to the ship which carries a separate receiver for each buoy. When operating, four instruments are spaced out over a distance of two miles and the ship drops depth charges at two-mile intervals as it proceeds on a straight course out for about 20 miles.

The author and Mr. J. C. Swallow, who assisted Hill in the development of the sono-radio buoy, employed Hill's technique on the world cruise of the survey ship "Challenger". Results from the various oceans are discussed.

13. *Salinity Meter for Sonar Measurements.*

K. E. Harwell & D. W. Hood, Electronics, Vol. 27, No. 1, pp. 172-174, Jan. 1954.

Precise measurement of the salinity of ocean water is necessary for computations of refraction gradients and sound velocities during seismic surveys over deep water. At constant temperatures, the conductivity of ocean water varies rapidly with salinity and can be used accurately to indicate the latter.

A salinity meter is described which uses R-F current. This provides the advantage that the electrodes need not be placed in direct contact with the water; thus eliminating corrosion and polarization problems. The precision of the instrument is ± 0.04 over a range of 5-35 parts per thousand.

14. *Processing of Photo-Recording Paper.*

H. F. Hieatt, Instruments & Automation, Vol. 27, No. 1, pp. 132-3, Jan. 1954.

The processing of photo-recording paper requires 5 steps—development, acid stop, fixing, washing and drying.

In developing, mixing directions must be closely followed. The developer should not be overworked. An acid stop bath, usually a dilute solution of acetic acid, will neutralize the developer and thus prolong the life of the acidic fixing solution. Acid stop should be replaced frequently. In fixing, again the directions must be closely followed. Records should be moved around in the solution to avoid stains forming. Stains will also occur if the records are not washed thoroughly. If there are no drying facilities in the field, records should be kept immersed in a separate bath of clean water and dried indoors later.

15. *Measurement of the Velocity of Sound in the Ocean.*

R. K. Brown, J. Acoust. Soc. Amer., Vol. 26, No. 1, p. 64, January, 1954.

An underwater sound velocity meter, which makes continuous recordings of the velocity of sound in the ocean as a function of depth, is described. A phase comparison system of measurement is employed at 500 kc. Several velocity and temperature records are given for comparison.

SEISMIC — INSTRUMENTAL

16. *Method of Sensitivity Control and Determination of Frequency and Amplitude Characteristics of Seismic Recording Channels by using a Magneto-Electric Generator* (In Russian).

N. Ye. Fedoseyenko & G. V. Groshevoy, Akad. Nauk SSSR Izv. Ser. Geofiz., No. 5, pp. 424-428, 1953.

To determine and adjust the sensitivity of seismic recording channels a small electrical generator has been constructed, especially designed for seismic work, to produce electric waves of pure sinusoidal shape; to operate with different frequencies used in seismic investigations, preserving the sinusoidal wave; finally, to remain free of external disturbances. The construction of the generator is described and response curves obtained in practical tests are reproduced.

(From Geophysical Abstracts 155, U.S. Geol. Survey).

17. *Dynamic Testing of Seismograph Galvanometers.*

R. M. Wilson, Am. Geophys. Un. Trans., Vol. 34, No. 4, pp. 600-602, 1953.

By using an ultra-low-frequency oscillator, a cathode-ray oscilloscope, and a high-frequency galvanometer it is possible to make frequency and phase calibrations of a seismograph galvanometer under simulated operating conditions both rapidly and simply. By combining such data with the mechanical and electrical constants of an ideal electro-magnetic seismometer and the results of a single shaking-table test, the over-all response curve may be obtained.

(From Geophysical Abstracts 155, U.S. Geol. Survey).

SEISMIC — INTERPRETATION

18. *A Universal Slide Rule for Computing the Dips of Reflecting Horizons on the Assumption of Linear Increase of Velocity.*

J. Daly, Geophysics, Vol. 18, No. 4, pp. 820-823, October, 1953.

A slide rule is described by which the dip of reflectors can be computed rapidly and accurately for the case where instantaneous velocity can be assumed to increase linearly with depth. Values for initial velocity Vo, rate of increase of velocity, k, and the spread distance Δx, can be introduced into the device easily and changed at will. In conjunction with a previously described instrument, normal move-out graphs and wave front charts can be constructed quickly and precisely.

(Author's Abstract).

19. *Problem Areas for the Seismologist.*

G. M. Conklin, Geophysics, Vol. 18, No. 4, pp. 827-843, October, 1953.

This paper describes interpretative problems encountered in four widely scattered areas: Southern Florida; Beaver County, Oklahoma; the Plainview Basin of the Texas Panhandle; and Hancock County, Mississippi.

Secondary refraction recordings offer problems, because refractions from deep beds are distorted and obscured by energy from shallow beds. The energy associated with the shallow refractors appears as multiples and is sustained for long periods of time. In Beaver County, Oklahoma, extreme variations in velocity cause distortion of reflections and introduce apparent dips which are erroneous. This velocity variation is thought to be due to differential salt solution from the Blaine-Cimarron interval. In the Plainview Basin and in Hancock County, multiple reflections are troublesome. These reflections are discussed and records and cross-sections illustrate these events. Some suggestions for the treatment of these problems are advanced.

(Author's Abstract).

20. *Nomogram for Computation of Exact Values of Normal Move-Out Times.*
O. Schneider-Riquelme, Geophysics, Vol. 18, No. 4, pp. 824-826, Oct., 1953.

A nomogram is presented for conveniently computing the exact value of normal move-out times in terms of the velocity at the near-surface datum, the rate of increase of velocity with depth, the reflection time, and the shot-receiver distance.

(Author's Abstract).

21. *Geophysical Prospecting and the Accuracy of the Interpretation Results* (In French).
M. Matschinski, Geofis Pura e Appl., Vol. 27, pp. 35-84, 1954.

Interpretation problems in geophysics are outlined, showing the difference between algebraic and statistical ones and the method of least squares. The problems are classified into four sections:

1) Choice of hypothetical geologic structure and its mathematical representation, using parameters. 2) Determination of the parameter numerical values. 3) Determination of all possible values. 4) Determination of the likelihood of the hypothesis itself.

The accuracy of the calculations is investigated and the general theory is applied to the determination of a fault from gravity data.

22. *Contouring is Important.*
E. J. Handley, World Oil, Vol. 138, No. 4, pp. 106-107, March, 1954.

From one set of basic geological and geophysical data, many different subsurface contour maps may be derived. A set of rules and guides is given which, it is hoped, will promote more accurate interpretations.

23. *Problems of Geophysical Interpretation in Alberta.*
J. A. Legge, Canadian Min. Met. Bull., Vol. 46, No. 489, pp. 10-12, 1953.

Most geophysical failures in oil prospecting in Alberta are due either to insufficient seismic control or to velocity effects both near surface and at depth. The decision as to the amount of detail to be worked out in an area must be based on previous geophysical leads and geological clues; exploration of an area should be planned on the basis of the size of anomalies expected, otherwise small reefs might be missed.

The use of isopach or isochron maps eliminates some of the adverse velocity effects. Surface corrections should be made as accurately as possible. Remaining anomalies should be analysed in the light of the regional geology so that at least the approximate magnitude of reef effects may be known.

(From Geophysical Abstracts 154, U.S. Geol. Survey).

SEISMIC — THEORY & RESEARCH

24. *Selection of Distances between Seismographs subdivided into groups for Weakening of Disturbing Background Noise* (In Russian).
P. S. Veitsman, Akad. Nauk SSSR Izv., Ser. Geofiz., No. 3, pp. 48-54, 1952.

Experiments were carried out to determine the optimum distance between individual seismographs or groups of seismographs placed along a seismic profile, so that the disturbing background becomes a minimum. Using the reflection method, the greatest disturbance is caused by microwaves propagating within the shallow upper layer of the earth. In the foothills of Tien Shan, investigations showed that these microwaves were 16 meters long; thus by placing seismographs at a distance of 8 meters their effect was almost eliminated.

25. *The Effect of Variations in Chemical Composition on the Velocity of Seismic Waves in Carbonate Rocks.*
C. Kisslinger, Geophysics, Vol. 18, No. 1, pp. 104-115, 1953.

To study variations in velocity in carbonate rocks, field measurements were made in dense, crystalline to lithographic, calcitic and dolomitic limestones in the St. Louis formation. Twelve geophones were used at a spacing of 50 cm. Comparison of chemical and velocity data indicates dolomitization may have an effect on velocity, but the effect apparently depends on the dolomitization process. Volume for volume replacement of calcite by dolomite tends to increase the velocity, but dolomitization giving rise to local porosity tends to decrease the velocity.

26. *The Dispersion of Surface Waves on Multilayered Media.*
N. A. Haskell, Bull. Seismol. Soc. Am., Vol. 43, No. 1, pp. 17-34, 1953.
A matrix formalism developed by W. T. Thomson is used to obtain the phase velocity dispersion equations for elastic surface waves of Rayleigh and Love type on multilayered solid media. The method is used to compute phase and group velocities of Rayleigh waves for two assumed three-layer models and one two-layer model of the earth's crust in the continents. The computed group velocity curves are compared with published values of the group velocities at various frequencies of Rayleigh waves over continental paths. The scatter of the observed values is larger than the difference between the three computed curves. It is believed that not all of this scatter is due to observational errors, but probably represents a real horizontal heterogeneity of the continental crusts.

27. *Crustal Structure and Surface-Wave Dispersion, Part III: Theoretical Dispersion Curves for Suboceanic Rayleigh Waves.*
W. S. Jardetzky & F. Press, Bull. Seismol. Soc. Am., Vol. 43, No. 2, pp. 137-144, April, 1953.
Theoretical Rayleigh wave dispersion curves for three different types of suboceanic basement layering are presented. Previous conclusions concerning the dispersion of Rayleigh waves across ocean basins are re-examined in the light of the new data.

28. *A Fourier Analyzer.*
F. J. McDonal, Rev. Sci. Instr., Vol. 24, No. 4, pp. 272-276, April, 1953.
An analog computer which provides Fourier analyses of transients encountered in seismic research. The integral $\int F(t) \sin \omega t dt$ is evaluated by analog computer elements which perform the generation of the functions $F(t)$ and $\sin \omega t$, multiply the two functions, and integrate the product. The function of $F(t)$, is generated from a variable area recording on film by a photocell and amplifier system simultaneously with the generation of the sine function, $\sin \omega t$, by mechanical means. Multiplication of these two functions is performed by the potentiometer method, and integration is accomplished by servo integrators. The instrument also includes control and calibration equipment which facilitates rapid and accurate analyses.

29. *Signal-To-Noise Ratio Improvements by Filtering and Mixing.*
H. R. Frank, & W. E. N. Doty, Geophysics, Vol. 18, No. 3, pp. 587-604, July, 1953.
This paper is concerned with the signal-to-noise (interference) amplitude ratio of seismograms. The problem of improving the signal-to-noise ratio by filtering and mixing is approached quantitatively. Records of known signal-to-amplitude ratio and known frequency content were made employing multiple-trace variable area equipment such that identical energy was reproduced and re-recorded through various filtering and mixing schemes and comparisons made. Equipment effects on wavelet character and stepout times are illustrated.

30. *Deep-Hole Geophone Study in Garvin County, Oklahoma.*
R. N. Jolly, Geophysics, Vol. 18, No. 3, pp. 662-670, July, 1953.

The results of a seismic well survey made with calibrated recording equipment are presented. This survey differed from the conventional type in that a geophone which could be locked to the wall of the bore-hole was used, thereby providing reliable amplitude data and permitting reflections to be recorded at depth. Consequently it was possible to observe the true shape and amplitude of the seismic pulses, both initial and reflected, over the major portion of their travel paths. Quantitative data were obtained on such factors as decrease of pulse amplitude with depth, location of reflecting horizons, and magnitude of reflection coefficients.

31. *Radiation from a Cylindrical Source of Finite Length.*
P. A. Heelan, Geophysics, Vol. 18, No. 3, pp. 685-696, July, 1953.

This paper presents the results of a theoretical study of radiation from a cylindrical source of finite length, the walls of which are subjected to symmetrical lateral and tangential stresses. Three divergent wave systems are generated, 'P', 'SV', and 'SH', and their amplitudes are calculated in terms of the stresses operative on the walls of the "equivalent cavity". The zonal distribution of amplitude in the three wave systems is calculated, and the total amount of energy in each is estimated. It is shown that under the action of a lateral pressure only, an 'SV' wave of amplitude 1.6 times the maximum amplitude of the associated 'P'-wave is beamed from the source in directions making angles of 45° with the axis of the source.

32. *Note on the Refracted Wave in a Layer.*
F. Press & M. Ewing, a paper read at the 23rd meeting of the S.E.G., at Houston, Texas, March, 1953. (Not yet published).

Refraction measurements give representative values for the velocity in a layer only when wavelengths are small compared with the layer thickness. Previous theoretical work on refractions assume an infinitely thick layer. Consideration of the theory for finite layer thickness leads to appropriate conditions on the wavelength when the velocity is to be determined to a prescribed accuracy. At large distances, these conditions arise from interference between the refracted wave and the wave reflected at grazing incidence from the bottom of the layer. Examples are given.

33. *The 'Sie' Electronic Shaking Table.*
L. W. Erath, a paper read at the 23rd meeting of the S.E.G., at Houston, Texas, March, 1953 (Not yet published).

The simulation of seismic motion has been a problem of geophysical laboratories for many years. This paper describes a shaking table that has been developed by the S.I.E. Research and Development Corporation. The S.I.E. shaking table is based on electronic and feed-back principles. The weight of the seismometer being tested is supported by a magnetic field and displacement is measured by a high frequency sensing element and is displayed by a special cathode-ray indicator. Calibration is accomplished by displacing the table with an ordinary micrometer screw. Excellent transient response allows tape recordings of ground motion and other phenomena to be displayed into the input circuit of the shaking table which provides the research engineer with a new and more accurate means of evaluating geophysical apparatus.

34. *Curved Path Delta T Analysis.*
J. T. Brustad, a paper read at the 23rd meeting of the S.E.G., at Houston, Texas, March, 1953 (Not yet published).

A rapid and accurate "curved path" delta-T velocity analysis may be calculated in a simple manner. The average velocities so obtained will, in most cases, be accurate to within ½ of 1% of theoretical, and will, in general, be far more accurate than those calculated using the "straight path" assumption.

The method is based upon a simple relationship: If T is the reflection time at zero offset and $T + M$ is the reflection time at an offset of S feet, then the quantity $K = S2T/2(M^2 + 2MT)$ is a close approximation of $\int_0^{\frac{1}{2}T} V^2 dT$. The distance between successive reflecting horizons, under the assumption of constant velocity in the interval, is then given by the square root of the product of the increment in K by half the increment in reflection time. The reflecting depths and corresponding average velocities can then be easily obtained.

GRAVITY — GENERAL

35. *On a Way of Calculating Isostatic Anomalies* (In French).
H. De Cizancourt, C. R. Acad. Sci. (Paris) 236, pp. 835-837, Feb. 23, 1953.

A method of calculating isostatic anomalies based on the equilibrium of vertical tensions produced by topographic loads, according to the relaxation hypothesis, and the pressures due to the deformation of the underlying material. The compensating masses are defined without arbitrary constants and the physical nature of isostatic equilibrium or disequilibrium can be studied.

36. *Gravity Measurements in North America with the Cambridge Pendulum Apparatus.*
G. D. Garland, Proc. Roy. Soc., A, Vol. 219, No. 1137, pp. 215-233, Aug. 25, 1953.

The Cambridge pendulum apparatus has been used to establish a line of nine fundamental gravity stations in North America, between Mexico City and Winnipeg. For this work considerable care was given to the elimination of magnetic disturbances; the most important precaution being the compensation of the vertical component of the earth's magnetic field by means of Helmholtz coils. The crystal frequency standard used to time the pendulums was rated for each observation against the precise carrier-wave frequencies broadcast by radio station WWV. In general, the values of gravity obtained are in agreement with those of previous observers, but detailed comparisons are difficult because of the need for a more consistent North American network. The total range in gravity covered by the line of stations is over 2,000 mgals, the extreme values being:

Mexico City: 'g' = 977.9415 cm/sec^2
Winnipeg: 'g' = 980.9952 cm/sec^2

relatively to the adopted base station value

Ottawa: 'g' = 980.6220 cm/sec^2

The standard deviation of the difference of gravity has a mean value of 0.0003 cm/sec^2.

37. *Gravity Measurements over the Northern Pennines.*
M. H. P. Bott & D. Masson-Smith, Geological Magazine, Vol. 90, No. 2, pp. 127-130, 1953.

In a gravity survey continuing the work of Hospers and Willmore a closed elongated area of negative Bouguer anomalies was outlined in the northern Pennines. The steep gradient indicates the anomaly cannot be of deep-seated origin and must be caused by a direct density contrast between lighter and denser masses of rock. The anomaly is assumed to be due to a covered acid intrusion. The origin of the intrusion is magnetic inasmuch as a negative anomaly must be produced by a total removal of actual mass, which in this area, could only have been downward.

38. *Gravity Measurements in Durham and Northumberland.*
J. Hospers & P. L. Willmore, Geological Magazine, Vol. 90, No. 2, pp. 117-126, 1953.

Gravity measurements were made in Durham and Northumberland in the region of the Alston block to determine whether such observations could help in elucidating geologic structure. Observations across the eastern part of the block are consistent with the idea that the 20 mile block between the Ninety Fathom dyke and Butterknowle fault is a horst. Observations across the western part are interpreted as due to a granite intrusion not yet exposed by erosion.

39. *Usefulness of High-Quality Gravity Surveys.*
S. Hammer, Oil & Gas J., Vol. 52, No. 21, pp. 106-110, Sept. 28, 1953.

Gravity is not uniformly successful in all areas, therefore we cannot lay down a blanket rule that a gravity survey should always precede leasing or other geophysical work. Rarely is gravity used alone without verification and additional detailing of the gravity prospects by other geological and geophysical methods. Gravity is mostly used in reconnaissance, followed by seismic work. Any guide that gravity may give greatly reduces the overall cost of an exploration program. Emphasis is placed on the need for high quality if a successful gravity survey is to result. Practical examples are given.

40. *Let's Look at Gravity's Discovery Record.*
E. V. McCollum, Oil & Gas J., Vol. 52, No. 21, pp. 111-113, Sept. 28, 1953.

Gravity has been particularly successful in indicating favourable structures in salt-dome provinces. In order to evaluate the importance of gravity methods, 27 structures are selected for review. Of these, 10 are considered as gravity discoveries and 8 more could have led to discovery with better siting of the test well.

41. *Gravity's Limitations.*
R. A. Weingartner, Oil & Gas J., Vol. 52, No. 21, pp. 113-114, Sept. 28, 1953.

Gravity has three main limitations; technical, interpretive, and psychological. The technical limitation is the terrain effect. As yet, no certain correction can be applied. The interpretation limitation is inherent in any data based on a total field method. The separation of local anomalies from regional effects is always difficult. The psychological limitations are many and include those due to the inability to convert gravity measurements to familiar geological terms; to the loss of confidence resulting from the varied interpretations by the trained interpreter and the criticism and interpretation by the inexperienced interpreters; and to the failure to secure the proper appreciation and the proper utilization of gravity in oil exploration.

42. *Pros and Cons of Gravity.*
P. L. Lyons, Oil & Gas J., Vol. 52, No. 21, pp. 114-116, Sept. 28, 1953.

No method is so well adapted for regional studies of any kind as the gravity method. Geophysicists should not fail to make use of the regional gravity picture by attaching importance to the regional gravity anomalies. The author describes some of the reasons that prevent much faith being placed in gravity surveys. Sources of error are discussed and solutions suggested.

43. *Adjustment of the Principal Gravity Observations in Great Britain.*
A. H. Cook, Mon. Not. Roy. Astronom. Soc., Geophys. Suppl., Vol. 6, No. 8, pp. 494-521, October, 1953.

The gravity surveys conducted in Great Britain to date depend on about 600 base stations, of which those in any one survey are connected by a strong network of first order measurements of gravity differences. There are sufficient connections between base stations of different surveys for all the surveys to be compared and combined into one uniform system. The largest discrepancies between surveys arise from errors in calibration factors of the gravimeters and the surveys have therefore been adjusted to six precise pendulum observations at stations between Aberdeen and Southampton.

44. *Present State of Absolute Measurements of Gravity and Possibilities of Their Development* (In German).
A. Berroth, Geofis. Pura e. Appl., Vol. 22, Fasc. 3-4, pp. 147-160, 1952.

Detection of an error of 13 mgal in the International Standard gravitational system based on Potsdam measurements, makes necessary a change in the procedures used in absolute determinations of gravity. Three possibilities are open: use of the present type of pendulum, with certain added improvements; use of a pendulum with string-supported bob; or observations of bodies falling freely in vacuum.

The second method is considered here. By introducing certain improvements it is possible to construct an instrument with an accuracy comparable to that of the usual pendulum, but with other advantages.

(From Geophysical Abstracts 154, U.S. Geol. Survey).

45. *The Principal Structural Characteristics of Northern Italy Deduced from Gravimetric Measurements* (In Italian).
O. Vecchia, Riv. Geofis. Appl., Vol. 13, No. 1, pp. 33-68, 1952.

Gravity maps of northern Italy have been plotted, representing both Bouguer and isostatic anomalies. The general geological interpretation of the gravity pattern is then developed by comparison with surface geology, seismicity, magmatism, thermo-mineral sources distribution and geomagnetism.

Every seismic zone of northern Italy, all thermo-mineral sources, its whole magmatic activity since the palaeozoic, coordinate with each other and find an explanation through the key furnished by the gravity pattern.

(From Geophysical Abstracts 154, U.S. Geol. Survey).

46. *On the Geologic Interpretation of Negative Anomalies of Regional Gravity in Sicily* (In Italian).
R. Fabiani, La Ricerca Sci., Vol. 23, No. 5, pp. 767-788, 1953.

Gravity surveys of Sicily during the last 50 years, with both pendulums and Worden gravimeters, have outlined negative anomalies of regional dimensions in the south-central part of Sicily with gravity minima around the city of Caltanissetta. The anomalies are attributed by some to the low density of the upper layers consisting of salty clays, rock salt, gypsum, sulphur and similar materials. A contributing factor may also be the numerous caverns known to exist in limestone formations. Others point out that the gravity pattern is not substantially changed if different density values are used in computations of Bouguer or isostatic reductions and conclude that the anomaly is an indication of a subcrustal trough, filled with low-density submarine masses that have been horizontally displaced from some point north of Sicily, thus producing the present topography of the island. Neither hypothesis can be proved correct although recent investigations for sulphur and hydrocarbons may provide information.

(From Geophysical Abstracts 154, U.S. Geol. Survey).

47. *Gravimetric Study of Algeria and Tunis* (In French).
J. Lagrula, Service Carte Geol. Alger. Bull., 4e Ser., No. 2, p. 111, 1951.

A compilation of the results of gravimetric studies in Algeria and Tunis since 1933. The instrument used, a Holweck-Lejay pendulum, is described and the results obtained are discussed.

(From Geophysical Abstracts 154, U.S. Geol. Survey).

48. *New Contribution to the Gravimetric Survey of the Central Sahara* (In French).
J. Lagrula, Acad. Sci. Paris Comptes Rendus, Tome 234, No. 22, pp. 2214-2216, 1952.

The gravimetric survey of the Sahara, begun with a Holweck-Lejay pendulum, has been completed with a Western gravimeter No. 53. Stations were uniformly 10 km apart. Some results are provisional, inasmuch as the topography of the Sahara is not known precisely; a few altitudes could be obtained only barometrically. In some places the resulting uncertainty in anomalies is as much as 10 mgal. Isostatic as well as Bouguer anomalies were calculated, according to the Airy system, with 'T' = 60 km. Data for 39 stations are given in a table. Correlation with geologic structure is striking, and is even better with a smaller value of 'T', for example, 20 km.

(From Geophysical Abstracts 154, U.S. Geol. Survey).

49. *Map of Density to Sea Level in Northern Italy* (In Italian).
O. Vecchia, Boll. Geodesia e Sci. Aff., Anno 11, No. 3, pp. 337-344, 1952.

A map of northern Italy and adjacent areas at a scale of 1 : 1,000,000 shows, by colour, average densities to sea level at intervals of 0.2. These have been calculated on the basis of present knowledge of stratigraphy and tectonics in the area. Densities of igneous, metamorphic, and sedimentary rocks, compiled from the literature, are given in three tables.

(From Geophysical Abstracts 154, U.S. Geol. Survey).

GRAVITY — INTERPRETATION

50. *The Indirect Effect and the Interpretation of Gravimetric Anomalies* (In French).
P. Lejay, Ann. Geophys., Tome 7, No. 3, pp. 175-198, 1951.

It is shown how geophysicists may apply the indirect effect in their gravity interpretations by using a simple supplementary correction (irregularities of less than 400 km assumed to be without effect). The magnitude of error introduced is shown to be of a much smaller order than those already resulting from other factors such as density and altitude.

51. *An Attempt to Interpret the Gravimetric Map of the Northern Part of the Moroccan Basin of Gharb. Maps of Residual Anomaly and First Derivative.*
Société Chérifienne des Pétroles & C. Aynard, Geophysical Prospecting, Vol. 1, No. 4, pp. 279-290, December, 1953.

The main features of the gravimetric map of the Gharb can be related to the shape of the basement, covered by cretaceous and miocene layers, with a total maximum thickness of 13,000 feet. For the interpretation of local features, in the northern part of the basin, first a regional anomaly has been drawn, then the map of the first derivative has been established. Both maps are compared with geological maps and seismic and electrical surveys.

As for method, the advantages and limitations of both processes are outlined. As for geological interpretation, it is suggested that most of the local features of the gravimetric map are due to the pre-Riffan tectonics.

52. *Residual Anomalies and Depth Estimation.*
S. Saxov & K. Nygaard, Geophysics, Vol. 18, No. 4, pp. 913-928, October, 1953.

The residual gravity anomaly at a point is defined as the difference between the average anomalies along two concentric circles whose centre is at the point, divided by the difference between the two radii or:

$$R(g) = \frac{\bar{g}(r_1) - \bar{g}(r_2)}{r_1 - r_2}$$

It is shown that the residual anomalies previously determined by the average circle or the average polygon method (Griffin, 1949) are included in the present definition.

The second vertical derivative of 'g' and, to some extent, the fourth vertical derivative of 'g' (Peters, 1949) are also included.

The relation between the residual anomalies and the depth of the subterranean masses is examined. It has been pointed out that the gravitational effect originating from a body with mass 'm' is clearly apparent when the centre of mass of the body has the depth $z = 2r = r_1 + r_2$. The influence from masses at a greater or lesser depth is almost eliminated.

By avoiding the use of the centre point in the figuring of the residual anomalies the influence of random errors is minimized.

(Author's Abstract).

53. *A Theory for the Regional Correction of Potential Field Data.*
F. S. Grant, Geophysics, Vol. 19, No. 1, pp. 23-45, January, 1954.

An analytical method based on the theory of statistical probability is developed for separating regional from local potential field effects. It is applied to an objective test on an artificial problem, as well as to a gravity survey that has already been the subject of studies of other averaging methods. It succeeds in both tests with good accuracy, and points up the danger of arbitrariness in the use of numerical methods.

(Author's Abstract).

54. *A Note on Downward Continuation of Gravity.*
C. A. Trejo, Geophysics, Vol. 19, No. 1, pp. 71-75, January, 1954.

Comparing calculated and exact values in an ideal example, it is shown that Peters' proposed method of downward continuation of gravity is far less suitable than a combination of Peters' procedure for upward continuation and a finite differences method for downward continuation. It is shown also how Peters' method can be substantially improved by considering only the closest values in the downward step of a continuation process.

(Author's Abstract).

55. *A Comparison of the Second Derivative Method of Gravity Interpretation with Reflection Seismics and Geological Findings in the Offenburg Area.*
O. Rosenbach, Geophysical Prospecting, Vol. 2, No. 1, pp. 1-23, March, 1954.

The aim of the investigation is to examine the significance of the second derivative for the purpose of the prospective determination of the geological properties of the district of Offenburg, which are relatively well-known as a result of both reflection seismic and bore profile findings.

The calculation of the second derivative is carried out by means of three approximation formulae, which are compared with each other. In contrast to the isogam map the second derivative shows some additional characteristics, whose structural significance illuminates the comparison with the results of reflection seismics.

A geological profile constructed on the basis of six wells completely confirms the geophysical findings.

(Author's Abstract).

56. *Gravity Maxima Corresponding with Sedimentary Basins.*
R. Martin, Geophysics, Vol. 19, No. 1, pp. 89-94, January, 1954.

Gravity work in Argentina has shown maximal values over the deepest part of some sedimentary basins. It is suggested that this unexpected result may be explained as a case of imperfect isostatic adjustment and may be of general interest in the interpretation of gravimetric surveys. It is also suggested that Airy's theory gives a better explanation of isostatic compensation over moderately large areas while the Pratt theory is applicable to enormous regions, of continental extent.

(Author's Abstract).

57. *A Universal Table for the Prediction of the Lunar-Solar Correction in Gravimetry (Tidal Gravity Correction).*

J. Goguel, Geophysical Prospecting, Vol. 2, Suppl., pp. 2-5, March, 1954.

Tidal gravity corrections increase the accuracy of stations and make it possible to obtain better closures on a base-network. These corrections may be obtained by multiplying the theoretical correction for a rigid globe by the factor 1.2. The author shows how tables have been compiled which enable an operator to read the correction to be applied to his measurements, as a function of the time and date of the observation. Correction tables for the period March-December, 1954, are given.

Tidal gravity corrections in graphical form have been calculated for the same period by C. Morelli and are included in the supplement.

58. *A Contribution to the Computation of the "Second Derivative" from Gravity Data.*

O. Rosenbach, Geophysics, Vol. 18, No. 4, pp. 894-912, Oct. 1953.

The theory and practical application of the second derivative method of gravity interpretation have been discussed by Elkins (1951) in a very interesting paper based partly on an earlier paper by Peters (1949). In this paper, Elkins shows how the second derivative may be computed at the centre of a series of concentric circles using the arithmetic means of the gravity values, assumed to be continuous, around each circle.

A method is here proposed which does not use a continuum of gravity values but instead requires only a series development. The approximation formulae needed for the routine calculations can be derived by a method different from that of Elkins and the least squares adjustments he used can be dispensed with.

Two hypothetical examples using the formulae derived by the series method are given and the results are compared with those computed by Elkins' formula.

(Author's Abstract).

GRAVITY — THEORY & RESEARCH

59. *Earth Tides.*

J. T. Pettit, L. B. Slichter, & L. Lacoste, Trans. Am. Geophys. Un., Vol. 34, No. 2, April, 1953.

The tidal variations of gravity have been observed throughout intervals of several weeks to several months at Los Angeles, Pasadena, Hawaii, and Attu. The term produced solely by the yielding of the earth (including its oceans) may conveniently be characterized by two parameters. One parameter expresses the time-phase, the other the amplitude. In the most extensive and reliable series of observations, at Pasadena and Los Angeles, these parameters were found to be nearly constant in time. Geographically, however, the phase shifts differ greatly at widely separated stations. Knowledge of the phase and amplitude parameters (when constant) enables the classical harmonic tidal constituents to be easily computed. Computation of the gravity tidal constituents for the Pasadena and Los Angeles data were carried through by the proposed simplified method, and compared with corresponding results obtained with the standard U.S. Coast and Geodetic Survey and British Admiralty computational procedures. Satisfactory agreement was obtained among the three methods.

60. *Approximations in the Calculation of the Form of the Geoid from Gravity Anomalies.*

A. H. Cook, Mon. Not. Roy. Astronom. Soc., Geophys. Supple., Vol. 6, No. 7, pp. 442-452, June, 1953.

The theory of the calculation of the detailed undulation of the geoid from gravity by Stoke's integral is usually given to first order, and there are some approximations which may be important in mountainous places. Some are trivial but the change of undulation with height is not. Discussion of this involves the definition of orthometric height and of the geoid. With suitable definitions the undulations of the geoid are the same as those of equipotential surfaces at external points, so that the latter may be calculated directly without additional correction for changes with height. The free-air correction to gravity is determined by these definitions and conditions; for geodetic purposes the fundamental quantity is not the change of gravity with height but the difference of geopotential. The correction derived in this paper thus differs slightly from those commonly in use and there are consequently some small errors in the figure of the earth derived with the use of the latter.

67. *Calculation of the Vertical Gradient of the Gravimetric Field* or *Measurement of the Magnetic Field at the Surface of the Earth.*
V. Baranov, Geophysical Prospecting, Vol. 1, No. 3, pp. 171-191, Sept. 1953.

It is known that good use can be made of calculating the second vertical derivative of gravitational and magnetic fields. The first derivative, or Vertical Gradient, has the same properties. Like the second derivative, it does not depend on the locally linear regional anomaly. Moreover, the gradient is less affected by experimental errors.

The report gives a practical method of calculating the vertical gradient. Its application is identical to that in general use for calculating the second derivative, except that the numerical coefficients are different. The method also allows the establishment of formulae for downward extension of the field and its derivatives.

MAGNETIC — GENERAL

62. *Airborne Magnetic Surveys.*
Nature, Vol. 173, No. 4398, pp. 281-283, February 13, 1954.

An account is given of a Geophysical Discussion held by the Royal Astronomical Society on November 27th, 1953. A review was made of the post-war development of the fluxgate method of carrying out magnetic surveys from the air, by measurements of three components of the geomagnetic field.

63. *An Estimate of the Time Taken for a Dyke to Cool Through its Curie Point.*
H. Manley, Geofis. Pura e Appl., Vol. 27, pp. 105-109, 1954.

The cooling rate of dykes is important in relation to their magnetic properties. Work on this question suggests that dykes such as the Pilandsberg and Tholeiite systems acquire their remanent magnetism in a period of 1-10 years. This means that such dykes will cool from, say 550° C to 450° C in that time period.

64. *About Possibilities and Limitations in Aeromagnetic Surveying.*
A. Lundbak, Geofis. Pura e Appl., Vol. 27, pp. 110-115, 1954.

Aeromagnetic surveying has been developed during more than 20 years. An outstanding result of this development is the airborne fluxgate magnetometer, which satisfies a plurality of demands.

Meantime, some problems appear, as the quantity measured by the common type of airborne fluxgate magnetometer is a component along the direction of the total magnetic force. For different purposes other components may be required. They can be obtained either by direct measurements or by computing procedures on the basis of the first-mentioned component; but in both cases difficulties arise. These difficulties are discussed, and some possibilities are set forward.

(Author's Abstract).

MAGNETIC — INSTRUMENTAL

65. *A New Inductive Method for the Determination of the Temperature Variation of Susceptibility of Rocks.*
H. Manley, Geofis. Pura e Appl., Vol. 27, pp. 98-104, 1954.

An inductive method for detecting the temperature variation of susceptibility of rocks has been developed. This method is more sensitive than any but the magnetometer. The latter, however, is not suited to town use, especially where stray magnetic fields are common. The new apparatus and its auxiliary equipment are described.

66. *Magnetic Gradiometer with a Fluxmeter* (In Russian).
A. G. Kalshnikov, Akad. Nauk SSSR Izv. Ser. Geofiz., No. 4, pp. 307-317, 1953.

Elimination of temporal effects, such as diurnal and other magnetic disturbances, in the precise measurement of magnetic vectors would be unnecessary, if instead of magnetic vectors their gradients were measured. The construction of a magnetic gradiometer, its operation, sensitivity, and sources of errors are described.

(From Geophysical Abstracts 155, U.S. Geol. Survey).

67. *On the Magnetic H-Balance for the Galathea Deep-Sea Expedition.*
J. Egedal, Geofis Pura e Appl., Vol. 25, pp. 26-28, 1953.

A brief description of an instrument designed to record the horizontal component of magnetism in the deep sea, and capable of functioning even if moved up and down following the movements of the ship and with changing orientation. The instrument is a balance and is a monad magnet; magnet, mirror, and knives are made of the same piece of steel. In order to measure the horizontal force the balance is placed in a vertical position resting with its knives on plane agate surfaces. The horizontal field at the balance is reduced to a negligible quantity by a compass placed at the proper distance below the balance. By means of a small magnet placed in a vertical position above the balance it is possible to change the vertical field and the scale value of the instrument. The whole instrument is constantly revolved on a vertical axis by means of a clock work.

(From Geophysical Abstracts 155, U.S. Geol. Survey).

MAGNETIC — THEORY & RESEARCH

68. *The Areal Distribution of Geomagnetic Activity as an Aeromagnetic Survey Problem near the Auroral Zone.*
L. W. Morley, Trans. Amer. Geophys. Un., Vol. 34, No. 6, pp. 836-40, Dec. 1953.

Aeromagnetic surveying within the auroral zone is complicated by the high incidence of severe magnetic disturbance. Although corrections for the time variations could be made by means of data obtained from a ground station located centrally within the survey area, the areal extent over which such corrections would be valid is not known. The paper gives magnetic-disturbance data obtained from two simultaneously operated ground stations, placed initially 130 ml apart, and later 87 ml apart, within the auroral zone. It is found that such corrections would be seriously in error for separations of this order between ground and air stations.

69. *Thermoremanent Magnetism of Rocks* (In Russian).
M. A. Grabovskiy, Akad. Nauk SSSR Izv. Ser. Geofiz., No. 3, pp. 215-224, 1953.

Every ferromagnetic rock is characterized by its induced (Ii) and remanent (Ir) magnetism. 'Ii' is that component of the magnetic vector which is generated in the rock by the action of the present geomagnetic field; 'Ir' is natural magnetization which cannot be produced by the existing geomagnetic field. According to the theory of ferromagnetism 'Ir' must be smaller than 'Ii', but there are many exceptions to this rule. This phenomenon is explained as the result of slow cooling of the rock in a magnetic field that creates conditions favourable to the irreversible process of magnetization.

The intensity of this thermoremanent magnetization caused by the cooling of the rock is determined by its magnetic properties, such as the coercive force, magnetic anisotropy, and magnetostriction. Reverse magnetization can be explained by the presence in the rock of two distinct magnetic components with different coercive forces and different Curie points.

(From Geophysical Abstracts 154, U.S. Geol. Survey).

ELECTRICAL

70. *Resistivity Curves for two Layers with Plane Contact Slightly Inclined with Respect to the Surface of the Earth* (In Italian).

R. Trudu, Riv. Geofis. Appl., Vol. 13, No. 2, pp. 95-110, 1952.

The problem of two layers with different resistivities separated by a plane surface and inclined with respect to the surface of the earth is reconsidered, using the method of electrical images. The problem is solved for a general distribution of electrodes at the surface, particularly for the single-pole method. The characteristics and possibilities of different measuring procedures, with a constant base, or by expanding or rotating electrodes, are considered and it is shown that the variables in the problem in each case reduce to two which may be determined by the Tagg method. The extension of the method to electrode configurations other than that with a single pole is considered.

71. *The Influence of the Time Lag of Electric Currents in the Earth on the Measurement of the Field in Electric Depth Sounding* (In Russian).

A. N. Tikhonov & B. S. Enenshtein, Dokl. Akad. Nauk SSSR, Vol. 88, No. 5, pp. 791-794, 1953.

An experimental investigation of the way in which the lag of the potential pulse on the current pulse in the normal four-electrode method of resistivity survey influences the answer in the case of a long baseline. It is shown that with the normal arrangement an error of up to 88 % can be produced for a 10,000 m baseline.

72. *On Geoelectrical Prospecting in Mountainous Areas. Relation of Strongly Ionized Water-Bearing Stratas* (In Italian).

F. Mosetti, Geophys. Observatory, Trieste, Publ. No. 31, 1953.

The results of a geoelectrical survey in mountainous areas, using the resistivity method, to determine the subsurface structure and the effect of the water-bearing stratas (strongly ionized because of the presence of a deposit of gypsum) which are situated in the proximity of an electrical generating station.

73. *Employment of Electric Methods of Prospecting for Interpretation of Magnetic Anomalies* (In Russian).

N. I. Khalevin, Akad. Nauk SSSR Izv. Ser. Geofiz., No. 1, pp. 61-68, 1953.

When interpreting the results of magnetic surveys often it is difficult to decide whether the observed magnetic effect is caused by a definite circumscribed ore body or by dissemination of magnetic particles in the formation. Only the first is economically important. The electric resistivity method, in addition to the magnetic survey, was used by Khalevin in several cases, so that both magnetic profiles and electric resistivity curves were available for the area. From analysis of both, it was possible to make a decision, which was subsequently confirmed by drilling.

74. *Sources of Error in Electrical Prospecting.*

T. S. West, Sr., & T. S. West, Jr., a paper read at the 23rd meeting of the S.E.G. at Houston, Texas March, 1953. (Not yet published)

This paper presents field data secured during the investigation of the Resistolog Method, an alternating-current method, the Wenner Method, and several of its various modifications. This work provides rather extensive data on surface and near-surface inhomogeneities in several areas in Texas, Kentucky, Michigan, and Oklahoma. The principal objective is to make available to workers in this field data on the usual nature and magnitude of shallow inhomogeneities under field conditions in oil productive areas.

Other sources of error are also discussed, such as polarization and natural earth currents in case of direct current methods, and induced eddy currents in case of radio frequency and other alternating current methods.

75. *Interpretation of Resistivity Data over Filled Sinks.*

K. L. Cook & R. G. Van Nostrand, a paper read at the 23rd meeting of the S.E.G. at Houston, Texas, March, 1953. (Not yet published).

Satisfactory general solutions of Laplace's equation in both prolate and oblate spheroidal coordinates are used to solve the problem of a resistivity survey over a filled hemispheroidal sink. Various methods of presenting the resistivity data are compared, with special emphasis on the application of these techniques to selected field examples. Conclusions are drawn concerning the value of such theoretical studies and the possibility of making satisfactory approximations. Such approximations of the edge effects are made for (1) a vertical dyke in case the width of the sink is small in comparison with its length and depth; and (2) a vertical fault in case the sink is large in comparison with the electrode separation. A careful study of the Lee and Wenner configurations indicates that the former gives additional information that more than justifies the extra time and expense involved.

76. *The Application of Resistivity Methods in Establishing the Base of the Water-Bearing Rocks in the Cannock Chase Coalfield.*

E. J. Polak, Geophysical Prospecting, Vol. 1, No. 3, pp. 197-207, Sept. 1953.

In the Cannock Chase Coalfield the rocks of the overburden are heavily water-logged, thus constituting a source of difficulty and even danger to the miner. In order to ensure maximum safety with the maximum use of reserves, the area has been investigated by boreholes and by resistivity surveys.

In this paper a short summary of the resistivity work is given, with special reference to electrode arrangements and methods of interpretation used. Where applicable, comparison between resistivity evidence and borehole data is shown.

OTHER METHODS

78. *Field Measurement of the Radioactivity of Rocks* in *the Application of Recent Counting Techniques to Geophysical Research.*

H. A. Slack, Amer. Geophys. Un. Trans., Vol. 35, No. 6, pp. 897-901, 1952.

Further development of a field gamma-ray counter suitable for measuring the radioactivity of ordinary rocks in place has resulted in greater sensitivity and portability The instrument was calibrated against prepared standard radioactive concrete blocks and used to investigate the radioactivity of the Kirkland Lake area in northern Ontario. Additional observations over the Round Lake batholith do not alter previous results. An area of higher radioactivity to the north is believed to be a separate geologic structure.

POSSIBILITIES AND LIMITATIONS IN APPLYING GEOELECTRICAL METHODS TO HYDROGEOLOGICAL PROBLEMS IN THE COASTAL AREAS OF NORTH WEST GERMANY *

BY

H. FLATHE **

Abstract

On the basis of results of extensive geoelectrical investigations in East Frisia as well as of theoretically calculated data, it is shown to what extent geoelectrics can furnish a contribution to success during the preliminary work for the establishment of water works, or for the enlargement of existing water works, in coastal areas. One of the most important tasks in this sphere is the search for permeable beds suitable for intake, the delimitation of their thickness and extent (catchment areas), and then the location of favourable places for wells. This task is rather difficult because of thickness variations in and change of facies of the old-pleistocene basin clay (Lauenburg clay) and the presence of Tertiary clay and fine clayey sands which, acting as impervious layers, often divide a permeable bed into several storage horizons. Further difficulties arise from the occurrence of brine bearing deposits near the coast, and water from the depths with a high salt content as a result of leaching processes around salt domes.

The problems arising in this connection are illustrated with the aid of examples from the Rheiderland. The following questions seem to be the most important:

a) the physical interpretation of the measurements with special regard to the principle of equivalence;

b) the correlation of the physical data with the subsurface geology.

This paper is not intended to be an example of a geoelectrical investigation. It is rather an attempt to present some general considerations governing the application of geoelectrical methods in Southern North Sea coastal areas, especially since similar geological conditions also occur in other coastal areas.

In previous years, extensive geo-electrical investigations have been carried out in coastal areas of the North Sea, especially in East Frisia. The purpose of this work was to obtain a general picture of the subsurface geology and thus to provide a basis for an estimation of how far geo-electrical methods can be applied in areas that are of interest for the establishment of new water wells or for the enlargement of already existing waterworks.

The geo-electrical problems in coastal areas, arising from the acute shortage of water, have been already outlined by Hallenbach (1953). The measurements in progress at that time have produced considerable results. Together with theoretical studies, the compilation of the present material now allows a general review of the potentialities of electrical resistivity measurements in hydrological exploration work in such areas. The space here does not permit a comprehensive treatment of all the problems arising in this connection and only a few points of special significance will be discussed.

---

* Presented at the Sixth Meeting of the European Association of Exploration Geophysicists, held in Copenhagen, 19/21 May, 1954.

** Amt für Bodenforschung, Hannover.

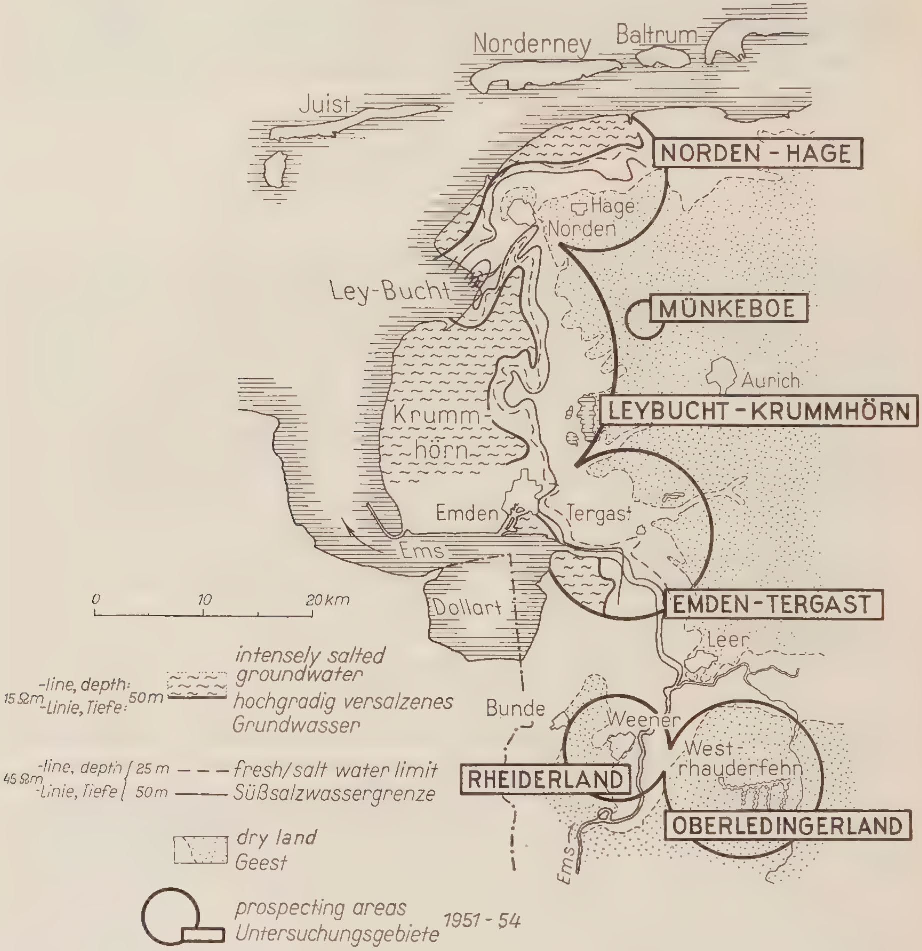

Fig. 1. Geoelectrical prospecting in East-Frisia. — Geoelektrische Untersuchungen in Ostfriesland.

Fig. 1 shows a part of the North Sea coastal area next to the German/Dutch border. Up to 1954 a total of nearly 600 resistivity soundings have been carried out in this area by the Amt für Bodenforschung. In the vicinity of Norden/ Emden, these soundings have provided valuable information concerning the distribution of groundwater salinity, down to depths of 60-80 m, and they are of the greatest importance for the water supply of the Krummhörn and the big new "Leybuchtpolder" of 1000 ha. The boundaries between fresh and saline waters at 25 and 50 m depth are marked in the figure and the areas of high salinity are indicated [1]. The rather interesting course of the boundary, especially in the area of the Leybucht where a tongue of freshwater advances from under the mud-cover into the shallows, has led to new conclusions concerning the movements of the fresh and saline water during the holocene. It should be mentioned that, because of the petrographic uniformity of the subsurface, resistivity variations inside the waterbearing sandy series can be interpreted as a result of variations in the electrolyte concentration (mainly Cl'). The problem, seen from the electrical point of view, is thus relatively simple, if conductivity measurements of the groundwater are carried out in addition. On the whole, electrical resistivity methods, in conjunction with several appropriately situated standard wells for the correlation of specific resistivity and chlorine content, seem to be the most suitable method of investigation in this case.

Difficulties arise, however, where the petrography of the subsurface undergoes considerable variations. This is the case in areas further inland, where old-pleistocene basin clay occurs. This so-called "Lauenburg Clay" is subject to unusual variations in thickness from nearly zero up to more than 80 m. These variations are partly caused by a preexisting landscape of strong relief, upon which the clay was diposited in channels and basins, by later, and very often far-reaching erosion processes, and partly by glacial action. Within the clay itself there are frequent changes of facies. It occurs partly as a rich clay, partly as a more or less sandy clay, and occasionally as a series of alternating fine sand and clay layers.

In addition to the normal coastal brine, often advancing deeply into the area where the Lauenburg Clay occurs (lower reaches of the river Ems), salt water occurs at greater depths as a result of leaching processes around salt domes (Bunde). All these factors cause a reduction in the number of possible freshwater-bearing permeable horizons. Apart from the old-pleistocene basin clay, late Tertiary clay horizons of small thickness very often bring about a horizontal separation of the permeable bed into several storage horizons. This separation is of great importance, if the groundwater in these storage horizons has different degrees of salinity. This is the case, for instance, near Emden—Tergast, where a clay horizon, only a few metres thick, at 50 m depth separates an upper storage horizon with brackish to salty groundwater from a lower fresh water-bearing horizon [2].

[1] The 45 Ω m-lines have been obtained by interpolation between the individual stations of the values of the true formation resistivities at depths of 25 and 50 m. According to the Archie-formula for permeable sands: rock resistivity $= K \cdot \rho_{water}$, the value of 45 Ω m for the formation resistivity corresponds to a chlorine content of the water of 250-300 mg/l, which is the so-called taste limit. Similarly, the formation resistivity of 15 Ω m corresponds to a chlorine content $>$ 1000 mg/l.

[2] This fact shows in the course of the fresh salt water boundary in Fig. 1, where the

These rather complicated problems lead to the question to what extent electrical resistivity methods can provide reliable results. To what extent can the structure of the subsurface be determined by a method which is based on the reduction of a three-dimensional problem to a two-dimensional one? This requires the elimination of a free parameter. Next to this purely physical problem comes that of the correct correlation of the physical data with the geology. These questions must be critically discussed, before a reasonably clear idea of the structure of the subsurface, based on geoelectrics, can be formed.

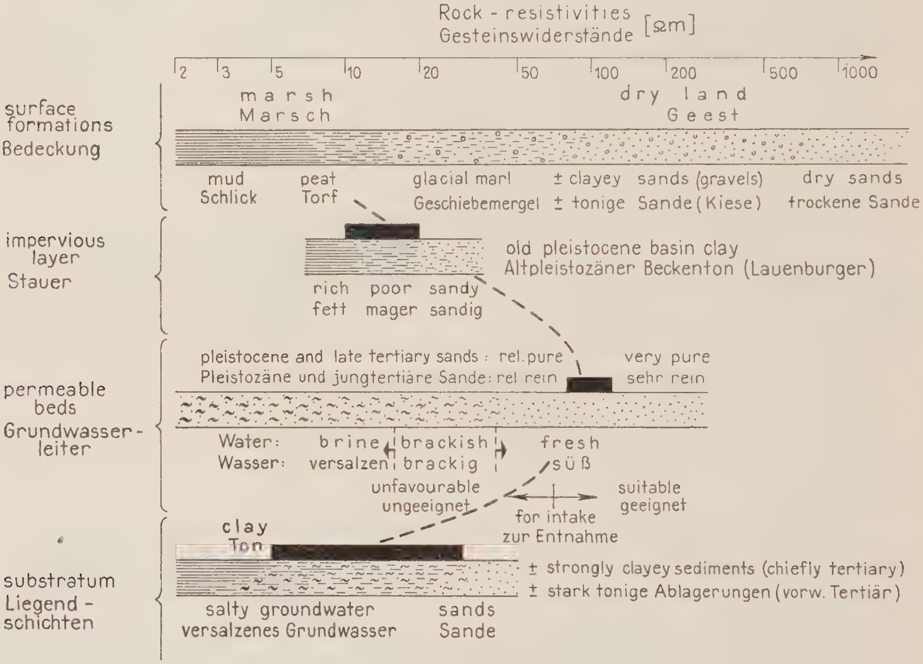

Fig. 2. Rock-resistivities in the lower River District of the Ems. — Gesteinswiderstände im Mündungsgebiet der Ems.

The *correlation between the electrical resistivities and the nature of the formations* is illustrated in Fig. 2, which is based on observations in the lower river area of the Ems. The permeable beds, consisting of freshwater-bearing sands and fine gravels, were found to have resistivities of 80-120 Ω m on an average. The material proved to be relatively clean and suitable for intake. Permeable horizons with higher resistivities, where a higher degree of purity could be expected, are rather scarce in this area. However, in some regions

---

45 Ω m line at 25 m depth runs further inland than that at a depth of 50 m, a fact, that cannot be regarded as a stable condition, unless a clay horizon is present. Geoelecrical measurements point here indirectly to the impermeable bed, which is not directly recognisable in the graphs.

resistivity values of the permeable beds as high as 300 Ω m were found (Hage). These values, being rather unusual for the coastal area, are attributed to groundwater with an exceptionally low electrolyte concentration (resistivities up to 65 Ω m), a relation proved by conductivity measurements of the pore waters. Water of this type is much sought after for water supply purposes.

If rock resistivities decrease to below 70 Ω m, an intake would be inadvisable in most cases. A better electrical conductivity points either to an increase of electrolyte concentration of the pore water in a petrographically uniform material, or to clayey/marly sediments; that is, either to saltwater-bearing permeable layers, or to more or less impervious horizons. Obviously, in both cases areas with such low resistivities are unsuitable for the establishment of waterworks. It is obviously of vital importance to know whether clay or salt water is involved, for clay as a dam has an influence upon the catchment area, whereas the presence of saltwater near a waterworks may become an acute danger during increased intake, when contamination of the wells may occur. In close co-operation with the geologist, this question can be solved in some cases by electrical resistivity methods, using an appropriate arrangement of the measuring grid. From the manner in which resistivity values vary over a larger area, certain conclusions can be drawn, especially if there are no appreciable variations in the risistivities of the clay bodies that may occur. This is not, however, the case in the coastal area under consideration.

The old-pleistocene basin clay is characterised by its great variation in resistivity, caused by frequent facies variations. It was found that Lauenburg Clay has resistivities ranging from 7 to 35 Ω m.

Layers at greater depths show an even wider range of resistivity values. There the fine, more or less clayey, Tertiary sands often contain salt water, originating from leaching processes around saltdomes. In these layers it is still more difficult to differentiate between clay and salt water. Because of the hydrological importance in the drilling of deep wells, it is essential to distinguish between a thick layer of Lauenburg Clay and a saltwater-bearing upper storage horizon, and drilling operations must be used to this end. Such exploration wells for determining the correlation between resistivity and geology are sometimes unavoidable, because, after all, the method applied is a physical one. Generally, one single well is sufficient, if drilled on the strength of geo-electrical results. At the end of this paper, an example of this will be given.

The resistivities of the surface formations vary over a wide range, from 1 to 10.000 Ω m, depending on whether the measuring point is located in rich mud or in dry quicksand. Although these surface formations are of small significance, they cannot, unfortunately, be neglected, because their extremely high as well as their extremely low resistivities very often mask the effect if the important deeper layers on the resistivity graph. This factor will also be illustrated later with the aid of some examples.

We now come to the actual *physical problem,* namely the interpretation of the recorded resistivity graph, that is the determination of the different rock layers, their thicknesses and their resistivities. We shall restrict ourselves solely to resistivity graphs obtained by the four electrode method, using direct current. These graphs represent the so-called "apparent" resistivity as a function of the half-distance of the current electrodes. It is well known that in the case of horizontal strata the thicker a rock layer is the more accurately its true resistivity can be determined from the resistivity graph. The values of the thickness and the resistivity of a layer in a horizontally stratified medium, the knowledge of which is essential to the interpretation, are included in the function Θ in the expression $V(r) = \frac{I\rho_1}{2\pi}\left(\frac{1}{r} + 2\int_0^\infty \Theta(\lambda, k_i, h_i)\, J_0(\lambda r)\, d\lambda\right)$ for the potential due to a point source at the surface of a parallely stratified semi-infinite space (Stefanescu, 1930). In practice, however, these values cannot be obtained directly from the values of the potential. For this reason, interpretation is generally done with the aid of standard curves calculated from the integral, with which the measured graphs are compared. In this procedure it is often found that a given measured graph can be matched equally well with more than one standard curve, different combinations of resistivity and thickness of a given layer being possible. This is known as the principle of equivalence. The importance of this principle of equivalence is only slight if the

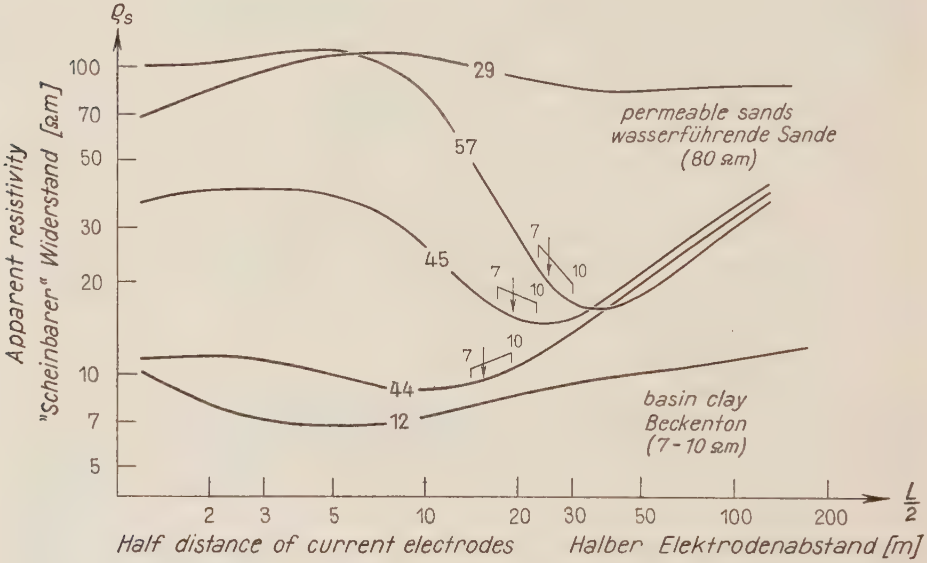

Fig. 3. Rheiderland. Permeable bed below basin clay. — Rheiderland. Grundwasserleiter unter Beckenton.

observed layer—in the present case generally the permeable bed—is sufficiently thick in comparison with its depth. Fig. 3 shows resistivity curves, measured in the Rheiderland, where a permeable bed (90 Ω m) of great thickness underlies the Lauenburg Clay. Curve No 12 was measured over outcropping clay, with a resistivity varying between 7 and 10 Ω m. The arrows on the graph indicate the upper surface of the permeable bed, the corresponding depth being read on the scale for the half distance of the current electrodes. These depth values are in accordance with the principle of equivalence, and the effect of anisotropy has been taken into account in their computation.

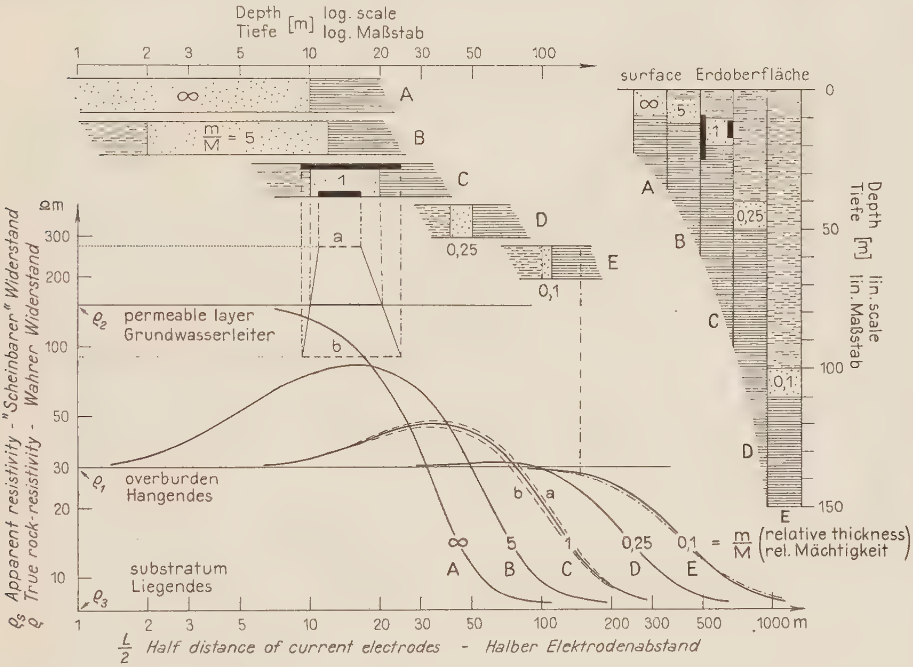

Fig. 4. Permeable bed of constant thickness at various depths. — Grundwasserleiter konstanter Mächtigkeit in verschiedenen Tiefen.

However, great thicknesses of the permeable bed, as would be desirable from the geological as well as from the geoelectrical point of view, are an exception. But whilst a permeable bed of 10 m thickness, for instance, would still suffice for intake, no matter whether it is situated at 5 or at 50 m depth, the depth of a horizon of a limited thickness is very important with regard to the interpretation of the resistivity curves. Owing to the fact that the resolving power decreases with the depth, the quotient m/M (m = layer thickness; M = thickness of the overburden) is, in electrical resistivity measurements, the standard for the detection of the layer, instead of the absolute layer thickness. In the following, this important quantity will be designated as the "relative" thickness of a layer.

Fig. 4 shows, moreover, some Schlumberger graphs calculated from the Stefanescu-integral. Let us assume there is a permeable bed of 10 m thickness, embedded in impervious strata at various depths. In the logarithmic representation, it can be seen immediately, how the resolving power decreases with increasing depth. The theoretical graphs show that even at a relative thickness of 1, the principle of equivalence plays a decisive part. Resistivity changes of 1 : 3 if accompanied by changes in thickness of nearly the same magnitude, result in only small changes of the resistivity curve (curves *a* and *b*). This variation lies already within the limits of possible error. At a relative thickness of 0,25 (layer at 40 m depth), the limits for recognizing the horizon in question are already reached. In such a case, no interpretation can be given if only one resistivity curve is available. But an example (to be given later) demonstrates that such a resistivity graph in a grid of measuring points is still of great value. A relative thickness of 0,1 shows a complete equivalence with a two-layer case, where the permeable bed is missing altogether.

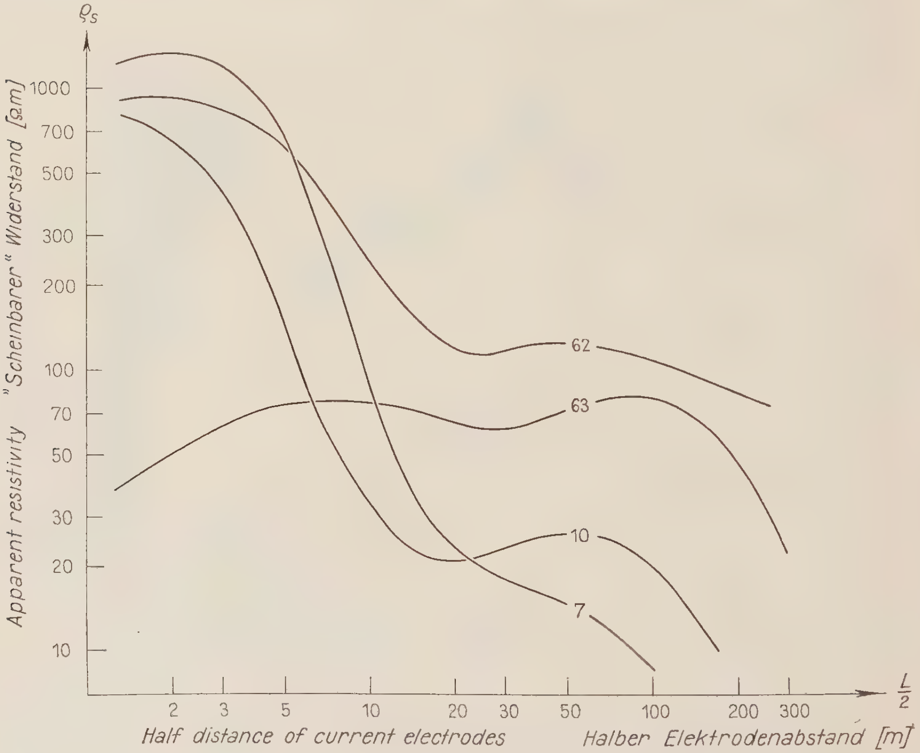

Fig. 5. Rheiderland. Typical sounding graphs from the South of Weener. — Rheiderland. Typische Sondierungskurven aus dem Raum südl. Weener.

In practice, the situation is more complicated, because the ideal theoretical three-layer case is never realized. Surface effects and deviations from horizontal stratification can to a large extent be eliminated by a careful choice of measuring points and an electrode line in the direction of the strike. With the Schlumberger arrangement, in which the potential electrodes are not moved, a smooth resistivity graph can be obtained with a maximum error of 3 %, provided good equipment is available. There are, however, no means of avoiding the influence of the surface formations and of the anisotropy. This is shown very clearly in Fig. 5. The resistivity graphs shown in this figure were mostly taken on dry land. In the right hand portions of the curves, which are no longer visibly influenced by the surface layer, one can recognize the theoretical cases just described. The graphs Nos. 63 and 10 show Lauenburg Clay underlain by a deeper permeable bed. The substratum is either very clayey, or salt-water-bearing, or both. In graph No 7, a permeable bed at approximately 40 m depth is, theoretically, still possible. A 70 m well in the immediate neighbourhood, however, shows only clay. The interpretation of graph No 62 is very difficult; a permeable bed is certainly present, as is disclosed by the maximum in the curve near L/2 = 50 m; but it cannot be ascertained whether this permeable layer is overlain by clay, above which is yet another groundwater-bearing horizon, or whether the overlying stratum consists only of fairly clayey sands,

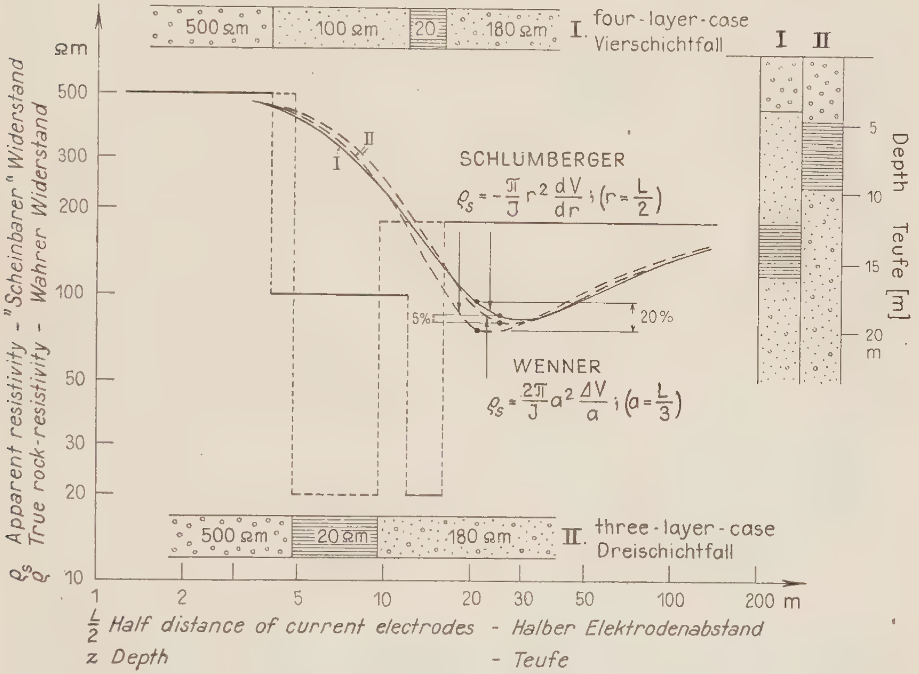

Fig. 6. Comparison of a 3-layer-case and a 4-layer-case (theoretically). — Gegenüberstellung eines 3-Schicht u. eines 4-Schichtfalles (theoretisch).

which do not act as a dam. How far-reaching the influence of the principle of equivalence is and to what extent hydrogeologically different cases can be related to similar types of curves, is shown in Fig. 6.

In this figure, a theoretical three-layer case is compared with a four-layer case. In the three-layer case, a higher-resistive covering (500 Ω m) is underlain directly by Lauenburg Clay (20 Ω m), in the four-layer case, a permeable bed (100 Ω m) occurs between the covering and the clay. In both cases the substratum consists of freshwater-bearing sands (180 Ω m). From the hydrological point of view the difference is very important. It is not desirable for a geophysicist to miss a possible groundwater storage horizon with a thickness of 8 m and to make a 100 % error in estimating the depth to a clayey horizon. The difference between the theoretical curves is at the most 20 %. In an interpretation of data by means of standard curves, such a difference must be conspicuous. But a comparison between the Wenner-graph for the three-layer case and the four-layer Schlumberger graph, which are nearly coincident; shows how much care is necessary to match the resistivity graph to the standard curves in the correct manner, and how strictly one has to distinguish between a

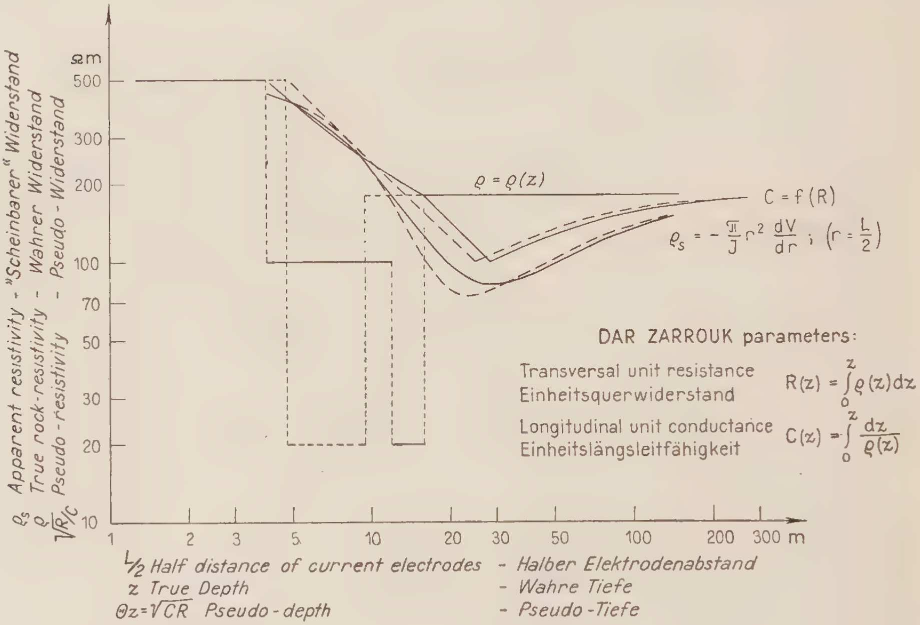

Fig. 7. Comparison of a 3-layer-case and a 4-layer-case (simultaneous representation of the theoretical Schlumberger sounding graph, the electrical logging-diagram and the Dar Zarrouk curve). — Gegenüberstellung eines 3-Schicht u. eines 4-Schichtfalles (gleichzeitige Darstellung der theoretischen Schlumberger-Kurve, des elektrischen Widerstandsprofils und der Dar Zarrouk-Kurve).

Wenner- and a Schlumberger arrangement (Deppermann 1954). The same point is illustrated again in Fig. 7. Here, the electrical logging diagrams, the Schlumberger graphs and the Dar Zarrouk-curves are represented in one diagram. Maillet (1947) has introduced the Dar Zarrouk parameters R and C, so named by him, and he uses them in the expression for the surface potential instead of the thicknesses and resistivities. By a simple transformation of variables, he was able to show that the knowledge of the so-called Dar Zarrouk function is sufficient to compute, in the case of horizontal strata, the distribution of the surface potential and hence the form of the electrical resistivity graph.

It should be noted here that the Dar Zarrouk curve, in areas where the resistivities of the layers are approximately known, can be a valuable help in evaluating the possibilities of applying geo-electrical methods to solve a problem. This method is only a make-shift solution as long as one is not in a position to acquire standard curves for a given geological situation without excessive calculation efforts. We cannot discuss, within this space, all details concerning this matter. Neither can the very difficult question of the anisotropy, which naturally plays an important part in the coastal area, be discussed in detail here. The anisotropy coefficient reaches greater values where the Lauenburg clay occurs as alternating layers of clay and fine sands. In the coastal area under investigation, the depth values obtained from the standard graphs had to be reduced by 10-20 % on the average, to correct for the anisotropy.

To illustrate the statements made so far, we will consider a practical example from the Rheiderland. This example was selected from among the many surveys that have been carried out, because it illustrates some of the main geo-electrical characteristics of the coastal area, although the actual area is *not* situated within the region of coastal salinity. Fig. 8 shows a portion of the district under investigation near Weener, with the limits of extension of the Lauenburg Clay and the depths of its base, as found by means of geo-electrical measurements and from wells in the town area of Weener. Because the actual Ems-marshes are a flooded area, the dry land south-west of Weener was originally intended for the establishment of a water works. Geo-electrical measurements disclosed that Lauenburg Clay of considerable thickness is present in a large part of this area. Waterbearing sands occur only locally in the overlying strata and are out of the question for intake purposes, because of the lack of a sufficiently large catchment area. Highly permeable layers were found flanking the clay in the underlying stratum. In the South, however, there is a substratum of good electrical conductivity, but it is not known whether this is due to clay or salt-water-bearing sediments. The possibility of the presence of salt-water from leaching processes could not be excluded from geophysical consideration because of the proximity of the Bunde Saltdome, found by refraction seismic investigations, whose anhydrite cap is situated at a depth of just over 100 meters. A well drilled nearly showed a more than 20-fold increase of the SO_4-contents in 60 metres. This, of course, excludes the southern part, and the district indicated by a clasped line remains as the catchment area, because it provides the necessary expectations for the establishment of a well gallery. For a better demonstration of the picture that can be formed after electrical investigations, Fig. 9 shows vertical sections of the measured district. The first profile is drawn in a W-E direction from the salt dome of Bunde to the river Ems; the second profile crosses the eastern flank of the clay occurrence in a SW-NE direction. On the left hand side of the W-E profile, Lauenburg Clay occurs directly above the anhydrite of the salt dome, which shows up at the end of graph No 20 as a marked increase of resistivity. The remaining three graphs on this profile show at the right hand end a steep slope. The question of clay or saltwater, was decided by the borehole "Weener I" which was drilled especially for this purpose. The well profile shows a very good agreement with the sounding graph No 78 taken at the same site. This may be seen by com-

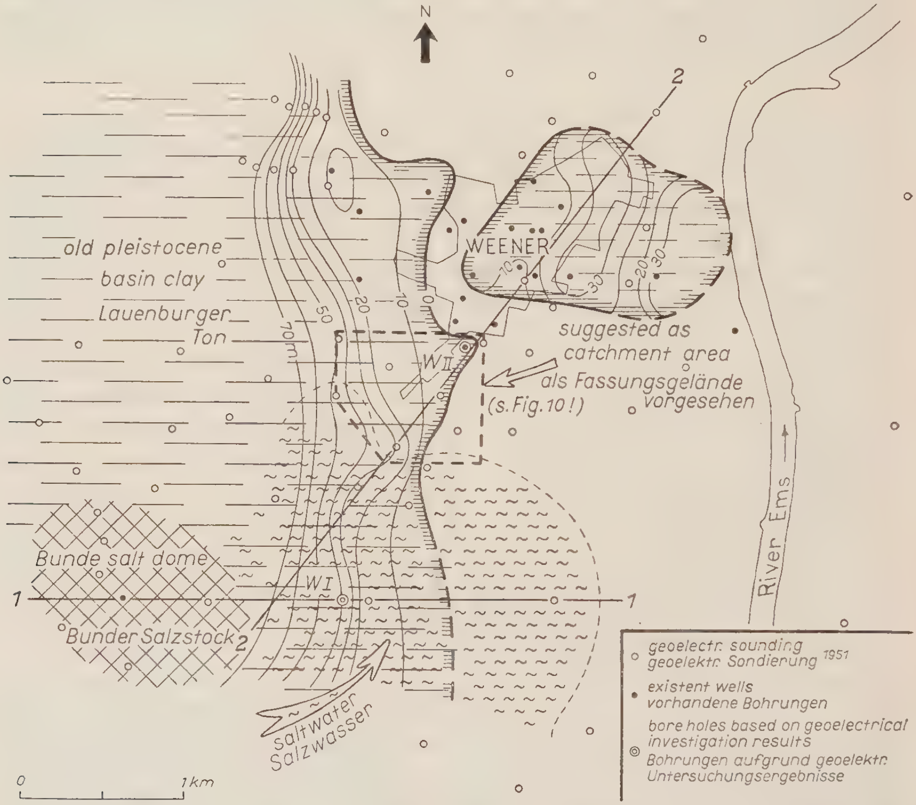

Fig. 8. Rheiderland. Extension and depth of base of Lauenberg clay. — Verbreitung des Lauenburger Tons und Tiefenlage seiner Unterfläche.
(after W. Richter and the author).

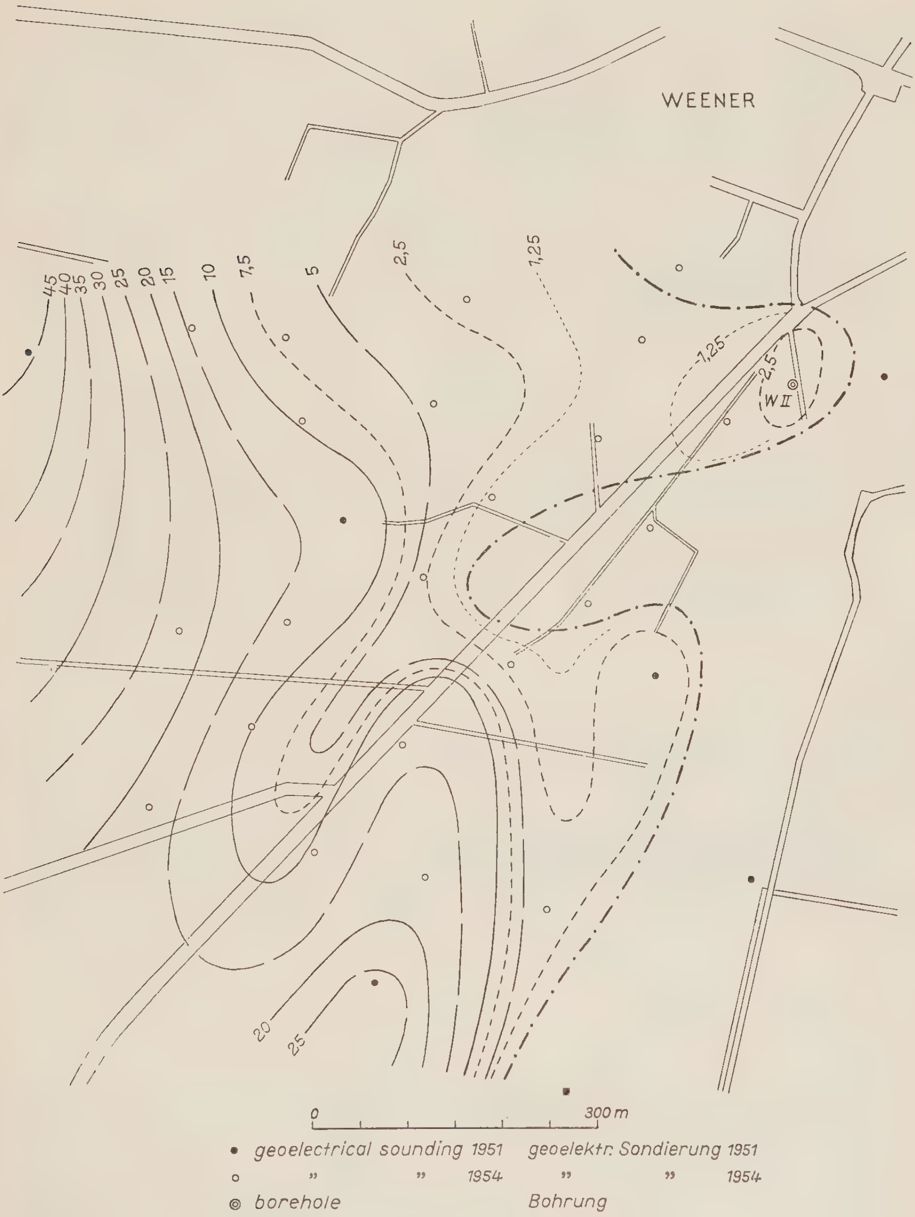

Fig. 10. Rheiderland. Catchment area in detail. Thickness of Lauenburg clay. — Fassungsgebiet (Detailvermessung). Mächtigkeit des Lauenburger Tons. (after W. Richter and the author).

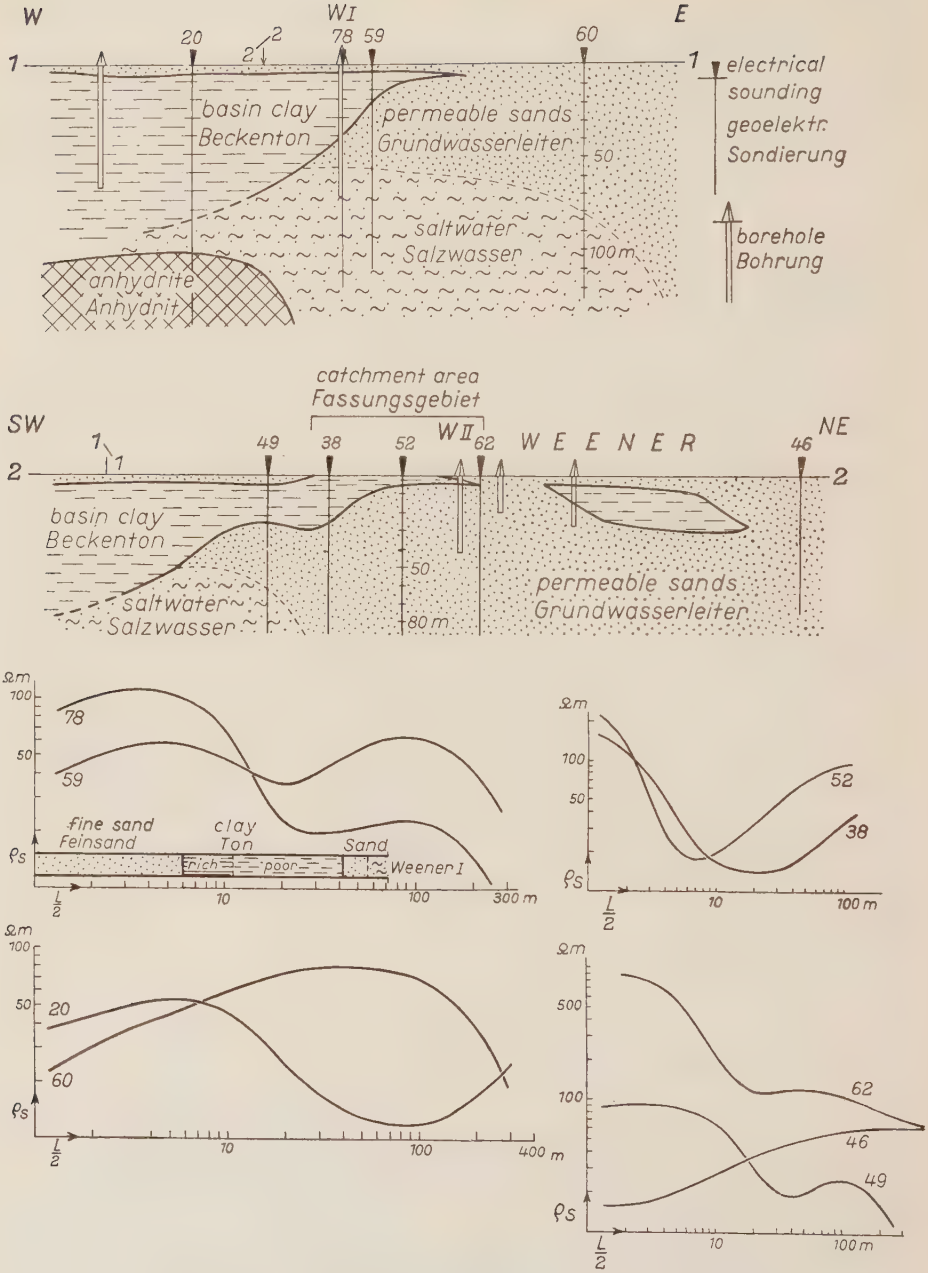

Fig. 9. Rheiderland. Vertical sections. — Rheiderland. Vertikalschnitte.

paring this curve with the theoretical curve for a permeable layer embedded in clay (relative thickness 0,25) shown in Fig. 4. The freshwater-bearing sands under the Lauenburg Clay cause a weak maximum in the curve which, however, can still be interpreted by comparison with graphs Nos 59 and 60 and assuming a value of 80 Ω m for the resistivity of the permeable bed. On its own, graph No 78 would admit of a wide variation in the interpretation.

On the second vertical section the position of the proposed catchment area is indicated. If the depth of the wells is restricted to 40 m, the saltwater from the Bunde salt dome should no longer be a danger. The flatly outcropping Lauenburg Clay provides a natural hygienic protection. The sands and fine gravels, whose resistivities vary between 100-180 Ω m, have a good permeability. The result of the test well "Weener II" has proved the suitability of the area for the establishment of a water-procuring plant, as suggested by the geoelectrical investigations. The measurements carried out in 1951 were supplemented in 1954 by a dense net of measuring points in the catchment area, after completion of the necessary preliminary hydrological works. This detail survey provided an accurate picture of the extent of the Lauenburg Clay. The results were represented in four maps:

1) Upper surface of the Lauenburg Clay
2) Base of the Lauenburg Clay
3) Thickness of the Lauenburg Clay
4) True resistivity of the lower sands.

Maps 1) and 2) are mainly of geological interest, because they give indications regarding the sedimentation and erosion of the Lauenburg Clay, whereas maps 3) and 4) represent the actual working material for the hydrologist. Map 3) is represented in Fig. 10. A comparison with the corresponding section in Fig. 8 shows a considerably more differentiated stratification of the clay, and underlines the necessity for detailed measurements, after the catchment area has been selected on the strength of the geoelectrical survey and considering the technical and economic points of view.

REFERENCES

DEPPERMANN, K., 1954: Die Abhängigkeit des scheinbaren Widerstandes vom Sondenabstand bei der Vierpunkt-Methode, Geophysical Prospecting, II, 262-273.

HALLENBACH, F., 1953: Geoelectrical Problems of the Hydrology of West German Areas, Geophysical Prospecting, I, 241-249.

MAILLET, R., 1947: The fundamental equations of electrical Prospecting, Geophysics, 12, 529-556.

STEFANESCU, S. C. et M. SCHLUMBERGER, 1930: Sur la distribution électrique potentielle autor d'une prix de terre ponctuelle dans un terrain à conches horizontales, homogènes et isotopes, Journal de physique et le rad. VII, 1, 132-140.

DISCUSSION

Mr. G. LEMASNE: We have been working ourselves on very similar problems in other parts of the world, and it is my impression that your conclusions are quite right.

Mr. C. MORELLI: Do you think that the tide has any influence on the height of the ground-water?

Mr. FLATHE: In the flat coastal areas under investigation, the ground water level lies practically within the surface layers, and the tide has therefore no influence on the reported electrical measurements.

DÉTERMINATION DES SALINITÉS DES EAUX DANS LE SOUS-SOL DU ZUIDERZEE PAR PROSPECTION GÉOPHYSIQUE *

PAR

A. VOLKER ** ET J. DIJKSTRA **

Abstract

The paper describes the determination of the chlorine content of deep ground water by means of the direct resistivity method using the Wenner electrode configuration. The purpose was to investigate the distribution of salinity in the brackish waters within a permeable sand of thickness 250 metres and which forms the deeper subsoil of the Ysselmeer areas.

Such a knowledge is of great value, firstly because the seepage of salt water into the proposed deep "polders" may reduce the crop yield, and secondly because it allows areas, where potable waters may occur, to be delineated.

To test the method, measurements were made near existing boreholes which extended to a depth of 350 metres. From these borings water samples from various depths were collected and it was found that the resistivity ρ_l of the porewater was closely related to their chlorine content. The resistivity ρ of the saturated sand was determined from the geo-electrical measurements. It was found that the resistivity ρ was given by $\rho = 4{,}5\ \rho_l$. From this relation, which is independent of the salinity, the chlorine content of the porewater could be estimated. These results are in close agreement with those of other observers. In the area ρ varied from 1 to 200 ohmmetres corresponding to a chlorine content changing from 12.000 to 15 mg per litre.

The method was adapted for working over water. Each of fourteen insulated conductors in a special cable terminated in an electrode, and these electrodes were spaced along the cable so that nine different Wenner spacings could be selected. The electrode separations varied from 44 metres up to 396 metres.

I — Introduction

Le barrage du Zuiderzee et l'asséchement de plusieurs polders dans cette mer transformée en bassin d'eau douce, le lac de l'Yssel, posent des problèmes hydrologiques dont le caractère est déterminé par la constitution géologique.

Les parties asséchées se trouvant à plusieurs mètres au dessous du niveau du lac, les eaux environnantes tendent à s'infiltrer à travers les digues et le sous-sol. Dans ses grandes lignes la constitution géotechnique peut être décrite de la façon suivante. Un paquet de sables perméables saturés d'eau d'une épaisseur de 250 mètres environ, est recouvert par des couches d'argile et de tourbe offrant une certaine résistance contre l'infiltration des eaux. Les assises du paquet perméable sont constituées par des argiles marines de l'ère tertiaire. Ainsi un large passage se trouve ouvert à l'eau en dessous du polder. Il est facile de se rendre compte du mouvement des eaux souterraines: pénétration dans les couches superficielles à partir de l'extérieur du polder; mouvement horizontal dans les sables perméables et remontée dans la couche arable (fig. 1).

---

* Presented at the Seventh Meeting of the European Association of Exploration Geophysicists, held in The Hague, 8/10 December 1954.

** Dienst der Zuiderzeewerken, The Hague.

Or, les eaux déjà présentes dans le sous-sol sont des eaux de mers fossiles dûes à des transgressions successives durant la période de sédimentation du paquet perméable.

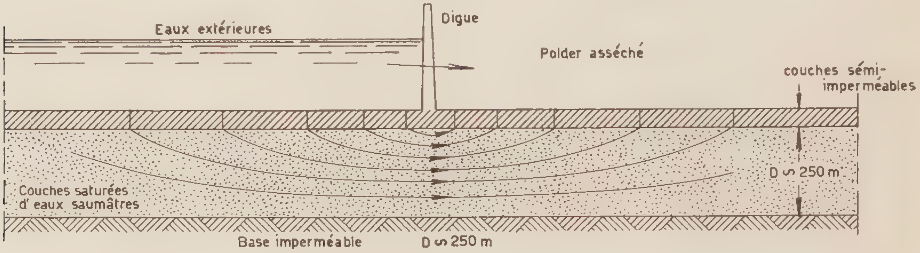

Fig. 1. Infiltration souterraine. — Underground infiltration.

Après l'asséchement d'un polder ce sont donc des eaux saumâtres qui montent dans la couche arable et qui peuvent être nuisibles aux récoltes. En outre les eaux d'infiltration des polders sont déversées par des stations de pompage dans l'Ysselmeer — grand réservoir d'eau douce, qui alimente une vaste partie du pays pendant les périodes arides. Il est donc nécessaire de connaître avant l'endiguement d'un nouveau polder la quantité d'eau qui s'infiltrera ainsi que la teneur en sel des eaux présentes dans le sous-sol.

Par contre, dans la partie méridionale du bassin du Zuiderzee on trouve dans le sous-sol des eaux douces qui peuvent servir à l'alimentation en eaux potables. Pour fixer l'emplacement des prises d'eau, il faut donc pouvoir délimiter cette région spéciale.

La méthode classique pour connaître la composition chimique des eaux souterraines consiste à forer au moyen de sondes. Dans les forages, on place des filtres munis de tubes, dans lesquels des échantillons d'eau sont prélevés. Vu la constitution géologique, il est nécessaire de pousser ces forages jusqu'à une profondeur de plus de 250 mètres, afin d'explorer tout le paquet perméable. Un assez grand nombre de forages profonds a ainsi été exécuté. Or, il se présente de grandes variations locales dans la composition des eaux. Il serait par conséquent nécessaire d'exécuter un grand nombre de ces forages afin d'explorer toute l'étendue du paquet ce qui provoquerait des dépenses considérables.

On est donc conduit à rechercher une méthode économique susceptible de donner rapidement une idée globale de la teneur en sel. Les méthodes géophysiques permettent de prospecter le sous-sol en effectuant des mesures physiques à la surface du sol. La méthode géo-électrique est tout indiquée pour notre cas, puisque la résistivité électrique est fortement influencée par la teneur en ions des eaux.

II — Principe de mesure des résistivités

La résistivité électrique du sous-sol peut être mesurée au moyen d'un dispositif bien connu, proposé par Wenner.

Selon ce procédé on opère avec quatre électrodes punctiformes placées dans un alignement à égale distance entre elles a. Les électrodes doivent être en contact avec les eaux souterraines.

Le courant continu I est injecté et mesuré entre les électrodes extérieures ; on mesure également la différence de potentiel ΔV entre les électrodes intérieures. Les valeurs de a, I et ΔV permettent de calculer la valeur de la résistivité apparente ρ_a. La méthode usuelle consiste à mesurer ρ_a pour différentes valeurs de a et à dresser un grafique.

En général la courbe ainsi obtenue est caractéristique pour une série de couches horizontales de résistivité différente.

La connaissance géologique du bassin, du Zuiderzee, obtenue par forages, justifie en effet l'hypothèse de départ de couches parallèles et horizontales. Elle justifie également le choix de la méthode Wenner; puisque en général les gradients de la salinité dans le sens horizontal sont très faibles.

En comparant la courbe obtenue à des courbes calculées théoriquement pour des conditions déterminées on peut arriver à une interprétation des résultats trouvés, interprétation qui fait conclure à la présence de deux ou trois, éventuellement quatre couches de telle ou telle résistivité.

Vu la profondeur de l'investigation à réaliser, il faut opérer avec une distance pour $3a$ d'un ordre de grandeur de 1500 m.

Le choix du courant continue a été dicté par la profondeur de l'investigation désirée : au moins 250 mètres et même 350 mètres de préférence. L'emploi d'un courant alternatif est dans ce cas impossible puisque le courant a tendance à se concentrer à la surface des conducteurs (effet de peau ou skin-effect).

Dans l'exécution des mesures, une difficulté spéciale provient des effects de polarisation sur les électrodes. Malheureusement l'utilisation d'électrodes impolarisables n'est pas possible pour les mesures à exécuter dans un point quelconque du lac. Par ailleurs une autre perturbation grande encore est dûe à l'existence de courants telluriques naturels et de courants vagabonds. Dans les instruments utilisés, ces effets sont éliminés de façon simple par un deuxième compensateur, placé en série avec le compensateur pour la mesure de la différence de potentiel ΔV, résultant du champ électrique engendré artificiellement.

III — Mesures pour la mise à l'épreuve et l'étalonnage de la méthode

La mise à l'épreuve et l'étalonnage ont été facilités par le fait que quelques forages à grandes profondeurs avaient été réalisés au préalable. Ces forages ont été exécutés selon le procédé classique de la soupape à clapet, procédé qui permet de placer, au fur et à mesure qu'on s'enfonce, des filtres munis de tubes destinés au prélèvement d'échantillons d'eau. Ainsi il est possible de déterminer la répartition des salinités dans les sables perméables. Pour chaque échantillon ont été déterminées la teneur en chlore, la teneur en autres ions et la conductivité électrique. Deux sondages I et II près de Harderwijk (fig. 2)

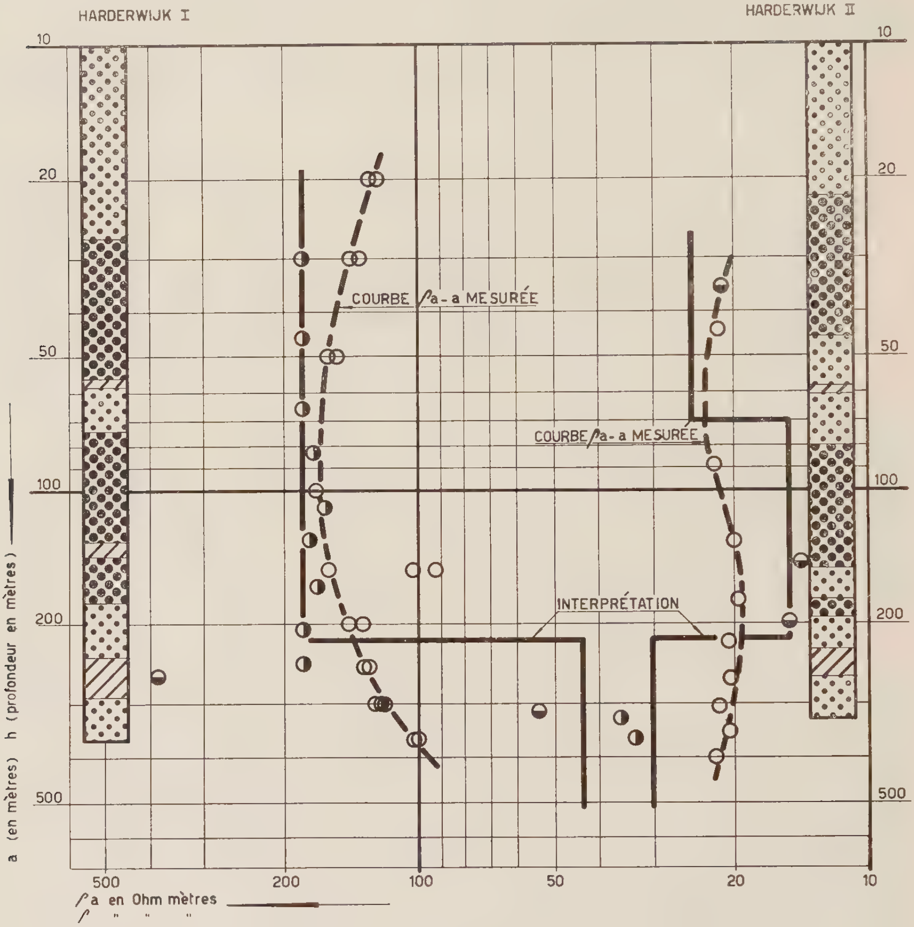

Echantillons d'eau pris dans les filtres
Water samples taken in the filters
◑ Harderwijk I ◒ Harderwijk II

Fig. 2. Mesures d'étalonnage. — Comparison measurements.

ont atteint une profondeur d'environ 350 mètres; les salinités en chaque point ne varient que très peu avec la profondeur: 20 milligrammes de Cl' par litre dans l'un des cas (I) et 1100 mg Cl'/litre dans l'autre (II). En outre, sont connus les résultats de deux sondages de plus de 200 mètres où l'on trouve des salinités augmentant avec la profondeur. Enfin une série de sondages entre les 80 et les 150 mètres fait également connaître la composition chimique de l'eau des pores des sables. En général les salinités varient entre 15 et 12000 mg Cl'/litre.

Les analyses démontrent qu'il existe une bonne corrélation entre la teneur en chlore et la résistivité électrique ρ_l du liquide des pores (fig. 3).

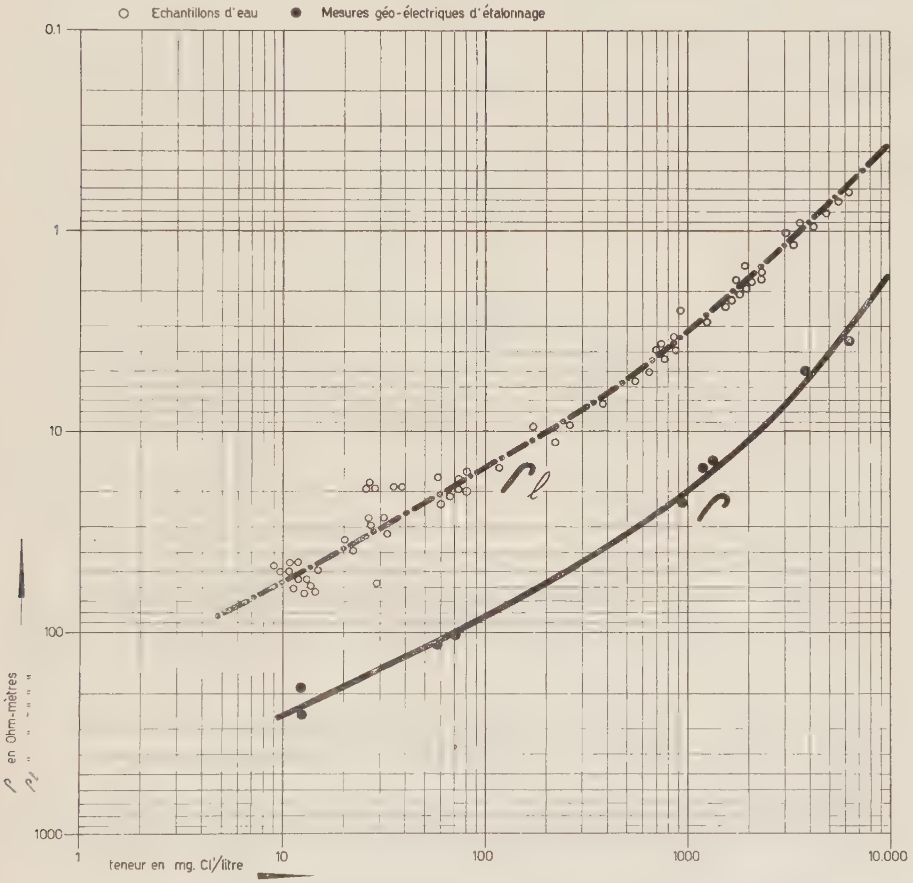

Fig. 3. Résistivité ρ des couches de sable en place. Résistivité ρ_l du liquide dans les pores. — Resistivity ρ of the sand beds. Resistivity ρ_l of the pore liquid.

Ceci s'explique par l'histoire géologique: les eaux saumâtres du sous-sol sont des eaux de mers fossiles de salinité plus ou moins affaiblie. Etant donné de plus que le chlore occupe la place la plus importante dans la composition, il est évident qu'on peut trouver une relation entre la teneur en chlore et la résistivité.

La résistivité ρ des couches de sable en place — constituées par les grains et les eaux des pores — est plus grande que ρ_l puisqu'une section à travers la masse est en partie constituée par les matériaux de grande résistivité que représentent les grains.

On a par conséquent:

$$\rho = \alpha\rho_l \qquad \text{où} \qquad \alpha > 1.$$

Les mesures géo-électriques permettent de déterminer ρ et non pas ρ_l. L'essentiel est donc d'obtenir la valeur de α, c'est à dire, la relation existant entre la résistivité des couches de sable en place et la teneur en chlore des eaux dans les pores. Mesurer cette résistivité au laboratoire sur un échantillon plus ou moins remué, n'aurait aucun sens. Ainsi que le remarque le prospecteur français M. Cagniard la résistivité doit être mesurée sur les formations en place, par les méthodes même qui servent à la prospection, ce qui offre aussi l'avantage — du fait qu'on opère sur un grand volume de terrain — de faire connaître une résistivité moyenne, beaucoup plus caractéristique que celle d'échantillons.

Il convient donc d'étalonner la méthode géo-électrique en effectuant des opérations de mesure à l'emplacement même des sondages mentionnés ci-dessus et de comparer les résultats obtenus. Les mesures font connaître, après interprétation des courbes $\rho_a — a$, les résistivités dans le sous-sol; ces valeurs ont été portées sur le même graphique que les teneurs en chlore obtenues par les échantillons d'eau prélevés dans les forages (fig. 3). On remarque que ρ est effectivement plus grand que ρ_l et que, compte-tenu de l'échelle logarithmique utilisée, la valeur de α est indépendante de la teneur en chlore, comme on devrait s'y attendre.

Ainsi un fait déjà bien connu par des expériences de laboratoire et par des considérations théoriques a été confirmé par ces essais à grande échelle.

Une expérience très intéressante pour la mise à l'épreuve de la méthode géo-électrique a été faite sur la digue de barrage du Zuiderzee. Cette digue sépare les eaux de mer — dans le „Waddenzee" — des eaux douces emmagasinées dans „l'Ysselmeer", lac artificiel de formation récente. En un point quelconque de la digue, on trouve une certaine salinité des eaux du sous-sol tandis que les couches supérieures influencées par les eaux de surface n'ont pas, de part et d'autre de la digue, les mêmes salinités.

Il était donc significatif d'exécuter deux mesures en un point déterminé de la digue, les électrodes plongeant successivement dans chacun des deux réservoirs contigus.

On obtient, comme on pouvait s'y attendre, des courbes $\rho_a — a$ entièrement différentes l'une de l'autre (fig. 4). En effet pour des petites valeurs de a, les courants se propagent dans les couches supérieures de résistivité selon qu'il s'agit d'un côté ou de l'autre de la digue (eaux de mer: 16000 mg Cl/litre contre 200 mg Cl/litre pour les eaux de l'Ysselmeer). Les deux courbes se rapprochent pour les grandes valeurs de a, car la couche supérieure ne joue alors qu'un rôle secondaire. L'interprétation des mesures permet de conclure à une même résistivité des couches à partir d'une certaine profondeur.

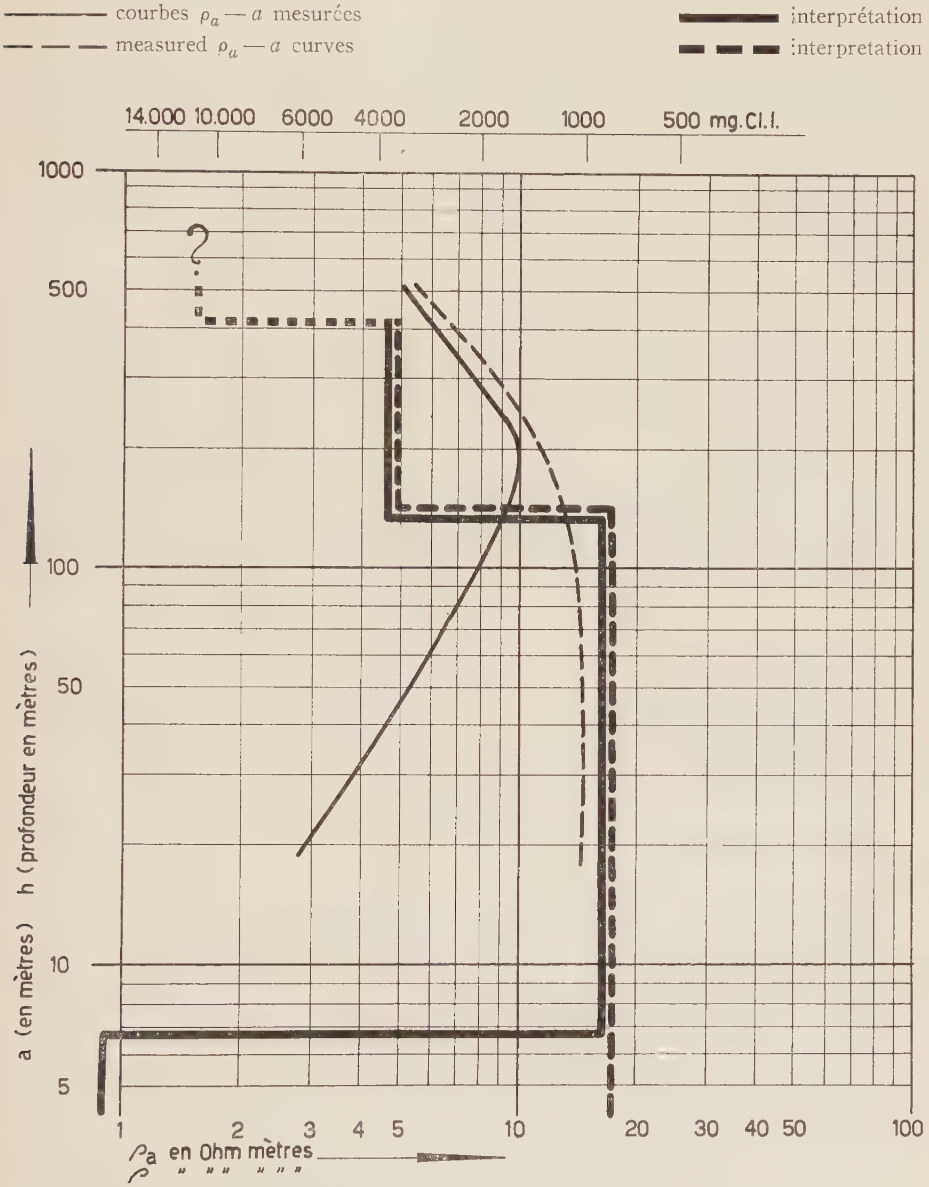

Fig. 4. Mesures des deux côtés de la digue de barrage du Zuiderzee. — Measurements on both sides of the enclosing dam of the Zuiderzee.

IV — RELATION ENTRE LA RÉSISTIVITÉ DES COUCHES DE SABLE ET LA TENEUR EN CHLORE DES EAUX DES PORES DE CE SABLE

D'après la fig. 3, la valeur de α serait:

$$\alpha = 5{,}35$$

et ceci, indépendamment de la salinité. Avant de comparer cette valeur avec les résultats obtenus par d'autres auteurs, il faut, du fait que les résistivités ρ_l et ρ ne se rapportent pas à la même température, effectuer des corrections. Les valeurs de ρ obtenues sur les formations en place se rapportent à la température moyenne des eaux dans le paquet perméable, soit à 10° C. Les valeurs de ρ_l déterminées dans des échantillons d'eau ont été étalonnées pour une température de 18° C.

Tenant compte de cette différence, on arrive à:

$$\alpha = 4{,}5$$

M. Sundberg (1932) essaie de calculer théoriquement cette valeur en estimant que les matériaux des grains en forme de sphères est isolant et en considérant la section de passage variable qui existe entre les grains comme conductrice du courant. Il arrive ainsi à la conclusion que la valeur de α est fortement influencée par le volume spécifique p des pores et que cette valeur est indépendante du diamètre des sphères. Pour la porosité dans le cas qui nous occupe ($p = 0{,}35$), M. Sundberg propose $\alpha = 4{,}7$.

Des essais de laboratoire ont conduit M. Klinkenberg (1951) à la formule simple:

$$\rho = \rho_l \, (L/p)$$

où p = porosité
L = coëfficiënt „lithologique".

Dans notre cas, nous arrivons à $L = 4{,}5 \times 0{,}35 = 1{,}6$. M. Klinkenberg a trouvé une valeur pour L de 1,4 à 2,0.

Enfin, le laboratoire géophysique de Delft a trouvé $\alpha = 4$ pour des échantillons de sable de la même porosité. Dans tous ces cas, il s'agit d'une saturation complète des pores par l'eau.

La valeur de α trouvée par les essais à grande échelle s'accorde donc suffisamment bien avec les résultats obtenus par d'autres auteurs.

La relation obtenue démontre que la résistivité est très sensible à la teneur en chlore. Ce fait justifie l'application de la méthode électrique pour le but envisagé.

D'autre part les résultats obtenus s'appliquent tous aux couches de sable du paquet perméable. Si la dimension des grains n'est pas la même pour toutes les couches, les porosités ne diffèrent que très peu, vu l'origine fluviale des sédiments.

On sait que le problème de la résistivité de l'argile et de la tourbe est beaucoup plus complexé que celui du sable. Heureusement on ne trouve que très rarement des argiles dans le paquet perméable. La relation entre la résistivité et la teneur en chlore des couches superficielles d'argile et de tourbe peut nous être indifférente, puisque nous avons le moyen de connaître les salinités de ces couches supérieures par des forages peu profonds et par conséquent assez économiques. Dans notre inventaire, ces couches figurent plus ou moins comme un perturbateur dont l'effet diminue rapidement en faisant agrandir la longueur a.

Il en est de même pour les assises plus ou moins argileuses en dessous de 250 ou 300 mètres. En effet, puisqu'aucun courant d'eau d'importance ne peut se produire dans ces couches, leur véritable teneur en sel ne présente pas de grand intérêt.

V — Mesure de la répartition des salinités dans le sous-sol

Après mise à l'épreuve et étalonnage, il a été possible d'entreprendre le véritable programme des recherches: détermination des salinités des eaux dans le sous-sol en des points quelconques. Les mesures donnent en premier lieu la graphique $\rho_a — a$; l'interprétation de ce graphique — c'est à dire son analyse pour conclure à l'existence d'une série de couches de telle et telle résistivité exige un travail spécial.

Dans le second paragraphe de cet article, nous avons parlé de l'emploi de courbes calculées théoriquement, en constituant un „catalogue", mais ce catalogue est toujours incomplet. Heureusement, les sondages de repère fournissent le moyen d'interpoler entre les mesures électriques d'étalonnage. En outre pour des cas où l'interprétation s'écarterait trop, du catalogue ou des mesures d'étalonnage, une série de courbes s'appliquant aux cas particuliers a été calculée par le „Mathematisch Centrum" d'Amsterdam.

Les mesures nécessaires dans le bassin du Zuiderzee ont été exécutés en partie dans les polders asséchés — les électrodes plongeant dans les eaux d'un canal ou fossé —, en partie sur les digues — les électrodes se trouvant dans l'eau du lac, enfin en partie dans un point quelconque du lac. Pour ces dernières mesures un dispositif spécial de câbles conducteurs a dû être construit. Il est en effet très difficile de placer les quatre électrodes en pleine mer exactement aux distances voulues.

Pour remédier à cet inconvénient, un câble contenant 14 brins isolés a été construit. Chaque brin de longueur différente se termine par une électrode, chaque électrode pouvant être séparément jointe aux instruments de mesure. Les distances ont été choisies de telle façon que neuf combinaisons peuvent être réalisées, chacune de ces combinaisons étant constituée par deux électrodes extérieures comme pôles de générateur et deux électrodes intérieures comme électrodes de potentiel (fig. 5). Pour chaque combinaison, les distances réciproques a des quatre électrodes employées doivent être chaque fois égales. La dimension de a diffère pour chaque combinaison. Pour les neuf combinaisons citées, cette distance varie entre $a = 44$ et $a = 396$ m. Ainsi neuf points peuvent être situés sur le graphique $\rho_a — a$.

Le câble, monté sur un treuil, est placé sur le gaillard arrière d'un petit remorqueur (fig. 6). Pour exécuter un sondage électrique le bout du câble était

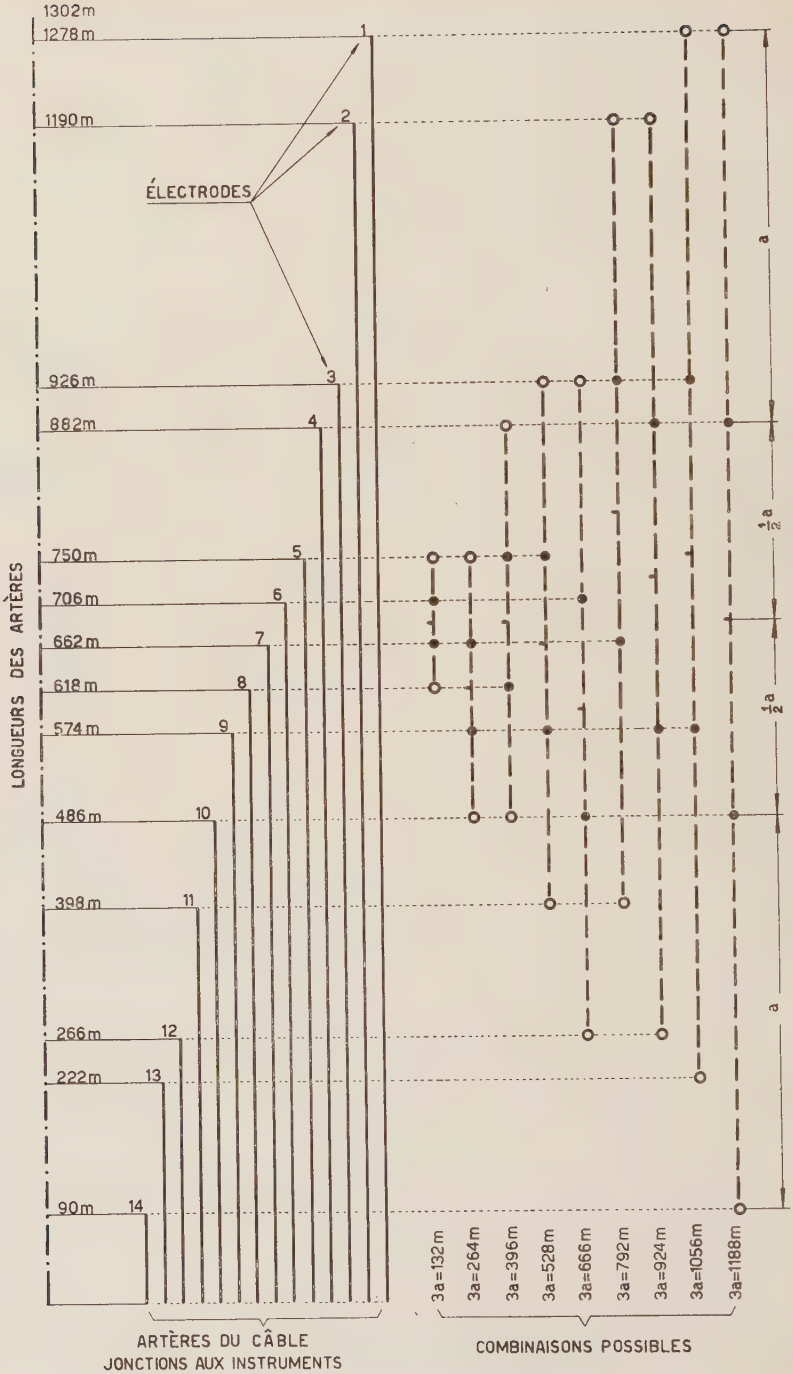

Fig. 5. Câble pour opération de mesures en pleine mer. — Cable for resistivity measurements at sea.

fixé à une ancre pourvue d'une bouée de reconnaissance et, tandis que le remorqueur navigait en ligne droite, le câble se déroulait pour couler jusqu'au fond du lac. Ensuite le remorqueur allait mouiller l'ancre.

Les différents raccordements étaient effectués au moyen d'un interrupteur.

La méthode de lancement du câble s'est avérée bonne, puisque même après avoir été employé une centaine de fois le câble n'était pratiquement pas détérioré. Dans des conditions favorables, on arrive à exécuter 4 sondages électriques par jour (fig. 7).

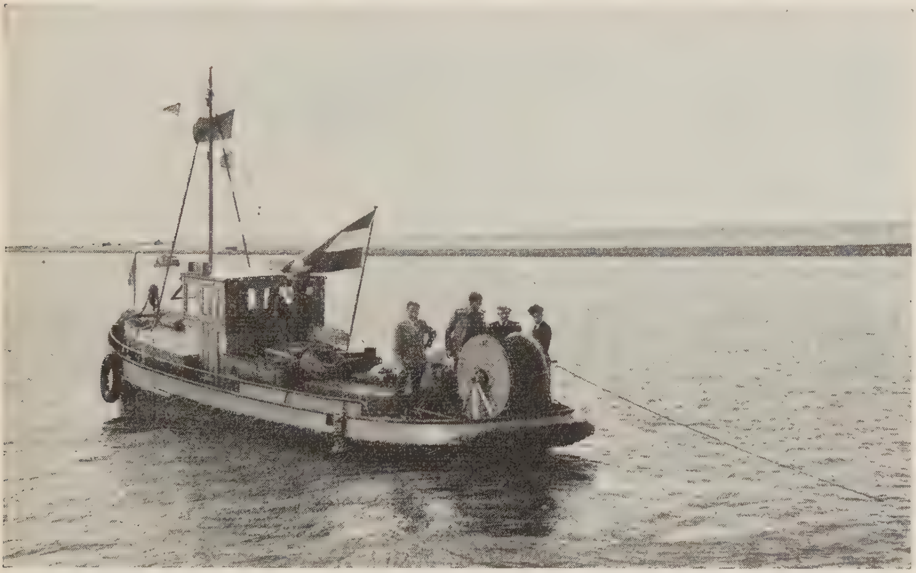

Fig. 6. Lancement du câble pour mesures dans l'IJsselmeer. — Laying out the cable for measurements in the IJsselmeer.

Afin de pouvoir opérer dans la zone côtière du lac où la profondeur est petite, le treuil a été installé également sur deux petits chalands accouplés avec un tirant d'eau ne dépassant pas 0,3 m (fig. 8).

Au total, 200 mesures ont été exécutées, dont 60 sur la terre ferme. En certains points, deux mesures avec des directions différentes du câble, furent effectuées, l'une en disposant le câble parallèlement, l'autre perpendiculairement à la direction des isohalines.

En 1951 et 1952, les mesures se sont pratiquement limitées à une partie du sud-est de l'Ysselmeer, en vue du programme de construction d'un nouveau polder: le „Flevoland", et de l'établissement éventuelle d'une prise d'eau pour l'alimentation en eau potable. Il a été constaté qu'il existe justement dans cette région de grandes différences de salinité, différences qui rendent l'application de la méthode électrique particulièrement indiquée.

Les renseignements obtenus permettent de distinguer dans le sous-sol, en de nombreux points, trois ou quatre couches avec des salinités différentes. Pour donner une esquisse simple de ces résultats, les moyennes des salinités dans la couche perméable ont été calculées (fig. 9).

Les eaux les moins saumâtres se trouvent du côté des collines sablonneuses du „Veluwe" où s'infiltrent des eaux de pluie. La répartition des salinités sur la carte montre quelques anomalies qui peuvent s'expliquer par la constitution et par d'autres données de caractère hydrologique.

Les mesures ont été complétées au cours de 1954.

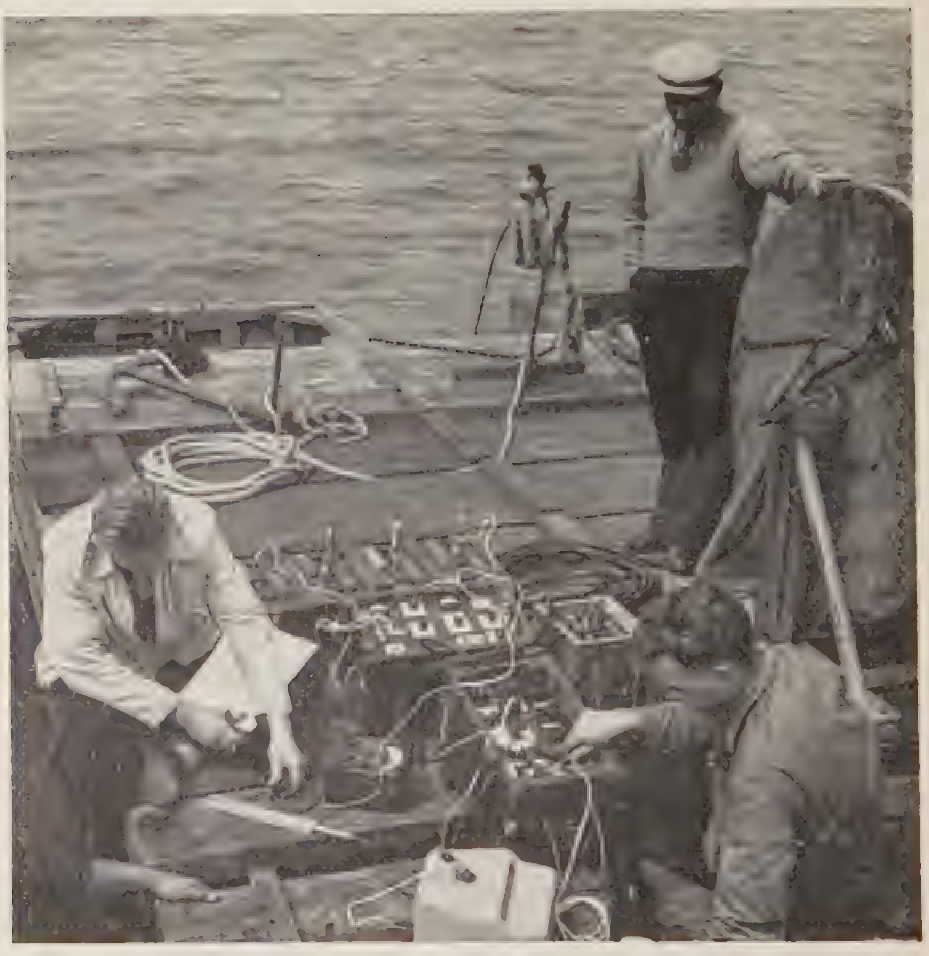

Fig. 7. Exécution d'une mesure. — The taking of a measurement.

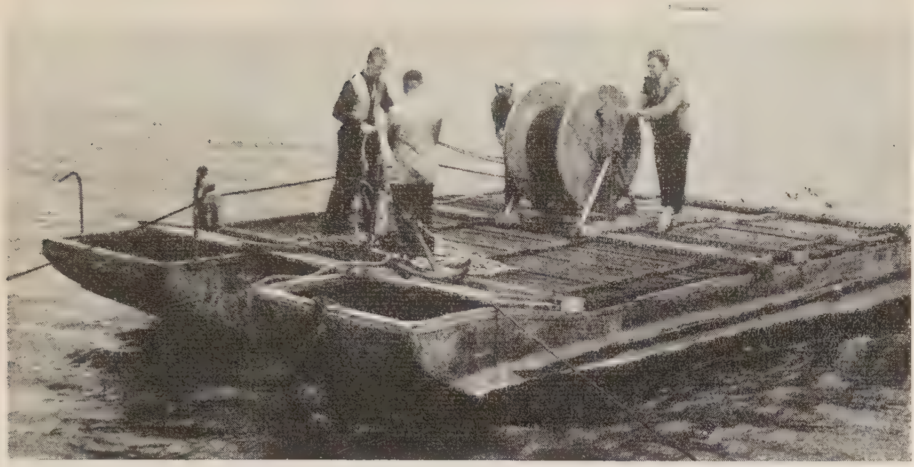

Fig. 8. Treuil placé sur chalands accouplés pour mesures dans des eaux peu profondes. — Reel placed on coupled flat-bottomed barges for measurements in shallow water.

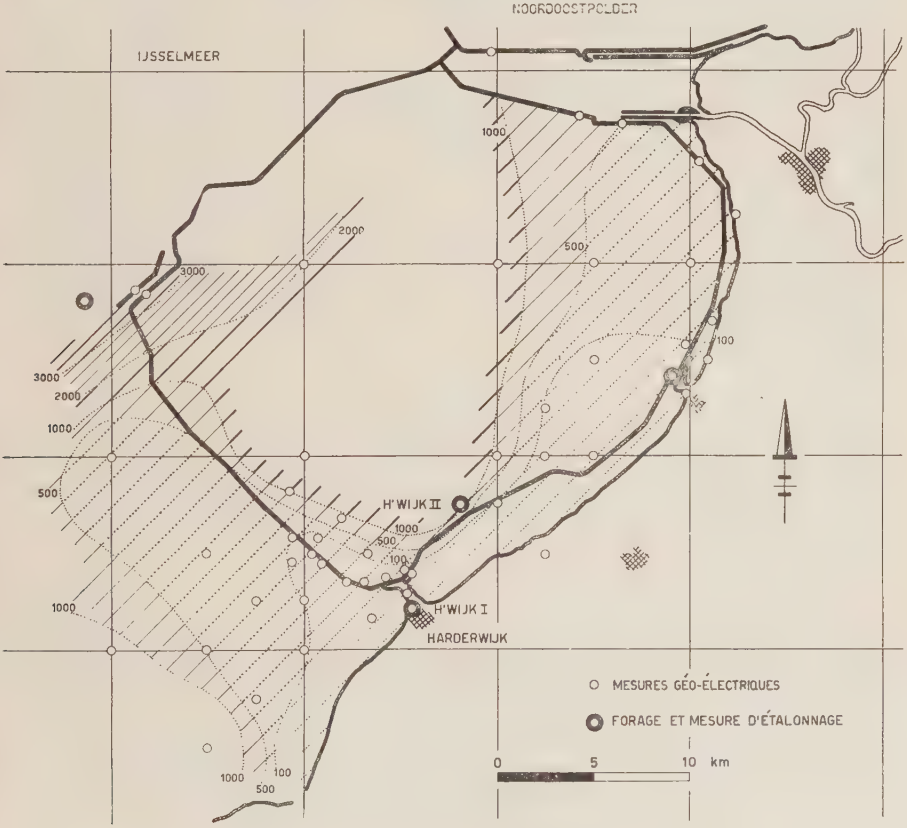

Fig. 9. Carte des moyennes des teneurs en chlore dans le paquet perméable (∾ 250 m). — Map showing the distribution of the chlorine concentrations in the permeable beds. (Averaged over approximately 250 m).

VI — Conclusion

L'application de la méthode géo-électrique pour certaines recherches hydrologiques est déjà bien connue, notamment pour le problème de la répartition des eaux douces et des eaux salées dans le sous-sol. Mais jusqu'ici les investigations se sont limitées à la recherche des lignes de séparation entre des eaux de salinité très différente.

Le présent article démontre qu'il est possible de déterminer aussi la teneur en sel elle-même et la répartition des couches dans le sous-sol avec des eaux de qualité différente. Pour cela il est indispensable de disposer d'une connaissance générale de la géologie du terrain ainsi que des résultats de quelques sondages de repère, donnant pour ces points une connaissance exacte de la composition chimique des eaux dans les pores.

Par des mesures géo-électriques à l'emplacement même de ces forages il est possible d'effectuer l'étalonnage du procédé en dressant un graphique de base pour la relation entre la résistivité électrique des formations en place et la teneur en sel des eaux dans les pores.

Enfin il a été démontré que des mesures en pleine mer ou dans les eaux d'un lac peuvent être réalisées à condition qu'on dispose d'un câble spécial.

L'initiative pour l'application de cette méthode économique a été prise par le Rijksinstituut voor Drinkwatervoorziening (Institut de l'État pour l'alimentation en eaux potables) à la Haye. Cet institut a mis les auteurs de cette communication en rapport avec M. J. Piket du Laboratoire Physique du Rijksverdedigingsorganisatie T.N.O. qui a fait construire les instruments nécessaires.

Nous nous acquittons volontier du devoir agréable de remercier M. Baars de la Bataafse Petroleum Maatschappij et M. Koefoed du Laboratoire de Géophysique de l'Université Technique à Delft, pour l'appui qu'ils ont bien voulu donner aux recherches.

Littérature

Klinkenberg, L. J., 1951 : Analogy between Diffusion and Electrical Conductivity in Porous Rocks, Bull. Geol. Soc. of America, 62, 559-564.

Sundberg, Karl, 1932 : Effect of Impregnating Waters on Electrical Conductivity of Soils and Rocks, Transactions Am. Inst. of Min. and Metall. Eng., Geoph. Prosp., 367-391.

Discussion

M. S. L. Astier : La Compagnie Générale de Géophysique a eu l'occasion de traiter en 1946 un problème assez semblable à celui qui vient de faire l'objet de l'intéressante communication de M. Volker. Il s'agissait de déterminer dans les sables dunaires de la presqu'île de Cap Vert les emplacements les plus favorables à l'établissement de nouveaux captages pour l'alimentation en eau douce de Dakar. Outre leur épaisseur, une campagne de sondages électriques a permis d'évaluer la résistivité des sables. A partir de cette résistivité on a pu tracer la limite de l'invasion de l'eau de mer vers l'intérieur des terres et indiquer des zones où l'eau d'imbibition des sables était très peu chargée en sels.

M. A. VOLKER : Il est connu depuis longtemps qu'il est possible de déterminer la ligne de séparation entre eaux douces et eaux salées par prospection géo-électrique.

Ce qu'il y a de nouveau dans la communication présentée c'est qu'elle démontre la possibilité de déterminer le degré de salinité, et même avec une certaine précision.

M. J. GOGUEL : Quelle est la résistivité des marnes tertiaires, sous les sables aquifères ? Avez-vous tenu compte, dans l'interprétation des sondages électriques, de leur influence, qui modifie la queue du profil ?

M. A. VOLKER : La résistivité des marnes tertiaires (dans lesquelles on trouve quelques couches de sable avec des salinités de quelques centaines de mg de Cl' par litre) avec des valeurs entre 9 et 60 Ohmmètres est plus petite ou parfois égale à la résistivité des couches de sable plistocènes.

La courbe des résistivités sera effectivement influencée par ces marnes, notamment en ce qui concerne la queue du profil.

Or, une comparaison entre les courbes déduites mathématiquement, les résultats des sondages et les courbes mesurées démontre que la partie supérieure de la courbe est à peine influencée par la troisième (et plus profonde) couche, de sorte qu'on peut considérer le problème comme le problème des deux couches.

KONSTRUKTIVE DARSTELLUNG VON SEISMISCHEN HORIZONTEN UNTER BERÜCKSICHTIGUNG DER STRAHLENBRECHUNG IM RAUM *

VON

J. BAUMGARTE **

Abstract

The paper describes a geometrical construction which allows the reflecting or refracting boundaries to be derived from seismic time observations.

In reflection work the construction makes use of the ray reflected from the boundary at normal incidence. For constant velocities of the beds, or for a linear increase of velocity with depth, the method leads to the construction of successive envelopes from which the reflecting interface and the rays are obtained. By using the idea of "stretching fictitious rays", the construction requires ruler and compasses only and is applicable to both plane and curved boundaries with any strike direction and in any number.

The same principles can be applied to refraction problems and again the construction of successive envelopes allows the indirect or Mintrop wave to be defined. The position of the refracting boundary and the velocity can be derived immediately. As in the reflection method any number of plane boundaries with any strike can be dealt with.

An appendix discusses the use of the method in reflection work with any type of velocity distribution.

Zusammenfassung

Es werden zeichnerische Verfahren zur Darstellung von Reflexions- und Refraktionshorizonten aus seismischen Laufzeitmessungen angegeben.

Die Konstruktionen der Reflexionsseismik verwenden stets die „seismischen Lote", d.h. die in sich reflektierten Strahlen. Für konstante Schichtgeschwindigkeiten und lineare Zunahme der Geschwindigkeit mit der Tiefe liefert schrittweises Tangieren die reflektierenden Horizonte sowie die gebrochenen Strahlenzüge. Die Einführung des „Prinzips der Streckung fiktiver Lotstrahlen" ermöglicht die Durchführung der Zeichnung nur mit Zirkel und Lineal, ohne Verwendung irgendwelcher Tafeln oder Nomogramme! Es lassen sich ebene und gekrümmte Horizonte beliebiger Streichrichtung und beliebiger Anzahl darstellen.

Die Konstruktionsprinzipien der Reflexionsseismik können für die Refraktionsseismik übernommen werden. Die Streckung fiktiver Lotstrahlen ermöglicht ein schrittweises Tangieren, das die Fronten der sogenannten indirekten oder Mintrop-Welle festlegt. Hieraus ergibt sich unmittelbar die Bestimmung der Refraktionshorizonte sowie der Schichtgeschwindigkeiten. Es lassen sich ebene Horizonte beliebiger Streichrichtung und beliebiger Anzahl darstellen.

---

* Doctors Thesis Bonn University. Part of this paper was presented at the Sixth Meeting of the European Association of Exploration Geophysicists, held in Copenhagen, 19/21 May 1954.

** Prakla G.m.b.H., Hannover, Germany.

Im Anhang wird kurz diskutiert, wie das Verfahren der sukzessiven Tangierung für die Reflexionsseismik auf allgemeine Geschwindigkeitsverteilungen erweitert werden kann.

INHALT

A. Einleitung 127

B. Konstruktive Darstellung von Reflexionshorizonten 129

1. Die Anfangsrichtung des Lotstrahls am Schusspunkt 129
2. Das Verfahren der sukzessiven Tangierung beim ebenen Problem . . . 131
3. Das Verfahren der sukzessiven Tangierung beim räumlichen Problem . . 134
4. Das Verfahren der Konstruktion in der Brechungsebene 142
5. Ein Beispiel falscher Konstruktion und einige Folgerungen hieraus . . . 145
6. Bemerkungen zur Konstruktion bei linearem Anstieg der Geschwindigkeit mit der Tiefe 147

C. Konstruktive Darstellung von Refraktionshorizonten 148

1. Behandlung des ebenen Falles durch sukzessive Tangierung von Fronten der Mintrop-Welle 148
2. Behandung des räumlichen Falles durch sukzessive Tangierung von Fronten der Mintrop-Welle in den Brechungsebenen 156

D. Anhang. Prinzipielle Bemerkungen zur Festlegung reflexions-seismischer Horizonte bei allgemeiner Geschwindigkeitsverteilung 158

Literatur 161

A. EINLEITUNG

Der Reflektionsseismik sind im Laufe der Zeit immer schwierigere Aufgaben gestellt worden. Eine zwangsläufige Folge hiervon war, dass auch die Auswertungs- und Konstruktionsmethoden verbessert werden mussten, um reflektierende Horizonte in Gebieten mit komplizierter Schollentektonik richtig darstellen zu können. Man war daher gezwungen, die Brechung der seismischen Strahlen zu berücksichtigen und so die Gesetze der geometrischen Optik auch in der geometrischen Seismik anzuwenden.

So lag es zuerst einmal nahe, in einem Untersuchungsgebiet mit einer Geschwindigkeitsverteilung zu rechnen, die nur eine Funktion der Tiefe z ist, also den Ansatz $v = v(z)$ zu machen. Es wurde die in einem Bohrloch gemessene Geschwindigkeitsverteilung als gültig für die Nachbarschaft derselben angenommen. Diese Verteilung wurde nun durch eine einfache mathematische Funktion angenähert, bei der der Strahlenweg rechnerisch oder zeichnerisch leicht darstellbar ist. In einer Arbeit von H. Kaufmann (1953) ist der Fall, dass die Geschwindigkeit im Messgebiet nur eine Funktion der Tiefe ist, eingehend behandelt worden.

Da aber die Reflexionshorizonte und damit die geologischen Schichten häufig stark geneigt sind, kann man mit einer Geschwindigkeitsfunktion $v = v(z)$ in vielen Fällen nicht rechnen.

Ist der Ansatz $v = v(z)$ nicht sinnvoll, so lässt sich jedoch folgendermassen verfahren: Man nimmt an, es sei eine Reihe verschiedener geologischer Schichten vorhanden und jede Schicht habe für sich eine konstante Schichtgeschwindigkeit; die Begrenzungsflächen der Schichten sind die Reflexionshorizonte.

Die Richtigkeit dieser Annahme haben die Bohrlochversenkungsmessungen weitgehend bestätigt.

Es ist nun Aufgabe der Reflexionsseismik, die Lage jeder Schichtgrenze aus der Kenntnis ihrer jeweiligen Reflexionszeiten und der gegebenen Schichtgeschwindigkeiten konstruktiv zu erfassen. Haben die Reflexionshorizonte alle gleiche Streichrichtung, wenn auch sonst verschiedene Neigung, so lässt sich dieses Problem relativ einfach behandeln. Weitaus schwieriger ist der allgemeine Fall, bei dem alle Reflexionshorizonte verschiedenes Streichen und Fallen im Raum haben, die Normalen dieser Horizonte also nicht komplanar sind. Mit diesem Problem haben sich bereits C. Dix und C. Lawler (1943) sowie H. Dürbaum (1953) und Th. Krey (1954) befasst. Dix und Lawler sowie Dürbaum entwickeln analytische Verfahren, deren Anwendung eine erhebliche Rechenarbeit und damit einen grossen Zeitaufwand verlangt. Krey beschreibt eine Näherungsmethode, die jedoch wenig befriedigende Ergebnisse liefert, wenn die reflektierenden Horizonte stärker gegeneinander geneigt sind. Demgegenüber behandelt die vorliegende Arbeit in Abschnitt B rein zeichnerische Verfahren, die sowohl unter den gemachten Voraussetzungen streng als auch in der praktischen Anwendung recht einfach sind. Die Dringlichkeit, ein Routineverfahren für die Darstellung von reflektierenden Horizonten ihrer räumlichen Lage nach zu finden, betonte kürzlich F. Romberg (1952) in einer Arbeit, die sich mit der Anwendung der Reflexionsseismik beim Kartieren von Verwerfungen befasst. Er führt dort unter anderem aus:

„Failure to measure wave front direction can be dealt with by shooting a cross-spread of some sort, but taking dip information fully into account in interpretation is more difficult. To-date, there exists no method for complete three-dimensional study of seismic information which is not too cumbersome for everyday use, though the ordinary subsurface map, with its fault blocks tilted in all directions, makes the need for such a method obvious. This is one of the frontiers of practical geophysics; an indeterminate improvement in daily work would surely result if a good way to treat three-dimensional data thoroughly were invented. It is the author's opinion that the art has lagged farther behind the potentialities of available technique in this matter than anywhere else in the industry."

Die in Abschnitt B entwickelten Verfahren zur Darstellung von Reflexionshorizonten beruhen auf sehr einfachen Konstruktionsprinzipien, deren Anwendungsmöglichkeit hiermit noch nicht erschöpft ist. Vielmehr wird in Abschnitt C gezeigt, dass sie sich nach leichter Modifikation auch für eine rein zeichnerische Behandlung der Refraktionsseismik verwenden lassen. Eine solche Behandlung bietet folgende Vorteile:

1) sie ist für den zweidimensionalen Fall einfacher als die übliche rechnerische,

2) sie lässt sich ohne grosse Schwierigkeit auf den dreidimensionalen Fall ausdehnen, der wegen seiner Kompliziertheit bisher ausser Betracht geblieben ist,

3) sie liefert überdies direkt die Front der Mintrop-Welle.

Damit ist dann eine weitgehend einheitliche konstruktive Darstellung von seismischen Horizonten unter Berücksichtigung der Strahlenbrechung im Raum erreicht, und zwar sowohl für die Reflexions- als auch die Refraktionsseismik.

B. Konstruktive Darstellung von Reflexionshorizonten

1. *Die Anfangsrichtung des Lotstrahls am Schusspunkt*

Wesentlich für alle Betrachtungen in der vorliegenden Arbeit ist die Festlegung der Anfangsrichtung der Lotstrahlen vom Schusspunkt zu einzelnen reflektierenden Horizonten. Es ist hierauf schon mehrfach in der Literatur eingegangen worden (z.B.: M. M. Slotnick (1936), C. Dix und C. Lawler (1943), H. Dürbaum (1953).

Im folgenden soll die Bestimmung dieser Anfangsrichtung nochmals durch eine physikalische Überlegung abgeleitet werden, die für alle späteren Ausführungen grundlegend ist. Hierbei wird aus Gründen der Einfachheit von speziellen Voraussetzungen ausgegangen, die jedoch für die angewandte Seismik von grosser Bedeutung sind und gleichzeitig für allgemeine Fälle den Ausgangspunkt der Behandlung bilden:

In der Erdkruste seien n reflektierende Horizonte $H_1, H_2 \dots H_n$ vorhanden, die Ebenen seien. Die Fortpflanzungsgeschwindigkeit der seismischen Impulse in der ersten Schicht, also zwischen der Oberfläche und dem ersten Horizont, sei v_1; sie sei v_2 in der zweiten Schicht zwischen H_1 und H_2; u.s.w. ... Alle Schichtgeschwindigkeiten v_i seien jeweils konstant und es gelte für jedes $i: v_i \neq v_{i+1}$. Auf der horizontal gedachten Oberfläche, die auch als Messebene bezeichnet wird, seien aus den Seismogrammen die Laufzeiten $T_1, T_2, \dots T_n$ der seismischen Impulse entlang den seismischen Loten, d.h. entlang den in sich reflektierten seismischen Strahlen zu den einzelnen Horizonten $H_1, H_2, \dots H_n$ bekannt. Hiernach ist $T_i = T_i\ (S)$ — $i = 1, 2, \dots, n$ — die Laufzeit der Impulse auf den doppelt durchlaufenen „Lotstrahlen" zum Horizont H_i, also vom Schusspunkt S in der Messebene zum reflektierenden Horizont und dann auf dem gleichen Wege zurück zur Messebene. Diese Zeiten $T_i = T_i\ (S)$ werden im folgenden als „Lotzeiten" des jeweiligen Horizontes H_i bezeichnet. In der Messebene lässt sich somit zu jedem Horizont H_i der zugehörige Isochronenplan $T_i = \text{const}$ angeben.

Es sei noch besonders hervorgehoben, dass die Ebenen $H_1, H_2, \dots, H_n$ beliebig gegenüber der Messebene gelegen sein können, allerdings mit der naturgemässen Einschränkung, dass von der jeweiligen Messstelle aus zu jedem Horizont überhaupt seismische Lote existieren. Die Lotstrahlen zum Horizont H_i werden an den Horizonten $H_1, H_2, \dots, H_{i-1}$ nach dem Brechungsgesetz von Snellius gebrochen. Sie bestehen also in Anbetracht unserer Voraussetzungen aus Streckenzügen, die nur dann alle in einer Ebene liegen, wenn die Horizonte gleiche Fallrichtung besitzen.

Es soll nun die Frage behandelt werden, welche Anfangsrichtung die Lotstrahlen zum Horizont H_i $(1 \leq i \leq n)$ in den Punkten der Messebene besitzen. Hierzu werde folgende physikalische Überlegung angestellt:

Zur Zeit $\tau = 0$ gehe vom Horizont H_i eine ebene Welle aus, deren Front mit H_i zusammenfalle. Die Welle laufe mit der Geschwindigkeit v_i zum Horizont H_{i-1}, werde hier gebrochen, laufe mit der Geschwindigkeit v_{i-1} weiter bis zum nächst höheren Horizont, u.s.w. Die Wellenfront ist zu Beginn der Bewegung eben. Sie bleibt es in jeder Schicht, da die Schichtgeschwindigkeiten als jeweils konstant und die Horizonte als Ebenen vorausgesetzt waren. Sie tritt also auch als ebene Welle an der Messebene zutage. Auf den Wellenfronten stehen die Wellenstrahlen senkrecht. Da bei Beginn der Bewegung die Wellenfront mit H_i zusammenfällt, sind gerade die seismischen Lotstrahlen auf H_i Wellenstrahlen unserer ebenen Welle, und zwar auf ihrem gesamten Wege von H_i bis zum Erreichen der Messebene. Gelangt die Welle zu einem Punkt der Messebene, so ist ihre Laufzeit demnach $\tau = \frac{1}{2} T_i$, wobei T_i die Lotzeit des Isochronenplanes für diesen Punkt ist. Die Front einer Welle besteht aus Punkten, in denen die Erregung gleichzeitig ankommt. Daher sind die Isochronen $T_i = \text{const}$ die Schnittlinien unserer Wellenfronten mit der Messebene zur Zeit $\tau = \frac{1}{2} T_i$. Da die Wellenfronten in der ersten Schicht Ebenen sind, die sich in Richtung ihrer Normalen mit der konstanten Geschwindigkeit v_1 fortpflanzen, sind somit die Isochronen

1) parallele Geraden,
2) für konstantes Zeitintervall gleichabständig.

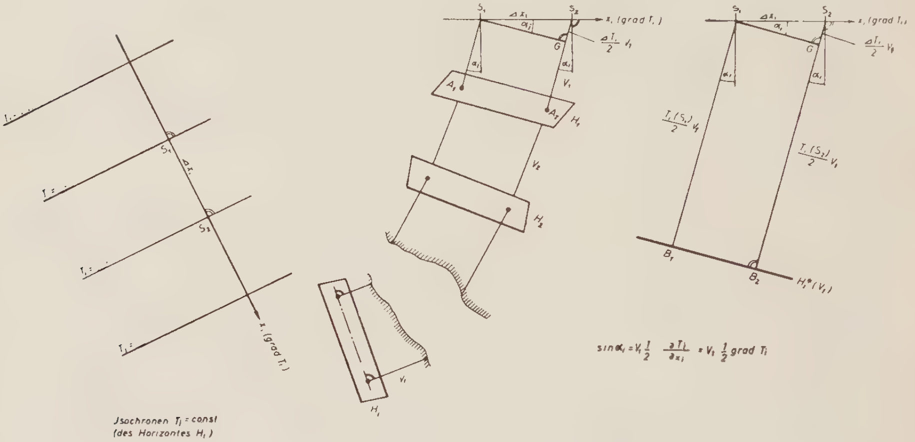

Fig. 1. Festlegung der Anfangsrichtung des Lotstrahles zum wahren Horizont H_i durch Konstruktion des fiktiven Horizontes $H_i^* (v_1)$. — Determination of the direction of emergence of a ray normal to the true interface H_i by constructing a fictitious interface $H_i^* (v_1)$.

Man denke sich nun die zum Horizont H_i gehörigen Isochronen gegeben;

dann ist nach Fig. 1 a-c aus den Isochronen und ihren Abständen die Richtung des Wellenstrahles in jedem Punkte der Messebene bestimmbar. Suchen wir z.B. die Strahlrichtung im Punkte S_1 der Messebene (Fig. 1 a), so lässt sich zunächst sagen, dass der Strahl in einem vertikalen Schnitt zur Messebene liegt, der durch den Punkt S_1 senkrecht zu den Isochronen $T_i = \text{const}$ entlang der x_i-Richtung geführt ist. Dieser Vertikalschnitt ist in dem oberhalb H_1 gelegenen Teil der Fig. 1 b dargestellt. Die Erregung ist in S_1 auf dem zugehörigen Strahl A_1S_1 zur Zeit $\tau = \frac{1}{2}\, T_i\,(S_1)$ eingetroffen. Zur gleichen Zeit hat sie auf dem zu A_1S_1 parallelen Strahl A_2S_2 den Punkt G erreicht. Es ist also S_1G der Schnitt der ebenen Wellenfront mit der Vertikalebene. Da die Erregung sich mit der Geschwindigkeit $v_1 = \text{const}$ in der ersten Schicht (oberhalb H_1) entlang des Strahles auf die Messebene hin bewegt, gilt

$$S_2\,G = \tfrac{1}{2}\,\Delta\,T_i\,v_1 = \tfrac{1}{2}\,\{T_i\,(S_2) - T_i\,(S_1)\}\,v_1$$

Hieraus ergibt sich für den Winkel α_i aus dem rechtwinkligen Dreieck S_1GS_2 die Beziehung

$$\sin\,\alpha_i = \Delta\,T_i\,v_1\,/\,2\,\Delta\,x_i$$

Diese Formel besagt, dass der Inzidenzwinkel α_i der Lotstrahlen zum Horizont H_i nur von der gemessenen Lotzeitverteilung T_i und der Geschwindigkeit v_1 in der ersten Schicht abhängt[1]. Damit ergibt sich sofort folgende einfache Konstruktion der Strahlrichtung im oberen Medium, die in Fig. 1 c veranschaulicht wird:

Man tangiere in üblicher Weise von S_1 und S_2 aus mit Verwendung der halben T_i-Zeiten und der Geschwindigkeit v_1; man tut also zunächst so, als ob in der Tiefe nur ein einheitliches Medium der konstanten Geschwindigkeit v_1 vorhanden wäre. Der erhaltene Horizont $H_i^*\,(v_1)$ hat für $i > 1$ keine reale Bedeutung, er werde daher als fiktiver Horizont bezeichnet. Jedoch treffen seine Lotstrahlen S_1B_1 bzw. S_2B_2 mit dem gesuchten Inzidenzwinkel α_i auf die Messebene; denn nach Konstruktion ist S_2G gleich $\frac{1}{2}\,\Delta\,T_i\,v_1$ wie in Fig. 1 b. Für $i = 1$ gilt offenbar $H_1^*\,(v_1) = H_1$.

Die Konstruktion des fiktiven Horizontes $H_i^*\,(v_1)$ legt also die Anfangsrichtung des wahren Lotstrahles zum Horizont H_i fest, und zwar zwischen der Messebene und dem ersten reflektierenden Horizont H_1; an letzterem findet die erste Brechung der Lotstrahlen zu den Horizonten H_i $(i > 1)$ statt.

2. *Das Verfahren der sukzessiven Tangierung beim ebenen Problem*

Die soeben eingeführte Konstruktion eines fiktiven Horizonts hat noch eine weitere wesentliche Bedeutung. Sie ermöglicht nämlich die rein zeichnerische Festlegung von reflektierenden Horizonten durch sukzessives Tangieren. Zur Erläuterung dieses Verfahrens diene ein einfaches Beispiel, und zwar ein ebenes Dreischichtenproblem. Es wird also vorausgesetzt, dass die drei Reflexionshorizonte gleiche Streichrichtung haben. Man konstruiert dann üblicherweise in einer zur Oberfläche vertikalen Ebene, die senkrecht zur allgemeinen Streichrichtung liegt. Sie ist die gemeinsame Brechungsebene sämtlicher von der Profillinie an der Oberfläche ausgehenden Strahlen.

---

[1] Diese Aussage gilt auch unter wesentlich allgemeineren Voraussetzungen; vgl. hierzu Anhang.

Zunächst seien die reflektierenden Horizonte Ebenen und die Schichtgeschwindigkeiten jeweils konstant. Es sei für diesen Fall in Fig. 2 das Schussprofil S_1S_2 senkrecht zum Streichen orientiert. Dann erscheinen im Zeitplan die Laufzeiten T_1, T_2 und T_3 entlang der seismischen Lote auf die Horizonte H_1, H_2 und H_3 als Geraden. Aus den gemessenen Lotzeiten T_1, T_2 und T_3 sowie den bekannten Geschwindigkeiten v_1, v_2 und v_3 ist die Lage der drei Horizonte zu ermitteln.

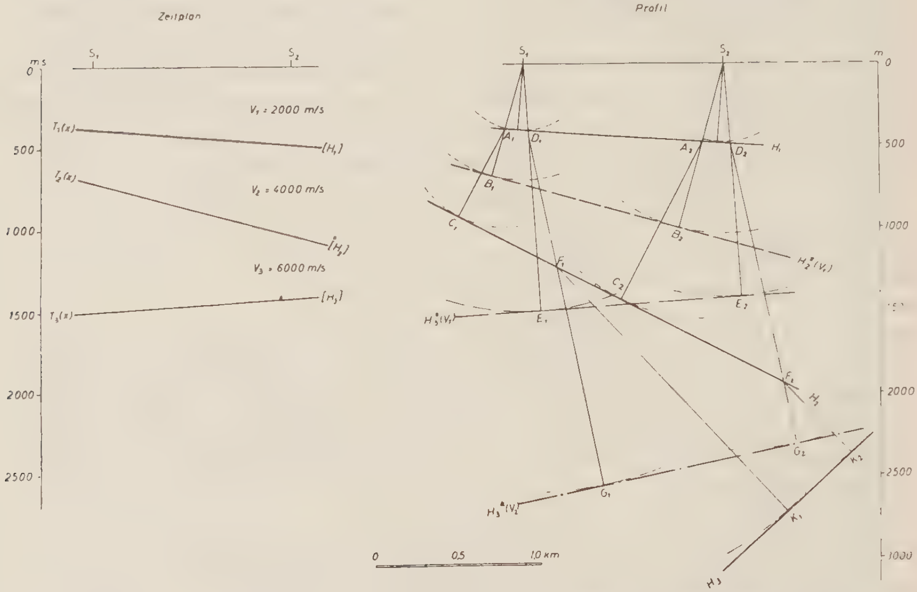

Fig. 2. Sukzessive Tangierung von drei ebenen Horizonten gleicher Streichrichtung. — Successive envelopes for three plane interfaces having the same strike direction.

Die Konstruktion erfolgt von den Schusspunkten S_1 und S_2 aus. Der Horizont H_1 wird wie üblich durch Tangieren gezeichnet, und zwar mit Verwendung der Geschwindigkeit v_1 und der halben Lotzeit $\frac{1}{2}\ T_1$ in S_1 bzw. S_2.

Um nun den Inzidenzwinkel der Lotstrahlen zum zweiten Horizont festzulegen, tangiert man gemäss dem vorigen Abschnitt B, 1 von S_1 bzw. S_2 mit den halben Lotzeiten $\frac{1}{2}\ T_2$ und der Geschwindigkeit v_1 in der ersten Schicht einen fiktiven Horizont $H_2{}^*$ (v_1). Er ist die Tangente B_1B_2. Nach dieser Konstruktion sind die Strecken S_1A_1 bzw. S_2A_2 bereits richtige Teile der seismischen Lote von S_1 bzw. S_2 auf den Horizont H_2. An den Punkten A_1 und A_2 auf dem Horizont H_1 setzt die Brechung ein. Wir betrachten nun den Horizont H_1 als neue Oberfläche und die Punkte A_1 und A_2 als neue Schusspunkte.

In diesen Punkten ist uns die Restlaufzeit T_r zum wahren Horizont H_2 bekannt. Sie beträgt für den einfachen Weg

$$T_r(A_1) = A_1B_1 / v_1\,;\; T_r(A_2) = A_2B_2 / v_1$$

Zur Bestimmung der wahren Lotentfernungen von A_1 bzw. A_2 zum zweiten Horizont sind diese Restzeiten mit der Geschwindigkeit v_2 des zweiten Mediums zu multiplizieren; d.h.:

Man multipliziert die Reststrecken A_1B_1 bzw. A_2B_2 der Lote auf den fiktiven Horizont $H_2^*(v_1)$ mit dem Verhältnis v_2/v_1 und bekommt so die Strecken A_1C_1 bzw. A_2C_2, mit denen man von A_1 bzw. A_2 aus tangieren muss, um den wahren Horizont H_2 festzulegen.

Es waren von den Loten S_1B_1 bzw. S_2B_2 auf den fiktiven Horizont $H_2^*(v_1)$ bereits die Teile S_1A_1 bzw. S_2A_2 physikalisch reell, jedoch die Reste A_1B_1 bzw. A_2B_2 nicht; diese sind nunmehr durch die Streckung im Verhältnis v_2/v_1 ebenfalls physikalisch reell geworden.

Sind die Horizonte H_1 und H_2 in der geschilderten Weise festgelegt, so erfolgt die Konstruktion des dritten Horizontes in drei Schritten. Beim ersten Schritt tangiert man von S_1 bzw. S_2 aus wieder mit der Geschwindigkeit v_1, jedoch gemäss Abschnitt B, 1 mit der halben Lotzeit $\frac{1}{2}\,T_3$ und erhält so den fiktiven Horizont $H_3^*(v_1)$.

Von den Strahlen S_1E_1 bzw. S_2E_2 gehören die Stücke S_1D_1 und S_2D_2 bereits zu den wahren Lotstrahlen von S_1 bzw. S_2 auf den dritten Horizont H_3. Für den zweiten Schritt werden die Reststrecken D_1E_1 und D_2E_2, die wieder physikalisch nicht reell sind, mit dem Quotienten v_2/v_1 gestreckt. Die so erhaltenen Längen sind D_1G_1 bzw. D_2G_2, mit denen um die Punkte D_1 bzw. D_2 tangiert wird; damit liegt der fiktive Horizont $H_3^*(v_2)$ fest. Von den Strahlen D_1G_1 bzw. D_2G_2 gehören die Stücke D_1F_1 bzw. D_2F_2 vom ersten zum zweiten Horizont wiederum zu den wahren Lotstrahlen von den Punkten S_1 bzw. S_2 zum Horizont H_3. Für den dritten Schritt werden die noch verbleibenden, physikalisch nicht reellen Reststrecken F_1G_1 bzw. F_2G_2 mit dem Quotienten v_3/v_2 gestreckt. Es ergeben sich die Strecken F_1K_1 bzw. F_2K_2, mit denen um F_1 bzw. F_2 tangiert wird, womit der wahre Horizont H_3 bestimmt ist.

Es ist hiernach evident, dass beim ebenen n-Schichten-Problem für die Konstruktion des n-ten Horizontes H_n notwendig ist, dass

1) die Horizonte H_1, H_2 bis H_{n-1} bereits festgelegt sind und

2) $(n-1)$ fiktive Horizonte $H_n^*(v_i)$, $i = 1, 2, \ldots, n-1$, gezeichnet werden müssen. Dann erst kann der wahre Horizont H_n festgelegt werden.

Das Verfahren ist ohne weiteres auch auf gekrümmte Horizonte gleicher Streichrichtung anwendbar, wenn die Geschwindigkeiten zwischen den Horizonten konstant sind. Bei der Konstruktion muss nur von genügend vielen, nicht zu weit voneinander entfernten Schusspunkten ausgegangen werden. Fig. 3 zeigt den Zeitplan und das zugehörige Konstruktionsprofil, bei dem von acht Schusspunkten aus konstruiert wird.

Wesentlicher Bestandteil des dargelegten Verfahrens ist offenbar das Prinzip, die physikalisch nicht reellen Anteile der „seismischen Lote" zu einem fiktiven Horizont mit den Quotienten zweier Geschwindigkeiten zu strecken. Es wird auch bei den Konstruktionsverfahren für räumliche Probleme, die hier entwickelt werden sollen, eine wesentliche Rolle spielen. Daher werde dieses Prinzip[2] als „Streckung fiktiver Lotstrahlen" gesondert benannt. Typisch für die geschilderte Konstruktion ist das schrittweise Tangieren mit Verwendung von Radien, die sich durch Streckung fiktiver Lotstrahlen ergeben. Die Konstruktion möge daher als „Verfahren der sukzessiven Tangierung" bezeichnet werden. Es ist bisher der Anschaulichkeit wegen für den sogenannten „ebenen Fall" erläutert worden. Jedoch lässt es sich auf den räumlichen Fall erweitern, dem wir uns nun zuwenden wollen.

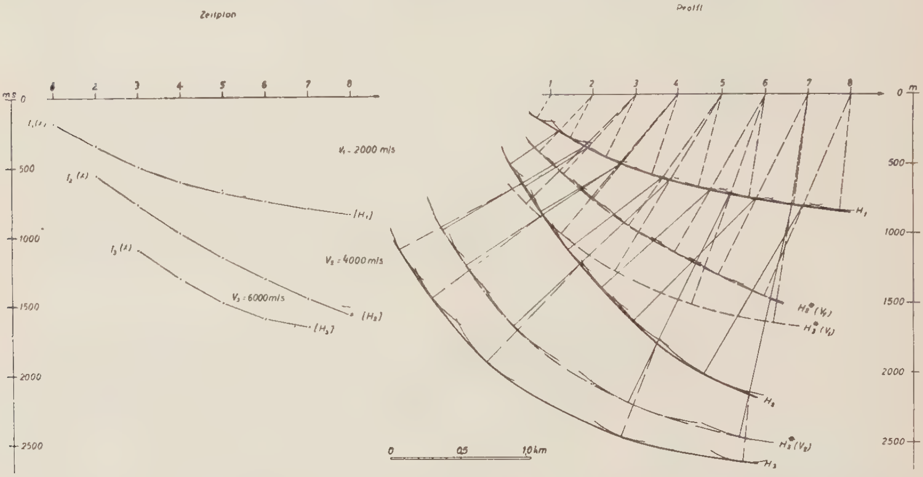

Fig. 3. Sukzessive Tangierung von drei gekrümmten Horizonten gleicher Streichrichtung. — Successive envelopes for three curved interfaces having the same strike direction.

3. *Das Verfahren der sukzessiven Tangierung beim räumlichen Problem*

Im räumlichen Fall haben die reflektierenden Horizonte jeweils verschiedene Streich- und damit auch Fallrichtungen. Die Konstruktion erfolgt naturgemäss nicht von einem einzigen Profil aus, sondern von mehreren. Ausgangspunkt ist eine flächenmässige Darstellung der Lotzeiten in der horizontalen Messebene, die als T-Isochronenplan bezeichnet wird. Die Isochronenscharen $T_1 = \text{const}$, $T_2 = \text{const}$ bis $T_n = \text{const}$ für die einzelnen Horizonte H_1, H_2 bis H_n sind nun nicht mehr untereinander parallel, wie es beim ebenen Problem der Fall ist.

---

[2] Ein ähnliches Prinzip benutzen auch Dienesch und Richard (1953) bei der Behandlung der Spiegelkonstruktion ebener Mehrschichten-Probleme mit Berücksichtigung der Brechung. Die Anwendung desselben ist jedoch relativ kompliziert, da für die Bestimmung der Brechungswinkel die Verwendung spezieller Diagramme notwendig ist.

Das Konstruktionsverfahren soll an einem einfachen Zweischichten-Problem erläutert werden. Fig. 4 zeigt die Isochronen $T_1 = \text{const}$ bzw. $T_2 = \text{const}$ der beiden reflektierenden Horizonte H_1 bzw. H_2. Die Isochronen sind jeweils untereinander parallel und für gleiches T-Intervall gleichabständige Geradenscharen. Die Geschwindigkeiten v_1 und v_2 seien wiederum konstant. Damit steht fest, dass die reflektierenden Horizonte H_1 und H_2 Ebenen sein müssen. Ihre Streichrichtungen fallen aber nicht zusammen, da die beiden Isochronenscharen nicht parallel zueinander verlaufen. In dem Isochronenplan sind noch zwei Schussprofile I und II eingetragen, auf denen eine reflexionsseismische Messung erfolgt sein könnte.

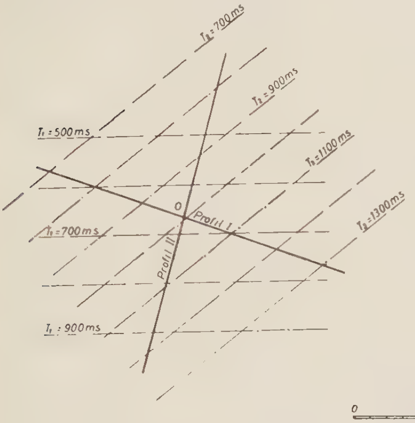

$T_1 = 500$ ms ... 900 ms: Isochronen des ersten Horizontes H_1. — Isochrones of the first interface H_1.
$T_2 = 700$ ms ... 1300 ms: Isochronen des zweiten Horizontes H_2. — Isochrones of the second interface H_2.

Fig 4. Isochronen zweier ebener Horizonte H_1 und H_2 verschiedener Streichrichtung. — Isochromnes for two plane interfaces H_1 and H_2 having different strike direction.

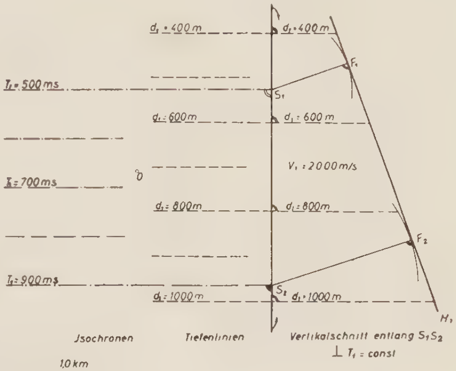

$T_1 = 500$ ms ... 900 ms: Isochronen des Horizontes H_1. — Isochrones of the interface H_1.
$d_1 = 400$ m ... 1000 m: Tiefenlinien des Horizontes H_1. — Depth Lines of the interface H_1.

Fig. 5. Konstruktion des wahren Horizontes H_1. — Construction of the true interface H_1. face H_1.

Die Festlegung des ersten Horizontes H_1 geschieht in Fig. 5 wie in dem bereits behandelten ebenen Fall. Man lege ein Konstruktionsprofil S_1S_2 senkrecht zu den Isochronen $T_1 = \text{const}$, d.h. man betrachte einen Vertikalschnitt zur Mess- bzw. Zeichenebene entlang S_1S_2. Im rechten Teil der Fig. 5 ist dieser Vertikalschnitt um S_1S_2 in die Zeichenebene geklappt. Die beiden Pfeile oberhalb und unterhalb dieser Zeichnung sollen die Klappung andeuten. Die Tangierung von S_1 bzw. S_2 mit den zugehörigen halben T_1-Werten und v_1 liefert die wahre Lage des Horizontes H_1 innerhalb dieses Schnittes. Ihm entnimmt man die wahren Tiefen des Horizontes H_1, d.h. die Tiefenlinien

d_1 = const (des mittleren Teiles der Fig. 5). Isochronen und Tiefenlinien sind getrennt voneinander gezeichnet, um klar hervortreten zu lassen, dass sie jeweils parallele und gleichabständige Geradenscharen sind, die natürlich auch zueinander parallel laufen.

Nun erfolgt die Konstruktion des zweiten reflektierenden Horizontes H_2 unter Berücksichtigung der Tatsache, dass die Lotstrahlen zum Horizont H_2 am ersten Horizont H_1 gebrochen werden. Für die Durchführung dieser Konstruktion benötigt man die soeben bestimmten Tiefenlinien des ersten Horizontes und die Lotzeiten T_2 zum zweiten Horizont. Es sind daher in Fig. 6 die Parallelenscharen d_1 = const bzw. T_2 = const zusammengezeichnet. Analog

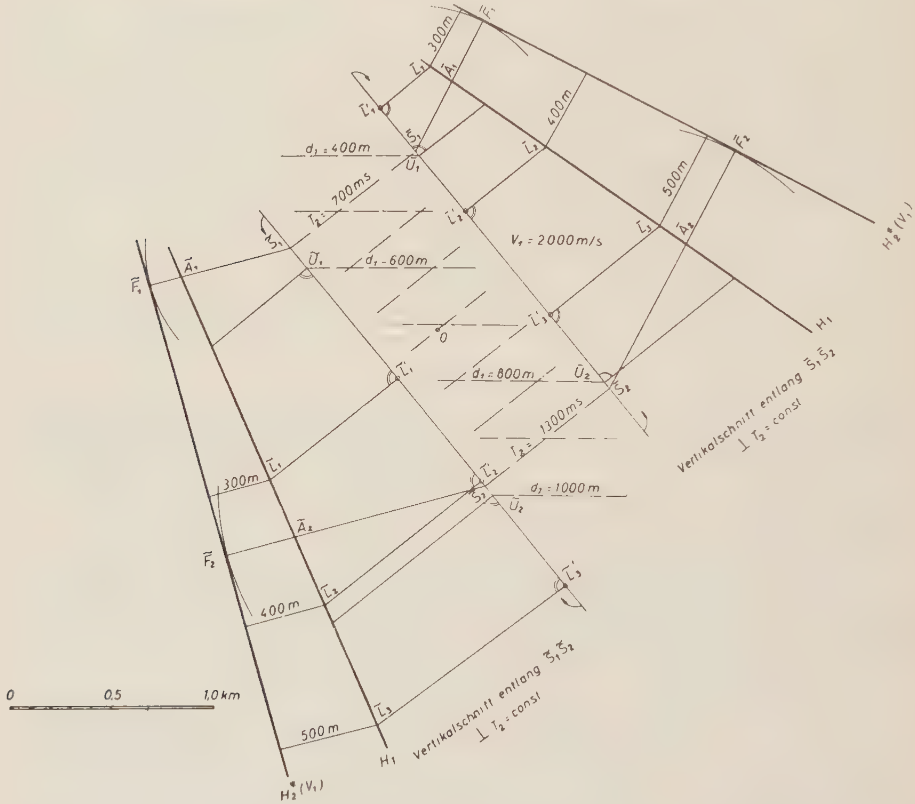

d_1 = 400 m ... 1000 m: Tiefenlinien des Horizontes H_1. — Depth lines of the interface H_1.
T_2 = 700 m ... 1300 m: Isochronen des Horizontes H_2. — Isochrones of the interface H_2.

Fig. 6. Konstruktion des fiktiven Horizontes $H_2^*(v_1)$ und Bestimmung der Lotentfernungen vom wahren Horizont H_1 zum wahren Horizont H_2. — Construction of the fictitious interface $H_2^*(v_1)$ and determination of the normal distances from the true interface H_1 to the true interface H_2.

zu dem bereits behandelten ebenen Fall lässt sich auch beim räumlichen Problem über die Lotstrahlen zum zweiten Horizont H_2 folgendes sagen:

1) Die Strahlen verlaufen oberhalb des ersten Horizontes H_1 in Vertikalschnitten zur Messebene, die senkrecht zu den Isochronen $T_2 = \text{const}$ geführt sind und

2) der Inzidenzwinkel der Strahlen hängt nur ab von der Geschwindigkeit v_1 oberhalb des Horizontes H_1 und den Lotzeiten T_2 in der Messebene, jedoch nicht von der Geschwindigkeit v_2 zwischen den Horizonten H_1 und H_2 und auch nicht von der räumlichen Lage des Horizontes H_1.

Die Spuren von zwei solchen Vertikalschnitten senkrecht zu den Isochronen $T_2 = \text{const}$ (Fig. 6) sind die Profillinien $\tilde{S}_1\tilde{S}_2$ bzw. $\bar{S}_1\bar{S}_2$. Die Vertikalschnitte sind um ihre Spuren in die Mess- bzw. Zeichebene geklappt. In ihnen lässt sich mit Hilfe der Tiefenlinien $d_1 = \text{const}$ jeweils der Schnitt mit dem ersten Horizont H_1 festlegen; z.B. liegt dieser Horizont 600 m unter dem Punkt $\tilde{U}_1$, 1000 m unter $\tilde{U}_2$ bzw. 400 m unter $\bar{U}_1$ und 800 m unter $\bar{U}_2$. Um nun die Lotstrahlen zum Horizont H_2 oberhalb H_1 festzulegen, tangiert man analog zum ebenen Fall von $\tilde{S}_1$ und $\tilde{S}_2$ bzw. $\bar{S}_1$ und $\bar{S}_2$ aus mit Verwendung von v_1 und $\frac{1}{2} T_2$; es ergibt sich so der fiktive Horizont $H_2{}^* (v_1)$. Vom Strahl $\tilde{S}_1\tilde{F}_1$ auf $H_2{}^* (v_1)$ ist das Stück $\tilde{S}_1\tilde{A}_1$ zwischen der Oberfläche und dem ersten Horizont bereits Teil des wahren Lotstrahles von $\tilde{S}_1$ zum Horizont H_2. Der wahre Lotstrahl wird im Punkte $\tilde{A}_1$ gebrochen und läuft zwischen H_1 und H_2 nicht mehr in dem betrachteten Vertikalschnitt. Entsprechendes gilt für die Strahlen $\tilde{S}_2\tilde{F}_2$, $\bar{S}_1\bar{F}_1$ und $\bar{S}_2\bar{F}_2$ und deren Anteile oberhalb des Horizontes H_1.

Man kann aber eine Aussage über die wahre Länge des Lotes vom Punkt $\bar{A}_1$ zum wahren zweiten Horizont H_2 machen. Diese Lotentfernung ergibt sich nämlich aus der Strecke $\bar{A}_1\bar{F}_1$ durch Streckung mit dem Quotienten v_2/v_1. Entsprechendes gilt für die Punkte $\bar{A}_2$, $\tilde{A}_1$ und $\tilde{A}_2$ sowie für jeden Punkt auf den Geraden durch $\bar{A}_1$, $\bar{A}_2$ bzw. $\tilde{A}_1$, $\tilde{A}_2$. So kann man z.B. von dem Punkt $\bar{L}_1$ in dem Vertikalschnitt $\bar{S}_1\bar{S}_2$ und von dem Punkt $\tilde{L}_1$ im Vertikalschnitt $\tilde{S}_1\tilde{S}_2$ sagen, dass ihre Lotentfernung zum wahren Horizont H_2 gleich $(v_2/v_1) \cdot$ 300 m ist, denn ihre fiktiven Lotstrahlen zwischen H_1 und dem fiktiven Horizont $H_2{}^* (v_1)$ haben die Länge 300 m. Ebenso ist für die Punkte $\bar{L}_2$ und $\tilde{L}_2$ die Lotentfernung $(v_2/v_1) \cdot 400$ m, schliesslich für die Punkte $\bar{L}_3$ und $\tilde{L}_3$ die Lotentfernung $(v_2/v_1) \cdot 500$ m.

Denken wir uns nun die Vertikalschnitte in ihre wahre räumliche Lage zurückgeklappt und z.B. durch das letztgenannte Punktepaar $\bar{L}_3$, $\tilde{L}_3$ eine Gerade gelegt, so lässt sich folgendes sagen:

1) Die Gerade liegt selbstverständlich im ebenen Horizont H_1,

2) alle ihre Punkte besitzen die gleiche Lotentfernung $(v_2 / v_1) \cdot 500$ m von Horizont H_2.

Entsprechendes gilt für die Geraden durch die beiden anderen Punktepaare $\bar{L}_1$, $\tilde{L}_1$ bzw. $\bar{L}_2$, $\tilde{L}_2$. Offenbar müssen diese drei Geraden jeweils gleicher Lotentfernung parallel und gleichabständig sein, denn die Horizonte sind eben und die Entfernungsintervalle einander gleich. Diese Eigenschaft der genannten Geraden bleibt bei senkrechter Projekten derselben auf die Messebene erhalten. Um die Projektionen in unserem Bild zu finden, braucht man nur die 3 Punktepaare jeweils gleicher Lotentfernung $\bar{L}_1$, $\tilde{L}_1 - \bar{L}_2$, $\tilde{L}_2 - \bar{L}_3$, $\tilde{L}_3$ in den umgeklappten Vertikalschnitten an die Oberfläche zu projizieren. Es ergeben sich so die Punktepaare $\bar{L}'_1$, $\tilde{L}'_1 - \bar{L}'_2$, $\tilde{L}'_2 - \bar{L}'_3$, $\tilde{L}'_3$ [3], die in Fig. 7 ge-

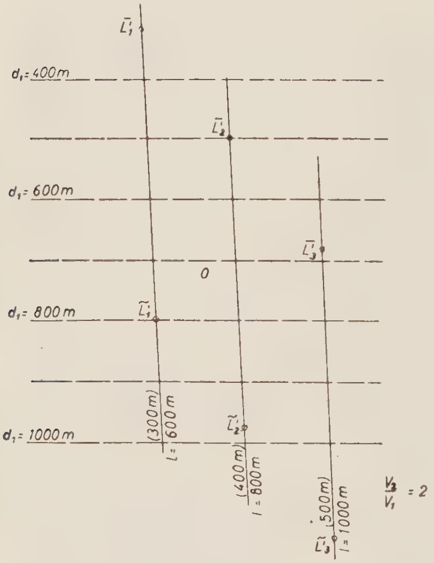

$d_1 = 400$ m...1000 m: Tiefenlinien des Horizontes H_1. — Depth lines of the interface H_1.
$l = 600$ m...1000 m: Linien gleicher Lotentfernung von H_1 zu H_2. — Lines of equal normal distance from H_1 to H_2.

Fig. 7. Tiefenlinien der Horizonte H_1 und auf die Messebene projizierte Linien gleicher Lotentfernungen von H_1 zu H_2. — Depth lines of the interface H_1 and projections on the plane of measurement of the lines of equal normal distance from H_1 to H_2.

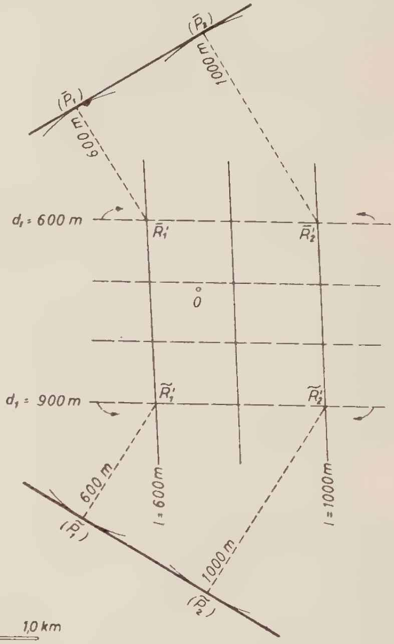

$d_1 = 600$ m...900 m: Tiefenlinien des Horizontes H_1. — Depth lines of the interface H_1.
$l = 600$ m...1000 m: Linien gleicher Lotentfernung von H_1 zu H_2. — Lines of equal normal distance from H_1 to H_2.

Fig. 8. Achsenschnitte der Kegel, deren Achsen die Tiefenlinien von H_1 sind. — Axial sections of the cones, the axes of which are the depth lines of H_1.

---

[3] Im folgenden wird stets die zu einem im Raume liegenden Punkt P gehörende Projektion auf die Messebene mit P' bezeichnet.

sondert gezeichnet sind; die Geraden durch diese Punktepaare sind parallel und gleichabständig, wie es sein muss.

In Fig. 7 sind ausser den auf die Messebene projizierten Linien gleicher Lotentfernung noch die Tiefenlinien des ersten Horizontes gezeichnet. Beide Scharen von parallelen Geraden stehen nahezu senkrecht aufeinander; diese Tatsache ist durch die spezielle Wahl unseres Beispiels begründet, sie hat also keine allgemeine Bedeutung. Die Schnittpunkte der beiden Parallelenscharen dienen der weiteren Konstruktion.

In Fig. 8 sind die Schnittpunkte $\bar{R}'_1$, $\bar{R}'_2$ sowie $\tilde{R}'_1$, $\tilde{R}'_2$ gewählt; diese liegen also in der Messebene. Da z.B. $\tilde{R}'_1$ auf der Tiefenlinie $d_1 = 600$ m liegt, befindet sich der zugehörige Punkt $\bar{R}_1$ in 600 m Tiefe auf dem ersten Horizont; dieser Punkt hat vom zweiten Horizont die Lotentfernung $l = 600$ m. Denken wir uns also um den Punkt $\bar{R}_1$ eine Kugel mit dem Radius $l = 600$ m gelegt, so muss diese den zweiten Horizont berühren. Ebenso liegt unter $\bar{R}'_2$ in 600 m Tiefe auf dem ersten Horizont der Punkt $\bar{R}_2$; eine Kugel um $\bar{R}_2$ mit dem Radius $l = 1000$ m berührt ebenfalls den zweiten Horizont. Legt man an diese beiden Kugeln einen tangierenden Kegel, so ist seine Achse die Verbindungslinie von $\bar{R}_1$ und $\bar{R}_2$ auf dem ersten Horizont; die Achse liegt also in 600 m Tiefe horizontal. Offenbar berührt der Kegel mit einer Mantellinie den zweiten Horizont. Jede Mantellinie kann durch einen Achsenschnitt des Regels erhalten werden; d.h. durch Schnitt des Kegels mit einer Ebene, die die Kegelachse enthält. Die den zweiten Horizont berührende Mantellinie wird gerade durch den Achsenschnitt geliefert, der senkrecht auf dem Horizont H_2 steht. Die Bestimmung seiner wahren Lage im Raum ist nicht unmittelbar möglich, jedoch lässt sich seine Gestalt leicht ermitteln, denn alle Achsenschnitte sind ja kongruent. Die Konstruktion geschieht in der Messebene von den Projektionen $\bar{R}'_1$, $\bar{R}'_2$ der Kugelmittelpunkte R_1, $\bar{R}_2$ aus; hierzu tangiert man mit den Radien $l = 600$ m bzw. $l = 1000$ m und erhält als wahre Gestalt des Achsenschnitts das Viereck $\bar{R}'_1\ \bar{R}'_2\ \overline{(P_2)}\ \overline{(P_1)}$. In gleicher Weise ergibt sich das Viereck $R_1\ \tilde{R}'_2\ (\tilde{P}_2)\ (\tilde{P}_1)$, das selbstverständlich zu dem vorigen kongruent ist.

Nach diesen Vorbereitungen ist es möglich, den zweiten Horizont H_2 durch seine Tiefenlinien festzulegen. Hierzu werden zwei zur Oberfläche vertikale Schnitte gelegt, und zwar gerade so, dass sie die Tiefenlinien $d_1 = \text{const}$ des Horizontes H_1 orthogonal treffen (Fig. 9). Zweckmässigerweise werden diese an sich beliebigen Schnitte durch die Punkte (P_1) und (P_2) gelegt. Diese Vertikalschnitte entlang $\overline{(P_1)}\ \bar{M}'_1\ \tilde{M}'_1\ (Q_1)$ sowie $\overline{(P_2)}\ \bar{M}'_2\ \tilde{M}'_2\ (Q_2)$ sind nach links bzw. rechts herausgerückt und in die Zeichenebene geklappt. In ihnen erscheint der Horizont H_1 als Schnittlinie $\bar{M}_1\,\tilde{M}_1$ bzw. $\bar{M}_2\,\tilde{M}_2$. Die Tiefen dieser Punkte unter der Messebene ergeben sich aus den Tiefenlinien $d_1 = 600$ m bzw. $d_1 = 900$ m des Horizontes H_1. Die beiden Kegel mit den Achsen $\bar{R}_1\,\bar{R}_2$ bzw. $\tilde{R}_1\,\tilde{R}_2$ werden kreisförmig geschnitten. Die Längen der Kreisradien

$\bar{M}_1 \bar{P}_1$ und $\tilde{M}_1 Q_1$ bzw. $\bar{M}_2 \bar{P}_2$ und $\tilde{M}_2 Q_2$ sind natürlich gleich den Strecken $\bar{M}'_1 \overline{(P_1)}$ und $\tilde{M}_1 (Q_1)$ bzw. $\bar{M}'_2 \overline{(P_2)}$ und $\tilde{M}_2 (Q_2)$. Der Horizont H_2 ist die tangierende Ebene an beide Kegel. In den hier betrachteten beiden Vertikalschnitten erscheint H_2 als tangierende Gerade an die kreisförmigen Kegelschnitte, nämlich $\bar{P}_1 Q_1$ und $\bar{P}_2 Q_2$. Aus ihrer Tiefenlage kann der Tiefenlinienplan für den Horizont H_2 gezeichnet werden; man entnimmt den beiden Vertikalschnitten je zwei Punkte der Geraden $d_2 = \text{const}$, z.B. die Punkte Z_1, Z_2 der Linie $d_2 = 1300$ m.

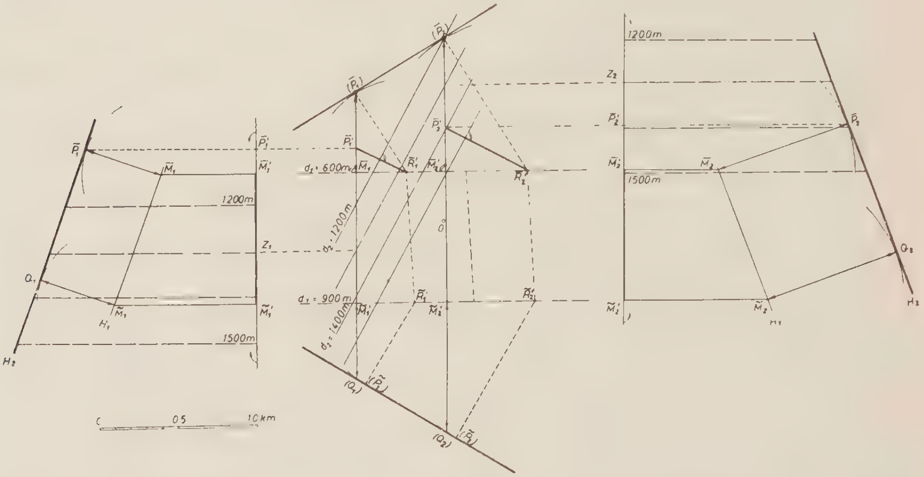

d_2 = 1200 m...1500 m: Tiefenlinien des Horizontes H_2. — Depth lines of the interface H_2.
$\bar{P}'_1\bar{R}'_1$ bzw. $\bar{P}'_2\bar{R}'_2$: Fallrichtung des Horizontes H_2. — Direction of dip of the interface H_2.

Fig. 9. Konstruktion des wahren Horizontes H_2. — Construction of the true interface H_2.

Als Zeichenkontrolle erhält man bei dieser Konstruktion die Fallrichtung des Horizontes H_2. Man braucht nur die Lote $\bar{R}_1 \bar{P}_1$ bzw. $\bar{R}_2 \bar{P}_2$, die von H_1 ausgehen und orthogonal auf dem Horizont H_2 stehen, senkrecht an die Oberfläche zu projizieren. Die Verbindungslinien der Projektionspunkte $\bar{R}'_1 \bar{P}'_1$ sowie $\bar{R}'_2 \bar{P}'_2$ liegen in der Fallrichtung, also senkrecht zu den Tiefenlinien des Horizontes H_2.

Zur Konstruktion der Achsenschnitte der Kegel gemäss Fig. 8 ist noch ergänzend zu bemerken: Wir haben dort der Anschaulichkeit halber die Linien gleicher Lotentfernung von H_1 zu H_2 benutzt, und zwar ihre Schnittpunkte mit den Tiefenlinien $d_1 = \text{const}$; das kann u.U. zu einer ungünstigen Situation bei der Zeichnung führen. Daher werde noch darauf hingewiesen, dass sich für die Konstruktion von Fig. 8 stets auch die Schnittpunkte der Tiefenlinien $d_1 = \text{const}$ mit den Profillinien $\bar{S}_1 \bar{S}_2$ bzw. $\tilde{S}_1 \tilde{S}_2$ der Fig. 6 verwenden lassen. Es müssen nur die richtigen Radien für die Tangierungskreise benutzt werden.

die leicht folgendermassen zu bestimmen sind: z.B. schneidet die Gerade $d_1 = 600$ m das Profil $\tilde{S}_1 \tilde{S}_2$ im Punkt $\tilde{U}_1$; 600 m unterhalb $\tilde{U}_1$ liegt auf H_1 ein Punkt, dessen Lotentfernung vom fiktiven Horizont $H_2^* (v_1)$ der Fig. 6 entnommen worden kann. Die Streckung dieses Lotes mit dem Quotienten v_2/v_1 liefert den Radius für den Tangierungskreis um $\tilde{U}_1$. — Sind die Achsenschnitte der Kegel in der soeben geschilderten Weise gezeichnet worden, so ist die weitere Bearbeitung gemäss Fig. 9 ohne irgendeine Änderung durchzuführen.

Das Prinzip der Streckung fiktiver Lotstrahlen lässt sich natürlich auch für die Kartierung gekrümmter Horizonte bei konstanten Schichtgeschwindigkeiten anwenden. Man muss nur in diesem Fall differenzierter verfahren. Sind die Isochronen $T_1 = \text{const}$ des Horizontes H_1 schon stärker gekrümmt, so muss der Tiefenlinienplan des Horizontes H_1 durch Konstruktion mehrerer kurzer Profile festgelegt werden. Dieses gilt genau so für die Ausgangskonstruktion des Horizontes $H_2^* (v_1)$ bei stark gekrümmten Isochronen $T_2 = \text{const}$. Auch hier wird eine Reihe kurzer Vertikalschnitte gelegt. Sodann werden die fiktiven Lote zwischen H_1 und $H_2^* (v_1)$ entnommen und mit v_2/v_1 gestreckt. Entsprechend Fig. 7 ergeben sich auf den Tiefenlinien von H_1 genügend Punkte mit bekannter wahrer Lotentfernung von H_1 zu H_2. Von vier benachbarten Punkten aus zeichnet man mit Hilfe der erläuterten Kegelkonstruktion den Tiefenlinienplan eines Ebenen-Elements. Hierbei werden zwei Punkte auf einer Tiefenlinie, die beiden anderen auf einer benachbarten Tiefenlinie des Horizontes H_1 gewählt. Es muss eine genügende Zahl von Ebenen-Elementen ihrer räumlichen Lage nach dargestellt werden, um den Tiefenlinienplan von H_2 hinreichend genau bestimmen zu können.

Das behandelte räumliche Zwei-Schichten-Problem lässt sich entsprechend dem ebenen Falle auch auf n Schichten von beliebiger räumlicher Lage erweitern. Jedes Mehr-Schichten-Problem kann man auf eine sukzessive Behandlung von räumlichen Zwei-Schichten-Problemen zurückführen.

Um den Horizont H_n aus seinen T_n-Isochronen zeichnen zu können, müssen die Tiefenlinienpläne der Horizonte $H_1, H_2, \ldots, H_{n-1}$ bereits vorliegen. Die Konstruktion von H_n erfolgt dann in n Schritten:

1. Schritt: Man lege Vertikalschnitte senkrecht zu den T_n-Isochronen und zeichne in diesen den Horizont H_1 (aus der Kenntnis seines Tiefenlinienplanes) und den fiktiven Horizont $H_n^* (v_1)$. Die fiktiven Lotstrahlen zwischen H_1 und $H_n^* (v_1)$ werden mit dem Quotienten v_2/v_1 gestreckt und ergeben die Länge der „seismischen Lote” zwischen H_1 und dem fiktiven Horizont $H_n^* (v_2)$. Die Tiefenlinien von H_1 und die Linien gleicher Lotentfernung von H_1 zu $H_n^* (v_2)$ geben analog zu dem ausführlich behandelten Zwei-Schichten-Problem die Fallrichtung des fiktiven Horizontes $H_n^* (v_2)$.

2. Schritt: Man lege Vertikalschnitte in Fallrichtung von $H_n^* (v_2)$ und trage die Horizonte H_1 und H_2 aus ihren Tiefenlinienplänen ein. Nunmehr wird in diesen Vertikalschnitten der fiktive Horizont $H_n^* (v_2)$ eingezeichnet; man erhält ihn durch Tangieren um Punkte des Horizonts H_1 mit Radien, die aus den Linien gleicher Lotentfernung zwischen H_1 und H_n^* (v_2) festliegen (vgl. 1. Schritt). Die Anteile der Lote von H_1 auf H_n^* (v_2), die zwischen H_1 und H_2 liegen, sind Teile der wahren Lotstrahlen zum Horizont H_n. Die fiktiven Rest-Lote zwischen H_2 und H_n^* (v_2) werden mit v_3/v_2 gestreckt. Die Tiefenlinien von H_2 und die Linien gleicher Lotentfernungen von H_2 zu H_n^* (v_3) geben wiederum analog zu dem ausführlich behandelten Zwei-Schichten-Problem die Fallrichtung des Horizonts H_n^* (v_3).

3. Schritt: Man lege Vertikalschnitte in Fallrichtung von H_n^* (v_3) und trage die Horizonte H_2 und H_3 aus ihren Tiefenlinienplänen ein. Nunmehr wird in diesen Vertikalschnitten von H_2 aus der fiktive Horizont H_n^* (v_3) eingezeichnet, u.s.w.

Beim n-ten Schritt ergibt sich dann die Kartierung des wahren Horizontes H_n.

In der praktischen Auswertung wird man, auch bei Vorhandensein einer grösseren Zahl reflektierender Horizonte, häufig mit der Behandlung von räumlichen Drei- oder sogar nur Zwei-Schichten-Fällen auskommen. Man muss hierzu auf Grund der bekannten Geschwindigkeitsverteilung drei bzw. zwei geeignete Schichtpakete bilden und ihnen repräsentative Geschwindigkeiten zuschreiben.

Hiermit werde die Schilderung des „Verfahrens der sukzessiven Tangierung" beendet und auf eine weitere Methode zur Lösung des räumlichen Problems der Reflexionsseismik eingegangen, bei der wiederum das Prinzip der Streckung fiktiver Lotstrahlen eine wesentliche Rolle spielen wird. Es handelt sich um das „Verfahren der Konstruktion in der Brechungsebene".

4. *Das Verfahren der Konstruktion in der Brechungsebene*

Die Konstruktion soll an dem Beispiel des soeben behandelten räumlichen Zweischichtenfalles der Fig. 4 erläutert werden. Hierbei wird der Verlauf des Lotstrahles von einem Punkt ausgehend zum Horizont H_2 ermittelt, und zwar in unserem Beispiel vom Schnittpunkt O der Profile I und II in Fig. 4. Die Konstruktion des ersten Horizontes erfolgt wie bisher (Fig. 5).

Ausgangspunkt für die räumliche Darstellung des zweiten Horizontes sind wiederum seine Isochronen $T_2 = \text{const}$ und die Tiefenlinien $d_1 = \text{const}$ des Horizontes H_1 (Fig. 10). Der Konstruktion dient eine Profillinie, die senkrecht zu den Isochronen verläuft und durch den Punkt O geht. Der Vertikalschnitt durch diese Linie wird in die Zeichenebene geklappt. Seine Schnittlinie mit dem ersten Horizont H_1 lässt sich wieder aus den Tiefenlinien $d_1 = \text{const}$ festlegen. Wiederum wird der fiktive Horizont H_2^* (v_1) gezeichnet; hierzu tangiert man z.B. um die Punkte X_1 und X_2 mit Verwendung von v_1 und den jeweiligen $\frac{1}{2}\,T_2$-Werten. Der vom Punkt O ausgehende Lotstrahl zum Horizont H_2 ist im ersten Medium die Strecke OD, denn sie ist Teil des Strahles OE^*, der senkrecht auf dem fiktiven Horizont H_2^* (v_1) steht. Durch Projektion des Punktes D an die Oberfläche erhält man den Punkt D'. Nun wird die Normale des Horizontes H_1 im Punkt D gesucht. Sie liegt in einem zur Messebene vertikalen Schnitt, der durch D' geht und ausserdem auf den Tiefenlinien $d_1 =$ const senkrecht steht. Ein solcher Vertikalschnitt ist in Fig. 10 links in die Zeichenebene geklappt. Die Normale zu H_1 in D schneidet die Messebene im Punkt N. Nach dem Brechungsgesetz von Snellius liegen einfallender Strahl, Schichtgrenzennormale und gebrochener Strahl in einer Ebene, der Brechungsebene. Denkt man sich die beiden Vertikalschnitte in ihre wahre räumliche Lage zurückgeklappt, so sieht man: Das Dreieck ODN liegt in dieser Brechungsebene; denn es waren ja die Seite OD der wahre Lotstrahl im obern Medium und die Seite DN das Lot auf dem Horizont H_1. Die Seite ON liegt in der Messebene; wir klappen um diese Seite die Brechungsebene (und damit das Dreieck ODN) in die Zeichenebene (Fig. 11).

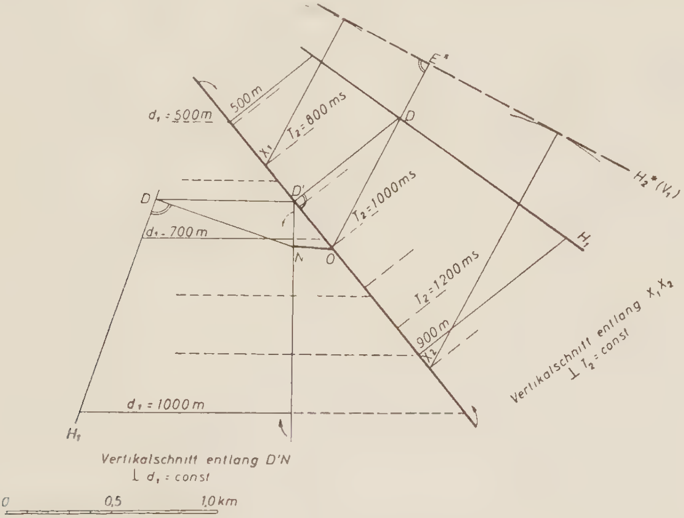

$T_2 = 700$ ms...1300 ms: Isochronen des Horizontes H_2. — Isochrones of the interface H_2.
$d_1 = 500$ m...1000 m: Tiefenlinien des Horizontes H_1. — Depth lines of the interface H_1.

Fig. 10. Konstruktion des fiktiven Horizontes $H_2{}^*$ (v_1) und der Normalen des Horizontes H_1 im Brechungspunkt D. — Construction of the fictitious interface $H_2{}^*$ (v_1) and the line normal to the interface H_1 at the point of refraction D.

In Fig. 11 wird auf der Linie ND in D die Senkrechte errichtet und so die Schnittlinie des ersten Horizontes H_1 mit der Brechungsebene erhalten. Wir ernehmen Fig. 10 noch die Strecke DE^* und verlängern mit ihr OD über D hinaus. Dann steht die Schnittlinie des fiktiven Horizontes $H_2{}^*$ (v_1) mit der Brechungsebene im Punkte E^* senkrecht auf der Strecke ODE^*. Nach dem Streckungsprinzip ist nun die wahre Lage des Horizontes H_2 in der Brechungsebene festzulegen. Parallel DE^* zeichnet man einen beliebigen zweiten fiktiven Strahl IK^*. Die fiktiven Lotstrahlen DE^* und IK^* werden mit dem Quotienten v_2/v_1 gestreckt und es wird mit diesen Längen um D und I tangiert. Die Tangente EK ist die Schnittlinie des Horizontes H_2 mit der Brechungsebene. Der Punkt E ist der wahre Fusspunkt des von O ausgehenden gebrochenen Lotstrahles auf dem zweiten Horizont, festgelegt in der Brechungsebene.

Da das Strahlenstück DE senkrecht auf H_2 steht, gibt seine Projektion an die Oberfläche die Fallrichtung von H_2. Zur Bestimmung derselben verlängert man in der Brechungsebene die Strecken ED und NO bis zu ihrem Schnittpunkt F, der gleichzeitig in der Messebene liegt. Durch F geht also die gesuchte Projektion der Normalen DE von H_2. — Ausserdem kennen wir auf Grund von Fig. 10 die Projektion D' des Punktes D auf der Messebene. Zeichnet man also nach Fig. 10 das Dreieck $D'NO$ und setzt nach Fig. 11 an die Seite NO die Strecke OF an, so ergibt in Fig. 12 die Richtung FD' die Fallrichtung des Horizontes H_2. Aus einem Vertikalschnitt entlang dieser Richtung sind leicht die Tiefenlinien von H_2 zu entnehmen; der Vertikalschnitt ist in der Fig. 12 in die Zeichenebene geklappt. Die Strecke $D'D$ ist ihrer Länge nach bekannt und steht senkrecht auf $D'F$. Die Strecken FD und DE sind nach dem Vorhergehenden ebenfalls bekannt. DE war die Normale auf dem Horizont H_2; daher ist die Senkrechte auf DE in E die Spur des Horizontes H_2 in unseren Vertikalschnitt. Da der Vertikalschnitt in der Fallrichtung von H_2 ge-

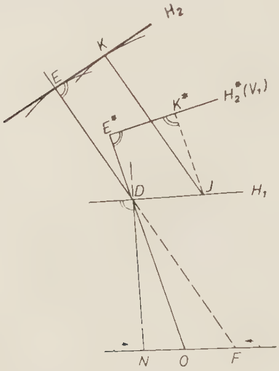

NOF: Spur der Brechungsebene in der Messebene. — Line of intersection of the plane of refraction with plane of measurement.

Fig. 11. Konstruktion des wahren Horizontes H_2 in der Brechungsebene. — Construction of the true interface H_2 in the plane of refraction.

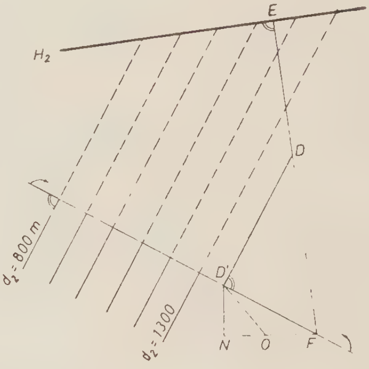

$d_2 = 1000$ m...1300 m: Tiefenlinien des Horizontes H_2. — Depth Lines of the Interface H_2.
D'F: Fallrichtung des Horizontes H_2. — direction or dip of the interfact H_2.

Fig. 12. Konstruktion des wahren Horizontes H_2 in einem Vertikalschnitt, geführt in Fallrichtung von H_2. — Construction of the true interface H_2 in a vertical plane through the direction of dip of H_2.

führt ist, können nunmehr die Tiefenlinien dieses Horizontes gezeichnet werden.

Auch dieses Verfahren der Konstruktion in der Brechungsebene lässt sich zwanglos für die Behandlung des n-Schichten-Problems erweitern.

Bei der konstruktiven Festlegung des n-ten Horizontelementes müssen wieder die $(n-1)$ höheren Schichtgrenzen in Gestalt ihrer Tiefenlinienpläne bekannt und in der Nachbarschaft des Strahlenausgangspunktes O auf der Messebene der Isochronenverlauf $T_n = \text{const}$ gegeben sein. Die räumliche Darstellung des n-ten Horizontstückes H_n erfolgt wieder in n Schritten.

1. Schritt: Man lege durch den betrachteten Punkt O der Messebene senkrecht zu den T_n-Isochronen einen ersten Vertikalschnitt und zeichne in diesem den Horizont H_1 sowie den fiktiven Horizont $H_n^*(v_1)$. Im Durchstosspunkt des von O ausgehenden Strahles durch den Horizont H_1 wird die Normale errichtet und so die Konstruktion in der ersten Brechungsebene ermöglicht. Analog zu dem ausführlich behandelten Zwei-Schichten-Problem ergibt sich in der Brechungsebene der fiktive Horizont $H_n^*(v_2)$; der gebrochene Teil des betrachteten Strahles (unterhalb H_1) wird bis zum Durchstoss der Messebene nach oben verlängert.

2. Schritt: Durch diesen Durchstosspunkt lege man in Fallrichtung von $H_n^*(v_2)$ einen zweiten Vertikalschnitt, in dem die Horizonte H_2 und $H_n^*(v_2)$ einzutragen sind. Im Durchstosspunkt des betrachteten Lotstrahles durch H_2 wird die Normale auf diesem Horizont errichtet und so die Konstruktion in der (zweiten) Brechungsebene ermöglicht. In dieser konstruiert man den fiktiven Horizont $H_n^*(v_3)$; der gebrochene Anteil des betrachteten Strahles (unterhalb H_2) wird bis zum Durchstoss der Messebene nach oben verlängert.

3. Schritt: Durch diesen Durchstosspunkt lege man in Fallrichtung von $H_n^*(v_3)$ einen dritten Vertikalschnitt, in dem die Horizonte H_3 und $H_n^*(v_3)$ einzutragen sind ... u.s.w.

Durch Fortsetzung der Konstruktion werden alle gebrochenen Strahlenstücke und die gesuchte räumliche Lage des Horizontelementes H_n zeichnerisch bestimmt.

5. *Ein Beispiel falscher Konstruktion und einige Folgerungen hieraus*

In den beiden vorstehenden Abschnitten sind zwei Verfahren zur konstruktiven Darstellung von Reflexionshorizonten unter Berücksichtigung der Strahlenbrechung im Raum beschrieben worden. Ausgangspunkt für die Behandlung war in beiden Fällen der Isochronenplan der Fig. 4. Ziel der Konstruktion war der Tiefenlinienplan des zweiten reflektierenden Horizontes H_2. Dieser ist auf Grund der Bearbeitung des Isochronenplanes

a) nach dem Verfahren der sukzessiven Tangierung in Fig. 9,
b) nach dem Verfahren der Konstruktion in der Brechungsebene in Fig. 12 dargestellt.

Nunmehr soll gezeigt werden, zu welchem unsinnigen Ergebnis eine Bearbeitung des gleichen Beispiels führt, wenn die Strahlenbrechung im Raum nicht berücksichtigt wird. Hierzu werde von den Profilen I und II der Fig. 4 aus gemäss Abschnitt B, 2 derart konstruiert, als ob ein ebenes Zwei-Schichten-Problem vorliegt. Bei jedem Profil wird also fälschlich angenommen, dass es senkrecht zur gemeinsamen Streichrichtung beider Horizonte orientiert sei, was natürlich dem wirklichen Isochronenverlauf (Fig. 4) widerspricht. Das Ergebnis dieser falschen Konstruktion ist in Fig. 13 dargestellt. Ersichtlich laufen die Tiefenlinien $d_1 =$ const bzw. $d_2 =$ const der Horizonte H_1 bzw. H_2 keineswegs jeweils parallel, vielmehr überschneiden sie sich.

Es ist also unsinnig, jedes Profil für sich zu konstruieren; die berücksichtigte Strahlenbrechung entspricht gar nicht den tatsächlichen Verhältnissen. — Vielmehr wäre in einem solchen Falle von zwei Schussprofilen I und II nach Fig. 4 so vorzugehen:

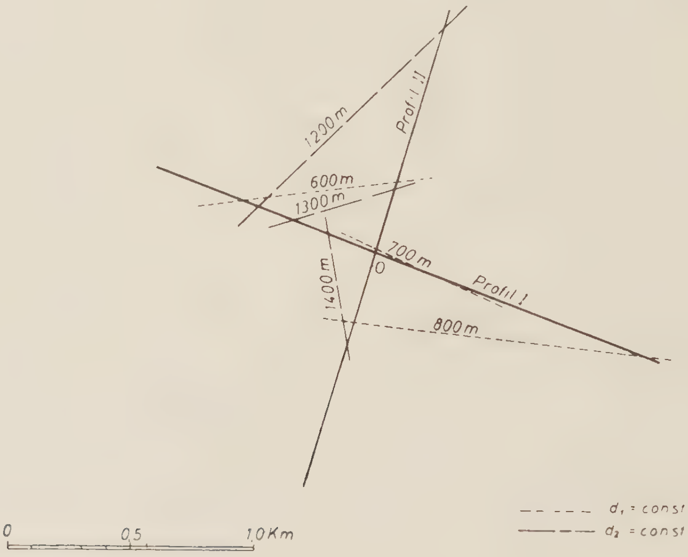

Fig. 13. Falsche Bearbeitung der Profile I and II (aus Fig. 4). Jedes Profil wurde für sich als ebenes Zweischichteproblem behandelt. — Erroneous interpretation of the profiles I and II (from Fig. 4). Each profile was treated independently of the other as a two-dimensional two layer problem.

1) Aus den gemessenen Lotzeiten wird für jeden Horizont ein übersichtsmässiger Isochronenplan gezeichnet.

2) Ein Vergleich des Verlaufs der Isochronen in beiden Plänen ermöglicht die Entscheidung, ob ein räumliches oder ebenes Konstruktionsproblem vorliegt.

3) Handelt es sich um ein räumliches Problem — d.h. die Isochronenscharen der einzelnen Horizonte überschneiden sich — so ist ein entsprechendes Konstruktionsverfahren anzuwenden. Eventuell müssen weitere Messungen zum Zwecke einer genügenden Sicherung der Isochronenpläne angesetzt werden.

4) Handelt es sich um ein ebenes Problem — d.h. die Isochronenscharen der einzelnen Horizonte sind zueinander parallel — so ist gemäss Abschnitt B, 2 in Vertikalschnitten zu konstruieren, die orthogonal zu den Isochronen geführt sind. Sind die Horizonte gleicher Streichrichtung stark gegeneinander geneigt, so können solche Profile, die nicht in Fallrichtung geschossen sind, nur der Sicherung der Isochronenpläne dienen.

6. *Bemerkungen zur Konstruktion bei linearem Anstieg der Geschwindigkeit mit der Tiefe*

Bei den bisherigen Betrachtungen wurden stets die Schichtgeschwindigkeiten als jeweils konstant vorausgesetzt.

Kann nun in einem Untersuchungsgebiet die Geschwindigkeitsverteilung als Funktion der Tiefe angesetzt werden, so lässt sich die Konstruktion eines jeden reflektierenden Horizontes für sich als ebenes Problem behandeln. Es werden wieder Vertikalschnitte senkrecht zu der gerade betrachteten Isochronenschar $T_i = \text{const}$ gelegt. Der seismische Strahl verbleibt dann immer in einem solchen Vertikalschnitt, also in der Ebene, die durch den Vektor der Anfangsrichtung des Strahles und den Gradienten der Geschwindigkeit gegeben ist.

Von gewisser Bedeutung für die Praxis ist die Geschwindigkeitsfunktion $v(z) = v_o + az$, $a > 0$; die Geschwindigkeit nimmt also linear mit der Tiefe z zu. Der Weg der seismischen Impulse ist für diese Funktion bekanntlich ein Kreis (cf. z.B.: Dix (1952), S. 141-162; Jakosky (1950), S. 683-690). Die Mittelpunkte dieser Kreise liegen in einer Ebene, die aus der Messebene durch Parallelverschiebung um die Strecke v_o/a nach oben entsteht. Für den Inzidenzwinkel des Lotstrahles zum Horizont H_i gilt wieder die Beziehung.

$$\sin \alpha_i = v_o \tfrac{1}{2} \left(\delta T_i \,/\, \delta x_i\right)_{z=o}$$

wobei die x_i-Achse senkrecht zu den Isochronen $T_i = \text{const}$ orientiert ist. Die Laufzeit T_i ist eine Funktion der Bogenlänge des kreisförmigen Strahles.

Eine solche idealisierte (stetige) Geschwindigkeitsfunktion bietet wenig Interessantes. In der üblichen Form ihrer Anwendung wird sie ja auch den physikalischen Realitäten keineswegs gerecht. Wesentlich interessanter ist bereits die folgende Geschwindigkeitsverteilung mit einer Unstetigkeitsfläche H_1:

Die Geschwindigkeit $v_1 = v_1(z) = v_o + az$, $a > 0$, nimmt linear mit der Tiefe zu bis zum Horizont H_1; unterhalb H_1 ist die Schichtgeschwindigkeit v_2 konstant bis zum Horizont H_2.

Die Konstruktion des Horizontes H_1 macht keine Schwierigkeiten.

Zur räumlichen Darstellung des Horizontes H_2 werden wieder Vertikalschnitte senkrecht zu den T_2-Isochronen gelegt. Analog zur Konstruktion im Abschnitt B, 3 geht man folgendermassen vor: In diesen Vertikalschnitten tangiert man von genügend vielen Punkten der Messebene aus einen fiktiven Horizont $H_2^*(v_1)$ mit Verwendung der Geschwindigkeit $v_1(z) = v_o + az$ und den halben Lotzeiten $\tfrac{1}{2}\, T_2$; die Tangierung erfolgt nach der üblichen Konstruktion für lineare Zunahme der Geschwindigkeit mit der Tiefe (cf. z.B.: Dix (1952), S. 141-162; Jakosky (1950), S. 683-690). Sodann zeichnet man in bekannter Weise die kreisförmigen Strahlen, die von den gewählten Konstruktionspunkten zum fiktiven Horizont H_2^* (v_1) laufen. Nunmehr wird in die Vertikalschnitte der Horizont H_1 auf Grund der Kenntnis seiner Tiefenlinien eingetragen. Wiederum sind die oberhalb H_1 gelegenen Anteile der Strahlen zum fiktiven Horizont H_2^* (v_1) bereits reelle Teile der Lotstrahlen zum wahren Horizont H_2. Damit lassen sich sofort die Restzeiten berechnen, die auf die Anteile der Lotstrahlen zwischen dem Horizont H_1 und dem wahren Horizont H_2 entfallen. Es sind die Linien gleicher Restzeiten auf H_1 wegen $v_2 =$ const gleichzeitig die Linien gleicher Lotentfernung von H_1 zum wahren Horizont H_2. Ausgehend von den Tiefenlinien des Horizontes H_1 und den Linien gleicher Lotentfernung von H_1 zu H_2 ist nun die Konstruktion gemäss Abschnitt B, 3 zu beenden.

Offenbar gestattet auch hier die Konstruktion des fiktiven Horizontes H_2^* (v_1) die Festlegung der Anfangsrichtung der Lotstrahlen rein zeichnerisch.

Für die bisher entwickelten Verfahren sind einige gemeinsame Gesichtspunkte massgebend, die sich leicht allgemein formulieren lassen. Eine solche allgemeine Formulierung ist jedoch für die Praxis nicht von unmittelbarer Bedeutung; sie wird daher im Anhang (Abschnitt D, 2) gebracht.

Hiermit sei die Behandlung der Konstruktionsverfahren zur Festlegung von Reflexionshorizonten beendet. Eine leichte Modifizierung der Konstruktionsprinzipien ermöglicht auch eine einfache, rein zeichnerische Darstellung von Refraktionshorizonten, die nunmehr erläutert werden soll.

C. Konstruktive Darstellung von Refraktionshorizonten

1. *Behandlung des ebenen Falles durch sukzessive Tangierung von Fronten der Mintrop-Welle*

Zunächst wenden wir uns dem ebenen Fall zu, bei dem also sämtliche Refraktionshorizonte gleiche Streichrichtung besitzen. In Anlehnung an die üblichen Voraussetzungen für eine rechnerische Behandlung werde angenommen, dass die Horizonte eben und die Schichtgeschwindigkeiten konstant sind. Die zeichnerische Darstellung erfolgt für ein Drei-Schichten-Problem:

Im Untergrund sind drei Schichten jeweils konstanter Schichtgeschwindigkeit $v_1 < v_2 < v_3$ vorhanden. Die beiden Grenzflächen zwischen den Schichten — also die Refraktionshorizonte — seien Ebenen gleicher Streichrichtung. Die Lage der Refraktionshorizonte sowie die Geschwindigkeiten v_1, v_2, v_3 sind aus einer refraktionsseismischen Vermessung entlang eines Profils senkrecht zur Streichrichtung zu bestimmen[4].

---

[4] Weicht die Lage des Profils wesentlich von der gemeinsamen Fallrichtung der Horizonte ab, so hat man es nicht mehr mit einem „ebenen" Problem zu tun; vielmehr liegt dann bereits der „räumliche" Fall vor, der in Abschnitt C, 2 behandelt wird.

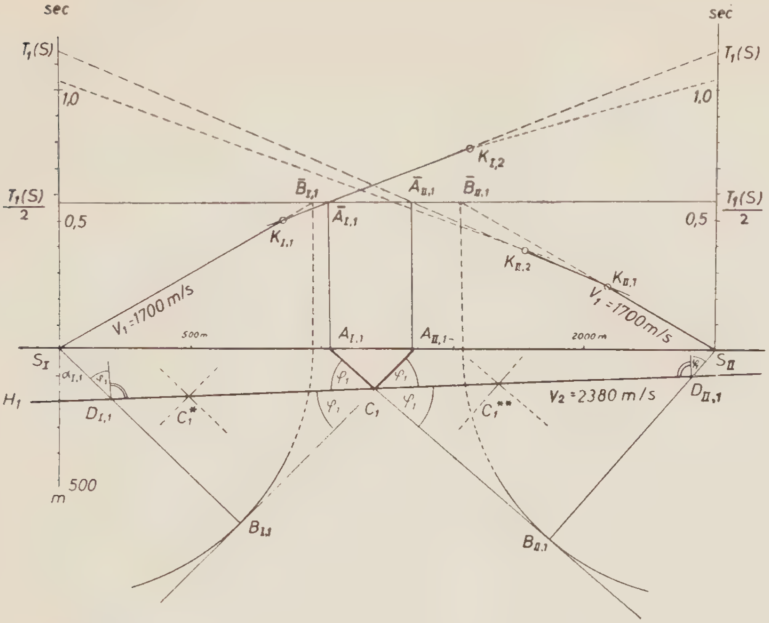

Fig. 14. Konstruktion des Refraktionshorizontes H_1 durch Tangierung von Fronten der Mintrop-Welle (ebener Fall). — Construction of the refracting interface H_1, by drawing envelopes for the fronts of the Mintrop wave (Two-dimensional case).

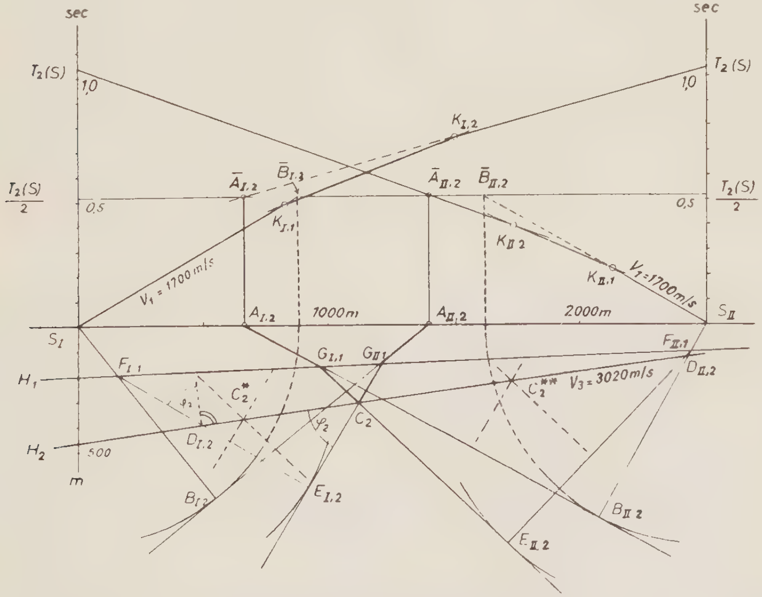

Fig. 15. Konstruktion des Refraktionshorizontes H_2 durch sukzessive Tangierung von Fronten der Mintrop-Welle (ebener Fall). — Construction of the refracting interface H_2 by drawing successive envelopes for the fronts of the Mintrop wave (Two dimensional case).

Auf unserem Profil seien von den Schusspunkten S_{I} und S_{II} aus zwei Laufzeitkurven durch Gegenschiessen aufgenommen, die in den Figuren 14 und 15 dargestellt sind. Die beiden Laufzeitkurven weisen je zwei Knickpunkte $K_{\mathrm{I},1}$, $K_{\mathrm{I},2}$ bzw. $K_{\mathrm{II},1}$, $K_{\mathrm{II},2}$ auf [5]; die einzelnen Laufzeitäste der ersten Einsätze sind Geradenstücke. Es sind also im Untergrund drei Schichten vorhanden, deren Grenzflächen wegen der vorausgesetzten Konstanz der Schichtgeschwindigkeiten Ebenen sind. Aus den Laufzeitkurven wird in Fig. 14 der erste Refraktionshorizont H_1 zwischen der ersten und zweiten Schicht konstruiert; sodann in Fig. 15 der zweite Refraktionshorizont H_2 zwischen der zweiten und dritten Schicht. Die Konstruktion erfolgt in einem Vertikalschnitt zur Messebene entlang unseres Refraktionsprofils $S_{\mathrm{I}}S_{\mathrm{II}}$; in diesem Schnitt liegen ja auf Grund der gemachten Voraussetzungen sämtliche seismischen Strahlen.

Die Neigung der ersten Äste der Laufzeitkurven $S_{\mathrm{I}}K_{\mathrm{I},1}$ bzw. $S_{\mathrm{II}}K_{\mathrm{II},1}$ ergibt sofort die Geschwindigkeit v_1 im ersten Medium.

Die zweiten Äste der Laufzeitkurven sind bedingt durch den Refraktionshorizont H_1 zwischen dem ersten Medium der Geschwindigkeit v_1 und dem zweiten Medium der Geschwindigkeit v_2. Daher dienen diese Äste der Bestimmung von H_1 und v_2, die durch einige Erläuterungen an Hand von Fig. 14 vorbereitet werden soll:

Wir betrachten den Strahl, der von S_{I} ausgeht und in $D_{\mathrm{I},1}$ unter dem Grenzwinkel der Totalreflexion φ_1 auf das zweite Medium auftrifft, sodann in der Grenzfläche H_1 verläuft und diese unter dem gleichen Winkel φ_1 zur Flächennormalen in $D_{\mathrm{II},1}$ verlässt, um in S_{II} wieder die Messebene zu treffen. Der auf diesem Weg von S_{I} nach S_{II} gelangende seismische Impuls bewegt sich im ersten Medium mit der Geschwindigkeit v_1, in der Grenzfläche mit der Geschwindigkeit v_2 fort. Die Laufzeit des Impulses ist $T_1\,(S_{\mathrm{II}})$. Durch den Gegenschuss läuft von S_{II} nach S_{I} ein Impuls auf dem gleichen Wege mit den gleichen Geschwindigkeiten auf den einzelnen Wegteilen; daher ist seine Laufzeit $T_1\,(S_{\mathrm{I}})$ gleich der vorherigen:

$$T_1\,(S_{\mathrm{I}}) = T_1\,(S_{\mathrm{II}}) = T_1\,(S)$$

In diesem Wert $T_1\,(S)$ treffen die verlängerten zweiten Äste der Laufzeitkurven die Zeitachsen bei S_{I} und S_{II}.

Denken wir uns nun zwei seismische Impulse, die von S_{I} bzw. S_{II} ausgehen und auf ihrem soeben beschriebenen Wege einander treffen, so ist in jedem Treffpunkt die Summe ihrer Laufzeiten offenbar gleich $T_1\,(S)$. Es lassen sich nun die auf H_1 gelegenen Treffpunkte solcher gegenläufiger Refraktionsimpulse aus den Laufzeitkurven konstruieren, und zwar als Schnittpunkte der Fronten der sogen. indirekten oder Mintrop-Wellen, die im ersten Medium von den entlang H_1 laufenden Impulsen nachgezogen werden. Um das einzusehen, bedarf es zunächst folgender Überlegungen:

---

[5] Im folgenden beziehen sich bei den Doppelindizes die römischen Ziffern stets auf die Schusspunkte, die arabischen Ziffern auf die Horizonte; z.B.: der Knickpunkt $K_{\mathrm{I},1}$ liegt auf der von S_{I} ausgehenden Laufzeitkurve und seine Existenz leitet sich aus derjenigen des Horizontes H_1 her.

Bekanntlich ergibt sich der Inzidenzwinkel $\alpha_{I,1}$ des Strahles $D_{I,1} S_I$ in Fig. 14 aus der Neigung des zweiten Astes der Laufzeitkurve, die vom Schusspunkt S_{II} aus aufgenommen worden ist; und zwar gilt

$$\sin \alpha_{I,1} = v_1 \, (\Delta T / \Delta x)_{s_I}$$

wobei x die Koordinate auf der Entfernungsachse ist. Da der zweite Ast der Laufzeitkurve eine Gerade ist, kann der Winkel $\alpha_{I,1}$ durch eine einfache Konstruktion festgelegt werden, die nachstehend ohne Beschränkung der Allgemeinheit für das spezielle $\Delta T = \frac{1}{2} T_1 (S)$ beschrieben wird: Man zeichne in den Laufzeitenplan der Fig. 14 die Gerade $T = \frac{1}{2} T_1 (S)$. Diese schneidet im Punkt $\bar{A}_{II,1}$ den zweiten Ast der von S_{II} ausgehenden Laufzeitkurve; der zugehörige Punkt auf dem Profil ist $A_{II,1}$. Es ist also die Strecke $S_I A_{II,1}$ das zu $\Delta T = \frac{1}{2} T_1 (S)$ gehörige Δx der obigen Formel für $\alpha_{I,1}$. Nun lässt sich über $S_I A_{II,1}$ als Hypotenuse ein rechtwinkliges Dreieck konstruieren, dessen eine Kathete $v_1 \,.\, \Delta T = v_1 \, \frac{1}{2} T_1 (S)$ ist, so dass der gegenüberliegende Winkel nach obiger Formel gerade $\alpha_{I,1}$ ist. Die Bestimmung der Kathetenlänge geschieht ohne Rechnung mit Hilfe des ersten Astes der von S_I ausgehenden Laufzeitkurve: Ist $\bar{B}_{I,1}$ der Schnittpunkt desselben mit der Geraden $T = \frac{1}{2} T_1 (S)$, so ist die Projektion der Strecke $\overline{S_I B_{I,1}}$ auf das Profil $S_I S_{II}$ gleich der gewünschten Länge $v_1 \,.\, \frac{1}{2} T_1 (S)$. Zeichnet man mit dieser Strecke um S_I einen Kreis und legt an ihn von $A_{II,1}$ eine Tangente, so ergibt sich das rechtwinklige Dreieck $S_I A_{II,1} B_{I,1}$, dessen Winkel bei $A_{II,1}$ gleich $\alpha_{I,1}$ ist. Hieraus folgt, dass die Kathete $S_I B_{I,1}$ den gesuchten Inzidenwinkel $\alpha_{I,1}$ des Strahles $D_{I,1} S_I$ festlegt. Das soeben konstruierte rechtwinklige Dreieck bietet aber noch mehr, nämlich durch seine zweite Kathete eine bei $A_{II,1}$ zutage tretende Wellenfront. Der in $A_{II,1}$ zur Zeit $\frac{1}{2} T_1 (S)$ von S_{II} aus registrierte Einsatz rührt doch von dem über den Refraktionshorizont H_1 gelaufenen Impuls her, indem er die indirekte oder Mintrop-Welle nach sich zieht. In unserem Schnitt ist die Front der Mintrop-Welle geradlinig; die Fronten zu verschiedenen Zeiten sind einander parallel, d.h. die Strahlen der Mintrop-Welle haben konstante Richtung. Diese Richtung ist aber bereits durch die Kathete $S_I B_{I,1}$ gegeben. Folglich ist der oberhalb des Horizontes H_1 gelegene Teil $C_1 A_{II,1}$ der Kathete $B_{I,1} A_{II,1}$ die Mintrop-Welle, die in $A_{II,1}$ zur Zeit $\frac{1}{2} T_1 (S)$ zutage tritt. Es haben also beide Katheten des rechtwinkligen Dreieckes $S_I A_{II,1} B_{I,1}$ ihre wesentliche Bedeutung:

1) Die Kathete $S_I B_{I,1}$ legt den Inzidenzwinkel $\alpha_{I,1}$ fest, unter dem die Strahlen der nach S_I laufenden Mintrop-Welle auf die Messebene treffen. Das Stück $S_I D_{I,1}$ der Kathete ist physikalisch reell; es ist der Strahl im Medium der Geschwindigkeit v_1, auf dem die Impulse von S_I abgehen bzw. dort ankommen, die am Horizont H_1 entlanglaufen. Das Stück $D_{I,1} B_{I,1}$ hat keine unmittelbare physikalische Bedeutung; es werde als fiktiver Strahl bezeichnet.

2) Die Kathete $B_{I,1}\,A_{II,1}$ legt eine Wellenfront fest. Das Stück $C_1\,A_{II,1}$ ist physikalisch reell; *es* ist die Front der Mintrop-Welle, die — von S_{II} aus erregt — in $A_{II,1}$ zur Zeit $\frac{1}{2}\,T_1\,(S)$ eintrifft. Das Stück $B_{I,1}\,C_1$ hat keine unmittelbare physikalische Bedeutung; es werde als fiktive Wellenfront bezeichnet.

Anm.: Vergegenwärtigen wir uns noch einmal kurz, wie das rechtwinklige Dreieck $S_I\,A_{II,1}\,B_{I,1}$ durch Tangierung entstanden ist, so ist ersichtlich, dass diese Konstruktion und ihre Bedeutung für unser Refraktionsproblem das Analogon zu der in Abschnitt B, 1 beschriebenen Tangierung in bezug auf die Reflexionsseismik bilden. Wieder erhalten wir neben einem Inzidenzwinkel auch Wellenfronten und -strahlen, die teils physikalisch reell und teils fiktiv sind.

Nach dem Vorhergehenden ist $C_1\,A_{II,1}$ die Front der Mintrop-Welle zur Zeit $\frac{1}{2}\,T_1\,(S)$; d.h. der von S_{II} ausgehende und am Horizont H_1 refraktierte Impuls ist zu dieser Zeit im Punkt C_1 eingetroffen. Sind von Fig. 14 nur die beiden von S_I und S_{II} ausgehenden Laufzeitkurven gegeben und hat man hieraus durch die angegebene Tangentenkonstruktion das rechtwinklige Dreieck $S_I\,A_{II,1}\,B_{I,1}$ erhalten, so ist die Lage des Punktes C_1 auf der Kathete $B_{I,1}\,A_{II,1}$ nicht bekannt; vielmehr ist diese Kathete der erste geometrische Ort für C_1. Der zweite geometrische Ort bestimmt sich aus der bereits eingangs dargelegten Tatsache, dass der von S_I ausgehende und am Horizont H_1 refraktierte Impuls zur Zeit $\frac{1}{2}\,T_1\,(S)$ ebenfalls in C_1 eingetroffen ist. Letzterer zieht nämlich die nach S_{II} hin laufende Mintrop-Welle $C_1\,A_{I,1}$ der Fig. 14 nach sich, die ihrerseits Teil der Kathete $A_{I,1}\,B_{II,1}$ des rechtwinkligen Dreieckes $S_{II}\,A_{I,1}\,B_{II,1}$ ist; dieses Dreieck kann aber in völlig analoger Weise wie $S_I\,A_{II,1}\,B_{I,1}$ aus dem zweiten Ast der von S_I und dem ersten Ast der von S_{II} ausgehenden Laufzeitkurven gezeichnet werden.

Sind somit von Fig. 14 nur die beiden Laufzeitkurven gegeben und zeichnet man hieraus die beiden rechtwinkligen Dreiecke $S_I\,A_{II,1}\,B_{I,1}$ bzw. $S_{II}\,A_{I,1}\,B_{II,1}$, so liegt der Schnittpunkt C_1 ihrer Katheten $A_{II,1}\,B_{I,1}$ bzw. $A_{I,1}\,B_{II,1}$ auf dem gesuchten Refraktionshorizont H_1. Es bedeuten ausserdem die Strecken $A_{I,1}\,C_1$ bzw. $A_{II,1}\,C_1$ die nach S_{II} bzw. S_I hin laufenden Fronten der Mintrop-Wellen zur Zeit $\frac{1}{2}\,T_1\,(S)$.

Die Festlegung eines beliebigen weiteren Punktes auf H_1 geschieht ebenfalls durch Bestimmung des Treffpunktes zweier einander entgegenlaufender Impulse, deren Laufzeitensumme gleich $T_1\,(S)$ ist. Dieser Punkt wird wieder als Schnitt der von den Impulsen mitgeführten Mintrop-Wellen bestimmt. Es ist aber nicht nötig, nochmals die entsprechenden Dreiecke zu konstruieren; vielmehr kommt man auf Grund folgender einfacher Überlegung wesentlich schneller zum Ziel: Die Fronten einer — z.B. der nach S_I hin laufenden — Mintrop-Welle zu verschiedenen Zeiten sind einander parallel. Man verschiebe die zur Zeit $\frac{1}{2}\,T_1\,(S)$ durch $A_{I,1}\,C_1$ gegebene Front parallel zu sich selbst um eine beliebige Strecke nach der Seite, auf der S_I liegt; damit ist dann die Lage der nach S_{II} hin laufenden Wellenfront zu einem um $\Delta\,T$ früheren Zeitpunkt $(\frac{1}{2}T_1\,(S) - \Delta\,T)$ fixiert. Die Parallelverschiebung der Front $A_{II,1}\,C_1$ nach der gleichen Seite um die gleiche Strecke wie soeben ergibt die Lage der nach

S_{I} hin laufenden Wellenfront zu dem um den gleichen Betrag ΔT späteren Zeitpunkt ($\frac{1}{2} T_1 (S) + \Delta T$). Es ist also die Laufzeitsumme der beiden durch Parallelverschiebung erhaltenen Wellenfronten gleich $T_1 (S)$, d.h. aber: ihr Schnittpunkt liegt auf dem Horizont H_1. Auf diese Weise sind z.B. die Punkte $C_1{}^*$ und $C_1{}^{**}$ in Fig. 14 bestimmt worden. — Zwei Punkte, z.B. C_1 und $C_1{}^*$, genügen zur Zeichnung des Horizontes H_1, die nunmehr ausgeführt sein soll.

Nach Fig. 14 schneidet H_1 in den Punkten $D_{\mathrm{I},1}$ bzw. $D_{\mathrm{II},1}$ die Katheten $S_{\mathrm{I}} B_{\mathrm{I},1}$ bzw. $S_{\mathrm{II}} B_{\mathrm{II},1}$, wodurch die beiden neuen rechtwinkligen Dreiecke $D_{\mathrm{I},1} C_1 B_{\mathrm{I},1}$ bzw. $D_{\mathrm{II},1} C_1 B_{\mathrm{II},1}$ entstehen. Diese Dreiecke sind ähnlich, denn der Horizont H_1 halbiert $\sphericalangle\, B_{\mathrm{I},1} C_1 A_{\mathrm{I},1}$, da ja nach Konstruktion von $C_1{}^*$ die Strecke $C_1{}^* C_1$ Diagonale in einem Rhombus ist. Nunmehr entnimmt man der Figur, dass der halbe Winkel, also z.B. $\sphericalangle\, D_{\mathrm{I},1} C_1 B_{\mathrm{I},1}$ gleich dem Grenzwinkel φ_1 der Totalreflexion zwischen erstem Medium der Geschwindigkeit v_1 und zweitem Medium der Geschwindigkeit v_2 ist. Es gilt somit

$$\sin \varphi_1 = v_1 / v_2 = D_{\mathrm{I},1} B_{\mathrm{I},1} / D_{\mathrm{I},1} C_1 = D_{\mathrm{II},1} B_{\mathrm{II},1} / D_{\mathrm{II},1} C_1$$

Da v_1 aus dem Anstieg der ersten Äste der Laufzeitkurven bekannt ist, lässt sich hiernach v_2 auf Grund einer Entnahme der Längen der Dreiecksseiten aus der Figur bestimmen.

Nach der obigen fortlaufenden Gleichung gilt

$$D_{\mathrm{I},1} C_1 = (v_2 / v_1)\, D_{\mathrm{I},1} B_{\mathrm{I},1}\,;\; D_{\mathrm{II},1} C_1 = (v_2 / v_1)\, D_{\mathrm{II},1} B_{\mathrm{II},1},$$

was folgendermassen interpretiert werden kann: Die Streckung der fiktiven Strahlen $D_{\mathrm{I},1} B_{\mathrm{I},1}$ bzw. $D_{\mathrm{II},1} B_{\mathrm{II},1}$ mit dem Quotienten v_2 / v_1 liefert die physikalisch reellen Strahlen $D_{\mathrm{I},1} C_1$ bzw. $D_{\mathrm{II},1} C_1$. Hierbei schrumpfen die fiktiven Wellenfronten $B_{\mathrm{I},1} C_1$ bzw. $B_{\mathrm{II},1} C_1$ auf den Punkt C_1 zusammen, in dem sich die physikalisch reellen Wellenfronten $A_{\mathrm{I},1} C_1$ bzw. $A_{\mathrm{II},1} C_1$ schneiden.

In den vorstehenden Ausführungen sind die einzelnen Schritte zur Konstruktion des refraktierenden Horizonts H_1 jeweils dort beschrieben worden, wo es die entsprechenden Überlegungen zu ihrer Herleitung erstmals zuliessen. Aus Gründen der Übersichtlichkeit mögen sie daher nachstehend nochmals zusammengestellt werden:

1) Man bringe in Fig. 14 die zweiten Äste der Laufzeitkurven mit den beiden Zeitachsen zum Schnitt, die im gleichen Wert $T_1 (S)$ getroffen werden.

2) Die Gerade $T = \frac{1}{2} T_1 (S)$ schneidet die ersten Äste der Laufzeitkurven in den Punkten $B_{\mathrm{I},1}$ bzw. $B_{\mathrm{II},1}$, die zweiten Äste in $A_{\mathrm{I},1}$ bzw. $A_{\mathrm{II},1}$.

3) Mit den Projektionen der gleich langen Strecken $S_{\mathrm{I}} B_{\mathrm{I},1}$ bzw. $S_{\mathrm{II}} B_{\mathrm{II},1}$ auf die Entfernungsachse zeichne man um S_{I} bzw. S_{II} Kreise; an diese sind von $A_{\mathrm{II},1}$ bzw. $A_{\mathrm{I},1}$ aus Tangenten zu legen, wodurch die rechtwinkligen Dreiecke $S_{\mathrm{I}} A_{\mathrm{II},1} B_{\mathrm{I},1}$ bzw. $S_{\mathrm{II}} A_{\mathrm{I},1} B_{\mathrm{II},1}$ entstehen.

4) Der Schnittpunkt C_1 der Tangenten ist der erste geometrische Ort für H_1. Die Tangenten werden parallel zu sich selbst um den gleichen Abstand verschoben, und zwar beide in Richtung auf den gleichen Schusspunkt — z.B.

S_I — hin. Der Schnittpunkt dieser Parallelen — z.B. C_1^* — ist der zweite geometrische Ort für H_1.

5) Die Geschwindigkeit des unterhalb H_1 liegenden zweiten Mediums

$$v_2 = v_1\,(D_{I,1}\,C_1\,/\,D_{I,1}\,B_{I,1}) = v_1\,(D_{II,1}\,C_1\,/\,D_{II,1}\,B_{II,1})$$

bestimmt sich durch Entnahme der Streckenlängen aus der Figur.

Im Gegensatz zu der üblichen rechnerischen Behandlung erfolgt hier die Konstruktion des Horizontes H_1 und die Bestimmung der Geschwindigkeit v_2 ohne Benutzung der Knickpunkte in den Laufzeitkurven und ohne Errechnung der Scheingeschwindigkeiten.

Nunmehr wenden wir uns einer weiteren Auswertung der Laufzeitkurven unseres Beispiels zu, nämlich der geometrischen Darstellung des zweiten Refraktionshorizontes H_2 zwischen zweiter und dritter Schicht. Die Konstruktion besteht in völliger Analogie zur Reflexionsseismik in einer sukzessiven Tangierung von Fronten der Mintrop-Welle, wobei die einzelnen Schritte durch die Anwendung des Prinzips der Streckung fiktiver Lotstrahlen gekennzeichnet sind.

Für unsere Aufgabe sind in Fig. 15 nochmals die Laufzeitkurven der Fig. 14 dargestellt; ausserdem ist der bereits festgelegte Horizont H_1 eingetragen. Der Auswertung dienen die ersten und dritten Äste der Laufzeitkurven. Nach dem Vorhergehenden ist nur eine geringfügige Erläuterung der Konstruktion nötig, so dass die einzelnen Schritte sofort aufgezählt werden können. Zunächst gilt:

a) Die dritten Äste der Laufzeitkurven schneiden die beiden Zeitachsen im gleichen Wert $T_2\,(S)$.

Wieder gilt für zwei von S_I bzw. S_{II} ausgehende Impulse, die sich auf dem Refraktionshorizont H_2 treffen, dass die Summe ihrer Laufzeiten gleich $T_2\,(S)$ ist. Der Treffpunkt ergibt sich wiederum als Schnittpunkt der Mintrop-Wellen, die von den gegeneinander laufenden Impulsen nachgezogen werden; er wird nachstehend für den Spezialfall ermittelt, dass die Laufzeit eines jeden Impulses gleich $\frac{1}{2}\,T_2\,(S)$ ist:

b) Die Gerade $T = \frac{1}{2}\,T_2\,(S)$ schneidet die ersten Äste der Laufzeitkurven in den Punkten $\bar{B}_{I,2}$ bzw. $\bar{B}_{II,2}$, die dritten Äste in $\bar{A}_{I,2}$ bzw. $\bar{A}_{II,2}$.

c) Mit den Projektionen der gleich langen Strecken $S_I\,\bar{B}_{I,2}$ bzw. $S_{II}\,\bar{B}_{II,2}$ auf die Entfernungsachse zeichne man um S_I bzw. S_{II} Kreise; an diese sind von $A_{II,2}$ bzw. $A_{I,2}$ aus Tangenten zu legen, wodurch die rechtwinkligen Dreiecke $S_I\,A_{II,2}\,B_{I,2}$ bzw. $S_{II}\,A_{I,2}\,B_{II,2}$ entstehen.

Die Katheten dieser Dreiecke schneiden den Horizont H_1 in vier Punkten. Es leuchtet sofort ein:

d) Die Kathetenanteile $S_I\,F_{I,1}$ bzw. $S_{II}\,F_{II,1}$ sind physikalisch reell; sie gehören zu dem am Horizont H_2 refraktierten Strahlenzug. Daher sind die Strecken $G_{II,1}\,A_{II,2}$ bzw. $G_{I,1}\,A_{I,2}$ die Fronten der Mintrop-Wellen, die unsere auf H_2 einander treffenden Impulse der Laufzeit $\frac{1}{2}\,T_2\,(S)$ nachziehen.

Nunmehr kommt das Streckungsprinzip zur Anwendung, das die fiktiven Strahlen $F_{I,1}\,B_{I,2}$ bzw. $F_{II,1}\,B_{II,2}$ in solche verwandelt, die von ihren Ausgangspunkten bis zu dem gesuchten Horizont H_2 physikalisch reell sind; hierdurch wird die Gültigkeit des Brechungsgesetzes in den Punkten $F_{I,1}$ bzw. $F_{II,1}$ gewährleistet.

e) Die Strahlen $F_{I,1}\,B_{I,2}$ bzw. $F_{II,1}\,B_{II2}$, werden im Verhältnis v_2 / v_1 gestreckt und als Radien für Kreise um $F_{I,1}$ bzw. $F_{II,1}$ verwandt; an diese Kreise sind von $G_{II,1}$ bzw. $G_{I,1}$ aus Tangenten zu legen, wodurch die rechtwinkligen Dreiecke $F_{I,1}\,G_{II,1}\,E_{I,2}$ bzw. $F_{II,1}\,G_{I,1}\,E_{II,2}$ entstehen.

Anm.: Es sei noch darauf hingewiesen, dass der Streckungsfactor v_2/v_1 ohne Kenntnis der Geschwndigkeiten selbst als Verhältnis zweier Dreiecksseiten der Fig. 14 entnommen werden kann (vgl. z.B. Schritt 5) der Konstruktion des Horizontes H_1.

Analog zu den entsprechenden Darlegungen in bezug auf H_1 lässt sich sofort einsehen:

f) Der Schnittpunkte C_2 der Tangenten $G_{II,1}\,E_{I,2}$ und $G_{I,1}\,E_{II,2}$ ist der erste geometrische Ort für H_2. Die Tangenten werden parallel zu sich selbst um den gleichen Abstand verschoben, und zwar beide in Richtung auf den gleichen Schusspunkt — z.B. S_I — hin. Der Schnittpunkt dieser Parallelen — z.B. $C_2{}^*$ — ist der zweite geometrische Ort für H_2.

Der Horizont H_2 schneidet die Katheten $F_{I,1}\,E_{I,2}$ bzw. $F_{II,1}\,E_{II,2}$ der beiden in e) konstruierten rechtwinkligen Dreiecke in den Punkten $D_{I,2}$ bzw. $D_{II,2}$. Es entstehen so die einander ähnlichen rechtwinkligen Dreiecke $D_{I,2}\,C_2\,E_{I,2}$ bzw. $D_{II,2}\,C_2\,E_{II,2}$, für die gilt:

g) $\sin \varphi_2 = v_2 / v_3 = D_{I,2}\,E_{I,2} / D_{I,2}\,C_2 = D_{II,2}\,E_{II,2} / D_{II,2}\,C_2$

wobei φ_2 der Grenzwinkel der Totalreflexion an H_2 ist. Hat man nach Schritt 5) der Konstruktion des Horizontes H_1 die Geschwindigkeit v_2 bestimmt, lässt sich nunmehr v_3 errechnen.

Es werde noch einmal besonders auf die physikalische Bedeutung folgender Streckenzüge der Fig. 15 hingewiesen:

α) Der Streckenzug $S_I\,F_{I,1}\,D_{I,2}\,D_{II,2}\,F_{II,1}\,S_{II}$ ist der Strahl, auf dem ein von S_I ausgehender, am Horizont H_2 refraktierter Impuls nach S_{II} gelangt; ebenso gilt diese Aussage für die Gegenrichtung von S_{II} aus nach S_I.

β) Der Streckenzug $A_{I,2}\,G_{I,1}\,C_2$ ist die Front der Mintrop-Welle, die von dem Refraktionsimpuls nachgezogen wird, der von S_I nach S_{II} läuft und sich zur Zeit $T = \frac{1}{2}\,T_2\,(S)$ in C_2 befindet.

γ) Der Streckenzug $A_{II,2}\,G_{II,1}\,C_2$ ist die Front der Mintrop-Welle, die von dem Refraktionsimpuls nachgezogen wird, der von S_{II} nach S_I läuft und sich zur Zeit $T = \frac{1}{2}\,T_2\,(S)$ in C_2 befindet[6].

---

[6] Es werde noch darauf hingewiesen, dass die beschriebene Konstruktion ohne Einschränkung durchführbar ist; so z.B. auch in folgenden Sonderfällen:

1) Einer der Punkte $A_{I,1}$, $A_{II,1}$ (Fig. 14) oder $A_{I,2}$, $A_{II,2}$ (Fig. 15) liegt nicht zwischen S_I und S_{II}.

2) Eine Scheingeschwindigkeit ist unendlich bzw. negativ, d.h. der Anstieg des zugehörigen Astes der Laufzeitkurve ist Null oder negativ.

Nachdem die Festlegung der Refraktionshorizonte H_1 und H_2 durch die Aufzählung der Konstruktionsschritte 1) bis 5) und a) bis g) ausführlich beschrieben ist, bietet die Erweiterung des Verfahrens auf das ebene n-Schichtenproblem keine Schwierigkeiten. Für die Konstruktion des n-ten Refraktionshorizontes H_n aus den $(n + 1)$-ten Ästen der Laufzeitkurven ist notwendig, dass die Horizonte $H_1, H_2, \ldots, H_{n-1}$ bereits vorliegen. Zunächst werden die von den Schusspunkten S_{I} und S_{II} ausgehenden gebrochenen Strahlenzüge festgelegt, und zwar durch $(n - 1)$maliges sukzessives Strecken fiktiver Lotstrahlen und Tangieren von den Schnittpunkten der Mintrop-Wellen mit den Horizonten. Sodann ergibt wieder eine Parallelverschiebung der Wellenfronten im Medium der Geschwindigkeit v_n die Lage des Horizontes H_n sowie das Geschwindigkeitsverhältnis v_n / v_{n+1}[7].

Die folgenden Eigenschaften dieses Verfahrens dürfen wohl als erhebliche Vorteile gegenüber den üblichen rechnerischen Methoden hervorgehoben werden:

1) Die Horizonte werden durch eine sukzessive Zeichnung schnell festgelegt; jeder Einzelschritt ist leicht durch die Anschauung kontrollierbar.

2) Jegliche Rechnungen und damit Vorzeichenfehler, die z.B. gerade bei Vorhandensein von entgegengesetzt einfallenden Horizonten leicht möglich sind, fallen fort.

3) Es werden keine Tabellen oder Diagramme benötigt.

4) Schliesslich liefert die Konstruktion eines Horizontes gleichzeitig die zugehörige Front der Mintrop-Welle in ihrem gesamten Verlauf, wodurch der Ablauf des physikalischen Vorganges anschaulich dargestellt wird.

2. *Behandlung des räumlichen Falles durch sukzessive Tangierung von Fronten der Mintrop-Welle in den Brechungsebenen*

Das soeben dargestellte Verfahren zur Festlegung von refraktionsseismischen Horizonten für den ebenen Fall hat über die bereits genannten vorteilhaften Eigenschaften hinaus noch die weitere, sich ohne grosse Schwierigkeit auf den dreidimensionalen Fall erweitern zu lassen, der wegen seiner Kompliziertheit in der einschlägigen Literatur bisher ausser Betracht geblieben ist. Die Erweiterung gelingt zwanglos durch Hinzunahme des in Abschnitt B, 4 beschriebenen Verfahrens der Konstruktion in der Brechungsebene zu der im vorigen Abschnitt dargelegten Methode. Es genügt, die Behandlung des räumlichen Falles der Refraktion nur zu skizzieren da die Grundlagen hierfür ausführlich in den Abschnitten B, 4 und C, 1 erörtert worden sind.

Es sollen also in der Erdkruste n aufeinander folgende Schichten mit den jeweils konstanten Schichtgeschwindigkeiten $v_1 < v_2 < \ldots < v_n$ vorhanden sein. Die Schichtgrenzen, d.h. die refraktierenden Horizonte $H_1, H_2, \ldots, H_{n-1}$

---

[7] Man vergleiche hierzu auch die bereits zitierte Arbeit von Dienesch und Richard (1953), in der die Festlegung der gebrochenen Strahlenzüge mit Hilfe der gleichen Diagramme erfolgt, die dort für die Spiegelkonstruktion der Reflexionsseismik entworfen wurden.

seien Ebenen, deren Normalen nun nicht mehr komplanar sind. — Durch Gegenschiessen seien auf einem Profil $S_{I}\,S_{II}$ und auf einem begleitenden Streifen desselben refraktionsseismische Laufzeitmessungen durchgeführt. Es ist nun die Aufgabe, aus den Zeitmessungen die Horizonte zu kartieren und die Schichtgeschwindigkeiten zu bestimmen. Die Lösung wird sofort für den Horizont H_i — $i = 1, 2, \ldots, n - 1$ — beschrieben unter der Voraussetzung, dass die darüberliegenden Horizonte bis H_{i-1} *bereits* ermittelt sind[8]. (Fig. 16).

Die von S_{I} bzw. S_{II} ausgehenden und am Horizont H_i refraktierten seismischen Impulse werden in den Bereichen um die Punkte Q_{I} bzw. Q_{II} als erste Einsätze registriert; ihre Laufzeiten $T_{I,\,i}$ bzw. $T_{II,\,i}$ sind den $(i+1)$-ten Ästen der Laufzeitkurven zu entnehmen. Zur Festlegung des Horizontes H_i ist es zunächst notwendig, die Inzidenzrichtungen der entsprechenden Strahlen sowohl an den Schusspunkten als auch an den Empfangspunkten aus den Zeitmessungen zu ermitteln. Hierzu dient die flächenhafte Vermessung in der Nachbarschaft von Q_{I} bzw. Q_{II}, deren Ergebnis in den Isochronenplänen $T_{I,i} = \text{const}$ bzw. $T_{II,i} = \text{const}$ ihren Niederschlag findet. Aus dem Isochronengradienten und der Geschwindigkeit v_1, die den ersten Ästen der Laufzeitkurven zu entnehmen ist, sind die Inzidenzrichtungen der Strahlen in den Punkten Q_{I} bzw. Q_{II} bestimmbar. Nunmehr erfolgt eine Parallelverschiebung der so in Q_{I} bzw. Q_{II} festgelegten Strahlen zu den Schusspunkten S_{II} bzw. S_{I} hin (Reihenfolge der Indizes beachten!). Damit kennt man die Richtungen, in denen die am Horizont H_i refraktierten Impulse die Schusspunkt verlassen

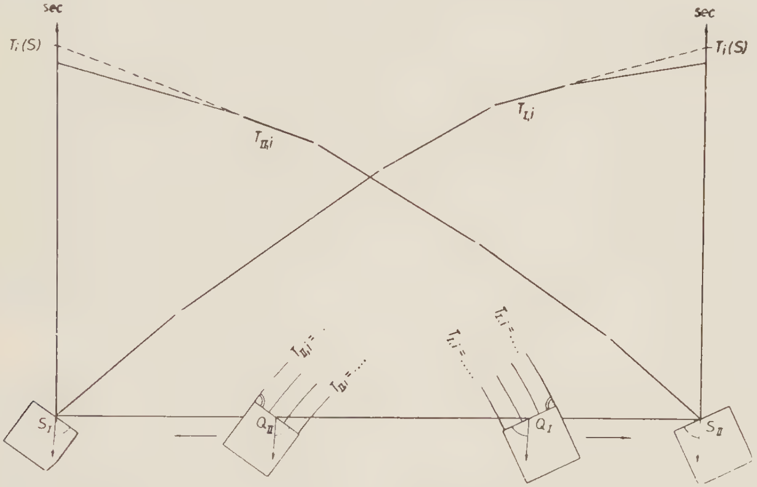

Fig. 16. Anfangsrichtung des zum Horizont H_i gehörenden Refraktionsstrahles im räumlichen Fall. — Direction of emergence in the three-dimensional case, of the refracted ray that corresponds to the interface H_i.

---

[8] Soll H_i für $i = 1$ bestimmt werden, so ist der darüberliegende Horizont H_0 die Messebene.

bzw. erreichen [9]. Die Laufzeit der von Schusspunkt zu Schusspunkt über H_i gelaufenen Impulse erhält man durch Verlängerung der T_i-Äste in den Laufzeitkurven bis zum Schnitt mit den Zeitachsen. Es gilt wiederum $T_{\text{I},i}\,(S_{\text{II}}) = T_{\text{II},i}\,(S_{\text{I}}) = T_i\,(S)$.

Aus den Richtungen der Strahlen in den Schusspunkten S_{I} und S_{II} ist der weitere Verlauf der gebrochenen Strahlenzüge bis in das Medium der Geschwindigkeit v_i sofort zu bestimmen; man benutzt hierzu die Methode der Konstruktion in der Brechungsebene ausgehend von den beiden Schusspunkten und setzt für jeden die Zeit $\frac{1}{2}\,T_i\,(S)$ an.

Durch sukzessives Strecken der fiktiven Lotstrahlen innerhalb der immer neu zu zeichnenden Brechungsebenen und Tangierung von Fronten der Mintrop-Wellen ergibt sich schliesslich die räumliche Lage der beiden von S_{I} bzw. S_{II} ausgehenden Strahlenteile im Medium der Geschwindigkeit v_i. Letztere müssen nun eine Ebene aufspannen, denn sie haben ja mit dem in H_i laufenden (total reflektierten) Strahl eine gemeinsame Brechungsebene. — Bei der praktischen Durchführung wird die Schwierigkeit auftreten, dass die genannten Strahlenteile schwach windschief verlaufen. Man muss dann ihre räumliche Lage ein wenig korrigieren, um zu erreichen, dass sie in einer Ebene liegen.

Innerhalb der so bestimmten gemeinsamen Brechungsebene wird die Spur des Horizontes H_i nach der für den ebenen Fall beschriebenen Konstruktion durch Parallelverschiebung der Wellenfronten festgelegt; entsprechend ermittelt man wie dort die Schichtgeschwindigkeit v_{i+1} unterhalb H_i.

Die gemeinsame Brechungsebene steht senkrecht auf dem Horizont H_i. Errichtet man also auf der soeben konstruierten Spur von H_i in der Brechungsebene eine Normale und projiziert diese senkrecht auf die Messebene, so erhält man die Fallrichtung des Horizontes. Nunmehr kann auch der Tiefenlinienplan des Horizontes H_i gezeichnet werden, womit unsere eingangs formulierte Aufgabe gelöst ist.

D. Anhang

Prinzipielle Bemerkungen zur Festlegung reflexionsseismischer Horizonte bei allgemeiner Geschwindigkeitsverteilung

In Abschnitt B sind Verfahren zur konstruktiven Darstellung von Reflexionshorizonten unter der Voraussetzung spezieller Geschwindigkeitsverteilungen entwickelt worden, und zwar solcher, die in der Praxis die wichtigste Rolle spielen. Zwei Konstruktionsprinzipien haben hierbei immer wieder Verwendung gefunden, nämlich

a) die Bestimmung der Inzidenzrichtung des seismischen Lotes zu einem reflektierenden Horizont H_i aus den Isochronen $T_i = \text{const}$ und der Geschwindigkeit in der Messebene,

---

[9] Die Parallelverschiebung liefert in den Schusspunkten die richtigen Inzidenzrichtungen, da wir ebene Horizonte und konstante Schichtgeschwindigkeiten vorausgesetzt hatten.

b) die Festilegung des gebrochenen Strahlenzuges eines seismischen Lotes durch Streckung fiktiver Lotstrahlen.

Nunmehr soll gezeigt werden, dass diese Prinzipien ihre Gültigkeit und Bedeutung auch für den allgemeinen Fall behalten, in dem eine beliebige Geschwindigkeitsverteilung $v = v\,(x, y, z)$ oberhalb des zu lokalisierenden Reflexionshorizontes H_i vorliegt, der im übrigen gekrümmt sein und eine beliebige Lage im Raum haben kann.

Zunächst ist also zu zeigen, wie sich bei allgemeiner Geschwindigkeitsverteilung $v = v\,(x, y, z)$ die Inzidenzrichtung eines seismischen Lotes bestimmt. Hierzu betrachten wir wieder die Lotstrahlen, die von den Schusspunkten in der Messebene ausgehen und auf den i-ten Horizont H_i senkrecht auftreffen, somit in sich selbst reflektiert werden. Die zugehörigen Lotzeiten T_i für den doppelt durchlaufenen Weg vom Schusspunkt zum Horizont und zurück sind aus den Seismogrammen bekannt. Die Anfangsrichtung des Lotstrahles am Schusspunkt ergibt sich wieder aus folgender Überlegung: Man denke sich zur Zeit $\tau = O$ die seismische Erregung vom Horizont H_i senkrecht ausgehend; es ist also H_i in diesem Zeitpunkt eine Wellenfront. Beim Lauf der Erregung bis zur Messebene stehen die Schallstrahlen stets senkrecht auf den Wellenfronten. Das ist die Aussage des Satzes von Malus; sie wird in der geometrischen Optik, deren Sätze wir üblicherweise als gültig für die geometrische Seismik betrachten, durch folgende Gleichung beschrieben:

$$v^2\,(\mathrm{grad}\,\tau)^2 = 1$$ [10].

Es bedeuten $\tau = \mathrm{const}$ die Wellenflächen, auf denen der Strahlvektor grad τ senkrecht steht. Ist die Geschwindigkeit v als Ortsfunktion gegeben, so kann mit Hilfe dieser Gleichung zu jeder gegebenen Wellenfläche die benachbarte konstruiert werden, so dass schliesslich die Gesamtheit aller Wellenflächen ermittelt werden kann. — In Vektorform lautet die obige Beziehung:

$$v\,\mathrm{grad}\,\tau = \vec{e}$$

wobei $\vec{e}$ der Einheitsvektor in Strahlrichtung und $\tau = \tau\,(x, y, z)$ die Laufzeit der seismischen Erregung auf dem Lotstrahl vom Horizont H_i zum Punkt (x, y, z) sind. Legen wir die x- und y-Achse in die Messebene, so interessiert uns dieser Ausdruck für einen Schusspunkt $S = S\,(x, y, O)$ derselben, in dem die Geschwindigkeit $v = v^S$ ist:

$$v^S\;(\mathrm{grad}\,\tau)^S = \vec{e}^{\,S}\,;\; S = S\,(x, y, O).$$

Wir zerlegen den Vektor $(\mathrm{grad}\,\tau)^S$ in die beiden Komponenten

$$(\mathrm{grad}^F\,\tau)^S,\;\; (\delta\tau\,/\,\delta z)^S\,;$$

---

[10] Diese Gleichung ist aus der geometrischen Optik — d.h. dem Teil der Optik, bei dem weder Beugung noch Polarisation eine Rolle spielen — in der Gestalt

$$(\mathrm{grad}\;E)^2 = N^2$$

als Eikonalgleichung bekannt. Hierbei bedeuten E das Eikonal und $N = N\,(x, y, z)$ den Brechungsindex.

hierbei ist der invariante Differentialoperator grad^F der zweidimensionale Gradient in der Messebene, der also aus $\tau = \tau\,(x, y, O)$ bestimmt wird. Da aber $\tau\,(x, y, O) = \frac{1}{2}\,T_i$ durch die reflexionsseismischen Messungen bekannt ist, erhält man die Komponente

$$(\text{grad}^F\,\tau)^S = \tfrac{1}{2}\,(\text{grad}\,T_i)^S$$

aus dem Verlauf der Isochronen $T_i = \text{const.}$ Hiernach ergibt sich wegen $|\,\vec{e}^{\,S}\,| = 1$ die Lage von $\vec{e}^{\,S}$ im Raume; schliesslich auch die Komponente $(\delta\tau\,/\,\delta z)^S$, die aber nicht weiter interessiert.

Der Einheitsvektor e^S des vom Schusspunkt S ausgehenden Lotstrahls liegt also in einem Vertikalschnitt zur Messebene, der die Isochronenrichtung in S senkrecht scheidet. Für den Inzidenzwinkel $(\alpha_i)^S$ am Schusspunkt, d.h. den Winkel zwischen Messebenen-Normale und Lotstrahl, gilt die Beziehung:

$$\sin\,(\alpha_i)^S = v^S\,\tfrac{1}{2}\,|(\text{grad}^F\;T_i)^S|.$$

Die Anfangsrichtung des Lotstrahls ist somit auch bei allgemeiner Geschwindigkeitsverteilung — in gleicher Weise wie für den Fall der konstanten Schichtgeschwindigkeit (s. Abschn. B, 1) und den Fall des linearen Anstiegs der Geschwindigkeit mit der Tiefe (s. Abschn. B, 6) — nur abhängig vom Zeitgradienten in der Messebene und der Anfangsgeschwindigkeit.

Hiermit ist die allgemeine Gültigkeit des eingangs erwähnten Konstruktionsprinzips a) erwiesen. Seine Bedeutung liegt wiederum darin, dass mit der Anfangsrichtung des Lotstrahls dieser automatisch vom Schusspunkt bis zum reflektierenden Horizont H_i festliegt. Das ist eine Folge des Prinzips von Fermat, nach dem der Strahl zwischen zwei Punkten P und Q bei vorgegebener Geschwindigkeitsverteilung aus der Bedingung

$$\int_P^Q \frac{ds}{v} = \text{Extremum}$$

bestimmt wird. — Die Eulerschen Differentialgleichungen für dieses Variationsproblem sind von zweiter Ordnung. Für $P = S = S\,(x, y, O)$ und beliebiges Q liefern ihre Lösungen sämtliche möglichen Strahlen mit dem Ausgangspunkt S, dem Schusspunkt. Aus dieser Mannigfaltigkeit wird der gesuchte Lotstrahl durch seine Anfangsrichtung eindeutig [11] ausgewählt. Schliesslich ergibt sich der Punkt auf dem Lotstrahl, der auch dem Horizont H_i angehört — in dem also die Reflexion stattfindet — aus der Kenntnis der Lotzeit T_i am Schusspunkt.

Z.B. sind die Extremalen des Variationsproblems Geraden für konstante Schichtgeschwindigkeit bzw. Kreise für lineare Zunahme der Geschwindigkeit mit der Tiefe. Diese beiden Fälle waren in Abschnitt B Gegenstand unserer

---

[11] Das ist bekanntlich der Fall, wenn $(\text{grad}\,v)\,/\,v$ im gesamten betrachteten Bereich eindeutig ist.

Betrachtung. Dort wurde die Anfangsrichtung der Lotstrahlen durch eine Tangentenkonstruktion zeichnerisch festgelegt. Das ist auch im allgemeinen Falle in entsprechender Weise immer möglich, wenn die Extremalen und Wellenfronten sich mit einfachem Gerät zeichnen lassen; andernfalls bleibt nur der Weg der Rechnung offen.

Weiterhin erfolgte in Abschnitt B die Lokalisierung der Reflexionshorizonte, die Unstetigkeitsflächen der Geschwindigkeit waren, durch sukzessive Tangierung, indem die gebrochenen Strahlenzüge der seismischen Lote mit Hilfe des Prinzips der Streckung fiktiver Lotstrahlen konstruiert wurden. Bei allgemeiner Geschwindigkeitsverteilung zwischen derartigen Horizonten kann man analog verfahren, was an folgender Aufgabe kurz beschrieben werden soll:

Es seien mehrere Reflexionshorizonte vorhanden, an denen die Geschwindigkeit sich sprungartig ändert. Zwischen diesen Unstetigkeitsflächen seien jeweils verschiedene Geschwindigkeitsfunktionen gegeben, für die eine zeichnerische Konstruktion der Extremalen und Wellenfronten möglich ist.

Sind sämtliche Horizonte bis H_{i-1} bereits festgelegt, so erfolgt die Konstruktion des Horizontes H_i in folgender Weise:

Aus den Isochronen $T_i = \text{const}$ in der Messebene und den Wellenfronten, die zur Geschwindigkeit $v_1 = v_1\,(x, y, z)$ des ersten Mediums (oberhalb H_1) gehören, wird durch Tangierung ein fiktiver Horizont $H_i^*\,(v_1)$ gezeichnet. An der ersten Unstetigkeitsfläche, also am Horizont H_1 sind die Restzeiten zu ermitteln, d.h. die Laufzeiten der seismischen Erregung entlang der fiktiven Lotextremalen zwischen H_1 und $H_i^*\,(v_1)$. Von H_1 aus wird nun mit Hilfe der Restzeiten und der Wellenfronten, die zur Geschwindigkeit $v_2 = v_2\,(x, y, z)$ des zweiten Mediums gehören, durch Tangierung der fiktive Horizont $H_i^*\,(v_2)$ konstruiert. An der zweiten Unstetigkeitsfläche, also am Horizont H_2, sind die Restzeiten zu ermitteln, d.h. die Laufzeiten der seismischen Erregung entlang der fiktiven Lotextremalen zwischen H_2 und $H_i^*\,(v_2)$; u.s.w.

Man kann in gewissem Sinne auch hier von einer „Streckung fiktiver Lotextremalen" sprechen. Natürlich ist diese „Streckung" jetzt nicht so einfach wie im Fall konstanter Geschwindigkeiten, also geradliniger Extremalen, bei dem der „Streckungsfaktor" als Quotient zweier Geschwindigkeiten gegeben war. Vielmehr muss man im allgemeinen Fall auf die Restzeiten zurückgreifen, um die „Streckung fiktiver Lotextremalen" durchführen zu können.

Verfasser dankt Herrn Dr. O. Rosenbach und Herrn Dr. F. Heimburg für wertvolle Anregungen und Hinweise, sowie der Prakla für die freundliche Genehmigung zur Veröffentlichung dieser Arbeit.

LITERATUR:

Dienesch, J. und Richard, H., 1953: "Procédés géométriques simples pour construction de coupes sismiques, application." Veröffentlichung der Compagnie Générale de Géophysique, vorgetragen auf der EAEG-Tagung, Paris.

Dix, C. Hewitt and Lawler, Reed C., 1943: "Computation of seismic dips below an unconformity." Geophysics VIII, 105-118.

Dix, C. Hewitt, 1952: "Seismic Prospecting for Oil", 141-162, Harper and Brothers, New York.

Dürbaum, H., 1953: "Possibilities of constructing true ray paths in reflection seismic interpretation." Geophysical Prospecting I, 125-139.

Jakosky, J. J., 1950: "Exploration Geophysics", 2nd Ed., Trija Publishing Company, Los Angeles.

Kaufmann, H., 1953: "Velocity functions in seismic prospecting." Geophysics XVIII, 289-297.

Krey, Theodor, 1954: "Extension to threedimensional problems concerning an approximate correction method for refraction in reflexion seismic prospecting." Geophysical Prospecting II, 61-72.

Romberg, Frederick, 1952: "Limitations of the seismic method of mapping faults." Geophysics XVII, 827-842, (insbesondere S. 835).

Slotnick, M M., 1936: "On seismic computations with applications, I." Geophysics I, 9-22.

ELECTRICAL HAZARDS IN SEISMIC PROSPECTING*

BY

A. M. SELEM** AND E. MERLINI**

ABSTRACT

Hazards due to powerlines, radiotransmitters and self-potentials in connection with weather conditions are considered. Voltage and current values are given for several measurements made under the most severe conditions of circuit arrangements. The necessity of general safety precautions is stressed.

INTRODUCTION

Electrical hazards in seismic prospecting are connected with the type of detonators used and vary with the general conditions of the area investigated.

This report considers the use of electrical seismic detonators, i.e. detonators which will not usually fire if subjected to a continous current of less than 250 ma. Since, however, for testing the continuity of the fuse head the current used in routine seismic work does not normally exceed 20 ma, this value is here considered as the highest safe current admissible. Similarly, since insulation tests prove that flash-overs take place when the potential difference between the fuse head and the metallic case of the detonators exceeds 1200 volts, a value of 200 volts is here admitted as the highest safe voltage.

Extraneous electrical conditions which may affect the safety of seismic shooting vary widely from the tropical deserts, where dust storms create dangerous statics and self-potentials due to particular ground formations may be encountered, to the highly industrialized areas of the temperate climates, where overhead powerlines, railways, radiotransmitters, other electrically operated equipment, ground and weather conditions may be simultaneous factors of the electrical hazard.

This report is limited to some measurements of the hazards which may occur in the industrialized areas of Western Europe because of induced voltages and leakages from powerlines and radiotransmitters and of self-potential distributions near powerlines or large metallic masses in connection with the weather situation.

INDUCED VOLTAGES UNDERNEATH AND NEAR A POWERLINE

Such voltages are due to electro-magnetic induction in the conducting elements of the blasting circuit and in the ground.

---

* Presented at the Fifth Meeting of the European Association of Exploration Geophysicists, held in Milan, 2/4 December 1953.

** AGIP Mineraria, Milan.

To check their distribution, r.m.s. values were measured using valve voltmeters with input impedances of about 5 megohms. In practice, such measurements may be considered as open circuit determinations.

The tests were carried in the vicinity of a 130.000 volt powerline where seismic recording had already shown strong disturbances.

Two 100 meter lengths of P.V.C. covered wire, having a section of 0,5 mm^2 and a resistance of 3,7 ohms, were laid out in a series of different arrangements over grass land wet from previous rain.

The first group of measurements was made with the two leads running parallel and underneath the powerline at a distance of 5 mm from each other.

Initially the two leads were shorted at one end and perfectly insulated at the other, this being the case of a circuit open at one end and connected with the detonator at the other end with perfect insulation everywhere.

The shorted terminal was then grounded, simulating the case when a contact occurs between the blasting circuit and the ground.

Finally, measurements were made with the two leads separated at both ends, but one lead was earthed at one of its ends. This case was made only to evaluate the approximate amplitude of the powerline disturbances affecting the seismic record.

The same measurements were with the two leads underneath the powerline and parallel to it, but separated by a distance of 1 meter.

Similar measurements were repeated with the two leads always running parallel to the powerline, but at a distance of 90 meters and then at 150 meters to one side of the line.

Table I shows the most significant values which were recorded. The highest

TABLE I

INDUCED VOLTAGES IN CIRCUIT PARALLEL TO POWERLINE

Circuit formed by two 100 meters leads running parallel to a 130.000 volts powerline. Voltage values in millivolts.

	Position relative to powerline	One end shorted and insulated	One end shorted and grounded	Both ends open. One lead grounded at one end
Distance between leads 5 millimeters	Beneath	0	0	27
	90 meters to one side	0	0	4
	150 meters to one side	0	0	3
Distance between leads 1 meter	Beneath	25	25	54
	90 meters to one side	3,3	4,5	4
	150 meters to one side	2,8	3,2	2,5

values are found for the two leads running at a distance of 1 meter from each other immediately beneath and parallel to the powerline. This value remains practically the same in the case of the two leads having their shorted end grounded as well as in the case where this terminal is insulated.

Considering the total resistance of the wires and of the detonator, the current originated by such voltages is within the safety limits.

Voltages due to leakages from powerlines

Leakages from powerlines due to special lack of insulation may lead to local voltage distributions in the ground.

To form some estimate of these, a series of tests was carried out in very damp weather conditions at the branching off point of a 130.000 volts powerline.

A lead 50 m in length was laid out on the ground so that its terminals were both underneath the two branches of the powerline; one terminal was tied to an iron pipe driven 1 meter into the ground, whilst the other terminal was connected to a 20 × 30 cm aluminium plate laid on the ground, thus reproducing the case of a blasting circuit in contact with the casing of a shot hole whilst the blaster is laid on the ground.

The measurements recorded with an AC valve voltmeter showed a maximum voltage of 2,5 volts and a maximum current of about 8 milliamperes.

Such a current is within the safety limits of the detonator, but it may increase dangerously during the summer season when the dust deposition on the powerline insulators is greater and a sudden increase in dampness may cover them with a wet film of relatively small ohmic resistance.

Voltages from powerlines during storms

A long series of tests was made near powerlines when storms were approaching in order to determine the effects of lightnings striking the powerlines or the ground close to them.

Because of the instantaneous character of such phenomena oscillographs were necessarily used.

Whenever it could be presumed that lightning was striking the powerline or the close surroundings of it within a distance of about 3 km from the observation station, the trace of the first pulse went beyond the limit of the oscillograph screen whilst the following smaller pulses were recorded.

Since, in the instrument used, the voltage for maximum deflection of the oscillograph spot was 12 volts, it may be assumed that the amplitude of the first instantaneous pulse is generally very great.

Smaller values were recorded as the storm area receded from the oscillograph, and at distances of more than 7 km the deflections on the oscillograph screen became negligible.

Such a distance is therefore believed to be quite a safe limit for carrying on seismic shooting, provided of course that the safety means on the powerlines are fully efficient.

RADIO-FREQUENCY TRANSMISSIONS

Low-power transmitters, such as those used in refraction prospecting, may be a source of hazard when the blaster is connected to the transmitter and the latter is not well grounded. In such case a 20 watt antenna transmitter may set up currents of 20 to 40 milliamperes on a blasting circuit 40 to 50 meters long, shorted and grounded at one terminal. It is therefore always advisable to insert by-pass condensers, separately grounded, in the blasting circuit.

Induced currents from low-power transmitters are negligible even if the antenna is parallel to the blasting circuits, provided that lengths tuned to the frequency of the transmitters are avoided.

For transmitters of higher power induced currents become more dangerous and whenever seismic shooting is carried out near broadcasting stations the limits of the dangerous area should be fixed in advance by proper lay-outs of circuits and thermo-ammeters determinations.

COMBINED EFFECTS OF SELF-POTENTIALS AND INDUCED VOLTAGES NEAR POWERLINES AND SMALL METALLIC MASSES

The self-potential distributions which are considered here are due to electro-chemical reactions between electrodes of different metals with the ground and between different ground formations. Since, however, electro-chemical contacts may give rise to the rectification of voltages induced by powerlines or arising from leakages from them, the sum of such effects must be considered.

Several tests were made near the pylons of a powerline and, to simulate the usual seismic shooting technique, a brass cylinder shaped as a detonator and an aluminium plate having the surface of a blaster were used. The brass cylinder, wrapped in paper and simulating a detonator placed in the explosive charge, was lowered into the 3½″ casing of a 10 meters deep hole.

The aluminium plate, laid on the ground at 15 meters from the hole, was connected to the brass cylinder by a lead running parallel to the powerline.

With a hole, drilled 4 meters from a powerline pylon and with the water table at 3 meters from the surface, a DC voltmeter (20,000 ohms/volt) inserted between the brass cylinder and the aluminium plate recorded 0,22 volt and 1,1 milliampere. A similar test with a hole 135 meters from the pylon gave 0,15 volt and 0,8 milliampere.

Measurements made with the bare brass cylinder lowered in the hole showed an increase of about 10 % in the above values.

Such effects are therefore well within the safety limits even if the shooting conditions are as severe as the one described above.

COMBINED EFFECTS OF SELF-POTENTIALS AND INDUCED VOLTAGES NEAR LARGE METALLIC MASSES

If however the surrounding metallic masses are large, quite dangerous hazards may occur. Such a situation occurred recently whilst proceeding to shoot a torpedo in a well cased to 1700 meters depth. The well was at a distance of about 9 km from a DC 3000 volts railway line. Before lowering the torpedo into the well, the potential difference between the casing of the well and the torpedo itself was checked. The torpedo was connected to the servicing truck, but this was not shorted to the metallic mass of the well. Values of 0,8 volt and of 22 milliamperes were recorded.

It is believed that such values were probably caused by special electromagnetic fields set up by trains running at the time along the railway, since a few hours later the measurements were repeated and only 0,3 volt and 1,3 milliampere were recorded.

In any case, the values stress the necessity, whenever such operations occur, of shorting the servicing truck to the casing of the well by large diameter leads with small ohmic resistance.

Conclusions

In appreciating the results of the above experiments, it must be borne in mind that the conditions that prevail in seismic field work—and consequently the hazards involved—vary over wide limits. In nearly all the situations which we have investigated, the usual hazards due to powerlines, to low-power radio transmitters and to self potentials were within the admissable safety limits by a factor of at least 2½. But a relatively inconspicuous change in conditions may cause these limits to be exceeded. Since it is impossible to carry out safety checks continuously during routine seismic operations, the wisdom of adhering to the following general safety rules is stressed.

1) Make up the charge at the shot hole, keeping the detonator wires shorted and as far as possible folded.

2) Connect the detonator wires to the lead wires only after the charge has been lowered some distance down the hole.

3) Keep the lead wires in a compact coil of minimum area with their free ends shorted and insulated.

4) As the charge is lowered down the hole unwrap the lead wires gradually and only as far as necessary.

5) Unshort the ends of the lead wires and connect them to the blaster only when ready to shoot.

6) Avoid laying out the blasting circuit parallel to nearby power lines.

7) Locate shot holes at a distance from power lines at least equal to the sum of the length of the lead wire and of twice the length of the detonator wires.

8) Stop shooting when storm approaches within 7 km.

9) When refraction shooting, connect the blaster to the radio transmitter only when ready to fire and avoid lengths of blasting circuit which cause resonance with the frequency transmitted.

10) When shooting near to large metallic masses short the servicing equipment to such masses.

A LOW-FREQUENCY REFRACTION GEOPHONE *

BY

W. M. JONES ** AND A. T. DENNISON **

Abstract

This paper describes a highly portable geophone, designed for large-scale refraction surveying, which uses a novel suspension system to obtain a natural frequency of about 1.85 c/s. The nominal output is 0.7 volts/cm/second into a 500 ohm load, the damping then being 0.7 of critical. Some typical recorded arrivals obtained with this geophone are illustrated.

As Dr. Germain-Jones (1954) has recently pointed out, certain seismic problems may be most readily solved by large-scale refraction surveys. The actual scale will naturally depend on the particular geological problem but we will consider here the cases where the distance from shot to geophone is greater than 20,000 ft rising perhaps to 100,000 ft in special cases. For distances of this order, the explosive charge becomes fairly large and it is desirable on economic grounds to obtain the maximum coverage of the refractor with each shot, subject of course to the contrary requirement of maximum detail. In practice this may result in geophone intervals of between 600 and 1,500 ft.

This brief summary outlines the general conditions of service of a refraction geophone and to these must be added the normal requirements of portability, ruggedness and field convenience. From the designer's view point these requirements must of course be translated into the required electrical and mechanical constants of the geophone. This conversion of field requirements is perhaps the most unsatisfactory step in design at the present moment because of the lack of the required basic information.

One debatable point is the lowest frequency of ground movement which it is necessary to record for optimum signal-to-noise ratio at the distances suggested. If this frequency can be established, then a geophone natural frequency of say half this value appears desirable if the system is to record a reasonable approximation to ground velocity. In general the predominant frequencies of ground movement become lower as the shot-geophone distance increases and records such as that in Fig. 5 indicate strong frequencies below 5 c/s at 50,000 ft. A geophone having a natural frequency of about 2 c/s therefore seems desirable for the longer distances: at shorter distances it will of course give a more faithful record of the ground movement than a higher frequency instrument.

---

* Presented at the Seventh Meeting of the European Association of Exploration Geophysicists, held in The Hague, 8/10 December 1954.

** British Petroleum Co. Ltd., Kirklington Hall, Newark, Notts.

The required geophone sensitivity depends on the minimum seismic background expected, which may be less than 10^{-6} cm/sec, and on the amplifier noise level , probably not less than 5×10^{-18} watts. A geophone giving 0.7 volts/cm/second into a 500 ohm load should give a clear record of ground unrest of 0.3×10^{-6} cm/sec which gives a reasonable margin for cable losses etc. A value of 500 ohms reduces the effect of resistive losses in the cables whilst giving a low impedance line not seriously affected by leakage in wet conditions.

The requirements of a refraction geophone may thus be summarized as a sensitivity of 0.7 volts/cm/sec across 500 ohms and a natural frequency of 2 c/s, the degree of damping being less than critical. The following sections describe one geophone which meets this specification whilst being highly portable and simple to operate.

Mechanical Principles

a) *Spring Suspension*

One of the main problems in designing a low frequency geophone is to achieve a suspension system of sufficiently low stiffness in a compact form which enables the total size of the instrument to be kept to the minimum determined largely by the size of the magnet assembly. Thus the use of a helical spring, with its necessary additional horizontal locating springs, gives a system which takes up a considerable amount of space and so increases the geophone size. The present suspension system [1], originated and developed by one of us (W.M.J.), achieves a minimum volume by the use of a single spring which is equally stressed at all points on its surface. This spring provides the necessary low vertical stiffness and also locates the coil in the magnet gap. The resultant 'open' construction makes the instrument readily accessible for field maintenance.

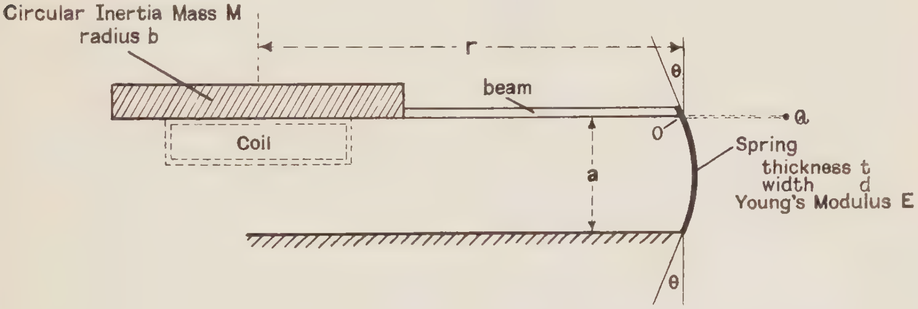

Fig. 1. Principle of Suspension System.

The principle of the geophone is shown diagrammatically in Fig. 1 and in more detail in Fig. 2. The flat spring runs the full width of the instrument and is clamped to angled faces on both the frame and the moving arm, the design being such that the inertia mass carried on the moving arm deflects the spring into a circular arc, the arm being horizontal in the equilibrium position. As described below, the natural frequency of the geophone is primarily dependent on the angular setting of the spring clamping surfaces and is about 1.85 c/s in the present case.

---

[1] Patent applied for.

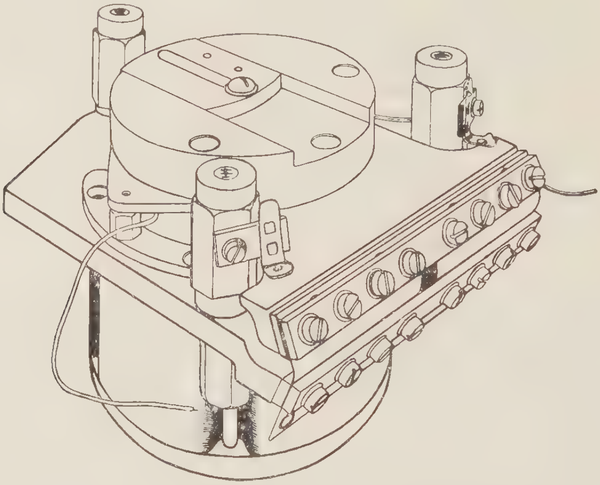

Fig. 2. Practical Construction of Geophone.

The coil and the inertia mass are fixed to the end of the moving arm so that the coil moves between the poles of a permanent magnet. The motion of the coil is not of course along a strictly vertical line, being more nearly along the arc of a circle, but this circle has a relatively large radius and the assumption of vertical motion will be generally satisfactory. The horizontal stiffness of the instrument is kept high by using a wide spring and by keeping the length of the spring (vertical dimension) as small as possible.

The effective sensitivity of the geophone depends of course on the size of the inertia mass and this in turn is limited by the ultimate strength of the spring material, the other dimensions being taken as fixed. In the present geophone a mass of 750 grams gives the required output without overstressing the spring.

b) *Theory of the suspension and the geophone equation*

The equation of the spring system at equilibrium with the beam horizontal is (Roark, 1943)

$$\theta = r\,(Mg/EJ)^{1/2}\ \tan\ (0.5\,a\,(Mg/EJ)^{1/2})$$

where J is the moment of inertia of the spring section and the other symbols have the meanings shown in Fig. 1. In this particular case we find that the tangent term is small and with an error of less than 1 % we may write

$$2\theta = r\,a\,Mg/EJ \quad \ldots\ldots\ldots\ldots \quad (1)$$

This becomes $\theta_1 + \theta_2 = r\,a\,Mg/EJ$

if the angles at the upper and lower ends of the spring, θ_1 and θ_2 respectively, are slightly different, as for example during movement of the system when θ_2 is fixed and θ_1, the angle to the vertical, varies.

The movement of the inertia mass will be along a circular arc and the natural frequency will be given by

$$2\pi\ f_0 = (EJ/I_o)^{1/2} \quad . \ . \ . \ . \ . \ . \ . \ . \ . \ . \ . \quad (2)$$

where I_o is the moment of inertia of the mass about the axis O. In practice the axis O itself moves as the spring deflects and it may be shown that for small angular deflections from the equilibrium position, the effective centre of rotation is an axis Q lying to the right of O at a distance

$$p = (a \cos \theta) / 2\,\theta$$

The effective moment of inertia I_Q is thus $M\,\{(r + p)^2 + (b/2)^2\}$.

Combining this with (1) and (2) we obtain

$$2\,\pi\,f_o = \{r\,g/2\,\theta\,[(r + p)^2 + 0.25\,b^2]\}^{1/2} \quad . \ . \ . \ . \ . \quad (3)$$

or, very approximately,

$$2\,\pi\ f_o = \sqrt{g\,/\,2\,\theta\,r}$$

We thus see that the natural frequency is determined primarily by the values of r and θ and depends very little on the elastic properties of the spring. Changes in spring characteristics vary the working length of the spring but this only changes the value of p, a small correction term: the resultant change in f_o is therefore slight but the spring dimensions must be carefully chosen to keep the maximum spring stress within safe limits. This maximum spring stress is given by

$$s_{max.} = Mgrt\,/\,2\,J \text{ or } \theta Et\,/\,a$$

These formulae agree well with the observed values. Thus with $r = 2.75$ inches and $\theta = 22°$ the calculated value of 1.82 c/s agrees with the measured value within the experimental error.

The slight rotational motion of the mass modifies the general geophone equation slightly since the mechanical force due to ground motion is a function of Mr_Q whereas the motion of the mass depends on the term I_Q.

Neglecting the inductance of the coil which is here about 0.5 henries, we have with the usual notation

$$\frac{d^2i}{dt^2} + \frac{K^2}{M'R}\,\frac{di}{dt} + \frac{S}{M'}\,i = \frac{K}{R}\,\frac{M}{M'}\,\frac{d^3s}{dt^3}$$

where $M' = I_Q\,/\,r_Q{}^2 = M\,k_Q{}^2/r_Q{}^2$, k_Q being the radius of gyration.

The geophone thus has a frequency response and damping characteristic corresponding to a mass M' rather than M. The effective ground motion and hence the sensitivity are however reduced by the factor M/M' which is approximately 0.94. These points must be borne in mind in making laboratory measurements.

MECHANICAL DETAILS

The general construction of the geophone is shown in Figs. 2 and 3. The circular magnet assembly carries a rectangular platform, one end of which forms the spring mounting face, inclined at 22° to the vertical. For convenience in assembly, two springs are used, each being 2″ wide and together forming a spring 4″ wide. These springs are rigidly held by clamping strips to their mounting faces and their upper end carries the moving arm with the inertia mass. The lower portions of the springs seen in the photograph are not functional but serve as spares which can be used in the event of spring failure and facilitate spring replacement.

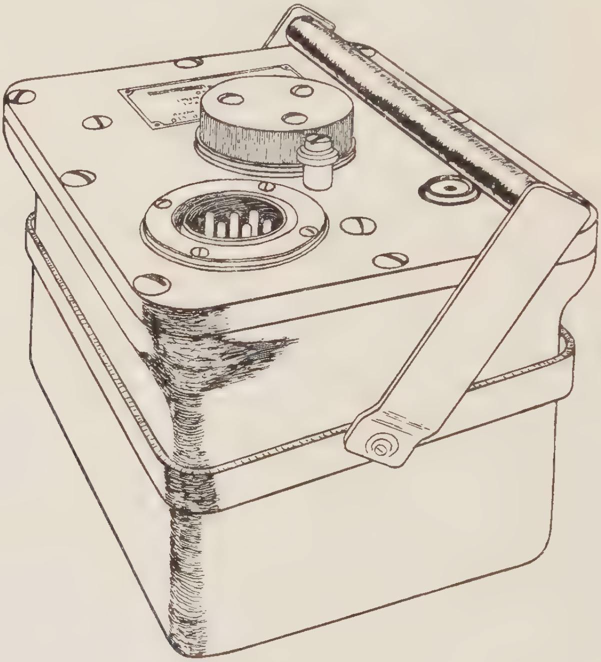

Fig. 3. Complete Geophone.

During assembly the spring length, i.e. the separation of the clamping strips, is adjusted so that the arm is horizontal: a fine adjustment is provided in the form of an adjustable rider in the top of the inertia mass. High carbon spring steel is used and the most satisfactory protection for this has proved to be a thin coating of a thermo-setting resin.

The coil is fixed to the underside of the inertia mass and moves in the air gap of the magnet, relatively large clearances being provided to simplify field adjustment. A non-metallic former is used to minimise internal damping and the winding is impregnated with Araldite resin to give protection against corrosion and to improve the mechanical strength. The inertia mass must of course be free from magnetic impurities if the expected characteristics are to be obtained.

The complete assembly is secured to the rectangular lid by three pillars, this lid containing the output plug, spirit level and clamping screw. Field experience showed that it was necessary to clamp the moving system very firmly during transport to avoid damage to the coil and excessive spring fatigue. A large coarse-threaded, finger-grip screw is therefore provided which on tightening presses down, via a rubber pad, on to the top of the inertia mass. The latter has two lobes on a transverse diameter with countersunk holes which locate on conical studs above the magnet. These form the bottom stop and hold the moving element firmly against any sideways motion.

The clamping screw upward travel is normally limited by a stop but if this is rotated, the screw can be removed to give access to the rider on the inertia mass without taking the instrument from its case. This also facilitates a field check to make sure that the coil is swinging freely in the gap.

The complete geophone measures 7″ × 5½″ × 4½″ high and by the use of light alloy castings the weight has been kept down to 14 lbs. the major part of this weight lying in the magnet assembly and the inertia mass. One of the main objects of the design was to produce an instrument which could be readily adjusted and dismantled in the field whilst providing an adequate degree of geophone matching. This has been achieved in a simple and compact form which is readily portable.

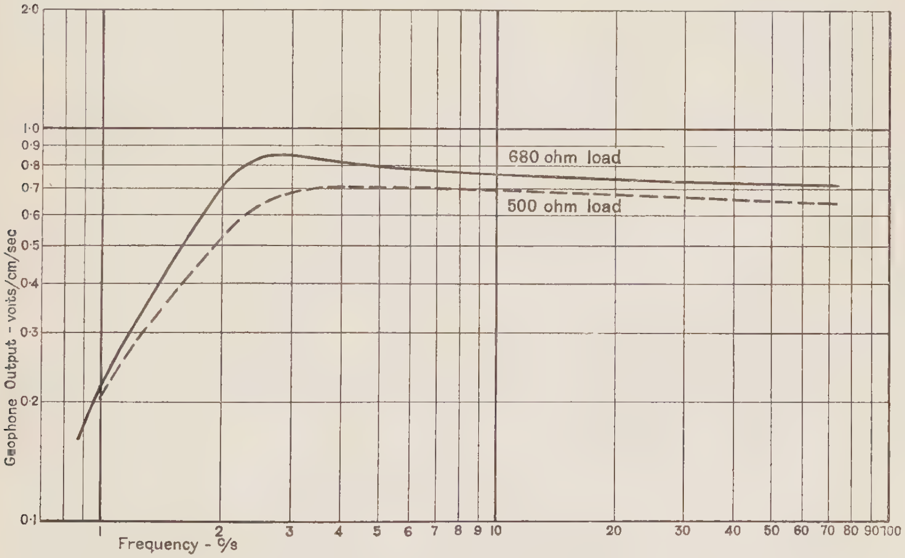

Fig. 4a. Geophone Output for Constant Velocity Input.

GEOPHONE PERFORMANCE

In its present form the geophone coil is wound with 38 s.w.g. wire to a resistance of 200 ohms. This gives the required output with a relatively low self-inductance, so minimising the loss in sensitivity at higher frequencies. Fig. 4 a shows the output-voltage/frequency characteristic with load resistors of 500 ohms and 680 ohms, corresponding to approximately 0.7 and 0.6 damping respectively. Fig. 4 b shows the corresponding phase/frequency responses: the angles shown here may be reduced by 180° if preferred since the geophone leads may be reversed.

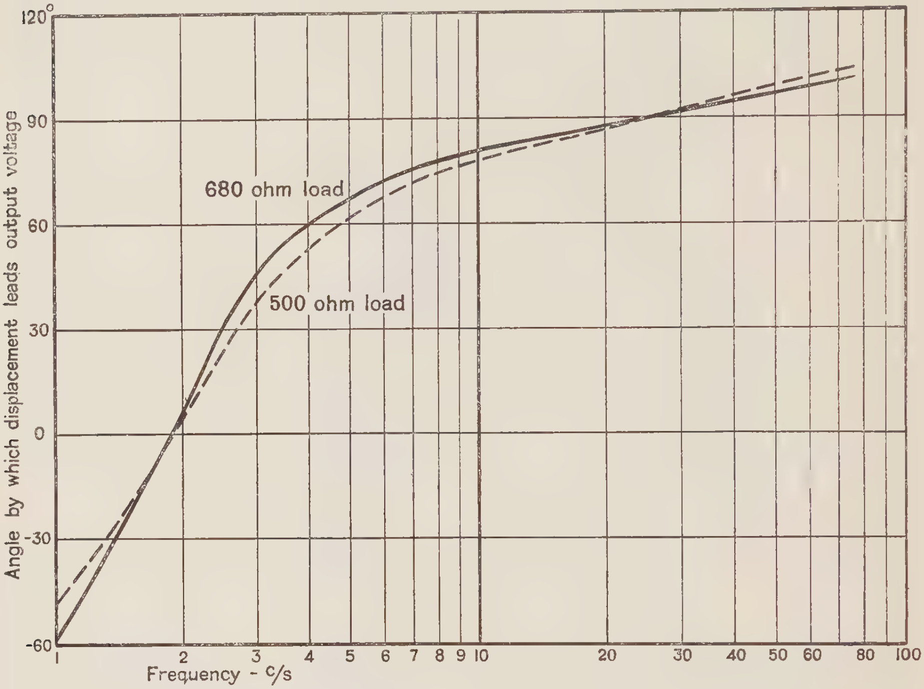

Fig. 4b. Geophone Phase Response.

The geophone has been successfully used in a number of areas and Fig. 5 shows tracings of arrivals recorded at various distances in some of these areas. It will be seen that trace (d) shows a very low frequency arrival even at the medium distance of 50,000 ft.

ACKNOWLEDGEMENT

The authors are indebted to the Chairman of the British Petroleum Co. Ltd. for permission to publish this paper.

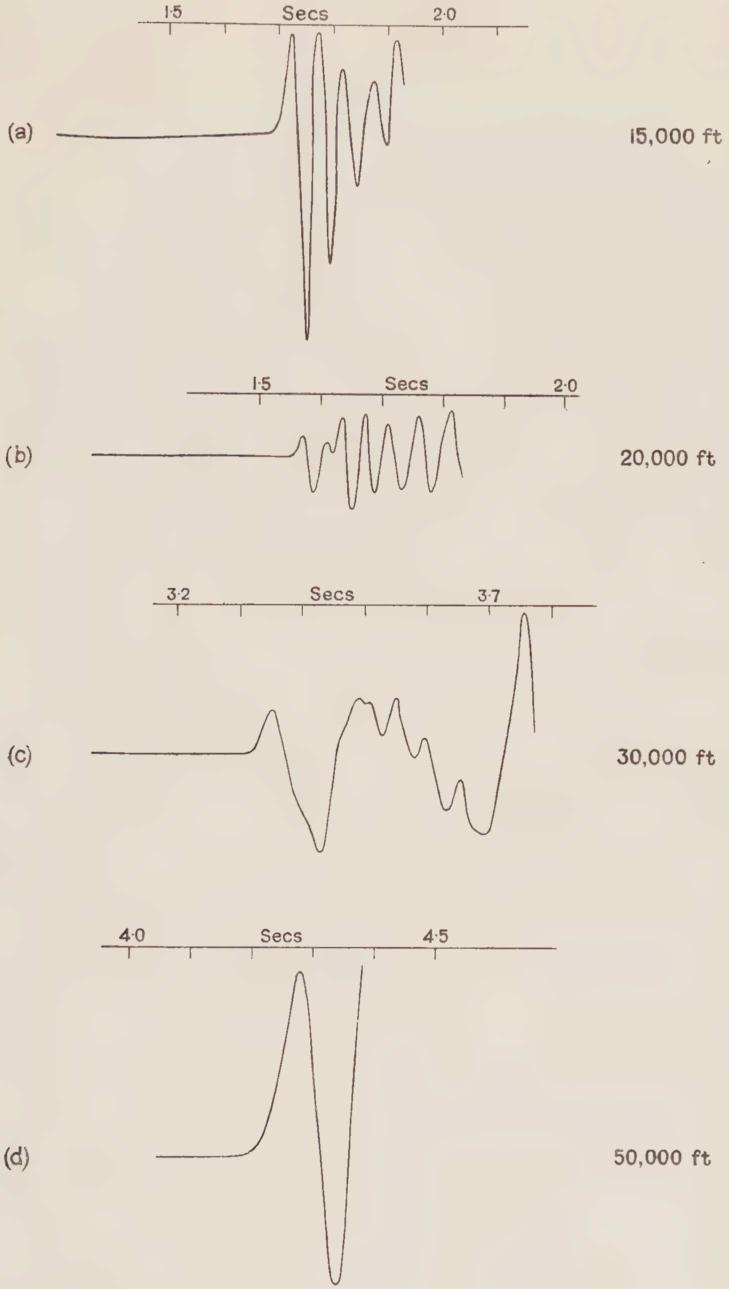

Fig. 5. Refraction Arrivals Recorded at Various Distances.

References

Germain-Jones, D. T., 1954: What is our Contribution?, Geophysical Prospecting, II, 177-184.

Roark, R. J., 1943: Formulas for Stress and Strain, p. 132, MacGraw-Hill.

Discussion

Mr. D. T. Germain-Jones: I should like to reinforce Dr. Dennison's plea for information on the types of geophones used by other workers on long distance refraction observations up to, say, 20 miles. Our own experience in past years in the foothills of S.W. Persia forced us then to conclude that geophones with a natural frequency of the order of 2 cycles per second, or less, were necessary. Such geophones have worked well, and we still use geophones with this order of frequency, though of better design and much lighter in weight in our present long range refraction work in other areas. We wonder, however, if we need to use such a low natural frequency in most cases and a programme of research is being undertaken by us, involving the determination of ground motion and analysis thereof, so that we can make a final decision. Until then, however, we shall continue to use a low frequency geophone which, on present evidence, appears to give us a better signal/noise ratio.

Mr. R. Geneslay: Mr. Germain-Jones asked if anybody could give some results of observations concerning the frequencies observed at large distances from the shot in refraction shooting.

My reply is: "We got good results in the Sahara even at larger distances than 50,000 feet, with geophones having a natural frequency of 4 to 5 c.p.s. Nevertheless I admit that geophones of lower natural frequency could possibly give better results and I think that the suggestion made by Mr. Germain-Jones of investigating the phenomena with tape recording is an interesting one. I hope that these investigations will throw some light on this rather obscure problem."

Mr. A. T. Dennison: It is of course clear that a higher frequency geophone will give some record at long distances: the frequency required to obtain the optimum signal-to-noise ratio may well depend on the type of noise background and hence on the particular area being surveyed.

MESURE DU BRUIT ET SISMOS MULTIPLES
(étude expérimentale dans les Landes) *

PAR

HENRI RICHARD ** ET MARCEL RIMBAUT ***

ABSTRACT

To improve the ratio of signal to noise resulting from the shot, seismologists have increased the number of geophones in each recording channel and have also increased the length of each spread. As a rule, however, the effectiveness of this multiple recording is based on theoretical considerations, and it appeared desirable to carry out an experimental investigation to obtain a direct measurement of the reduction in noise as a function of the geophone pattern etc. The work was done in the Landes where experience had shown that recording was difficult.

The experimental arrangement, which allowed the accurate measurement of the noise without interference from reflected energy, is described.

Shots, repeated under apparantly identical conditions, revealed the random nature of the noise and pointed to the necessity of a large number of experiments to yield an accurate result. Two geophone patterns were employed, one of 12 geophones in a straight line and the other of two parallel lines of geophones, the directions of the geophone lines being either along the shot line, perpendicular to the shot line or at some intermediate angle.

The results obtained in two widely spaced locations were in good agreement and allowed definite conclusions to be drawn. When the 12 geophone line is long enough the noise is reduced by a factor of 0.36 and with two lines, each 55 metres long and containing 12 geophones, the reduction was 0.29, if the lines were sufficiently widely separated. The results agree with the factor $K N^{-1/2}$ for the reduction in noise where N is the number of geophones per trace and K is a factor close to unity. The results also show the influence of the length of the geophone line its orientation and its mean distance from the shot.

Dans les régions où les mouvements parasites de surface provoqués par l'explosion masquent plus ou moins les ondes réfléchies, la tendance à „multiplier" les sismographes se généralise de plus en plus.

Pour diminuer artificiellement le niveau du „bruit" c'est-à-dire l'amplitude des parasites, la théorie et l'expérience démontrent en effet qu'il est nécessaire d'augmenter dans de fortes proportions le nombre de sismographes branchés sur une trace et d'accroître dans une certaine mesure la longueur ou la surface couverte par celle-ci.

En 1936 P. W. Klipsch précisait déjà dans le Geophysics que, en vue d'obtenir une amélioration du rapport signal/bruit voisine de 10, il faudrait 100 sismographes par trace, soit 600 sismographes pour un enregistreur à 6 traces, mais il ne posait pas le problème du dispositif optimum.

---

* Presented at the Seventh Meeting of the European Association of Exploration Geophysicists, held in The Hague, 8/10 December 1954.

** Compagnie générale de Géophysique.

*** Société Nationale des Pétroles d'Aquitaine.

Actuellement, on peut utiliser par trace, grâce aux progrès réalisés dans la fabrication des appareils :

des simples, doubles ou triples lignes de 12 à 36 sismographes, couvrant jusqu'à 120 mètres.

des étoiles ou autres figures groupant 24, 36 ,48 sismographes et même davantage, le diamètre variant de 30 à 120 mètres.

Si la multiplication prend une importance technique et économique de plus en plus grande, l'étude de son influence sur l'atténuation du bruit reste assez souvent *théorique* ou *qualitative.*

Or cette étude ne peut pas être théorique tant que dans les terrains où la multiplication s'impose à forte dose, les lois de propagation et d'entretien de tous les parasites qui constituent le bruit sont encore mal connues. En outre, elle doit être objective et quantitative de manière à chiffrer l'efficacité de la multiplication et à choisir rapidement et sans hésitation un bon dispositif.

Bref, le meilleur moyen est de procéder à des expériences et, plus précisément, de mesurer effectivement le niveau du bruit.

En un point donné il faut donc exécuter un assez grand nombre de tirs permettant de *mesurer l'atténuation du bruit en fonction des différents schémas de multiplication.*

Les mesures présentées ont été réalisées dans les Landes, région difficile où depuis plusieurs années on emploie systématiquement 6 à 36 sismographes/trace combinés avec 1 à 10 explosions simultanées.

Conditions de surface dans les Landes. La région est une plaine sablonneuse et uniforme principalement couverte de forêts, ou en dehors des dunes côtières, le niveau hydrostatique se trouve à quelques mètres de profondeur. Le sable à stratification entrecroisée y est souvent traversé à faible profondeur par un banc d'alios. Les essais ont été exécutés en deux stations A et B, distantes de quelques dizaines de kilomètres.

Exploitation sismique normale. Dans les deux secteurs on enregistre des réflexions pendant les deux secondes qui suivent l'explosion, en opérant comme suit :

24 sismographes par trace, répartis sur deux lignes longitudinales parallèles de 12 sismographes, 5 mètres entre sismographes, 55 mètres par ligne, 20 à 30 mètres entre lignes.

45 à 60 mètres entre traces.

tirs multiples à 8-12 mètres de profondeur.

Des réflexions plus profondes n'apparaissent pas.

Modifications expérimentales. Pour que la mesure de bruit et de son atténuation soit correcte, il est nécessaire d'apporter au schéma habituel quelques modifications remplissant deux conditions ne pas trop s'écarter des normes d'exploitation courante sinon les conclusions perdraient une grande partie de leur intérêt.

garantir l'absence absolue d'énergie réfléchie, sinon les mesures seraient faussées.

Dans ce dessin :

les charges expérimentales sont enterrées à une profondeur un peu plus petite que la profondeur habituelle ; elles sont cependant placées *sous le niveau hydrostatique.*

l'explosion est *unique* et non multiple.

l'explosion a lieu chaque fois dans un trou *vierge.*

les trous où ont lieu les explosions successives sont *assez écartés* pour éviter que l'effet d'un tir soit altéré par l'effet des tirs environnants.

la charge expérimentale est du *même ordre de grandeur* que la charge habituelle.

les traces sont placées à une distance convenable de l'explosion : 5 à 6 traces s'échelonnent de *250 à 400 mètres* des points de tir. Au cours des expériences, la position des différentes explosions par rapport aux sismographes ne change pratiquement pas. On a d'ailleurs vérifié que, à cette distance, le bruit varie peu en fonction de l'éloignement.

le bruit est mesuré de *2 à 3 secondes après l'explosion,* c'est-à-dire à un moment où, en cours d'exploitation, aucune énergie réfléchie n'est enregistrée.

le réglage de fréquence et de sélectivité des amplificateurs est le *réglage normal.*

Sans insister sur tous les détails, on notera cependant que les AVC des amplificateurs sont supprimés, des précautions sont prises contre la saturation de l'appareillage, les sismographes sont placés avec beaucoup de soin, les expériences en un secteur donné doivent être réalisées dans la même journée sans changer les réglages, les sensibilités, le volume des charges, etc.

Plan de position (fig. 1)

On groupe à l'intérieur d'un rectangle de 16 sur 56 mètres de côté, 24 points d'explosion écartés de 8 mètres.

A 250-400 mètres de ce rectangle sont déroulées deux bases sismographiques de 5 ou 6 traces chacune. Pendant toute la durée des tirs, on enregistre simultanément sur ces deux bases. L'une sert de *base de référence* : chaque trace est équipée avec une ligne longitudinale de 12 sismographes couvrant 55 mètres (5 mètres entre sismographes) et immuable. Aucun sismographe ne doit être déplacé, aucun branchement ne doit être changé.

La seconde base, *dite expérimentale,* est déportée latéralement à 30 mètres de la précédente. Pour une explosion donnée, toutes les traces ont le même dispositif sismographique. A chaque explosion, on essaie un nouveau schéma et on compare son efficacité à celle du dispositif de référence. La liste des dispositifs expérimentés sur toutes les traces de cette base est la suivante :

1) *Une ligne longitudinale* de 12 sismographes, la distance entre sismographes

variant de 0 à 5 mètres et la couverture passant en conséquence de 0 à 55 mètres.

2) *Deux lignes longitudinales et parallèles* de 12 sismographes chacune. Dans ce cas, la couverture de chaque ligne est constante: 55 mètres, mais on fait varier l'écartement latéral entre lignes.

3) *Une ligne transversale* de 12 sismographes, de couverture variant de 0 à 55 mètres comme au 1). Nous entendons par „transversale" une ligne perpendiculaire à l'axe de tir.

4) *Deux lignes transversales et parallèles* de 12 sismographes chacune, à écartement variant comme au 2).

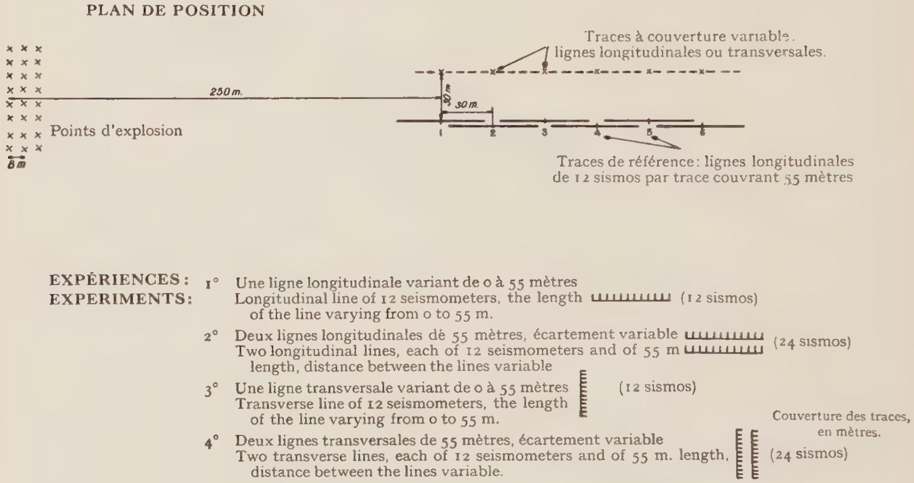
PLAN DE POSITION
Traces à couverture variable. lignes longitudinales ou transversales.
250 m.
30 m.
30 m.
Points d'explosion
8 m
1
2
3
4
5
6
Traces de référence: lignes longitudinales de 12 sismos par trace couvrant 55 mètres
Couverture des traces, en mètres.

EXPÉRIENCES:
EXPERIMENTS:

1° Une ligne longitudinale variant de 0 à 55 mètres
Longitudinal line of 12 seismometers, the length of the line varying from 0 to 55 m. (12 sismos)

2° Deux lignes longitudinales de 55 mètres, écartement variable
Two longitudinal lines, each of 12 seismometers and of 55 m length, distance between the lines variable (24 sismos)

3° Une ligne transversale variant de 0 à 55 mètres
Transverse line of 12 seismometers, the length of the line varying from 0 to 55 m. (12 sismos)

4° Deux lignes transversales de 55 mètres, écartement variable
Two transverse lines, each of 12 seismometers and of 55 m. length, distance between the lines variable. (24 sismos)

Fig. 1. Bruit et sismos multiples. — Noise and multiple seismometers.

A — Expériences à la Station A

Base de référence. La base de référence, immuable pendant toute la série de tirs conduit à des observations très importantes.

Comparaison entre le rendement sismique d'une explosion et le niveau du bruit après cette explosion.

Il est connu que des charges du même volume explosant dans des conditions en apparence identiques ne produisent pas exactement le même effet sismique. Mais il a été vérifié que la déviation de l'impétus de la première onde refractée arrivant à des sismographes assez éloignés varie de la même façon sur tous les sismographes et constitue un excellent critère du rendement sismique, critère que, à un coefficient près, nous convenons d'appeler un peu sommairement „l'énergie" dégagée par l'explosion.

Nous avons donc le moyen de mesurer à un coefficient près, en plusieurs points de la base, „l'énergie" dégagée par les explosions successives et de la comparer au niveau du bruit mesuré 2 à 3 secondes après l'explosion.

Le niveau du bruit enregistré pendant un certain temps après l'explosion est égal à l'aire couverte par la trace de part et d'autre de sa position moyenne.

Sur la figure 2, on a porté en ordonnée, pour une dizaine d'explosions:

„l'énergie" arrivant en deux points P et Q de la base de référence (impétus de l'onde réfractée).

le bruit mesuré en ces deux points, de 2 à 3 secondes après l'explosion.

On constate que, à 3 % près au maximum, les deux courbes d'énergie se superposent. Par contre, d'une explosion à l'autre le rapport des bruits varie d'une manière très désordonnée, le bruit en P pouvant être supérieur de 20 % au bruit en Q (tir N° 6) ou inférieur de 12 % (tir N° 8). En outre les variations de bruit sont loin de suivre fidèlement les variations d'énergie.

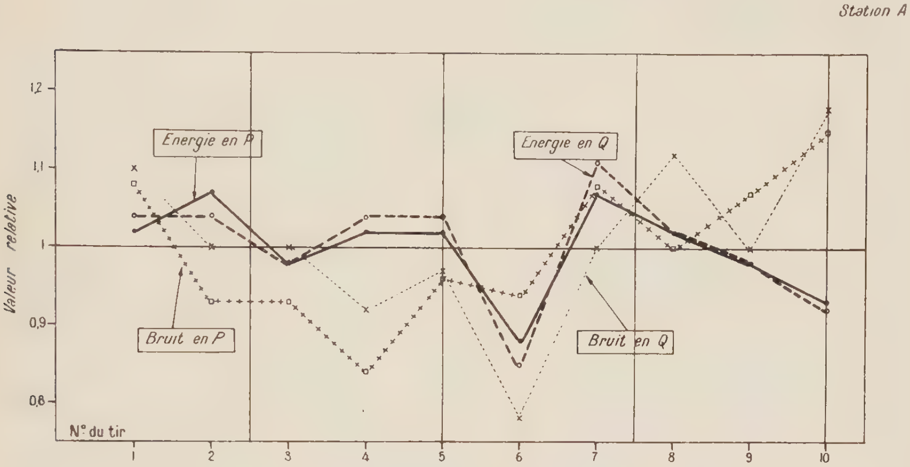

Fig. 2. Base de référence. — Measurement at reference base.

Ce caractère capricieux est encore mis en relief sur la figure 3 où l'on a étudié en fonction des traces, le niveau du bruit relatif à plusieurs explosions. De la trace 1 à la trace 6, le bruit va tantôt en croissant, tantôt en décroissant. Parfois, il reste à peu près constant.

Une manière de suivre la dispersion consiste à calculer pour chaque explosion le rapport du bruit enregistré par deux traces écartées de 30 mètres, deux traces écartées de 60 mètres, etc.

Sur la figure 4 on observe nettement que la dispersion du rapport:

$$\frac{\text{bruit sur la trace 5}}{\text{bruit sur la trace 3}} \quad \text{(60 mètres entre les deux traces)}$$

est plus grande que celle du rapport:

$$\frac{\text{bruit sur la trace 5}}{\text{bruit sur la trace 4}} \quad \text{(30 mètres entre les deux traces)}$$

Sur 18 exploisions par exemple il a été calculé que pour toutes les traces espacées de 60 mètres, l'écart moyen arithmétique du rapport était de 0,095. Il est de 0,063 pour les traces écartées de 30 mètres. La différence s'explique en bonne partie par le fait que les traces distantes de 30 mètres se chevauchent partiellement et sont *moins indépendantes* entre elles que les traces plus espacées.

Base de référence. — Reference base

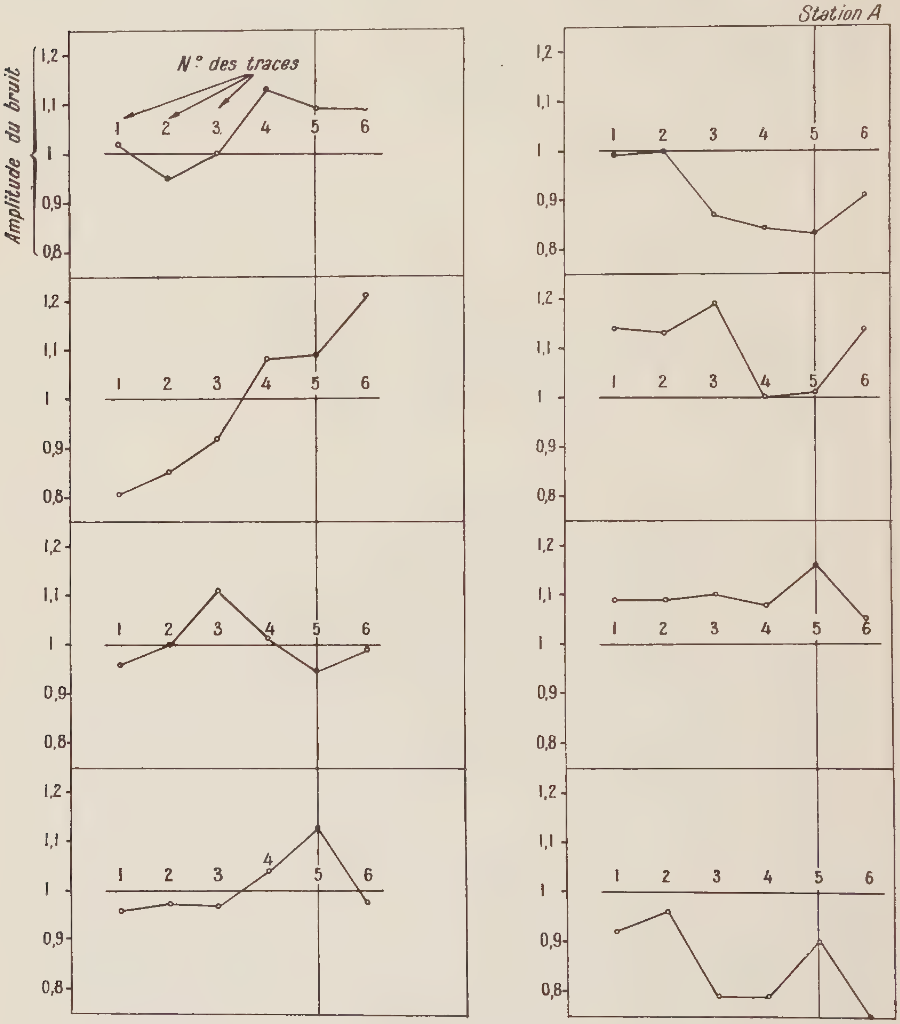

Fig. 3. Amplitude de bruit mesurée sur 6 traces étalon au cours de plusieurs explosions. — Noise recorded on 6 traces during several explosions.

Enfin, si au lieu de considérer le bruit enregistré par chaque trace, on évalue la moyenne du bruit sur l'ensemble des traces, on constate, (*sommet de la figure 5*), que la moyenne des bruits et l'énergie suivent de très près les mêmes fluctuations. *Au bas de la figure 5*, on compare les rapports (moyenne des bruits sur 6 traces/énergie), au rapport (bruit sur une trace/énergie).

Le rapport faisant intervenir la moyenne varie très peu et il est probable que si les mesures étaient plus nombreuses, il serait constant. Au contraire, le rapport établi pour une seule trace varie de 1,2 à 0,86.

Base de référence. — Reference base

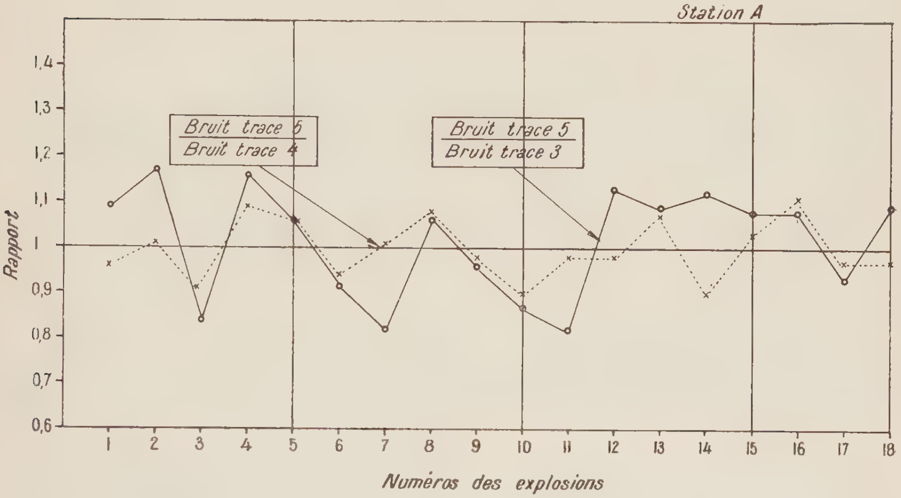

Ecart moyen arithmétique :

La moyenne de l'écart = 0,095 (si les traces sont espacées de 60 mètres).
La moyenne de l'écart = 0,063 (si les traces sont espacées de 30 mètres).

Average deviation :

The average deviation = 0,095 (for a distance of 60 m between the traces).
The average deviation = 0,063 (for a distance of 30 m between the traces).

Fig. 4. Rapport des bruits enregistrés par deux traces. — Ratio of the noise recorded on pairs of traces.

De toutes ces mesures on déduit que :

1) Sur une trace, le niveau du bruit mesuré de 2 à 3 secondes après l'explosion se distingue par son caractère aléatoire. D'une explosion à l'autre il varie entre de larges limites.

2) Le niveau du bruit varie également d'une manière imprévisible d'une trace à l'autre.

3) L'infidélité se manifeste bien que les traces examinées groupent chacune 12 sismographes couvrant 55 mètres. Il a été controlé que, comme il fallait s'y attendre, la dispersion était encore plus importante lorsque l'on opérait avec un seul sismographe, ou lorsque mesurait le niveau du bruit pendant un temps

plus court. Les constations précédentes sont en étroite relation avec un phénomène souvent observé au cours d'une prospection. Lorsque l'opérateur exécute au même endroit deux tirs pratiquement identiques, les parasites ne troublent pas toujours les réflexions avec la même intensité en des points homologues

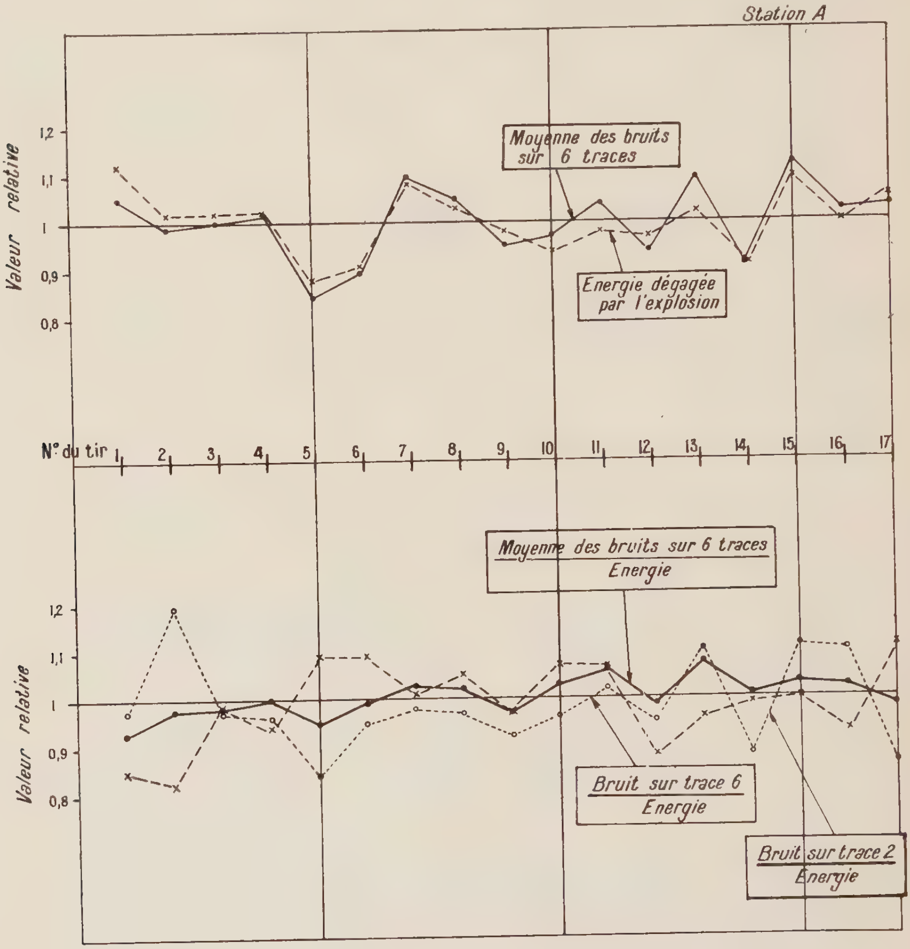

Fig. 5. Base de référence. — Measurements at reference base.

des deux enregistrements. Par exemple une rèflexion déterminée sera surtout perturbée sur les traces 1 et 3 du premier enregistrement, tandis que sur le deuxième, cela se produira sur les traces 2 et 5.

4) Sur l'ensemble des traces, sous réserve qu'elles soient assez nombreuses, la moyenne du bruit se révèle en gros proportionnelle au „rendement sismique" de l'explosion.

Remarque: Il a paru nécessaire d'insister sur ces différents points, car ils démontrent clairement que par suite de son caractère erratique, l'étude systématique et précise du bruit exige des statistiques assez nombreuses. Et comme dans toute interprétation statistique, il convient d'être prudent, car il faut exécuter un grand nombre de mesures dans des conditions aussi constantes que possible, ce qui, nous le savons, se réalise assez difficilement dans l'expérimentation sismique.

AMPLITUDE DU BRUIT SUR LES TRACES À COUVERTURE VARIABLE

On a établi précédemment que, pour un tir donné, la moyenne des bruits enregistrés sur toute la base de référence était à peu prés proportionnelle au „rendement sismique" de l'explosion. Pour chaque tir l'amplitude du bruit mesurée sur les traces à dispositif variable doit donc être rapportée à cette moyenne afin d'éliminer les variations imputables au fait que toutes les explosions ne sont pas rigoureusement identiques.

Ligne longitudinale de 12 sismographes

L'amplitude du bruit ainsi chiffrée pour chaque trace de la base expérimentale est reportée en ordonnée sur la figure 6. En abscisse, on porte la longueur couverte par la ligne. Dans le cas de deux lignes, on considère leur écartement.

Cas d'une seule ligne longitudinale

Les mesures ont été faites pour des longueurs de:

55 mètres (5 mètres entre sismographes) comme sur la base de référence
44 mètres (4 mètres entre sismographes)
33 mètres (3 mètres entre sismographes)
22 mètres (2 mètres entre sismographes)
11 mètres (1 mètre entre sismographes)
1 mètre (0 m 09 entre sismographes).

Cas de deux lignes longitudinales parallèles

L'écartement entre lignes a été de: 0, 2 m 50, 10 m, 20 m, et 30 m.

Chaque trace donne des courbes assez sinueuses, en accord avec la dispersion notée sur la base de référence.

Lignes transversales de 12 sismographes

La figure 7, établie comme la figure 6, se prête aux mêmes observations.

Moyenne sur les 5 traces à couverture variable (Fig. 8)

La moyenne des résultats apportés par toutes les traces définit une courbe régulière montrant l'atténuation du bruit en fonction de l'allongement d'une ligne, ou de l'écartement entre lignes.

Comme à la base de référence, il apparaît qu'une moyenne établie sur plusieurs traces diminue rapidement le degré de dispersion. Les courbes sont commentées plus loin, après confrontation avec les résultats de la station B.

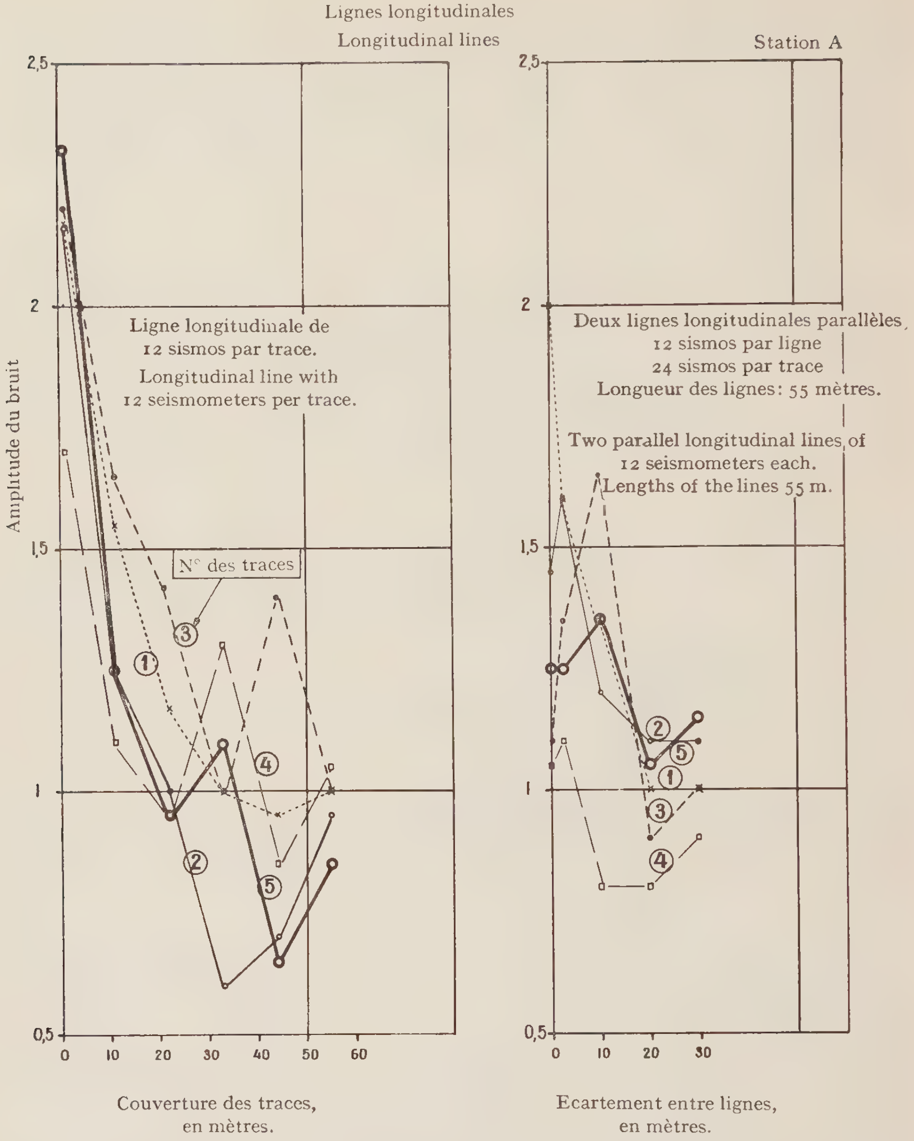

Fig. 6. Amplitude du bruit mesurée sur 5 traces à couverture variable. — Noise amplitude on 5 traces with varying multiple spacing.

B — EXPÉRIENCES À LA STATION B

Les expériences à la station B ont été exécutées suivant le même processus qu'en A, mais on s'est limité à l'étude de la simple ligne longitudinale et transversale. Une mesure a été exécutée sur une ligne oblique; inclinée à 50 grades sur l'axe de tir.

La fig. 9 reproduit les résultats sur les 5 traces à couverture variable. Les observations en B sont analogues aux observations déjà faites à la station A.

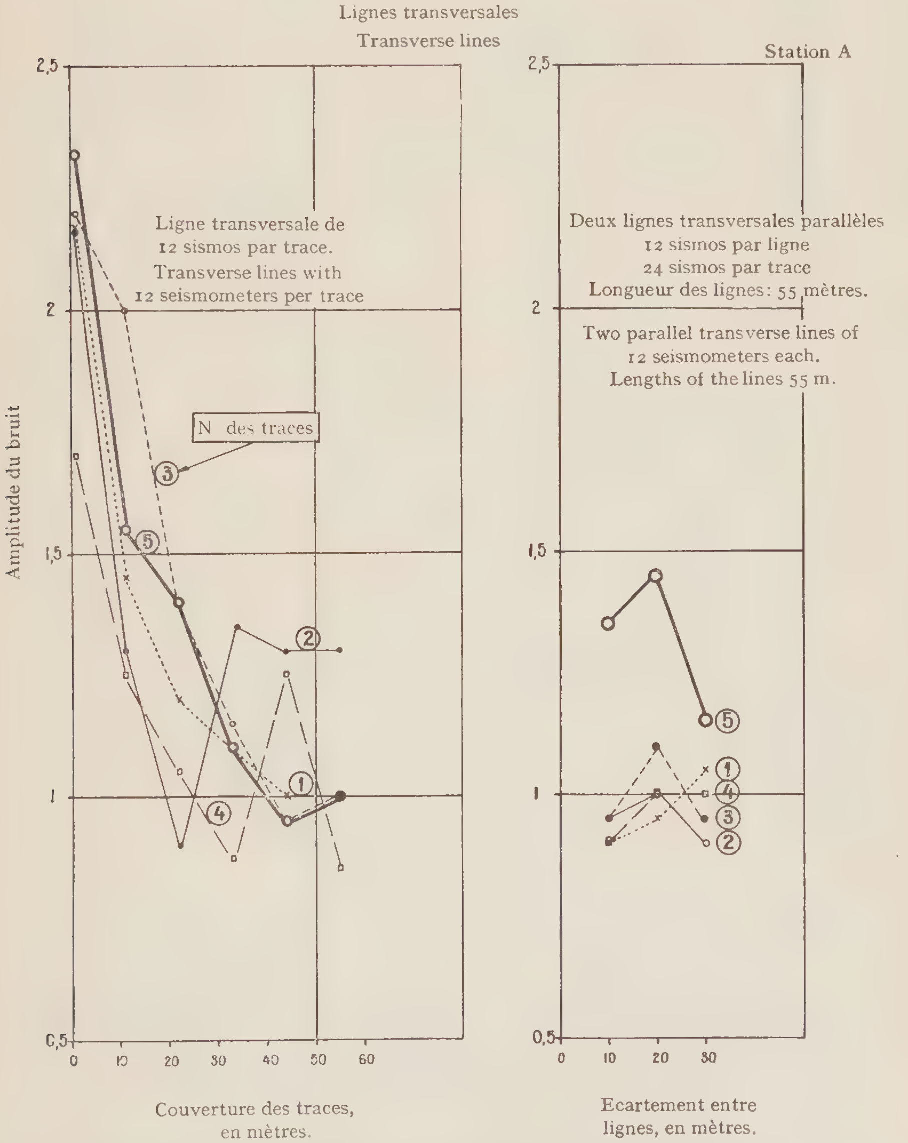

Fig. 7. Amplitude du bruit mesurée sur 5 traces à couverture variable — Noise amplitude recorded on 5 traces with varying multiple spacing.

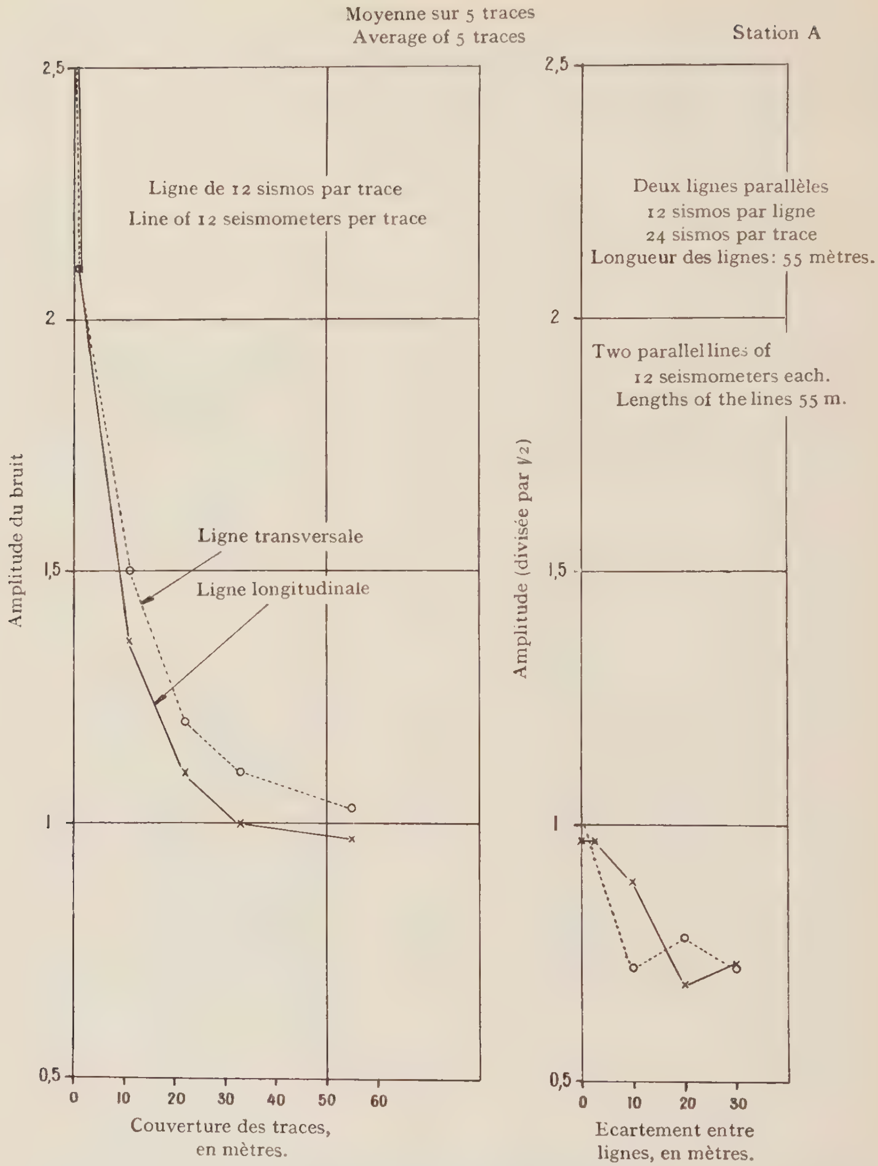

Fig. 8. Amplitude du bruit en fonction de la longueur couverte. — Noise amplitude as a function of the length of the line.

Le côté gauche de la fig. 10 montre que la moyenne sur les traces donne des courbes très comparables à celles de A (côté gauche de la fig. 8). Dans les deux séries de mesures, la courbe de la ligne transversale se place nettement au-dessus de la longitudinale. La mesure sur la ligne oblique se place à mi-chemin entre les deux courbes.

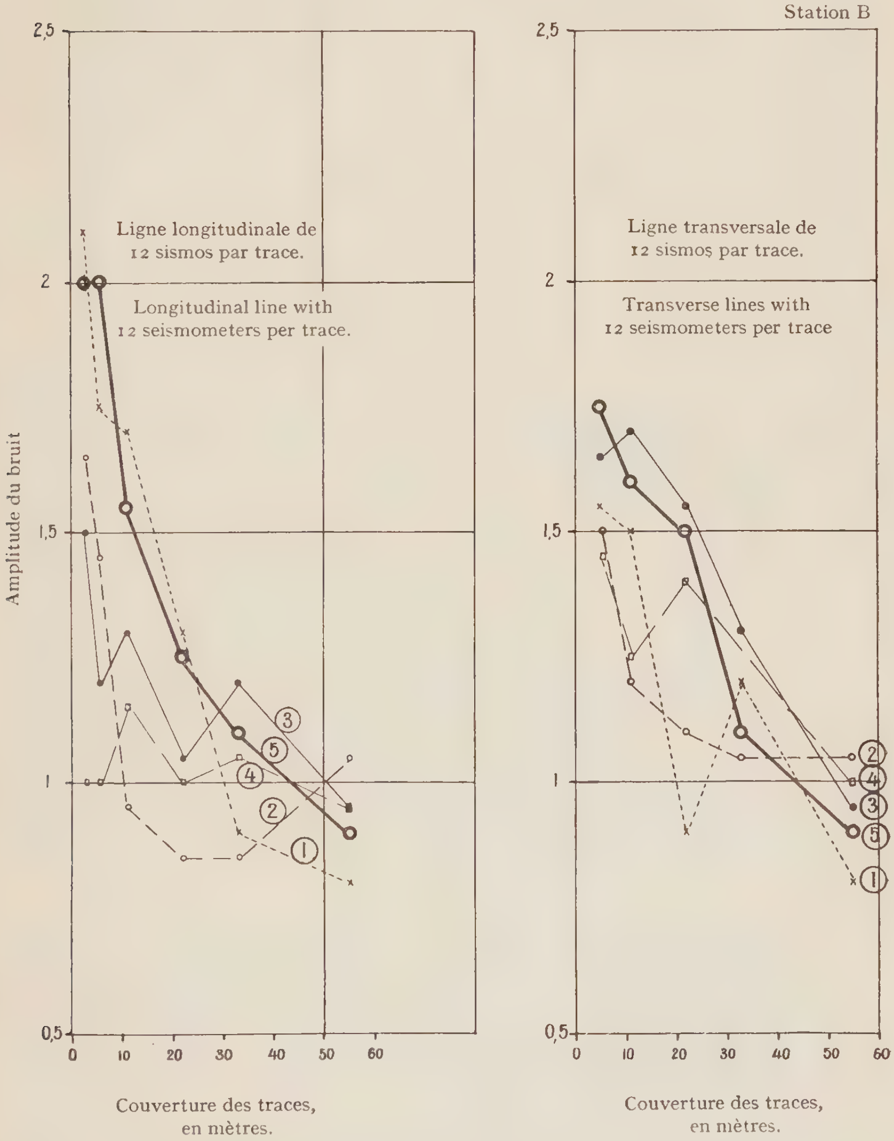

Fig. 9. Amplitude du bruit mesurée sur 5 traces à couverture variable. — Noise amplitude recorded on 5 traces with varying multiple spacing.

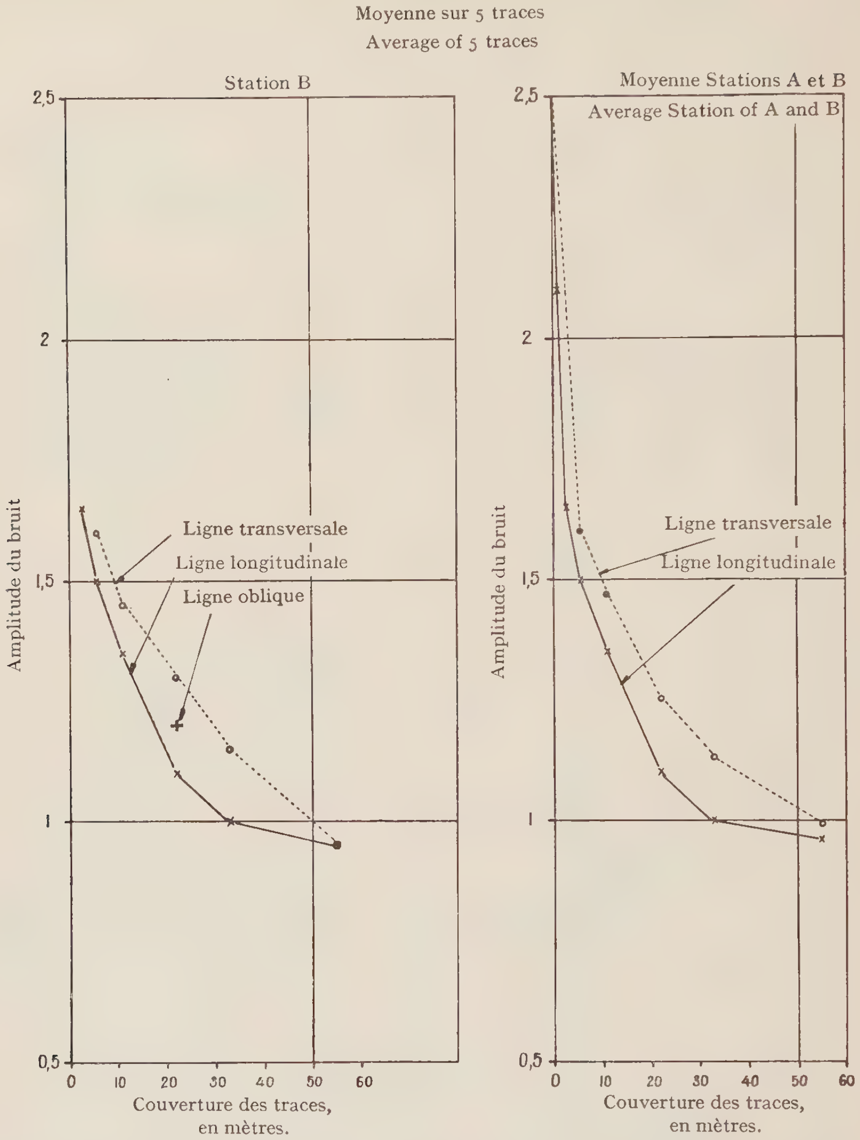

Moyenne sur 5 traces
Average of 5 traces

Station B

Moyenne Stations A et B
Average Station of A and B

Fig. 10. Amplitude du bruit en fonction de la longueur couverte. — Noise amplitude as a function of the length of the line.

Comparaison entre les valeurs moyennes mesurées en A et B

Pour les dispositifs de A et de B identiques, les valeurs moyennes aux deux stations diffèrent peu comme le souligne le tableau ci-après:

Amplitude du bruit

	en A	*en B*	*Ecart en %*
Ligne longitudinale de 11 mètres	1,36	1,35	négligeable
Ligne longitudinale de 22 mètres	1,10	1,10	„
Ligne longitudinale de 33 mètres	1,10	1,0	„
Ligne longitudinale de 55 mètres	0,97	0,95	„
Ligne transversale de 11 mètres	1,50	1,45	„
Ligne transversale de 22 mètres	1,20	1,30	10 % environ
Ligne transversale de 33 mètres	1,10	1,15	5 % environ
Ligne transversale de 55 mètres	1,03	0,95	5 à 10 % environ

Il paraît par conséquent tout à fait licite de construire les courbes moyennes combinant les résultats des deux stations. On obtient ainsi les graphiques du côté droit de la fig. 10.

C — Synthèse des résultats

Depuis le début des mesures on a adopté comme niveau de bruit unité le bruit enregistré sur une base immuable où chaque trace était équipée avec 12 sismographes couvrant 55 mètres.

Il s'avère plus rationnel de rapporter les courbes au niveau de bruit enregistré lorsque tous les sismographes sont concentrés: longueur de la ligne réduite à 0. Ce problème a priori assez délicat, car aucun artifice ne permet de grouper 12 sismographes dans un espace de dimension nulle, se résout par comparaison avec le bruit enregistré par un seul sismographe.

Sur la fig. 11 il est finalement possible de tracer les diagrammes qui représentent les „courbes de réponse" de la multiplication en fonction de:

la longueur d'une ligne de 12 sismographes

l'orientation de la ligne: longitudinale ou transversale

l'écartement entre deux lignes.

Les courbes construites quand la couverture varie de 0 à 55 m sont très régulières et s'extrapolent sans difficulté jusqu'à près de 100 mètres.

Dans l'hypothèse de deux lignes les résultats assez concordants autorisent à adopter la courbe moyenne donnée par les dispositifs longitudinaux et transversaux.

Conclusions pratiques

Ligne de 12 sismographes

On constate:

1) Que la ligne soit longitudinale ou transversale, le bruit tend asymptotiquement vers la même limite: 0,36 atteinte pour une longueur de l'ordre de 100 mètres.

Cette limite 0,36 peut se mettre sous la forme $1{,}24/\sqrt{12}$, valeur largement supérieure à $1/\sqrt{12}$.

Voici une interprétation de ce résultat. Les bruits enregistrés par chacun des 12 sismographes accouplés s'assimilent entre chaque sismographe à des

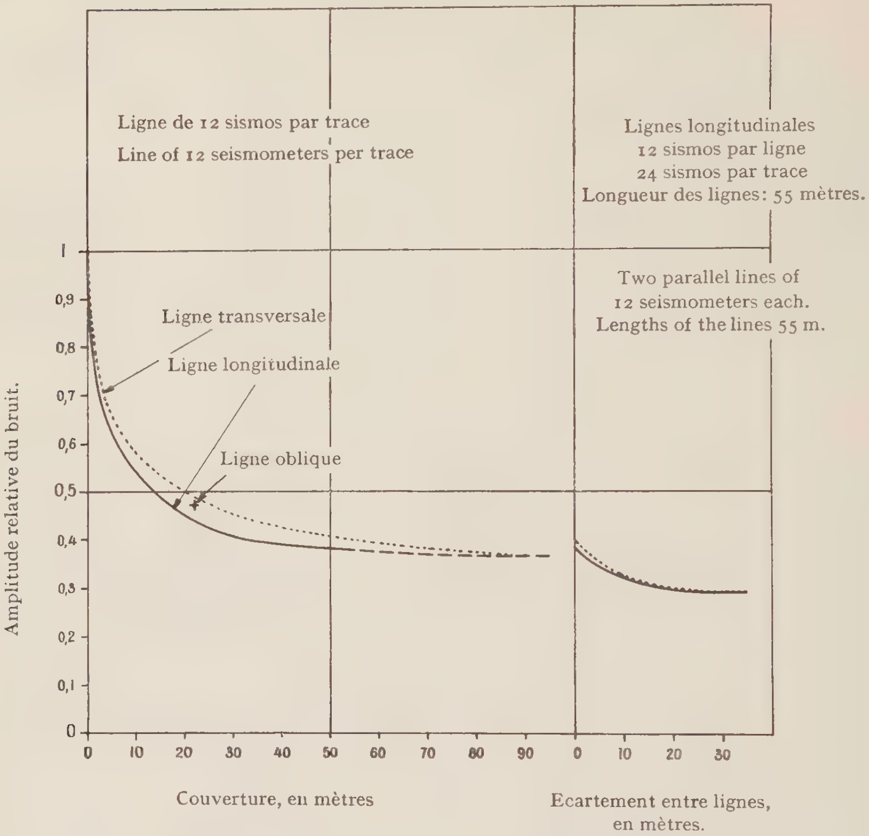

Fig. 11. Synthèse des mesures — Synthesis of the measurement.

phénomènes sinusoïdaux indépendants lorsque la ligne couvre une centaine de mètres, mais la résultante n'est pas atténuée dans le rapport $1/\sqrt{12}$ parce que les sismographes n'enregistrent pas des niveaux de bruits d'amplitude égale. L'effet de cette dispersion, qui serait facile à calculer à partir de données statistiques plus nombreuses, introduit le facteur correctif $K = 1{,}24$.

2) Le bruit décroît rapidement de 0 à 30 mètres. Au-delà, sa diminution n'est perceptible qu'avec une statistique assez poussée.

3) L'effet d'une ligne longitudinale de 30 mètres équivaut approximativement à celui d'une transversale de 55 mètres.

4) Avec 12 sismographes, il ne s'avère pas très fructueux de dépasser une longueur de 50 à 60 mètres sur ce périmètre.

Deux lignes de 12 sismographes (longueur des lignes: 55 mètres)

On constate:

1) Que les lignes soient longitudinales ou transversales, le bruit tend vers la même limite: 0,29 pour un écartement voisin de 15-20 mètres.

Cette limite est à comparer à la valeur: 0,39 enregistrée lorsque les deux lignes de 55 mètres sont confondues.

Le rapport 0,29/0,39 = peut s'écrire: $1,06/\sqrt{2}$. Ceci laisse supposer que l'indépendance des lignes est complète. Le facteur correctif K = 1,06 est encore dû au fait que les deux lignes n'enregistrent pas des niveaux de bruit d'amplitude égale.

Cette dispersion a été signalée avec insistance au début de la note.

2) L'effet de deux transversales de 55 mètres équivaut à celui de deux longitudinales de 55 mètres dès que les écartements atteignent une dizaine de mètres.

3) Il n'est pas opportun d'avoir un écartement de plus de 30 mètres.

4) Selon les problèmes, il peut y avoir intérêt pour améliorer le rapport signal/bruit à adopter des lignes longitudinales, transversales ou obliques.

Résumé

Au cours de ces dernières années, de nombreux tâtonnements ont retardé dans les Landes la mise au point de la multiplication.

On a d'abord observé que les résultats s'amélioraient sensiblement quand l'écartement entre sismographes passait de 1 à 2 puis à 3 mètres, quand la ligne était longitudinale au lieu d'être transversale. Ensuite, on a constaté progressivement qu'un écartement de 5 mètres paraîssait plus avantageux. Enfin, il est apparu que dans bien des secteurs, il fallait utiliser par trace 12, 24 ou 36 sismos combinés judicieusement avec des tirs simples ou multiples.

A l'inverse de ces observations, les graphiques de la fig. 11 sont déduits d'expériences dont la durée a été très brève et qui peuvent se répéter facilement. Malgré cette brièveté, les laborieuses conclusions des travaux antérieurs sont non seulement contrôlées, mais encore chiffrées avec précision.

En effet, les courbes démontrent sans ambiguïté que l'influence de la multiplication sur l'atténuation du bruit est ici relativement petite, certainement inférieure à $\sqrt{n}$ (n étant le nombre de sismographes). Il en résulte que, lorsque les conditions de surface deviennent à peine plus médiocres ou lorsque l'intensité de l'énergie réfléchie diminue, si par exemple l'amplitude du bruit double, il ne faut pas hésiter à multiplier par 4 ou 5 le nombre de sismographes ou de tirs. Les graphiques démontrent aussi qu'une solide statistique basée sur la mesure directe du bruit et de son atténuation aboutit à une conclusion indiscutable quand on recherche l'influence de l'allongement ou de l'écartement des lignes, le dispositif le plus efficace etc.

La variation du bruit, en fonction des différents paramètres, longueur, écartement, orientation des lignes étant alors chiffrée avec certitude, le sismicien doit et peut en outre tenir compte de ces données numériques lorsqu'on lui demande

de s'adapter à certains problèmes géologiques: structures faillées, pendages accusés, etc.

Discussion

Mr. A. J. Farando: What is the influence of the direction of the geophone line on the increase or decrease of the noise?

What is the influence of multiple reflections in the time interval chosen to measure the noise level?

Mr. H. Richard: I think that the direction of the geophone line has no great influence on account of permanent local conditions.

The locations of the stations have been so selected that no multiple reflections are present.

Mr. J. Goguel: Vous présentez vos résultats en fonction du nombre de sismos utilisé, alors qu'en fait, c'est leur distance que vous avez fait varier.

Pouvez-vous distinguer entre l'effet du nombre de sismos, et de la longueur qu'ils occupent?

Mr. H. Richard: Les expériences ont été conduites seulement avec 12 et 24 sismos par trace. Il a paru préférable de se limiter à ces deux nombres 12 et 24 de manière à réaliser un plus grand nombre d'expériences et à obtenir une statistique plus fournie. Mais la méthode s'applique que l'on fasse varier le nombre de sismos ou la surface couverte par un nombre donné de sismos.

BOOK REVIEW

A. S. Eve and D. A. Keys. — Applied geophysics in the search for minerals. Cambridge University Press. Fourth edition 1954.

In running to a fourth edition 25 years after the first, this introductory textbook must be unique in the literature of applied geophysics. The book retains its attractive size, now 362 pages, whilst presenting a comprehensive introduction to the main branches of the subject.

The balance of the book is unusual by modern standards in that more than half of its content is devoted to magnetic, electrical and electro-magnetic methods, whilst only 90 pages are allotted to gravitational and seismic methods. It will therefore tend to recommend itself more to geologists and metal mining students than to those interested in the search for oil.

The book contains descriptions of a wealth of methods for producing geophysical maps which, in many cases, has meant that space for methods of interpretation has been restricted. This is particularly so in the chapter on gravitational methods, most of which is taken up with details of the construction and operation of torsion balances. With the inclusion of the gravimeter in the present edition, it is perhaps unfortunate that space could not have been found for a discussion of the corrections normally applied to gravimeter observations.

Chapter 2, which deals with magnetic methods, has been augmented by a description of the airborne magnetometer and two examples of field survey results.

By rearrangement of the matter, Tagg's method of interpretation for the 'two-layer resistivity problem' has now been included in the chapter on electrical methods. A good deal of reference is made in this chapter to interpretation based on the 'electrode spacing equals depth rule' and although cautionary footnotes are added, these would hardly appear to be adequate. The rôle of empirical rules is not clearly stated and it is regrettable that greater space is not devoted to more modern quantitative developments. Regarding the self potential section of this chapter, the experimenal errors in Fig. 29 (National Earth Currents at Fisher Hill) are of surprising magnitude and it would appear from the text that these might be due to neglecting stake resistance effects when using microammeter methods. Only in the last paragraph of this chapter is the application of resistivity methods to the investigation of ground water resources mentioned.

Many electromagnetic methods are described in chapter 4 and to these is now added a brief description of aerial work by Lundberg.

The chapter on seismic work, which includes both refraction and reflection methods is still very brief, that part devoted to reflection being now increased to 12 pages. Of the space available, fan shooting appears to occupy an excessive share, and methods of timing by using the air blast seem out of place. A method of well shooting is mentioned using a shot fired in an old well, but the reverse procedure of using detectors in the well is not given.

Radioactive methods now have a short and very helpful chapter to themselves.

Well-logging has also developed into a separate rather condensed chapter, dealing with its applications to correlation and identification of formations.

In order to retain the character of this textbook, much of the early pioneering work, —and the book is dedicated 'to all pioneers'—has remained, the new edition taking mainly the form of additions. Quantitative interpretation methods tend to receive scanty treatment and the text could profitably be more critical of those which are given. How far some of the older material merits its place in a modern textbook must remain questionable.

A minor point regarding the production is that Fig. 114 has unfortunately been printed upside down in my copy.

G. M. H.

E.A.E.G. ABSTRACT SERVICE

EXPLORATION — GENERAL

79. *Accuracy of the Results of Geophysical Prospecting.* (In French).

M. Matschinski, Geophysical Prospecting, Vol. 2, No. 1, pp. 38-51, March, 1954.

The problems of geophysical interpretation are classified. Four fundamental problems are distinguished and methods of solving them are indicated. Among these are classical methods and methods based on the author's theoretical work.

The geophysical examples are developed, as well as the very simple numerical examples. Methods of enumeration are also referred to. The whole object is to show that the practical application of the geophysical methods suggested will not give prospectors any difficulty.

(Author's Abstract).

80. *How to Plan an Exploration Campaign.* (Part 2).

E. B. Noble, World Oil, Vol. 138, No. 2, pp. 90-92, February 1, 1954.

The two points emphasized in this paper are:

(1) Costs for the exploration programme must be estimated accurately.

(2) Personnel must be selected with much particularity.

Advice is given on these two important points.

81. *Oil Exploration in Surinam.*

W. K. Link, Geol. en Mij., Jaarg. 15, No. 6, pp. 249-50, 1953.

Geophysical exploration of Surinam for oil was begun in 1939, when 15 refraction profiles were shot. In an exploratory well the basement complex was found at 1,500 m; just 100 m deeper than predicted on the basis of seismic work. No indication of oil or gas was found. A fluorescent survey following the seismic exploration gave very discouraging results, which were confirmed by drilling.

(From Geophysical Abstracts 154, U.S. Geol. Survey).

82. *Contouring is Important.*

E. J. Handley, World Oil, Vol. 138, No. 4, pp. 106-107, March, 1954.

From one set of basic geological and geophysical data, many different subsurface contour maps may be derived. A set of rules and guides is given which, it is hoped, will promote more accurate interpretations.

83. *Use and Maintenance of Oscilloscopes.*

J. Dobrin, Instruments and Automation, Vol. 27, No. 3, pp. 449-451, March, 1954.

Oscilloscopes are used for observing waveform, frequency, phase, voltage and time. If not maintained properly they develop troubles which cause defective output. A list of common faults which may be traced by observation, is given, and a routine servicing schedule for the instruments is outlined.

84. *Studies on Origin of Petroleum: Occurrence of Hydrocarbons in Recent Sediments.*

P. V. Smith, Jr., Bull. A.A.P.G., Vol. 38, No. 3, pp. 377-404, March, 1954.

Research on recent sediments has indicated the presence of liquid naphtha, paraffin, and aromatic components in both salt- and fresh-water deposits. Free hydrocarbons in quantities of 12,000 per 1,000,000 parts of dry sediment have been shown.

Estimates based on cores from the floors of the Gulf of Mexico off Louisiana and the Santa Cruz Basin off California give from 4,500,000 to 10,400,000 barrels of crude oil per cubic mile of sediment.

85. *Marine Exploration comes of Age.*
C. H. Johnson & J. W. Wilson, World Petroleum, Vol. 25, No. 3, pp. 74-77, March, 1954.

Since the passing of the U.S. Tidelands Bill, there has been an impressive increase in marine exploration. At the end of 1953, geophysical parties operating on the U.S. continental shelf numbered 28 (24 seismic and 4 gravity). Operating methods are described.

86. *The Exploration of the Ocean Floor.* (In German).
O. Pratje, Geol. Rundschau, Band 39, Heft 1, pp. 152-176, 1951.

A discussion of methods of exploration and present knowledge of the ocean floor, including the submarine portions of the earth's crust. A 9-page bibliography is included.

(From Geophysical Abstracts 155, U.S. Geol. Survey).

87. *Deep-Sea Investigations of the Earth's Crust.* (In German).
O. Pratje, Umschau, Jahrg. 52, Heft 6, p. 165, 1952.

A brief account of the geophysical investigation of the structure of the crust underlying ocean basins. Next to gravity and magnetic measurements, the seismic refraction method is most prominent.

(From Geophysical Abstracts 155, U.S. Geol. Survey).

SEISMIC — GENERAL

88. *Proper Plugging of Shot Holes a Must.*
J. Deupree, World Oil, Vol. 138, No. 2, pp. 87-88, Feb. 1, 1954..

Proper plugging of shot holes insures a better relationship with the land owners and leaves no basis for damage claims. The various plugging methods at present in use are described.

89. *Deep Seismic Sounding of the Earth's Crust.* (In Russian).
G. A. Gamburtsev, Akad. Nauk SSSR Doklady, Tom. 87, No. 6, pp. 943-945, 1952.

During 1949-50 extensive seismic surveys were made in the northern part of the Tien Shan to explore the deep structure of the region, and determine its seismic properties. The reflection method was used at first but later the method of correlated refracted waves was used almost exclusively. To increase the depth of sounding, the length of profiles was increased to 400 km. Simultaneously the sensitivity of the seismographs was improved, greater amplification was introduced, and the geophones were distributed with optimum distance between them, suppressing the effect of background noise. It was found advantageous to use lower frequencies, down to 10 c/sec for longitudinal waves and still lower frequency for transverse ones. Explosive charges were not increased, but the shots were usually made in holes covered with water and 20 to 25 m deep.

(From Geophysical Abstracts 154, U.S. Geol. Survey).

90. *Seismic Surveys in Western Steiermark.* (In German).
H. Lackenschweiger, Berg- und Hüttenmänn. Montash., Jahrg. 97, Heft 6, pp. 111-113, 1952.

Details are given of a seismic survey in western Steiermark, made as the first step in exploration for new coal seams. Velocities measured in various formations were 2,100-2,800 m/sec in Tertiary, 3,200-3,800 m/sec in Cretaceous, 4,200-5,000 m/sec in Palaeozoic, and 5,500 m/sec in crystaline rocks. Data were compiled in isochron maps with related profiles. Favourable structures were then drilled, but all proved barren.

(From Geophysical Abstracts 154, U.S. Geol. Survey).

91. *Seismic Observations in the Eastern Atlantic, 1952.*
M. N. Hill & A. S. Laughton, Proc. Roy. Soc., Vol. 222, No. 1150, pp. 348-56, 18 March, 1954.

The seismic refraction shooting experiments undertaken in the eastern Atlantic and on the neighbouring continental shelf are briefly described, and the results compared with previous work. The deep-sea results show that basaltic rocks lie immediately below the sedimentary layer, which is variable in thickness, with a mean of about 1 km. The basaltic rocks extend to the Mohorovicic discontinuity at a depth of between 9 and 13 km below sea level.

The results from the stations on the continental shelf at the mouth of the English Channel confirm that the basement rocks slope gently seaward; the value of this slope and the nature of the sedimentary cover vary with position.

(Author's Abstract).

92. *Seismic Refraction Work by H. M. S. Challenger in the Deep Oceans.*
T. F. Gaskell, Proc. Roy. Soc., Vol. 222, No. 1150, pp. 356-361, 18 March, 1954.

An account is given of the seismic work carried out on the world cruise of H. M. S. Challenger. At most of the stations in the deep ocean a material giving a seismic velocity of 6.3 to 6.6 km/sec was found covered by about 0.5 km of sediment. Some stations nearer the continents gave velocities resembling those found on land. Near volcanic islands 1.5 to 3 km of material giving a velocity of 4 to 5 km/sec was found overlying material giving 6.5 to 7.0 km/sec.

(Author's Abstract).

93. *Seismic Exploration at Sea.* (In German).
H. Menzel, Umschau, Jahrg. 53, Heft 21, pp. 650-652, 1953.

A review of the seismic reflection and refraction methods as applied to marine surveying. This field of geophysics is invaluable both in exploration for oil on the continental shelf and in purely scientific investigation of the sea floor.

(From Geophysical Abstracts 155, U.S. Geol. Survey).

SEISMIC — THEORY & RESEARCH

94. *Ghost Reflections Caused by Energy first Reflected above the Level of the Shot.*
F. A. Van Melle & K. R. Weatherburn, a paper read at the 23rd meeting of the S.E.G., at Houston, Texas, March, 1953 (Not yet published).

A recorded event which has not travelled a simple reflection path, but has undergone a previous reflection from the base of the weathering or from the surface of the earth above the shotpoint, may, by analogy with optical ghosts, be called a ghost reflection. A method is described for determining the reflection coefficient at interfaces above the level of the shot. Values as high as 0.7 have been found in Beaumont clay surface in Harris County, Texas. With reflection coefficients of this magnitude the ghost reflections influence the character of seismograms noticeably.

95. *A Study of Well Velocity Data in North West Germany.*
W. Von Zur Mühlen & G. Tuchel, Geophysical Prospecting, Vol. 1, No. 3, pp. 159-170, September, 1953.

This article is based on data from 74 seismic well velocity surveys in N.W. Germany. The effect of overburden is illustrated by means of diagrams representing interval velocities against depth. To eliminate observational errors and lithological variations from well to well, interval velocities from about the same depth are averaged. Thus, relatively uniform curves are obtained for Lower Tertiary, Upper Cretaceous, and Lower Cretaceous (Albian), making the effect of overburden better evident than from individual observations. The vertical gradients of velocity for these geological sections are given. Furthermore, they are compared with curves for Lower Tertiary and Cretaceous obtained in N. America. Due to its high lime content, the Upper Cretaceous of N.W. Germany has a much higher velocity than that observed in the Cretaceous of N. America. The curves for shales of the Lower Tertiary and Lower Cretaceous (Albian), however, are similar in both countries. In older formations, on the other hand, e.g. Jurassic and Triassic, lithologic character has the dominant influence and the effect of overburden is rather small and often scarcely noticeable.

The data considered cover a depth range down to 2,700 m. The interval velocities are generally based on the use of various equal intervals.

96. *A Device for Overcoming the Effects of Static on Seismic Shot Signals.*
F. A. Roberts and A. T. Dennison, Geophysical Prospecting, Vol. 1, No. 3, pp. 192-196, September, 1953.

When refraction time signals are transmitted over a radio link between shooter and observer there is a serious risk of interference from electrical storms. This risk can be minimised by sending a series of signals at fixed time intervals and the paper describes a simple device which will do this with the required accuracy.

97. *Love Waves in a Surface Layer of Varying Thickness.*
S. Homma, Geophys. Mag., Tokyo, Vol. 24, No. 1, pp. 9-14, Aug., 1952.

The author considers asymptotic expressions for particular solutions of wave equation in a surface layer of linearly varying thickness, and concludes that a Love wave can be transmitted in an approximate sense. Distance of transmission without much change in wave form depends on wave length. The problem is of interest in connection with seismic waves.

98. *On High-Frequency Seismometry.* (In Russian).
G. A. Gamburtsev, Dokl. Akad. Nauk SSSR, Vol. 88, No. 5, pp. 787-789, 1953.

Experiments were made in Northern Tien Shan using the reflected wave method and frequencies of 10-30 c/s. It is shown that reliable results can be obtained with these higher frequencies.

99. *Travel-Time of Love Waves in 'Study of Surface Waves, Part 7'.*
Y. Sato, Tokyo Univ. Earthquake Research Inst. Bull., Vol. 30, Pt. 4, pp. 305-317, 1952.

Expressions are derived for the travel times of Love waves as well as for the critical distances of arrival. The author investigates the case of a single superficial horizontal layer above a semi-infinite medium when the focus is located respectively in and below the layer. For the latter case it is shown that the travel time is independent of the depth of focus. Two numerical evaluations are made resulting in a plot of the critical distance and arrival time as a function of the period.

100. *Theory of the Combination Seismograph.* (In German).
M. Weber, Zeit. Ang. Math. u. Phys., Vol. 4, Fasc. 1, pp. 57-81, 1953.

The combination seismograph consists of a mechanical seismometer combined with an electromechanical transducer and electronic amplifier with recorder. The electromechanical transducer transforms minute displacements of the vibrating element into electric impulses by corresponding changes of electrical capacities or by generation of voltages employing piezoelectric or magnetostrictive effects. Magnification is achieved by electronic amplification. The detailed theory of the mechanical movements of different parts of the seismometer is presented, followed by the discussion of the functioning of the transducer. Possibilities of measuring displacements, velocities, or accelerations with the described instruments are discussed.

101. *Construction of Master Charts for Boundary Velocities of Seismic Waves.* (In Russian).
A. M. Yepinat'yeva, Akad. Nauk SSSR Izv. Ser. Geofiz. No. 2, pp. 124-130, 1953.

The velocity of the seismic wave propagating along the boundary plane between two media can be determined along profiles that are collinear with or perpendicular to the line of shots. The latter procedure is necessary in studying vertical stratification, but greater accuracy can generally be obtained from collinear profiles, especially when reverse travel-time curves are used. Expressions for this boundary velocity have been derived analytically; in the present paper graphic procedures for its determination are suggested and applied to two examples.

The author points out that sometimes the observed boundary velocity may be not that of the wave refracted by the plane separating the formations, but that of a thin intermediate layer of high seismic velocity embedded in the upper formation. This ordinarily can be discovered by other seismic evidence.

102. *Some Questions related to Interpretation of Travel Time Curves of Refracted Waves Obtained along the Profile Perpendicular to Vertical Boundary Planes.* (In Russian).
A. M. Yepinat'yeva, Akad. Nauk SSSR Izv. Ser Geofiz. No. 1, pp. 17-25, 1953.

When the medium through which seismic waves are propagated is stratified vertically, the shape of travel-time curves of refracted waves, taken along a line perpendicular to the plane of stratification, is different from the hyperbolic pattern obtained in horizontally stratified media characterized by constant velocities. Old methods for the determination of velocities do not yield accurate values. Theoretical analysis as well as experiments show that the effective values of the boundary velocity V_b and the increase of the depth Δh can be computed accurately enough if sections of the travel-time curves sufficiently remote from the boundary plane are used. Otherwise the values obtained are always lower than the true ones. The problem cannot be solved for a medium with several parallel vertical strata.

103. *Concerning Multiple Reflections in Seismic Exploration.* (In German).
R. Meinhold, Gerlands Beitr. Geophys., Band 63, Heft 1, pp. 59-70, 1953.

Multiple reflections can considerably distort and falsify geologic evaluation. They occur especially at shallow variable surfaces with strong velocity contrasts. Strong echoes were observed during work over a salt dome in northern Germany, where the energy was reflected between the anhydrite cap, lying at a depth of 350 m, and the groundwater table. Formulae are derived for the time factor, for calculating the impulse time of echoes from the arrival time of the original reflection; also for the time gradients of echoes for both horizontal and inclined strata, under the assumption that the energy is multiply reflected between the reflector and the earth's surface.

104. *Statistical Study of Waves from Blasts Recorded in the United States.*
E. H. Vestine & S. E. Forbush, J. Geophys. Research, Vol. 58, No. 3, pp. 381-400, Sept. 1953.

Computational methods are described for analyzing a time series into two new time series, these comprising one having systematic quality and stationary autocorrelation, and the other having the properties of random noise. The methods are illustrated by application to seismic records. When a spike signal is expected in a certain interval of record, a significant test for the reality of an observed spike signal is applied.

It is shown that seismic records obtained many kilometers from the source have a remarkably stationary autocorrelation over considerable intervals of time. The random noise level is high. After analysis, in one case a spike signal due to the reflection of a compressional wave from the Mohorovicic discontinuity was probably found, although it is not distinguishable among other similar pulses in the record.

105. *Note on Analytical Tests for Distinguishing Types of Seismic Waves.*
E. H. Vestine, J. Geophys. Research, Vol. 58, No. 3, pp. 401-4, Sept., 1953.

It is pointed out that surface gradients of ground displacements should prove of assistance in identifying and distinguishing the nature of seismic signals. Several theoretical relationships expected for surface disturbances are noted. These can be tested experimentally.

GRAVITY — GENERAL

106. *Gravimetric Study of a Chromite Deposit.* (In French).
Y. Crenn & J. Metzger, Ann. Geophys., Tome 8, Fasc. 3, pp. 269-274, 1952.

Gravimetric prospecting for chromite in mountainous terrain in southern New Caledonia showed an anomaly restricted to a zone 100 m in diameter, with a maximum of 0.60 mgal, which was attributed to a body of 70,000 tons of chromite. Subsequent exploitation disclosed the lens responsible for the anomaly. The fact is stressed that only large ore bodies, of the order of 50,000 tons or more, can safely be determined gravimetrically, and that detailed gravimetric prospecting is justified only after a preliminary study consisting of two or three profiles; anomalies indicating ore should be apparent in these even if topographic corrections are neglected.

(From Geophysical Abstracts 154, U.S. Geol. Survey).

107. *Diurnal Variations of Gravity in Europe. First Note: Observational Data.* (In Italian).
C. Morelli, Ann. Geofis., Vol. 6, No. 1, pp. 113-124, 1953.

The increasing precision of gravimetric measurements, now ± 0.01 mgal, makes it necessary to take into account the lunisolar effect on gravity. Computations of such corrections in an individual survey are very lengthy, and therefore the Osservatorio Geofisico di Trieste is preparing such corrections for stations in northern Italy. These data are also applicable to Central Europe and with slight modifications to nearly all Europe. The computations have been assuming a rigid earth and with deformation taken into account by applying a factor 1.22 to computed amplitudes, as suggested by Baars.

(From Geophysical Abstracts 154, U.S. Geol. Survey).

108. *Gravimetric Prospecting in the Paris Basin.* (In French).
J. Goguel, Soc. Geol. France Comptes Rendus, No. 16, pp. 339-341, 1952.

Gravimetric prospecting has been carried on in the Paris basin since 1944 by the Bureau des Recherches géologiques et géophysiques, the Compagnie Générale de

Géophysique, and the Bureau de Recherches des Pétroles, using Thyssen and North American gravimeters. Complete coverage of the sedimentary basin is expected within a few months. Stations are spaced closely, never less than 1 per 7 km^2, often 1 per 2 or 3 km^2, and in the oil basin of the north, 1 per km^2. Many small anomalies were revealed which would have been missed with less dense coverage.

(From Geophysical Abstracts 154, U.S. Geol. Survey).

109. *The Results of a Gravity Survey in the Country between the Clee Hills and Nuneaton.* A. H. Cook, J. Hospers, & D. S. Parasnis, Geol. Soc. London Quart. J., Vol. 107, Pt 3, pp. 287-306, 1951 (1952).

A gravity survey made between the Clee Hills and Nuneaton shows close correlation of change of anomaly with thickness of the Coal Measures, and a somewhat less close relation with the thickness of the Triassic over the Forest of Arden. The corresponding density differences agree with densities of rocks measured at the surface. The remaining anomalies indicate about 4,000 feet of rather light rocks, probably Coal Measures, below the Triassic in the Forest of Arden, and about 2,500 feet of Triassic at Kidderminster.

(From Geophysical Abstracts 155, U.S. Geol. Survey).

110. *Seismic and Gravity Investigations on the Malaspina Glacier, Alaska.* C. R. Allen & G. I. Smith, Am. Geophys. Un. Trans., Vol. 34, No. 5, pp. 755-760, 1953.

During July and August 1951, seismic and gravity surveys were made on the Malaspina Glacier, southeastern Alaska, to determine the thickness of the ice and the configuration of the glacial floor. Seismic reflection along a 10-mile profile approximately parallel to the assumed direction of ice flow indicate ice thicknesses ranging from 1,130 to 2,050 ft. The subglacial floor is below sea level along the entire profile, 700 feet below in the central part. The ice becomes thinner northward toward the mountains and southward toward the ice margin. Gravity measurements along the central 3 miles of the seismic profile indicate the trend of subglacial topographic features is northwest-southeast. Seismic refraction measurements beyond the glacial margins indicate that the proglacial deposits are more than 500 feet thick.

(From Geophysical Abstracts 155, U.S. Geol. Survey).

GRAVITY — INTERPRETATION

111. *Geophysical Prospecting and the Accuracy of the Interpretation Results.* (In French). M. Matschinski, Geofis. Pura e Appl., Vol. 27, pp. 35-84, 1954.

Interpretation problems in geophysics are outlined, showing the difference between algebraic and statistical ones and the method of least squares. The problems are classified into four sections: 1) Choice of hypothetical geologic structure and its mathematical representation, using parameters. 2) Determination of the parameter numerical values. 3) Determination of all possible values. 4) Determination of the likelihood of the hypothesis itself.

The accuracy of the calculations is investigated and the general theory is applied to the determination of a fault from gravity data.

112. *Solution of the Inverse Gravimetric Problem.* (In Russian). A. K. Malovichko, Akad. Nauk SSSR Izv. Ser. Geofiz., No. 3, pp. 228-31, 1953.

The determination of the shape of a buried geologic body gravimetric data can be reduced to the solution of a non-linear integral equation of the first kind. A method of solving this equation by successive approximations is presented; the procedure is applied to the problem of determining the outline of the surface separating two underground formations on the basis of the gravimetric anomalies on the horizontal surface of the earth over this area, limiting the problem to the two-dimensional case. Ordinarily only a few approximations have to be computed to obtain a sufficiently accurate solution. As an example, the anomaly of a buried parallelepiped body of infinite length is analysed.

(From Geophysical Abstracts 155, U.S. Geol. Survey).

113. *The Use of Multiples in Gravimetric Interpretation.*
R. J. Miller & D. M. Rodriguez, Compass, Vol. 30, No. 1, pp. 34-38, 1952.

Tables and graphs of gravitational anomalies of ore bodies having forms, dimensions, and depths, and designated as structures having multiples equal to one, are computed and drawn for selected parametric values. Then, for each type of structure a multiplier —a simple formula—is derived. By selecting various parameters better suited to the geology (or where previous experience gives us further information) in the area under investigation, the values of multipliers can be rapidly computed and the corresponding gravitational anomalies scaled off from the graphs.

(From Geophysical Abstracts 155, U.S. Geol. Survey).

GRAVITY — THEORY & RESEARCH

114. *A Determination of the Earth Tide from Tilt Observations at two places.*
R. H. Corkan, Mon. Not. Roy. Astronom. Soc., Geophys. Suppl., Vol. 6, No. 7, pp. 431-441, June, 1953.

The paper gives a method of analysing observations of the tilting of the earth's surface. Observations from two places are combined and it is assumed only that the body tilt due to the direct yielding to the attractive forces is simply related to the equilibrium form, but with a constant phase lag, and that the semidiurnal constituents in the load tilt have the same ratios as in the loading tide. It is shown that these ratios are very stable over large parts of the oceans, and a useful table is given for the main seas and oceans. This method avoids the uncertainties of computation of the loading tide which have caused many difficulties in previous investigations, and it automatically eliminates the greater part of the secondary effects of the more distant oceanic tides.

115. *Approximations in the Calculation of the Form of the Geoid from Gravity Anomalies.*
A. H. Cook, Mon. Not. Roy. Astronom. Soc., Geophys. Suppl., Vol. 6, No. 7, pp. 442-452, June, 1953.

The theory of the calculation of the detailed undulation of the geoid from gravity by Stokes's integral is usually given to first order, and there are some approximations which may be important in mountainous places. Some are trivial but the change of undulation with height is not. Discussion of this involves the definition of orthometric height and of the geoid. With suitable definitions the undulations of the geoid are the same as those of equipotential surfaces at external points, so that the latter may be calculated directly without additional correction for changes with height. The free-air correction to gravity is determined by these definitions and conditions; for geodetic purposes the fundamental quantity is not the change of gravity with height but the difference of geopotential. The correction derived in this paper thus differs slightly from those commonly in use and there are consequently some small errors in the figure of the earth derived with the use of the latter.

ELECTRICAL

116. *Basic Theory of the Magneto-Telluric Method of Geophysical Prospecting.*
L. Cagniard, Geophysics, Vol. 18, No. 3, pp. 605-635, July, 1953.

From Ampere's Law (for a homogeneous earth) and from Maxwell's equations using the concept of Hertz vectors (for a multilayered earth), solutions are obtained for the horizontal components of the electric and magnetic fields at the surface due to telluric currents in the earth. The ratio of these horizontal components, together with their relative phases, is diagnostic of the structure and true resistivities of subsurface strata. The ratios of certain other pairs of electromagnetic elements are similarly diagnostic.

Normally, a magneto-telluric sounding is represented by curves of the apparent resistivity and the phase difference at a given station plotted as functions of the period of the various telluric current components. Specific formulae are derived for the resistivities, depths to interfaces, etc. in both the two- and three-layer problems.

117. *Induced Polarization: a Method of Geophysical Prospecting.*
D. F. Bleil, Geophysics, Vol. 18, No. 3, pp. 636-661, July, 1953.

Laboratory experiments have shown certain fundamental relationships concerning the induction of a polarization potential on a metallic body in an electrolyte. The potential induced is a linear function of the potential drop across the body in the energizing field up to a saturation potential of 1.2 vols. Diffusion of ions and chemical action are the predominant factors which determine the rate of growth or decay of the polarization potential. Polarization occurs only at the boundaries of electrically conducting minerals. The results of the laboratory experiments provide an explanation of the induced polarization potential of a homogeneous, uniformly-mineralized earth. This potential falls off as $1/r$ from a point electrode. Induced polarization susceptibility is defined and a method of analyzing field data is described. Field measurements over two mineralized zones (pyrrhotite and magnetite) substantiate the theory as developed.

118. *The Field of a Magnetic Dipole in the Presence of a Conducting Sphere.*
H. W. March, Geophysics, Vol. 18, No. 3, pp. 671-684, July, 1953.

Formulae are derived for the components of the distorted field of a magnetic dipole in the presence of a conducting sphere in a homogeneous medium. In the method employed the field is resolved into two partial fields for the first of which the radial component of the magnetic vector vanishes and for the second of which the radial component of the electric vector vanishes. From the general formulae approximate formulae are derived for the field components in the special case in which the conductivity of the medium is low, the radius of the sphere is not too large, and both the dipole and the observer are in the vicinity of the sphere. These approximate formulae are within limits applicable to the problem of locating a spherical body of ore buried in a mass of rock.

DE QUELQUES SUJÉTIONS DE LA GÉOPHYSIQUE MINIÈRE *

PAR

JEAN GOGUEL **

Mes chers confrères,

Au cours de la réunion qui vient de s'ouvrir vous allez entendre et discuter des communications fort diverses portant sur la technique de nos appareils et de nos méthodes et je ne doute pas que vos entretiens, pendant les interruptions de séance ne prolongent le programme officiel qui vous a été communiqué.

Si notre règlement impose au président sortant de s'adresser à vous, c'est je pense, non pour vous faire entendre une communication technique supplémentaire, mais pour fournir l'occasion d'un coup d'oeil un peu plus général.

Vous êtes certainement tous conscients du fait que l'art que nous pratiquons est en continuelle expansion, non seulement du fait des perfectionnements incessants dont vous allez avoir quelques aperçus, mais plus encore parce que l'échelle sur laquelle il est fait appel aux méthodes confirmées va en croissant d'année en année. Si satisfaisante que soit cette constatation, je ne crois cependant pas qu'il y ait grand profit à nous appesantir sur des statistiques de mois-équipe, qui ne feraient que développer un sentiment d'auto-satisfaction auquel l'homme n'est que trop enclin. Je crois plus utile de rechercher ce qui, dans ce mouvement de croissance, reste en arrière, ne serait-ce que relativement, et de tâcher d'en analyser les raisons.

Il n'est pas besoin de fouiller bien profondément les statistiques pour se rendre compte que l'essentiel de la croissance de la géophysique est dû à la recherche du pétrole. Bien que les applications de la géophysique à la recherche des Mines, les Travaux publics, la recherche de l'eau aillent également en se développant, la proportion de notre travail consacrée à ces questions, pourtant essentielles, parait décroître, et j'ai le sentiment qu'elle est très en dessous de ce à quoi les possibilités de la géophysique, d'une part, les besoins existants dans ces domaines, de l'autre, devraient conduire.

Parmi les raisons de ce retard — tout relatif, car de beaux progrès ont été réalisés dans ces branches, comme certaines communications présentées ici-même vous le montreront — il en est une qui apparait immédiatement: la croissance des prospections pour pétrole absorbe tous les moyens, et en particulier les hommes disponibles, et ne permet pas de consacrer au développement des autres branches l'effort qu'elles mériteraient.

---

* Presidential Address delivered at the Fourth Annual Meeting of the European Association of Exploration Geophysicists, held in Paris, 18-20 May, 1955.

** Bureau des Recherches Géologiques, Géophysiques et Minières, Paris.

Mais il s'agit là d'une limitation essentiellement temporaire, qui n'introduit qu'un simple ralentissement dans la croissance de ces branches, et ne modifie pas les conditions de celle-ci.

L'un des attraits, pour une entreprise de prospection géophysique, des problèmes posés par la recherche du pétrole, est qu'ils comportent en général des campagnes beaucoup plus étendues que les autres. Le travail d'adaptation des méthodes à chaque cas particulier, voir le choix des méthodes, de même que les questions pratiques posées par le déplacement et l'installation des équipes, ne représentent donc qu'une proportion plus réduite par rapport au travail de routine d'exécution des mesures, et celui-ci, suffisamment prolongé, peut être organisé de manière à obtenir un meilleur rendement. Je pense qu'il s'agit là d'une différence essentielle, destinée à subsister: Pour tout problème, qu'il s'agisse d'eau, de travaux publics ou de mine, on peut estimer, au moins grossièrement, la valeur des renseignements que l'on peut attendre de la géophysique, donc le montant des sommes qu'il est raisonnable d'y investire, et on se rend compte que les grandes campagnes resteront l'exception, et que nous aurons toujours à répondre à des nombreuses demandes de campagnes de courtes durées. Pour chacune de celles-ci, il faut choisir les méthodes, mettre au point leur mise en oeuvre, les étalonner ; en un mot, entreprendre un travail qui demande du chef d'équipe des qualités de jugement, d'initiative, voire d'intuition, alors que la brièveté du travail ne justifiera pas la dissociation de la mise au point, et de l'exécution des mesures de routine, que permettent des campagnes très longues. Il y a là une difficulté propre à ces problèmes non pétroliers, qui constitue en même temps un attrait pour des ingénieurs désireux de montrer ce dont ils sont capables.

La prospection du pétrole n'a retenu, en fin de compte, qu'un nombre limité de méthodes, parmi celles qui lui étaient proposées. Les autres problèmes peuvent être de natures tellement variées qu'ils peuvent avoir à faire appel à tout l'arsenal des méthodes existantes. Le jeu imprévisible de l'invention peut nous en offrir d'autres, dont il est difficile de dire à priori à quelle catégorie de problèmes ils s'appliqueront. Mais, si l'invention d'un principe ne surgit pas sur commande, sa mise en oeuvre exige un long travail, et des investissements, auxquels on consent d'autant plus volontiers qu'on voit mieux le nombre des problèmes particuliers auxquels s'appliquera la méthode à développer. La prospection du pétrole permet beaucoup plus facilement une telle appréciation, que les problèmes beaucoup plus fragmentaires et dispersés que posent le Génie civil ou la recherche de mines ; il ne faut cependant pas méconnaître le volume total de travail qu'ils peuvent offrir. Pour ne citer qu'un exemple, je suis convaincu que l'adaptation d'une méthode sismique à l'auscultation du rocher, ou du sol de fondation, à très faible profondeur, aurait un très grand nombre d'applications, susceptible de justifier des investissements de mise au point notables, même si chaque application ne représente qu'un travail d'importance médiocre.

Les études géophysiques non pétrolières posent, à cause de la variété d'origine et de formation des responsables qui ont à faire appel à elles, certains problèmes psychologiques sur lesquels je voudrais attirer votre attention.

En matière de prospection pétrolière, les clients sont des sociétés importantes, qui possèdent leurs propres géophysiciens — ils voisinent ici avec les membres des entreprises — et qui sont parfaitement au courant des possibilités de la Géophysique. Ils peuvent se montrer exigeants, mais ils ne demanderont pas l'impossible, et savent apprécier la portée exacte des résultats qui leur sont apportés. Entre l'entrepreneur et le client — sans parler du cas où celui-ci est son propre entrepreneur — peut ainsi s'établir une collaboration confiante et féconde sur le plan technique.

Il n'en est malheureusement pas de même pour les autres applications de la géophysique. Les responsables des recherches auxquelles nous avons à apporter notre contribution ont à faire face à trop de problèmes divers, et surtout, le recours à la Géophysique est pour eux beaucoup trop occasionnel, pour qu'on puisse attendre d'eux une parfaite connaissance de notre discipline.

Sans doute ne devons nous pas nous résigner à cet état de choses — je parle ici au nom de ceux qui sont responsables de la formation des ingénieurs — Nous devons nous efforcer de faire comprendre aux élèves de nos Ecoles quelles sont les possibilités et les méthodes de la prospection géophysique. Nous avons dans la formation des ingénieurs, deux tâches tout à fait distinctes à remplir : aux futurs géophysiciens, nous devons donner une solide connaissance des sciences de base, et une formation aussi poussée que possible dans les disciplines avec lesquelles ils se trouveront en contact, sans avoir la possibilité de les approfondir, au cours de leur activité professionnelle — je pense en particulier à la Géologie et à la Métallogénie, voire à certaines branches de l'art du constructeur. Tout au moins en France, où la carrière future de nos étudiants reste mal déterminée jusqu'à la fin de leurs études, nous estimons que nous n'avons pas à leur enseigner le détail des techniques à mettre en oeuvre, qu'ils apprendront dans leurs Compagnies, ou au cours de stages appropriés.

A ceux qui, sans être géophysiciens eux-mêmes, peuvent avoir occasionnellement besoin de la Géophysique, c'est-à-dire à tous les ingénieurs qui peuvent avoir affaire au terrain, nous devons donner quelques notions sur les domaines d'application et les possibilités de la Géophysique, en laissant de coté bien entendu tout ce qui concerne la réalisation des appareils, ou les tours de main techniques.

Mais, les programmes d'enseignements sont déjà si chargés, et la procédure de leur réforme est si lourde, qu'il nous est difficile de faire accorder à cet enseignement général de la Géophysique la place qui nous parait nécessaire. Des efforts patients et méthodiques devront être poursuivis, et pendant longtemps encore les Géophysiciens auront parfois affaire à des Ingénieurs n'ayant que des notions rudimentaires sur les possibilités de leur art. Je me suis référé au cas de la France, mais je suis bien certain que la situation n'est guère différente dans d'autres pays.

Cette ignorance du client peut avoir des conséquences tout au long de la prospection. Et tout d'abord, elle risque d'entrainer l'absence de toute prospection, si le responsable ne se rend pas compte que le problème qui le préoccupe peut recevoir une solution par la géophysique. Aucune statistique ne nous dira le nombre des occasions manquées, les sommes dépensées en prospections au hasard, en recherches d'eau vaines, et qu'une prospection géophysique préalable aurait pu économiser. Parce que l'information des responsables du pétrole est satisfaisante, que le travail qu'il nous fournissent suffit à nous occuper, devons nous nous tenir pour satisfaits? Je ne le crois pas. Il y a un effort, je ne dis pas de propagande, ce mot ayant mauvaise réputation, mais d'information auprès de milieux techniques assez variés, qui doit être entrepris, et dont nous devons nous sentir responsables, chacun dans son pays.

Lorsque, ce premier écueil ayant été franchi, le maître de l'oeuvre fait appel au Géophysicien, celui-ci se heurte souvent à une difficulté d'un autre ordre. Il s'aperçoit que, sur la foi d'une information trop sommaire, on le croit capable de résoudre tous les problèmes et, suivant une formule classique, de "voir par transparence" à traverse le terrain. Tant qu'il est si surchargé de travail qu'il n'arrive pas à faire face aux demandes, il lui est assez facile de repousser celles qui ne lui paraissent pas impliquer une chance raisonnable de succès. Mais que survienne un ralentissement de la demande, ou que le Géophysicien craigne de voir interprété son refus comme une dérobade, et de compromettre ainsi des affaires ultérieures plns intéressantes, la tentation serait forte de céder à l'insistance du client, et d'accepter de faire des mesures, tout en sachant qu'aucun résultat utile ne peut s'en dégager. Pour un profit immédiat, ce serait compromettre gravement l'avenir. Bien que, et c'est fort sage, les contrats soient toujours rédigés de telle sorte que nous vendions du travail de mesure, et non des résultats, nous sommes moralement engagés à ne faire de mesures qu'en vue du résultat qui nous est indiqué. Plus on nous fait confiance, en nous laissant libre du choix des instruments ou des méthodes à mettre en oeuvre, plus nous devons nous montrer scrupuleux dans leur choix. La connaissance que possède le Géophysicien des possibilités exactes de chacun de ses instruments n'est définie par aucun contrat, mais quelle impression produira-t-il si il réclame l'emploi d'un instrument nouveau, pour reconnaître au premier essai qu'il ne s'applique pas?

Une fois les mesures faites, il s'agit de les interpréter; nous apportons des données, qui doivent être combinées avec toutes les connaissances antérieures, afin d'arriver à l'interprétation la plus vraisemblable. C'est un travail qui devrait être effectué en étroite collaboration avec le maitre de l'oeuvre, finalement responsable des décisions à prendre. Lorsque, ignorant les servitudes de la technique que nous appliquons, il nous laisse effectuer seuls cette interprétation, dont il accueillera les résultats avec une confiance aveugle, il peut nous mettre dans une situation délicate. Nous ne voulons pas être considérés comme des sorciers ou des thaumaturges, dont les oracles sont indiscutés, mais nous tenons à faire saisir exactement le degré de certitude — parfois faible — des conclusions tirées de nos mesures, à faire comprendre les raisonnements plus ou moins indirects qui nous y ont conduits, et la manière dont toute modification des hypothèses de travail admises réagirait sur elles. Nous souhaitons trouver chez le maître de l'oeuvre une compréhension suffisante pour qu'il puisse admettre que — le cas se présente malheureusement quelques fois — les résultats sont totalement inutilisables, et que pourtant il n'était pas injustifié d'entreprendre les mesures. Et c'est cependant là un aveu bien difficile à faire pour le prospecteur. A défaut d'une compréhension préalable, qui serait désirable, il faut que les explications que nous aurons données honnêtement, avant et pendant les mesures, fassent comprendre au client la nature de nos opérations, et le préparent au besoin à un tel échec.

Il faut que le Maître de l'oeuvre comprenne que les conclusions tirées de nos mesures n'ont pas un degré de certitude correspondant à la précision des instruments employés, et qu'elles doivent simplement s'ajouter aux autres données en sa possession, et se combiner avec elles. On trouve encore parfois un Maître de l'oeuvre qui se croit habile en dissimulant au Géophysicien une partie des renseignements acquis par les recherches antérieures, pour voir si celui-ci les retrouvera. Raisonnement enfantin, qui méconnait la nature tout à fait différente des informations fournies par des procédés d'investigation différents et le fait qu'elles ne se recouvrent pas, mais doivent être combinées ensemble.

Le responsable d'une recherche minière souhaiterait parfois qu'une prospection électrique aboutisse comme conclusion à l'indication des emplacements de sondages à entreprendre. Je ne crois pas, cependant, que ses conclusions puissent, ni doivent, s'exprimer toujours sous cette forme. Sans doute, il peut arriver qu'une anomalie électrique se présente avec une netteté telle, que sans autre information, il paraisse opportun d'en vérifier l'origine par un sondage; mais beaucoup plus souvent, ce n'est qu'en discutant les rapports de cette anomalie avec la minéralisation connue et la structure géologique, que pourront apparaître les directions selon lesquelles une recherche parait avoir le maximum de chances de succès — étant entendu qu'il ne s'agit pas d'une certitude, mais d'une simple probabilité, de l'ordre de celles sur lesquelles les mineurs ont l'habitude de fonder leur action, mais améliorée par rapport à ce qu'aurait été cette même probabilité avant la prospection géophysique.

Il faudrait aussi que le Mineur comprenne que, si les conclusions apportées à l'issue de la prospection représentent la combinaison la plus vraisemblable des connaissances géologiques acquises, et des mesures géophysiques, celles-ci subsistent indépendemment des hypothèses de travail dans le cadre desquelles elles ont été interprétées, et que, lorsque des travaux ultérieurs auront précisé ou modifié les idées admises, il pourra être nécessaire de reprendre ces résultats, et de voir comment ils peuvent s'interpréter à la lumière des idées nouvelles — ce qui exige évidemment que le Maître de l'oeuvre conserve tout le détail des mesures.

Il serait normal que ce soit le Maître de la recherche, responsable des décisions et des risques à prendre, qui effectue cette synthèse des connaissances géologiques acquises et des données géophysiques, pèse les probabilités qui en résultent, et fasse son choix. Mais souvent, faute pour lui de pouvoir apprécier exactement la portée et la valeur des indications fournies par la Géophysique, il laissera au Géophysicien le soin de tirer les conclusions. Mais un inconvénient inverse se présente alors : mis au courant des hypothèses de travail utilisées par le mineur, le Géophysicien risque de surestimer leur valeur, de les considérer comme démontrées, et de les utiliser comme un cadre dans lequel il situera l'interprétation de ses mesures. Et le mineur, à son tour, risque de croire que celles-ci démontrent une hypothèse qu'il n'avait lui-même avancée que sous toutes réserves. Il est bien d'autres cas — je ne citerai que, tout près de nous, les rapports entre la Physique du Globe et la Géologie — où deux disciplines voisines se prêtent mutuellement leurs hypothèses les plus aléatoires, et les retrouvent ensuite, sans reconnaître leur origine, parées d'un prestige qui leur fait attribuer une certitude illusoire.

Bien que son rôle soit de prendre des risques — risques calculés, bien entendu — le responsable d'une recherche est parfois heureux de se décharger sur d'autres du choix qui doit être fait. Il est des cas où il importe plus d'aller de l'avant — que ce soit en sondage ou en galerie — que de choisir judicieusement une direction que rien m'indique. Je pourrais citer au moins un exemple où un procédé, soit disant géophysique, mais en réalité plus proche de la sourcellerie, les mesures ne pouvant avoir aucune relation avec la minéralisation cherchée, a pu rendre un réel service au mineur, en affirmant ce qui n'était pour lui qu'une hypothèse à laquelle il n'osait se fier, et en lui fournissant ainsi l'énergie nécessaire pour avancer dans une des deux directions possibles, alors que, comme l'âne de Buridan, il hésitait sans rien entreprendre, sûr moyen de ne rien trouver.

Il faudrait n'avoir aucune foi en la Géophysique — et tel n'est pas mon cas — pour accepter de la voir réduite à un tel rôle. Mais pour éviter ce risque, il faut obtenir la collaboration du Maître de l'oeuvre, la lui imposer même, obtenir de lui tous les renseignements nécessaires sur la valeur des données géologiques, et lui expliquer à la fois la valeur des indications géophysiques obtenues, et les doutes subsistant dans leur interprétation. Il faut, dans ce travail, que le Géophysicien sache raisonner en Géologue ou en Mineur. L'intervention d'un conseil, indépendant des deux parties peut constituer entre elles un lien précieux.

Je viens d'emprunter des exemples à la recherche minière, domaine où l'action se fonde, d'une manière parfaitement justifiée, sur des probabilités très inférieures à l'unité. En matière de travaux publics ou de recherche d'eau, on exige des probabilités beaucoup plus élevées — très voisines de l'unité pour les travaux publics, assez fortes pour les recherches d'eau, pour lesquelles on ne peut se permettre qu'une très faible proportion d'échecs.

La probabilité des interprétations de la Géophysique ne correspond pas, le plus souvent, au degré de certitude ainsi exigé, mais là encore, la Géophysique n'est pas seule à intervenir. Elle se place dans un cadre géologique, où il ne reste qu'à lever certaines indéterminations ; surtout en matière de Travaux publics, son rôle n'est pas, en général, d'apporter des réponses définitives, mais d'orienter des recherches par sondages ; il ne faudrait pas en conclure que ce rôle soit faible. Au contraire, on ne peut jamais aussi bien chiffrer la valeur des renseignements apportés par une prospection géophysique, que lorsqu'on peut comparer le coût des sondages implantés grâce à elle à ce qu'aurait été le prix des sondages nécessaires pour obtenir les mêmes renseignements, sans indications préalables. Les données ainsi recueillies permettent d'affirmer que le domaine des applications de la Géophysique aux Travaux publics est encore très loin d'être complètement exploré.

Les recherches d'eau ne portent pas, en realité, sur la présence même de ce fluide, mais sur les conditions dans lesquelles il circule ou pourrait circuler, après mise en dépression. La recherche directe par les procédés géophysiques parait donc impossible mais il est de nombreux cas où une recherche indirecte — précisant, par exemple, la nature ou l'épaisseur des alluvions — peut se montrer extrêmement féconde. Mais les recherches d'eau sont très nombreuses et très dispersées, leurs promoteurs sont en but aux sollicitations des sourciers, et un sérieux effort d'information est nécessaire pour faire comprendre exactement aux cadres techniques responsables, à la fois les possibilités et les limitations des méthodes géophysiques, ceci d'autant plus que, vu le caractère indirect des recherches, la collaboration entre le Géophysicien et le Géologue est particuliérement nécessaire.

Si je voulais résumer d'un mot les considérations qui précédent, je dirais que l'une des difficultés des prospections géophysiques autres que celles pour pétrole, est que nous n'y sommes plus entre nous. Il nous faut à la fois comprendre des préoccupations très différentes et surtout — c'est le plus difficile — faire comprendre la nature et la valeur de ce que nous apportons, sans susciter des espoirs immodérés, qui ne pourraient engendrer que des déceptions.

Mais je crois que cette servitude doit, pour des esprits ouverts, constituer un attrait supplémentaire dans un domaine où nous avons la perspective d'élargir encore considérablement l'importance et la variété des travaux qui nous appellent.

RELATIVE DETERMINATION OF THE DENSITY OF SURFACE ROCKS AND THE MEAN DENSITY OF THE EARTH FROM VERTICAL GRAVITY MEASUREMENTS *

W. DOMZALSKI **

ABSTRACT

The gravity difference between two stations, one at the surface and the other underground vertically below the former and at a given distance from it, depends on the mean density of the earth, σ_m, as well as on the density of the layer of rock contained between the two stations. When one of these densities is known, the other can be computed from this gravity difference. The reliability of this determination depends on the relative accuracies with which σ_m and σ can be obtained.

These accuracies are discussed in the paper. The mean density of the earth has been determined with an accuracy of approximately 0.01 gr/cm^3. The determination of the density of a layer of rock depends on density determinations of rock samples which are not representative of the layer as a whole. Thus the accuracy of the value of σ based on a number of sample determinations will depend on many factors, including the method of averaging the density values obtained from the samples and the degree of uniformity in the geology.

To investigate the problem discussed above, three sets of gravity measurements were made under differing conditions. In each instance a number of pairs of stations vertically above each other were occupied on the surface and underground. The results computed from the data on each pair of stations in a set of measurements were considered as repeated measurements of the same quantity, and the most probable value was calculated.

The results demonstrated that the accuracy varied with the conditions prevailing in the area where the observations were made. In Godstone Quarries the dip of the strata was negligible, the rocks fairly uniform and structural conditions undisturbed. Consequently, although the rock layer between the surface and underground stations was only of the order of a hundred feet, the mean density of the earth computed from the average density of the rock samples, was very close to the accepted standard value of 5.52 gr./cm^3. This agreement, however, was easily upset when only one random sample density was assumed as representative of a given formation.

In a different locality in Cumberland the observations were made in a mine and on the surface. The rock layer between the surface and the underground stations was approximately a thousand feet thick. One set of measurements followed a line parallel to a fault, the other a line crossing this fault. The results differed appreciably from the standard value of σ_m, particularly in the latter case.

It is concluded that the gravity difference between a surface and an underground station can be used satisfactorily to determine the average density of a rock layer in situ and en bloc, using the standard value for the mean Earth density.

---

* Presented at the Seventh Meeting of the European Association of Exploration Geophysicists, held at The Hague, 8-10 December 1954.

** Mining and Geophysical Services Ltd., London.

SYMBOLS AND NOTATION USED IN THE TEXT

G	Universal Gravitational Constant
σ	density
h	difference in elevation
r	radius
Rm	mean radius of the Earth
Δr	thickness of a layer (h and Δr are equal numerically)
Δg	difference of observed gravity between two stations, vertically above each other
σ_m	mean Earth density

INTRODUCTION

The term vertical gravity measurement used in this paper refers to a measurement taken in the same plan position on the surface and underground. The experiments were conducted in a disused quarry in Surrey, and in a mine in Cumberland. In the former the thickness of the ground layer between the pairs of stations was of the order of a hundred feet, whilst in the latter it was of the order of a thousand feet. The geology of the two locations differed appreciably as regards both the type of rock and in its structural aspects. These diverse conditions serve as an illustration of the possibilities and limitations inherent in the method of measurement.

The densities of the surface rocks were determined in the laboratory from hand specimens. The analysis of the results of gravity measurements leads to a value of the mean density of the Earth, or conversely to the average density of a layer of surface rorks if a certain value of the mean density of the Earth is assumed.

GENERAL CONSIDERATIONS

1. The problem of rock densities is equally important both in exploration geophysics and in geophysics applied to geodetic problems. These densities are required for the reduction of the observed values of gravity, which includes the influence of elevation and of the terrain, and for the interpretation of the gravity anomalies.

The terrain corrections compensate for 1) the attraction of the material which is not considered in the Bouguer correction, and which is above the upper plane of the infinite slab whose attraction is $2\pi G\sigma h$, 2) the overcompensation caused by applying the Bouguer correction which assumes the space filled with material, where actually there is none. These corrections require the densities of those rocks which constitute the topography around the stations considered and whose densities generally differ from the densities obtained from the measurements on samples. The elevation correction for a surface station has the form

$$[F - 2\pi G \sigma]\, h \quad . \; . \; . \; . \; . \; . \; . \; . \; . \; . \; . \qquad (1)$$

and for an underground station

$$[F - 4\pi G \sigma]\, h \qquad \ldots\ldots\ldots \qquad (2)$$

Expression (2) is directly applicable to the vertical gravity measurements discussed here. In fact, if the gravity values at the two stations vertically above each other were corrected for the effect of the surface topography and any local anomaly, then the difference in the value of gravity between these two stations would be

$$\Delta g = [F - 4\pi G \sigma]\, h \qquad \ldots\ldots\ldots \qquad (3)$$

2. In order to appreciate fully the assumptions made when expressions (1) and (2) are used, and to investigate the ratio of the density of the surface rocks and the mean density of the Earth, some theoretical aspects are necessary.

The attraction of a sphere at its surface is

$$g = G\, M/r^2 \qquad \ldots\ldots\ldots \qquad (4)$$

where M is the mass of the sphere assumed to be concentrated in its centre and r is the radius. In using expression (4) it has been assumed that the Earth is a non rotating sphere, so that neither flattening nor the centrifugal effect have been taken into account.

The rate of change of gravity along the radial direction is given by

$$dg/dr = d\,(G\, M/r^2)/dr \qquad \ldots\ldots\ldots \qquad (5)$$

Before the differentiation is carried out, it is necessary to discriminate between the rate of change above the free surface and below it.

If the change above the free surface is required, the only variable is the distance r whereas, for the rate of change below, it is necessary to take into account the change in the mass M, since M is a function of r, say $M\,(r)$.

Above the free surface

$$dg/dr = G\, M\ [d\,({}^1/r^2)/dr] = -2\, G\, M/r^3 \qquad \ldots\ldots \qquad (6)$$

giving

$$dg/dr = -2\, g/r \qquad \ldots\ldots\ldots \qquad (7)$$

Here the minus sign implies that gravity decreases when moving away from the centre

For the rate of change below the surface, the final expression will also include the effect of the traversed layer of rock. The rate of change will be

$$dg/dr = d\ [G\, M\,(r)/r^2]/dr \qquad \ldots\ldots\ldots \qquad (8)$$

Since the mass of the Earth as a function of the radius is given by

$$M(r) = 4\pi \int_0^r \sigma\, r^2\, dr \qquad \ldots\ldots\ldots \qquad (9),$$

$$d\, M(r)/dr = 4\pi\, \sigma\, r^2 \qquad \ldots\ldots\ldots \qquad (10)$$

where σ is the density of the layer $d\,r$.
Hence

$$dg/dr = 4\,\pi\,G\,\sigma - 2\,G\,M\,(r)/r^3 \qquad (11)$$

In this, the radius should be that of the inner sphere of the mean density σ_m. In practice, however, $d\,r$ is very small compared with r and no appreciable error is introduced by the continued use or r. Thus

$$dg/dr = 4\,\pi\,G\,\sigma - 2\,g/r \qquad (12)$$

Expression (12) differs from (7) by the term $4\,\pi\,G\,\sigma$ which, as already indicated, represents the effect of the layer of rock traversed on the way downwards. The term

$$F = 2\,g/r \qquad (13)$$

is the free air correction, which is constant for all practical purposes. The accurate form of it would be

$$F = (2\,g/r)\ (2 + dr/r)/2\ (1 + dr/r)^2 \qquad (14)$$

Again however, the highest elevation on the Earth's surface is approximately 1/700 of the Earth's radius and $d\,r$ can be neglected so that the expression (13) is sufficiently accurate. The variation of the vertical gradient due to the changes in the latitude is even less than its variation with elevation. The accurate formulae which take these effects into consideration are listed in Appendix I.

The total elevation correction for the underground stations is obtained from expression (12). For the surface stations the term $2\,\pi\,G\,\sigma$, known as the Bouguer correction must be used, giving a total elevation correction

$$-\Delta\,g = [2\,\pi\,G\,\sigma - 2\,g/r]\,\Delta\,r \qquad (15)$$

It is to be noticed that $4\,\pi\,G\,\sigma$ is exactly double the Bouguer correction because the downward attraction a the top of a layer is changed into an upward one below the layer. The sign of the free air correction is always opposite to the sign of the other term in expressions (12) and (15), the actual signs depending on whether the gradient $d\,g/d\,r$ is considered towards the centre, or away from it.

For a finite interval $\Delta\,r$, expression (12) becomes

$$-\Delta\,g = [4\,\pi\,G\,\sigma - 2\,g/r]\,\Delta\,r \qquad (16)$$

and the gravity within a uniform solid sphere changes in proportion to the distance from the centre (Ramsay 1952):

$$g = 4/3\,\pi\,G\,\sigma_m\,r \qquad (17)$$

As the density of the Earth is not uniform (Bullen 1936, Jeffreys 1937) gravity changes non-uniformly (Benfield 1937, Olczak 1938, Saxov 1952, Stewart) within the Earth so that σ_m will be used to denote the man density within the sphere of radius r. This effect is negligible in the work considered here.

Substituting (17) in (16), a formula connecting the superficial density σ with the mean density of the Earth σ_m is obtained.

$$\Delta g = 4\pi G\,[2/3\,\sigma_m - \sigma]\,\Delta r \quad . \; . \; . \; . \; . \; . \; . \; . \; . \quad (18)$$

Finally it must be remembered that the term $4\pi G \sigma$ applies to an infinite layer of rock, but in practice this requirement is satisfied if the ratio of the horizontal dimensions to the thickness is more than ten (Domzalski 1955).

With the aid of expression (18) it is possible to compute the density σ of the layer of rock of thickness Δr, or the mean density of the Earth σ_m, if one or the other is known.

3. A comparison of the relative accuracies of σ, or σ_m will decide which computation is more reliable.

The determination of the mean density of the Earth σ_m, is based on the measurements of the universal constant of gravitation and the acceleration of gravity at the Earth's surface. The former has been re-determined with increasing accuracy many times, since the original Cavendish experiment, and a re-determination by Heyl (1930) gave the value of $G = (6.670 \pm 0.004) \times 10^{-8}$ c.g.s. The value adopted here is the mean, of several determinations by different observers. Thus Kaye & Laby (1952) give $G = (6.659 \pm 0.005) \times 10^{-8}$ c.g.s. whilst in the geophysical literature the value most commonly used is Hayford's value of 6.667×10^{-8} c.g.s. Another later re-determination by Zahradnicek (Champion and Davy 1937) gave $G = 6.659 \times 10^{-8}$ c.gs. The difference between the two extreme, modern values is therefore 0.011×10^{-8} c.g.s. which is equivalent to an accuracy of 1 : 600 but Heyl's value alone is accurate to 1 in 1700.

The other quantity affecting directly the determination of the mean density of the Earth is the value of the gravitational acceleration at the Earth's surface. Determinations of the absolute value of gravity have been made at several base stations, and a great number of other stations have been tied in by relative pendulum observations. These measurements permit the determination of the spheroid approximating to the shape of the Earth, because the flattening of this spheroid can be derived on the basis of Clairaut's Theorem (Stokes 1883). From the distribution of gravity over the Earth's surface the spheroid can be determined. Several formulae which use different methods of analysis giving slightly different coefficients are in existence (Appendix I). The one now in universal use is the International Formula, derived by Heiskanen and Cassinis.

The preceding discussion shows that the accuracy with which the gravity to be used for the mean density calculation is known, depends on the accuracy of absolute pendulum measurements and the accuracy of the estimation of gravity from the gravity formulae referred to. It is known that some of the absolute gravity measurements such as the Potsdam system may be in error by 10 to 13 milligals (Kaye and Laby 1952). However the overall accuracy is of the order of 1 to 5 in 10^5 and the error in the estimation of the Earth radii (spheroid) is of the same order. Thus the inaccuracy in the value of the mean density of the Earth is due mainly to the uncertainty in the determination of the universal gravitational constant. (about 1 in 10^3). The mean density of the Earth can be derived from the expression

$$\sigma_m = 3\, g \times 1.0014\, (1/4\, \pi\, G\, R_m) \quad . \; . \; . \; . \; . \; . \; . \; . \quad (19)$$

where Rm is its mean radius and g the gravitational acceleration at 45° latitude, has been increased by the factor 1.0014 to allow for the centrifugal force and ellipticity. (Kaye and Laby 1952). The resulting σ_m depends on the adopted numerical values of G, R_m and g, and the comparison of the two following values of the mean density of the Earth $\sigma_m = 5.517$ (Jeffreys 1952) and $\sigma_m = 5.526$ (Kaye and Laby 1952) provides a measure of the accuracy, equivalent to 1 in 600.

The mean density of the horizontal layer of rock separating two stations one above the other can only be estimated from measurements on samples. As a layer of rock of finite thickness and considerable extent is rarely uniform, the accuracy of the value of σ finally used depends not only on the actual accuracy of the laboratory determination, but also on the method of selection, the statistics employed and the structural conditions near the observation points.

The laboratory determination of the density of a sample can be made to within ± 0.005 gr/cm^3, which is comparable with the range of the quoted values for the mean density of the Earth. The average density of a layer of rock, however, would only be equivalent to the density of a random sample if the material was perfectly uniform. To obtain the best value for the density in the case of a non-uniform layer, it would be necessary to obtain a large number of samples and have a satisfactory method of correcting for variations in porosity, degree of compaction, lithology and moisture content. Furthermore, the unknown existence of anomalous structural conditions in the vicinity of the points of the gravity measurements, e.g., a fault, may cause a substantial difference between the actual and estimated values of the average density of the layer, so that, whilst the individual determinations of density may be relatively accurate, the accuracy of the average density of the layer will be much lower and cannot be predicted, unless the the local conditions are known in detail.

It is thus concluded that the determination of the average density σ of a rock layer from expression (18) after subsitution of the value for σ_m, is generally more reliable than the determination of σ_m from the average density σ. An equivalent degree of accuracy could only be achieved if the rock layer was uniform and no structural anomalies were present in the vicinity.

EXPERIMENTAL RESULTS

1. Three series of measurements were carried out at surface and underground stations. In Godstone Quarries the thickness of the intervening layer was of the order of a hundred feet, and it was composed of uniform strata, whereas in Cumberland, the thickness of the layr was about a thousand feet and the strata were dipping and faulted.

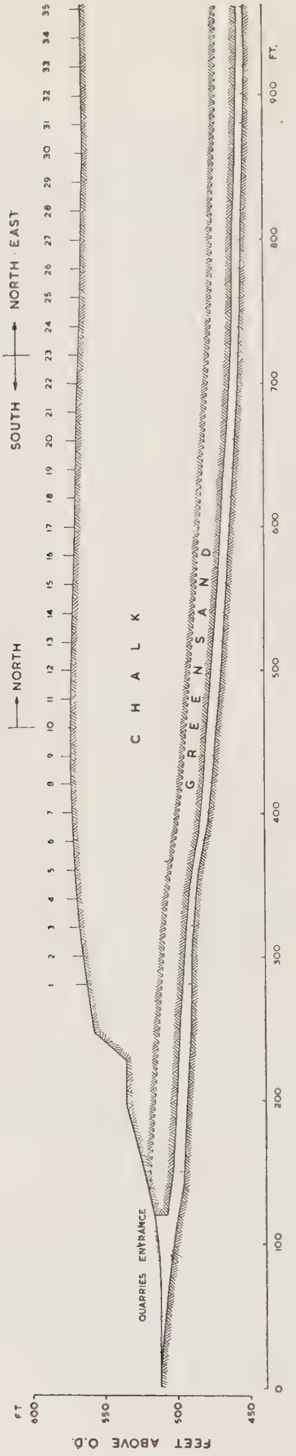

Fig. 1
Geological section of Goldstone Quarries.

2. *Measurements in Godstone Quarries*

This site is a disused hearthstone mine near Godstone in Surrey, England and the access is gained along a gently dipping incline. Inside the workings the headings were driven in the beds of hearthstone so that the dip of the headings is indicative of the average dip of the strata. (Fig. 1). The layer of ground between the stations on the surface and underground is composed of Chalk and Greensand. The thickness of the Greensand formation was found by trenching near the entrance to the quarries, and because of the uniform and gentle dip of the strata, it is reasonable to assume that this thickness remained unchanged along the 600 feet of traverse. The Greensand formation is composed of three distinct beds; viz. Greensand, soft sandstone and hard sandstone and their densities, as determined in the laboratory, are 1.88 gr/cm^3, 1.71 gr/cm^3 and 2.30 gr/cm^3 respectively. The relative thickness of these beds was measured in a nearby exposure and found to be in the prolayer 15 feet thick gives values of 12, 1.5 portion 7.5 : 1 : 1. Applying these values to a and 1.5 feet respectively, so that the weighted average density for the whole layer of Greensand formation is 1.91 gr/cm^3. The determination of the density of the chalk was made from several samples obtained from outcrops and shallow pits. Their values varried between 2.08 gr/cm^3 and 2.20 gr/cm^3 and the average of 2.14 gr/cm^3 was used in the computations below.

The gravity meter readings were corrected for the terrain effects and the readings taken underground were also corrected for the effects of tunnels, headings and the loose material filling the spaces where hearthstone had been excavated. The effect of the underground excavations on the gravity field at the surface was so small, that even a detailed surface survey failed to reveal it and so it was neglected. Altogether 35 pairs of stations were occupied along the traverse, but the first nine have not been considered, due to the proximity of uneven surface topography (Fig. 1). The traverse runs approximately north between stations 10 and 23 and then turns to the north-east between stations 23 and 35. As the surface elevation increases towards the east average thickness of the ground layer contained between the pairs of stations is 98 feet for the section 10-23 and 106 feet for the section 23-35. As the thickness of the Greensand layer is believed to remain constant the increased thickness of the ground layer must be due entirely to the increased thickness of the chalk. The average weighted density of the whole ground layer for each of the two sections can be computed using the densities previously determined and the known thicknesses of the chalk and Greensand beds. These average densities for the two sections differed by less than 0.01 gr/cm^3 so that one value of 2.10 gr/cm^3 was adopted for stations 10 to 35; this value together with the measured gravity difference between a pair of the vertical stations permit the determination of the mean density of the Earth from expression (18). Bearing in mind all the assumptions and limitations discussed in the first part of this paper, the mean density of the Earth

$$\sigma_m = 3/2\,[(\Delta g/\Delta r)\,(1/4\pi G) + \sigma] \quad . \quad . \quad . \quad . \quad . \quad . \quad (20)$$

Table I contains the data and the results for individual pairs of stations. Each entry in column 3 is the difference between the values of gravity, observed at the surface and underground stations in the same plan position. The differential terrain correction in column 4 is the difference between the effects of the surface topography on the surface and underground stations respectively ($T_u - T_s$) whilst column 5 includes the effects of the excavations and filled spaces on the underground values of gravity. The corrected gravity difference in column 6 is given by $\Delta g = \Delta g_o + [T_u - T_s] - Du$.

The values of σ_m derived in column 8 for the different pairs of stations were considered as repeated measurements of the same quantity and the least squares method was used for the computation of the most probable value, which is 5.52 ± 0.03 gr/cm^3. Although this is in remarkable agreement with the generally accepted value, it must be borne in mind that a different method of averaging the sample densities might easily lead to a somewhat different average density of the ground layer and consequently to a different value of σ_m. To illustrate this point, the calculations were repeated for the lowest value for the density of chalk, namely 2.08 gr/cm^3, and also for the highest value (2.20 gr/cm^3). The average densities of the ground layer between the surface and underground gravity stations then become 2.06 gr/cm^3 and 2.16 gr/cm^3 respectively and the corresponding values of σ_m are 5.46 ± 0.04 gr/cm^3 and 5.61 ± 0.04 gr/cm^3.

The values of σ_m obtained from measurements at stations 10-26 are, with one exception, above 5.50 gr/cm^3, whilst those obtained at stations 27-35 are all below this figure. The separate groups lead to values of 5.55 ± 0.02 gr/cm^3

TABLE I

Derivation of σ_m from the average density of rock layer.
Measurements in Godstone Quarries

1 No. of pair of stations	2 Δr Vertical distance in feet	3 Δg_0 Gravity difference in milligals	4 ΔT Differential Terrain corrections in milligals +	5 D_u Total correction for Effect of underground excavations in milligals —	6 Δg Corrected Gravity difference in milligals	7 $\frac{\Delta g}{\Delta r} \times \frac{1}{4\pi G}$	8 σ_m gr/cm^3
10	98.53	4.20	0.02	0.17	4.05	1.61	5.57
11	101.27	4.26	0.02	0.13	4.15	1.60	5.55
12	102.01	4.29	0.02	0.14	4.17	1.60	5.55
13	102.69	4.32	0.02	0.17	4.16	1.59	5.54
14	103.61	4.35	0.02	0.17	4.20	1.59	5.54
15	104.13	4.42	0.02	0.13	4.31	1.62	5.58
16	105.11	4.46	0.02	0.17	4.31	1.61	5.57
17	106.16	4.49	0.02	0.14	4.37	1.61	5.57
18	107.60	4.58	0.02	0.13	4.47	1.63	5.60
19	108.86	4.66	0.02	0.13	4.55	1.64	5.61
20	109.19	4.55	0.02	0.16	4.41	1.58	5.52
21	110.39	4.63	0.02	0.15	4.50	1.60	5.55
22	110.51	4.61	0.02	0.14	4.49	1.59	5.54
23	110.46	4.54	0.02	0.17	4.39	1.56	5.49
24	110.25	4.55	0.02	0.13	4.44	1.58	5.52
25	110.35	4.54	0.01	0.13	4.42	1.57	5.51
26	110.39	4.54	0.01	0.13	4.42	1.57	5.52
27	109.99	4.53	0.01	0.15	4.39	1.56	5.49
28	109.76	4.46	0	0.13	4.33	1.54	5.46
29	109.90	4.38	0	0.14	4.24	1.51	5.42
30	109.54	4.49	0	0.13	4.36	1.56	5.49
31	111.34	4.52	0	0.13	4.39	1.54	5.46
32	112.95	4.61	0	0.13	4.48	1.55	5.48
33	112.58	4.58	0	0.14	4.44	1.54	5.46
34	111.89	4.54	0	0.17	4.37	1.53	5.45
35	111.97	4.51	0	0.16	4.35	1.52	5.43

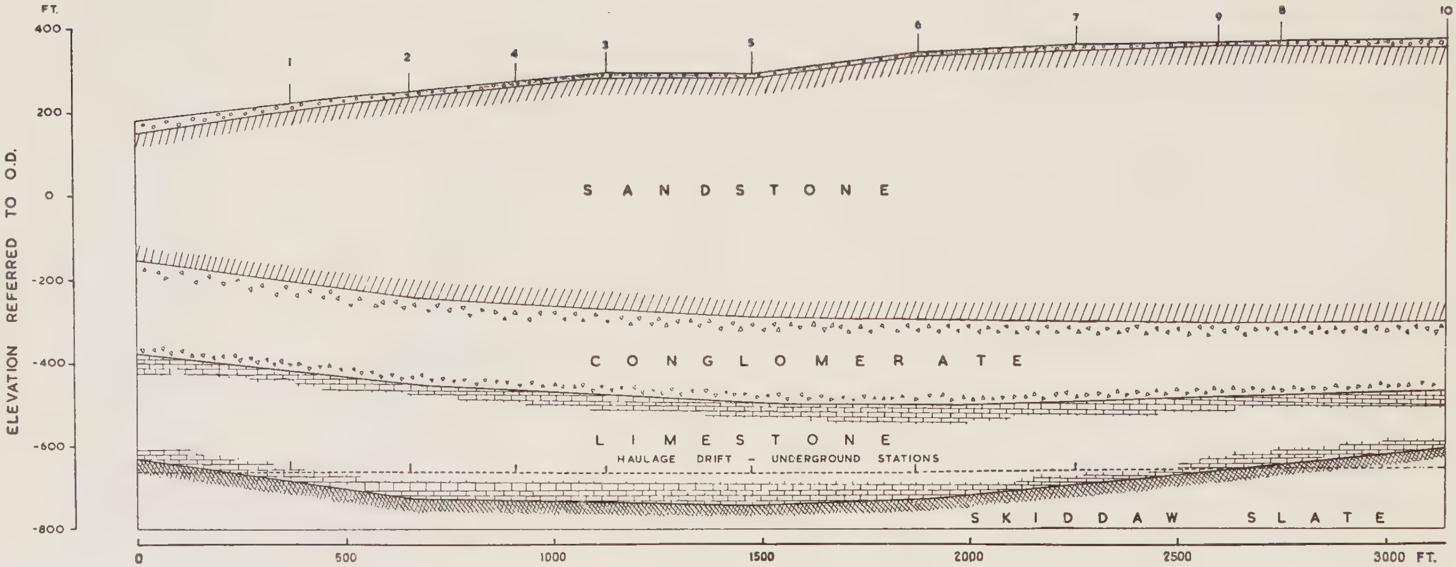

Fig. 2

Geological section of Florence Mines, parallel to the fault.

and 5.46 ± 0.02 gr/cm³ respectively for σ_m. The progressive nature of this change along the traverse particularly apparent with the change in direction, suggests that the variations in the relative thicknesses of the beds may be responsible.

3. *Measurements in Florence Mines*

Measurements in very different conditions to those in the Godstone Quarries, were made in the haematite mines in Cumberland, where the vertical distance between the stations was of the order of a thousand feet. The sequence and thicknesses of the different strata were obtained from boreholes, whilst the density of the rocks was determined from samples obtained from surface exposures from underground and from borehole cores. The adopted value of the density for each type of rock is an average of the determinations on samples from different locations and different depths. These values are (in correct sequence)

Overburden:	2.10 gr/cm³
Sandstone:	2.46 gr/cm³
Conglomerate:	2.60 gr/cm³
Limestone:	2.70 gr/cm³
Slate:	2.76 gr/cm³

A system of faults of varying magnitude crosses the area in approximately an east-west direction.

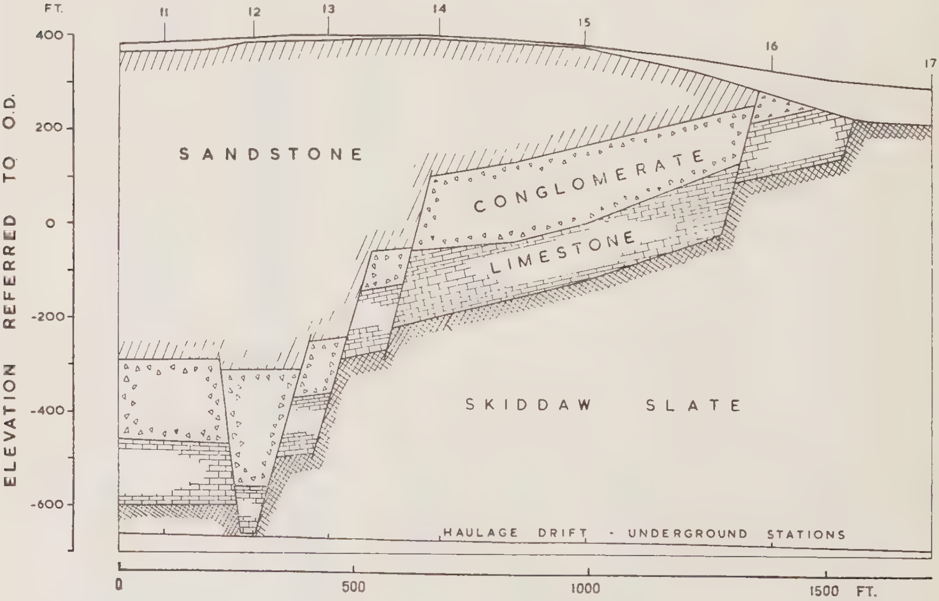

Fig. 3
Geological section of Florence Mines, crossing the fault.

The measurements were carried out along two traverses. Stations 1-10 were on an east-west traverse running approximately parallel to and about 600 feet south of a major fault. Stations 11-17 were on a north-south line crossing this fault which had an approximate throw of 400 feet to the south. The sections along the two traverses are shown in Figs 2 and 3. It is evident that, although the relative thicknesses of the formations along the first traverse change somewhat, the variations are gradual and uniform along its whole length of 3200 feet (Fig. 2). The average density of the whole layer of rocks between the surface and underground stations on traverse 1, computed from the listed average densities of the formations and weighted by their corresponding thicknesses, leads to a value of 2.53 gr/cm^3. A similar procedure was adopted in the derivation of the average density of the layer of rocks along the second traverse giving a value of 2.63 gr/cm^3, which will differ most from the real local value at the ends of the section where one type of rock is predominant.

The observated gravity values were corrected as before and the results are tabulated in Table II. The most probable values are 5.58 ± 0.04 gr/cm^3 obtained from the measurements on traverse 1 and 5.69 ± 0.06 gr/cm^3 from the measurements on traverse 2.

DISCUSSION OF RESULTS AND CONCLUSIONS

The result obtained in Godstone Quarries, namely 5.52 ± 0.03 gr/cm^3 is in accord with the acepted value but an average density based on an insufficient number of samples would lead to a different value of σ_m and this would also occur if the calculations were based on certain stations only. It appears that even with the very favourable conditions of uniform thickness, gentle dip, and undisturbed structural aspect, a representative average density can only be obtained with a sufficient number of stations to compensate for possible local deviations from uniformity.

In the previous discussion of the accuracy with which different quantities are known, no mention was made of the effect of inaccurate gravity observations which may be due to a faulty instrument, observer's mistakes or an erroneous calibration, last one being a systematic error. If any errors are involved in the gravity measurements, the erorrs in the resulting values of density will depend on the vertical distance between the stations (Domalski 1954). The grater this distance, the less effect will the error in the gravity observations have on the resultant density. Similarly the errors in the determination of this vertical distance will also affect the resultant density less if the vertical distance is great. Thus the observations in the Florence Mines, involving a rock layer of 1000 feet will be less affected by any inaccuracies in the gravity measurements than the observations in Godstone Quarries, where the vertical distance was a tenth that at Florence. As the results obtained in Godstone tend to be more accurate, it is seen that uneven dips and discontinuities affect the results very adversely. A comparison of the two values of σ_m

TABLE II

Derivation of σ_m from average density of rock layer. Measurements in Florence Mines

1 No. of pair of stations	2 Δr Vertical distance in feet	3 Δg_0 Gravity difference in milligals	4 ΔT Differential Terrain corrections in milligals +	5 D_u Total correction for Effect of underground excavations in milligals —	6 Δg Corrected Gravity difference in milligals	7 $\frac{\Delta g}{\Delta r} \times \frac{1}{4\pi G}$	8 σ_m gr/cm³
1	885.83	24.83	0.30	0.11	25.02	1.11	5.46
2	920.37	27.08	0.31	0.13	27.26	1.16	5.54
3	965.94	29.17	0.37	0.13	29.41	1.19	5.58
4	932.14	27.06	0.31	0.12	27.25	1.14	5.51
5	962.67	29.03	0.40	0.11	29.32	1.19	5.58
6	1013.76	31.91	0.45	0.12	32.24	1.25	5.67
7	1024.95	32.26	0.49	0.14	32.61	1.25	5.67
8	1031.13	31.59	0.54	0.14	31.99	1.21	5.61
9	1010.60	30.95	0.56	0.11	31.40	1.22	5.63
10	1036.03	31.29	0.58	0.15	31.72	1.20	5.60
11	1040.19	31.52	0.58	0.11	31.99	1.20	5.75
12	1054.01	32.16	0.58	0.11	32.63	1.21	5.76
13	1063.74	32.56	0.57	0.11	33.02	1.22	5.78
14	1068.83	32.45	0.57	0.11	32.91	1.21	5.76
15	1055.37	30.84	0.58	0.11	31.31	1.16	5.69
16	1005.19	27.22	0.65	0.11	27.76	1.08	5.57
17	980.00	25.59	0.71	0.13	26.17	1.05	5.52

obtained in the Florence Mines, i.e. 5.58 ± 0.04 gr/cm³ and 5.69 ± 0.06 gr/cm³, confirms this supposition. The measurements which contributed to the calculation of these two values were carried out over (and under) the same type of rocks and the same average density of a given formation was used in both instances. The different result, therefore, is solely due to the fact that measurements in one case were along a traverse parallel to a fault and some distance away from it, and in the second case across this fault. Apart from the difficulty already discussed of obtaining a representative average density of a ground layer containing a horizontal discontinuity, the existence of a fault zone with its crushed and fissured material will further alter the overall average density "en bloc". In the interpretation of the gravity results it is this average bulk density which has to be known. Accordingly, it is desirable to use expression (18) and to determine σ from σ_m, since this would appear to involve less uncertainty.

To illustrate somewhat this point, the average densities of the ground layer were computed using $\sigma_m = 5.52$ gr/cm³. The results are Godstone 2.10 ± 0.02 gr/cm³, Florence 2.49 ± 0.03 gr/cm³ from traverse 1 and 2.53 ± 0.04 gr/cm³ from traverse 2. The comparison of these with the laboratory determinations of density on the samples, and the averaged densities based on these determinations as discussed, is instructive.

APPENDIX

FORMULAE REFERRED TO IN THE TEXT

CLAIRAUT'S THEOREM

$f + k = 5/2\ m$ where f = geometric flattening
k = gravitational flattening
m = ratio of the centrifugal force to the acceleration of gravity on the equator.

MEAN DENSITY OF THE EARTH FROM THE THEORY OF THE FIGURE OF THE EARTH

$$M = [g_e R^2{}_e/G]\ (1 + 3/2\ m - f)$$

$$\sigma_m = [3\, g_e/4\, \pi\, G\, R_e]\ (1 + 3/2\, m - f)$$

M = mass of Earth
R_e = equatorial radius
g_e = acceleration of gravity on the equator
m, f = see above

GRAVITY AS A FUNCTION OF LATITUDE

Helmert's formula:

$$g_o = 978.030\ (1 + 0.005302\ \sin^2 \emptyset - 0.000007\ \sin^2 2\ \emptyset)$$

U.S. Coast and Geodetic Survey formula:

$$g_o = 978.039\ (1 + 0.005294\ \sin^2 \emptyset - 0.000007\ \sin^2 2\ \emptyset)$$

International formula:

$$g_o = 978.049\ (1 + 0.0052884\ \sin^2 \emptyset - 0.0000059\ \sin^2 2\ \emptyset)$$

g_o = gravity at sea level; $\emptyset$ = latitude

THEORETICAL VERTICAL GRADIENT OF GRAVITY

G. Cassinis, P. Dore, S. Ballarin:
(Fundamental Tables for reduction of gravity observed values, Milan 1937)

$$\frac{dg}{dH} = -0.308552 - 0.000220\ \cos 2\ \emptyset$$

U.S. Coast and Geodetic Survey

$$\frac{dg}{dH} = -0.30855 - 0.00022 \cos 2\,\emptyset + 0.000144H$$

S. Hammer (based on Helmert's derivation)

$$\frac{dg}{dH} = -0.308550 - 0.000227 \cos 2\,\emptyset + 0.000145H$$

$\emptyset$ = geocentric latitude (sufficient approximation is effected by use of geodetic latitude); H: elevation in Kilometers above 1924 International Ellipsoid (sufficient approximation is effected by reference to sea level).

ACKNOWLEDGEMENTS

The investigations described in this paper were carried out with the kind permission of the Directors of Mining and Geophysical Services Limited, who sponsored all the aspects of the undertaking.

The author wishes to thank Prof. J. M. Bruckshaw of the Imperial College for his remarks and criticism throughout the different stages of the investigations.

Thanks are also due to the Management of the Florence Mines for the permission to operate underground, and for the facilities provided, and also to the Caterham County Council for permission to enter the Godstone Quarries.

REFERENCES

Benfield A. E., 1937, "Note on the Variation of Gravity with Depth", Zeitschrift fur Geophysik Vol. XIII. Heft 4/5.

Bullen K. E., 1936, "The Variation of Density and the Ellipticities of Strata of Equal Density within the Earth", M.N.R.A.S. Geophysical Supplement Vol. 3. No. 9, p. 395.

Champion F. C., 1937, & Davy N., Properties of Matter, pp. 38-41, Prentice-Hall Inc. N.Y.

Domzalski, W., 1954, "Gravity Measurements in a Vertical Shaft", Bulletin I.M.M. June 1954. (Tansactions I.M.M. Vol. 63, 1953/4 part 9) pp. 429-445).

——, 1955, "Three Dimensional Gravity Survey" Geophysical-Prospecting Vol. 3. No. 1. pp. 15-55.

Heyl, P. R., 1930, "A Redetermination of the Constant of Gravitation", American Bureau of Standards, Journal of Research Vol. 5, pp. 1243-1290.

Jeffreys H., 1937, "On the Materials and Density of the Earth's Crust", M.N.R.A.S. Geophysical Supplement Vol. IV No. 1, pp. 50-61.

—— 1952, "The Earth", Cambridge University Press.

Kayes G. W. C. & Laby T. H., 1952, "Tables of Physical and Chemical Constants", Longmans, Green & Co.

Olczak T., 1938, "On the Mass of the Earth and on Gravity within the Earth", Acta Astronomica, Serie C. Vol. 3. Gracovie 1938. pp. 81-85.

Ramsay A. S., 1952, "An Introduction to the Theory of Newtonian Attraction", Cambridge University Press.

Saxov S., 1952, "The Variation of Gravity within the Earth", Tellus Vol. 4. No. 2.

Stewart R. M., "Gravity in the Interior of the Earth", Journal of the R.A.S. of Canada, Vol. XLIII No. 4, pp. 129-137.

Stokes G. G., "On Attractions and on Clàiraut's Theorem", Mathematical & Physical Papers 1883. pp. 116.

DISCUSSION

Mr. SCHLEUSENER: In gravity surveys in mines the measured gravity differences at the two levels are used for the calculation of the densities. Mr. Domzalski has been lucky with the reasonably uniform chalks and could get a remarkable good value of the mean density of the earth.

It seems to me that the only layer which is uniform enough to give an even better control of σ_m or σ is water which has an exactly known density and compressibility. We are free of many assumptions if we choose for example the Boulder Dam whose water level changes as far as I remember about 200 m, which will bring about 8 milligals change in gravity. These 8 milligals can be measured nowadays within about 1 : 600 with a marine gravimeter. The gravity at the ground should be measured with high and low water against a reference point a few hundred meters from the shore.

Mr. DOMZALSKI: As Mr. Schleusener points out the value of the mean density of the Earth, calculated from vertical gravity measurements, depends primarily on the uniformity of the intervening layer and on the accuracy with which its true bulk density is known. I have endeavoured to stress this fact throughout the text and the analysis of the results confirms the existing uncertainty and tallies with the conclusions which Mr. Schleusener drew from his experiments.

Water would undoubtedly be the most uniform medium available for such measurements. The practical difficulty might arise in connection with observations at the surface in position vertically above the station at the bottom, where measurements could be taken with an underwater gravity meter. Measurements at sea would be still more satisfactory from the point of view of an infinite horizontal extent of the layer. If pendulum measurements were accurate enough or if a gravity meter could be used successfully in a submarine, it would be an interesting experiment to take such submarine measurements at different depths under the surface.

UN INTÉGRATEUR POUR LE CALCUL DES CORRECTIONS TOPOGRAPHIQUES *

PAR

R. BOLLO** et J. GOGUEL**

ABSTRACT

When gravimetric prospecting is concerned with a region featuring broken relief the calculation of topographical corrections becomes vitally important, for these rectify apparent anomalies completely. It is essential that they should be calculated as exactly as possible. By the classic method this takes an extremely long time and may in the long run involve an outlay actually higher than that expended on operations on the terrain.

It has thus been felt necessary to seek methods which would speed up calculation, and, bearing that in mind, the use of a polar integrator has been envisaged. With this the contour lines of a map can be followed between two fixed radii, the pole corresponding to the location of the position. Two integrator roulettes will give the values of the first two terms of the expansion in terms of the quotient of the height divided by the distance, the second of the terms resulting from the curvature of the earth. Unless there are escarpments very close to the position, the use of these two terms will be sufficient.

Polar integration will deal successively with different contour lines and a subsidiary graph will be plotted, giving the value of each of the integrals in terms of the height. By means of this subsidiary graph the values of the corrections will be obtained with a planimeter and a moment integrator. It is envisaged that the same operation could be repeated in the case of two maps with different scales, for instance, 1-20,000 and 1-200,000 the effect of the areas in the immediate neighbourhood of the position being taken into account by the observer. It is hoped that in this way the calculation of topographical corrections will be made quicker, more exact and less laborious.

Le calcul des corrections topographiques par la méthode classique des zones de Hayford constitue, dès que l'on aborde des régions un tant soit peu accidentées, un travail extrêmement lourd et il est des cas — nous en avons eu un exemple récent dans le SE de la France — où ce calcul est beaucoup plus coûteux que l'exécution des mesures elles-mêmes sur le terrain; les corrections trouvées sont d'ailleurs d'une importance telle qu'il serait impossible, en leur absence, de se rendre compte même grossièrement de l'allure des anomalies.

La mise au point d'une méthode qui permettrait d'alléger ce calcul et d'en réduire le prix, tout en augmentant si possible la précision du résultat, ne tend pas seulement à réaliser une économie. C'est une condition préalable qui doit être remplie avant que puisse être abordée d'une manière systématique l'étude des régions à relief accidenté, dont la structure pose le plus souvent des problèmes pour lesquels la gravimétrie pourrait être d'un grand secours.

---

* Presented at the Eighth Meeting of the European Association of Exploration Geophysicists, held in Paris, 18-20 May 1955.

** Bureau des Recherches Géologiques, Géophysiques et Minières, Paris.

Le calcul d'une correction topographique se ramène à celui d'une intégrale, étendue à un volume qui est défini par les cartes en courbes de niveau dont nous disposons. Dans la méthode classique, cette intégration est effectuée d'abord suivant la verticale, à l'aide de tables, mais pour des éléments de surface dont l'étendue est loin d'être négligeable et dont chacun exige une appréciation de l'altitude moyenne qui demande expérience et jugement, et constitue la part la plus lourde du travail. Il est d'ailleurs peu satisfaisant de se borner à considérer l'altitude moyenne alors que la loi suivant laquelle interviennent les différentes parties de la fraction de zone considérée est beaucoup plus complexe.

Dans la méthode dont nous allons indiquer le principe, on s'est efforcé d'adapter cette intégration à la forme sous laquelle nous sont données ses limites, c'est-à-dire des courbes de niveau, en rendant par ailleurs l'intégration aussi automatique que possible. On effectuera donc l'intégration l'abord par tranches d'altitude constante, et ensuite seulement suivant la verticale. L'effet d'un elément de volume correspondent à la surface ds entre les altitudes z et $z + dz$, situées à la distance horizontale r de la station O d'altitude z_0, peut s'obtenir ainsi : sa distance au plan horizontal de O est : $h = z - z_0 - \frac{r^2}{2a}$ (a, rayon de la Terre).

La composante verticale de l'attraction de cet élément de volume est proportionnelle à : $ds\, dz\, h\, (h^2 + r^2)^{-3/2}$ ou en développant :

$$ds\, dz \left[\frac{z - z_0}{r^3} - \frac{1}{2\,ar} + \ldots\ldots\right]$$

Dans un premier stade on déterminera par intégration graphique pour l'altitude z les quantités $A = \int \frac{ds}{r^3}$ et $B = \int \frac{ds}{r}$, et dans le second stade, on effectuera l'intégration par rapport à z selon la formule :

$$\int A\ (z - z_0)\ dz - \frac{1}{2a} \int B\ d\ z$$

L'intégration ne peut évidemment se faire d'un seul coup pour tout le plan, d'autant qu'on est amené d'ordinaire à utiliser deux cartes à des échelles différentes pour les zones proches et les zones lointaines. Pour les zones très proches de l'instrument jusqu'à un rayon r_1 les cartes topographiques sont inutilisable ; entre les rayons r, et r_2 on utilisera une première carte et une deuxième entre les rayons r_2 et r_3.

Au-delà du rayon r_3 la correction peut, soit être négligée, soit être bloquée avec la correction isostatique correspondante et calculée pour un petit nombre de stations par les méthodes classiques.

L'appareil que nous nous proposons de construire donnera simultanément les intégrales A et B prises entre deux rayons r_1 et r_2. Il est de type polaire (fig. 1), le pôle étant placé à l'emplacement de la station sur la carte et il suffira de suivre avec un traceur le contour fermé constitué par une courbe de niveau et, éventuellement, des arcs de cercle de rayons r_1 et r_2 ; des butées limitent d'ailleurs la course du traceur et permettent de suivre l'un ou l'autre de ces cercles sans qu'ils soient tracés sur la carte. Il pourra être commode d'équiper celle-ci en distinguant par des couleurs appropriées certaines courbes de niveau.

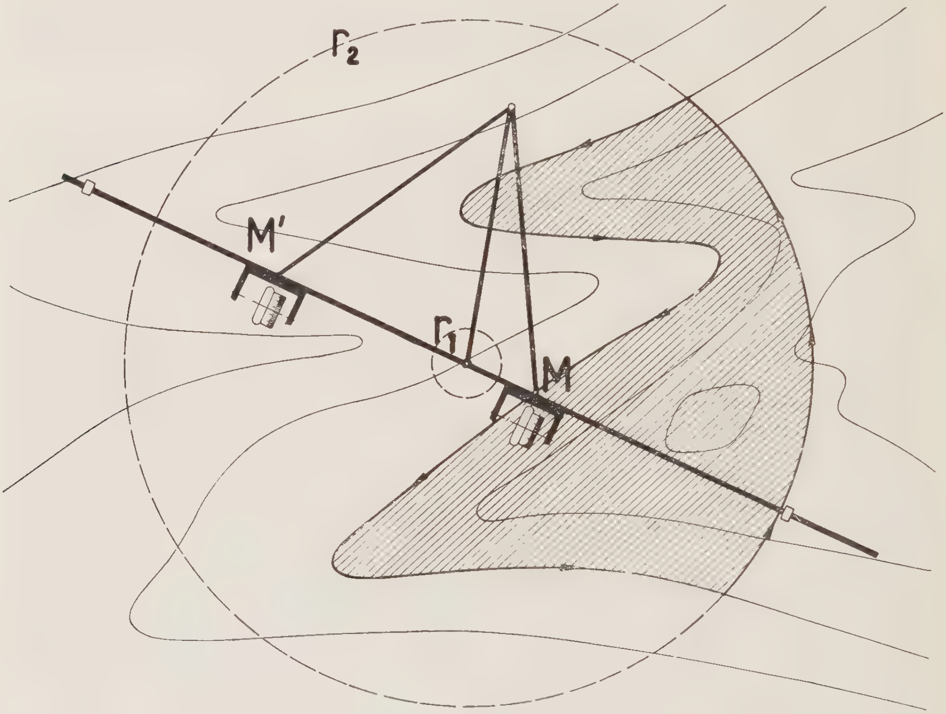

Fig. 1. Illustration du principe de l'intégrateur. — Illustration of the principle of the integrator.

L'appareil (fig. 2) comporte une règle parallèle à OM et pivotant autour du point O, et le long de laquelle coulisse un charriot lié au traceur M et portant une roulette intégratrice d'axe de rotation parallèle à OM. Après parcours d'un contour fermé, la quantité dont a tourné cette roulette est proportionnelle à l'intégrale $B = \int \frac{ds}{r}$ D'autre part, si M' est l'inverse de M dans une inversion de centre O et de constante K^2, une roulette liée de la même manière au point M' fournira la valeur de

$$K^2 A = K^2 \int \frac{ds}{r^3}$$

Le charriot portant cette seconde roulette est de construction identique au premier et lui est assujetti par un dispositif articulé comportant trois tiges et qui n'est autre chose qu'un demi-inverseur de Paucelier. Des dispositions de construction très simples fournissent un dégagement suffisant pour permettre à l'un ou à l'autre des charriots de s'approcher aussi près que possible du centre *O*. La longueur utile de la tige médiane de l'inverseur est réglable, de manière à fixer la valeur de la constante K^2 en fonction des valeurs des rayons r_1 et r_2. La butée déterminant le rayon intérieur r_1 limitera en fait la course du charriot *M'* et non celle de *M*. Pour chacune des échelles usuelles de cartes et pour les rayons correspondants r_1 et r^2 choisis une fois pour toutes, des crans de réglage permettront de retrouve immédiatement les positions des butées et la longueur de la tige médiane. L'intégration sera effectuée pour les contours fermés déterminés par un certain nombre de courbes de niveau, choisies par l'opérateur en fonction de l'expérience acquise dans les calculs antérieurs, et qui ne seront d'ailleurs pas nécessairement les mêmes pour les cartes des zones proches ou lointaines, ni pour toutes les stations.

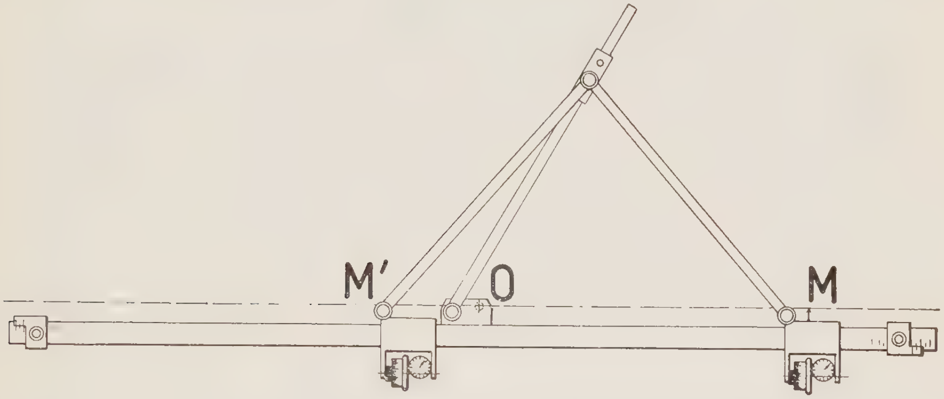

Fig. 2. Diagramme de l'intégrateur. — Diagram of the integrator.

Pour effectuer le deuxième stade de l'intégration, selon l'altitude, on utilisera également une méhode graphique. Des diagrammes tout préparés (fig. 3) comporteront en ordonnées une échelle linéaire des ultitudes, et de part et d'autre d'un axe, les valeurs de chacune des intégrales *A* ou *B* pour les domaines relatifs à deux échelles, les graduations étant établies directement en lecture de l'appareil, pour les échelles des cartes utilisées. Un simple planimètre permettra de tirer du diagramme la valeur du terme

$$\frac{1}{2a}\int B dz$$

à la fois pour les deux cartes (l'influence des zones proches étant d'ailleurs très faible). Pour le terme $A\ (z - z_0)\ dz$, on utilisera un intégrateur à moment

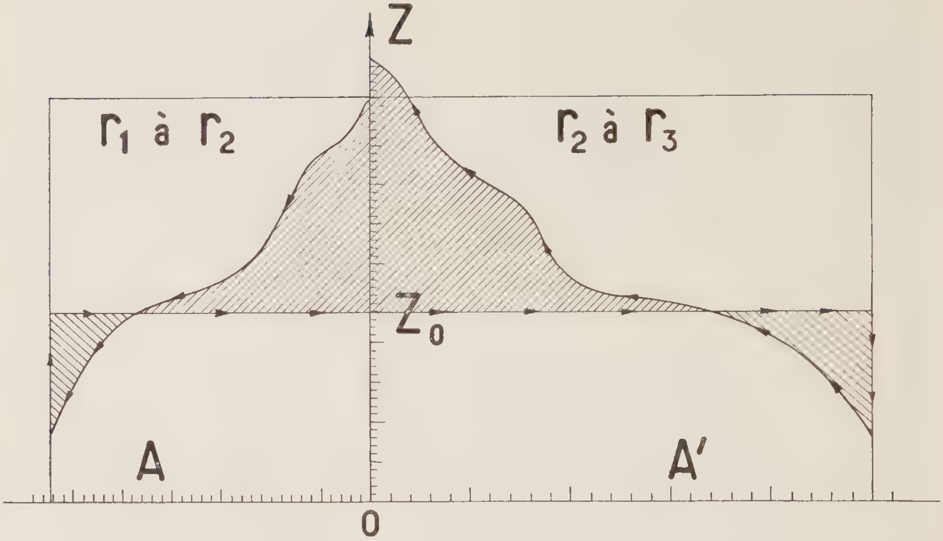

Fig. 3. Diagramme pour l'intégration suivant la verticale. — Diagram for the vertical integration.

de type classique, dont la base sera placée à l'altitude z_0 de la station, altitude qui n'intervient pas avant ce stade des opérations

On espère, avec l'organisation du travail qui vient d'être indiquée, parvenir à rendre les opérations beaucoup plus automatiques que par le passé et en même temps utiliser toute la finesse des indications fournies par les courbes de niveau. La durée du travail dépendra évidemment du nombre de courbes de niveau pour lesquelles devra être effectuée l'intégration. Mais si, au fur et à mesure, on porte sur le second diagramme les valeurs trouvées, on se rendra compte assez rapidement du nombre de valeurs nécessaires pour assurer avec une précision suffisante le tracé du diagramme qui sera planimétré dans la seconde phase de l'opération. Il sera ainsi possible de proportionner exactement le travail à fournir à la précision nécessaire.

Les détails de construction de l'instrument, qu'il n'est pas nécessaire de préciser ici, ont été étudiés en collaboration avec les Etablissements CORADI qui doivent en effectuer la réalisation.

Discussion

Mr. Hammer: How long will it take to compute the topographic correction at a station with this integrator? To what extent is the inclusion of the term for the curvature effect of the earth of practical importance?

Mr. Goguel: La durée du calcul — qui dépendra du nombre de courbes intégrées — ne pourra être précisée qu'après réalisation de l'instrument, qui n'est encore qu'en projet.

Le terme tenant compte de la courbure de la Terre peut être utile pour certains calculs géodésiques, portant sur des zones lointaines ; il est faible pour les zones proches, et aurait peut être pu être négligé pour les seules applications à la prospection, où l'on aurait pu admettre que son effet ne se ferait sentir que sur la part régionale de l'anomalie. Mais sa suppression n'aurait entrainé qu'une très petite simplification dans la réalisation de l'instrument, et il a paru préférable de maintenir la roulette intégratrice correspondante, l'usager ayant évidemment toujours la faculté de ne pas la lire.

Mr. SAXOV : What will the accuracy be if you use a map in the scale 1/20 000 or something like this ?

Mr. GOGUEL : La précision dépendra du nombre de courbes de niveau pour lesquelles sera effectuée l'intégration, et il sera facile de l'adapter aux besoins.

Mr. SELEM : I wish to mention that we have the same problems of rough topography and that we have adopted a method based on an integrator of normal commercial production. The method has been used for detailed gravimetric surveys and we are pleased with the accuracy of the results. The saving in time proved to be over 50 % in comparison with the previous correction technique. Details of the method will be given in a paper to be presented at the next meeting.

RAPPORTEUR POUR LA CONSTRUCTION RAPIDE DU RAYON REFRACTE *

PAR

J. SCHOEFFLER** et E. DIEMER **

Abstract

In this paper we describe a protractor which provides a very simple method of constructing refracted rays in a vertical plane. Another advantage of this apparatus is that it can be made locally in any computing office.

La Société Chérifienne des Pétroles possède un dossier d'une centaine de sismo-sondages qui permettent de connaître les vitesses des terrains sédimentaires qu'elle prospecte. Nous avons été placés devant le problème suivant: un manteau d'épaisseur très variable de marnes miocènes ou crétacées de vitesse lente, correspondant à un accroissement linéaire de la vitesse avec la profondeur, recouvre du Jurassique, calcaire, marneux ou détritique, dont la vitesse est relativement constante et s'établit autour de 3.600 ou 4.000 mètres par seconde.

Il est indispensable dans certains cas, de tenir compte du dioptre séparant ces deux milieux, qui donne souvent d'ailleurs des réflections totales.

Nous raisonnerons dans un plan vertical, les structures étant supposées cylindriques et d'axe perpendiculaire à la coupe sismique.

La restitution d'une coupe temps en coupe profondeur à l'aide d'une loi $V = f(P)$ ou $V = f(\tau)$ (V étant la vitesse, P la profondeur et τ le temps vertical) est une opération relativement rapide. La réfraction d'un rayon sismique au passage d'une surface séparant deux milieux de vitesse constante est également facile à déterminer. Il suffit de tracer sur un disque de Kodatrace, les angles réfractés r correspondant aux angles d'incidence, i, pris de 5 en 5° pour le rapport V_1/V_2 considéré. Mais le problème que nous voulons résoudre est le suivant: déterminer la réfraction subie par un rayon ayant parcouru un milieu dans lequel la vitesse est fonction de la profondeur et pénétrant dans un deuxième milieu à vitesse constante. On peut toujours résoudre le problème à la règle à calcul: c'est une méthode longue et fastidieuse; le rapporteur que nous allons décrire accélère de beaucoup cette opération.

---

* Presented at the Seventh Meeting of the European Association of Exploration Geophysicists, held in The Hague, 8/10 December 1954.

** Société Chérifienne des Pétroles, Petitjean, French Morocco.

Principe (Figure 1).

Soit un demi-cercle de rayon $K = OA$. Un rayon sismique d'angle d'incidence égal à i coupe la circonférence en un point A; en supposant qu'il pénètre en O dans un milieu de vitesse différente, il subit une réfraction d'angle r telle que $\sin r = (V_2 V_1) \sin i$, V_1 et V_2 étant les vitesses du premier et du deuxième milieu. Si le point H est la projection de A sur le diamètre CD et B, l'intersection avec AH de la droite représentant la direction du rayon réfracté, nous avons:

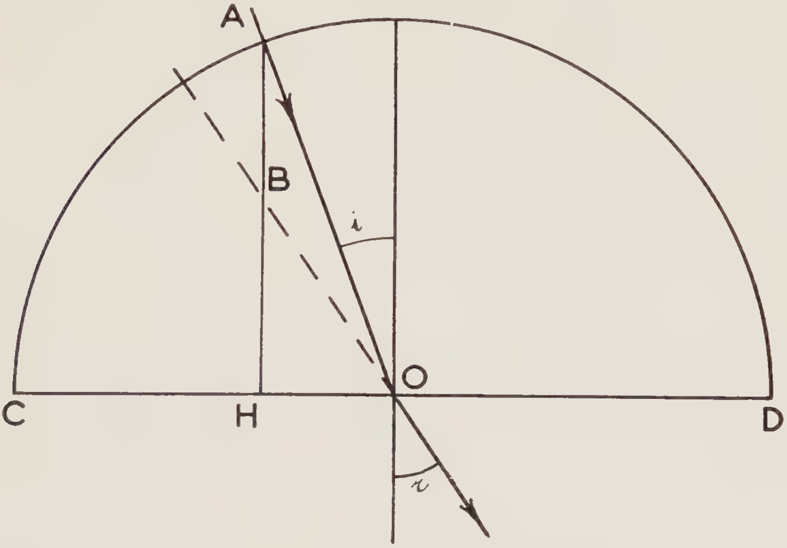

Fig. 1. Illustration du principe de la méthode.
Illustration of the Principle of the Method.

$$OH = OA \sin i \text{ et } OH = OB \sin r$$

$$\text{ou} \quad OB = OH/\sin r = OA \sin i/\sin r = OA.\ V_1/V_2$$

$$\text{c'est à dire } OB/OA = V_1/V_2 \text{ ou } OB = KV_1/V_2.$$

Description de l'Appareil (Figure 2)

Sur un demi-cercle de rayon K, nous traçons des traits perpendiculaires au diamètre CD, traits dont le but est d'indiquer cette direction perpendiculaire à CD; ils seront équidistants sauf si la connaissance numérique de l'angle i est nécessaire; ils seront alors tracés à la distance $OH = K \sin i$, de 0 à 90° et de 5° en 5° par exemple.

Autour de O pivote une réglette en plexiglass dont une branche est graduée en KV_1/V_2; la ligne médiane de cette branche possède une rainure, dont l'utilité apparaîtra plus loin.

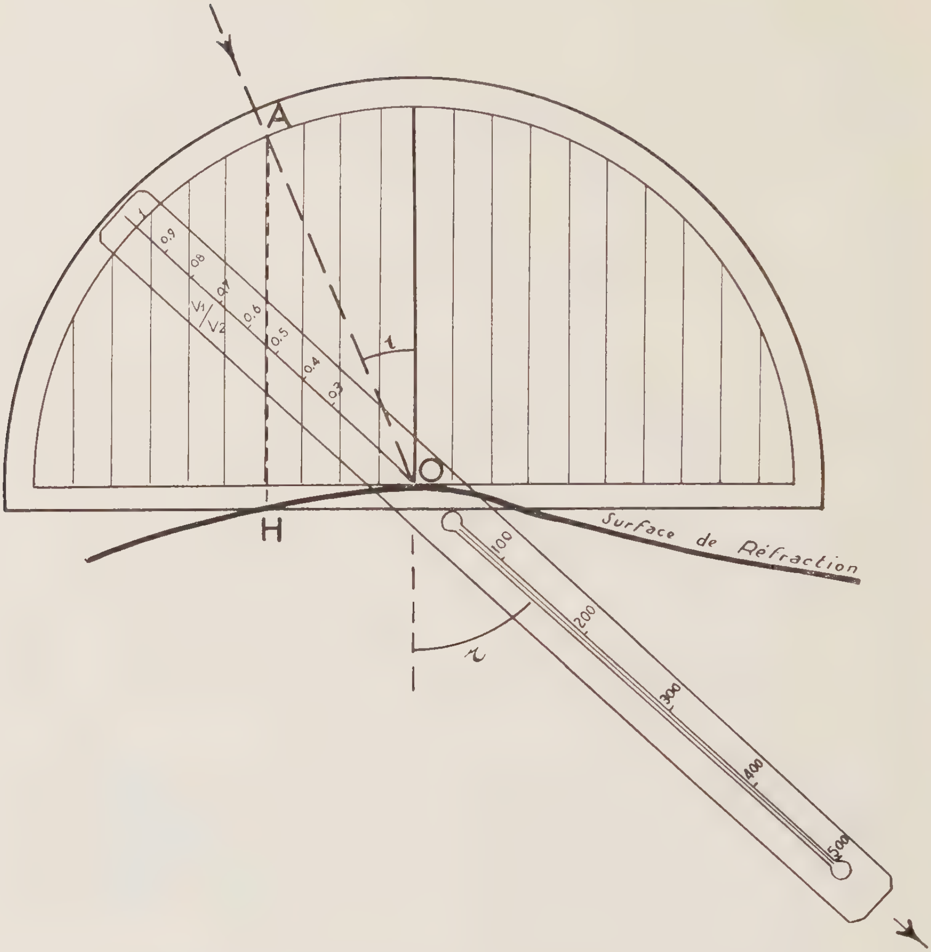

Fig. 2. Diagramme du rapporteur.
Diagram of the Protractor.

La deuxième branche comporte une fente longitudinale permettant le tracé du rayon réfracté; sur cette branche on peut porter une graduation en millisecondes à la distance $P = VT$, à partir de l'axe O, V étant la ou les vitesses habituellement employées dans le 2ème terrain.

MISE en OEUVRE — PREPARATION de L'ABAQUE (Figure 2-3)

A l'aide d'un abaque de restitution, nous traçons la tangente à un rayon incident en O, point de rencontre de ce rayon avec la surface de réfraction. Nous plaçons notre rapporteur de telle façon que son diamètre tangente la surface

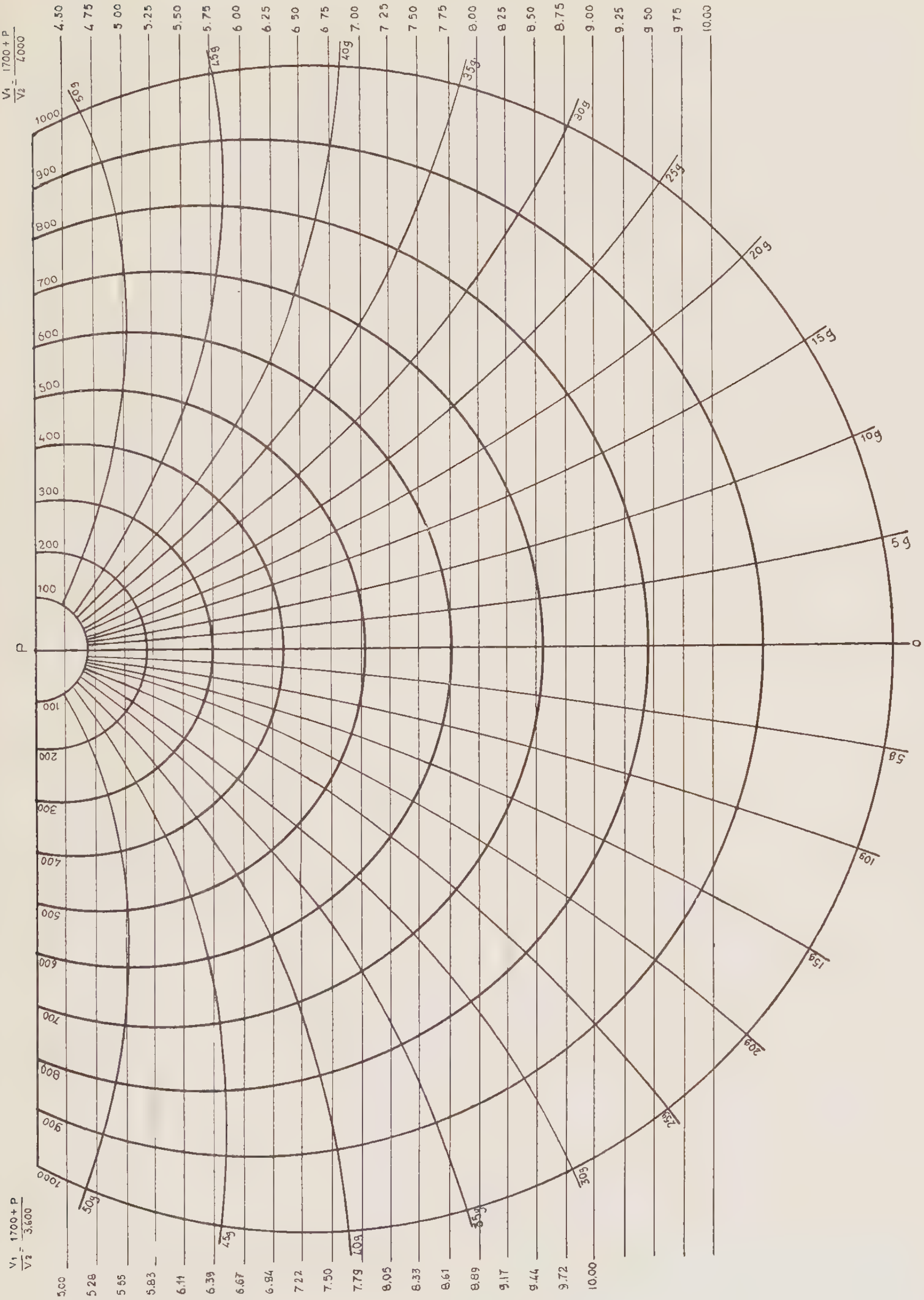

Fig. 3. Abaque indiquant les valeurs de V_1/V_2.
Wave Front Chart with the Values of V_1/V_2 indicated.

réfraction en ce point O. La tangente au rayon incident coupant la circonférence de rayon K en un point A, le rayon réfracté sera obtenu en faisant coïncider par rotation de la réglette, la valeur du rapport V_1/V_2 et la perpendiculaire abaissée de A sur le diamètre. Il est commode de placer la pointe d'un crayon dans la rainure au point correspondant à la valeur V_1/V_2 en question et de faire ainsi pivoter la réglette par l'intermédiaire du crayon. On trace ensuite le rayon réfracté et l'on repère la position du miroir grâce à la graduation figurant sur la deuxième branche de la réglette et connaissant le temps à parcourir dans le deuxième terrain et la vitesse de ce milieu.

La réglette étant graduée en V_1/V_2, il importe de faire apparaître la valeur de ce rapport sur l'abaque employé. Dans le cas d'une loi $V = V_0 + kP$ ou $V = V_0 + a\tau$ les lignes d'équi-valeur de ce rapport sont des droites parallèles à la surface du sol. Nous avons l'habitude de tracer ces lignes tous les 100 m et d'y afficher la valeur du rapport sur chacune d'elle.

L'abaque dont nous présentons une reproduction correspond à la loi $1700 + P$ et est gradué pour les vitesses du deuxième terrain les plus couramment employées dans notre région, à savoir 3.600 m/s et 4.000 m/s (figure 3).

REMARQUE

L'axe de la réglette doit être extrêmement fin pour ne pas gêner la lecture. On pourrait également remplacer l'axe par un pivot encastré en plexiglass, mais ceci nécessite une réalisation industrielle soignée, alors que notre rapporteur peut être construit dans n'importe quel bureau.

DISCUSSION

Mr. BRAUCH: I would like to call attention to my publication: „Gedanken zur Auswertung in der Reflexonsseismik" in "Die Bergbauwissenschaften" 1954, Heft 6 S. 178. There a similar instrument is shown. The main difference to the one just shown is, that I use the rays of *two* neighbouring shot points for construction of the refracted ray.

Mr. FAVRE: signale qu'il a fabriqué un appareil analogue à celui de M. Schoeffler, en ce qui concerne du moins la réfraction d'un rayon sismique à la traversée d'un interface séparant deux milieux de rapport de vitesses V_2/V_1.

Cet appareil présente sur celui de M. Schoeffler le seul avantage d'être *continu*.

Le principe en est le suivant: sur le schéma, on a:

$$\frac{V_2}{V_1} = \frac{\sin i_2}{\sin i_1} = \frac{OC/OB}{OC/OA} = \frac{OA}{OB}$$

à condition que AB soit perpendiculaire à l'interface, ceci étant réalisé très simplement par un parallélogramme déformable $OBB'O'$. Il suffit de graduer

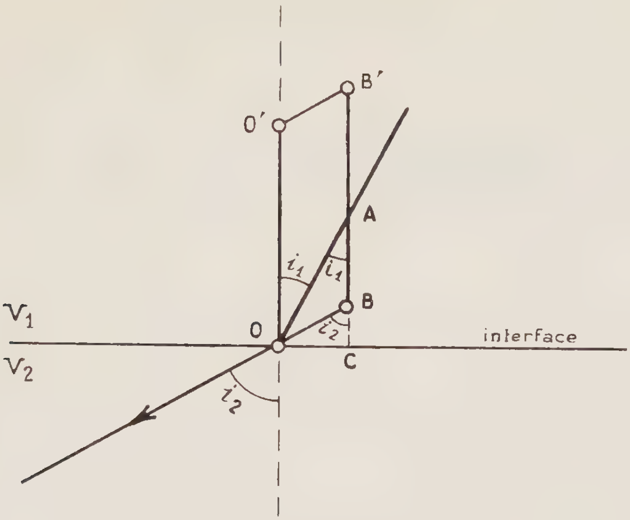

directement la ligne OA en valeurs de V_2/V_1 en prenant la longueur fixe OB comme unité.

ETUDE THEORIQUE DE LA VITESSE DES ONDES DE COMPRESSION DANS LES VASES *

PAR

I. D'ERCEVILLE **

Abstract

It has been noted that in water-saturated silt, the velocity of propagation of longitudinal waves is very low. The purpose of this paper is to suggest a theoretical explanation for this phenomenon.

The medium under study is assumed to consist of identical solid spheres piled one upon the other in a regular array, with the fluid filling the interstices. First the velocity of propagation is calculated for the system of the solid particles alone; then, utilizing the results obtained for this case, the velocities for the solid-fluid system are calculated. Two velocities are obtained, one of them being higher and the other lower than in the case where no fluid is present.

Resumé

On a constaté dans des milieux imbibés d'eau, des vitesses basses pour les ondes de compression.

On suppose qu'un tel milieu se compose d'un empilement régulier de sphères solides baignant dans du liquide. Calculant d'abord la vitesse d'une onde de compression verticale, en l'absence de liquide, on part de ce résultat pour calculer cette vitesse dans l'ensemble solide-liquide. On trouve deux vitesses possibles, l'une élevée et l'autre plus basse que quand il n'y a pas de liquide.

On a été conduit expérimentalement à admettre, pour les ondes de compression, des vitesses très basses dans des vases, celles-ci pouvant être considérées comme composées de particules solides baignant dans de l'eau. Ce résultat peut paraître paradoxal, puisque chacun des constituants donne une vitesse élevée.

Pour tenter d'expliquer, au moins qualitativement, le phénomène, imaginons le modèle mathématique simple suivant:

des grains sphériques, tous identiques entre eux, sont composés d'un matériau possédant une densité ρ et possédant, en masse, une vitesse d'onde longitudinale C. Ces grains sont empilés régulièrement et leurs intervalles sont remplis par un fluide de densité ρ' et de vitesse C'.

---

* Presented at the Seventh Meeting of the European Association of Exploration Geophysicists, held in The Hague, 8-10 December 1954.

** Compagnie Générale de Géophysique, Paris.

Etudions la vitesse d'une onde plane de compression se propageant verticalement et ce à une profondeur h au-dessous du sol.

I. Rappelons, d'abord, ce qui se passerait si le fluide était supprimé, ce qui fournit un modèle de WZ.

Les sphères étant supposées régulièrement empilées par couches horizontales, il en résulte que chacune d'elles est en contact avec douze sphères dont les centres sont les sommets d'un icosaèdre régulier convexe, dont trois appartiennent à la couche supérieure et trois à la couche inférieure. Si a est leur rayon commun, chacune de ces sphères correspond à une section horizontale $\sqrt{12}\,a^2$ et à un volume $4\sqrt{2}\,a^3$.

Il en résulte que la densité du milieu granulaire est $(\pi/3\sqrt{2})\,\rho$, soit $0{,}74\,\rho$. Mais, en réalité, les sphères de deux couches superposées sont appuyées l'une contre l'autre par une pression statique $P = 0{,}74\,\rho g h$. Il en resulte une force F de contact égale à $\sqrt{12}\,a^2 P / 3 \sin I$, I désignant l'angle d'une arête d'un tétraèdre régulier avec les faces.

La diminution du rayon au point de contact d'après une formule classique est :

$$y = 0{,}77\,a \sqrt[3]{\frac{12\,P^2}{9\,k^2\rho^2 C^4 \sin^2 I}} \quad \text{avec } k = E/\rho C^2$$

(E module d'Young).

Supposons maintenant une compression p, petite par rapport à P et due à une onde ; il en résulte une variation δy

$$\delta y = \frac{0{,}77 \times 2\,a}{3} \sqrt[3]{\frac{4}{3\,k^2\rho^2 C^4 \sin^2 I\,P}}\,p \quad . \; . \; . \; . \; . \quad (1)$$

La contraction cubique ε est $\delta y / a \sin^2$ I. D'autre part, $\sin^2$ I $= 2/3$, $P = 0{,}74\,\rho g h$

$$\varepsilon = 0{,}77 \sqrt[3]{\frac{2}{0{,}74}}\; k^{-\frac{2}{3}}\, C^{-\frac{4}{3}}\, (gh)^{-\frac{1}{3}}\, \frac{p}{\rho} \quad . \; . \; . \; . \; . \quad (2)$$

Si v est la vitesse de propagation cherchée

$$\varepsilon = p/0{,}74\,\rho\,v^2 \quad . \; . \; . \; . \; . \; . \; . \; . \; . \; . \quad (3)$$

de (2) et (3), il résulte :

$$\boxed{v = 1{,}12\,(k\sqrt{hg}/C)^{-1/3}\,C} \quad . \; . \; . \; . \; . \quad (4)$$

Ce résultat est indépendant de la densité et du rayon des grains, mais non de l'hypothèse faite sur la sphéricité et l'identité des grains. Quant à k, c'est un coefficient numérique ne dépendant que du coefficient de Poisson σ et égal à $(1 + \sigma)\ (1 - 2\sigma)/(1 - \sigma)$.

Prenant $\sigma = 0{,}25$, $k = 5/6$, nous aurons alors

$$v = 1{,}06\ (\sqrt{hg/C})^{1/3}\ C \quad \ldots\ldots\ldots \quad (5)$$

Si nous prenons $h = 5$ m, $C = 3000$ m/sec, nous trouvons $v = 420$ m/sec.

On remarque aussi que, dans un milieu donné:

$$v = Kh^{\frac{1}{6}} \text{ d'où } dt = (1/K)\, h^{-1/6}\, dh \quad \ldots\ldots \quad (6)$$

d'où pour traverser une couche finie h, un temps: $t = (6/5K)\ h^{5/6}$

$$\frac{h}{t} = K\frac{5}{6}h^{\frac{1}{6}} = K\left[\left(\frac{5}{6}\right)^{6} h\right]^{\frac{1}{6}} = K\left(\frac{h}{2{,}99}\right)^{\frac{1}{6}} \quad \ldots\ldots \quad (7)$$

La vitesse moyenne obtenue est donc la vitesse vraie, sensiblement au tiers de la couche à partir de la surface.

II. Réintroduisons le fluide dans les interstices. Toute compression exercée sur ce milieu composite se partagera en deux parties, l'une p correspondant aux forces de contact des grains solides, l'autre p' étant transmise par le fluide.

Supposons, en particulier, une pression sinusoïdale de la forme $C^{ste}\ e^s$ dans laquelle s est de la forme $2\pi fi\ (t - z/w)$, z étant la profondeur considérée comme variable, f la fréquence et w la vitesse inconnue de propagation. Les pressions transmises par les grains et par le fluide seront pe^s et $p'e^s$.

Les élongations des grains et du fluide seront de même ue^s et $u'e^s$.

Ecrivons les équations du mouvement des grains. Soit v la vitesse sans le fluide, nous pouvons la calculer comme il a été indiqué ci-dessus, à condition de remplacer h par $h\ (1 - \rho'/\rho)$ pour tenir compte, dans la pression statique, de la poussée d'Archimède. Nous aurons une contraction cubique

$$p\ e^{s\prime} 0{,}74\ \rho v^2$$

D'autre part, la pression du fluide fait varier le rayon des grains et entraîne un réarrangement de ceux-ci. La dimension du rayon étant

$$(p'e^s/\rho C^2)\ \{(1 - \sigma)/(1 + \sigma)\}\, a = ({}^3/{}_5)\ p'ae^s/\rho C^2$$

en prenant $\sigma = 0{,}25$, la contraction cubique qui en résulte est de $0{,}9\ p'e^s$. D'où la contraction cubique totale:

$$\varepsilon = e^s\left(\frac{p}{0{,}77\,\rho\, v^2} + \frac{0{,}9\, p'}{\rho\, C^2}\right) \quad \ldots\ldots \quad (8)$$

Mais nous avons la condition $-\, \partial\ (ve^s)/\partial z = \varepsilon$, ce qui entraîne

$$2\pi i f \frac{\rho u}{w} = \frac{p}{0{,}74\, v^2} + \frac{0{,}9\, p'}{C^2} \quad \ldots\ldots \quad (9)$$

D'autre part, on a dynamiquement

$$-0{,}74\,\rho\,\frac{\partial^2 (ue^s)}{\partial t^2} = \frac{\partial (pe^s)}{\partial z} + 0{,}74\,\frac{\partial (p'e^s)}{\partial z} \quad . \; . \; . \; . \; . \quad (10)$$

d'où

$$0{,}74\,\rho\; 4\pi^2 f^2 u = -\frac{2\pi i f}{w}\,(p + 0{,}74\,p') \quad . \; . \; . \; . \; . \quad (11)$$

Eliminant u entre (9) et (11), nous trouvons:

$$p\left(\frac{1}{w} - \frac{w}{v^2}\right) = 0{,}74\,p'\left(\frac{0{,}9\,w}{C^2} - \frac{1}{w}\right) \quad . \; . \; . \; . \; . \; . \quad (12)$$

Par ailleurs, considérons le fluide. Nous étudierons son mouvement, en négligeant la viscosité et le frottement et en admettant qu'il se déplace dans des canaux verticaux dont la section est la fraction 0,26 de la surface. Nous avons

$$-\rho'\,\frac{\partial^2}{\partial t^2}(u\,e^s) = \frac{\partial (p'e^s)}{\partial z} \quad . \; . \; . \; . \; . \; . \; . \; . \quad (13)$$

$$4\pi^2 f^2 \rho' u' = \frac{2\pi i f}{w}\,p' \quad . \; . \; . \; . \; . \; . \; . \; . \quad (14)$$

en négligeant la contraction cubique due aux forces de contact. Enfin, remarquons que la contraction cubique totale est ε, tandis que la contraction cubique du solide et du liquide est de:

$$\varepsilon' = \left(\frac{0{,}74 \times 1{,}8\,p'}{\rho C^2} + \frac{0{,}26\,p'}{\rho' C'^2}\right) e^s \quad . \; . \; . \; . \; . \; . \quad (15)$$

la différence $\varepsilon - \varepsilon'$ représente le volume de fluide expulsé qui est

$$0{,}26\,\frac{\partial (u'\,e^s)}{\partial z}$$

$$\frac{p}{0{,}74\,\rho\,v^2} - p'\left(\frac{0{,}26}{\rho' C'^2} + \frac{0{,}43}{\rho\,C^2}\right) = -0{,}26\,\frac{2\pi f i}{w}\,u' \quad . \; . \; . \quad (16)$$

Eliminant u' entre (14) et (16), il vient:

$$\frac{p}{\rho\,v^2} = 0{,}74\,p'\left(\frac{0{,}43}{\rho C^2} + \frac{0{,}26}{\rho' C'^2} - \frac{10{,}26}{\rho' w^2}\right) \quad . \; . \; . \; . \; . \quad (17)$$

En écrivant que (12) et (17) sont compatibles, on trouve l'équation en $1/w^2$

$$\frac{1}{w^4} - \frac{1}{w^2}\left[\frac{1{,}7\,\rho'}{\rho\,C^2} + \frac{1}{C'^2} + \frac{1}{v^2}\left(1 + \frac{3{,}9\,\rho'}{\rho}\right)\right] + \frac{1}{v^2}\left(\frac{5{,}1\,\rho'}{\rho\,C^2} + \frac{1}{C'^2}\right) = 0 \quad (18)$$

Comme, en fait, v est beaucoup plus petit que C, l'équation a deux racines réelles positives, ce qui donne deux vitesses possibles.

Traitons un cas numérique. Prenons $\rho'/\rho = 0{,}4$, $v = 400$ m/sec, $C = 3000$ m/sec, $C' = 1500$ m/sec: on trouve 247 m/sec, vitesse basse et 2090 m/sec, vitesse intermédiaire entre celle des constituants.

Remarquons, avant de quitter l'équation (18), que si l'on fait tendre ρ'/ρ vers 0 (cas de l'air dans les interstices) on trouve bien à la limite v et C'.

En se souvenant que, pour une couche d'épaisseur donnée, la fréquence propre est proportionnelle à la vitesse, l'on voit que le couplage entre le „système grains" et le fluide écarte les fréquences propres, résultat très général.

D'autre part, en remontant à l'équation (12), on voit pour la basse vitesse que w_1, p et p' sont du même ordre de grandeur, mais de phases opposées.

Au contraire, pour la grande vitesse w_2, les deux pressions sont en phase, mais p est très petit par rapport à p' (1 à 2 %) et, en pratique, la pression n'est pas transmise par les forces de contact entre grains.

Pour faire le partage entre les deux modes de vibration, il faut faire intervenir les conditions aux limites. D'ailleurs, les deux ondes étant de nature différente peuvent affecter de façon fort dissemblable les appareils de mesure.

III. En négligeant la viscosité, nous nous sommes certainement éloignés fortement de la réalité. Pour l'introduire dans les calculs, il suffit d'introduire dans les équations dynamiques (10) et (13) une force proportionnelle à la différence des vitesses $(u' - u)\, e^s$. On trouve ainsi deux vitesses complexes, c'est-à-dire que l'on obtient, comme il fallait s'y attendre, des ondes amorties et dont la propagation dépend de la fréquence. En négligeant $1/C^2$ et $1/C'^2$ devant $1/v^2$, on trouve pour la basse vitesse la quantité complexe

$$w = \frac{v}{\sqrt{1 + 3{,}9\,\rho'/\rho - 11{,}4\,Mi/2\pi\rho f}} \quad \ldots\ldots \quad (19)$$

en désignant par M le coefficient de proportionnalité des forces aux vitesses.

La viscosité diminue encore la vitesse. Mais l'évaluation théorique du coefficient M est difficile, car elle fait intervenir la taille des grains; or, ceux-ci ne sont pas, a priori, les particules obtenues par dessiccation car celles-ci peuvent s'agglomérer en grains plus gros se comportant élastiquement comme un grain solide.

Il n'y a pas lieu, d'ailleurs, de chercher à obtenir des résultats numériques précis, le modèle adopté n'ayant pas la prétention de traduire fidèlement la réalité. Le but de cette étude est seulement de montrer que des basses vitesses dans un milieu granulaire solide gorgé d'eau sont possibles.

DISCUSSION

Mr. KREY: Krey rappelle l'assemblée à la publication de Gassmann "Elastic Waves through a Packing of Spheres", Geophysics XVI, 4. Gassmann arrive à des vitesses, qui ne sont pas beaucoup plus petites que celles de l'eau, quand les espaces intermédiaires sont remplies de l'eau ou d'une liquide similaire. En outre les qualités élastiques de son "Packing of Spheres" ne sont pas isotropes. Peut-être on peut expliquer les différences des résultats d'Erceville de l'une côté et de Gassmann de l'autre côté par les faits suivants: Chez d'Erceville la liquide est supposée de migrer entre les interstices pendant les vibrations. Chez Gassmann — au contraire — la liquide doit rester dans les interstices. Il semble à Krey que la supposition de Gassmann est plus justifiée que celle d'Erceville parce que la longueur des ondes est beaucoup plus grande que les interstices.

Krey croit que le modèle pour la vase choisi de Monsieur d'Erceville n'est pas très convenant. Il rappelle au fait que les vitesses du caoutchouc sont très petites et il lui semble que la structure de la vase est comparable avec celle du caoutchouc ou d'une autre matière gélatineuse.

Mr. D'ERCEVILLE: Gassmann considère une sorte de "corps moyen" de sorte que l'adjonction d'un fluide ne peut évidemment qu'augmenter la vitesse. Mais il est sûr que le solide et le liquide doivent chacun de leur côté obéir aux lois de la mécanique. L'anisotropie disparaît si on suppose qu'à l'instar de ce qui se passe dans un fluide, les sphères d'une même couche horizontale exercent entre elles des forces égales à celles qui s'exercent entre sphères de couches différentes. Alors peu importe la force de l'icosaèdre considérée.

Il y a bien des sortes de vases mais le cas du caoutchouc me paraît distinct. Sa basse vitesse s'explique soit par le fait de vacuoles remplies d'air et aux parois très élastiques (caoutchouc mousse) d'où une grande compressibilité apparente, soit par le fait que le corps peu compressible mais très déformable ne se présente pas en masse pouvant être considéré comme indéfini.

Mr. VOLKER: M. d'Erceville a assumé une relation entre la pression et le rapprochement des centres des grains. Cette relation ne s'accorde pas avec les théories de la mécanique du sol où l'on part d'une relation logarithmique. On peut se demander quelle est l'influence de cette théorie sur le résultat des calculs de M. d'Erceville, notamment sur les deux racines de la solution. Disparaîtraient-elles?

Mr. D'ERCEVILLE: La formule utilisée pour le rapprochement des centres de deux sphères appuyées par une force l'une contre l'autre est tirée de la théorie de l'élasticité (voir Timoshenkoy, Théorie de l'élasticité et résistance des matériaux). Je ne vois pas la formule de mécanique des sols à laquelle fait allusion M. Volker. En différenciant cette dernière on doit pouvoir en déduire le rapprochement des grains en fonction d'une compression très petite. On peut ainsi calculer des vitesses peut-être numériquement différentes mais l'existence de deux vitesses théoriques résulte du couplage mécanique entre le système grains et le fluide et ne dépend pas de la formule utilisée.

REFLECTION SURVEY IN ROUGH TOPOGRAPHY *

A. M. SELEM **

ABSTRACT

The problems connected with reflexion surveys in areas of rough topography consist of choosing proper equipment and of making careful near-surface corrections. This paper illustrates some solutions to these problems that have been adopted in a survey which has recently started in a hily coastal area, in Southern Italy.

As the area is characterized by a youthful and very actively eroded topography of Post-Miocene clays and litoral clastic sediments, both rotary and percussion drilling were necessary whilst all the seismic equipment had to be light to allow straight lines to be shot as far as possible. Details are given of the truckmounted, light equipment which has been designed for this special purpose.

In connection with the youthful topography of the area being surveyed, the criteria for the proper computation of the near-surface corrections is discussed. The great differences in elevation, combined with variations in the surface and near-surface materials, necessitated a careful analysis before deciding the thickness of the correction zone. The results are shown of the preliminary tests carried out in order to determine the average thickness of the low-velocity zone. The solution adopted for drawing the reference surface determining the base of the correction zone for the whole of the area is subseqently explained.

Reference datum is drawn so as to follow gently, and with segments of constant slopes, the general features of the rough topographic relief at a depth ranging from 30 to 60 metres from the surface. Criteria for the routine checking of velocity variations in the correction zone are illustrated. Such checks are based on both uphole time analyses and refraction "first breaks" plots, with deeper shot holes at constant intervals.

Unsatisfactory results necessitate longer spreads for "low velocity tests" and uphole shooting from deeper holes and the reference datum is deepened for the particular area where this becomes necessary.

The final cross-sections are shown and although, as yet, no deep holes are available to check the seismic data, the general appearance of the cross-sections seems to indicate that subsurface data are free from the influence of topography and of the velocities in the near-surface formations.

MOBILITY

Rough topography has been always a serious limiting factor to reflection surveys, because of the difficulty of manoeuvring the rather heavy seismic equipment and also because of the problems connected with the sharp differences in elevation and the near surface corrections.

Yet there are so many mountainous and hilly areas of interest to oil prospection that we believe there lies in this sector one of the most promising possibilities for the future developments of the seismic techniques.

---

* Presented at the Seventh Meeting of the European Association of Exploration Geophysicists, held in The Hague, 8-10 Dec., 1954.

** AGIP Mineraria, Milan.

The literature on the subject however is very scarce so that it would seem to be little experience available, in spite of the practical and theoretical interest of the problems connected with it.

This paper is presented mainly as an attempt to start discussion on such problems by showing what we have recently done and how we have attempted to overcome some of the difficulties connected with reflection shooting in a hilly area in Southern Italy.

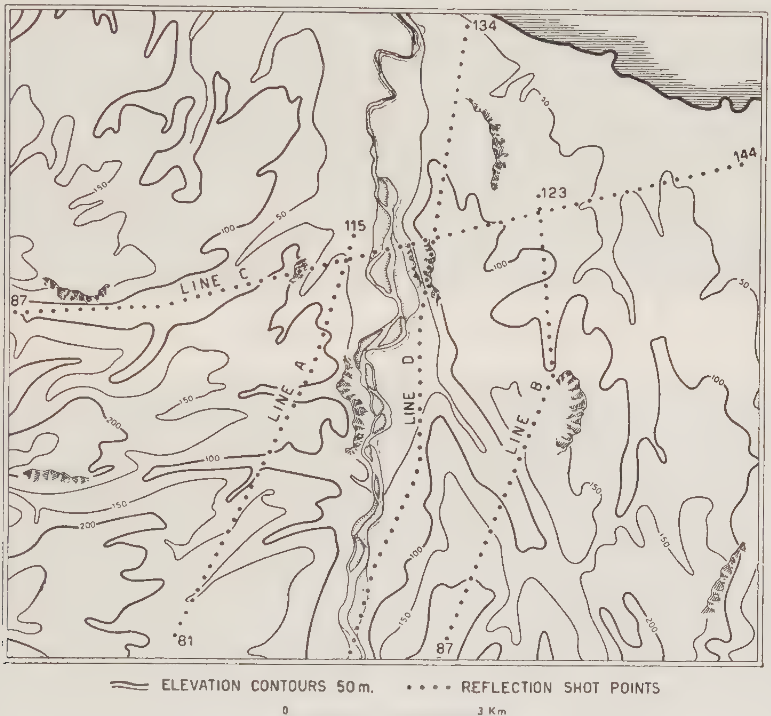

Fig. 1. Topographic map of a part of the surveyed area.

The area of the survey is characterized by an actively eroded hilly topography, with elevations ranging from sea level to nearly 300 metres over distances of 5 to 10 Kms, with many reversals, scarps and local slopes of over 25°. Figs. 1 and 2 illustrate the features of the topography. Lithologically the surface and near surface formations are mostly Post-Miocenic clays, but marly and molassic stringers and clastic litoral sediments are often present (Figs. 3 and 4).

As a consequence, the seismic equipment had to be light to allow manoeuvring on the difficult terrain, shooting over straight continuous traverses without breaks, and at the same time powerful drills were often required.

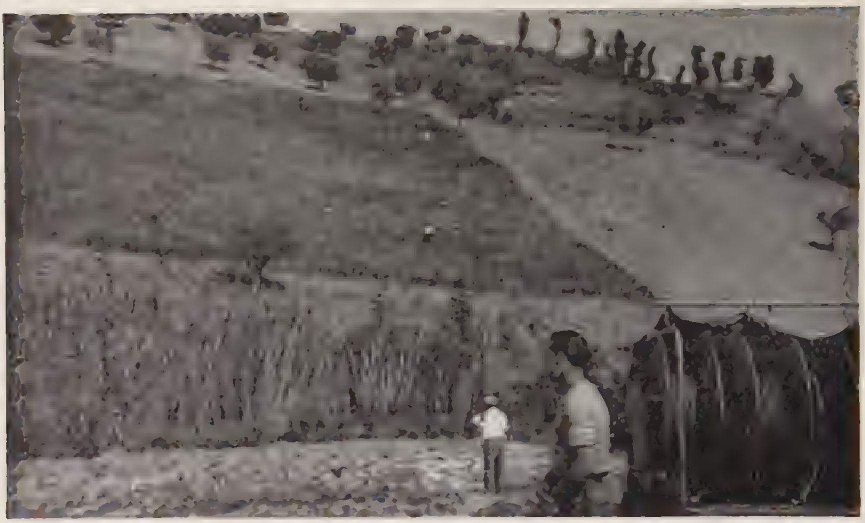

Fig. 2. Illustration of the topographic relief of the surveyed area.

Fig. 3. Illustration of the near surface lithology.

The recording equipment presented no difficulties. An SIE P-II portable recorder was installed on a cabin-mounted jeep and geophone cable extensions made possible the recording by the jeep even at 200 metres from the seismic traverses.

The cable reels were mounted independently on a second jeep and this

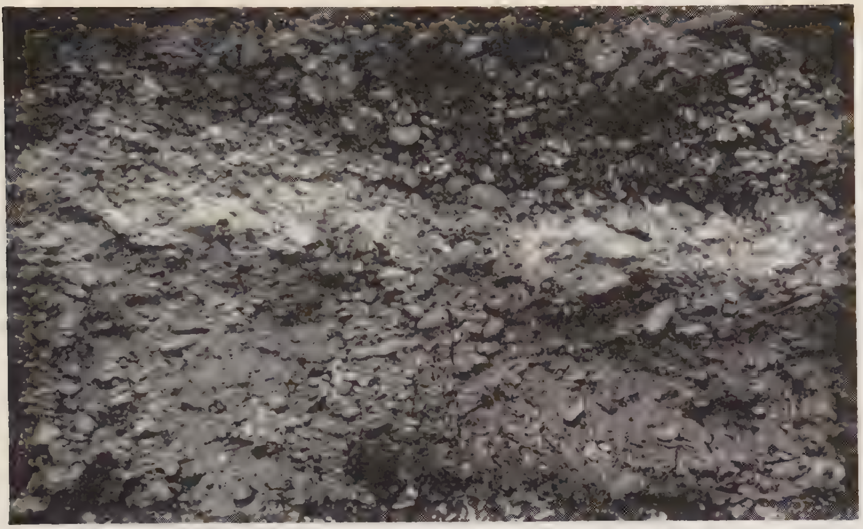

Fig. 4. Illustration of the near surface lithology.

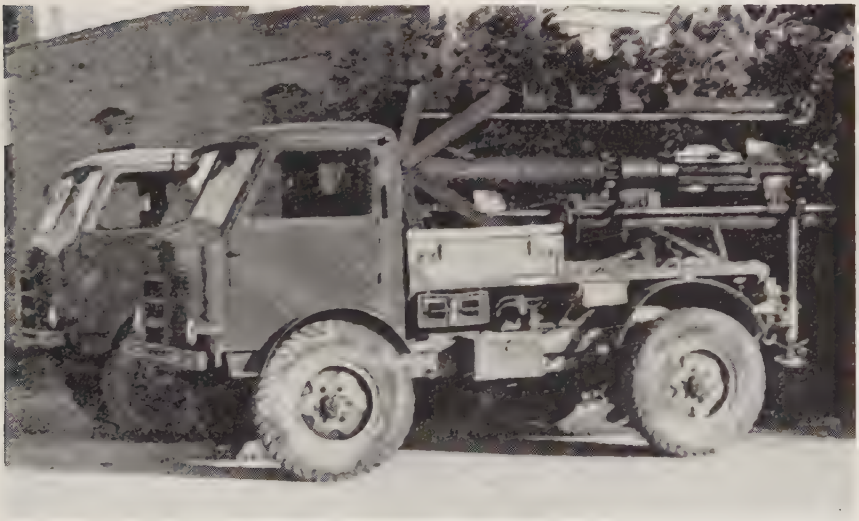

Fig. 5. Truck mounted percussion drill.

allowed for laying out the spreads in advance, thus speeding up recording operations. Whenever the jeep was unable to manoeuvre, portable cables were used.

The drilling equipment had to be as light as possible because, of necessity, it was the only equipment which had to operate on each shot point location. For drilling in clays a Konrad Stork Solite drill was used. This drill was mounted on a jeep but could easily be made portable. The drilling in the molassic and in the clastic formations required, however, the use of a heavier drill.

The best solution was reached by using a casing percussion Diesel hammer which was the most appropriate drill for operating in gravel formations and its weight (about 2 tons) and compactness (length of mast 3,9 metres) allowed it to be mounted on a 2 ton truck (Fig. 5).

Two ton trucks were also used for the hydraulically operated casing extracting equipment, for the water tenders and for the shooting car. To supply the water at shot points which could not be reached by truck, light canvas hoses were used and the water was pumped along them under a head of up to 100 metres.

The performance of this equipment has been satisfactory and the average production of the party was about 90 shot points recorded per month in summer time.

This production was partially due to the field procedure and the performance of the field personnel but most of the credit lies with the particular types of vehicle which were used.

The advantage of using jeeps can be easily appreciated since the performance of those vehicles is well known. Their use however is limited seriously by their small carrying capacity.

Much more advantageous has been the use of a special type of a 2 ton truck, built by Lancia for army needs. This truck develops 68 HP at 3200 R.P.M., but gives a much better performance than trucks normally used in seismic routine work of similar capacity but of greater power. It is able to manoeuvre in very difficult terrain, climbing slopes up to 50°, rarely getting stuck and proving of astonishing durability in spite of the rough work demanded. This is due mainly to such factors as the many gear ratios (12 ratios, low speed first gear 4 Kms/h — high speed fifth gear 60 Kms/h), the No-Spin differentials (which increase the power transmitted to the wheel under greater stress), the special elastic chassis, the independent spiral sprung frontwheels, the compact body (4,50 × 2,00 × 2,20 metres) and the turning radius (5,50 metres).

What has been said so far demonstrates that, without need of tractors or caterpillars, a seismic party can carry out in dry weather reflection surveys in rough topography, such as the one described here, with a satisfactory output and with due attention to the fundamental needs of the layouts of the survey, provided the right vehicles are used.

Surface corrections

The problems connected with the near-surface corrections are the second major difficulty in rough topography. Although division is usually made between youthful and mature topography, in practice all topographies are varying combinations of the two and can be described in terms of the stage of maturity.

In the case of the present survey a rather youthful topography was involved, with active vertical erosion leading to overall differences in elevation up to 170 metres along the 7 to 12 Kms. traverses, with abrupt changes, frequent reversals and steep slopes up to 25°. The situation was further complicated by evidences of lithological changes in the very near surface formations.

Scattered up-hole shooting and short refraction spreads recorded at the beginning of the survey at several points proved that, with the exception of some limited sectors where higher velocities were found, an average velocity ranging from 1600 m/sec. to 1800 m/sec. was present underneath the single or multiple weathering, and was practically constant down to depths of 100 metres and more. A constant control of the velocities a depths greater than 40-60 metres was, however, impossible since split spreads of 400 m. length were required. In any case, since the results of the scattered seismic tests were in general agreement with the geological assumptions, i.e. that the lithological changes were occurring in the thin litoral sediments near the surface only, the datum surface determining the limit of the correction zone was so chosen to follow the general features of the topographic relief. Its depth ranged on an average from 30 to 60 metres and its shape took the form of a series of segments of constant slope.

Constant control of the near surface velocities in the correction zone was maintained by a careful analysis of the "first break" obtained from routine reflection records and by up-hole shooting from deeper holes drilled at approximately constant intervals along each traverse where outcrops or topographic features suggested physical changes in the near-surface conditions. Sometimes these deeper holes for up-hole shooting were drilled after the recording had been made in order to check the information from the first break data.

Fig. 6 illustrates some of the most significant topographic and near-surface conditions encountered during the routine work. On the section of Line A, single layer weathering with 500 m/s velocity was constantly found with a practically constant velocity of 1750 m/s below it. The youthful topography characteristic of clay areas is clearly evident.

Along the section shown of Line B two low-velocity layers, with 500 m/s and 900 m/s respectively, occur above the formation with constant velocity of 1750 m/s. It may be noted that the 900 m/s layer begins with the scarp between shot points 101-102 and that the general picture seems to indicate a slightly mature topography which has been rejuvenated.

The part of Line C shown on the same figure has the character of a more mature topography, particularly East of shot point 139, where a higher velocity formation of 2000 m/s outcrops nearly at the surface. West of shot point 139 the same conditions of Line B may be noted, but the second low-velocity formation rises to a value of 1100 m/s whilst underneath it a velocity of 1700 m/s is constantly recorded.

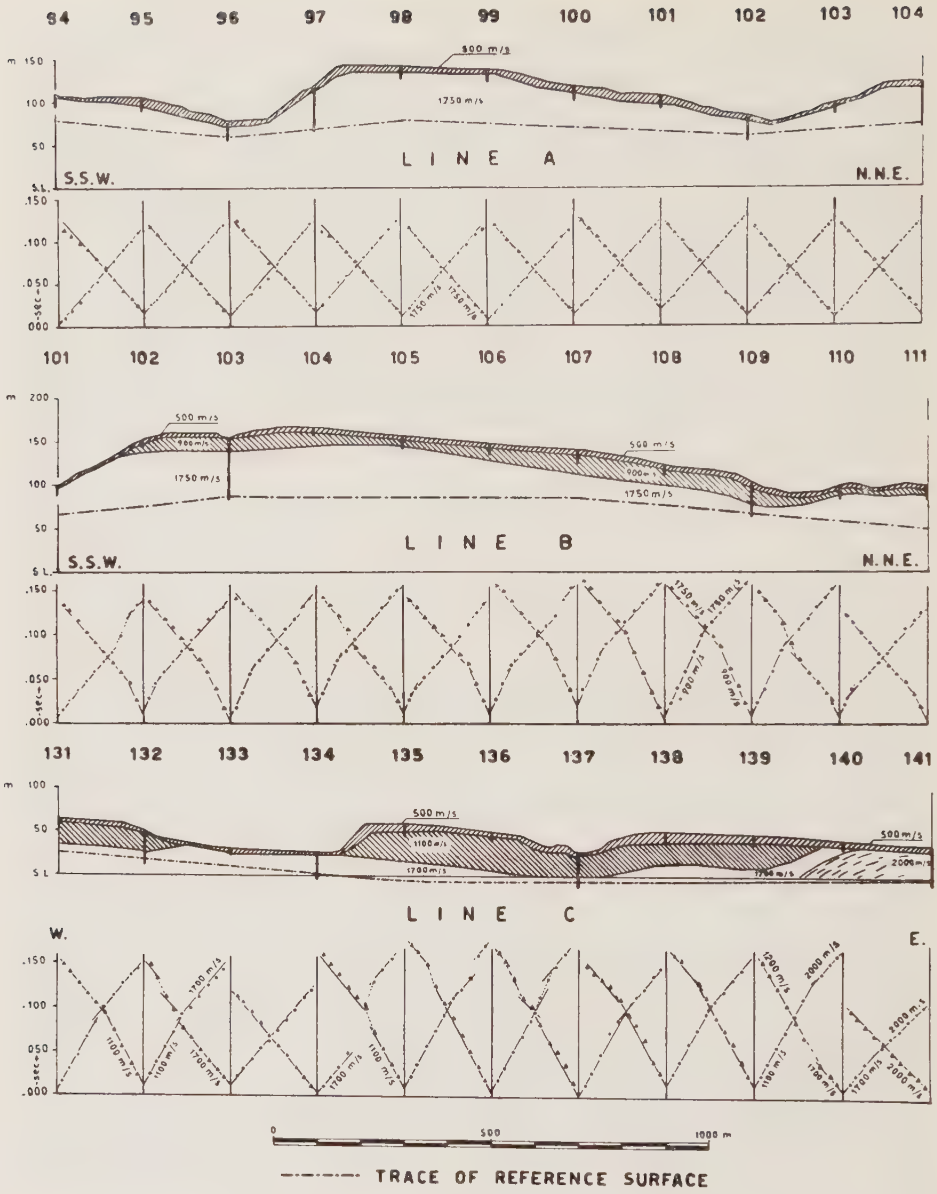

Fig. 6. First break graphs illustrating the near surface conditions.

The information just shown clearly indicates that in the North-Eastern sector of the area two low velocity layers are evident whilst close to the sea lateral erosion of mature topography develops. Further West and South the youthful topography of clay areas is apparent.

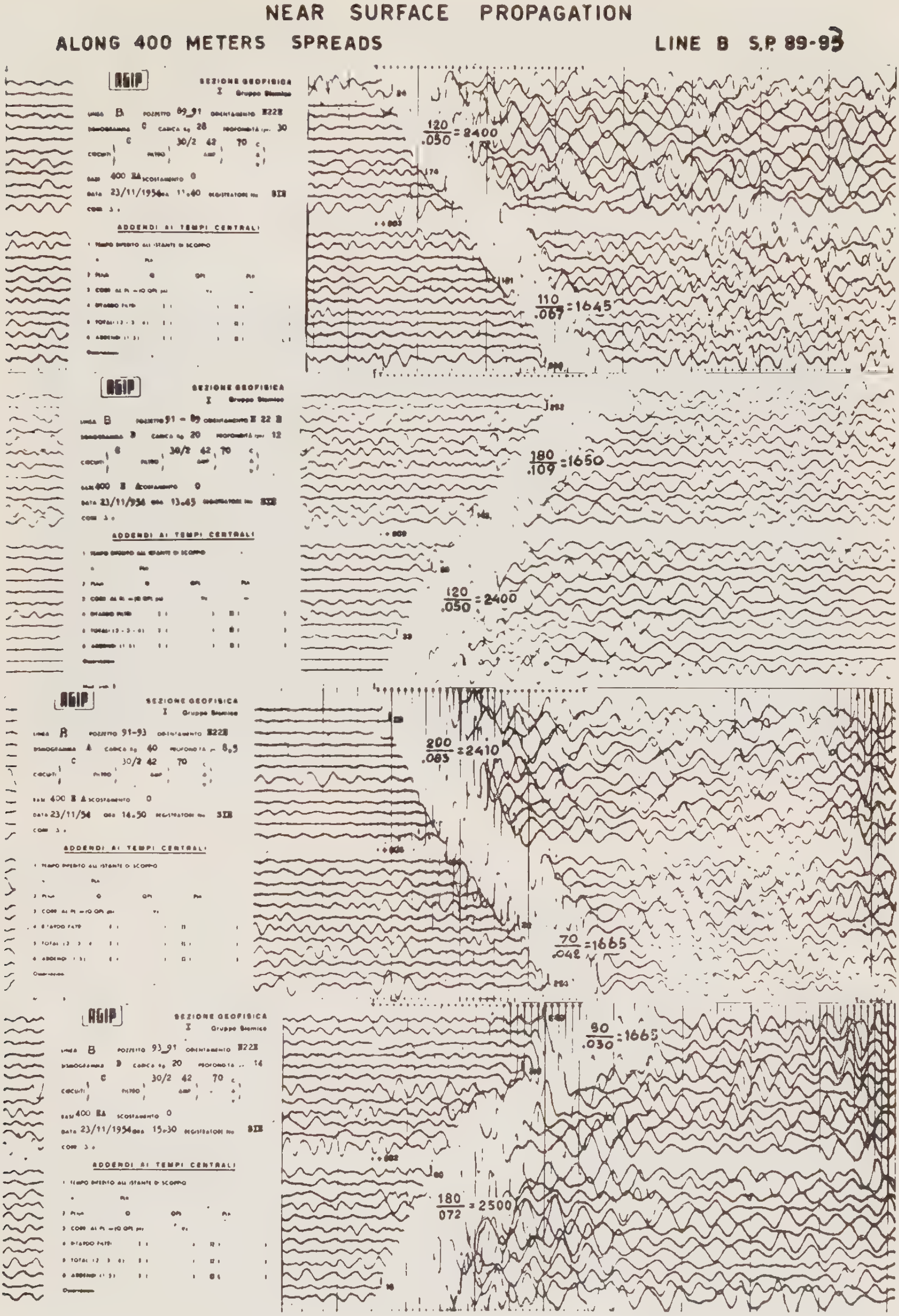

Fig. 7. Seismograms illustrating the near surface propagation of seismic energy.

In this sector however some unusual characteristics in the near-surface energy propagation were recorded. Fig. 7 shows some of he records obtained whilst shooting for control, over short refraction tests of 400 metres spread between shot points 89-95 of Line B. On each of those records up to shot point 93 on the first 9-13 traces a 2400-2500 m/s velocity is clearly evident,

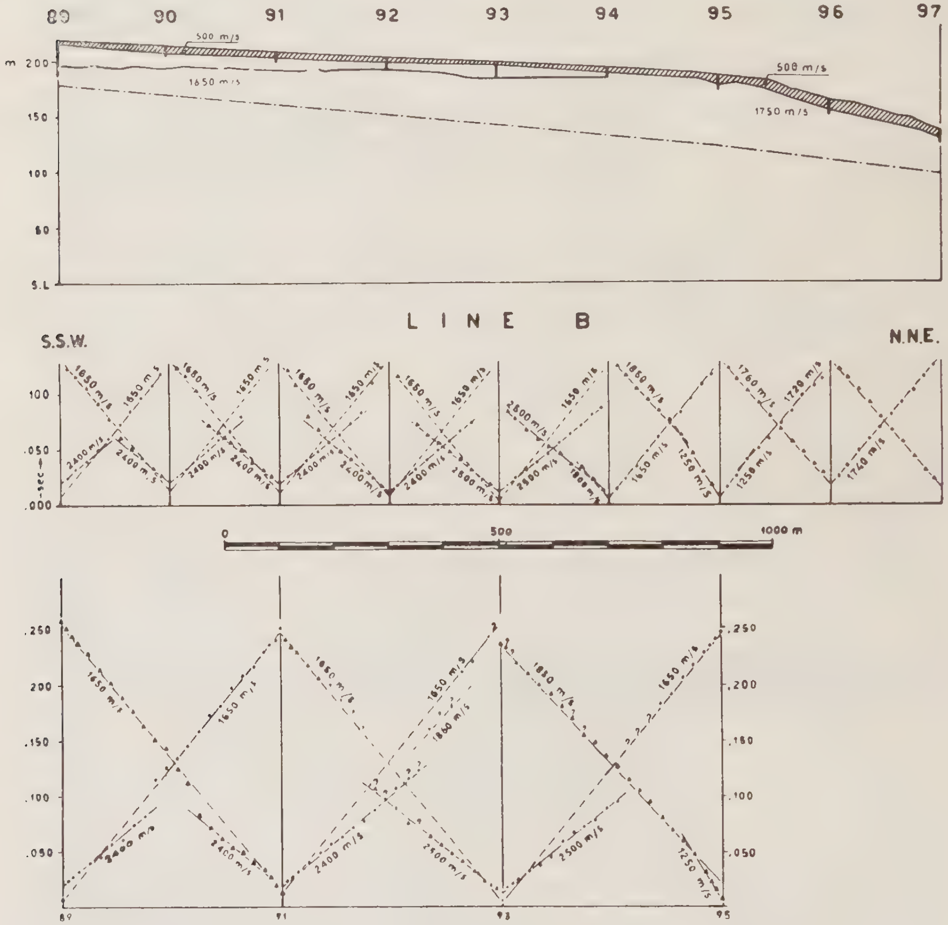

Fig. 8. First break graphs illustrating the near surface propagation of seismic energy.

whilst the traces more remote from the shot point show a lower velocity around 1650 m/s. The graphs are shown on Fig. 8. The tests were made in order to check the first break graphs obtained from routine 400 metres split spread records. These graphs are also shown on Fig. 8, together with the topography and the near surface cross-section of this part of the line.

It may be noted that the longer the spread and, in consequence, the greater the charge, the distance over which the high velocity breaks are detected, becomes greater. There is some lack of evidence of the 1650 m/s velocity on the 400 metres split spreads around shot point 92-94 where a higher value of 1850 m/s appears. NNE of shot point 95 underneath the weathering a velocity around 1750 m/s is constantly recorded.

The 2400-2500 m/s velocity slopes up to shot point 94 are certainly due to stringers through which the energy is propagated with difficulty, as it may be in the case of the broken marly beds visible on the surrounding outcrops and lying within the clay formation (Fig. 9). This has been checked by an up-hole shooting test recorded at each meter interval at shot point 89 and by the drill cuttings. The distribution of the stringers is indicated in Fig. 8.

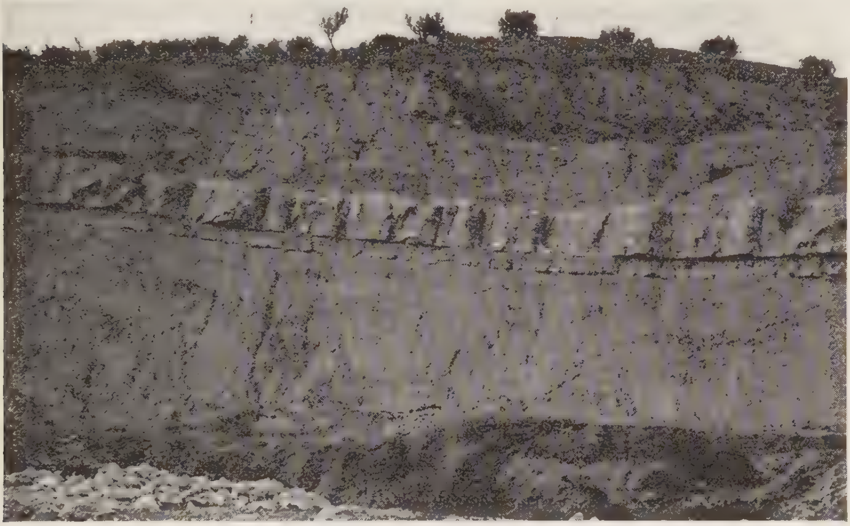
Fig. 9. Outcrop of a marly stringer.

Their thickness however has been proved to be very small and their influence on the elevation correction has been consequently neglected.

The corrections problems discussed illustrate how much care the operator should take when shooting in rough topography to recognize unusual and changing conditions. Every means of control should be considered, from drilling logs to frequent up-hole shooting and short refraction checks. The surface geology of the area should be known as far as possible and the lay-outs of the spreads should be so chosen to give the best control of the near surface energy propagation. Offsets of shot points from the spread should be avoided in rough topography.

Apart from the accuracy of the near surface corrections, a major problem is always represented by the proper selection of the reference surface.

This surface is usually a plane located at a depth below the velocity variations

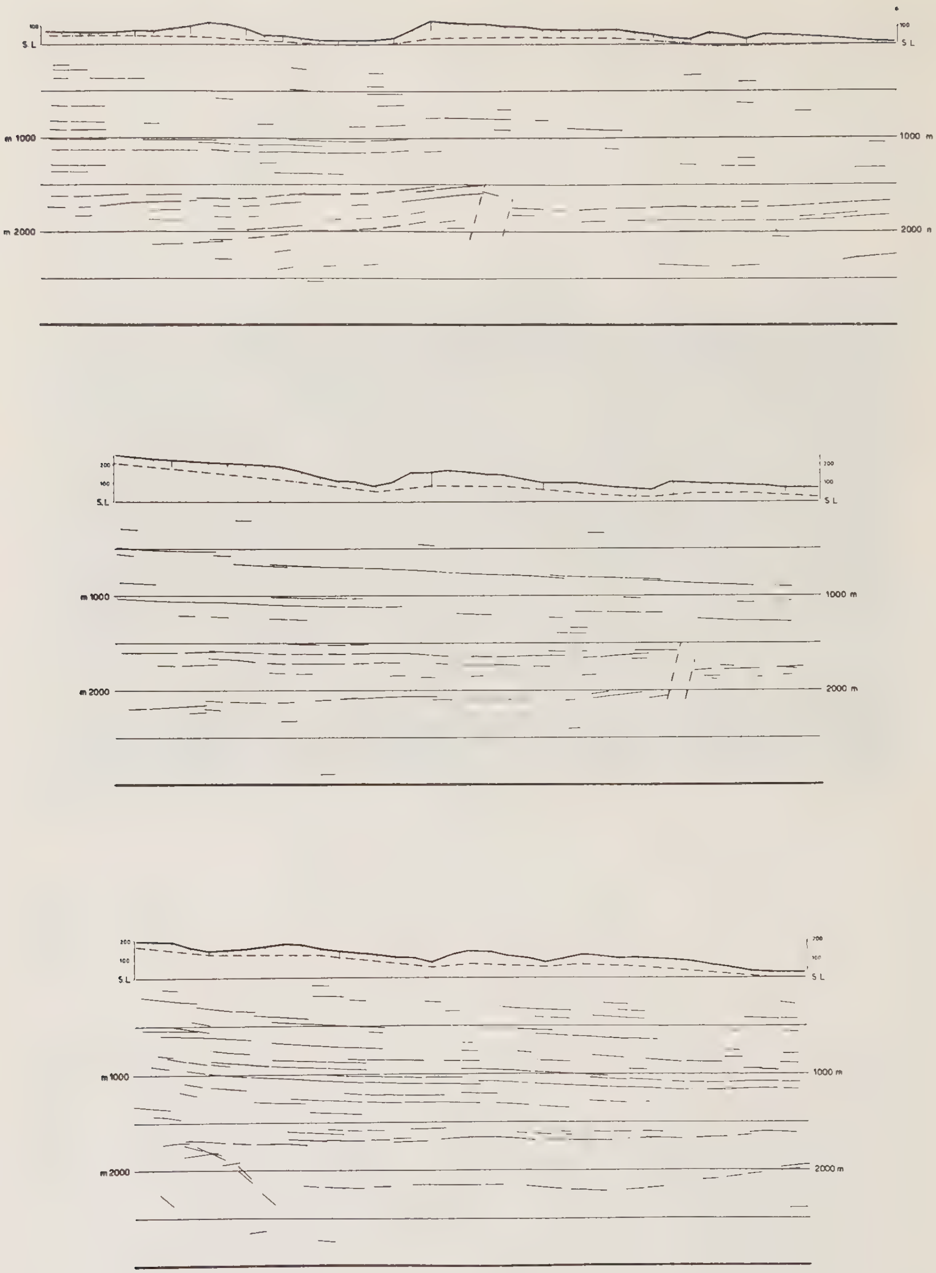

Fig. 10.
Examples of reflection sections.

occurring near the surface. In rough topography however the adherence to this condition often leads to excessive thicknesses of the correction zone, so that the velocity variations occurring in it cannot be fully controlled. The solution to the problem is, therefore, always a compromise based on the actual physical conditions characterizing the area and may vary from horizontal reference planes, to floating datum planes or to the use of lateral velocity variations.

In the case of the present survey it was known that the Post-Miocenic clays were lithologically mainly uniform and that only their higher section was complicated by changing litorál sedimits.

It was therefore decided to use a floating reference surface for the whole area drawn with segments of constant slopes at such a depth to keep it as much as possible within the uniform deeper clays and yet within the range of the near surface velocity control allowed by the length of the spread. This decision resulted in easy computations and in reasonably accurate reflection ties and the cross-sections obtained (Fig. 10) do not appear to be influenced by topographic relief. The method of course may have its disadvantages where abrupt changes in elevation cause the correction zone to become too thin or too thick, but it is believed to be a practical and a fairly reasonable approach to a reliable interpretation of a first reconnaissance survey.

Acknowledgement

The author whishes to thank the AGIP Mineraria S.p.A. for permission to publish this paper.

RESISTIVITY CURVES FOR A CONDUCTING LAYER OF FINITE THICKNESS EMBEDDED IN AN OTHERWISE HOMOGENEOUS AND LESS CONDUCTING EARTH *

BY

O. KOEFOED **

ABSTRACT

A method is described for computing master resistivity curves. It is a modification of that devised by Ehrenburg and Watson, but is superior as a shorter time is required for the computations. A collection of 31 master curves for the three layer case is presented.

INTRODUCTION

It is generally recognized that standard curves for the three layer case form an invaluable tool in the interpretation of observations with the resistivity method. Collections of such curves have been published in past decades by Wetzel and McMurry (1937), and by Watson (1934), but this comparatively small collection has proved inadequate for general use. It is, therefore, very gratifying to learn that, in the last few months, very much larger callections of three layer and four layer master curves have been published (Compagnie Générale de Géophysique, 1955) or are being prepared for publication (Mooney, 1954, and Mooney and Wetzel).

Compared with the publications of the Compagnie Générale de Géophysique and of Mooney and Wetzel the work of the present author is quite negligible, but publication is still justified for two reasons. Firstly, although the publication of the C.G.G. contains *Schlumberger* type curves for most of the cases presented in this paper, *Wenner* type curves for these cases have not yet been published. Secondly, the computational method presented in this paper contains certain simplifications, which differ in detail from those considered in the recent papers of Flathe (1955) and Deppermann and in that by Mooney and Wetzel.

NOTATION

Throughout this paper the following notation is used.

d_1 and d_2 are the thicknesses of the first and the second layer.

---

* Adapted from a paper presented at the Seventh Meeting of the European Association of Exploration Geophysicists, held in The Hague, 8-10 December 1954.

** N.V. De Bataafsche Petroleum Maatschappy, The Hague (Royal Dutch Shell Group) and Technical University at Delft.

ρ_1, ρ_2 and ρ_3 are the resistivities of the first, second and third layer.

k_1 is the reflection coefficient between the first and the second layer, defined by $k_1 = (\rho_2 - \rho_1)/(\rho_2 + \rho_1)$.

k_2 is the reflection coefficient between the second and the third layer.

c is double the layer thickness when the subsurface is considered to consist of a number of homogeneous layers of equal thickness and in which adjacent layers do not necessarily differ in resistivity.

I is the intensity of the current that flows from the electrode.

Q is the strength of an image pole when the strength of the real pole on the surface is taken as unity.

R is the distance between a current electrode and a potential electrode.

a is the electrode distance in a Wenner configuration.

V is the total potential at a point.

$\Delta_n V$ is the contribution to the potential from an image pole of strength $I\ Q_n$ at a depth nc.

ρ_a is the apparent resistivity in a Wenner configuration.

$\Delta_n \rho_a$ is the contribution to the apparent resistivity from an image pole of strength IQ_n at a depth nc.

COMPUTATION METHOD OF EHRENBURG AND WATSON

The method, used in computing the resistivity curves presented in this paper, is a modification of the method first published by Ehrenburg and Watson (1932) and described in greater detail by Watson (1934).

The method of Ehrenburg and Watson considers the case in which the thicknesses of all the resistivity layers are either equal to, or some multiple of, a constant thickness $c/2$. The electrical images of the surface electrode all lie at equal distances of c apart in this case. (Some of the shallower image poles may have zero strength.)

The strengths of these electrical image poles, which are denoted Q, may be obtained by a recurrence formula that may be found in the article by Watson (1934). For the three layer case, considered in the present paper, this recurrence formula assumes a particularly simple form in which the strength of each image pole is obtained as a sum of three terms only.

When the strength of each image pole is known, the potential at a point on the surface can be found by adding the contributions of all the image poles to that of the pole on the surface. The following expression is thus obtained for the potential V at a point on the surface at a distance R from the electrode.

$$V = \frac{\rho_1 I}{2\pi} \left\{ \frac{1}{R} + \frac{2Q_1}{\sqrt{R^2 + c^2}} + \frac{2Q_2}{\sqrt{R^2 + (2c)^2}} + \frac{2Q_3}{\sqrt{R^2 + (3c)^2}} + \dots \right\} \qquad (1)$$

The factors 2 inside the brackets result from the fact that, in addition to the image poles of strength Q_n in the subsurface, there is a series of image poles of equal strength in the air above the electrode.

Watson (1934) remarks that for the purpose of computing the potential by equation (1) it is convenient to construct tables giving the values of the reciprocals of the square roots that occur in this equation. In the calculations presented below the values of the potentials at points on the surface have not been computed, but for each image pole its contribution to the apparent resistivity in a Wenner electrode configuration has been calculated. The expression for this contribution follows easily from equation (1). When the electrode spacing is a, the contribution to the apparent resistivity of an image pole of strength Q_n located at a depth $n\,c$ is found to be

$$\Delta_n \rho_a = \rho_1 Q_n \left(\frac{4}{\sqrt{1 + n^2 c^2/a^2}} - \frac{4}{\sqrt{4 + n^2 c^2/a^2}} \right) \quad . \quad . \quad . \quad (2)$$

Tables have been prepared for the values of the expression in brackets in equation (2). It has been found that, when n increases, the values in these tables become negligible more rapidly han those in the tables described by Watson.

SEPARATION OF SINGLE POLE EFFECT FROM DIPOLE EFFECTS

The objection has been raised against the method of Ehrenburg and Watson that the computations are rather time consuming. This is due primarily to the fact that the values of the strength of the image poles, in many cases, approach zero only very slowly as the depth of the image pole increases.

This difficulty however, is at least partially apparent. The individual image poles have different signs, so that the values of their strength oscillate about zero. It is true that the amplitude of this oscillation often remains appreciable to considerable depths, but in evaluating the contribution of the neglected image poles to the apparent resistivity one should also take into consideration the effect of the partial cancellation that results from the difference in sign of the image poles. Obviously, this cancellation would be at a practical optimum when he aggregate strength of the neglected image poles is zero.

Now the aggregate strength of all the image poles can be computed in an extremely simple manner, as may be seen by the following considerations regarding the apparent resistivity at an infinite value of the electrode distance.

Consider an image pole of strength Q_m at a great but finite depth mc. Suppose this image pole to be split up in two parts, of strength Q_{m1} and Q_{m2}, in such a manner that the aggregate strength of Q_{m2} and all the image poles at greater depth equals zero. The series of image poles from Q_{m2} downward is then equivalent to a series of dipoles of length c. We now consider one of these dipoles at a depth nc which is infinite of the same order as the electrode distance a; it may be easily shown that the contribution of this dipole to the apparent resistivity for infinite electrode distance is of the order of Q_n/n. Since the number of these dipoles is of the order of n, the aggregate contribution of all the dipoles to the apparent resistivity at infinite electrode distance is of the order of Q_n. Since, moreover, Q_n approaches to zero as n approaches to infinity, it follows that the series of dipoles gives no contribution to the apparent resistivity at infinite electrode distance.

We now turn to the contribution of the image poles from Q_{m1} upward to the apparent resistivity at infinite electrode distance. Since these image poles are located at a *finite* depth it follows from eq. (2) that the contribution of one of them to the apparent resistivity at infinite electrode distance is $2\ \rho_1\ Q$, and the aggregate contribution of all the image poles to the apparent resistivity is, therefore,

$$2\,\rho_1 \sum_{n-1}^{n=\infty} Q_n \quad . \quad . \quad . \quad . \quad . \quad . \quad . \quad . \quad . \quad (3)$$

In this expression the summation extends from 1 to infinity because the aggregate strength of the image poles down to Q_{m1} is equal to the aggregate strength of all the image poles.

At the same time it is generally known that, as the electrode distance approaches infinity, the apparent resistivity in a three layer case approaches to the resistivity of the third layer. A rigorous proof of this statement has been given by Muskat (1933). From this consideration it follows that the aggregate contribution of the image poles to the apparent resistivity at infinite electrode distance must be

$$(\rho_3 - \rho_1) \quad . \quad . \quad . \quad . \quad . \quad . \quad . \quad . \quad . \quad . \quad . \quad . \quad (4)$$

Obviously, the expressions (3) and (4) must be equal to each other. Solving, we find

$$\sum_{n=1}^{n=\infty} Q_n = (\rho_3 - \rho_1)/2\,\rho_1 \quad . \quad . \quad . \quad . \quad . \quad . \quad . \quad (5)$$

and by this equation the aggregate strength of the image poles can easily be computed.

Care must be taken to see that, in the computations of the apparent resistivities, the computations are broken off in such a manner that the aggregate strength of the neglected image poles in zero. To this end the value of the strength of the deepest image pole which is included in the computation must be replaced by a value which is chosen in such a manner that the total strength of the image poles included in the computation becomes equal to the value according to eq. (5).

In order to have a check on the convergence of the computations it is convenient to divide the image poles into a number of groups. This is done by occasionally splitting an image pole into two parts, and assigning one of these parts to the group above it and the other part to the group below it. This should be done in such a manner that the aggregate strength of the first group is equal to the aggregate strength of *all* the image poles, while the aggregate strength of each of the other groups is zero. The computations of the apparent resistivities may then be broken off at the end of each of these groups. A check on the convergence of the computations may be obtained by computing separately the total contribution to the apparent resistivity of the image poles within each group. It has been found that the contributions of these groups to the apparent resistivity converge much more rapidly than those of the individual image poles.

SERIES EXPANSION FOR THE EFFECT OF THE DEEPER POLES

In the computation of the contributions of the deeper poles to the apparent resistivity a further simplification may be obtained by utilizing a well known series expansion for the reciprocal of a distance. With the notation of figure 1 and provided that p is greater than q, the reciprocal of r can be expanded in a convergent series of the form

$$\frac{1}{r} = \frac{1}{p} - \frac{1}{2}\frac{q^2}{p^3} + \frac{3}{8}\frac{q^4}{p^5} + \ldots\ldots \quad . \quad (6)$$

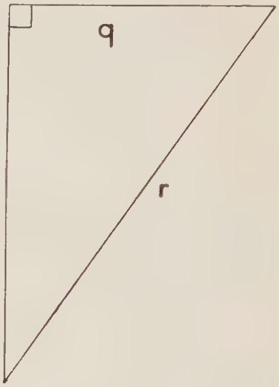

Fig. 1. Illustration of notation

Now suppose that, in figure 1, the vertex opposite r represents a current electrode on the surface, the vertex opposite q an image pole, and the vertex opposite p a voltage electrode on the surface. We may then apply equation (6) to find the contribution of an image pole to the potential in a point on the surface at a distance R from the current electrode. This yields

$$\Delta_n V = \frac{\rho_1 I}{2\pi} 2 Q_n \left\{ \frac{1}{n\,c} - \frac{1}{2}\frac{R^2}{(n\,c)^3} + \frac{3}{8}\frac{R^4}{(n\,c)^5} + \ldots\ldots \right\}$$

From this equation we then find the expression for the contribution of an image pole to the apparent resistivity in a Wenner configuration

$$\Delta_n \rho_a = \rho_1 Q_n \left\{ 6\, a^3/(nc)^3 - \frac{45}{2}\, a^5/(nc)^5 + \ldots\ldots \right\}$$

The contribution of a group of image poles to the apparent resistivity may thus be written in the form

$$\sum_n \Delta_n \rho_a = 6\,\rho_1 (a/c)^3 \sum_n (Q_n/n^3) - \frac{45}{2}\rho_1 (a/c)^5 \sum_n (Q_n/n^5) + \ldots\ldots \qquad (7)$$

Equation (7) presents the great advantage that the individual series involve the strengths and the depths of the image poles only and are independent of the electrode distance. Therefore we may compute the contributions of a certain group of image poles to the apparent resistivities at different electrode distances by the following procedure. We compute, for this group of image poles, the expressions

$$\sum_n (Q_n/n^3), \sum_n (Q_n/n^5), \text{etc.}$$

and we multiply these expressions with the appropriate factors

$$6\,\rho_1\,(a/c)^3, \frac{45}{2}\,\rho_1\,(a/c)^5, \text{etc.}$$

where different values may be substituted for the electrode distance a.

It has been stated above that the series expansion of eq. (6) converges only if p is greater than q. In order that the convergence shall be rapid enough for practical purposes the ratio p/q must be at least 2 or, using the notation of eq. (7), nc must be greater than $4a$, since in the determination of an apparent resistivity at an electrode spacing of a a distance of $2a$ between current electrode and voltage electrode is involved.

The method must therefore be applied only to image poles at a depth greater than $4a$. In most of the cases which we have computed, the contributions of the groups of image poles to the apparent resistivity had become negligible befor this depth has been reached. In those cases where the convergence of the contributions of the groups of image poles to the apparent resistivity is comparatively slow, the present procedure leads to a valuable reduction in the time required for the calculations. Provided that the condition $nc > 4a$ is satisfied, the convergence of the series in eq. (7) is very rapid indeed. In none of the cases which we have computed has it been necessary to include terms higher than that in $(a/c)^5$.

RESULTS OF THE CALCULATIONS

Resistivity curves have been computed for three layer cases in which

$$\rho_3 = \rho_1$$
$$\rho_2/\rho_1 = 2/3,\ 3/7,\ 1/4,\ 3/17 \text{ and } 1/9,$$

and for different values of the ratio of the thicknesses of the layers. The results of these computations are presented in tables 1-5. For the majority of the above cases, resistivity curves are contained in the collection that was published by the Compagnie Générale de Géophysique (1955). Nevertheless it is considered worth while publishing the present data, since our computations refer to a Wenner electrode configuration whereas the curves published by the Compagnie Générale de Géophysique refer to a Schlumberger electrode configuration.

The values of the apparent resistivities are given in the tables to three decimal figures; the last decimal figure, however, may be in error by a few points.

TABLE I

Apparent resistivities for $\rho_1 = \rho_3 = 1$ and $\rho_2 = 2/3$

$(k_2 = -k_1 = 0.2)$

a/d_1	$\frac{1}{2}$	1	$1\frac{1}{2}$	2	$2\frac{1}{2}$	3	4	5	6	8	12	16	20
$d_2 = 5d_1$	0.985	0.928	—	0.810	—	0.753	0.732	0.729	0.737	0.765	0.822	0.866	0.900
$d_2 = 3d_1$	0.985	0.930	0.866	0.818	—	0.772	0.771	0.783	0.800	0.837	0.894	0.928	0.944
$d_2 = 2d_1$	0.986	0.932	0.873	0.833	0.810	0.801	0.810	—	0.852	0.883	0.930	0.962	—
$d_2 = d_1$	0.987	0.941	0.896	0.871	0.863	0.865	0.883	—	0.922	0.947	0.971	—	—
$d_2 = \frac{1}{2} d_1$	0.990	0.956	0.928	0.916	0.916	0.922	0.938	—	0.961	0.974	—	—	—

a/d_1	1/3	2/3	1	$1^1/_3$	$1^2/_3$	2	$2^2/_3$	4	$5^1/_3$	$6^2/_3$
$d_2 = \frac{1}{3} d_1$	0.997	0.984	0.965	0.951	0.942	0.938	0.942	0.958	0.971	0.980

a/d_1	2/5	4/5	$1^1/_5$	$1^3/_5$	$2^2/_5$	$3^1/_5$	4
$d_2 = \frac{1}{5} d_1$	0.997	0.983	0.970	0.963	0.962	0.968	0.975

TABLE II

Apparent resistivities for $\rho_1 = \rho_3 = 1$ and $\rho_2 = 3/7$

$(k_2 = -k_1 = 0.4)$

a/d_1	$\frac{1}{2}$	1	$1\frac{1}{2}$	2	$2\frac{1}{2}$	3	4	5	6	8	12	16	20
$d_2 = 5d_1$	0.971	0.862	—	0.642	—	0.542	0.515	0.518	0.532	0.577	0.666	0.734	0.784
$d_2 = 3d_1$	0.971	0.864	0.743	0.655	—	0.575	0.568	0.588	0.620	0.685	0.779	0.840	0.884
$d_2 = 2d_1$	0.972	0.867	0.753	0.676	0.634	0.622	0.634	—	0.711	0.774	0.848	0.894	—
$d_2 = d_1$	0.974	0.883	0.794	0.743	0.724	0.729	0.764	—	0.834	0.884	0.933	—	—
$d_2 = \frac{1}{2} d_1$	0.980	0.910	0.851	0.825	0.822	0.831	0.865	—	0.916	0.942	—	—	—

a/d_1	1/3	2/3	1	$1^1/_3$	$1^2/_3$	2	$2^2/_3$	4	$5^1/_3$	$6^2/_3$
$d_2 = \frac{1}{3} d_1$	0.994	0.967	0.928	0.896	0.878	0.871	0.875	0.906	0.935	0.953

a/d_1	2/5	4/5	$1^1/_5$	$1^3/_5$	$2^2/_5$	$3^1/_5$	4
$d_2 = \frac{1}{5} d_1$	0.993	0.965	0.935	0.918	0.916	0.928	0.942

TABLE III

Apparent resistivities for $\rho_1 = \rho_3 = 1$ and $\rho_2 = 1/4$
$(k_2 = -k_1 = 0.6)$

a/d_1	$\frac{1}{2}$	1	$1\frac{1}{2}$	2	$2\frac{1}{2}$	3	4	5	6	8	12	16	20
$d_2 = 5d_1$	0.958	0.800	——	0.491	——	0.361	0.329	0.330	0.346	0.394	0.490	0.568	0.632
$d_2 = 3d_1$	0.958	0.801	0.629	0.505	——	0.395	0.385	0.409	——	0.513	0.624	0.703	0.761
$d_2 = 2d_1$	0.960	0.805	0.640	0.528	0.468	0.444	0.456	——	0.543	0.619	0.724	0.798	——
$d_2 = d_1$	0.961	0.823	0.685	0.603	0.578	0.573	0.611	——	0.706	0.779	0.863	——	——
$d_2 = \frac{1}{2}d_1$	0.968	0.856	0.758	0.711	0.703	0.716	0.760	——	0.837	0.885	——	——	——
a/d_1	1/3	2/3	1	$1\frac{1}{3}$	$1\frac{2}{3}$	2	$2\frac{2}{3}$	4	$5\frac{1}{3}$	$6\frac{2}{3}$			
$d_2 = \frac{1}{3}d_1$	0.990	0.945	0.880	0.825	0.790	0.775	0.778	0.828	0.874	0.906			
a/d_1	2/5	4/5	$1\frac{1}{5}$	$1\frac{3}{5}$	$2\frac{2}{5}$	$3\frac{1}{5}$	4						
$d_2 = \frac{1}{5}d_1$	0.988	0.940	0.887	0.855	0.846	0.867	0.891						

TABLE IV

Apparent resistivities for $\rho_1 = \rho_3 = 1$ and $\rho_2 = 3/17$

$(k_2 = -k_1 = 0.7)$

a/d_1	$\frac{1}{2}$	1	$1\frac{1}{2}$	2	$2\frac{1}{2}$	3	4	5	6	8	12	16	20
$d_2 = 5d_1$	0.952	0.769	0.568	0.422	—	0.279	0.244	0.245	0.260	0.303	0.390	0.465	0.529
$d_2 = 3d_1$	0.952	0.771	0.576	0.433	—	0.309	0.294	0.315	0.346	0.412	0.521	0.603	—
$d_2 = 2d_1$	0.952	0.775	0.584	0.454	—	0.357	0.363	0.397	0.440	0.518	0.630	0.708	—
$d_2 = d_1$	0.955	0.791	0.626	0.526	—	0.478	0.515	—	0.615	0.693	0.792	—	—
$d_2 = \frac{1}{2}d_1$	0.961	0.825	0.701	0.637	0.621	0.632	0.680	—	0.772	0.833	—	—	—

a/d_1	1/3	2/3	1	$1^1/_3$	$1^2/_3$	2	$2^2/_3$	4	$5^1/_3$	$6^2/_3$
$d_2 = \frac{1}{3}d_1$	0.988	0.932	0.849	0.778	0.731	0.708	0.707	0.764	0.818	0.858

TABLE V

Apparent resistivities for $\rho_1 = \rho_3 = 1$ and $\rho_2 = 1/9$

$(k_2 = -k_1 = 0.8)$

a/d_1	$\frac{1}{2}$	1	$1\frac{1}{2}$	2	$2\frac{1}{2}$	3	4	5	6	8	12	16	20
$d_2 = 5d_1$	0.945	0.740	—	0.354	—	0.202	0.164	0.164	0.174	0.208	0.279	0.344	0.404
$d_2 = 2d_1$	0.946	0.745	0.530	0.380	—	0.264	0.259	—	0.324	0.391	0.501	0.584	—
$d_2 = \frac{1}{2}d_1$	0.953	0.788	0.632	0.543	0.514	0.519	0.566	—	0.670	0.746	—	—	—

a/d_1	2/5	4/5	$1^1/_5$	$1^3/_5$	$2^2/_5$	$3^1/_5$	4
$d_2 = \frac{1}{5}d_1$	0.980	0.898	0.802	0.737	0.702	0.729	0.769

ACKNOWLEDGMENTS

The author is indebted to Mr. J. G. van Ewyk for his valuable help in the numerical calculations, and to N.V. De Bataafsche Petroleum Maatschappij for permission to publish this paper.

REFERENCES

Compagnie Générale de Géophysique, 1955, Abaques de sondage électrique, Geophysical Prospecting, 3, supplement III.

Deppermann K., On the calculation of resistivity curves, to be published in Geophysical Prospecting, III, 4.

Ehrenburg D. O. and Watson R. J., 1932, Mathematical theory of electrical flow in stratified media with horizontal, homogeneous and isotropic layers, Am. Inst. Min. Metall. Eng. Trans. Geoph. Prosp., 423-438.

Flathe H., 1955, A practical method of calculating geo-electrical model graphs for horizontally stratified media, Geophysical Prospecting, 3, 268-294.

Mooney H. M., 1954, Depth determinations by electrical resistivity, Mining Engineering, 915-918.

—— H. M. and Wetzel W. W., in press, Potentials about a point electrode and apparent resistivity curves for a four-layer earth, University of Minnesota Press.

Muskat M., 1933, Potential distribution about an electrode on the surface of the earth, Physics, 4, 129-147.

Watson R. J., 1934, A contribution to the theory of the interpretation of resistivity measurements obtained from surface potential observations, Am. Inst. Min. Metall. Eng. Trans., 110, 201-232.

Wetzel W. W., and McMurry H. V., 1937, A set of curves to assist in the interpretation of the three layer resistivity problem, Geophysics, 2, 329-341.

DISCUSSION

Mr. VOLKER: What time does the computing work for Mr. Koefoed's new procedure take?

Mr. KOEFOED: For the case where $\rho_1 = \rho_3$ the time required for one type curve is about five hours, for the case where $\rho_1 \neq \rho_3$ six hours. These figures do not include the time required for preparing the tables of reciprocal distances.

A PRACTICAL METHOD OF CALCULATING GEOELECTRICAL MODEL GRAPHS FOR HORIZONTALLY STRATIFIED MEDIA *

BY

H. FLATHE **

ABSTRACT

For the quantitative interpretation of field resistivity curves it is necessary to possess theoretically calculated standard graphs. The problem of calculating such graphs for certain parallel stratified media has been solved long ago. The methods developed so far, however, require facilities, which are not normally available to the geophysicist in the field. It has been shown by experience, that the catalogues of graphs, which have been made available for practical use, are inadequate, when the number of layers exceeds three. For this reason endeavours are made to find a method, to allow the geophysicist to calculate model graphs suited to any given special geological situation, with ordinary field facilities and without too great an expenditure of time. The principle of equivalence implies that such a model graph be known with a high accuracy.

To this end, a method for the calculation of model graphs for a series of parallel beds is described. This method is sufficiently simple — no series need to be summed up — to be applied by the geophysicist in practice, even during field work. The study of the kernel function in Stefanescu's integral representation of the "apparent" resistivity leads to a basis for the set of graphs. The prime elements of this basis form a one-parametric curve-system, by means of which the graph for any multi-layer sequence of strata can be obtained to any degree of approximation by linear combination.

The importance of this method in practice is demonstrated with the help of examples.

INTRODUCTION

1. Experience shows that in geo-electric prospecting the quantitative evaluation of apparent resistivity graphs represents the main task. This is, however, impracticable without theoretically calculated standard curves. Since virtually it is not possible to deduce directly from the measured graph the resistivities and thicknesses of layers in the subsoil, it is necessary to apply the method of curve comparison. For this reason, efforts have been made over a number of years, to develop methods for computing standard curves, the ability of a geophysicist to interpret geo-electrical measurements depending to a high degree, apart from a certain amount of experience, on the evaluation material

---

* Presented at the Eighth Meeting of the European Association of Exploration Geophysicists, held in Paris, 18/20 May 1955.

** Amt für Bodenforschung, Hannover.

placed at his disposal. As well as the indispensible two-layer diagrams, a set of three-layer graphs, as complete as possible, seems absolutely necessary for the interpretation of geo-electrical investigations over a horizontally stratified medium. In principle, there are no difficulties in applying the calculation methods to multi-layer cases as well. There is, on the other hand, some difficulty in the choice of the thickness and resistivity ratios. Because of the increasing number of parameters it follows that a catalogue of four- and more layer cases must show considerable gaps, if it is to remain in a convenient form, and it is more than likely that each geophysicist engaged in geo-electrical surveying will experience that just those standard curves which he requires for the interpretation of field measurements are not contained in his catalogue. In order to rectify this deficiency, as the first step towards an interpretation use is made of the well-known auxiliary point methods, the bases of which are more or less empirical. Each geophysicist employing such methods of solution will consider it desirable to be able to check the result of the evaluation thus achieved, at least at the interesting points of the area, by exactly calculated model graphs. Here, however, the calculation methods known so far will fail, for with the means normally at his disposal in the field, the geophysicist cannot compute one single standard graph. Also the lack of time would make it a practical impossibility for him to sum up a relatively badly converging series, this process being necessary for each point on the curve. Consequently there was, up to now, no simple method of controlling the interpretation of an apparent resistivity graph for which the catalogue did not contain the appropriate standard graph.

The aim of the investigations described in this paper, is to provide a method to enable the geophysicist in the field, to calculate sufficiently *exact* special model graphs for each particular area, without a great expenditure in time, and with the simplest means of computation, such as a slide rule and a table of logarithms. The method shown here avoids the summing of series. On the basis of three theorems, proved in the theoretical section below, a method is developed, permitting the construction of a resistivity graph in a relatively simple manner, by the aid of a single set of prime curves, representing a fundamental system for the total of all resistivity graphs over a series of parallel beds. Although the algebraic treatment of the problem has very many interesting theoretical aspects, here it is restricted solely to that which is necessary for the evaluation. In the second part of the paper, practical applications of the method are indicated and techniques of computation shown. The possibilities of the method as far as this can be done within the compass of this publication, are demonstrated by means of several selected examples.

THEORY

2. *The theorem of formation for the kernel function in* STEFANESCU'S *integral.*

Consider a series of parallel stratified, conducting media where ρ_1, ρ_2, ……

are the specific resistivities of the individual layers, and h_1, h_2, ... the depths of the interfaces (Fig. 1). Instead of the resistivities ρ_i we use, following HUMMEL, the quantities $k_i = (\rho_{i+1} - \rho_i) / (\rho_{i+1} + \rho_i)$ in the calculations.

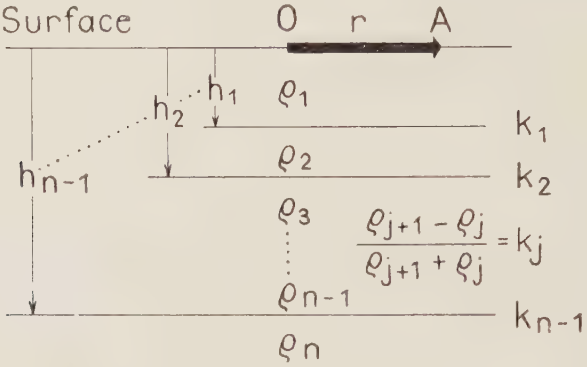

Fig. 1.

For the potential of a point source at the surface of space, STEFANESCU (1930) has given the integral representation

$$V(r) = \frac{I \rho_1}{2\pi} \left(\frac{1}{r} + 2 \int_0^\infty \Theta_1 (\lambda, k_i, h_i) \, J_0 (\lambda r) \, d\lambda \right)$$

where I is the current intensity, r the distance between the point source O and the space point A, J_0 the Bessel function of the order O. From this potential function the term for the so-called "apparent" resistivity ρ_s, according to the definition by SCHLUMBERGER, may be obtained by differentiation:

$$\rho_s (r) \underset{Def.}{=} - \frac{2\pi}{I} r^2 \frac{dV}{dr} = \rho_1 \left(1 + 2 r^2 \int_0^\infty \Theta_1 (\lambda) \, J_1 (\lambda r) \, \lambda \, d\lambda \right) \quad . \quad . \quad (1)$$

This quantity is usually plotted as an apparent resistivity curve using the four-point method with direct current in the Schlumberger arrangement ($r = L/2$, half distance of current electrodes). The resistivities and thicknesses of the individual layers are included in the quantities k_i and h_i in the kernel function Θ_1 (λ), which is calculated for the n-layer case, according to STEFANESCU, by the aid of CRAMER's rule from the system of boundary conditions

$$
\begin{aligned}
&\Theta_1 - \Psi_1 &&= 0 \\
&e^{-\lambda h 1}\,\Theta_1 + e^{\lambda h_1}\,\Psi_1 - e^{-\lambda h_1}\,\Theta_2 - e^{\lambda h_1}\,\Psi_2 &&= 0 \\
&-e^{-\lambda h_1}\,\Theta_1 + e^{\lambda h_1}\,\Psi_1 + \frac{\rho_1}{\rho_2}\,e^{-\lambda h 1}\,\Theta_2 - \frac{\rho_1}{\rho_2}\,e^{\lambda h_1}\,\Psi_2 &&= \left(1 - \frac{\rho_1}{\rho_2}\right) e^{-\lambda h_1} \\
&\qquad\qquad\vdots \qquad\qquad \vdots &&\quad \vdots \\
&e^{-\lambda h_{n-1}}\,\Theta_{n-1} + e^{\lambda h_{n-1}}\,\Psi_{n-1} - e^{-\lambda h_{n-1}}\,\Theta_n - e^{\lambda h_{n-1}}\Psi_n &&= 0 \\
&-e^{-\lambda h_{n-1}}\,\Theta_{n-1} + e^{\lambda h_{n-1}}\,\Psi_{n-1} + \frac{\rho_{n-1}}{\rho_n}\,e^{-\lambda h_{n-1}}\,\Theta_n - \frac{\rho_{n-1}}{\rho_n}\,e^{\lambda h_{n-1}}\,\Psi_n &&= \left(1 - \frac{\rho_{n-1}}{\rho_n}\right) e^{-\lambda h_{n-}} \\
&\Psi_n &&= 0
\end{aligned}
$$

For the 2-layer case:

$$\Theta_1(\lambda) = \frac{k_1 e^{2\lambda h_1}}{1 - k_1 e^{-2\lambda h_1}},$$

and for the 3-layer case:

$$\Theta_1(\lambda) = \frac{k_1 e^{-2\lambda h_1} + k_2 e^{-2\lambda h_2}}{1 + k_1 k_2 e^{-2\lambda(h_2 - h_1)} - k_1 e^{-2\lambda h_1} - k_2 e^{2\lambda h_2}}.$$

Without modifying the generality, the depths h_i can be chosen rational to each other. If we take the highest common factor as unit thickness and also as unit length for the electrode distance, then h_i are integers. Then $\Theta_1(\lambda) = \Theta(\lambda)$ (in the following, the index will be left out) is a rational function of $e^{-2\lambda} = u$:

$$\Theta = \frac{P_n(u)}{Q_n(u)}$$

The index n gives the number of layers. Numerator and denominator are polynomials of the degree h_{n-1} in u. As the numerator $P_n(u)$ occurs in a negative form in the denominator, it is best to introduce the auxiliary function $H_n(u) = Q_n(u) + P_n(u)$. For the two-layer case is valid:

$$H_2(u) = 1; \qquad P_2(u) = k\,u$$

The possibility for a recurrence formula of the kernel function Θ for an arbitrary layer sequence is given by the following theorem:

Theorem 1: (Law of formation)

> Proceeding from the n- to the $(n + 1)$-layer-case by adding at the top of he substratum an $(n + 1)$ *th* layer with the data k_n and h_n, the kernel function
>
> $$\Theta(\lambda) = \frac{P(u)}{H(u) - P(u)}$$
>
> with $u = e^{-2\lambda}$ satisfies the equations
>
> $$\begin{aligned} P_{n+1}(u) &= P_n(u) + H_n(u^{-1})\, k_n\, u^{h_n} \\ H_{n+1}(u) &= H_n(u) + P_n(u^{-1})\, k_n\, u^{h_n} \end{aligned} \qquad (3)$$
>
> For the denominator $Q = H - P$, especially
>
> $$Q_{n+1}(u) = Q_n(u) - Q_n(u^{-1})\, k_n\, u^{h_n}$$
>
> is valid.

Proof: We put $e^{-\lambda} = u^{1/2} = x$ and introduce the determinants

$$\tilde{P}_n(x) = \left|\begin{array}{c|ccccccccc} -x^{h_1} & -x^{h_1} & -x^{-h_1} & 0 & 0 & 0 & \cdot & \cdots & \cdot & 0 \\ x^{h_1} & \frac{\rho_1}{\rho_2} x^{h_1} & -\frac{\rho_1}{\rho_2} x^{-h_1} & 0 & 0 & 0 & \cdot & \cdots & \cdot & 0 \\ 0 & x^{h_2} & x^{-h_2} & -x^{h_2} & -x^{-h_2} & 0 & \cdot & \cdots & \cdot & 0 \\ 0 & -x^{h_2} & x^{-h_2} & \frac{\rho_2}{\rho_3} x^{h_2} & -\frac{\rho_2}{\rho_3} x^{-h_2} & 0 & \cdot & \cdots & \cdot & 0 \\ \vdots & & & \vdots & & & & & & \vdots \\ & & & & & & & & & 0 \\ 0 & \cdot & \cdot & \cdots & \cdot & \cdot & 0 & x^{h_{n-1}} & x^{-h_{n-1}} & -x^{h_{n-1}} \\ 0 & \cdot & \cdot & \cdots & \cdot & \cdot & 0 & -x^{h_{n-1}} & x^{-h_{n-1}} & \frac{\rho_{n-1}}{\rho_n} x^{h_{n-1}} \end{array}\right| \qquad (2a)$$

$$\tilde{H}_n(x) = \left|\begin{array}{c|ccccccccc} x^{-h_1} & \cdot & \cdot & \cdot & \cdot & \cdot & \cdot & \cdots & & \cdot \\ x^{-h_1} & \cdot & \cdot & \cdot & \cdot & \cdot & \cdot & \cdots & & \cdot \\ 0 & \cdot & & & & & & & & \cdot \\ \vdots & \vdots & & & & & & & & \vdots \\ 0 & \cdot & \cdot & \cdot & \cdot & \cdot & \cdot & \cdots & & \cdot \end{array}\right| \qquad (2b)$$

which only differ in the first column.

From the system of the boundary conditions (eq. 2) it may be shown that

$$\Theta = \frac{\tilde{P}_n}{\tilde{H}_n - \tilde{P}_n}$$

To prove this, substitute the first equation of the system ($\Psi_1 = \Theta_1$) in the second and third equation and substitute the last equation ($\Psi_n = 0$) in the previous two equations. The remaining system of $2n$-2 equations is then solved for Θ_1 by the aid of Cramer's rule. The denominator of this solution (the determinant of he homogeneous system) is immediately seen to be the difference $\tilde{H}_n$-$\tilde{P}_n$. The numerator of the solution (the determinant that is obtained by replacing the terms in the first column of the homogeneous system by those on the right hand side of the inhomogeneous system) is identical with $\tilde{P}_n\,(x)$. This becomes apparent if in (2*a*) all even columns are subtracted from the first column.

Furthermore we note that the determinants $\tilde{P}_n\,(x)$ and $\tilde{H}_n\,(x)$, by substituting the last column $(0, \ldots\ldots, 0, -x^{h_{n-1}}, \frac{\rho_{n-1}}{\rho_n}x^{h_{n-1}})$ by $(0, \ldots\ldots, 0, -x^{-h_{n-1}}, -\frac{\rho_{n-1}}{\rho_n}x^{-h_{n-1}})$, change over to $\tilde{H}_n\,(x^{-1})$ and $\tilde{P}_n\,(x^{-1})$ resp. To demonstrate this, exchange the 2*m-th* column with the $(2m+1)$ *-th* $(m = 1, \ldots, n\text{-}2)$, and also alter the sign of the even lines and of the first column; as the number of these operations is even, the sign of the determinants does not alter.

By adding a $(n+1)$ *th* layer, we get

$$\tilde{P}_{n+1}\,(x) = \begin{vmatrix} & & & 0 & 0 \\ & & & \vdots & \vdots \\ & \left(\tilde{P}_n(x)\right) & & 0 & 0 \\ & & & -x^{-h_{n-1}} & 0 \\ & & & -\frac{\rho_{n-1}}{\rho_n}x^{-h_{n-1}} & 0 \\ 0 & \ldots & 0 \quad x^{h_n} & x^{-h_n} & -x^{h_n} \\ 0 & \ldots & 0 \quad -x^{h_n} & x^{-h_n} & \frac{\rho_n}{\rho_{n+1}}x^{h_n} \end{vmatrix}$$

and by appropriate transformation

$$\tilde{P}_{n+1}\,(x) = \begin{vmatrix} & & & & 0 & 0 \\ & & & & \vdots & \vdots \\ & \left(\tilde{P}_n(x)\right) & & & 0 & 0 \\ & & & & -x^{-h_{n-1}} & 0 \\ & & & & -\frac{\rho_{n-1}}{\rho_n}x^{-h_{n-1}} & 0 \\ 0 & \ldots\ldots & 0 & 0 & 0 & -x^{h_n} \\ 0 & \ldots\ldots & & -\left(1-\frac{\rho_n}{\rho_{n+1}}\right)x^{h_n} & \left(1+\frac{\rho_n}{\rho_{n+1}}\right)x^{-h_n} & 0 \end{vmatrix}$$

By developing with respect to the last line, we get

$$\tilde{P}_{n+1}\,(x) = \left(1+\frac{\rho_n}{\rho_{n+1}}\right)\tilde{P}_n\,(x) + \left(1-\frac{\rho_n}{\rho_{n+1}}\right)x^{2h_n}\,\tilde{H}_n\,(x^{-1})$$

The same is valid for $\tilde{H}_{n+1}$. By the substitution

$$\tilde{P}_n(x) = P_n(u)\prod_{j=2}^{n}\left(1+\frac{\rho_{j-1}}{\rho_j}\right) \quad ; \quad \tilde{H}_n(x) = H_n(u)\prod_{j=2}^{n}\left(1+\frac{\rho_{j-1}}{\rho_j}\right)$$

with $u = x^2$ results (3) are demonstrated.

3. *Decomposition of the kernel function into partial fractions.*

The rational function Θ can, according to a fundamental theorem of algebra, be decomposed into a sum of real and complex partial fractions

$$\frac{P_n(u)}{Q_n(u)} = \sum_{i=1}^{h_{n-1}} \beta_i \frac{c_i u}{1-c_i u} \quad . \; . \; . \; . \; . \; . \; . \; . \quad (4)$$

and pairs of conjugate complex partial fractions can be combined to give real fractions whose numerators and denominators are of second degree. These fractions may correspond to kernel functions of integrals representing apparent resistivity curves, provided that they satisfy the equation for $\Theta_1(\lambda)$ in the 3-layer case given on page 271. In this case the following equation must be satisfied

$$\beta_i \frac{c_i u}{1-c_i u} + \beta_i' \frac{\bar{c}_i u}{1-\bar{c}_i u} = \alpha_i \frac{\dfrac{c_i+\bar{c}_i}{1+c_i\bar{c}_i}\, u - c_i\bar{c}_i u^2}{1-(c_i+\bar{c}_i)\,u + c_i\bar{c}_i u^2} \qquad (5)$$

where the term on the right hand side is the kernel function multiplied by a weight factor α_i.

In general, however, solutions for α_i which satisfy this equation for all values of u do not exist. Thus, the decomposition into partial fractions leads to

$$\frac{P_n(u)}{Q_n(u)} = \sum_{i=1}^{l} \alpha_i \frac{K_i u}{1-K_i u} + \sum_{i=l+1}^{\frac{h_{n-1}-l}{2}} \alpha_i \frac{K_i^{(1)} u + K_i^{(2)} u^2}{1-K_i^{(1)}(1-K_i^{(2)})\,u - K_i^{(2)} u^2} + R_n \quad (6)$$

where the first two summations on the right hand side correspond to two-layer cases and simple three-layer cases of the relative thickness 1 ($h_1 = 1$, $h_2 = 2$), and the last term, R_n, represents no apparent resistivity curves in our sense. If only real roots occur, then obviously a decomposition into a finite number of two-layer cases is possible. The existence of the integral demands that $|K_i| \leq 1$ is valid, because the integrand must not have any singularities in the λ-integration interval $(0, \infty)$. The set of curves which are separable into real two-layer cases contain, for instance, the three-layer minimum types $\rho_1 > \rho_2 < \rho_3$ with $h_1 = 1$, $h_2 = 2$; at a greater number of layer units, complex roots usually occur. The following paragraph is restricted to multiple layer cases with a perfectly conducting or a perfectly insulating substratum. In this special case, as will be shown below, the kernel function can always be resolved into partial fractions corresponding to three layer cases only.

4. *The case* $k_{n-1} = \pm 1$.

All cases in which $k_{n-1} = \pm 1$ can be transformed into the case of an *even* number of layer units overlying a perfectly *conducting* substratum. To this end it suffices to insert an additional interface with $k_n = -1$ at an *even* depth h_n, greater than the depth to the original substratum.

For the resolution into partial fractions this means that only complex roots of the denominator polynomial are involved. The two possible real roots ± 1, corresponding to two-layer cases, have merely been expanded to three-layer cases by a transformation of the kernels

$$\frac{\pm u}{1 \mp u} = \frac{\pm u - u^2}{1 \mp 2u + u^2} \quad . \quad . \quad . \quad . \quad . \quad . \quad . \quad . \quad . \quad . \qquad (7)$$

If we lay down

$$\frac{P(u)}{Q(u)} = \sum_{i=1}^{h_{n/2}} \alpha_i \frac{\varkappa_i u - u^2}{1 - 2\varkappa_i u + u^2} \quad . \quad . \quad . \quad . \quad . \quad . \quad . \quad . \qquad (8)$$

we get under consideration of $Q = H - P$ and $\Sigma \alpha_i = 1$

$$Q = H - P = \prod_i (1 - 2\varkappa_i u + u^2)$$

$$P = \sum_{i=1}^{h_{n/2}} \alpha_i (\varkappa_i u - u^2) \prod_{j \neq i}{}' (1 - 2\varkappa_j u + u^2)$$

$$H = \sum_{i=1}^{h_{n/2}} \alpha_i (1 - \varkappa_i u) \prod_{j \neq i}{}' (1 - 2\varkappa_j u + u^2)$$

$$H + P = (1 - u^2) \sum_{i=1}^{h_{n/2}} \alpha_i \prod_{j \neq i}{}' (1 - 2\varkappa_j u + u^2) \qquad (9)$$

and with this

$$\frac{\frac{H+P}{1-u^2}}{H-P} = \sum_{i=1}^{h_{n/2}} \frac{\alpha_i}{1 - 2\varkappa_i u + u^2} \quad . \quad . \quad . \quad . \quad . \quad . \qquad (10)$$

It follows from the law of formation (3) that for $k_n = -1$ the polynomials $\frac{H+P}{1-u^2}$ and $H - P$ are symmetrical with respect to their coefficients,* the coefficent of the *p*th term from the beginning equal to that of the *p*th term from the end.

Writing (10) in the form

---

* In the symmetric form of the denominator reflects that all its roots have the same modulus, which is 1.

$$\frac{1}{u}\,\frac{u^{-(h_n/2-1)}\dfrac{H+P}{1-u^2}}{u^{-h_n/2}\,(H-P)}=\frac{1}{u}\sum_{i=1}^{h_n/2}\frac{\alpha_i}{(u+u^{-1})-2\varkappa_i}$$

and substituting $u + u^{-1} = z$
(recurrence formula: $u^{\mu} + u^{-\mu} = z\,(u^{\mu-1} + u^{-(\mu-1)}) - (u^{\mu-2} + u^{-(\mu-2)})$)
the *symmetric form*

$$\boxed{\frac{p\,(z)}{q\,(z)}=\sum_{i=1}^{h_n/2}\frac{\alpha_i}{z-z_i}} \quad \ldots\ldots\ldots \quad (11)$$

is obtained, where p and q are polynomials in z of degree $\left(\frac{h_n}{2}-1\right)$ and $\frac{h_n}{2}$ respectively. The resistivity quantities $\varkappa_i$ which according to (8) are necessary for the decomposition are related to the roots z_i by

$$\varkappa_i=\frac{z_i}{z} \quad \ldots\ldots\ldots\ldots\ldots \quad (12)$$

Solutions for α_i satisfying eq. 11 do exist. They may be found by substituting $z \rightarrow z_i$ in eq. 11 and applying l'Hôpital's rule. This gives

$$\alpha_i=\frac{p\,(z_i)}{\left.\dfrac{d}{dz}\,q\,(z)\right|_{z\,=\,z_i}} \quad \ldots\ldots\ldots \quad (13)$$

The result is contained in

Theorem 2: (Theorem of decomposition)

> Each horizontal layer case with a finite number of layers of uniform conductivity and a substratum either perfectly insulating or perfectly conducting can be referred to three-layer cases of he relative thickness 1 ($h_1 = 1$, $h_2 = 2$) with an ideally conducting substratum. The apparent resistivity $\rho_s\,(r)$ can be expressed as a linear combination of a finite number of prime elements:
>
> $$\rho_s\,(r)=\rho_1\sum_i \alpha_i D\,(\varkappa_i, r) \quad \ldots\ldots\ldots \quad (14)$$
>
> with
>
> $$D\,(\varkappa, r)\underset{Def.}{=}1+2\,r^2\int_0^{\infty}\frac{\varkappa\,u-u^2}{1-2\,\varkappa\,u+u^2}\,J_1\,(\lambda r)\,\lambda\,d\lambda \quad \ldots \quad (15)$$
>
> $$(\varkappa\ \text{real};\ |\varkappa| \leq 1)$$
>
> The prime elements $D\,(\varkappa, r)$ form a one-parametric set of curves. (Fig. 2).

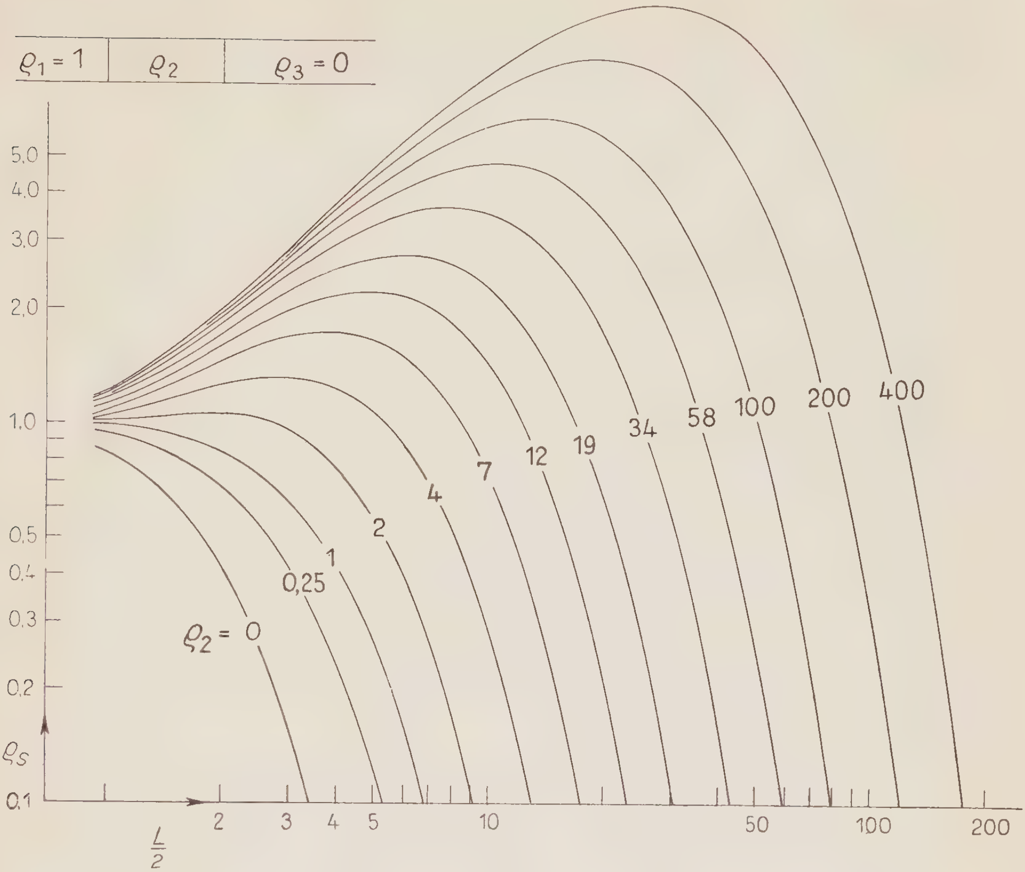

Fig. 2. The set of prime curves.

The fundamental system of the prime element $D\ (\varkappa, r)$ can be calculated, most easily, according to DEPPERMANN by the aid of the tabulated Hankel functions $H_1{}^{(1)}$ * from

$$D\,(\varkappa, r) = -\frac{\pi}{4} r^2 \Big(\varphi\, H_1^{(1)} (-i\,\varphi \frac{r}{2}) + \sum_{n=1}^{\infty} (2n\pi - \varphi)\; H_1^{(1)}[\, i\,(2n\,\pi - \varphi) \frac{r}{2}\,] + (2n\pi + \varphi)\, H_1^{(1)}\,[i\,(2n\,\pi + \varphi]\,\frac{r}{2}\,] \Big)$$

where $\varkappa = \cos\varphi$.

It is seen that, for great values of r, $D\ (\varkappa, r)$ may be represented by the first term $-\frac{\pi}{4} r^2\, i\,\varphi\, H_1^{(1)} (-\varphi\, \frac{r}{2})$ alone. For the smaller electrode distances,

---

* e.g. JAHNKE-EMDE, Tables of higher functions, Leipzig 1952.

instead of the case $h_1 = 1$, $h_2 = 2$, the congruent case $h_1 = 2$, $h_2 = 4$ with the same resistivity data is calculated by decomposing into partial fractions, with already known prime elements, according to *Theorem 2*. Since $p(z) = z$ and $q(z) = z^2 - 2\,(1 + \varkappa)$, this decomposition is:

$$D\,(\varkappa, r) = \frac{1}{2}\left[\,D\left(+\sqrt{\frac{1+\varkappa}{2}}, 2\,r\right) + D\left(-\sqrt{\frac{1+\varkappa}{2}}, 2\,r\right)\right]$$

The prime elements on the right, with the argument $2\,r$, are known already; and in this manner, the set of prime elements can, without any trouble, be extended from large to small electrode distances.

The set of prime elements can be calculated, therefore, without having to sum up a series.

The decomposition into partial fractions itself is independent of the electrode arrangement. With the same data α_i and $\varkappa_i$ of the decomposition, the Wenner curve can be calculated, provided the fundamental system of the prime elements for the Wenner arrangement is taken as a basis.

5. *The general case: k_{n-1} arbitrary* ($|k_{n-1}| \leq 1$)

The basis found in the former paragraph for the special cases $k_{n-1} = \pm 1$, consisting of the one-parametric curve set of the prime elements $D\,(\varkappa, r)$ represents also a basis for the total of all horizontal layer cases. This is expressed in

Theorem 3: (Theorem of approximation)

> Each horizontal layer case, with an *arbitrary* conductivity of the substratum, can be approximated to by the aid of the prime elements D $(\varkappa, r)$. Suppose $\rho_s\ (r)$ is an arbitrary multiple layer graph: for every $\varepsilon > 0$ and for maximum electrode distance R, there exist $N\ (\varepsilon, r)$ functions $D\ (\varkappa_1, r)$, $D\ (\varkappa_2, r)$, ..., $D\ (\varkappa_N, r)$, from the set of prime elements $\{D(\varkappa,\ r)\}$ and real numbers $\alpha_1, \alpha_2, \ldots, \alpha_N$, where $\Sigma\,\alpha_i = 1$, such that for $r \leq R$
>
> $$\left|\,\log \rho_s(r) - \log\left(\sum_{i=1}^{N} \alpha_i\, D\,(\varkappa_i, r)\right)\right| < \varepsilon \quad . \quad . \quad . \quad . \quad (16)$$

The theorem points out that in a finite r-interval a sequence of linear combinations from prime elements can always be found converging towards the given function. Thus

$$\rho_s\,(r) = \lim_{N \to \infty} \sum_{i=1}^{N} \overset{(N)}{\alpha_i}\; D\,(\overset{(N)}{\varkappa_i}, r) \quad . \quad . \quad . \quad . \quad . \quad . \quad . \quad (17)$$

The proof is given directly by constructing such a sequence. In the given n-

layer case, the substratum of which may begin at h_{n-1}, an additional interface, is intercalated at $h_n > h_{n-1}$, on top of an assumed ideally conducting substratum ($\rho_{n+1} = 0$). According to the law of formation (3), this $(n + 1)$-layer case is obtained from the given n-layer case by

$$\begin{aligned} P_{n+1}(u) &= P_n(u) - H_n(u^{-1})\,u^{h_n} \\ H_{n+1}(u) &= H_n(u) - P_n(u^{-1})\,u^{h_n} \end{aligned} \qquad (18)$$

As the depth of the auxiliary interface is increased, i.e. $h_n \to \infty$, the kernel function of the $(n + 1)$ layer case tends towards the kernel function of the given n-layer case within the integration interval $|u| < 1$. An alternative procedure is to insert an additional interface at a depth $h_n > h_{n-1}$ on top of an assumed perfectly *insulating* substratum ($\rho_{n+1} = \infty$). For $\rho_{n+1} = 0$, the given n-layer graph will be approximated from below, for $\rho_{n+1} = \infty$ from above. (Fig. 3). This approximation from both sides gives an estimation of errors. It follows that *Theorem* 3 is proved, because the $(n + 1)$-layer cases used for approximation are exactly representable, according to *Theorem* 2.

With Theorem 3, the problem of the theoretical calculation of an arbitrary horizontal layer graph is reduced to solving an algebraic equation with only real roots, as long as one possesses the one-parametric curve set of prime elements.

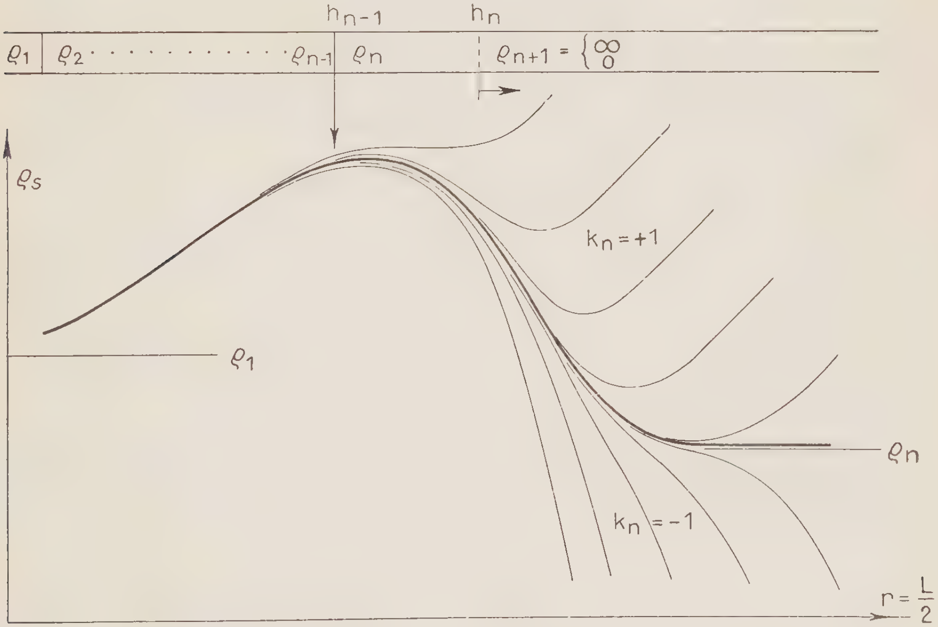

Fig. 3. Schematic representation of the Theorem of approximation.

THE PRACTICAL CALCULATION OF MODEL GRAPHS

6. *General Remarks*

The transformation of the kernel function into a symmetric form has two decided advantages in practice:

a) Reduction of the degree of the denominator polynomial $Q(u)$ by half.

b) All roots of the denominator $q(z)$ are real.

Although the calculations are considerably simplified by these two facts, the degree of the denominator polynomial should not be chosen too high for the calculation of graphs carried out in the field, in order that a slide rule and a table of logarithms will suffice for the calculations. Generally in a sequence of layers the surface layer has the least thickness, and, if this layer is taken as standard thickness, the degree of the denominator polynomial will often increase considerably. If the surface layer is thin relatively to the second layer, it will be useful to either disregard the top layer entirely, or if that leads to serious errors, to apply the principle of equivalence with respect to the surface layer.

Although the graph for any arbitrary horizontal layer case can be calculted by *Theorem* 3, it is obvious that the calculation of such cases is the simplest when the resistivities of the substratum are either very low or very high; and fortunately these cases occur rather frequently in practice.

In most cases of hydrological investigations, the impervious rocks consist either of clayey sediments, whose pore waters are often extremely saline, giving rise to good conducting properties, or of crystalline bodies with high resistivities. In areas where such extremes do not occur, the application of electrical prospecting is questionable anyway, because, in such cases, the permeable beds are often electrically indistinguishable from the impervious substratum.

7. *The Procedure of the Calculation*

For the calculation of the model graph, the resistivity values $\varkappa_i$, characterizing the prime elements, and the weights α_i, with which the prime elements are to be multiplied are found. Both of them result from the symmetric polynomials $p(z)$ and $q(z)$ of the kernel function according to (11), (12) and (13). The construction of the model graph is performed, therefore, in the following four stages:

I. The calculation of the symmetric polynoms $p(z)$ and $q(z)$.

II. The determination of the roots $z_i = 2\,\varkappa_i$ of the denominator polynomial $q\,(z)$.

III. The calculation of the weights $\alpha_i = p\,(z_i)/q'\,(z_i)$.

IV. The determination of the apparent resistivities

$$\rho_s = \rho_1 \sum \alpha_i D\,(\varkappa_i\,, r)$$

Some examples to illustrate the numerical manipulations, are shown at the end of the paper.

I. The calculation of the symmetric polynomials $p(z)$ and $q(z)$ is achieved by the use of the law of formation (3) in *Theorem* 1. The polynomials $H(u)$ and $P(u)$ are obtained using this recurrence formula, after having increased, if necessary, the number of layer units for the case under review, to an even number with an ideally conducting substratum. This completion is effected solely by inserting an additional interface at $h_n > h_{n-1}$ with the resistivity value $k_n = -1$, such that h_n is the next even number to h_{n-1}. $(H + P)$ and $(H - P)$ are set up and $(H + P)$ divided by $1-u^2$. Numerator and denominator of the quotient $\dfrac{(H + P)/(1-u^2)}{H - P}$ are now symmetrical in the coefficients. Analogous to the proof of *Theorem* 2, both polynomials are divided by half the highest power of u and in order to get $p(z)$ and $q(z)$, the substitution $u + u^{-1} = z$ according to the recurrence formula

$$u^{\mu} + u^{-\mu} = z\,(u^{\mu-1} + u^{-(\mu-1)}) - (u^{\mu-2} + u^{-(\mu-2)})$$

is carried out.

For calculations up to 20 layer units the following scheme results:

$$\begin{aligned}
u &+ u^{-1} = z \\
u^2 &+ u^{-2} = z^2 - 2 \\
u^3 &+ u^{-3} = z^3 - 3z \\
u^4 &+ u^{-4} = z^4 - 4z^2 + 2 \\
u^5 &+ u^{-5} = z^5 - 5z^3 + 5z \\
u^6 &+ u^{-6} = z^6 - 6z^4 + 9z^2 - 2 \\
u^7 &+ u^{-7} = z^7 - 7z^5 + 14z^3 - 7z \\
u^8 &+ u^{-8} = z^8 - 8z^6 + 20z^4 - 16z^2 + 2 \\
u^9 &+ u^{-9} = z^9 - 9z^9 + 27z^5 - 30z^3 + 9z \\
u^{10} &+ u^{-10} = z^{10} - 10z^8 + 35z^6 - 50z^4 + 25z^2 - 2
\end{aligned}$$

If the number of layer units is 7 or more the above calculation is the most useful, (see example No. 2), but for a smaller number of layer units the following scheme, where all layers have an equal thickness, is more advantageous:

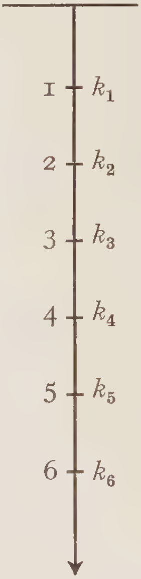

4 layer units

Perfectly conducting substratum:

$$p(z) = z + (a_1 - a_3)$$
$$q(z) = z^2 + (a_1 - a_2)\,z + 2\,(b_1 - b_2)$$

Perfectly insulating substratum:

$$p(z) = z^2 + (a_1 + a_2)\,z + 2\,(b_1 + b_2)$$
$$q(z) = [z + (a_1 + a_3)]\,(z^2 - 4)$$

Coefficients: $a_1 = k_2\,(k_3 + k_1)$ $b_1 = k_1 k_3 - 1$
$a_{\substack{2\\3}} = k_3 \pm k_1$ $b_2 = k_2\,(k_1 k_3 + 1)$

6 layer units

Perfectly conducting substratum:

$$p(z) = z^2 + (a_1 - a_3)\, z + (b_2 - b_4)$$
$$q(z) = z^3 + (a_1 - a_2)\, z^2 + (b_1 - b_3)\, z + 2\,[(c_1 - c_2) - (a_1 - a_2)]$$

Perfectly insulating substratum:

$$p(z) = z^3 + (a_1 + a_2)\, z^2 + (b_1 + b_3)\, z + 2\,[(c_1 + c_2) - (a_1 + a_2)]$$
$$q(z) = [z^2 + (a_1 + a_3)\, z + (b_2 + b_4)]\,(z^2 - 4)$$

Coefficients:

$$a_1 = k_2\,(k_3 + k_1) + k_4\,(k_3 + k_5)$$
$$a_{\substack{2\\3}} = k_5 \pm k_1$$
$$b_{\substack{1\\2}} = k_3\,(k_5 + k_1) + k_2\,k_4 (k_1\,k_3 + k_1\,k_5 + k_3\,k_5 + 1) - 2 \mp (1 - k_1\,k_5)$$
$$b_{\substack{3\\4}} = k_3\,(k_5 \pm k_1)\,(k_4 + k_2) + (1 \pm k_1\,k_5)\,(k_4 \pm k_2)$$
$$c_1 = k_1\,k_4\,(1 + k_3\,k_5) + k_2\,k_5\,(1 + k_1\,k_3)$$
$$c_2 = k_3\,(1 + k_1\,k_5) + k_2\,k_4\,(k_1 + k_3 + k_5) + k_1\,k_2\,k_3\,k_4\,k_5.$$

In this scheme, since those k_i are eliminated which are zero, the symmetric polynomials $p(z)$ and $q(z)$ are obtained directly, without having to do a substitution (see example No. 1).

II. For the *calculation of the zeros* of a polynomial, an extensive literature is already in existence. There is a special case here in that all roots are real and their modulus is ≤ 2. When the degree is not too high the simplest procedure seems to be that of successive approximations by iteration or by NEWTON's method and to decrease the degree step-by-step by division. Generally there are roots near to $+2$ and -2, for which a first approximation can be assumed. It should be noted that the roots near $+2$ must be carefully determined, because the appropriate elements vary considerably in this region with small variations of $\varkappa_1 = z_i/2$. Less accuracy is required for the calculation of negative roots.

III. *The determination of the weights* $\alpha_i = p(z_i)/q'(z_i)$ is best effected by HORNER's scheme, since by this method each z_i can be firmly adjusted on the slide rule (see example No 2). The relation $\Sigma\alpha_i = 1$ provides a check on the accuracy of the calculation. With an insulating substratum ($k_{n-1} = +1$) the weight α_1, belonging to the prime element $D\,(1, r)$, is very small. It must, however, be known exactly in order that the true position of the curve branch ascending under 45° can be obtained. Generally, the accuracy of the slide rule is not sufficient for the calculation of p and q' in this case. However, this is a minor matter, since as the electrode separation increases, all prime elements tend towards zero, with the exception of $D\,(1, r)$. It follows that the weight must equal the reciprocal of the longitudinal unit conductance $C = \Sigma\, m_i/\rho_i$ (so-called Dar Zarrouk-variable according to Maillet, 1947), and it may be easily calculated, therefore, from the resistivities and thicknesses (see example No 2).

IV. *The apparent resistivities* $\rho_s = \rho_1\, \Sigma\, \alpha_i\, D\ (\varkappa_i, r)$, are obtained using the calculated data α_i and $\varkappa_i$, from the diagram D of the prime elements. In contrast to Fig. 2, the apparent resistivities ρ_s, for fixed electrode distances, are plotted here as functions of the resistivity quanties $\varkappa_i$. Only the weight α_i, or directly $\rho_1\ \alpha_i$, is to be set on the slide rule and to be multiplied with the ρ_s-values taken along the ordinate to the appropriate value $\varkappa_i$ (see example No 2). The total shows the ρ_s-values for the required graph as function of $r = L/2$. For the transformation of the graph from distances measured in unit layer thicknesses to their true values in meters, only a translatory shift along the abscissa is necessary.

EXAMPLES

8. *Synopsis*

The choice of model graphs to be calculated depends entirely on the intended purpose: as mentioned in the introduction their major use is in the confirmation of an interpretation carried out over an object of interest; but, as well as this, other uses may be seen and three possible applications are

a) the interpretation itself (see example No 1).

b) to be able to judge beforehand whether the geo-electrical treatment of an object is promising, and to what extent geological questions can be answered (example No 2).

c) for the interpretation of anomalies in measured graphs, which might be caused for instance, by intercalated horizons of deviating conductivity (example No 3).

For the purpose a) of the interpretation, complete sets of graphs will be calculated, for b) special types will be chosen, which are characteristic for the particular object, and for c) again special graphs will be computed.

Two of the following examples concern hydro-geological problems, while the third originates from an investigation of a clay deposit. Example No 4 does not really come within the compass of this paper: it is included to give some idea of the possibilities opened up by the method described in this paper, for fundamental investigations of geo-electrical resistivity curves (principle of equivalence, anisotropy etc).

9. *Example No 1*

This example originates from geo-electrical operations in the north-west German coastal area. In 1954, the extension of the freshwater lens on the North Sea isle of Norderney was investigated. The fresh/saltwater interface, of interest in this connection, runs within pleistocene sands and gravels (Fig. 4). Under relatively clean near-surface sands with average resistivities of 180 Ω m, there are interglacial fine clayey sands with low resistivities (about 60 Ω m) at a depth of 15-30 m. Below 30 m come glacial course sands and small gravels probably originating from the Elster glacial period. For the interpretation, several cases were calculated. Fig. 4 shows a set of model graphs, and the following table contains the data α_i and $\varkappa_i$ for the decomposition:

graph No	α_1	$\varkappa_1$	α_2	$\varkappa_2$	α_3	$\varkappa_3$	
1	1	— 1	.	.	.	.	$D\,(-1, r)$
2	0,8	+ 0,25	0,2	— 1	.	.	$D\,(-0.5, r)$
3	1	— 0,5	.	.	.	.	
4	0,198	+ 0,826	0,691	— 0,076	0,111	— 1	
5	0,3075	+ 0,625	0,6925	— 1	.	.	
6	0,248	+ 0,806	0,752	— 0,931	.	.	
a)	0,247	+ 0,765	0,753	— 0,915	.	.	
b)	0,249	+ 0,846	0,751	— 0,946	.	.	
7	0,218	+ 0,875	0,182	— 05	0,6	— 1	
8	0,197	+ 0,911	0,106	— 0,071	0,696	— 0,965	

The true resistivity of glacial gravels within the freshwater region is rated at 180 Ω m, this value having been taken as the most likely from a consideration of all of the graphs; it undergoes, however, a certain amount of variation making it necessary to calculate also other model graphs, with different resistivities for the third layer. This has been indicated in the graphs 6a) and 6b). The hatched section demonstrates the region over which the curve 6 can vary under uniform thickness conditions, if the resistivity of the glacial gravels ranges between 140 and 240 Ω m.

The set of graphs in Fig. 4 shows clearly an equivalence to 3-layer cases in the centre. The second layer with a resistivity of 60 Ω m and the third layer with one of 180 Ω m appear combined as one layer with a mean resistivity; but the evaluation of this feature using a three-layer catalogue would lead to an error of 20 %. The fact that a 4-layer case exists on Norderney is, on the one hand, known from geology (drillings); on the other hand, however, it may be seen from the measured graphs recorded there, for these, when compared with the calculated set of graphs in Fig. 4, show a gap between the graphs 3 and 4. This gap is produced due to the fact that the descending branch of the graph is immediately shifted to the right as soon as the fresh/saltwater interface is lowered below 30 m, (that is, when the freshwater lens penetrates into the glacial gravels).

In order to indicate the simplicity of the computation for a set of curves as in Fig. 4, the numerical calculation for graph No 6 is shown below. Using the scheme given in 7. I. for four layer units over an ideally conducting substratum, results in

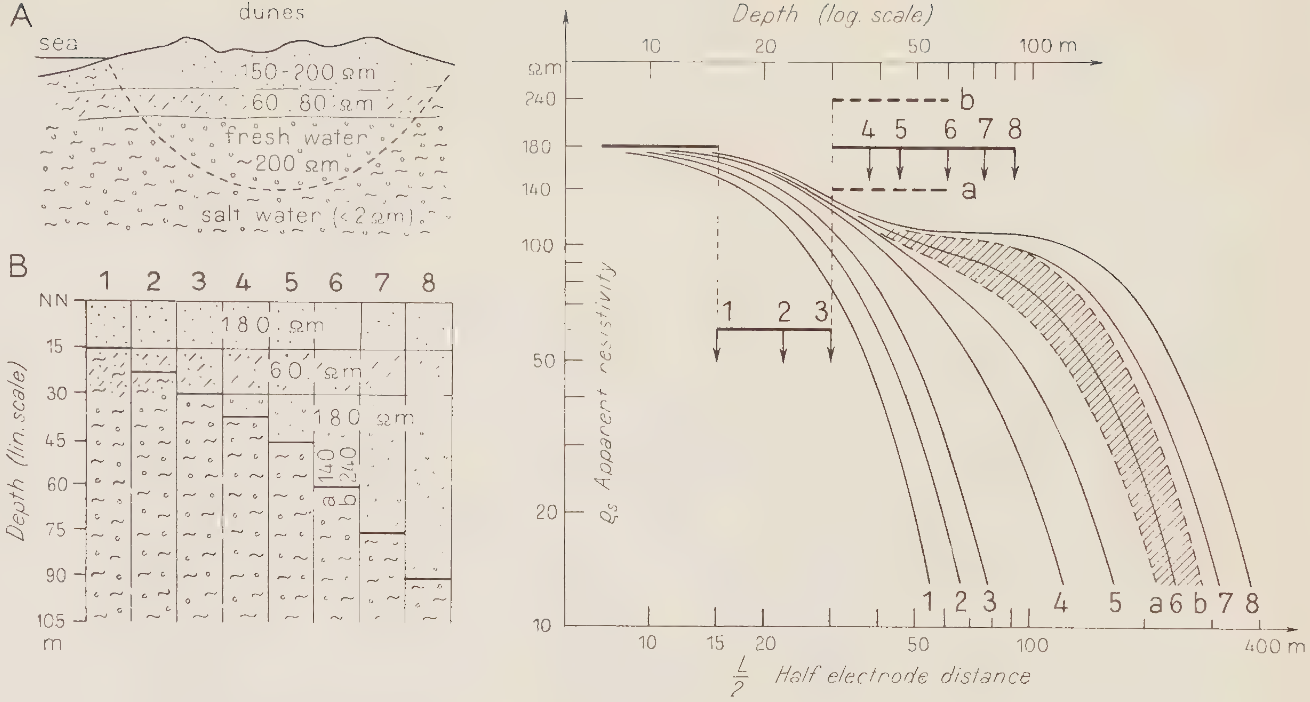

Fig. 4. Example No 1: Fresh/saltwater interface on the isle of Norderney.

$$
\begin{array}{llll}
k_1 = -0{,}5 & a_1 = -0{,}25 & b_1 = -1 & p(z) = z - 0{,}75 \\
k_2 = +0{,}5 & a_{\substack{2\\3}} = \mp\ 0{,}5 & b_2 = +0{,}5 & q(z) = z^2 + 0{,}25\,z - 3 \\
k_3 = 0 & & & q'(z) = 2z + 0{,}25
\end{array}
$$

$$z_1 = +1{,}612 \qquad \varkappa_1 = +0{,}806 \qquad \alpha_1 = \frac{0{,}862}{3{,}474} = 0{,}248$$

$$z_2 = -1{,}862 \qquad \varkappa_2 = -0{,}931 \qquad \alpha_2 = \frac{2{,}612}{3{,}474} = 0{,}752$$

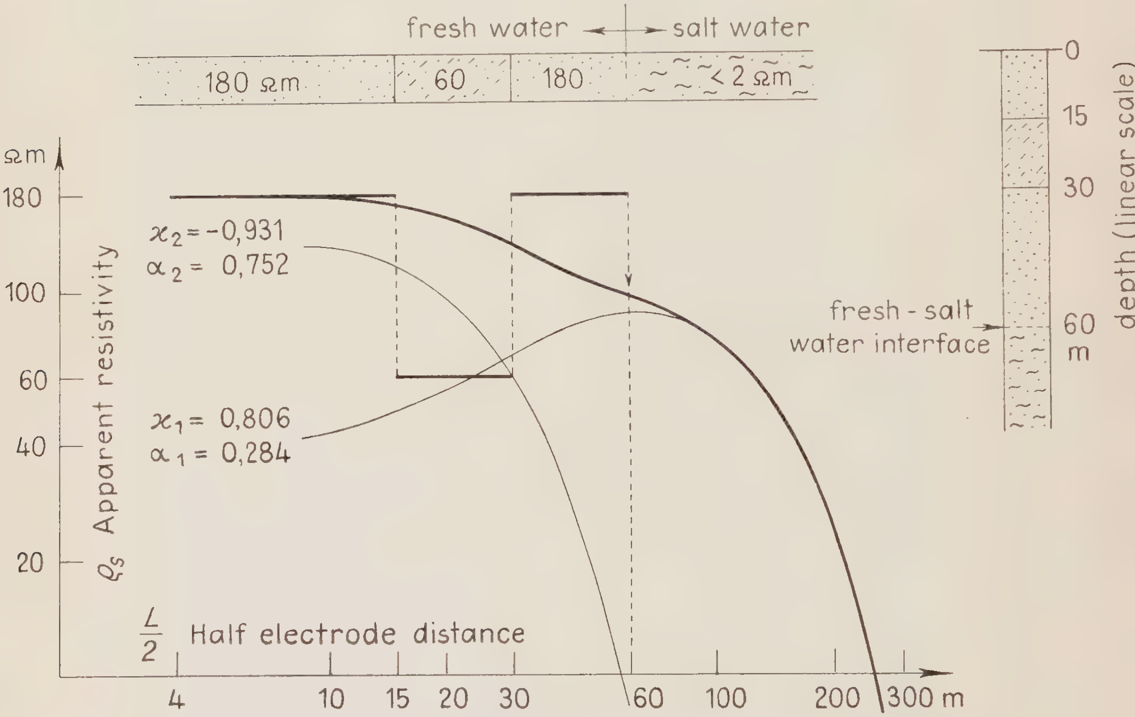

Fig. 5. Construction of a model graph to a sequence of layers on the isle of Norderney (4-layer case).

By the aid of the diagram *D* of the prime elements, the graph can be plotted immediately. Fig. 5 shows the curve together with the two partial curves plotted according to their weights. The calculation takes about 10 minutes. The calculation of the complete set in Fig. 4 can be effected in less than two hours.

10. *Example No 2*

The search for permeable beds is one of the main tasks of electrical prospecting. This example concerns a problem which often occurs in south-German areas. The geological conditions are represented schematically under *A* in

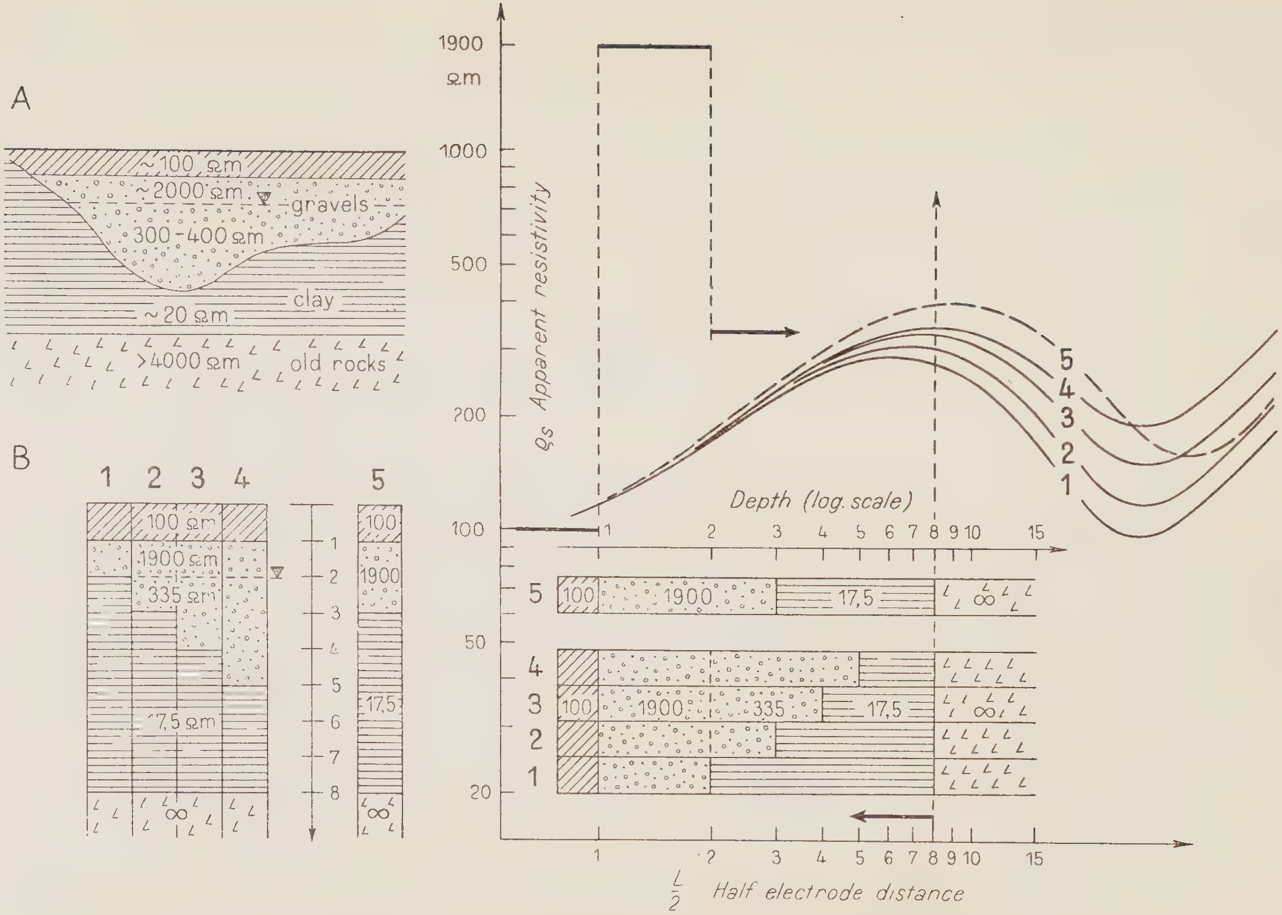

Fig. 6. Example No 2: Model graphs concerning a hydro-geological problem.

Fig. 6. A trough filled with gravels cuts into clayey sediments overlying old rocks; the gravels are covered by clayey sands. The problem is to determine the thickness of the permeable gravels; it is possible that they do not lie completely in the groundwater.

In order to get a general idea of the possibilities of performing an electrical investigation, empirical values were introduced for the conductance of the individual horizons, and model graphs were calculated for the profiles given under *B*. The graphs are plotted on the right in Fig. 6, the data α_i and $\varkappa_i$ of the decomposition, calculated wih the slide-rule, being shown in the following table:

graph No	α_1 $\varkappa_1$	α_2 $\varkappa_2$	α_3 $\varkappa_3$	α_4 $\varkappa_4$	α_5 $\varkappa_5$	$\Sigma\, \alpha_i$
1	0,0285 + 1,0	0,968 + 0,9	0,0029 + 0,494	0,0005 — 0,502	0,0001 — 1,0	1,0000
2	0,0336 + 1,0	0,957 + 0,913	0,0015 + 0,317	0,0026 — 0,78	0,0064 — 1,0	1,0011
3	0,0412 + 1,0	0,934 + 0,924	0,0109 + 0,085	0,0151 — 0,244	0,0001 — 1,0	1,0013
4	0,0528 + 1,0	0,894 + 0,932	0,0487 + 0,337	0,0026 — 0,504	0,0028 — 1,0	1,0009
5	0,0339 + 1,0	0,94 + 0,949	0,0015 + 0,307	0,0 — 0,806	0,025 — 1,0	1,0004

With a uniform cover and horizontal groundwater level, the downward slope of the valley floor is indicated by the upward slope of the curve minima. The differences are not very large, because the badly conducting gravels considerably influence the form of the curve by giving it a striking maximum. The comparison curve No 5 shows that for this particular region the curves are extremely sensitive to an alteration of the ratio: depth of the groundwater level/thickness of the top stratum. This ratio is 2 : 1 at he curves 1-4, and 3 : 1 at curve No 5 in Fig. 6. It can be seen that with minor variations of this thickness ratio the solution of the problem of the thickness of the permeable bed becomes questionable, and more so when resistivity variations in the individual horizons have to be considered.

As an example of the numerical calculation of a 5-layer case with 8 layer units, the graph No 4 is computed below; the course of the calculation runs according to § 7.

$$\begin{array}{llll}
h_1 = 1 & k_1 = +0{,}9 & P(u) = & k_1 u^{h_1} + k_2 u^{h_2} + k_3 u^{h_3} + k_4 u^{h_4} + k_1 k_2 k_3 u^{h_3 - h_2 + h_1} + k_1 k_2 k_4 u^{h_4 - h_2 + h_1} \\
h_2 = 2 & k_2 = -0{,}7 & & + k_1 k_3 k_4 u^{h_4 - h_3 + h_1} + k_2 k_3 k_4 u^{h_4 - h_3 + h_2} \\
h_3 = 5 & k_3 = -0{,}9 & H(u) = & 1 + k_1 k_2 u^{h_2 - h_1} + k_1 k_3 u^{h_3 - h_1} + k_1 k_4 u^{h_4 - h_1} + k_2 k_3 u^{h_3 - h_2} + k_2 k_4 u^{h_4 - h_2} \\
h_4 = 8 & k_4 = +1 & & + k_3 k_4 u^{h_4 - h_3} + k_1 k_2 k_3 k_4 u^{h_4 - h_3 + h_2 - h_1}
\end{array}$$

$$H + P = (1 + u^8) + 0{,}27\,(u + u^7) - 0{,}7\,(u^2 + u^6) - 0{,}27\,(u^3 + u^5) - 0{,}486u^4$$
$$H - P = (1 - u^8) - 1{,}53\,(u - u^7) + 0{,}7\,(u^2 - u^6) - 0{,}27\,(u^3 - u^5)$$

$$p(z) = z^4 + 0{,}27\,z^3 - 4{,}7\,z^2 - 1{,}08\,z + 3{,}157$$
$$q(z) = (z^3 - 1{,}53\,z^2 - 1{,}3\,z + 1{,}26)\,(z^2 - 4)$$
$$q'(z) = 5z^4 - 6{,}12\,z^3 - 15{,}9\,z^2 + 14{,}76\,z + 5{,}2$$

roots $z_i = 2x_i$;

$z_1 = +\ 2{,}0$

z	1	− 1,53	− 1,3	+ 1,26
+ 1,9		+ 1,9	+ 0,703	− 1,134
	1	+ 0,37	− 0,597	+ 0,126
+ 1,86		+ 1,86	+ 0,614	− 1,275
	1	+ 0,33	− 0,686	− 0,015
z_2 = + 1,864		+ 1,864	+ 0,623	− 1,262
	1	+ 0,334	− 0,677	− 0,002

$$z^2 + 0{,}334\,z - 0{,}677 = 0$$
$$z_{\substack{3\\4}} = -0{,}167 \pm \sqrt{0{,}028 + 0{,}677}$$
$$z_3 = +0{,}673$$
$$z_4 = -1{,}007$$

weights $\alpha_i = p(z_i)/q'(z_i)$:   Dar Zarrouk parameter: $C = 1 + 1/19 + 3/3{,}35 + 3/0{,}1768 = 18{,}91$

$\alpha_1 = 1/C = 0{,}05285$

z_i	$p(z)$					$q'(z)$					$\alpha_i = \frac{p(z_i)}{q'(z_i)}$	$x_i = z_i/2$
	+ 1	+ 0,27	− 4,7	− 1,08	+ 2,914	+ 5	− 6,12	− 15,9	+ 14,76	+ 5,2		
+ 2,0		+ 2	+ 4,54	− 0,32	− 2,8		+ 10	+ 7,76	− 16,28	− 3,04	0,0528	+ 1,0
	+ 1	+ 2,27	− 0,16	− 1,4	+ 0,114	+ 5	+ 3,88	− 8,14	− 1,52	+ 2,16		
+ 1,864		+ 1,864	+ 3,98	− 1,343	− 4,515		+ 9,32	+ 5,97	− 18,51	− 6,99	0,894	+ 0,932
	+ 1	+ 2,134	− 0,72	− 2,423	− 1,601	+ 5	+ 3,2	− 9,93	− 3,75	− 1,79		
+ 0,673		+ 0,673	+ 0,634	− 2,735	− 2,568		+ 3,365	− 1,86	− 11,94	+ 1,9	0,0487	+ 0,337
	+ 1	+ 0,943	− 4,066	− 3,815	+ 0,346	+ 5	− 2,755	− 17,76	+ 2,82	+ 7,1		
− 1,007		− 1,007	+ 0,742	+ 4,01	− 2,952		− 5,035	+ 11,22	+ 4,71	− 19,6	0,0026	− 0,504
	+ 1	− 0,737	− 3,958	+ 2,93	− 0,038	+ 5	− 11,155	− 4,68	+ 19,47	− 14,4		
− 2,0		− 2	+ 3,46	+ 2,48	− 2,8		− 10	+ 32,24	− 32,68	+ 35,84	0,0028	− 1,0
	+ 1	− 1,73	− 1,24	+ 1,4	+ 0,114	+ 5	− 16,12	+ 16,34	− 17,92	+ 41,04		

control: $\Sigma = 1{,}0009$

$\rho_1 = 100$ $r = L/2$

x_i	$\rho_1\,\alpha_i$	1	1,5	2	2,5	3	4	5	6	8	10	12	15	20	25	30	40	50	60
+ 1,0	5,28	6,5	8,3	10,7	13,2	15,8	21,1	26,4	31,7	42,2	52,8	63,3	79,2	106	132	158	211	264	317
+ 0,932	89,4	106,4	131,4	161	189	215	257	283	298	302	282	250	197	113	64,5	33	8,5	1,8	
+ 0,337	4,9	5,1	5,2	5,2	5,1	4,7	3,8	2,8	2	0,9	0,4	0,1							
	$\rho_s =$	118,0	144,9	176,9	207,3	235,5	281,9	312,2	331,7	345,1	335,2	313,4	276,2	219	196,5	191	219,5	265,8	317

The entire calculation just shown, for which only a normal slide rule was used, requires 1-1¼ hours, which is hardly more than would be required for the measuring of such a curve in the field.

11. *Example No 3*

The example shown in Fig. 7 originates from work concerning the search for and the delimination of clay deposits, by aid of geo-electrical measurements; it refers to the northern Hümmling in the Ems region, where over a clay deposit curves were obtained which, in general, did not show ideal minima. It had to be concluded that sandy intercalations were present. One single intercalated horizon would produce a 5-layer case, the interpretation of which by a catalogue of 3-layer graphs would be certain to fail. As the substratum of he basin clay consists of very pure sands and gravels, in part lying above

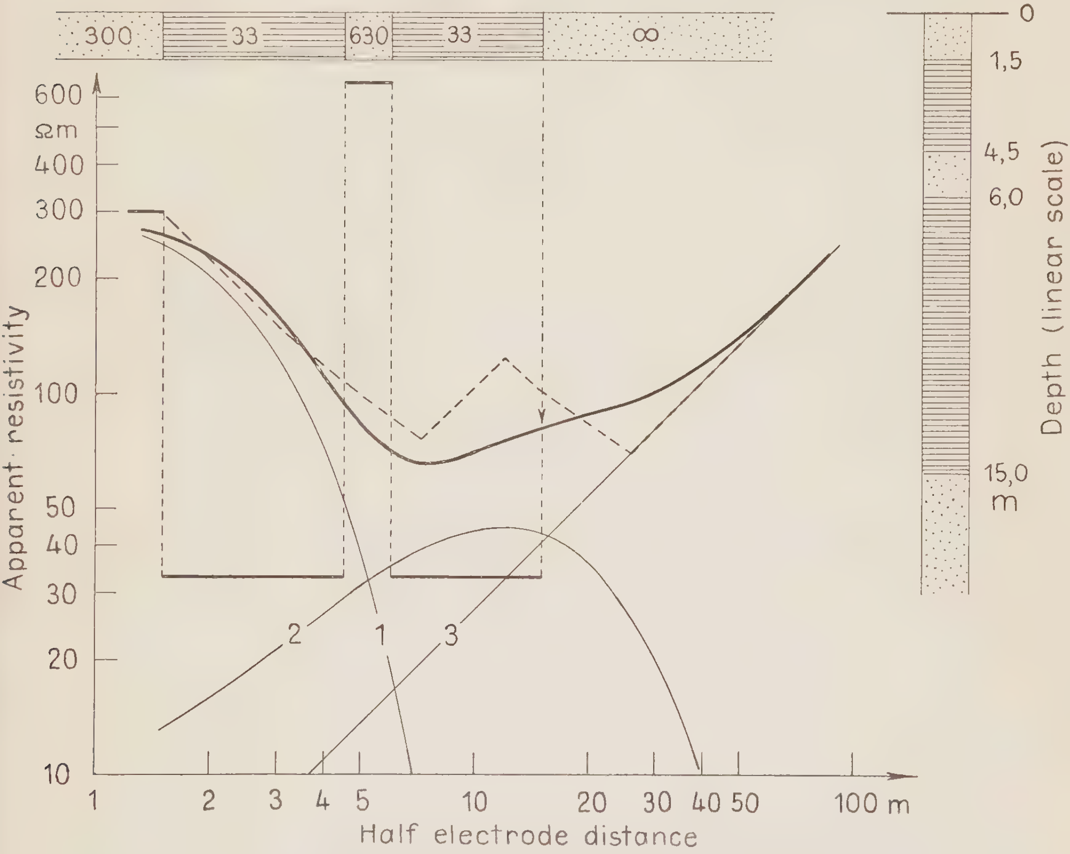

Fig. 7. Example No 3: Clay deposits with an interbedded sandy horizon (5-layer case).

the groundwater level, the recorded resistivity curves show a positive slope of nearly 45° at the end branch. The conditions, therefore, are very favourable for the application of our calculation method. By variation of depth, thickness and resistivity of the intercalated sandy horizon, it is possible to find the model graphs appropriate to many measured curves, and thus get a clear idea of the underground structure; this was by no means possible with the auxiliary point interpretation methods. In this particular case, the profile shown on the right of Fig. 7 has been taken as starting point. The appropriate theoretical graph has been obtained by superposition of 6 prime elements, three of which can be neglected because their weights are too small. This example shows clearly that, although with an increasing degree of the denominator polynomial the number of zeros will increase, only a few of them will provide a noticeable contribution. To illustrate this fact, the curves $p(z)$, $q(z)$ and $q'(z)$ are represented in Fig. 8.

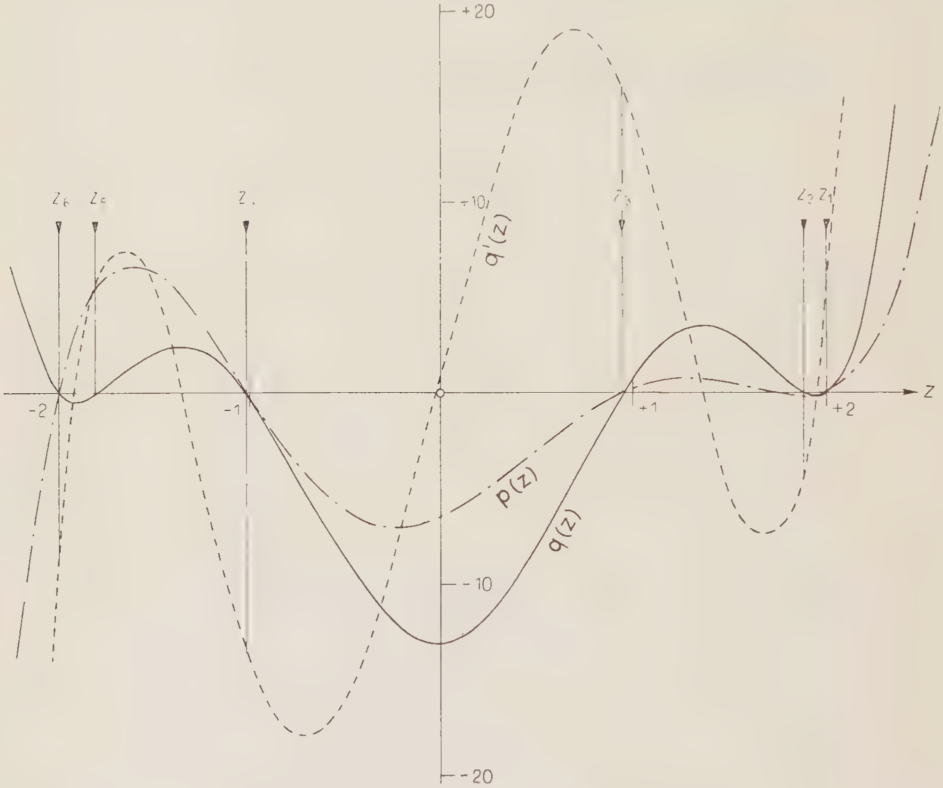

Fig. 8. The symmetrizised polynomials to the model graph of the example No 3.

The data of the decomposition are given in the following table:

$$\begin{array}{ll|l} h_1 = 1 & k_1 = -0{,}8 & p(z) = z^5 - 1{,}61\,z^4 - 5{,}072\,z^3 + 8{,}06\,z^2 + 4{,}316\,z - 4{,}46 \\ h_2 = 3 & k_2 = +0{,}9 & \\ h_3 = 4 & k_3 = -0{,}9 & q(z) = (z^4 - 0{,}01\,z^3 - 4{,}368\,z^2 - 0{,}16z + 3{,}268)\,(z^2 - 4) \\ h_4 = 10 & k_4 = +1 & \end{array}$$

α_i	0,0136	0,04	0,001	0,0004	0,941	0,004
$\varkappa_1$	+ 1,0	+ 0,943	+ 0,473	— 0,507	— 0,903	— 1,0

This example, shows how the three prime curves provided with different

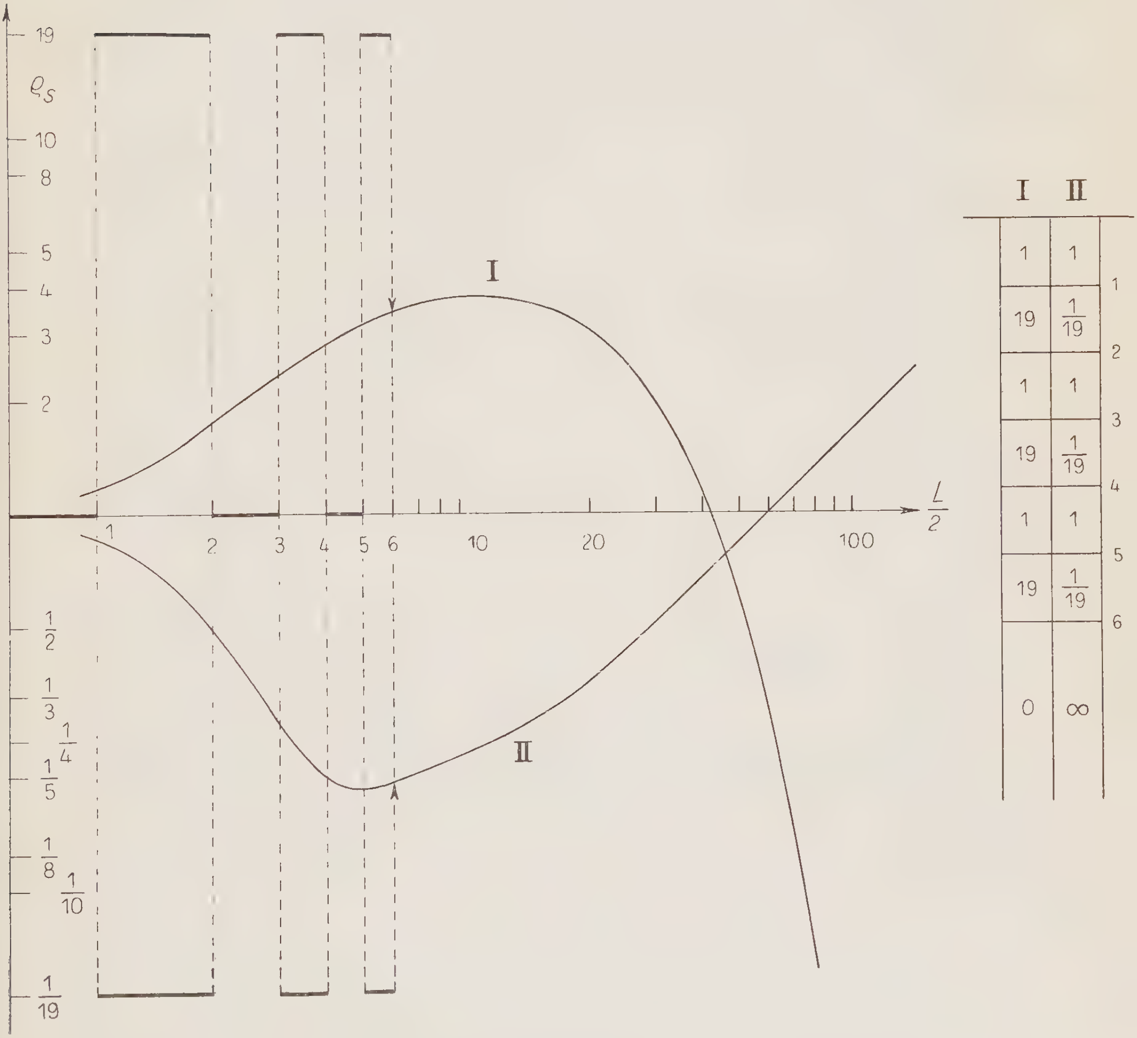

Fig. 9. Example No 4: Theoretical graphs over an interbedding of good and bad conductors (7-layer case).

weights determine the form of the 5-layer graph; each of the partial curves models a certain section of the entire curve. The plotted model graph is exact; the importance of possessing such exact graphs for comparison is shown by the Dar Zarrouk curve (dotted line), calculated for this example according to MAILLET, 1947, from which a much more characteristic sounding graph would have been expected.

12. *Example No 4*

The example shown in Fig. 9 has not been taken from practice: it is meant to illustrate anisotropy and the principle of equivalence, as they occur in an interbedding of good and bad conductors of equal thickness. Cases have been computed for 6 layers, with conductivity discontinuities of 1 : 19 ($k = \pm 0{,}9$), in one case overlying a perfectly conducting, and in the other case a perfectly insulating substratum. Both curves are exact and they give a good illustration of the resolving power of the geo-electrical method. For the decomposition result the following data:

graph No	α_1 $\varkappa_1$	α_2 $\varkappa_2$	α_3 $\varkappa_3$	α_4 $\varkappa_4$
I	0,52716 + 0,98065	0,35596 + 0,8491	0,11688 + 0,68975	
II	0,016667 + 1	0,026247 + 0,905	0,009718 + 0,715	0,947368 — 1

In this special case, which is mainly of theoretical interest, the calculation was carried out in 6 figures, after setting $p(z)$ and $q(z)$ according to the scheme under 7. I.

REFERENCES

Deppermann, K., 1955: On the calculation of resistivity curves, to be published in *Geophysical Prospecting,* III, 4.

Maillet, R., 1947: The fundamental equations of electrical prospecting, *Geophysics,* 12, 529-556.

Stefanescu, S., C. et M. Schlumberger, 1930: Sur la distribution électrique potentielle autour d'une prise de terre dans un terrain à couches horizontales, homogènes et isotropes, *Journal de Physique et le Rad.*, VII, 1, 132-140.

BOOK REVIEW

H. FAUL. — Nuclear Geology. A Symposium on Nuclear Phenomena in the Earth Sciences. John Wiley and Sons, Inc., New York, 1954. Price $ 7.00.

The release of nuclear energy has already been applied in geology nearly ever since it has been known. The process of emitting alpha, beta and gamma radiation in the uranium and thorium series has been used and is being used in geology for age determinations. The results of these determinations were not very accurate due to lack of fundamental knowledge. Although in the course of time further improvements were made, it is only during the last 10 to 15 years that physicists and chemists have made great progress in the understanding of the nuclear processes. Applications of these processes have been made in all directions and it was a good idea of the editor to compile all information relevant to geology together in one book, except the geology of stable isotopes, as this was already extensively covered in some other books.

In reading this book two points stand out quite clearly; firstly: the main application is still in the field of age determinations, and secondly: the amount of work is still too small and many of the underlying assumptions have not yet been proven fully in most cases to come to definite conclusions.

The book begins with an introduction to nuclear physics. The subject matter treated in the book requires such an introduction but it has been kept simple and short.

Then a few chapters are devoted to the occurrence and distribution of uranium, thorium and other radioactive elements in different types of rocks and oceans. Nothing, however, is mentioned of the geographical distribution of the main occurrences of the various radioactive minerals.

A good chapter on heat produced by radioactive elements and its implications on the theory of the "cooling earth" follows, much of which is speculative. Many more data on heat conductivity and thermal gradients are necessary.

In the chapter on Radiation Damage and Energy Storage some more information could perhaps be given of the use of X-ray diffraction technique and of thermoluminescence for correlation purposes.

The next chapter gives a short account of a previous A.P.I. project on the effect of radioactivity in the genesis of petroleum, the result of which was that hydrocarbons are formed by the effect of radioactivity but the amounts are far too small.

The application of radioactivity as a geophysical tool is two-fold; as a surface method and as a well logging method. A good analysis is given of the factors influencing the readings in the case of surface prospecting, showing that gamma ray intensity maps without the proper corrections may be very misleading.

The determination of absolute age is the most important chapter of the whole book. It gives a short but very useful account of every method in use for age determination with its advantages and disadvantages. The main points for inaccuracy are: leakage, contamination, migration and leaching. Included in this chapter is a very useful table of age determinations in order of increasing age (the older measurements have been discarded as being too inaccurate).

The book concludes with a short chapter on the origin of the earth.

As a whole the editor has succeeded in bringing out a good book which will interest the graduate student and the practising professional geologist for whom it is intended. The symposium form of this book has its disadvantages, as it does not make for easy reading, but it gives up-to-date information on the different aspects. The book also clearly outlines and indicates what is factual infomation and what still requires proof.

Printing and figures are, as usual, very clear.

B. B.

E.A.E.G. ABSTRACT SERVICE

EXPLORATION — GENERAL

119. *Geophysical Management looks at Safety as a Public Relations Factor.*
C. H. Green, a paper read at the 7th Annual Midwestern Meeting of the S.E.G., Dallas, Texas, November, 1953. (Not yet published).

The public relations value of a good safety programme is stressed. Public relations is not just something that can be turned on and off at will — every company in every industry has it — whether it is wanted or not.

It has only recently become clearly appreciated that every safety activity has public relations value — good or bad. Just doing a good job on safety is not enough; the job is not complete untill the public and clients are made aware of the fact.

A worthy objective of safety then should be to create the most favourable human relations possible. The prevention of accidents by inreasing safety activity within the industry is but one of the factors leading to betterment of public and employee relations within the geophysical exploration industry.

120. *The Application of Geophysical Methods in New Brunswick.*
S. H. Ward, a paper read at the Eastern Meeting of the S.E.G., Boston, Mass., December, 1953. (Not yet published).

A brief discussion concerning the applicability and limitations of several geophysical methods in New Brunswick is presented. An assessment is given of the use of the airborne magnetic, ground magnetic, electromagnetic, electrical resistivity, self-potential, and geochemical methods in the exploration for economic deposits of sulphide mineralization. A general discussion of the future applications of geophysical techniques in New Brunswick concludes the article.

121. *What's New in Geophysics.*
W. M. Rust, World Oil, Vol. 138, No. 5, pp. 80-88, April, 1954.

A review of geophysical developments over the past two years. The principal subjects are: multiple geophones and pattern shooting, offshore seismic prospecting, surveying, magnetic recording, and electronic computers.

122. *Highly Skilled Professionalism.* by J. N. Walstrum. *Confidence and Patience.* by C. H. Green. World Oil, Vol. 138, No. 5, pp. 100-104, April, 1954.

General articles on what an oil company and its geophysical contractor can reasonably expect of each other. The two authors represent opposite sides of the question.

123. *Geophysical Activity Drops in U.S., Canada.*
S. Hammer, Oil & Gas J., Vol. 52, No. 50, pp. 147-150, April 19, 1954.

Throughout the World, in 1953, 1,100 geophysical crews were in operation. They included 941 seismic, 129 gravity, 19 magnetic and 16 other methods. Charts show the distribution of activity, by countries, for the U.S. and for the World. Graphs show monthly variations of activity in the U.S. and Canada over the past ten years.

124. *Geophysical and Geological Investigations in the Gulf of Mexico.*
M. Ewing, J. L. Worzel, D. B. Ericson & B. C. Heezen, a paper read at the Annual Meeting of the S.E.G., at St. Louis, 1954. (Not yet published).

In 1953 the research vessels Vema and Atlantis spent about 3 weeks in the Gulf of Mexico. Coring, seismic refraction, and topographic studies were undertaken. The results point to the southern half of the Gulf as a typical ocean basin with a profound change at the foot of the continental slope. Many sediment cores longer than 30 feet were taken in the Sigsbee deep. The abrupt change separates approximately 3 feet of recent sediments from Wisconsin in which all cores ended.

125. *Our Expanding Horizons.*
R. L. Lay, Geophysics, Vol. 19, No. 2, pp. 191-201, April, 1954.

Exploration assignments today are more challenging than ever before. The emphasis is on smaller structures and more accurate and deeper interpretations. Many of the more difficult areas, formerly not considered amenable to geophysical exploration, reveal a similarity of problems in widely separated geological and geographical provinces. Geologists and geophysicists are continually broadening their view-points because they realize more and more that few areas are unique.

Geophysics has made and is continually making substantial contributions to basic geology. Exploration thinking is broadening steadily toward more definite evaluation of the many types of oil-bearing traps.

Explorationists are learning the principles of sound business risk and thereby expanding their horizons by becoming good business men as well as highly trained specialists. The opportunity to expand our horizons further was never more promising than at the present. (Author's Abstract).

126. *Current Status of Marine Exploration.*
C. H. Johnson, a paper read at the 7th Annual Midwestern Meeting of the S.E.G., Dallas, Texas, November, 1953. (Not yet published).

Marine exploration for oil is expanding and promises to expand further, even though land exploration may be in a period of adjustment. Political weather is favourable for such expansion; geological factors are highly promising and continued maintenance of reserves demands such expansion. Technical advances in the art of marine exploration and in marine drilling make such expansion logical and feasible.

127. *Oil Exploration in the French Union.*
Petroleum Times, Vol. 58, No. 1488, pp. 859-861, August 20, 1954.

A concise but comprehensive history is given of the exploration for oil in France and her overseas territories, from the pre-war Pechelbronn fields production onwards. The more important concession companies are mentioned, with details of their operating areas and production figures.

SEISMIC — GENERAL

128. *Seismic and Gravity Investigations on the Malaspina Glacier, Alaska.*
C. R. Allen & G. I. Smith, Am. Geophys. Un. Trans., Vol. 34, No. 5, pp. 755-60, 1953.

During July and August 1951, seismic and gravity surveys were made on the Malaspina Glacier, southeastern Alaska, to determine the thickness of the ice and the configuration of the subglacial floor. Seismic reflections along a 10-mile profile approximately parallel to the assumed direction of ice flow indicate ice thicknesses ranging from 1,130 to 2,050 feet. The subglacial floor is below sea level along the entire profile, 700 feet below in the central part. The ice becomes thinner northward toward the mountains and southward toward the ice margin. Gravity measurements along the central 3 miles of the seismic profile indicate the trend of subglacial topographic features is northwest-southeast. Seismic refraction measurements beyond the glacial margins indicate that the proglacial deposits are more than 500 feet thick. (From Geophysical Abstracts 155, U.S. Geol. Survey).

129. *Mapping Water-Saturated Sediments by Sonic Methods.*
W. O. Smith & H. B. Nichols, Sci, Monthly, Vol. 77, No. 1, pp. 36-41, 1953.
A new method of geophysical investigation is based on the velocity with which sound waves of very low frequency penetrate water-saturated sediments. The instrumentation is based on the sonar principle, using a sonic signal given off by a transducer slung out over the side of a vessel.
(From Geophysical Abstracts 155, U.S. Geol. Survey).

130. *Doodlebuggers Afloat.*
W. H. Newton, World Petroleum, Vol. 25, No. 2, pp. 32-35, February, 1954.
Since the U.S. Tidelands dispute was recently settled in favour of state ownership, seismic reflection crews have been very active in the Gulf of Mexico, especially off the coasts of Texas and Louisiana. The planning, outfitting, and operations of a typical party are described.

131. *Seismic Refraction Measurements in the Atlantic Ocean, part VI: Typical Deep Stations, North America Basin.*
M. Ewing, G. H. Sutton, & C. B. Officer, Jr., Bull. Seismol. Soc. Am., Vol. 44, No. 1, pp. 21-38, January, 1954.
In the Spring of 1951, 33 deep-sea refraction stations were made by members of the Lamont Geological Observatory, Columbia University, on the research vessels Atlantis and Caryn of the Woods Hole Oceanographic Institution. This paper contains the results of six of these stations, three of which were made in the region to the south of Bermuda and three in the region to the northwest of Bermuda. The crustal structure reported in this paper is considered to be typical of the crust of the western North Atlantic.

132. *Seismic Problems in Williston Basin.*
J. A. Kornfeld, Oil & Gas J., Vol. 52, No. 50, pp. 196-200, April 19, 1954.
The subsurface and surface geological characteristics of the area are summarised, with notes on regional deformations. The quality of records generally obtained is good in most areas, but there are certain field problems, such as localised thick Tertiary and Quarternary cover, which necessitate deep drilling of shot-holes.
A table is given of wells shot for velocity in the Williston Basin, showing the date and depth of survey in each case.

133. *Geophysical Costs Go up as Profits Sag.* by C. W. Smith.
How to Cut Seismic Exploration Costs. by N. Clayton.
Experimental Crews Can Cut Seismic Exploration Costs. by R. M. Bradley.
World Oil, Vol. 138, No. 5, pp. 90-98, April, 1954.
Three general articles on reduction of the cost of seismic exploration.

134. *Velocity Measurements in Shotholes in Northern Germany.*
T. Krey & G. Teudesmann, Erdöl und Kohle, Heft 9, pp. 548-550, September, 1954.

SEISMIC — INSTRUMENTAL

135. *Response Curves of an Electromagnetic Seismograph by Sine-Wave Simulator Method.*
L. M. Murphy, R. M. Wilson, L. R. Burgess, & T. H. Pearce, Bull. Seismol. Soc. Amer., Vol. 44, No. 1, pp. 7-19, January, 1954.
Little is known of the response characteristics of electrical-type seismographs, since most of the data are derived from theoretical assumptions. Experiments here described have shown that if a harmonic motion is impressed on a seismometer boom by means

of a sine-wave simulator, the resultant motion can be recorded with measurable amplitudes. This permits a relationship to be established between ground movement and galvanometer readings of the seismograph.

136. *New Exploration Tool.*
Oil & Gas J., Vol. 52, No. 47, pp. 61, March 29, 1954.

Continuous velocity logging can now be carried out using a new sonic tool. The continuous-logging tool contains both a transmitter and receiver, separated by an insulator, and generates and records pulses at such a rate that it obtains a continuous record. A brief description ef the construction and function of the tool is given.

137. *Patents.*
Abstracts in Geophysics, Vol. 19, No. 2, p. 323, April, 1954.

U.S. 2,656,422.	20 October, 1953.	Gain control system for seismic amplifiers.
U.S. 2,657,373.	27 October, 1953.	Apparatus for eliminating ground roll.
U.S. 2,657,374.	27 October, 1953.	Suspension system for seismometers.
U.S. 2,658,578.	10 November, 1953.	Seismic system in which the three components of ground motion are recorded on separate traces.
U.S. 2,658,579.	10 November, 1953.	Apparatus for analysing a group of seismic records.
U.S. 2,659,064.	10 November, 1953.	A variable air-gap condenser type rotational seismometer.
U.S. 2,659,065.	10 November, 1953.	Suspended-coil seismometer.
U.S. 2,661,464.	1 December, 1953.	Seismic recording system in which dip of the reflecting horizon is indicated on the record.
U.S. 2,662,126.	8 December, 1953.	Seismic amplifier mixing circuit.
U.S. 2,663,002.	15 December, 1953.	Attenuator for seismic gain control.

138. *Problems in the Application of Transistors to Seismic Equipment.*
R. W. Olson, a paper read at the 7th Annual Midwestern Meeting of the S.E.G., Dallas, Texas, November, 1953. (Not yet published).

Brief general theory of operation of transistors, movement of current carriers through crystal lattices, limits to vacuum tube analogy, circuit elements, parameters, amplifier configurations, performance characteristics and possibilities, and future possibilities are discussed.

139. *The Electrical Aspects of Connecting Geophones in Multiple.*
L. W. Erath, a paper read at the 7th Annual Midwestern Meeting of the S.E.G., Dallas, Texas, November, 1953. (Not yet published).

This paper discusses, broadly, electrical problems of impedance matching between geophones and input circuits of geophysical amplifiers. It deals more specifically with the effect on energy transfer, frequency response, and damping of using a large number of geophones. Response curves and circuit diagrams are presented. No reference is made to the seismic considerations of multiple geophones.

140. *What about Reproducible Seismic Recording?*
K. Beeman, World Oil, Vol. 138, No. 5, pp. 86-88, April, 1954.

A manufacturer's appraisal of the future of magnetic tape recording systems. Whilst the initial outlay is expensive it is estimated that, eventually, survey costs will be lowered using this equipment.

141. *Adjustable Magnetic Control for Seismographs.*
J. J. Dowling, J. Sci. Instr., Vol. 31, No. 6, pp. 222, June, 1954.

A magnetic spring control permits the adjustment of a seismograph pendulum without touching it. It is applicable to almost any type of seismograph, vertical or horizontal.

SEISMIC — FIELD TECHNIQUE

142. *New Seismic Tool.*

W. P. Sterne, Oil & Gas J., Vol. 52, No. 46, pp. 106-7, March 22, 1954.

A new seismic method has been developed in which an integrating recorder takes soundings from a 6,000 lb. weight dropped by a special truck. The recorder integrates the vertically travelling events but tends to suppress the undesirable horizontal events.

Among the advantages of this — the Geograph — method are: soundings can be more widely scattered and thus better records obtained; costs are less since no drilling or dynamite is necessary; the method is speedier; no set pattern is required for the soundings.

143. *Symposium on Current Seismic Techniques Used in Pattern Shooting.*

B. F. Rummerfield, A. E. McKay, J. W. Hammond, & F. F. Reynolds, Oil & Gas J., Vol. 52, No. 50, pp. 136-146, April 19, 1954.

An introductory article, "Why This Symposium?", by B. F. Rummerfield, puts the point of view of the two schools of thought that exist to explain the efficacy of multiple geophone techniques, and makes certain generalisations concerning the method.

"Record-Improvement in Bad Reflection Areas", by A. E. McKay, discusses the improved records obtained in two areas where poor record quality is attributed to near-surface high frequency interference.

"How to Recognize and Eliminate Record Disturbances", by J. W. Hammond, concludes, from several discussed examples, that properly spaced multiple geophones will reduce interfering energy, and that multiple holes improve signal-tonoise ratio.

The final article of the symposium is an evaluation of "Design Factors for Multiple Arrays of Geophones", by F. F. Reynolds.

144. *Recording of Seismic Waves in Bore Holes.*

E. T. Howes, a paper read at the Annual Meeting of the S.E.G., at St. Louis, 1954. (Not yet published).

Reflected and refracted seismic waves are normally detected by a horizontal spread of geophones placed at the surface of the ground. However, these same seismic waves can be detected by a vertical spread of geophones suspended in a fluid-filled bore hole. Equipment specially designed for use as a vertial spread in shallow bore holes is described. Sample records are shown. The relative advantages and operating problems are also discussed.

145. *Patents.*

Abstracts in Geophysics, Vol. 19, No. 2, p. 322, April, 1954.

U.S. 2,654,874.	6 October, 1953.	Seismic recording system in which the effect of ground roll is cancelled in pickup of the airborne wave.
U.S. 2,656,003.	20 October, 1953.	Seismic system where a grooved explosive disc is detonated above the ground.

146. *Review of Pattern Shooting.*

A. E. McKay, a paper read at the 7th Annual Midwestern Meeting of the S.E.G., Dallas, Texas, November, 1953. (Not yet published).

Patterns of shot holes and patterns of seismometers are now standard technique in many areas currently being surveyed by seismograph. This paper reviews some of these pattern arrangements and shows comparison records in a number of areas such as New Mexico, West Texas, western Oklahoma, Mississippi, and others. Pattern shooting is a useful technique but is by no means a cure-all.

SEISMIC — INTERPRETATION

147. *Time Method of Migrating Steep Dips.*

R. B. Rice, a paper read at the 7th Annual Midwestern Meeting of the S.E.G., Dallas, Texas, November, 1953. (Not yet published).

This paper presents a time-resolution method of performing reflection seismograph computations which is particularly useful in steep-dip areas. Two of the principal advantages of this method are that it is simple and fast to use and that it allows the use of any desired velocity gradient or the rapid change from one velocity function to another. In addition, examples of actual cross sections computed by this method are presented.

148. *Different Basic Assumptions for Weathering Corrections.*

E. J. Handley, a paper read at the 7th Annual Midwestern Meeting of the S.E.G., Dallas, Texas, November, 1953. (Not yet published).

The mathematical computations involved in making weathering corrections are commonly based on the assumption that the near-surface sedimentary rocks are stratified into rather well defined "layers", with velocities of longitudinal seismic waves being considered as a constant for each layer. The basic data used in making weathering corrections are the measured values for first arrival refraction times and distances, and up-hole times and depths. It is shown that the assumption can be made that the velocity continuously increases with depth, and that when layers occur, they may be considered zones in which the velocity increases at different rates. It is pointed out that the basic data may fit such assumptions equally well. The assumption by Blondeau that the velocity $V_Z = CZ^{1}/n$ is discussed and some of the mathematical relationships involved are shown to be so simple that they can easily be applied to making weathering corrections.

149. *Evalution of Linear Operators in Seismogram Analysis.*

E. A. Robinson, a paper read at the Eastern Meeting of the S.E.G., Boston, Mass., December, 1953. (Not yet published).

The usefulness of linear operators in the analysis of seismograms is dependent among other considerations on geologic and mathematical limitations.

Certain of the more significant limitations are discussed and illustrative examples on seismic records are shown.

150. *Reflection Quality, a Fourth Dimension.*

B. F. Rummerfield, a paper read at the Annual Meeting of the S.E.G., at St. Louis, 1954. (Not yet published).

The quality of seismic reflection results has a direct relation to newer petroleum provinces in the North American Continent. An approach is suggested whereby a local seismic study of changes of physical characteristics of subsurface reflecting horizons can be attempted. The changes in the quality of deeper reflecting horizons in relation to a persistent shallow, or "control", horizon may be able to add a fourth dimension to present seismic interpretations.

151. *Devices for the Construction of Refracted Rays.*

R. Vajk, Geophysics, Vol. 19, No. 2, pp. 237-241, April, 1954.

Simple devices constructed from such readily obtainable items as triangles, protractors, plastic rulers, and steel straight edges are described for the graphical solution of two problems which often arise in seismic computations. One problem is to find the minimum-time path between two points located in media with different seismic velocities separated by a plane interface. The other is to find the refracted ray where the incident ray to an interface and the velocities of the media on either side are known.

(Author's Abstract)

152. *Determination of Dips and Depths of Geological Layers by the Seismic Refraction Method.*

L. Mota, Geophysics, Vol. 19, No. 2, pp. 242-254, April, 1954.

Equations are developed for computing depths and dips of 1, 2, 3, ...,n inclined interfaces from seismic refraction data without the aid of graphical techniques.

(Author's Abstract)

153. *Delta-t Formula for Obtaining Average Seismic Velocity to a Dipping Reflecting Bed.*

J. C. Pflueger, Geophysics, Vol. 19, No. 2, pp. 339-341, April, 1954.

A formula is derived for obtaining average velocity to a reflecting bed independent of the dip of the bed. For this velocity between two shot points it is shown that:

$$\overline{V} = x/\sqrt{T_3^2 - T_1T_2}$$

where $\overline{V}$ is the average velocity,

x is the distance between shot points,

T_1 and T_2 are the two-way normal times to the reflecting bed from the two shot points,

T_3 is the reflection time from one shot point down to the reflecting horizon and up to the other shot point.

When $T_1 = T_2$, the fomula becomes:

$$\overline{V} = x/\sqrt{T_3^2 - T_1^2} \text{ or } \overline{V} = x/\sqrt{\Delta T(2T_1 + \Delta T)}$$

which is the usual flat-bed delta-time formula.

SEISMIC — THEORY & RESEARCH

154. *The variation of the Elastic Constants of Rocks with Frequency.*

Dr. J. Bruckshaw & P. C. Mahanta, Petroleum, Vol. 17, No. 1, pp. 14-18, January, 1954.

A method has been developed for the measurement, in the laboratory, of the variation of the elastic properties of rocks, in the frequency range 40-120 c.p.s. In addition, the observations yield information concerning the internal dissipation of energy over this range. A number of rock specimens have been examined and the results are compared with those of other investigators.

155. *On the Seismic Effect of Deeply Set Explosive Charges. (In German).*

W. Muhlen, Geol. Jahrb., Band 66, pp. 425-432, 1952.

Seismic waves undistorted by secondary reflected or refracted waves were obtained by detonating charges at depths of 15, 200, 280, and 340 m in a drill hole. The resulting direct waves were recorded by a series of mechanical seismographs. The nearest of these, at 7200 m, gave quantitatively useful results. The first and only useful impulses in the seismograms showed a decrease in amplitude and increase in frequency with depth. The 15 m shot, only, indicated surface waves.

Further results indicate that frequency depends on depth of charge as well as on travel time and distance, as shown by Ricker. Mühlen suggests that the reason for this may be due to the propagation of elastic waves in material under differing degrees of compression.

(From Geophysical Abstracts 154, U.S. Geol. Survey).

156. *Seismic Model Study.*
E. T. Howes, L. H. Tejada-Flores & L. Randolph, J. Acoust. Soc. Amer., Vol. 25, pp. 915-921, Sept. 1953.

A method has been developed for studying seismic sound pulses in reduced scale models which simulate geophysical seismic exploration methods. Use is made of a tank of water for transmission of the acoustic wave from a source to a faulted limestone stratum and returning to a pressure sensitive receiver. Results obtained demonstrating the geometric aspects of the propagation, reflection, refraction and diffraction of sound pulses are described and illustrated on accompanying plates.

(From Physics Abstracts, Sec. A, January, 1954).

157. *Dispersive Properties of Stratified Elastic and Liquid Media: A Ray Theory*
I. Tolstoy & E. Usdin, Geophysics, Vol. 18, No. 4, pp. 844-870, October, 1953.

The interference principle of wave guide propagation is applied to the derivation of the period equations for a number of problems involving both elastic and liquid strata. In the case of undamped steady state propagation in a solid or liquid stratum two arbitrarily chosen points at the same depth must be indistinguishable on an amplitude basis. This well known principle combined with the knowledge of the reflection coefficients enables us to derive in a few simple steps the period equations for a number of multilayer cases which heretofore had been avoided on account of algebraic difficulties. The period equations obtained by this method exhibit a singular simplicity and unity of form. As a consequence of this one may distinguish formally the M1 and M2 waves discovered by Sezawa and understand their physical significance.

(Author's Abstract).

158. *On the Theory of Head Waves.*
P. A. Heelan, Geophysics, Vol. 18, No. 4, pp. 871-893, October, 1953.

When a combined longitudinal and transverse disturbance, diverging from a localized source, strikes a plane boundary between two solid elastic media, several systems of head waves and secondary boundary waves are generated, each associated with grazing incidence of one or the other of the reflected or refracted waves. Associated with grazing incidence of P_1P_2, the refracted P-wave, is the head wave system comprising $P_1P_2P_1$ (the "refracted wave" of seismic prospectors), and $P_1P_2S_1$ (a transverse head wave) in the upper medium, and $P_1P_2S_2$ (a transverse head wave) in the lower medium. There is no boundary wave in the lower medium. These three waves with the second-order term of P_1P_2 (the first-order term is zero on the boundary) satisfy conditions of continuity of stress and displacement at the boundary. Moreover, the energy of the three head waves is derived completely from the second-order component of P_1P_2, which possesses a component of energy flow normal to the boundary. The amplitudes of $P_1P_2P_1$, $P_1P_2S_1$ and $P_1P_2S_2$ are calculated for certain cases.

(Author's Abstract).

159. *The Underwater Spark as a Source of Sound Impulses.* (In German).
H. Drubba & H. H. Rust, Arch. Elect. Übertragung, 7, pp. 429-440, Sept., 1953.

Account of investigations into behaviour of sparks, produced by discharging a condenser charged to voltages between 0.5kV and 5kV, across an underwater spark-gap with a length of 0.1 or 0.3 mm. Results given include photographs, curves of current against time, and information about propagation of sound waves through the water.

(From Physics Abstracts, Sec. A, February, 1954).

160. *A Practical Example of an Anisotropic Velocity-Layer.*
J. G. Hagendoorn, Geophysical Prospecting, Vol. 2, No. 1, pp. 52-60, March, 1954.

The results obtained from a number of seismic velocity well-logging surveys and adjacent refraction sections are compared. The velocities derived by these two methods for a certain layer are found to differ appreciably. This is shown by presenting the time-depth relations of the well-surveys and the time-distance relations of the refraction sections at three locations, plotted on graphs with sloping depth- and distance-axes. (Author's Abstract).

161. *Extension to Three-Dimensional Problems Concerning an Approximate Correction Method for Refraction in Reflection Seismic Prospecting.*

T. Krey, Geophysical Prospecting, Vol. 2, No. 1, pp. 61-72, March, 1954.

The formulae derived by the author in a preliminary paper for taking into consideration refraction when dealing with the problem of a vertical plane are extended to the three-dimensional case. Vector analysis is extensively applied. Among others it is shown that in the general case the three horizontal two-dimensional vectors, i.e.

1) the gradient of the time of reflection,
2) the direction of true dip,
3) the vector from the shot point to the projection of the reflecting point, point into three different directions.

(Author's Abstract).

162. *The Refraction Arrival in Water Covered Areas.*

C. B. Officer, Jr., Geophysics, Vol. 18, No. 4, pp. 805-819, October, 1953.

A solution is given for the refraction arrival in water covered areas in terms of the evalution of a branch line integral for an impulsive point source. The physical significance of the mathematical solution is discussed, and an experimental verification of the theoretical predictions is presented. The character, frequency, and range dependence of the refraction arrival agree with theory.

Using the results of this theory and the conventional interpretation techniques for refraction seismograms, it is possible to determine the velocities and depths of the seismic refraction horizons from the record of a single receiver. The velocities of the refraction layers can be determined from the frequency of the refraction arrivals, the depth of water, and the velocity of sound in water. Then, from the travel times the depths of the horizons can be computed.

This method could be of importance in reconnaissance measurements of geologic structure over the continental shelves.

(Author's Abstract).

163. *Relations Between the Propagation of Longitudinal and Transverse Waves in Relaxation Media. I.* (In German).

W. Kuhn & S. Vielhauer, Z. Phys. Chem., Vol. 202, pp. 124-160, July, 1953.

A theoretical treatment is given of the velocity of propagation and absorption of longitudinal and transverse waves in an amorphous medium which changes from a vitreous solid state to a liquid state as the temperature is raised. Several cases are worked out on the basis of different assumptions regarding the relaxation processes. The bearing of these results on the nature of the earth's core is briefly discussed. (From Physics Abstracts, A, April, 1954.)

164. *Relations between the Propagation of Longitudinal and Transverse Waves in Relaxation Media. II.* (In German).

W. Kuhn & S. Vielhauer, Z. Phys. Chem., Vol. 202, pp. 161-190, Oct., 1953.

The velocities of longitudinal and transverse waves were measured in a resin at a range of temperatures passing through the softening point. A reduction in the longitudinal velocity at the softening point is explained by the relaxation of the shear stresses, associated with a 30% relaxation in the compressibility modulus. These observations are applied to a consideration of the properties of seismic waves in the earth's interior, with special reference to the discontinuity in the velocity of propagation at a depth of 2,900 km., and of the properties of the earth's core.

(From Physics Abstracts, A, April, 1954.)

165. *On the Indicator Equation of a Seismometer.* (In German).

M. Weber, Geofis. Pura e Appl., Vol. 23, pp. 1-5, 1953.

The indicator equation is the differential equation representing the relation between the oscillations of the mechanical system and the output voltage of a seismometer. The differential equations are derived, one controlling the oscillations of mechanical system, another determining the observed electric voltage as a function of the displacements of the mechanical system. From these two equations the final indicator equation is derived replacing the data on the stiffness of the system and its friction by values obtained from the observation of the decay of free vibrations of the system. An equivalent linear indicator equation is then calculated with these results.

(From Geophysical Abstracts 155, U.S. Geol. Survey).

166. *Third and Fourth Dimensions in Exploration.*

J. Daly, Bull. Am. Ass. Petr. Geol., Vol. 38, No. 2, pp. 319-332, Feb., 1954.

The trend in exploration toward the investigation of deeper and geologically more complex structures, necessitates a keener appreciation of the three-dimensional factors involved in evaluating them. For the deep structures, in which dips of 5° - 10° are common, it is necessary to migrate the dips to their true position. It is particularly necessary to do this with fault problems; otherwise, the fault trace may be mislocated by ½ mile or more.

By using some of the seismograph instruments at an angle to the line of shot holes, three-dimensional control can be obtained simultaneously with normal continuous profiling methods.

A seismograph interpretation of a faulted structure may be correct geometrically and may still not appear geologically sound until a fourth dimension, geologic time, has been added.

Closer co-operation between the geologist and geophysicist must eventually come, because it is an economic necessity.

(Author's Abstract).

167. *Laboratory Measurements of Seismic Velocities in Ocean Sediments.*

A. S. Laughton, Proc. Roy. Soc., Vol. 222, No. 1150, pp.336-341, 18 March, 1954.

Laboratory measurements have been made of the compressional wave velocities in samples of deep-sea sediments using ultrasonic methods. The variation of velocity with compaction pressure has been determined. From the results it has been concluded that a vertical gradient of velocity exists in the sedimentary layer of the ocean.

(Author's Abstract).

168. *An Oscillographic Method for Determining Velocities of Detonation in Explosives.*

F. C. Gibson, Rev. Sci. Instr., Vol. 25, No. 3, pp. 226-231, March, 1954.

The method and apparatus are described for determining velocities of detonation over one to five adjacent segments of an explosive charge. Time intervals are determined to the nearest 0.1 microsecond, which permits an accuracy of the order of 1 % where distances of 10 cm. are employed in 7,000 m./sec. explosives. Representative data are included to show the accuracy of the method as well as application techniques.

(Author's Abstract).

169. *Wave Propagation in a Randomly Inhomogeneous Medium. III.*

D. Mintzer, J. Acoust. Soc. Amer., Vol. 26, No. 2, pp. 186-90, March, 1954.

The coefficient of variation for a series of sound pulses and the correlation function for successively received sound pulses are evaluated for arbitrary pulse length, using the assumption that the correlation function of the refractive index inhomogeneities is expressible as the product of time- and space-dependent functions. For the case of pulse length much less than the time constant of refractive index correlation function, the coefficient of variaton is found to be independent of the pulse length, and the pulse correlation function is found to be identical with the time-dependent part of the refractive index correlation function. Comparison is made with data obtained from Sheehy. An approximate calculation shows that the motion of source and receiver will distort the pulse-correlation function so that little information can be obtained from the data concerning the time dependance of he refractive index.

(Author's Abstract).

170. *Measurements of Sound Absorption in Aqueous Salt Solutions by a Resonator Method.* O. B. Wilson, Jr., & R. W. Leonard, J. Acoust. Soc. Amer., Vol. 26, No. 2, pp.223-226, March, 1954.

This paper presents the results of measurements of the sound absorption in aqueous solutions of several salts. While magnesium sulphate is the salt of primary interest in this case, some results for sea water at different temperatures, solutions of magnesium acetate, zinc sulphate, and berillium sulphate are given. The frequency range of the measurements is approximately 50-500 kc. Although the resonator method used is not very precise, it is the only known laboratory method which is able to give reliable absorption measurements in water and water solutions in this low-frequency range where the sound absorption in these liquids is extremely small.

(Author's Abstract).

171. *The Backscattering of Sound from a Harbour Bottom.* R. J. Urick, J. Acoust. Soc. Amer., Vol. 26, No. 2, pp. 231-235, March, 1954.

When underwater sound strikes the bottom of the sea in shallow or deep water, a portion of its intensity is scattered back toward the source of sound. A study of the backscattering from the bottom as a function of pulse length, frequency, and tilt-angle at several locations in a harbour along the east coast of America, was made by using a tiltable transducer mounted on a barge. The results are expressed in terms of a quantity called the "scattering strength" of a unit area of bottom.

The results suggest that the backscattering of sound from a natural bottom is due more to its roughness rather than to the fact that it consists of sedimentary particles. Even at normal incidence the bottom of a sea or bay appears sufficiently rough so that little sound is returned by specular reflection. Some evidence in support of these conclusions is given.

(Author's Abstract).

172. *Wave Propagation in a Randomly Inhomogeneous Medium. I.* D. Mintzer, J. Acoust. Soc. Amer., Vol. 25, No. 5, pp. 922-27, September, 1953.

The propagation of sound pulses from a source in a medium where the index of refraction varies randomly is studied by means of the Born approximation to the wave equation. The coefficient of variation (standard deviation of the amplitude of a series of pulses, expressed as a percentage of the mean amplitude of the series) is evaluated for pulse lengths short compared with the time in which the refractive index varies significantly, and for ranges large compared with the wavelength of the sound. The results are in agreement with Sheehy's experiments.

(Author's Abstract).

173. *Wave Propagation in a Randomly Inhomogeneous Medium. II.* D. Mintzer, J. Acoust. Soc. Amer., Vol. 25, No. 6, pp. 1107-11, November, 1953.

The region of validity o the single-scattering approximation used in Part I is found by considering the next higher approximation; it is valid for $k_0^2 ar \alpha^2 \ll 1$, where k_0 is the wave number of the incident sound, r is the range from source to observer, a is the mean size of the inhomogeneities, and α is the *rms* value of the refractive index variations. Some approximate results are given for the case of wavelength large compared with inhomogeneity size. By consideration of the intensity variations, it is found that ray theory is valid for $(k_0a^2/r) \gg 1$, as has been found for plane waves.

(Author's Abstract).

174. *The Propagation of Waves in An Imperfect Elastic Medium.* (In French).
M. Matschinski, C. R. Acad. Sci. (Paris), Vol. 238, pp. 203-205, January 11th, 1954.
An approximate method is given for determining the change in waveform and the absorption due to the imperfect elasticity of the medium (plasticity is excluded).
(From Physics Abstracts, A, May, 1954).

175. *Boundary Disturbances in High-Explosive Shock Tubes.*
R. G. Shreffler & R. H. Christian, J. Appl. Phys., Vol. 25, No.3, pp. 324-331, March, 1954.
High-velocity disturbances are observed to propagate along the walls of a high-explosive operated shock tube in advance of the plane shock. Experiments are presented which determine the dependence of the geometry, energy and velocity of the disturbance on such variables as the gas contained in the shock tube, the shock strength and the roughness and composition of the supporting boundary. A model is constructed to explain the flow within the disturbance. Arguments are presented which show the disturbance to result from radiation originating in the luminous plane shock.
(Author's Abstract).

176. *Screening Action of a Thin Elastic Layer.* (In Russian).
V. Babich & A. Alekseev, Dokl. Akad. Nauk SSSR, Vol. 91, No. 4, pp. 763-765, 1953.
When a wave is propagated in laminated media, it occasionally occurs that the wave is incident on a thin layer at an angle exceeding that for total internal reflection but, in spite of this, the disturbance partially penetrates the screening layer. The penetration becomes greater when the thickness of the layer is reduced and the angle of incidence approaches the critical value. The problem is studied theoretically in the present paper, the solution of the problem in the theory of elasticity being constructed by the method of incomplete separation of variables. For simplicity, it is assumed that the velocities in the material above and below the screening layer are equal and lower than that in the layer. It is found that the results obtained cannot be explained by theories based on geometrical optics and it is concluded that future progress in this field of geophysics depends on the full application of the dynamical theory of elasticity.
(From Physics Abstracts, A, May 1954).

177. *New Method for Measuring Wave Velocities in Stone.* (In German).
E. Müller, Naturwissenschaften, Vol. 41, No. 4, p. 85, 1954.
A brief reference is made to a method for measuring the longitudinal and transverse wave velocities in stone specimens about 3 cms. long and a few mm. thick by taking spark photographs of the motion of the waves set up in a fluid in which the stone is immersed. The velocities and elastic constants of ten common stones are given; the values agree with those found in seismic practice.
(From Physics Abstracts, A, June 1954).

178. *Energy Distribution in Explosion-Generated Seismic Pulses.*
B. F. Howell, Jr., a paper read at the Eastern Meeting of the S.E.G., Boston, Mass, December 1953. (Not yet published).
Three separate pulses were recognized on a group of seismograms of ground motion

resulting from explosions measured at distances ranging from 10 to 1, 172 feet from the shotpoint. It is believed that the first pulse represents primarily body waves, the second pulse coupled waves formed by internal reflections in the low velocity surface layer, and the third pulse Rayleigh and Love waves arriving simultaneously. The ratios of the energies of the various pulses are given for several distances. The rates of attenuation of the three pulses are expressed as exponential functions and also as inverse power functions.

179. *Note on the Nature of a Seismogram — I.*
H. E. Tatel & M. E. Tuve, J. Geophys. Research, Vol. 59, No. 2, pp. 287-288, June 1954.
Coherent patterns obtained from multiple seismograms have indicated that there could be strong conversion of compressional waves to surface waves at the earth's uneven surface. In addition, ground motion studies have shown the presence of Rayleigh waves after the P arrival and before the S arrival. This conversion could account for much of the ground motion in a typical seismogram.

180. *Note on the Nature of a Seismogram — II.*
H. E. Tatel, J. Geophys. Research, Vol. 59, No. 2, pp. 289-294, June, 1954.
Model experiments have verified Lamb's calculations. Also they have corroborated the conversion hypothesis of Part I, in which compressional waves produce strong Rayleigh waves at a surface discontinuity. In addition, the reciprocity theory is shown to be valid, and the generation of Rayleigh waves from deep focus sources has been studied. Apparently, any obstacle in the path of a plane (compressional) wave acts as a scattering contre, and if at the surface produces Rayleigh waves.

181. *Underwater Exposion Shock Wave Parameters at Large Distances from the Charge.*
A. B. Arons, J. Acoust. Soc. Am., Vol. 26, No. 3, pp. 343-346, May, 1954.
A series of experimental measurements, with explosives TNT and pentolite, has been made to extend the knowledge of underwater shock wave parameters at large distances. The results are shown (together with earlier work by R. H. Coles et al) in the form of simularity curves.

182. *Note on "The Primary Seismic Disturbance in Shale"* by N. Ricker and W. A. Sorge.
F. A. Van Melle, Bull. Seismol. Soc. Am., Vol. 44, No. 2A, pp. 123-125, April 1954.
The author describes practical and theoretical work which provides evidence that the 'law of decay of velocity amplitude from small explosions with the -5/2 power of the travel time' which Mr. Ricker advocates has a rather narrow range of validity.

183. *One-Dimensional Transducers for Seismic Models.*
L. Knopoff & G. L. Brown, a paper read at the Pacific Coast Meeting of the S.E.G., Los Angeles, November, 1953. (Not yet published).
The surface excitation of seismic models imposes certain conditions upon the nature of the source and receiving transducers to be used. Among these conditions are those of size, stability, directivity, adaptability, and efficiency. This investigation determines the physical properties of transducer materials most ideally suited for use in seismic models and the proper use of these materials in the production of pressure pulses of the desired type and in the detection of the resultant motion. As an example of the several types of electro-mechanical transducer materials, attention is limited to the class exhibiting elastic, piezoelectric properties. The conditions of adaptability and stability in a one-dimensional source are satisfied by a suitable choice of source material, excitation wave form, and load impedance. An indication is made of the techniques employed for a solution to the three-dimensional problem. Materials pos-

sessing properties satisfying a large number of the one- and three-dimensional conditions are described.

184. *Forces and Effects of Explosives in Submarine Geophysical Exploration.*
F. J. Hortig, a paper read at the Pacific Coast Meeting of the S.E.G., Los Angeles, November, 1953. (Not yet published).

Normal application of explosions as the requisite point source of high-intensity low-frequency energy in submarine geophysical exploration has necessitated controls on steepness of pressure wave front and peak pressure amplitude to minimize damage to marine life and eliminate contended damage to marine and onshore physical structures.

Limited quantitative measurements have been made of the forces and effects of "jet" and "open" submarine shots on marine and onshore physical structures to permit establishment of practical operating control limits. In addition, measurements of force amplitudes and effects resulting from railroad and highway transportation were made for comparison with the effects of geophysical explosions at comparable measurement distances. Concurrent observations and analyses of damage to marine life were also conducted.

185. *Notes on the Use of Multiple Geophones.*
L. V. Lombardi, a paper read at the 7th Annual Midwestern Meeting of the S.E.G., Dallas, Texas, November, 1953. (Not yet published).

The use of multiple geophones, which has been largely empirical, serves two primary funtions: cancellation of random and other unwanted energies, and improved sampling of the wave front. Curves are presented showing surface-wave-cancellation effectiveness of several different spreads. The results also apply to mixed records. Cancellation of random energies follows conventional sampling theory, varying with the square root of the number of geophones in the spread. Sampling of the wave front is more complex because the samples are not mutually independent.

186. *Pressure Field around Distributed Charges.*
N. R. Sparks & D. Silverman, a paper read at the 7th Annual Midwestern Meeting of the S.E.G., Dallas, Texas, November, 1953. (Not yet published).

The pressure field in the earth around a long continuous distributed charge depends primarily upon the velocity of detonation of the explosive. When the detonation velocity matches the velocity of the surrounding formations, the initial pressure is most intense in the direction of detonation and may be 20 to 30 times the pressure in the opposite direction and to the side of the charge. This pressure ratio falls to approximately 6 : 1 when the detonation velocity is 20% higher or lower than the formation velocity. Matched velocity charges exhibit strong directional characteristics with respect to reflection as well as with respect to pressures in the vicinity of the charge.

187. *Seismic Wave Types in a Shallow Bore Hole.*
E. D. Riggs, a paper read at the 7th Annual Midwestern Meeting of the S.E.G., Dallas, Texas, November 1953. (Not yet published).

Field measurements of near-surface velocity, using a multiple seismometer array within the bore hole, indicates the presence of a well developed secondary event. This type of wave has been generated under controlled conditions and from its characteristics identified as an interface type, generally known as a bound tube wave. Some practical aspects of near surface velocity surveys and up-hole measurements are considered.

188. *A. Brief Summary of Three Years of Seismic Field Research.*
J. W. Hammond & H. M. Thralls, a paper read at the 7th Annual Midwestern Meeting of the S.E.G., Dallas, Texas, November 1953. (Not yet published).

The first objective of a seismic field research unit is to determine a procedure which will hold constant all variables except the one being investigated. The results of field research are, in a large measure, dependent on the attainment of this objective. Given proper instrumentation the competent field research engineer can reach conclusions and develop solutions if positive control over variables is established.

Field research, like other research, must be divorced completely from the bustle of a commercial survey. Efficiency is highly desirable but cost per unit of subsurface coverage is of no importance during the research period.

This paper outlines the factors to be considered in a field research programme and describes in brief some of the results obtained in three years of field operations in various localities of North America.

189. *Lamb's Problem with Internal Dissipation. I.*
M. Newlands, J. Acoust. Soc. Am., Vol. 26, No. 3, pp. 434-448, May, 1954.

A theoretical investigation is made of the response of an elastic half-space to a vertical impulse at the surface. Dissipation properties are incorporated in the medium and dissipation coefficients λ', μ' varying as the nth power of the frequency are assumed. These lead to dispersion and absorption. The response may be described by components of the three distinct types, P-, S-, and R-. Each is observed at the surface as a train of waves culminating in a characteristic phase about the instants r/α, r/β, and r/γ, respectively where α, β, and γ are the velocities of propagation of P-, S-, and R-waves in nondissipative media and r is the focal range. These phases are discussed in detail; their "amplitude" and "span" are defined and the variations of each of these quantities and their ratios with r, density ρ and the material constants are derived. A schematic determination of λ and μ (the elastic constants), n, λ', and μ' from experimental data is outlined.

(Author's Abstract).

190. *Spall Effects produced by a Cylindrical and a Spherical charge of High Explosive.*
W. A. Allen & W. Goldsmith, J. Appl. Phys., Vol. 25, No. 6, pp. 813-14, June, 1954.

An experiment has been performed to verify the equivalence of the spall effects produced when cylindrical and spherical charges are detonated in contact with a steel plate. The results, which showed unusual similarity of those effects that occur near the free surfaces, are discussed.

191. *Short Range Propagation of Mechanical Disturbances in the Ground.*
B. J. Starkey, & C. M. Lock, J. Appl. Phys., Vol. 25, No. 6, pp. 816-17, June, 1954.

The phenomena of the propagation of mechanical vibrations through the earth are of practical importance in seismological and geological investigations but knowledge of the precise origin of the oscillatory nature is usually of secondary interest. Hence little is known of the mechanism of the oscillatory response.

From an extensive series of experiments in propagation over distances from 0-50 ft., in which as much as possible was done to eliminate instrumental influences, it was found that the oscillations are closely connected with the stratified nature of the soil. The experiments and conclusions are discussed.

192. *Two-Dimensional Model Study.*
J. Oliver, F. Press & M. Ewing, Geophysics, Vol. 19, No. 2, pp. 202-219, April, 1954.

The solutions of many problems in seismology may be obtained by means of ultrasonic pulses propagating in small-scale models. Thin sheets, serving as two-dimensional models are particularly advantageous because of their low cost, availability, ease of fabrication into various configurations, lower energy requirements, and appropriate dilatational-to-shear-velocity ratios. Four examples are presented:—flexural waves in a sheet, Rayleigh waves in a low velocity layer over-lying a semi-infinite high velocity layer, Rayleigh waves in a high velocity layer overlying a semi-infinite low velocity layer, and body and surface waves in a disc.

(Author's Abstract).

193. *A Three Dimensional Seismic Wave Model with Both Electrical and Visual Observation of Waves.*

J. F. Evans, C. F. Hadley, & D. Silverman, Geophysics, Vol. 19, No 2, pp. 220-236, April, 1954.

The short wave lengths required in a seismic model to give wave-front patterns geometrically similar to those in a large prototype (the earth) can only be obtained by using high frequency sound waves. As sources and detectors of such high frequency waves, piezoelectric crystals are used, primarily because under identical stimuli they are capable of almost perfect duplication. Such duplication is made use of in displaying on an oscilloscope stationary patterns which are characteristic of transient particle motion at a point in the model. Also, it has made possible the direct visual observation of transient wave fronts in transparent models, techniques for which are described, and sample photographs given. As an example of quantitative use of the described model techniques, the results are presented showing symmetric and antisymmetric wave propagation in a free elastic plate. Good agreement is found between many features of the experimental record and theoretical predictions.

(Author's Abstract).

194. *A Study of Wave Motion in the Elastic Region near the Shotpoint.*

F. Troseth, a paper read at the 7th Annual Midwestern Meeting of the S.E.G., Dallas, Texas, November, 1953. (Not yet published).

An understanding of the mechanics by which elastic waves are initiated in rocks is a primary aim of basic seismic research. Much of the experimental work done on the subject has been inconclusive because the investigators found it necessary to assume a "probable" pressure distribution on the surface between regions of elastic and non-elastic deformation.

A mathematical analysis of wave propagation indicates that the assuming of a pressure distribution may be avoided by making measurements in the elastic region surrounding a shotpoint and extrapolating the information gained back to the desired surface. Experimental studies of wave propagation in a large tank of pitch show that the mathematical method of extrapolating measured information from one point to another in an elastic medium can be applied to an actual physical system.

195. *The Impulsive Response of Planted Geophones.*

R. G. Piety, a paper read at the Annual Meeting of the S.E.G. at St. Louis, 1954, (not yet published).

In the interaction between the ground and the geophone, experimental observations can show a wide range of variation in field practice. In general a tightly planted geophone is much more highly damped than a geophone resting on the surface. The impulsive response is obtained by dropping a small steel ball on the planted geophone. It is observed that in some cases the behaviour indicates that reciprocity between the reception and transmission of a pair of differently planted geophones holds true.

196. *A Magnetic Compounder for Directional Discrimination of Seismic Waves.*

C. C. Lash, T. H. Gilmartin & J. D. Eisler, a paper read at the Annual Meeting of the S.E.G., at St. Louis, 1954, (not yet published).

The magnetic compounder is a multiple-trace magnetic recording and playback device which provides discrimination between seismic waves based on their direction of arrival. The device makes a temporary recording of the signals from 12 groups of seismometers. The continuously moving magnetic tracks carry the signals to a large array of pickup coils before erasing. These coils are connected so as to add their output with a systematic pattern of time delays. By this means, the recording is analysed into components on the basis of movement, i.e., differences in arrival time.

The magnetic compounder has been tested with procedures intended to lead to routine field use. Since the device is inherently capable of improving the ratio of reflected energy to the extraneous seismic noise by virtue of its directional sensitivity, the instrument was field tested in various areas to evaluate its capability of resolving dip as well as to carry correlation analysis.

The use of the magnetic compounder in research work is illustrated as a method for emphasizing and separating surface waves.

197. *Recent Results of the Model Seismology Programme at the Lamont Geological Observatory,*

J. E. Oliver, F. Press & M. Ewing, a paper read at the Annual Meeting of the S.E.G., at St. Louis, 1954. (not yet published).

At the Lamont Geological Observatory elastic wave propagation is investigated by means of pulses of ultrasonic freguencies traveling through small scale models. The use of two-dimensional rather than three-dimensional models greatly enlarges the scope of investigations. Two-dimensional models are cheaper and more readily available, require less space, are easy to fabricate, require less elaborate electronics, and have a favourable ratio of compressional to shear velocity. Current applications of the seismic model, or analog computer, to specific problem of surface wave dispersion and reflection and refraction of body waves are discussed.

198. *Seismic Interpretation Theory for an Elastic Earth.*

L. B. Slichter, Proc. Roy. Soc., Vol. 224, No. 1156, pp. 43-63, 9th June 1954.

The seismic interpretation problem for an isotropic spherical earth is analysed on the basis of elastic theory, under the assumption that the three independent elastic parameters are unknown continuous functions of the depth. It is shown that solutions for these functions may be obtained in the form of Taylor's series.

Algebraic checks are obtained by comparing the general solutions with the corresponding results for two special cases in which the elastic parameters vary in a prescribed manner in the interior of the sphere. Practical application of elastic theory to the direct interpretation of seismograms requires further development of the theory, with probable utilization of modern high-speed computing methods.

199. *Early Arrivals in Seismic Prospecting.*

F. F. Evison, Nature, Vol. 173, No. 4413, p. 1047, May 29th 1954.

A brief note on the development of an electromechanical seismic source (ref. N.Z. J. Sci. Tech., Vol. 35, No. 4, 1953) for better control of the generated impulse in seismic surveying. The confusion normally found in the early part of a record is avoided. Development of a shallow-reflection technique is considered possible.

200. *A Field Evalution of the Electromagnetic Reflection Method.*

R. V. Nostrand & A. Orsinger, a paper read at the Annual Meeting of the S.E.G., at St. Louis, April 1954 (not yet published).

Equipment has been assembled for field investigations on the theory of electromagnetic wave propagation. Two large loops, one for transmitting and the other for receiving, are laid on the surface of the ground. A pulsed current is passed through the transmitting loop. A similar arrangement of loops is placed on the surface of a metallic model and the signals received by the two receiving lips are mixed in opposition.

The layering in the model is then manipulated until the difference signal is a minimum, which condition signifies that the actual earth has been approximated in the model considering the appropriate scaling factors. Using this technique at five stations in Dallas County, Texas where the depth of the Austin chalk-Eagle Ford shale contact varies from 50 to 400 feet, this depth was determined within an average accuracy of about 5%.

201. *Transmission Characteristics of Near-Surface Layers, Barton County, Kansas.*
R. B. Fisher, a paper read at the Annual Meeting of the S.E.G., at St. Louis, April 1954 (not yet published).

Pulses are recorded at several depths in the earth adjoining a shot hole. The recorded pulses are analysed by means of a Henrici rolling sphere analyser to obtain their Fourier spectra. Point-by-point division of two spectra yielded the transfer characteristics of the earth materials between two geophone positions.

The high-fequency components of the waves in the very shallow layers of the earth were found to attenuate extremely rapidly.

GRAVITY — GENERAL

202. *Gravity Measurements and Oceanic Structure.*
B. C. Browne, Proc. Roy. Soc., Vol. 222, No. 1150, pp. 398-400, 18 March, 1954.

The observed isostatic balance between continents and oceans is consistent with the seismic results and depends mainly on the shallowness of the Mohorovicic discontinuity under the oceans.

The gravity anomalies over flat parts of the ocean floor show a greater scatter than do those over flat continental areas. This is believed to be due to varying thicknesses of sediment which conceal the underlying topography.

(Author's Abstract).

203. *The British Fundamental Gravity Station.*
Nature, Vol. 173, No. 4409, pp. 794-5, May 1, 1954.

At its meeting on June 30, 1952, the British National Committee for Geodesy and Geophysics resolved that the British Fundamental Gravity Station should be at the National Physical Laboratory, Teddington, Middlesex. The geodetic coordinates and height of the pillar are:

Lat. 51° 25′ 13.6″N. Long. 00° 20′ 21.4″W.
Height (Newlyn datum) 9.23 m.

Two subsidiary sites are also delineated.

204. *Tables of Corrections for Lunisolar Effects to be Applied to Gravimetric Observations in Mexico.* (In Mexican).
H. De Castro, Ciencia (Mexico), Vol. 12, No. 11-12, pp. 301-310, 1953.

The method based on the formulae of spherical astronomy is developed to determine the effect of the moon and the sun on the force of gravity measured at a point on the surface of the earth, and numerical values are given for different points in Mexico. In computing these corrections, the deformation of the globe due to the tidal effect is not taken into consideration.

(From Geophysical Abstracts 155, U.S. Geol. Survey).

205. *Present State of Gravimetric Measurements in Belgium and the Belgian Congo.* (In Belgian).
P. Sanders, Ciel et Terre, 68e ann., Fasc. 7-8, pp. 151-164, 1952.

This paper begins with a theoretical discussion on absolute gravity measurements, and the adoption of g = 981, 131.0 mgals for Uccle, which is the basis of the gravimetric network of Belgium. The minimum value measured in Belgium is 980,975.6 ± 0.2 mgals at Saint-Hubert; the maximum is 981, 203.2 ± 0.8 mgals at Heist. Measurements were made with a pendulum.

(From Geophysical Abstracts 155, U.S. Geol. Survey).

206. *Gravity Anomalies of Texas, Oklahoma, and The United States.*
L. L. Logue, Oil & Gas J., Vol. 52, No. 50, pp. 132-135, April 19, 1954.

A structural interpretation of the geology of Texas and Oklahoma based upon gravity data, is presented in map form. The maps, seven in all, are discussed in detail.

207. *Variations of the Total Vector of Gravity at Winsford (Cheshire) Part I. General Results and Maritime Load Influences.*
R. Tomaschek, Mon. Not. Roy. Astronom. Soc., Geophys., Suppl. Vol. 6, No. 9, pp. 540-556, April 1954.

Simultaneous measurements of the vertical component and two perpendicular horizontal components of gravity have been made in the I.C.I. salt mine at Winsford (Cheshire) over the period 1951, April 16 to 24. Apart from the gravitational tide the measurements show a well developed influence of the variations in the maritime loading, especially in the horizontal components. A common drift in all components indicates the influence of meteorological pressure variations over a large area. Furthermore, diurnal variations of presumably meteorological origin have been observed. The "load tilt" has been determined. It is elliptical with an azimuth of N. 47° W. of the main axis and has an amplitude of 1.65 millisec per foot tide at Liverpool (5.5 msec/m). The load influences in the vertical component are only 2.4% of those in the horizontal direction and indicate the influence of more distant oceanic areas.

GRAVITY — INSTRUMENTAL

208. *Patents.* Abstracts in Geophysics, Vol. 18, No. 4, p. 952, October 1953.
U.S. 2,634,610. 14 April 1953. A system for compensating a pendulum or gravimeter against accelerations of its transporting vehicle.
U.S. 2,638,001. 12 May 1953. An underwater gravimeter.

209. *Patents.* Abstracts in *Geophysics,* Vol. 19, No. 1, p. 156, January 1954.
U.S. 2,648,055. 4 Aug. 1953. Instrument functioning as gravimeter or seismometer.
U.S. 2,650,991. 1 Sept. 1953. Gravimeter-accelerometer.

210. *Patents.* Abstracts in Geophysics, Vol. 19, No. 2, p. 321, April 1954.
U.S. 2,657,581. 3 Nov. 1953. Borehole gravimeter having a suspended transversely-oscillating mass.
U.S. 2,660,062. 24 Nov. 1953. A vertical acceleration-compensating system for a gravimeter.

GRAVITY — INTERPRETATION

211. *The Least Squares Approach to the Residual Analysis of Gravity Data.*
T. J. Bevan, a paper read at the Annual Meeting of the S.E.G., at St. Louis, 1954. (Not yet published).

The primary purpose of residual analysis is to bring out local anomalies of relatively small magnitude that would otherwise be over-looked or under-evaluated because of the "shadowing" of a large regional gradient. It is extremely difficult to draw accurately a graphical estimation of the regional gradient and, at best, it contains considerable human error. By fitting a cubic surface to the regional pattern with a least squares process the residual values can be calculated analytically eliminating these human errors. Control points on the residual map can be made identical with the station control. The method is economical if punched cards and electronic calculators are used.

Examples of results are shown from the Rocky Mountain, Williston Basin, southern Oklahoma, and Gulf Coast provinces.

212. *Least Squares Polynomial Fitting to Gravitational Data and Density Plotting by Digital Computers.*

S. M. Simpson, Geophysics, Vol. 19, No. 2, pp. 255-269, April 1954.

The fitting of a 'n'th order polynomial in 'x' and 'y' to gravity data by least squares is discussed. A consideration of the normal equations for the general case shows certain simplifications resulting from rectangularity in data distribution. Some sample residual maps are constructed. Density plotting, made possible by the digital computer, is described and illustrated. It is shown that this process can serve as a substitute for contouring when only a qualitative picture is desired.

(Author's Abstract).

213. *Analysis of Potential Fields.*

L. L. Nettleton, a paper read at the 7th Annual Midwestern Meeting of the S.E.G., Dallas, Texas, November 1953. (not yet published).

Geophysical measurement of potential fields include the sum of all effects below the level measurement. The separation of these into regional and residual components is a basic problem in the interpretation of such measurements. We have no definite criterion for a "correct" regional because the source of potential fields is ambiguous. It is shown that the several analytical and mathematical or "grid" systems do not provide such criterion because of choices or assumptions which must be made at certain steps in the derivation of the numerical factors by which such systems are reduced to practice. Several of the published systems are compared with each other and with a graphical residual system by a table of relative weights of their coefficients and by application to the same map.

In spite of the limitations and empirical nature of any method of determining a regional it is possible to make very effective use of one or more approaches to the regional problem. An understanding of the possibilities and limitations of the several possible methods is necessary for the proper application and for any interpretation of the resulting "anomalies."

GRAVITY — THEORY & RESEARCH

214. *The Correlation Between Pre-Cambrian Rock Densities and Bouguer Anomalies near Parry Sound, Ontario.*

C. G. H. Oldham, Geophysics, Vol. 19, No. 1, pp. 76-88, Jan. 1954.

A gravity survey and a survey of rock densities have been carried out over an area of two thousend square miles near Parry Sound. A closed positive Bouguer gravity anomaly of thirty milligals was delineated, and a considerable variation was found to exist in the densities of pre-Cambrian gneisses. In most previous interpretations of gravity over the Canadian Shield the gneisses have been assumed to possess a uniform density and anomalies have been attributed to changes in the thickness of horizontal crustal layers. In this paper it is shown that the Parry Sound anomaly can be explained in terms of structures within the crust taking the form of projections downward of the sensity variations found at the surface. The postulated structure is a nearly circular basin of dense gneisses. The shape is reasonable and agrees with such geological evidence as is available.

(Author's Abstract).

215. *The Tides of The Solid Earth and Their Geophysical and Geological Significance.*
R. Tomaschek, Nature, Vol. 173, No. 4395, pp. 143-145, Jan. 23, 1954.

After a discussion on the theoretical values of the tides of the solid Earth, the methods of obtaining characteristic values of the elastic yielding of the earth are described and a table of the most probable values is given. From observations in the British Isles, examples of the influence of the maritime loading and of meteorological load differences of large extent are given. The parallelism in the behaviour of the gravimeter and horizontal pendulums in certain cases is shown. The uniform reduction of former tilt measurements on the continent shows that the residuals of the M_2 tide are not only due to the tides of the ocean, but are distinctly influenced by the tectonic structure of the continent and are, therefore, a suitable means of locating such structures. As the tilt movements are the expression of stresses in the upper layers of the earth, a certain parallelism with periods in the productivity of oil wells and with the periodicity of earthquakes seems possible.

216. *Negative Gravity Anomalies over Acid "Intrusions" and Their Relation to the Structure of the Earth's Crust.*
M. H. P. Bott, Geol. Mag., Vol. 90, No. 4, pp. 257-267, 1953.

The almost invariable association of acid intrusions with negative Bouguer anomalies is certainly often caused by direct density contrast between the acid intrusive and the denser country rock. Theoretical consideration of these observations suggests that a gravity survey may provide a criterion for testing the genetic type of a granite, as follows: A large negative anomaly may indicate magmatic origin; various patterns with no large anomaly may indicate granitization; a large positive anomaly may indicate association with a basic intrusion below, which has given rise to the "granite" either by differentiation, or by melting and reintrusion of the intruded sialic rocks. The paper includes a brief summary of the mechanics of intrusion.

(From Geophysical Abstracts 155, U.S. Geol. Survey).

217. *Tables for the Computation of the Tidal Accelerations of the Sun and Moon.*
J. T. Pettit, Trans. Am. Geophys. Un., Vol. 35, No. 2, pp. 193-202, April 1954.

Tables are provided for facilitating the computation of the tidal acceleration of the sun and moon at a point on the surface of a rigid earth. Without interpolation, the tables provide an accuracy of one microgal in the resultant computation. Higher accuracy is readily obtained by interpolating.

(Author's Abstract).

MAGNETIC — GENERAL

218. *Airborne Magnetometer Profile from Portland, Oregon to Albuquerque, New Mexico.*
W. B. Agocs, J. C. Rollins & E. Bangs, Geophysics, Vol. 19, No. 2, pp. 270-280, April 1954.

An airborne magnetometer profile of the variations of the earth's anomalous total magnetic field was obtained using a wing-tip magnetometer installation in a flight from Portland, Oregon to Albuquerque, New Mexico. The magnetic data were obtained by flying at barometric altitudes ranging from 7,000 to 10,000 feet above mean sea level.

The variations in the total magnetic field are tied to the known geology along the flight path, and the possible interpretations of the magnetic data are reviewed in light of the known general geology.

(Author's Abstract).

219. *Rock Magnetism and the Earth's Magnetic Field during Paleozoic Time.*
J. W. Graham, J. Geophys. Research, Vol. 59, No. 2, pp. 215-222, June 1954.

A brief appraisal is given of the observations and arguments that are advanced in support of the opinion that during Paleozoic time the earth's magnetic field retained approximately its present orientation, and, except for possible brief excursions, its present sense.

MAGNETIC — INSTRUMENTAL

220. *The Gulf Airborne Magnetic Gradiometer.*
W. E. Wickerham, Geophysics, Vol. 19, No. 1, p. 156, January 1954.

An instrument capable of measuring magnetic gradients as encountered in airborne magnetometer operations has possible applications as an interpretational aid. Its usefulness, particularly for qualitative analysis is discussed briefly. The design of a spacial-type airborne gradiometer of adequate precision can be shown to be quite impractical. An instrument based on the time derivative of the magnetic intensity variations provides a useful alternative and is described.

221. *Patents.* Abstracts in Geophysics, Vol. 19, No. 1, p. 156, January 1954.
U.S. 2,648,042. 4 Aug. 1953. A magnetic orientation system.
U.S. 2,648,046. 4 Aug. 1953. A piezoelectric magnetometer.
U.S. 2,649,568. 18 Aug. 1953. A saturable-core magnetometer.
U.S. 2,649,569. 18 Aug. 1953. A semiconductor magnetoresistive magnetometer.

222. *Patents.* Abstracts in Geophysics, Vol. 19, No. 2, April 1954.
U.S. 2,659,859. 17 Nov. 1953. Method and apparatus for aeromagnetic prospecting.
U.S. 2,661,455. 1 Dec. 1953. Magnetic flux measuring system.
U.S. 2,663,843. 22 Dec. 1953. Magnetic gradiometer.

MAGNETIC — FIELD TECHNIQUE

223. *Patents.* Abstracts in Geophysics, Vol. 18, No. 4, p. 952, October 1953.
U.S. 2,635,134. 14 April, 1953. A prospecting method in which several magnetometers are suspended from a blimp to make simultaneous intensity measurements several hundred feet above ground.
U.S. 2,642,479. 16 June, 1953. A magnetic gradiometer.

MAGNETIC — INTERPRETATION

224. *Employment of Electric Methods of Prospecting for Interpretation of Magnetic Anomalies* (In Russian).
N. I. Khalevin, Akad. Nauk SSSR Izv. Ser. Geofiz., No. 1, pp. 61-68, 1953.

When interpreting the results of magnetic surveys, often it is difficult to decide wheter the observed magnetic effect is caused by a definite circumscribed ore body or by dissemination of magnetic particles in the formation. Only the first is economically important. The electric resistivity method, in addition to the magnetic survey, was used by Khalevin in several cases, so that both magnetic profiles and electric resistivity curves were available for the area. From analysis of both, it was possible to make a decision, which was subsequently confirmed by drilling.

(From Geophysical Abstracts 153, U.S. Geol. Survey).

225. *Analysis of Potential Fields.*
L. L. Nettleton, a paper read at the 7th Annual Midwestern Meeting of the S.E.G., Dallas, Texas, November 1953 (not yet published).

Geophysical measurements of potential fields include the sum of all effects below the level of measurement. The separation of these into regional and residual components is a basic problem in the interpretation of such measurements. We have no definite criterion for a "correct" regional because the source of potential fields is ambiguous. It is shown that the several analytical and mathematical of "grid" systems do not provide such criterion because of choices or assumptions which must be made at certain steps in the derivation of the numerical factors by which such systems are reduced to practice. Several of the published systems are compared with each other and with a graphical residual system by a table of relative weights of their coefficients and by application to the same map.

In spite of the limitations and empirical nature of any method of determining a regional it is possible to make very effective use of one or more approaches to the regional problem. An understanding of the possibilities and limitations of the several possible methods is necessary for the proper application and for any interpretation of the resulting "anomalies."

MAGNETIC — THEORY & RESEARCH

226. *Application and Principles of the Magnetic Method of Exploration.* (In Mexican). J. A. Sharpe, Petrol. Mexicanos, 2ª Epoca, Tomo 1, No. 9, pp. 711-715, 1953.

The different factors contributing to the production of a magnetic anomaly and the four main types of magnetic anomalies caused respectively by a deep intrusion of igneous rock, by such an intrusion almost reaching the surface of the earth, by an intrusion protruding out of the surface of the earth, and by a topographic elevation on the surface, are discussed. Magnetic profiles corresponding to each of these types of anomalies are discussed to aid in interpreting the results of magnetic surveys. (From Geophysical Abstracts 155, U.S. Geol. Survey).

227. *Review of the Development of the Airborne Magnetometer.*
R. F. Beers, Beers & Heroy, a paper read at the Eastern Meeting of the S.E.G., Boston, Mass., December 1953. (Not yet published).

Equations are developed for the general form of expression of the total intensity of the earth's magnetic field as measured by the airborne magnetometer. Existing models of magnetometers are examined to reveal the special cases which they represent in terms of the general equations. The examples selected include significant references published in the periodical and patent literature.

228. *The Permanent Magnetisation of Horizontal Volcanic Sheets.*
T. Hatherton, J. Geophys. Research, Vol. 59, No. 2, pp. 223-232, June 1954.

The magnetisation of igneous rocks is often largely due to thermoremanent components. Several horizontal sheets of acid tuffs in New Zealand exhibit similar magnetisation patterns. Each sheet has a basic minimum Q value; super-imposed on this is an amplitude of polarisation pattern which, for one sheet examined in detail, is found to vary with depth in a similar manner to the inverse ratios of the computed cooling times over the temperature range $T_0 \rightarrow 0.75\ T_0$, T_0 being the instantaneous temperature of deposition of the lava.

ELECTRICAL

229. *A Resistivity Investigation into a Washout Feature in Coal Measure Strata.*
G. M. Habberjam & J. T. Whetton, Geophysical Prospecting, Vol. 2, No. 1, pp. 24-37, March, 1954.

An account of a resistivity investigation into an old river valley in Coal Measure strata. This valley denuded several of the upper coal seams leaving behind unconsolidated material and it was the purpose of the work described to investigate how far the extent and nature of this material could be determined by resistivity methods conducted at the surface. As such the survey fits into a wider programme of research instigated by the National Coal Board.

The feature, which is quite well-known geologically, was surveyed by conventional methods and the results obtained are discussed in relation to the above project.

Thus, the investigations succeeded in tracing the approximate centre line of the feature and in yielding some information on the nature and order of thickness of the deposits. Limitations of the method and its future application are also discussed.

(Author's Abstract).

230. *A New Kind of Natural Electric Field in the Ground.* (In Russian).
A. V. Veshev et al, Akad. Nauk SSSR Doklady, Tom. 87, No. 6, pp. 939-41, 1952.

Regular diurnal variations of the value of electric self potential at a point in the ground have been observed. It has been suggested that a correlation exists between these variations and the changes of temperature of the air and of the ground because the corresponding graphs of each show great similarity.

(From Geophysical Abstracts 154, U.S. Geol. Survey).

231. *Patents.* Abstracts in Geophysics, Vol. 18, No. 4, p. 952, October, 1953.

U.S. 2,642,477. 16 June, 1953.	An eletromagnetic prospecting system in which the phase difference between a low-frequency field signal and a high frequency carrier signal is measured.

232. *Geolectrical Investigation of Ground Structure.* (In German).
V. Fritsch, Umschau, Jahrg. 52, Heft 11, pp. 330-331, 1952.

This paper describes the physical principles and the techniques of electrical exploration methods, illustrated by three practical examples.

(From Geophysical Abstracts 155, U.S. Geol. Survey).

233. *The Measurement of Telluric Currents.* (In German).
K. Jung, Umschau, Jahrg. 51, Heft 3, pp. 74-75, 1951.

This is a discussion of the principles and application of the geoelectric "four-point" method, pioneered by Schlumberger, which makes use of natural earth currents in obtaining data on underground structure.

(From Geophysical Abstracts 155, U.S. Geol. Survey).

234. *Patents.* Abstracts in Geophysics, Vol. 19, No. 1, p. 156, January, 1954.

U.S. 2,652,530. 15 Sept., 1953.	A low-frequency electromagnetic induction method of prospecting.
U.S. 2,653,220. 22 Sept., 1953.	An electromagnetic wave transmission system.

235. *On The Relation between Telluric Currents and the Earth's Magnetic Field.*
J. R. Wait, Geophysics, Vol. 19, No. 2, pp. 281-289, April, 1954.

The validity of Cagniard's analysis of the behaviour of telluric earth currents is questioned in view of the fact that the harmonic components of the electric field and the magnetic field tangential to the ground are only proportional to one another if the fields are sufficiently slowly varying over the surface of the ground. His result is extended to include the effects of a layered ground with both conductivity and susceptibility variations. Finally the corresponding transient problem is solved for a two-layer horizontally stratified earth.

(Author's Abstract).

236. *Mutual Coupling of Loops Lying on the Ground.*
J. R. Wait, Geophysics, Vol. 19, No. 2, pp. 290-296, April, 1954.

The theory of a method to measure electrical ground constants by mutual coupling of loops is outlined. Curves are given in parametric form showing the dependence of the mutual impedance on conductivity, dielectric constant, frequency and separation. An expression is derived in the appendix for the field of a circular wire loop laid on a homogeneous conducting ground.

(Author's Abstract).

237. *Sub-Surface Electrical Measurements about two Plane Interfaces.*
G. O. Buckner, Geophysics, Vol. 19, No. 2, pp. 297-309, April, 1954.

Many response curves have been calculated for multiple-electrode logging devices through thin beds (Guyod, 1944, parts 5, 6, 7, 8, 9, 10 & 11). For conditions where one can assume equal resistivity material above and below the thin bed, all electrodes in a line normal to the interfaces, and bore hole effects negligible, a function $G_A(x)$ is introduced to make possible rapid computations. Tables and examples are included.

(Author's Abstract).

238. *Patents.* Abstracts in Geophysics, Vol. 19, No. 2, p. 321, April, 1954.

U.S. 2,657,380.	27 October 1953.	Prospecting system in which a fractional micro-second pulse is transmitted through the ground.
U.S. 2,659,882.	17 November 1953.	Prospecting system in which a high frequency pulse is transmitted through the ground.
U.S. 2,661,466.	1 December 1953.	Apparatus and method for electromagnetic prospecting.

239. *New Oil Exploration Method Developed.*
A. Gibbon, World Oil, Vol. 138, No. 6, pp. 99-101, May 1954.

A new method of oil exploration (the "Lee Method") has been developed and field tested. Based on the same set of factors as those used in electrical logging, the method detects and measures the same electrical effects through a system of electrodes driven into the surface of the ground. The data obtained are used to produce "polarization index numbers", which are plotted on polarization charts, or "Longcologs". Favourable areas show strong polarization, and within these areas the best drilling locations are those of "negative" polarization (below zero on the Longcolog).

It is claimed that production depths and multiple horizons can be determined from the logs, and that there is no depth limitation.

240. *Some Practical Examples of Interpretation of Telluric Methods in Languedoc (South-Eastern France).*
M. Mainguy & A. Grepin, Geophysical Prospecting, Vol. 1, No. 4, pp. 233-40, December, 1953.

In the region covered by the paper, electrical methods have been applied in four different zones:

a) Ales-Maruejols Basin (resistive lower Oligocene blanketed by conductive Upper Oligocene);
b) Ledignan and Vaunage-Lunel anticlines (faulted structures in the marly and limy Cretaceous, with different resistivities;
c) Carmague (thick series of conductive sediments);
d) Beziers Basin (highly complicated structures in the Mesozoic, sidely blanketed by conductive Miocene).

It may be assumed that electrical methods can yield valuable information enabling one to define the rugged subsurface topography of resistive strata buried under a reasonably thick cover of conductive sediments especially when a part of the lower formation outcrops even if the part exposed be small. Faults may be delineated and much more information is obtainable than can be expected from gravity meter surveys at a price not very much higher.

241. *Geo-Electrical Problems of the Hydrology of West-German Areas.*
F. Hallenbach, Geophysical Prospecting, Vol. 1, No. 4, pp. 241-49, December, 1953.

The supply of drinking water for general use in the towns and communities of Western Germany is in many cases insufficient. In order to eliminate the difficulties in the supply of water, geophysical methods have been applied to a large extent since the end of the war. The most important hydrological problems, which were solved successfully by geoelectrical measurements, were as follows:

1) Search for, and delimitation of, areas with salty ground water.

2) Investigation of the geological situation in catchment areas for large waterworks, and the finding of suitable places for the establishment of new plants, and in particular:

3) Search for and determination of the thickness and nature of water-bearing sands and gravels and of the relief of the underlying impervious strata.

GEOCHEMICAL.

242. *Hydrochemical Prospecting for Petroleum Reservoirs.* (In Polish).
J. J. Glogoczowski & K. Szypulowa, Nafta (Krakow), 8, pp. 145-147, 1952.

At the present it is impossible to draw definite conclusions about the meaning of relative values of the ions found in water in three different geological formations, but it seems a promising indication of presence of hydrocarbons at greater depths. The ions considered are HCO_3^-, Cl^-, $SO_4^=$, Ca^{2+}, and Mg^{2+}. Three tables give numerical results.

(From J. Inst. Petrol., February 1954.)

243. *Reconnaissance Geochemical Surveys for Base Metal Mineralization Carried out in Lemieux Township, Gaspe Peninsula, Quebec.*
J. E. Riddell, a paper read at the Eastern Meeting of the S.E.G., Boston, Mass., December, 1953. (not yet published).

During the field season of 1953, geochemical soil and water surveys were employed to outline zones of mineralization containing base metals, in a selected portion of Lemieux township of about 20 square miles in extent.

This area is located in a maturely dissected upland region, underlain by moderately folded and faulted Paleozoic sediments and volcanics which have been intruded by acidic and basic igneous formations of Devonian age. The known bese-metal mineralization is confined to quartz-carbonate veins carrying sphalerite, galena, chalcopyrite and pyrite.

Soil samples were taken at the base of side slopes along the valleys. These samples were analysed for their content of readily soluble copper, lead, and zinc using standard laboratory procedures.

Water samples were taken at appropriate intervals along the main streams and their tributaries. These samples were analyzed in the field using a modified monocolor technique with dithizone as a reagent.

The results of the geochemical surveys show that both soil and water contain greatly increased amounts of base metals in the vicinity of the showings. The areal distribution of the geochemical anomalies indicates that base metallization has been confined to a limited portion of the area surveyed.

OTHER METHODS

244. *Radioactivity as a Guide to Ore.*
W. H. Gross, Economic Geology, Vol. 47, pp. 722-742, 1952.

The author suggests the use of 'higher than normal' natural radioactivity of surface rocks within the confines of a stock or batholith as an indicator of structural deformation within the pluton, and possibly as an indicator of ore mineralization. The basic assumption is a theory of ore genesis (not universally accepted) that demands that pegmatite and ore solutions (the former which are highly radioactive) both originate as a residual liquid from the cooling of the same acid or intermediate magma. Structures that localize one also localize the other. The residual solutions will pass through the mesh of early formed crystals as the solutions move down a pressure gradient caused by structural deformation.

A decreasing pressure gradient may be accompanied by a decreasing temperature gradient which will cause precipitation along the migration path. The 'higher than normal' radioactivity should indicate low pressure areas along which ore may occur.

245. *Detection of Radioactive Minerals.*
D. W. McInnes, Mining & Geol. J., Vol. 4, No. 6, pp. 11-13, 1952.

Descriptions of the Geiger-Müller counter and scintillometer are given, with instructions for their use and maintenance. Wiring diagrams are included.

246. *Geophysical Prospecting of Yugashima Gold Mine. (In Japanese with English summary).*
S. Kunori & T. Saito, Geol. Survey Japan Bull., Vol. 3, Nos. 4-5, pp 28-34, 1952.

Gold and silver occur in veins with gauge minerals of quartz, calcite, and rhodochrosite. Gamma-ray and geochemical methods gave most satisfactory results.

247. *Laboratory Scintillation Counters Applied to some Geophysical Problems in the Application of Recent Counting Techniques to Geophysical Research,*
K. Whitham, Amer. Geophys. Un. Trans., Vol. 33, No. 6, pp. 902-11, 1952.

The development and operation of a laboratory scintillation counter capable of analyzing the separate uranium and thorium contents of radioactive minerals is described. A gamma-gamma analysis was used. An analysis of laboratory experimental data has shown that in measuring the distribution of radioactivity in geologic formations, and in estimating the radioactive heat production in rocks from field observations, scintillation counters using the gamma-gamma counting technique could be used to eliminate the uncertainties due to the presence of potassium, and such a counter would be at least 20 times more sensitive than that described by Slack (see E.A.E.G. abstract no. 78).

248. *The New Counters.*
S. C. Curran, Science Progress, Vol. 42, No. 165, pp. 32-45, January, 1954.

The prototype of the modern scintillation counter was introduced by Curran and Baker during 1944, when they coupled a photomultiplier tube to a scalling unit. This provided a counter much more rapid than the Geiger. The scintillation method has since proceeded at a great rate and is the dominant one in present use. Gas-filled proportional tubes, for counting and analysing radiations, have progressed at the same time and also are a more rapid counter than the Geiger. Recent developments in all three methods are discussed. The conduction, semi-conduction and Cerenkov types of counter are also described briefly.

249. *Geomicrobiology in Petroleum Industry.* (In Polish).
A. Luchterowa, Bull. Polish Inst. Petrol., 2, pp. 7-8, 1952.

Geomicrobiology is being employed to solve the questions of origin of petroleum, its separation from sedimentary rocks, and petroleum prospecting. The various breeds of bacteria are briefly described, and their appearance in known oil-bearing areas points to a new way of prospecting. The metabolism of various kinds of these bacteria enables some to reduce sulphates, some to consume paraffins, other to oxidize aromatics, but paraffins with 10-16 C atoms are easiest to attack. Presence of gaseous paraffins in subsoil over petroleum reservoirs is affected by these bacteria. In the Soviet Union some 18,000 samples, half from known areas, are being correlated with the known subterranean structure.

(From J. Inst. Petrol., February, 1954).

250. *New Oil Finding Method Tested.*

R. B. Pratt, World Oil, Vol. 137, No. 6, pp. 98-105, November 1953.

Oil is sought by a radio technique. A transmitter is fixed in one position. It generates waves, at constant frequency and amplitude, which are picked up by a receiver placed at varying distances on a straight traverse. An oil deposit would be indicated by anomalies on the edge of the transmitter curves.

The operating and interpretation methods are described and illustrated with diagrams and profiles.

251. *Delineation of Petroleum Areas by Radioactive Emanation Survey.*

R. A. Stothart, World Petroleum, Vol. 25, No. 4, pp. 78-79, April, 1954.

A short review, in general terms, of the usefulness of radioactive surveys, and some of the difficulties to be expected. Reference is made to previous articles on the subject, and it is concluded that radioactive surveys should not be used alone in delineating unproven terrain, but are most useful in supplementing records obtained by seismic, gravity, or magnetic surveys.

252. *Radioactive Prospecting for Uranium Minerals* (In French).

C. Lallemant, Onde Elect., Vol. 33, pp. 547-552, October 1953.

A summary of principles with a table of properties of principal uranium minerals, followed by a review of apparatus developed by the Commissariat de l'Energie Atomique. Prospecting for uranium minerals in French territory is referred to.

(From Physics Abstracts, A, May, 1954).

253. *Patents.* Abstracts in Geophysics, Vol. 19, No. 2, April, 1954.

U.S. 2,656,470. 20 October 1953. Method of airborne radioactivity prospecting.
U.S. 2,656,471. 20 October 1953. Method of airborne radioactivity prospecting.

254. *Summary of A.E.R.E (Harwell) Equipment for Use in Prospecting and Assaying Radioactive Ores.*

Atomic Energy Res. Estab. (Harwell) Mem. EL/M83, 1953

Equipment described includes portable ratemeters, borehole logging equipment, (car or airborne) radioactivity detecting equipment and laboratory assey equipment. A brief description of the various instruments is given and some indication of the applications.

(From Physics Abstracts, A, June 1954).

255. *Oil Detection by Scintillation Counters.*

G. Hare, World Petroleum, Vol. 25, No. 3, p. 94, March 1954.

Oil pools may be delineated by the haloes of radioactive soil formed on the surface directly above. Characteristic radioactive patterns of this nature are caused by numerous metal ores. In fact, virtually all rocks and soils are radioactive in some degree. Alpha, beta, and gamma rays are emitted. The latter are most important since they occur in the greatest quantities and are less affected by the interference of cosmic rays. The invention of the scintillation counter has made it possible, only recently, to measure gamma rays. This instrument is a hundred times more sensitive than the Geiger counter, and is designed to detect very small variations in gamma ray activity.

The correlation of radioactivity data with all available geological and geophysical data is advised and such correlation is discussed here.

256. *Propagation of Radio Frequency Energy through the Earth.*
F. M. McGehee, a paper read at the 7th Annual Midwestern Meeting of the S.E.G., Dallas, Texas, November 1953 (Not yet published).

The results of measurements of some propagation characteristics of 1614 and 1700 kc radiation through the earth are reported. In experiments conducted at Carlsbad Caverns, N. M., and Mammoth Cave, Ky., transmitters were set up on the surface 700 and 280 feet above unwired tunnels, and the signal strength measured at many points in the tunnels. The data are interpreted to show that the radiation is approximately equal over an underground hemisphere and that the attenuation is about 0.014 and 0.05 to 0.1 nepers/meter at the two locations respectively. These values are in good agreement with theory.

257. *Radioactivity Measurements in Los Angeles Basin.*
H. W. Hoylman & W. L. Morris, a paper read at the Pacific Coast Meeting of the S.E.G., Los Angeles, November 1953 (Not yet published).

The paper discusses some of the results obtained during the past two years from gamma radiation surveys which have been studies as geophysical data reflecting certain geological conditions. The problem of determining gamma ray anomalies with a continuous recording scintillation counter is discussed. Cross sections and contour maps will be shown of gamma radiation measurements, on the ground and in the air, across certain oilfields and geological structures in the Los Angeles Basin. Some correlations of radioavtivity and aeromagnetics with geology are shown.

258. *Gamma Ray Exploration Comes of Age.*
D. S. Lobdell, E. F. Buckley & J. W. Merritt, World Oil, Vol. 139, No. 2, pp. 107-Aug. 1, 1954.

A general survey is made of the method of detecting surface gamma radiation associated with buried hydrocarbons. Some typical gamma ray profiles across producing fields are shown. Instrumentation factors, and the limitations to good instrumentation, are discussed.

It is shown how the shape and size of the patterns obtained may help to determine the nature of the oil accumulation below. Exceptional patterns, and interference patterns, are briefly considered.

TEMPLATES FOR FITTING SMOOTH VELOCITY FUNCTIONS TO SEISMIC REFRACTION AND REFLECTION DATA *

BY

J. G. HAGEDOORN **

Abstract

Velocity functions can be grouped into families, any one of which results in seismic pictures differing among themselves only in their scales of time and distance but similar in all other respects. For any one of these families it follows that curves drawn on logarithmic scales of time and distance to represent a particular relationship between seismic quantities will be similar in shape. This leads to the use of templates with logarithmic scales for fitting a smooth velocity function to a set of seismic data. Suitable templates for fitting refraction and reflection data to velocity distributions linear with either depth or vertical time are presented. An insight into the uncertainties involved is obtained with the aid of numerical examples.

General

The data obtained in seismic exploration work consist primarily of travel-times from explosive sources to geophones. In order to be able to transform these data from time values to depth values, the velocities in the media transversed must be evaluated.

The simplest and most straightforward manner of determining velocities is by velocity surveys in wells drilled through the formations involved. By measuring the travel-times, from a shotpoint at the surface near the well to a geophone lowered to successively greater depths, it is possible to obtain an accurate vertical velocity distribution. A template for obtaining an approximating smooth velocity distribution to fit time-depth values obtained in this manner has been presented in "A Process of Seismic Reflection Interpretation", chapter V (Hagedoorn 1954 b).

Templates based on similar considerations can also be developed for determining smooth velocity distributions from the other two main sources of seismic information, the refraction- and the reflection methods. Credit is due to J. McG. Bruckshaw of Imperial College, London, for recognizing the possibilities of templates and for making use of them to determine smooth velocity distributions from refraction data. A template for the same purpose is presented here. The mathematical basis for it is simpler and it has the merit that time-distance points can be plotted directly on logarithmic scales.

---

* Presented at the Eight Meeting of the European Association of Exploration Geophysicists, held in Paris, 18/20 May 1955.

** N.V. De Bataafsche Petroleum Maatschappy, The Hague (Royal Dutch Shell Group).

The determination of velocity distributions from seismic data obtained from well surveys and from refraction- and reflection shooting is an established routine procedure in seismic interpretation. The ultimate test for the applicability of any solution is by observing whether this solution would, by working back, lead to the original data to within an acceptable margin of error. This statement may appear too obvious, but erroneous solutions may not be suspected until this test is applied. An example is given in "A Process of Seismic Reflection Interpretation", chapter V, 1. The difficulties arise from the fact that it is desirable, for the sake of ease in interpretation, to approximate to an actually discontinuous velocity distribution by a smooth velocity function in those cases where the errors incurred by the approximation are permissible.

Thus the most reliable method of obtaining smooth velocity functions from seismic data is by trial and error; of testing different continuous functions until a reasonable fit to the observed values is obtained. In this way it is possible to observe the accuracy of fit directly. In order to reduce the amount of work involved, it is best carried out in the reverse direction by comparing the data to the results from a number of possible velocity functions, which have been prepared beforehand in the form of templates.

The mathematical derivation of suitable templates can be developed as follows. If the velocity does not change laterally, as has been assumed to be the case in figure 1, it is a function of depth only and, according to Snell's law, a ray is determined by

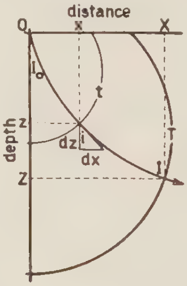

Fig. 1. Depth-Distance-Time relationship.

$$\sin i/\sin I_o = V_z/V_o$$

The velocity V_z, as a function of the depth z, can always be expressed as

$$V_z/V_o = f(z/L)$$

The function f may be any function, continuous or not. By defining f, a family or group of velocity functions is chosen, any particular member being fixed by the choice of V_o and L. One of the advantages of arranging all possible velocity functions into such groups will be seen to be that the templates for each group become extremely simple.

If the inverse function of f is F, giving the depth as a function of velocity,

then $$z/L = F(V_z/V_o) = F(\sin i/\sin I_o) = G(I_o, i)$$

and $$Z/L = G(I_o, I).$$

Then $$\frac{X}{L} = \int_0^X \frac{dx}{L} = \int_0^Z \tan i \frac{dz}{L} = \int_{I_o}^I \tan i \frac{dG}{di} di = H(I_o, I)$$

and $$T\frac{V_o}{L} = \int_0^T \frac{V_o}{L} dt = \int_0^Z \frac{V_o}{L} \frac{dz}{V_z \cos i} = \int_{I_o}^I \frac{\sin I_o}{\sin i \cos i} \frac{dG}{di} di = K(I_o. I)$$

This is a parametric relationship between Z, X and T with I_o and I as parameters. In principle, I_o and I can always be eliminated from these three equations, resulting in one single relationship

$$M(z/L, x/L, tV_o/L) = 0.$$

Thus the family of velocity distributions $V_z/V_o = f(z/L)$ results in one single function M to describe the seismic picture and this picture is the same for all these velocity functions if x and z are scaled in units of L and t is scaled in units of L/V_o.

A wavefront at time T is given by the function M with $t = T$, the refraction time-distance curve is given by the function M for $z = 0$ and the relationship between vertical reflection time and the reflection time to a horizontal distance X, the t, Δt relationship, is given by elimination of z from two equations, one of which is M with $x = 0$ and the other M with $x = X$.

Thus it is clear that any relationship between two of these variables, when represented by a graph on logarithmic scales of time and distance, has exactly the same shape for all velocity functions of one family. Only the position of a curve will differ from those of its neighbours so that, by observing the amount a curve is shifted relative to a curve representing the relationship for known values of V_o and L, the values of V_o and L applicable to any particular case can be determined. This means that a template for determining a velocity function can consist of a logarithmic coordinate system with only one master curve for each family of velocity functions, if the relationship used is a simple relation of time with depth or distance.

This procedure has been worked out for the case where the time-depth relationship has been determined from a well survey in "A Process of Seismic Reflection Interpretation", chapter V. This template consists of a logarithmic coordinate system on which experimentally determined time-depth points can be plotted on a transparent overlay that can then be shifted to where the plotted points fit one of the master curves, thereby determining which family fits the velocity distribution best and also the values of V_0 and L.

THE TEMPLATE FOR REFRACTION DATA

In figure 2 the seismic refraction picture is shown for the case of the two families of smooth velocity functions most widely used in practice, the "linear" velocity distribution $V_z/V_0 = 1 + z/L$, where the velocity increases linearly with depth (continuous lines) and the "parabolic" velocity distribution $V_z/V_0 = \sqrt{1 + 4z/L}$, where the velocity increases linearly with vertical time (broken lines).

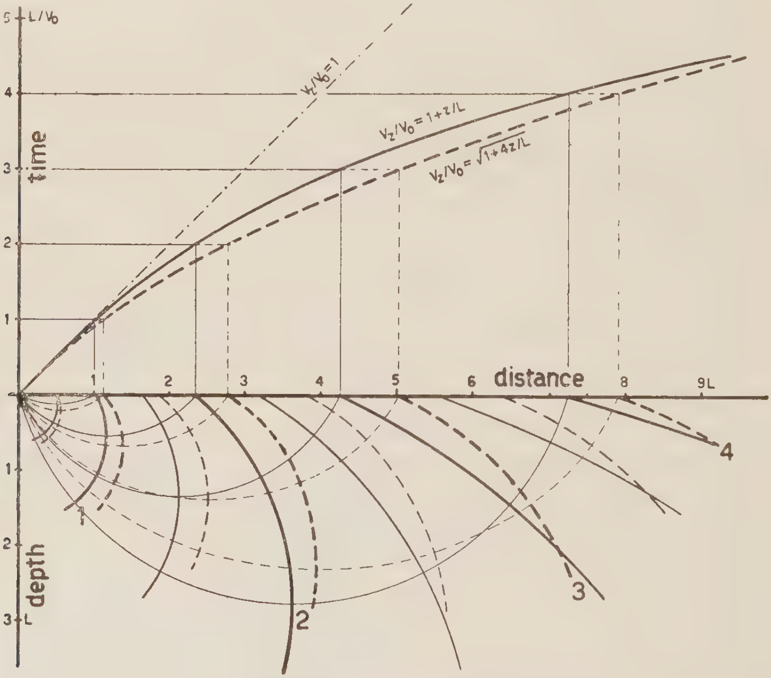

Fig. 2. The general refraction Depth-Distance-Time relationship for all linear and for all parabolic velocity distributions.

Figure 2 is a universal picture, corresponding to all possible functions belonging to these two families of velocity functions, because the times have been scaled in units of L/V_0 and the distances in units of L. A template for determining smooth velocity distributions, belonging to one of the two families under consideration would consist, in principle of the t, x curves of figure 2 plotted on logarithmic scales.

A detailed account of the considerations leading to a practical template can be omitted here because it would be exactly the same as the procedure, described elsewhere (Hagedoorn 1954b), for deriving a template for time-depth data.

A serviceable template is presented on enclosure *D*. The time-distance points must be plotted on a transparent overlay on which the V_o- and L-axes are also traced. This overlay is then shifted, keeping the traced axes parallel to those on the template, to a position where the plotted points fit one of the master curves as closely as possible. The values of V_o and L can then be read off on the V_o- and L-scales respectively at the intersections of the translated axes.

Uncertainties of refraction interpretation

It is a well-known fact that the determination of a velocity distribution from refraction data is a rather uncertain procedure. Layers with relatively lower velocities will not yield first-arrivals, and layers with intermediate velocities will only do so if they are thick enough. It is seldom that time-distance curves lead to a complete knowledge of the velocity distribution; this would only be derivable if the velocity were to increase monotonously with depth at a rate continuous within definite limits so that a smooth time-distance curve could be observed. However, in practice, refraction work is usually carried out under circumstances where fairly abrupt changes in velocity occur, so that refraction interpretation is to some extent undetermined. Another uncertain factor is the fairly common anisotropy; the velocities in the horizontal direction, as they are determined from a refraction time-distance relationship are quite often as much as 10% higher than in the vertical direction (Cholet & Richard 1954, Hagedoorn 1954a).

Even when anisotropy is not taken into account and under apparently straightforward circumstances, the velocity determinations from refraction data will still contain an uncertainty.

In order to arrive at a quantitative picture of these uncertainties, a numerical example has been worked out in figure 3. As point of departure it has been assumed that an overburden with a linear velocity distribution $V_z = 1.77 (l + z/2.44)$ Km/sec overlies a basement at 2.10 Km depth having a constant velocity of 5 Km/sec. These magnitudes are within the ranges generally encountered in practice. The first-arrival time-distance curve in figure 3*A*, resulting from a shot at *O*, consists of a curved part from *O* to *D* and a straight line from *D* onwards, the surface of the basement being assumed horizontal. Conversely, this time-distance curve would be the data from which the velocity distribution would have to be determined in practice.

The observational error in refraction work of this magnitude usually lies in the order of from 5 to 10 milliseconds. An interpretation of the velocity distribution which resulted in the same first-arrival time-distance curve t_o within this error would be considered a possible interpretation. In the particular case of figure 3 the velocity distributions $V_z = 1.75\sqrt{1 + z}$ and $V_z = 1.79e^{z/2.96}$ would result in time-distance curves, which do not deviate

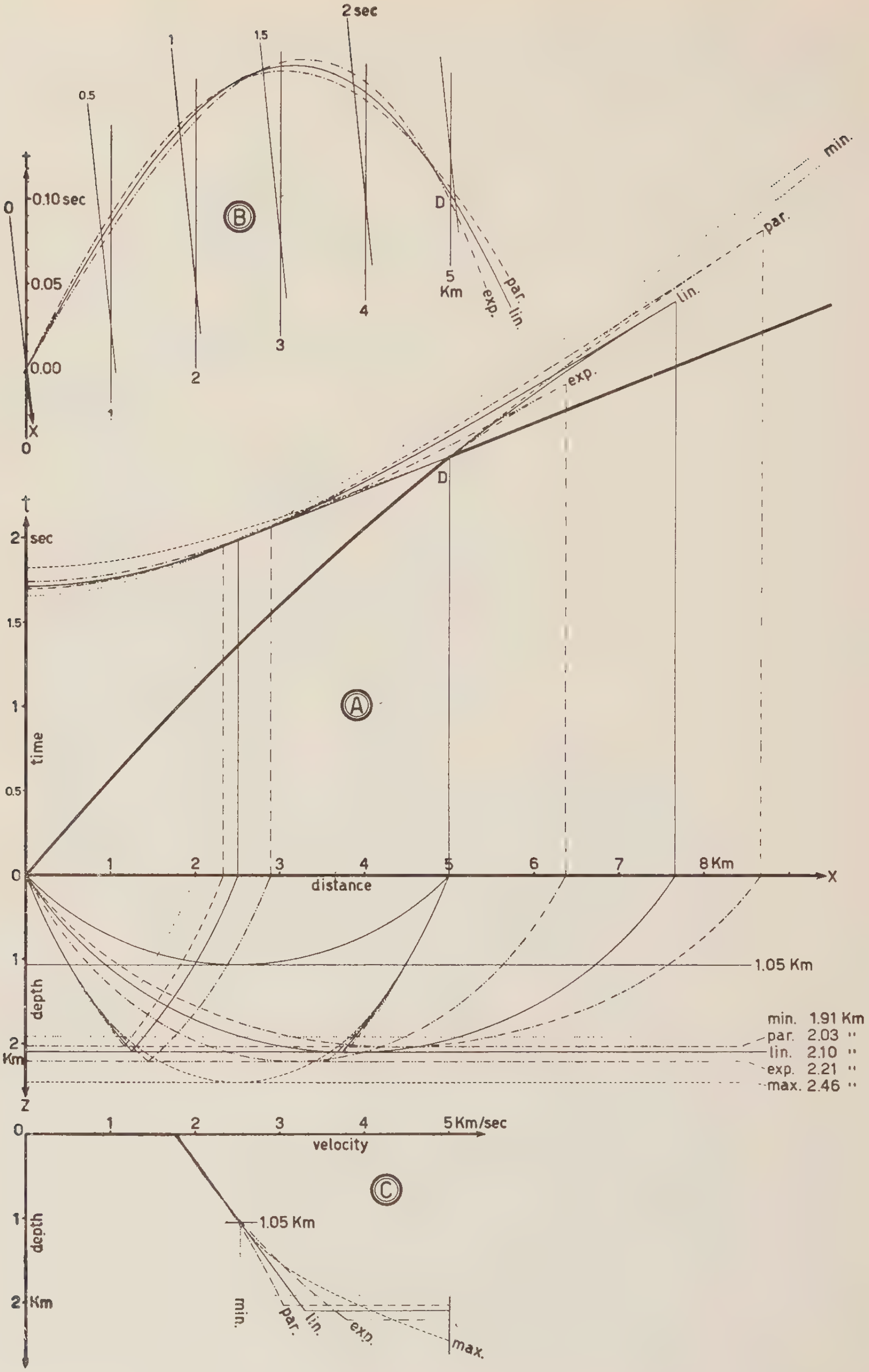

Fig. 3. Five different velocity distributions resulting in nearly the same first-arrival time-distance curves.

more than 5 and 6 millisecoids, respectively, from the result of the original velocity distribution $V_z = 1.77\ (1 + z/2.44)$ up to a distance of 5 Km.

This means that it would not be possible to differentiate between a parabolic, a linear or an exponential velocity distribution on the evidence given by the first-arrival time-distance curve of figure 3. This statement refers to this particular example, but it can be seen in a wider sense by formulating it in terms of times and distances expressed in units of V_o and L. Thus, it would not be possible to differentiate between a parabolic $(V_z = V_o\sqrt{1 + 2z/L})$, a linear $(V_z = V_o\ (1 + z/L))$, or an exponential $(V_z = V_o e^{z/L})$ velocity distribution from the evidence of a first-arrival time-distance curve with its deflection point at a distance of up to about $2L$, if the observational error is as much as $0.004\ L/V_o$. This will include nearly all practical cases, so that a distinction between the types of velocity function is usually only possible from other evidence as, for example, from well data obtained in adjacent areas.

In figure 3*B*, in which the time scale is ten times that in figure 3*A* and the distance axis is inclined in order to show a clear graphical picture, the three time-distance curves, corresponding to the three above mentioned velocity functions, are shown up to the deflection point *D*. It will be seen that, by a suitable choice of the two variables V_o and L, these curves can be made to cut each other twice, just as do the curves representing the velocities as a function of depth in figure 3*C*.

In figure 3*C* the three velocity distributions, the parabolic, the linear and the exponential one, are seen to deviate only slightly down to about half the depth to the basement, but below this depth the deviations are seen to increase considerably. These result in appreciably different depth values (2.03,2.10 and 2.21 Km) when the depth of the basement is derived from the first-arrival time-distance curve on the assumption of the three different velocity distributions in the overburden.

The reason for these appreciably different depths is clear by observing that the curved part of the first-arrival time-distance curve, from *O* to *D* in figure 3*A*, only refers to a depth of penetration to 1.05 Km. Energy from the shotpoint, penetrating to depths in the overburden from 1.05 Km down to the basement, will register at the surface beyond the distance of the deflection point at 5 Km and could only be observed as second arrivals after the first refraction impulses from the basement have arrived. In practice these second arrivals, which have been drawn in figure 3*A*, can hardly ever be observed within the reverberations from the first-arrival refraction impulses.

This masking effect will always occur when a basement having a relatively higher velocity is investigated. In this numerical example no knowledge can be gained on the velocities in the lower half of the overburden. This is the order of magnitude of masking effect commonly met in practice and, to a greater or lesser extent, this masking of velocities is unavoidable in nearly all refraction interpretations.

The determination of a velocity distribution in an overburden, from the time-distance curve up to the deflection point, for example with the aid of the template on enclosure *D*, actually means that a fairly accurate solution of the velocity distribution in the upper half of the overburden is extrapolated all the way to the basement. The velocity distribution in the lower part could, however, be appreciably different, resulting in a quite erroneous interpretation of the depth.

The unknown velocities in the lower half of the overburden will, however, lie within certain bounds. As a practical minimum, the velocity could be assumed to remain constant at the value attained at the deepest known point. This case has been included in figure 3*A* and *C* (dotted lines) and it results in an interpretation giving a minimum depth of 1.91 Km to the basement.

The theoretical maximum velocity distribution below 1.05 Km, which would still result in the same first-arrival time-distance curve as for the linear velocity distribution down to 2.10 km depth, would be a limiting case where all energy from *O*, penetrating to depths between 1.05 Km and that of the basement, would converge at the deflection point *D*. This case can be approximated by assuming a large number of layers below 1.05 Km depth, each with a velocity such that its refraction time-distance graph passes through the deflection point *D*. In this way the maximum depth case (dashed lines) was derived in the example of figure 3. The velocity is seen, in figure 3*C*, to increase continuously up to the basement velocity of 5 Km/sec at 2.46 Km depth.

On the supposition that the velocity increases monotonously with depth, and without taking into account observational errors, the conclusion is that the first-arrival time-distance curve in figure 3*A* can refer to a basement lying at a depth anywhere between 1.91 and 2.46 Km below the surface, an uncertainty of 25 per cent. This is the order of magnitude of the uncertainty to be expected in general in refraction work.

This large uncertainty only refers to the interpretation of the absolute depths and certainly does not mean that simple structures, for instance with a magnitude of 5% of their depth, could not be found. If the lateral changes in velocity are not too large, the relative depth picture of a structure can often be quite accurately determined by refraction work.

It is, however, clear that it is pointless to try and obtain a very accurate velocity distribution from seismic refraction data alone. A velocity function found from the time-distance curves with the aid of the template must only be accepted as a probably better approximation to the actual distribution than, for example, a constant velocity, because it implies a probable increase in velocity in the lower part of the overburden continuous with that in the upper part.

THE TEMPLATE FOR REFLECTION DATA

In figure 4 the general reflection picture is shown for the velocity distribution linear with depth and for horizontal reflectors. This is, of course, a highly idealized picture and, again, it must be regarded only as an approximation which is mathematically workable and which leads to practical routine

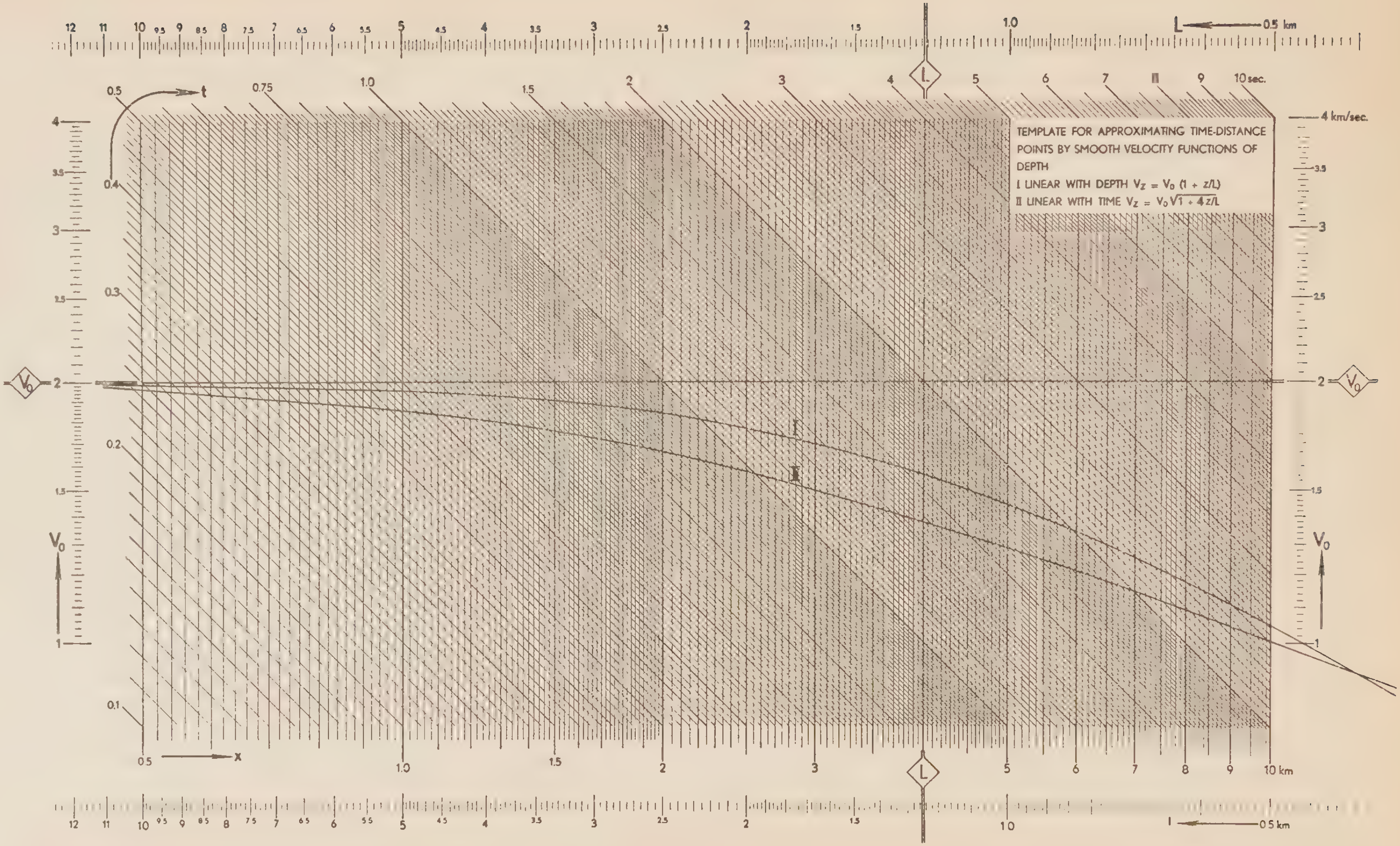

TEMPLATE FOR APPROXIMATING TIME-DISTANCE POINTS BY SMOOTH VELOCITY FUNCTIONS OF DEPTH

I LINEAR WITH DEPTH $V_Z = V_0 (1 + z/L)$

II LINEAR WITH TIME $V_Z = V_0 \sqrt{1 + 4z/L}$

Enclosure D

interpretations in a number of actual cases where the errors incurred by the approximations are acceptable.

A vertical time-depth relationship and a refraction time-distance relationship each result in one curve for a particular velocity distribution, so that the templates contain only one curve for each family of velocity distributions $V_z V_o = f(z/L)$. The reflection time-distance relationship, however, requires a curve for each horizontal reflector, one of which, for the limiting case of a reflector at zero depth, is the refraction time-distance curve. This means that the reflection template, even for one family of velocity functions, would have to contain a large number of curves, enough, in actual practice, to enable fitting of a curve starting at any value of the vertical reflection time t_o.

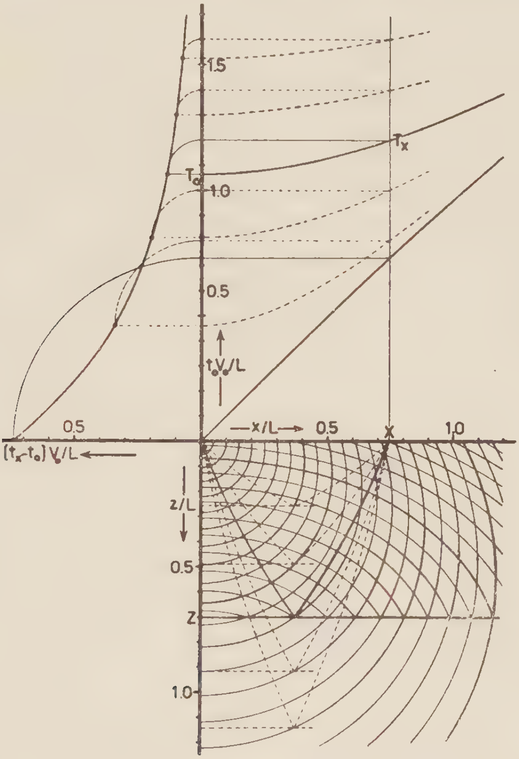

Fig. 4. The general reflection Depth-Distance-Time relationship for all linear and for all parabolic velocity distributions.

The reflection template for all velocity distributions linear with depth could consist, in principle, of the curves of the top right hand graph of figure 4 plotted on logarithmic scales of time and distance. This solution would, however, be unacceptable as the vertical reflection times could not be plotted because a logarithmic graph cannot contain the time axis at distance zero.

In actual practice a "t, Δt" process, based on regular reflection profiles, is used extensively for the determination of velocity distributions (Steele 1941). This process enables rapid statistical use of a large number of reflections on records obtained over a fairly large area where no appreciable lateral change in velocity is assumed. The reason that such a statistical approach is so attractive can be appreciated by observing the relatively very small change of reflection time with distance for the deeper reflections in the example of figure 4, where the shooting distance has been chosen greater than in most cases in actual practice.

The statistical data are obtained in the form of two time observations from each reflection, one at a short distance and one at the largest practical distance, for example, the mean times of the nearest four and the furthest four seismometers of each spread. By always using the mean values of times from pairs of symmetrical shots a first order correction is made for the effect of dipping reflectors.

The time values for the short distances can be transformed to time values at zero distance by assuming the time-distance relationship to be hyperbolic:

$$\left.\begin{aligned} t_1 &= \sqrt{t_0^2 + p x_1^2} \\ t_2 &= \sqrt{t_0^2 + p x_2^2} \end{aligned}\right\} \qquad t_0 = \sqrt{\frac{x_2^2 t_1^2 - x_1^2 t_2^2}{x_2^2 - x_1^2}}$$

The errors incurred by this assumption of a hyperbolic relationship are negligeable for most practical velocity distributions. The error in the value of t_0 will be appreciably smaller than when assuming the time-distance relationship to be the more convenient parabolic one:

$$\left.\begin{aligned} t_1 &= t_0 + q x_1^2 \\ t_2 &= t_0 + q x_2^2 \end{aligned}\right\} \qquad t_0 = t_1 - (t_2 - t_1)\left(x_2^2/x_1^2 - 1\right)$$

It will, however, be found that this parabolic relationship can be used in a great number of practical cases. In order to evaluate the error incurred by this approximation this error was derived for the velocity distributions linear with depth and linear with vertical reflection time. The value of t_0 is too large by approximately:

$$0.05\,\frac{x_1^2 x_2^2}{t_0^4}\,\frac{L}{V_0^5} \qquad \begin{aligned} &\text{for } V_z = V_0(1 + z/L) \\ &\text{and for } V_z = V_0\sqrt{1 + 2z/L} \end{aligned}$$

The seismic data, from which the velocity distribution must be derived, then consist of pairs of values, the times for zero distance and the times for a fixed distance x. These can then be plotted in a t_o against t_x-t_o, or t, Δt, graph as shown in the top lefthand graph in figure 4. Only one curve has been drawn, corresponding to one shooting distance x/L. It is clear that a t, Δt template must contain a large number of curves for different values of x/L on logarithmic scales. In contradistinction to the vertical time-depth template and the refraction time-distance template, both scales of this $t, \Delta t$ template are time scales. This means that, when a particular $t, \Delta t$ relationship is fitted to the curves of the template, the graph has to be shifted the same amount along both axes, depending on the value of V_o/L corresponding to the particular case. A transparent overlay, on which the obtained $t, \Delta t$ points have been plotted, may only be moved in one direction, along lines where t and Δt change proportionally. Thus the amount of shift will only furnish the value of V_o/L of the approximating velocity distribution. The value of L/x, and hence L, is found by observing to which particular curve the plotted points must be shifted in order to obtain the best fit.

A template for this purpose is presented on enclosure E. This contains a set of curves for the velocities linear with depth $V_z/V_o = 1 + z/L$ (full-drawn curves) and a set of curves for the velocities linear with vertical time $V_z/V_o = \sqrt{1 + 4z/L}$ (dashed curves). These curves have been drawn for $V_o/L = 0.5$, so that the points at this value on the V_o/L scales must be marked on the transparent overlay on which the $t, \Delta t$ points are plotted. This transparent overlay must then be shifted, keeping these marked points at equal values on the two V_o/L scales, to a position where the best fit of the points to one of the curves is obtained.

For completeness, a curve (circle-dash line) has been included for fitting t_o, $t_x - t_o$ points to a constant velocity. The $t_x - t_o$ relationship for a constant velocity V_c can be derived from the following formula

$$t_x - t_o = \sqrt{t_o^2 + x^2/V_c^2} - t_o$$

The curve on the template has been plotted for $V_c/x = 5$. If both the t_o and the $t_x - t_o$ values, corresponding to a velocity $V_c/x = a$, were multiplied by $5/a$ these points would be plotted on the circle-dash curve on the template. Conversely, the amount that a set of points must be shifted to fit this curve, in a direction where t_o and $t_x - t_o$ remain proportional, determines the value of V_c/x.

Uncertainties of velocities derived from reflection data

The uncertainties of velocity determinations from refraction data were seen to be due mainly to anisotropy and to the fact that a time-distance curve usually does not contain information about the whole depth column. These sources of error do not affect reflection interpretations because the energy always travels in a nearly vertical direction and, in most cases, information is obtained about the whole depth column from a number of reflections from successively greater depths.

A reflection observed on a record results from an impulse of fairly simple form, transformed by the amplifying system with more or less filtering, to a wave-train consisting of from about two to ten peaks and troughs, superimposed on a background of noise of the same order of magnitude. A series of correlating troughs or peaks on successive traces are picked bnd certainly not the first moments of arrival. The interval between the first arrivals and the picked peaks or troughs will usually be in the order of from 10 to 40 milliseconds, depending on the filters used and on the amplitude of the reflection in regard to the noise background. Because of the variable circumstances it is difficult to correct for this error. It is an error in the total time and not in the step-out time, or Δt, except in those cases where the frequency of the recorded impulse changes appreciably with distance. This last effect may, however, become a source of errors when especially long distances are shot for the purpose of obtaining large step-out times for accurate velocity determinations. It is a point in favour of using statistical data from regular reflection profiles, rather than to shoot special long distance profiles only for the purpose of determining the velocities.

It is clear that the fact that reflections are always picked too late will not result in a large error in the velocity distribution, but will result in horizons being plotted too deep. The t_o, $t_x - t_o$ curve will only be shifted by small, but not necessarily constant amounts in the direction of the t_o-axis.

The main source of uncertainty of the velocity determinations from reflection data is the observational error in the step-out times. A single value of a step-out time can, for example, have been obtained from two pairs of time values each of which are the mean of four time readings. In practice, the error in on step-out time will hardly ever be less than one millisecond and will contain an uncertainty due to a dip or change in dip of the reflector. This error can be, and is, reduced by using the statistical mean of a number of reflections. This means, however, that an average is taken over a certain area where a lateral change in velocity may occur. The wide variety of circumstances met in practice make it impossible to predict to what degree of accuracy the step-out times can be obtained, but some idea of the magnitude of the uncertainty can be derived from the scattering of the individual values.

In order to obtain some insight into the influence of the observational errors on the determination of the velocities and the resulting errors in the depth values found, a numerical example is presented in figure 5. The velocity distribution linear with depth $V_z = 1.755\ (1 + z/2.44)$ and the velocity distribution linear with vertical travel time $V_z = 1.75\sqrt{1 + z}$ (continuous curves) are seen to result in $t_o, t_x - t_o$ relationships (dot-dot-dash curves) where the difference (dot-dash curves) between the values of $t_x - t_o$ is less than 0.0003 sec

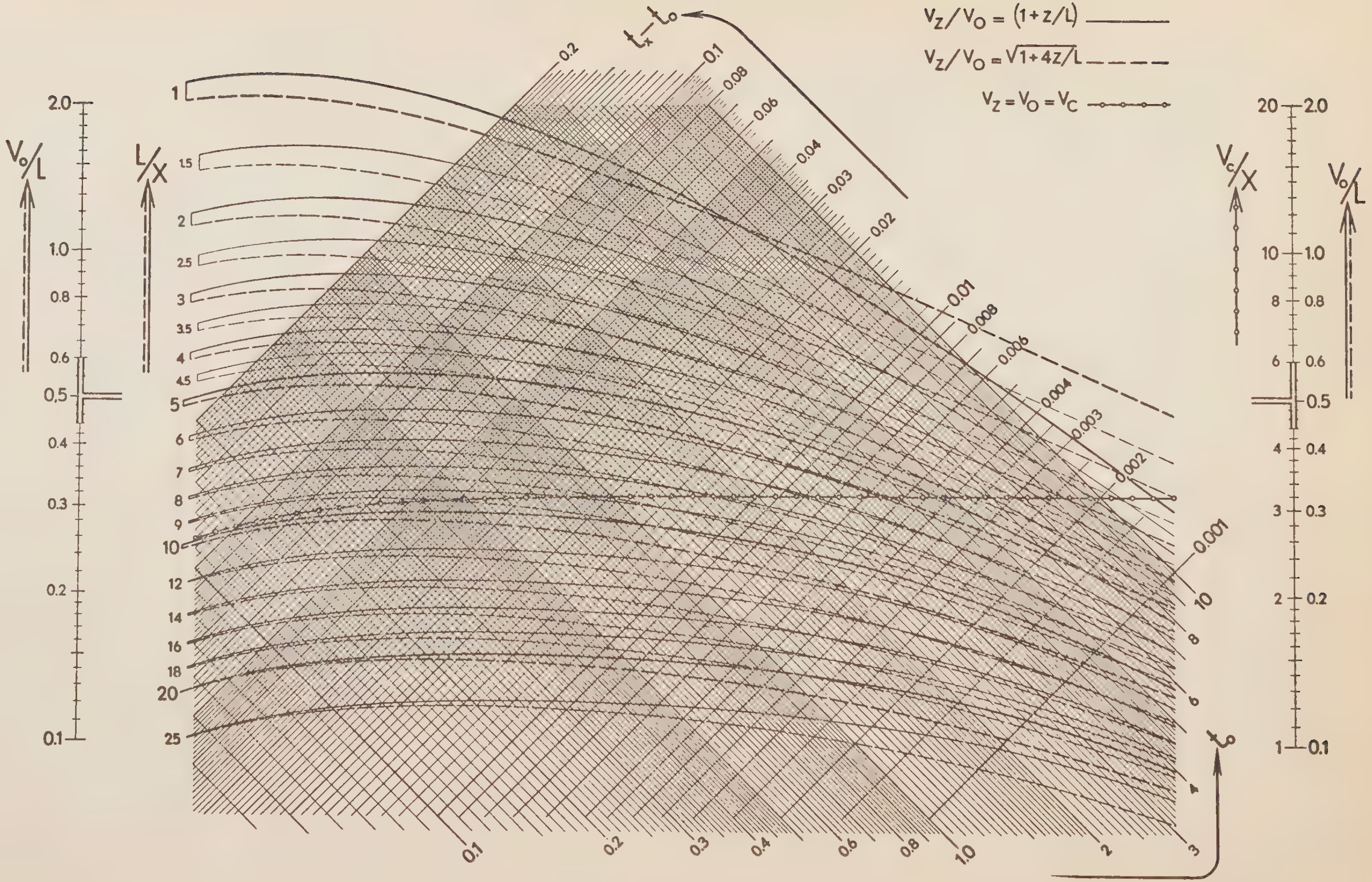
$V_Z/V_O = (1+Z/L)$
$V_Z/V_O = \sqrt{1+4Z/L}$
$V_Z = V_O = V_C$
$t_x - t_o$
t_o
V_o/L
L/X
V_c/X
V_o/L
2.0
1.0
0.8
0.6
0.5
0.4
0.3
0.2
0.1
20
10
8
6
4
3
2
1
1
1.5
2
2.5
3
3.5
4
4.5
5
6
7
8
9
10
12
14
16
18
20
25
0.2
0.1
0.08
0.06
0.04
0.03
0.02
0.01
0.008
0.006
0.004
0.003
0.002
0.001
10
8
6
4
3
2
1.0
0.8
0.6
0.4
0.3
0.2
0.1

Enclosure E

and 0.0011 sec respectively for shooting distances of $x = 0.25$ Km and $x = 0.50$ Km respectively.

The particular case of figure 5 is of the order of magnitude of what may be found in actual practice. The result can be stated in general by scaling all distance values in units of L and all time values in units of L/V_o: The step-out times for two velocity distributions $V_z = V_o \sqrt{1 + z/L}$ and $V_z = 1.003\, V_o\, (1 + z/2.44L)$ with always differ less than about $0.01\, (x/L)^2 L/V_o$.

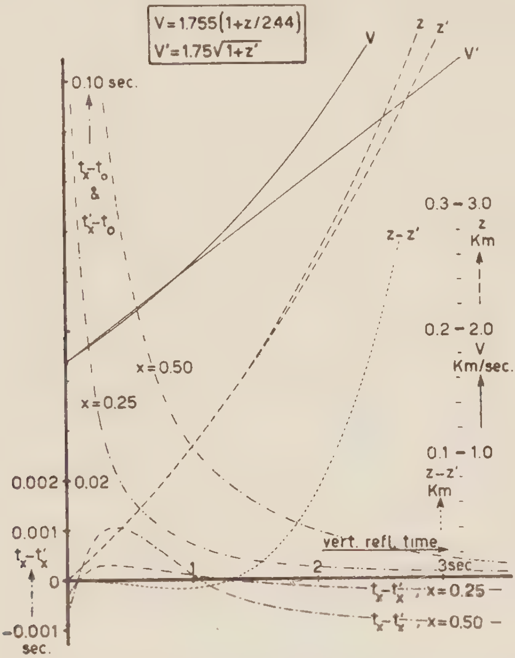

Fig. 5. A linear and a parabolic velocity distribution resulting in nearly the same time-delta-time relationship.

Conversely, from a t, Δt relationship, it would not be possible to determine which of the two types of smooth velocity distributions is the best approximation to the actual one, if the observational error is of this order of magnitude. Probably, in most cases in actual practice, a choice between the two can hardly ever be made solely from reflection data alone, the same as was the case in refraction interpretation.

This means that if a set of t_o, $t_x - t_o$ points obtained in practice fits one of the sets of curves on the template on enclosure E reasonably well, it will probably fit the other set just as closely. The choice of the type of velocity distribution will usually depend upon computational convenience except when additional information from well surveys in adjacent areas is available.

The use of a wrong velocity distribution for plotting a depth section will manifest itself by the occurrence of "washboarding" when the reflection times are plotted vertically. Depending on the quality of the reflections, this washboarding can usually be observed only if the error in the step-out time is in excess of about 2 to 10 milliseconds. Conversely, this means that if a set of t_o, $t_x - t_o$ data can be fade to fit a curve on the template to within this range, the use of the corresponding smooth velocity distribution will not result in observable washboarding.

This is the great advantage of using such a direct method of fitting values to a template over less direct methods where the closeness of a fit at some point in the process is not seen in direct connection to the results eventually plotted.

When fitting data to logarithmic templates the best procedure is not to plot points but to plot line segments showing the magnitude of the probable uncertainty or of the permissible variation. For t_o, $t_x - t_o$ points this means plotting line segments at the t_o values with a length corresponding to an acceptable variation of the $t_x - t_o$ values.

Acknowledgements

The author is indebted to the Bataafsche Petroleum Maatschappij for the permission to publish this paper.

References

CHOLET J. & RICHARD H., 1954, A Test on Elastic Anisotropy Measurement at Berriane, Geophysical Prospecting, 2, 232-246.

HAGEDOORN J. G., 1954a, A Practical Example of an Anisotropic Velocity Layer, Geophysical Prospecting, 2, 52-60.

——, 1954b, A Process of Seismic Reflection Interpretation, Geophysical Prospecting, 2, 85-127.

STEELE W. E. Jr, 1941, Comparison of Well Survey and Reflection "Time-Delta-Time" Velocities, Geophysics, 6, 370-377.

Discussions

Mr. VON HELMS: I would like to speak about the exact calculation of the depth of a layer from refraction data. We have seen that it will be possible to have a mistake in the depth of 25% between the different velocity-functions which you assume for the overburden. Such a value in the mistake (25%) is too high for practical work. If you have already a mistake of 25% for the depth of the first layer, how big may be the mistake for the 2nd, 3rd layers and so on?... Another trouble is that the velocity functions for the overburden near the shot point can be quite different in distances of 10, 20 km... for refraction points. Therefore it would be the best to use the values of the average-velocity of the overburden obtained by well shooting for calculating the depth of the layer. For reflection calculations the danger of making big mistakes is much smaller because the shot points and the geophones are close together.

Mr. HAGEDOORN: It is, of course, best to use a velocity distribution obtained from a well survey whenever available. In practice, however, the drilling of wells usually comes after seismic exploration, the location of the wells being the aim of this exploration.

DÉTERMINATION DE LA POSITION DANS L'ESPACE D'UN MIROIR SITUÉ SOUS UN RÉFRACTEUR SÉPARANT DEUX MILIEUX DE VITESSES DIFFÉRENTES, À PARTIR DES DONNÉES D'UN TIR EN CROIX ISOLÉ *

PAR

B. FAVRE **

ABSTRACT

The problem is considered of how to determine, from dip shooting data, the position in space of a reflecting horizon located underneath a refracting interface between two media of different velocities.

The author proposes a combination between a geometric solution and an analytic one, to obtain the quickest result.

La détermination dans l'espace d'un miroir M_2 situé au-dessous d'un horizon réfracteur M_1 (discontinuité de vitesse à la traversée de M_1) a déjà retenu l'attention de plusieurs géophysiciens, notamment parmi les membres de l'E.A.E.G.

Nous apportons ici une contribution à ce problème, dans le cas particulier de l'exploitation d'un tir en croix isolé. Ceci peut être utile lorsque les tirs en croix ont été effectués dans une région à tectonique compliquée, pour pallier l'incertitude ou la discontinuité des coupes sismiques. Nous supposons connues les lois de vitesse au-dessus et au dessous de l'horizon M_1, et admettons que celui-ci est localement plan dans la zone où il intervient comme réflecteur et réfracteur.

Désignons par t_1 le temps double observé pour la trajectoire EA (fig. 1) issue du point d'explosion E et normale au miroir M_1, par t_2 le temps double observé pour la réflexion sur le miroir M_2 (trajectoire EBC, atteignant M_2 normalement en C, après s'être réfractée en B à la traversée de M_1). Désignons par $\vec{g_1}$ et $\vec{g_2}$ les gradients-temps résultants observés respectivement pour les réflexions sur M_1 et sur M_2. Nous supposons effectuées les corrections de surface.

1°) Examinons d'abord le cas de *deux milieux à vitesses constantes*, V_1 entre le *D.P.* et M_1, V_2 entre M_1 et M_2. Ce cas se présente notamment à Lacq (Aquitaine), où l'on observe, grâce à un certain nombre de carottages sismiques, une vitesse sensiblement constante $V_1 \sim 2500$ m/sec. entre la surface du sol et le niveau M_1 des calcaires à silex (toit du Sénonien inférieur, roche réservoir du gisement superficiel de pétrole), et une vitesse sensiblement constante $V_2 \sim 5400$ m/sec. entre celui-ci et le niveau M_2 du toit du Néocomien, roche réservoir du gisement profond de gaz.

---

* Presented at the Eighth Meeting of the European Association of Exploration Geophysicists, held in Paris, 18-20 May, 1955.

** Institut Français du Pétrole, Paris.

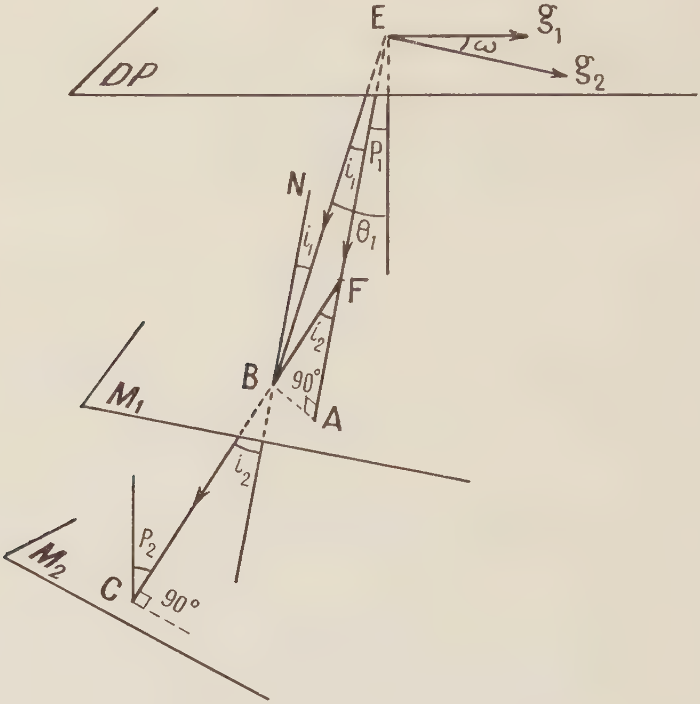

Fig. 1. Schéma d'ensemble. — General diagram.

Le problème de la restitution de M_2 ne présente pas de difficultés théoriques; mais l'obtention d'une solution suffisamment rapide du point de vue pratique est moins évidente.

Le procédé que nous proposons (*c*) combine des calculs élémentaires à une représentation graphique de certains des éléments de la fig. 1. Son principe repose sur la remarque très simple suivante: le plan d'incidence P en B (défini par le rayon incident EB et la normale BN) contenant aussi la normale EA (parallèle à BN et passant par le point E de ce plan), il s'ensuit que le rayon réfracté BC, situé également dans le plan P, rencontre, si on le prolonge vers le haut, le rayon EA en un certain point F. C'est la considération de ce point F qui représente la nouveauté de la méthode proposée.

Nous allons examiner d'abord une solution descriptive et une solution par les calculs, avant de décrire la solutation mixte utilisée.

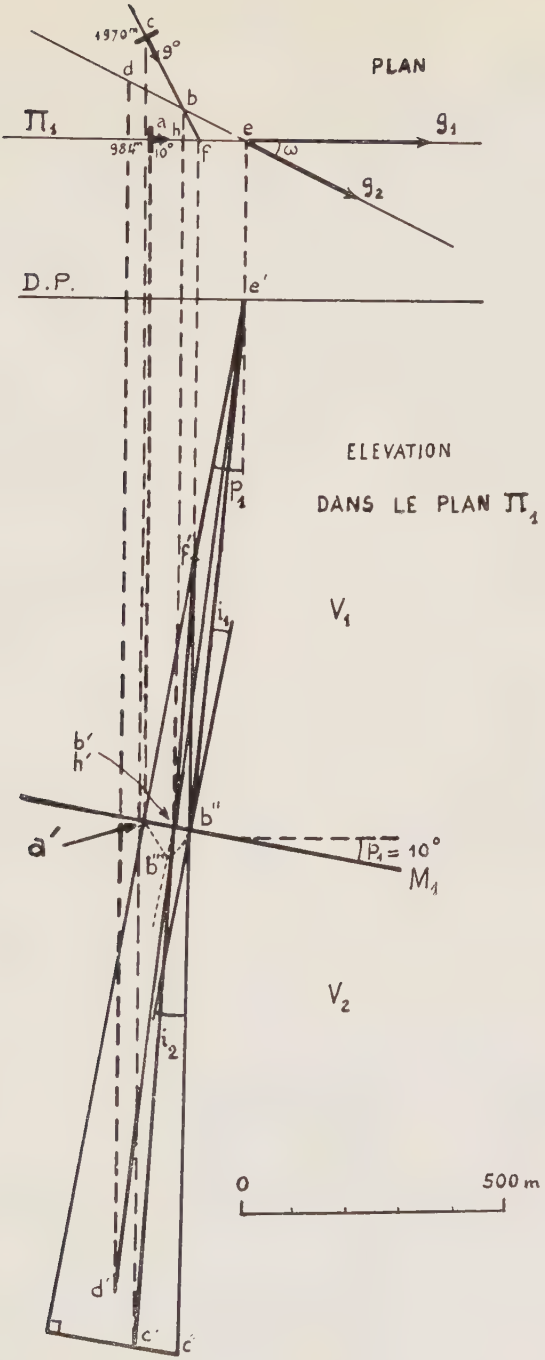

Fig. 2. Solution descriptive, dans l'exemple numérique suivant: — Projective solution, in the following numerical example:

$V_1 = 2.500$ m/sec., $V_2 = 4500$ m/sec, $t_1 = 0{,}800$ sec, $t_2 = 1{,}240$ sec
$g_1 = 72.10^{-6}$ sec/m, $g_2 = 50.10^{-6}$ sec/m, $\omega = 27°$.

a) *Solution descriptive*

Sur la fig. 2, nous donnons un exemple théorique de solution graphique, en utilisant une réprésentation sur deux plans de projection, l'un horizontal (DP), l'autre vertical (plan vertical Π_1 contenant la droite support de $\overrightarrow{g_1}$). Dans ce système, la représentation de M_1 est immédiate en projection verticale:

Nous déterminerons ensuite la projection verticale $e'd'$ de la direction EB dont nous connaissons la projection horizontale (suivant g_2), et l'angle $\theta_1 = \arcsin\ (V_1\, g_2)$ qu'elle fait avec Ez : $e'\,d'$ coupe M_1 en b', projection verticale de B, *d'où* la projection horizontale correspondante b.

Nous amenons ensuite le plan P en coïncidence avec Π_1, par une rotation de l'ensemble de la figure de l'espace autour de la droite EA commune à ces deux plans. Tous les éléments du plan P se présentent alors en vraie grandeur: b' vient en b'' (tel que $\overline{a'b''} = \overline{a'b'''} = \overline{AB}$) et on lit l'angle d'incidence $i_1 = \widehat{a'\,e'b''}$, d'où l'angle réfracté $i_2 = \arcsin\ ((V_2/V_1).\ \sin\ i_1)$ qui nous définit la projection verticale f' de F (d'où f sur la droite support de $\overrightarrow{g_1}$).

On a par ailleurs

$$\overline{BC} = V_2\, t_{BC} = V_2\left(\frac{t_2}{2} - t_{EB}\right) = V_2\left(\frac{t_2}{2} - \frac{\overline{e'b''}}{V_1}\right)$$

d'où c'' en portant $\overline{b''c''} = \overline{BC}$ sur $f'b''$ prolongé.

Dans la rotation inverse autour de EA, f' ne bouge pas, et la projection verticale c' de C se place sur $f'b'$ prolongé et sur la perpendiculaire abaissée de c'' sur $e'a'$. On en déduit la projection horizontale c (sur fb) et la cote de C. Le pendage de M_2 est donné par

$$p_2 = \arcsin\ \frac{\overline{bc}}{\overline{BC}}$$

b) *solution analytique*

Sur la fig. 3, nous présentons une suite de calculs pour arriver à la détermination des éléments de M_2 (coordonnées de C, et pendage p_2), sans faire la construction graphique précédente, mais en en conservant les notations. La nouvelle donnée introduite, ω, représente l'angle de $\overrightarrow{g_1}$ avec $\overrightarrow{g_2}$. Il y a d'autres façons de conduire les calculs.

Nous avons pris comme axe des x la droite support de $\overrightarrow{g_1}$ (dans le sens opposé à g_1): cela simplifie le calcul de $\cos\ i_1$ par la somme des produits des cosinus directeurs de EA et de EB (le cosinus directeur de EA par rapport à Ey étant nul).

Cette solution par le calcul est beaucoup trop lourde, même en nous contentant, comme nous l'avons fait sur la fig. 3, de calculer les quantités successives de proche en proche en fonction des quantités déjà calculées. On pourrait en déduire aisément les valeurs cherchées p_2, x_c, y_c, z_c en fonction des données

$$V_1 = \qquad t_1 = \qquad g_1 = \qquad \omega = \qquad \cos\omega =$$

$$V_2 = \qquad t_2 = \qquad g_2 = \qquad \sin\omega =$$

$$\begin{array}{c} \overline{EA} \\ \text{ou} \\ \overline{NB} \end{array} \begin{cases} \sin p_1 = V_1 g_1 = \\ 0 \\ \cos p_1 = \end{cases} \qquad \begin{array}{l} p_1 = \\ \operatorname{cotg} p_1 = \\ \overline{EA} = \dfrac{V_1 t_1}{2} = \end{array} \qquad A \begin{cases} x_A = \overline{EA} \sin p_1 = \\ y_A = 0 \\ z_A = \overline{EA} \cos p_1 = \end{cases}$$

$$\overline{EB} \begin{cases} V_1 g_2 \cos\omega = \\ (V_1 g_2 \sin\omega) \\ \sqrt{1 - V_1^2 g_2^2} = \cos\theta_1 = \end{cases} \qquad \theta_1 = \qquad \sin\theta_1 = \qquad \operatorname{cotg}\theta_1 =$$

$$\cos i_1 = \sin p_1 \cdot V_1 g_2 \cos\omega + \cos p_1 \cos\theta_1 = \qquad i_1 = \qquad \sin i_1 = \qquad \operatorname{tg} i_1 =$$

$$\sin i_2 = \frac{V_2}{V_1} \sin i_1 = \qquad i_2 = \qquad \operatorname{tg} i_2 =$$

$$\overline{AB} = \overline{EA} \operatorname{tg} i_1 = \qquad \overline{af} = \frac{\overline{AB}}{\operatorname{tg} i_2} \sin p_1 = \qquad \overline{BF} = \frac{\overline{AB}}{\sin i_2} =$$

$$\overline{eb} = \frac{\overline{EA}}{\cos i_1} \sin\theta_1 = \qquad t_{EB} = \frac{t_1}{2\cos i_1} = \qquad \overline{BC} = V_2\left(\frac{t_2}{2} - t_{EB}\right) =$$

$$B \begin{cases} x_B = \overline{eb} \cos\omega = \\ y_B = \overline{eb} \sin\omega = \\ z_B = \overline{eb} \operatorname{cotg}\theta_1 = \end{cases} \qquad F \begin{cases} x_F = x_A - \overline{af} = \\ y_F = 0 \\ z_F = x_F \operatorname{cotg} p_1 = \end{cases}$$

$$\overline{bf} = \sqrt{(x_B - x_F)^2 + (y_B - y_F)^2 + (z_B - z_F)^2} =$$

$$\sin p_2 = \frac{\overline{bf}}{\overline{BF}} = \qquad \boxed{p_2 =} \qquad \cos p_2 =$$

$$\left.\begin{array}{ll} x_B + (x_B - x_F)\dfrac{\overline{BC}}{\overline{BF}} = & \boxed{x_C =} \\ y_B + (y_B - y_F)\dfrac{\overline{BC}}{\overline{BF}} = & \boxed{y_C =} \\ z_B + \overline{BC} \cos p_2 = & \boxed{z_C =} \end{array}\right\} C$$

Fig. 3. Tableau de calculs (solution analytique). — Table of calculations (analytic solution).

initiales V_1, V_2, t_1, t_2, g_1, g_2 et ω, mais les expressions trouvées sont longues et ne présentent aucun avantage pratique.

La solution graphique de la figure 2, même facilitée en travaillant sur papier millimétré pour éviter les lignes de rappel, est impraticable aussi, parce que surchargée à l'échelle nécessairement réduite de travail (M_2 devant tenir dans les limites du dessin).

c) *Solution mixte*

De la fig. 2, nous ne conservons que la *projection horizontale seule,* en utilisant en pratique le graphique même sur lequel nous avons effectué la com-

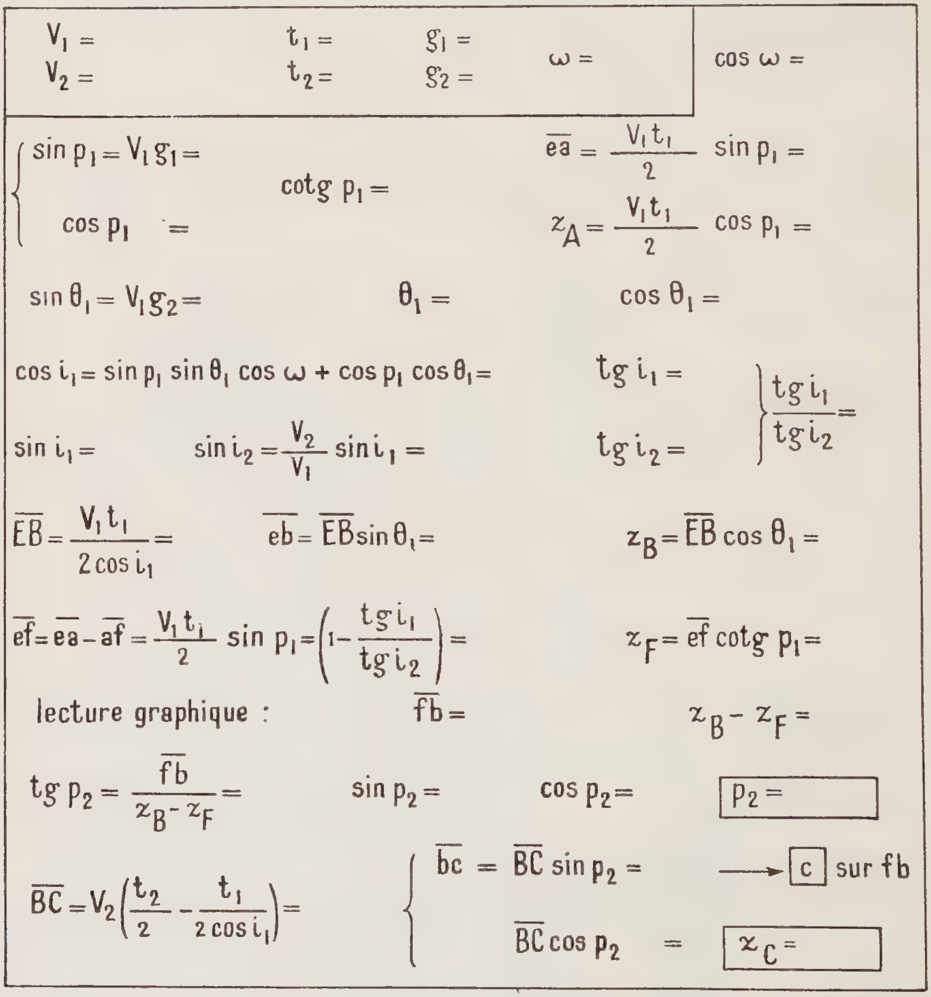

$V_1 =$ $\quad t_1 =$ $\quad g_1 =$ $\quad \omega =$ $\quad \cos\omega =$

$V_2 =$ $\quad t_2 =$ $\quad g_2 =$

$\left\{\begin{array}{l}\sin p_1 = V_1 g_1 = \\ \cos p_1 = \end{array}\right.$ $\quad \operatorname{cotg} p_1 =$ $\quad \overline{ea} = \frac{V_1 t_1}{2} \sin p_1 =$ $\quad z_A = \frac{V_1 t_1}{2} \cos p_1 =$

$\sin\theta_1 = V_1 g_2 =$ $\quad \theta_1 =$ $\quad \cos\theta_1 =$

$\cos i_1 = \sin p_1 \sin\theta_1 \cos\omega + \cos p_1 \cos\theta_1 =$ $\quad \operatorname{tg} i_1 =$

$\sin i_1 =$ $\quad \sin i_2 = \frac{V_2}{V_1} \sin i_1 =$ $\quad \operatorname{tg} i_2 =$ $\quad \left.\begin{array}{l} \\ \\ \end{array}\right\} \frac{\operatorname{tg} i_1}{\operatorname{tg} i_2} =$

$\overline{EB} = \frac{V_1 t_1}{2\cos i_1} =$ $\quad \overline{eb} = \overline{EB} \sin\theta_1 =$ $\quad z_B = \overline{EB} \cos\theta_1 =$

$\overline{ef} = \overline{ea} - \overline{af} = \frac{V_1 t_1}{2} \sin p_1 = \left(1 - \frac{\operatorname{tg} i_1}{\operatorname{tg} i_2}\right) =$ $\quad z_F = \overline{ef} \operatorname{cotg} p_1 =$

lecture graphique : $\overline{fb} =$ $\quad z_B - z_F =$

$\operatorname{tg} p_2 = \frac{\overline{fb}}{z_B - z_F} =$ $\quad \sin p_2 =$ $\quad \cos p_2 =$ $\quad \boxed{p_2 = \quad}$

$\overline{BC} = V_2\left(\frac{t_2}{2} - \frac{t_1}{2\cos i_1}\right) =$ $\quad \left\{\begin{array}{l}\overline{bc} = \overline{BC} \sin p_2 = \longrightarrow \boxed{c} \text{ sur } fb \\ \overline{BC} \cos p_2 = \boxed{z_C = \quad}\end{array}\right.$

Fig. 4. Tableau de calculs (solution mixte). — Table of calculations (mixed solution).

position des gradients-temps observés sur les deux directions de dispositifs. Dans la solution descriptive, par contre, l'orientation de lignes de rappel dépendait de la direction trouvée pour $\vec{g_1}$, ce qui imposait une deuxième feuille de papier millimétré.

Les calculs représentés fig. 4, sont notablement allégés par rapport à ceux de la figure 3: nous déterminons successivement p_1, $\overline{ea}$, z_A, θ_1, i_1, i_2, $\overline{EB}$, z_B, puis $\overline{eb}$ et $\overline{ef}$ qui nous définissent, sur les droits supports de $\vec{g_2}$ et de $\vec{g_1}$ respectivement, les points b et f dont *nous mesurons graphiquement la distance* $\overline{fb}$. En calculant encore z_F, $z_B - z_F$, $\overline{BC}$ et $\overline{bc}$, nous en déduisons les éléments définissant le miroir cherché: son pendage p_2, sa position c en plan sur le prolongement de fb et sa cote z_C.

Ces calculs sont assez rapides, en utilisant la règle à calcul et une table des valeurs naturelles des fonctions circulaires. A partir des données de départ, il faut 20 à 25 minutes en tout pour obtenir les résultats cherchés.

Nous donnons fig. 5, 6, 7 des exemples réels tirés de l'étude du champ profond de Lacq. Sur les deux derniers, on peut remarquer que les miroirs profonds sont restitués parfois en des positions qu'il était malaisé de prévoir.

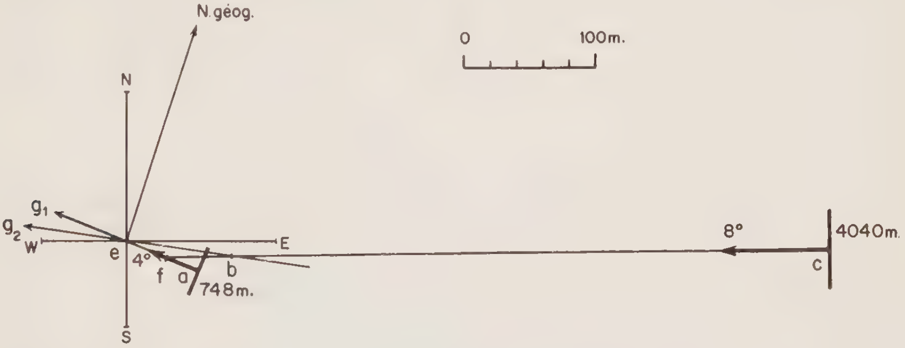

Fig. 5. Premier exemple, sur le champ de Lacq. — First example, from the Lacq oil field.
$V_1 = 2500$ m/sec, $V_2 = 5400$ m/sec, $t_1 = 0{,}600$ sec, $t_2 = 1{,}833$ sec
$g_1 = 31.10^{-6}$ sec/m, $g_2 = 41.10^{-6}$ sec/m, $\omega = 14°$.

L'échelle de travail sur papier millimétré doit être aussi grande que possible, par exemple 1/2.000, de façon à estimer la longueur et la direction de fb avec une précision raisonnable.

Toutefois, la réduction de format imposée pour la publication dans "Geophysical Prospecting" rend fb exagérément petit, et nous a fait renoncer à représenter le fond millimétré.

2°) *Cas où la vitesse V_1 est variable dans le milieu supérieur, la vitesse V_2 étant constante dans le milieu inférieur* —

Nous reprenons (fig. 8) une représentation par projections analogue à celle

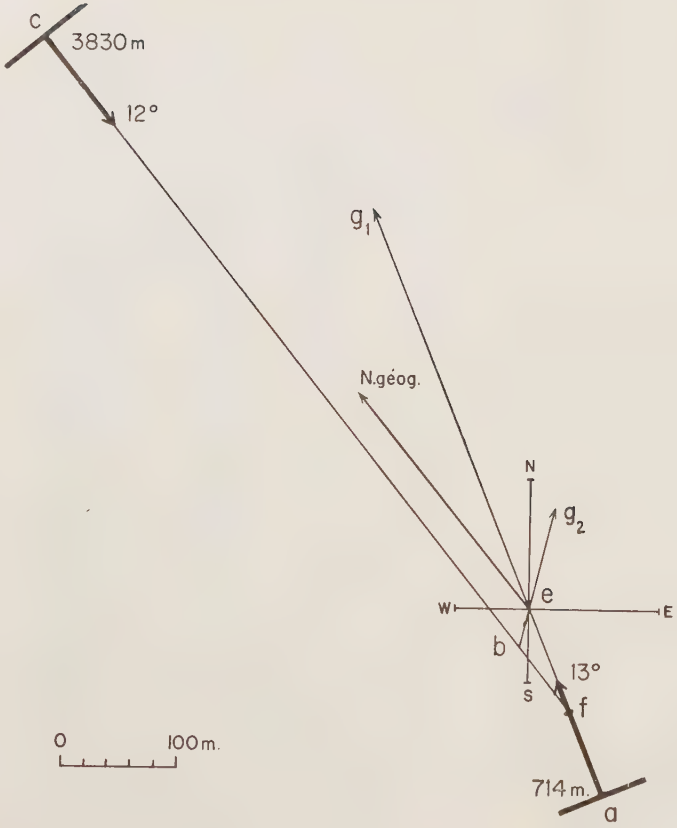

Fig. 6. Deuxième exemple (Lacq.). — Second example (Lacq). $V_1 = 2500$ m/sec, $V_2 = 5400$ m/sec, $t_1 = 0{,}588$ sec, $t_2 = 1{,}768$ sec. $g_1 = 93{,}2.10^{-6}$ sec/m, $g_2 = 22{,}4.10^{-6}$ sec/m, $\omega = 36°40$.

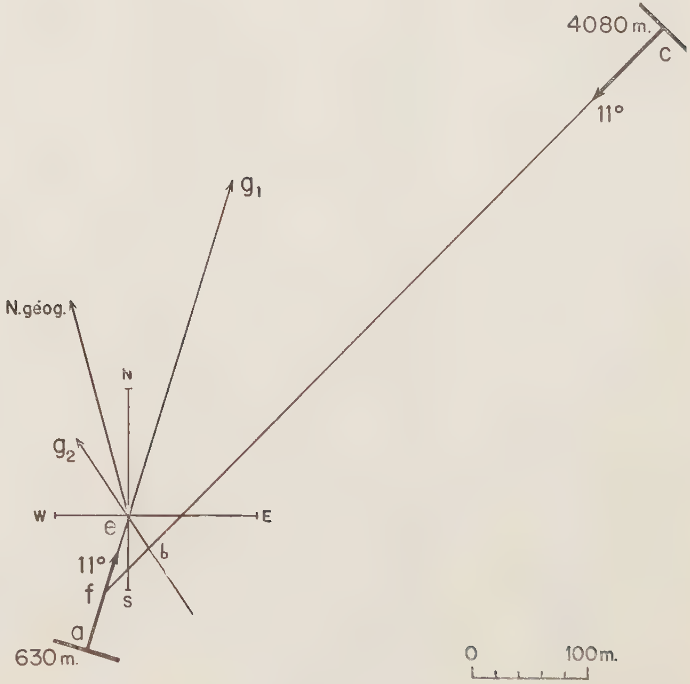

Fig. 7. Troisième exemple (Lacq.). — Third example (Lacq). $V_1 = 2500$m/sec, $V_2 = 5400$ m/sec, $t_1 = 0{,}513$ sec, $t_2 = 1{,}812$ sec $g_1 = 77{,}5.10^{-6}$ sec/m, $g_2 = 20{,}5.10^{-6}$ sec/m, $\omega = 51°$.

de la figure 2, mais cette fois les trajectoires sont courbes entre le *DP* et le miroir M_1. En admettant une loi de vitesse fonction de la profondeur seule, par exemple $V_1 = V_0 + kz$, on restitue M_1 sur le plan Π_1 (projetant verticalement $\vec{g}_1$) à l'aide d'un abaque ordinaire de restitution. L'angle ω de

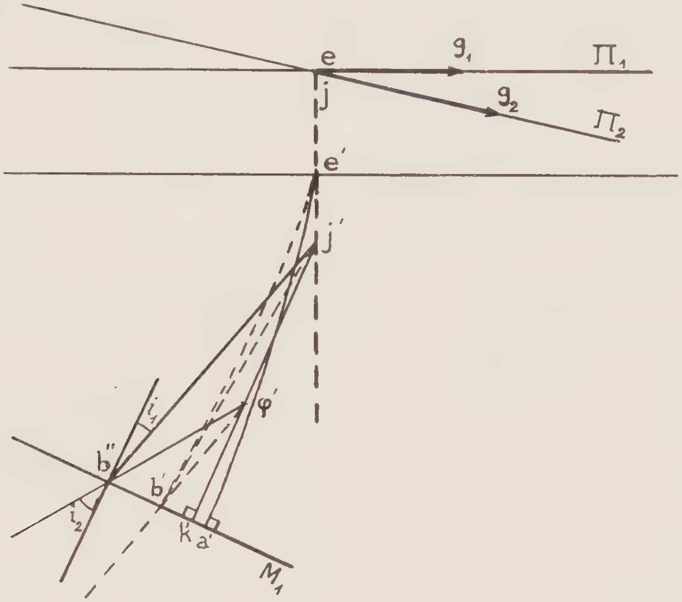

Fig. 8. Cas où la vitesse varie en fonction de la profondeur entre la surface du sol et l'horizon M_1. — Case in which the velocity changes with depth between the surface and the horizon M_1.

$\overrightarrow{g_1}$ et de $\overrightarrow{g_2}$ est aussi l'angle que fait Π_1 avec le plan Π_2 (projetant verticalement $\overrightarrow{g_2}$). Si d'après l'abaque, *D* est le déplacement réel et *z* la cote d'un point courant de la trajectoire de gradient-temps g_2, on peut déterminer la projection de la trajectoire courbe *EB* sur le plan Π_1 par points ($x = D \cos \omega, z$) ce qui nous fixe b' sur M_1 avec la précision désirée, ainsi que le point *b* correspondant en projection horizontale. La cote de b' nous permet de lire t_{EB} sur l'abaque.

Si nous voulons amener le plan *P* (plan d'incidence en *B*) en coïncidence avec Π_1 pour que ses éléments se présentent en vraie grandeur, nous ne pouvons pas opérer exactement comme nous l'avions fait sur la figure 2. Le plan *P* contient la normale *BN* et la tangente en *B* à la trajectoire *EB*. Cette tangente, située aussi dans le plan Π_2 coupe la verticale de *E* (intersection de Π_1 et de Π_2) en un point *J* de cote lisible graphiquement (j'). *BJ* ne coupe pas *EA*. Mais la perpendiculaire *JK* abaissée de *J* sur M_1 est évidemment située dans le plan Π_1, et aussi dans le plan *P* (car elle est parallèle à la droite

BN du plan *P*, et passe par un point *J* de ce plan). Par une rotation autour de *JK*, on peut donc amener *P* en coïncidence avec Π_1 ; la lecture de i_1 en b'' permet de calculer i_2 et de dessiner le rayon réfracté qui, situé dans le plan *P*, coupe la droite *JK* du même plan en un point **Φ** équivalent du point *F* du problème précédent.

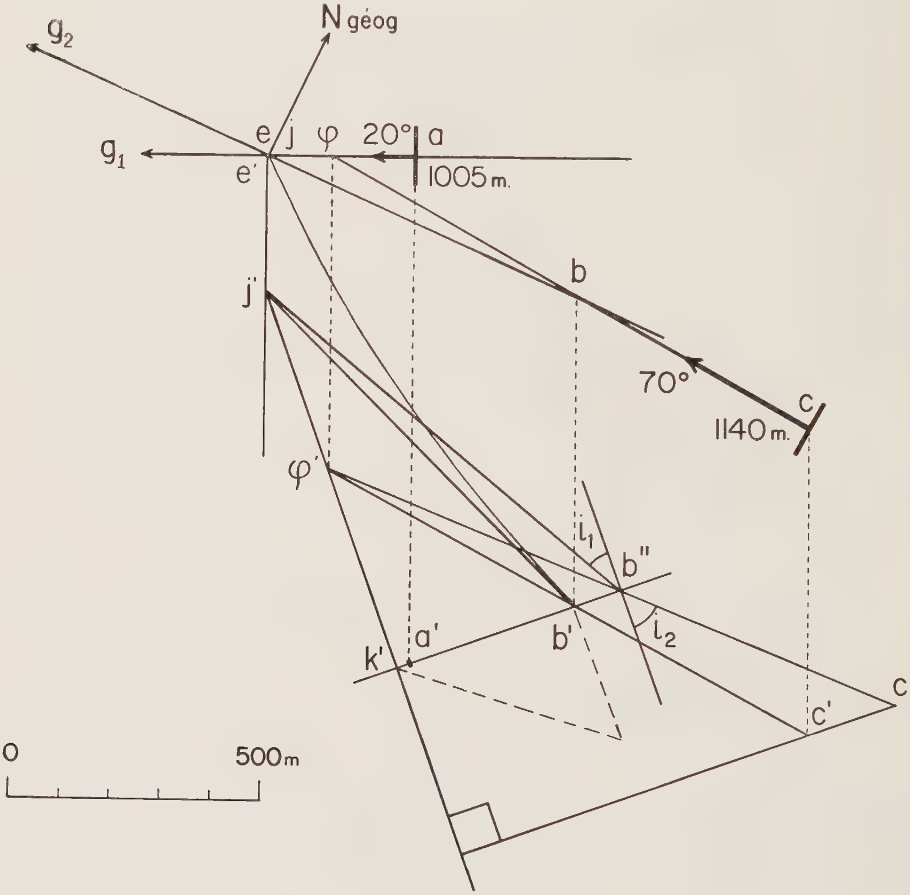

Fig. 9. Exemple extrait du Maroc. — Example taken from Morocco.
$V_1 = 1700 + 1{,}2z$ m/sec, $V_2 = 4000$ m/sec, $t_1 = 0{,}465$ sec
$t_2 = 0{,}666$ sec
$g_1 = 117{,}5.10^{-6}$ sec/m, $g_2 = 264.10^{-6}$ sec/m, $\omega = 24°$.

Nous donnons figure 9 un exemple tiré du Maroc, dans une région où l'horizon M_1 sépare les marnes miocènes dont la loi de vitesse est voisine de $V_1 = 1700\,\text{m} + 1{,}2z$, des calcaires jurassiques de vitesse assez proche de 4000 m/sec.

Cette solution graphique permet certes d'aboutir au résultat mais sa lourdeur la condamne en pratique.

3°) Dans le *cas ou la vitesse V_2 varierait aussi avec la profondeur* dans le milieu inférieur, la mesure de l'angle θ_2 que fait avec la verticale la tangente en B au rayon réfracté BC peut s'obtenir comme ci-dessus. A partir de ce point la trapectoire reste dans le plan vertical contenant cette tangente, et le déplacement en fonction de la profondeur au-dessous de B s'obtient sur l'abaque de restitution relative à la loi de vitesse du terrain inférieur, en y choisissant la courbe qui, à la profondeur où à la vitesse est $(V_2)_0 + k_2 z_B$, fait avec la verticale l'angle θ_2).

Ce cas est compliqué, et doit d'ailleurs se présenter rarement, le taux d'augmentation de la vitesse diminuant en pratique à partir d'une certaine profondeur.

En conclusion, c'est pour le seul cas où V_1 et V_2 sont sensiblement constants que nous avons pu présenter un procédé acceptable pour restituer correctement le miroir inférieur M_2 dans l'espace.

En outre, nous devons avouer que les gradients-temps sont rarement connus avec une bonne précision : c'est un inconvénient général des tirs en croix, qui ne bénéficient pas, comme les profils continus, du contrôle des pendages basé sur l'allure statistique des éléments de miroir à niveau donné.

A RATIONAL APPROACH TO THE DESIGN OF ELECTRICAL FILTERS AND OF SHOT-HOLE AND GEOPHONE PATTERNS IN SEISMIC REFLECTION PROSPECTING [*]

BY

F. MUIR [**] and F. W. HALES [**]

Abstract

The authors develop an optimum filtering theory for seismic reflection recording. A criterion of record improvement is applied to a mathematical model consisting of a set of wavelets superimposed on a random noise backgruond. This leads to the design of electrical filters and geophone and shot-hole patterns with optimum filtering characteristics.

Introduction

Areas of no reflection or, more properly, areas where the noise level is sufficiently high to obscure record line-ups, are a major problem in seismic reflection prospecting and in an effort to secure meaningful results from these areas increasing use is being made of geophone and shot-hole patterns. Their use is justified by field experience and their design based on the argument that over the area of a pattern the reflection signals will be received in phase whilst the noise signals will not. This paper presents a more precise analysis which leads to the synthesis of optimum linear electrical filters and to the design of geophone and shothole patterns which combine economy with freedom those dangers attendant on pattern shooting which were discussed in a previous paper read before this Association (Hales and Edwards 1955).

Criterion of Record Improvement

Reflections are identified by three qualities:

(i) Alignment
(ii) Relative amplitude
(iii) Character

of which the last two are the counterparts of Elevation and Essential Copy in the Gaby grading system (Gaby 1947). The first two qualities, alignment and relative amplitude, are inter-related since the amount of shift of a reflection peak or through due to noise is directly proportional to the noise level.

---

[*] Presented at the Eighth Meeting of the European Association of Exploration Geophysicists, held in Paris, 18-20 May 1955.

[**] Seismograph Service Limited, London.

Accordingly we define our optimum filter, whether it be an electronic device, a geophone pattern or a shot-hole pattern, as that one which maximizes the ratio between peak signal amplitude and the root-mean-square noise amplitude. We shall show later that such a filter will also be near optimal under a character-preserving criterion.

The Seismic Model

The model of the disturbance at a point due to a shot to which we shall apply the criterion is compounded of a set of unevenly-spaced reflection pulses superimposed on a random noise background.

Each pulse is defined by an equation:

$$\psi_r = \left[1 - \frac{T_r^2}{2}\right] e^{-T_r^2/4} \quad . \; . \; . \; . \; . \; . \; . \; . \quad (1)$$

which relates the particle velocity amplitude Ψ_r to a dimensionless time variable T_r, itself defined by the relation:

$$T_r \equiv \omega_r \left[t - t_r\right] \quad . \; . \; . \; . \; . \; . \; . \; . \; . \quad (2)$$

where ω_r is the characteristic angular frequency of the pulse

t_r is the travel time of the pulse

and t is the usual time variable.

The form of these pulses and the form of their associated Fourier transforms:

$$\varphi_r = \Omega_r^2 \, e^{1-\Omega^2_r} \quad . \; . \; . \; . \; . \; . \; . \; . \; . \; . \quad (3)$$

where

$$\Omega_r \equiv \omega / \omega_r \quad . \; . \; . \; . \; . \; . \; . \; . \; . \; . \quad (4)$$

are illustrated in Figs. 1 and 2.

These model pulses are based directly on Ricker's Wavelet Theory of Seismogrom Structure (Ricker 1951). In this theory Ricker asserts that seismic waves are propagated according to Stokes' equation:

$$\nabla^2 \left[\theta + \frac{1}{\alpha} \cdot \frac{\partial \theta}{\partial t}\right] = \frac{1}{\beta^2} \cdot \frac{\partial^2 \theta}{\partial t^2} \quad . \; . \; . \; . \; . \; . \; . \; . \quad (5)$$

which differs from the classical wave equation:

$$\nabla^2 \theta = \frac{1}{\beta^2} \cdot \frac{\partial^2 \theta}{\partial t^2} \quad . \; . \; . \; . \; . \; . \; . \; . \; . \quad (6)$$

in that it contains a viscous damping term.

Using an initial impulsive boundary condition to describe the shot, Ricker has obtained a set of solutions to Stokes' equation amongst which is one which describes the earth particle velocity at a point and it is this function that we use for our model wavelet. It was chosen because it derives from the only

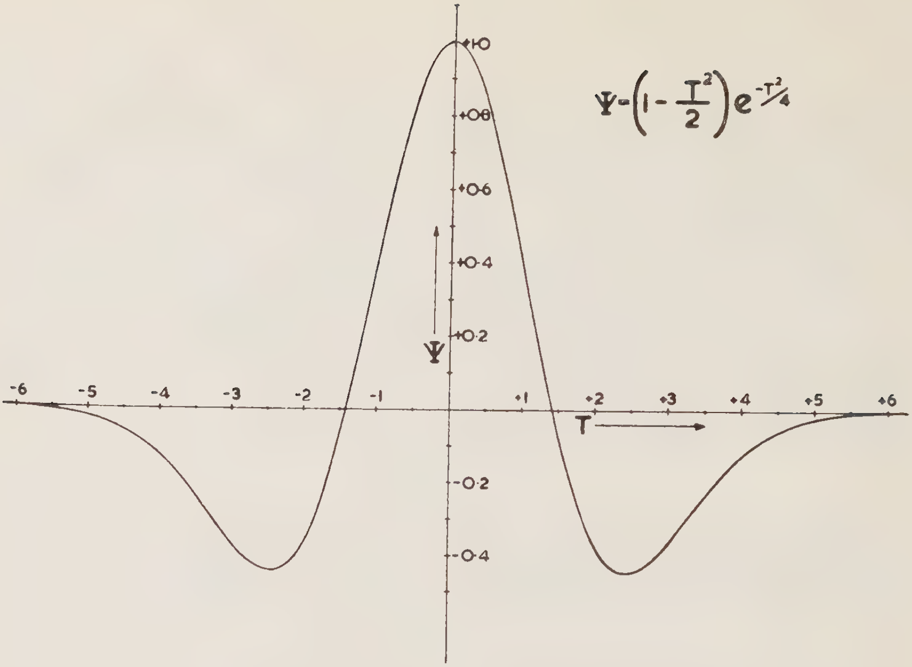

Fig. 1. Model seismic velocity wavelet.

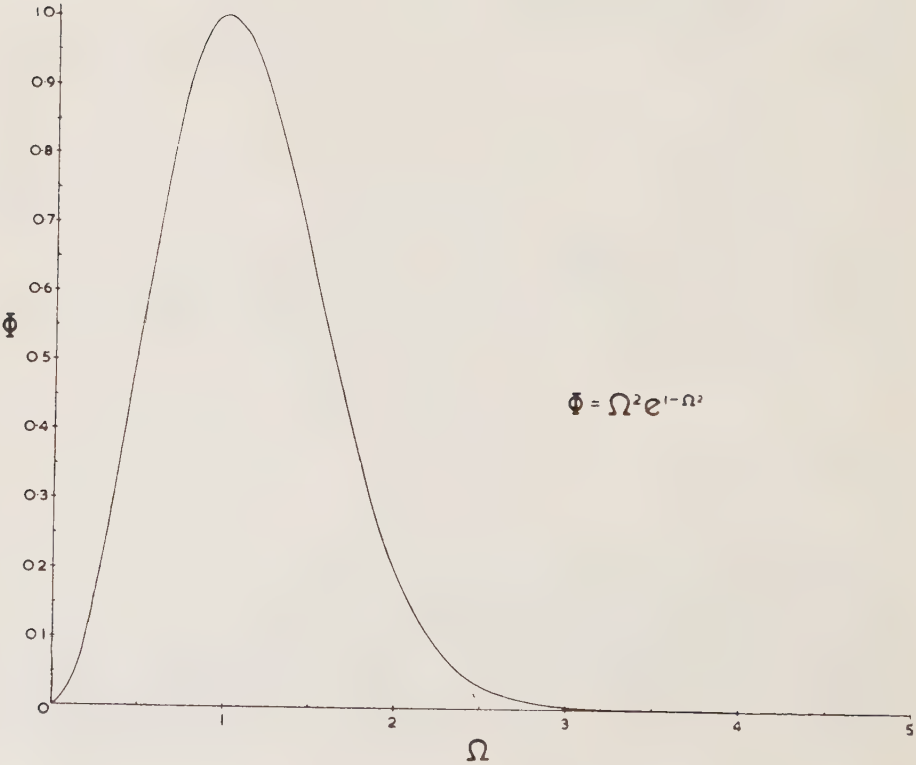

Fig. 2. Model wavelet frequency spectrum.

experimentally corroborated theory, Ricker himself having obtained good agreement as to:

(i) the form of the disturbance
(ii) the law of broadening
(iii) the law of amplitude decay
(iv) the spectrum of the disturbance.

We further define the random noise background as having a flat frequency spectrum. This is not necessarily true of every noise trace but it is an accurate representation of our present pre-knowledge of the random noise spectrum.

The Optimum Filter

Dwork (1950) has shown that for the general case of a known pulse superimposed on an arbitrary noise background the frequency response of that linear device which gives a maximum value for the ratio between the peak amplitude of the pulse and the root-mean-square of the noise is biven by:

$$H(\omega) = \frac{F^*(\omega)e^{-i\omega k}}{[\sigma(\omega)]^2} \quad . \; . \; . \; . \; . \; . \; . \; . \; . \; . \quad (7)$$

where $H(\omega)$ is the frequency response of the device,

$F^*(\omega)$ is the complex conjugate of the Fourier transform of the pulse, that is the Fourier transform of the pulse reversed in time,

$\sigma(\omega)$ is the frequency distribution of the noise, and k is the time delay of the device.

In the case of our model, since $\sigma(\omega) = 1$ by definition and $F^*(\omega) = \varphi^*(\omega) = \varphi(\omega)$ by symmetry (Eq. 3),

$$H(\omega) = \varphi(\omega)\, e^{-i\omega k} \quad . \; . \; . \; . \; . \; . \; . \; . \; . \quad (8)$$

That is, the optimum linear device has a frequency response equal to the frequency spectrum of the reflection wavelet itself. Wiener (1949) has shown that for high noise levels a device with this characteristic is near optimal also under a minimum distortion criterion which requires that the integrated root-mean-square error between the impressed message, i.e., signal less noise, and the filtered signal shall be at a minimum.

Optimum Electrical Linear Filter

As the only variable in the spectrum of a reflection wavelet is its characteristic angular frequency, the optimum electrical linear filter is best realised as a resistance/capacitance network, since it is only with such a filter that frequency shift may be obtained by a uniform change of a single set of elements. Guillemin (1949) has shown that an RC network can be synthetized to approximate arbitrarily closely to any required attenuation characteristic, and one practical method of synthesis has been described by Orchard (1951). *Fig. 3* illustrates the frequency response of such an optimum filter in a form more familiar to electronic engineers, that is with decibel attenuation plotted against the frequency on a logarithmic scale.

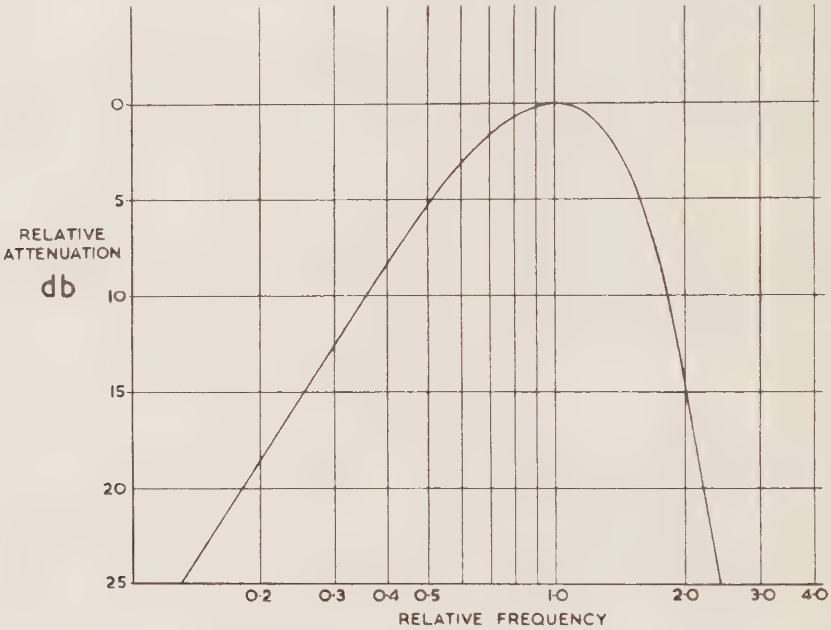

Fig. 3. Optimum overall response.

OPTIMUM PATTERNS

The application of this theory to the design of optimum geophone patterns is more complex since the frequency-attenuating effect of a pattern on a reflection wavelet is a function not only of the shape and size of the pattern but also of the apparent horizontal velocity of the wavelet; while the shape of a pattern determines the form of a frequency response, it is the wavelet velocity that positions this response on the frequency scale. This consideration suggests the following design requirements:

(1) The pattern must consist entirely of positive elements. Just as the frequency response of the optimum filter is equal to the frequency spectrum of the reflection wavelet so, properly, in the time domain should the geophone density along the line of travel be equal to the amplitude of the wavelet itself. But as the integral of the wavelet over all time is zero, so should the pattern contain an equal number of positive and negative elements and such a pattern would completely cancel out signals arriving with zero step-out. Thus, the function of the pattern is that of a low-pass filter and in its design we are

limited to ensuring that the attenuation characteristic for the higher frequencies only is optimum.

(2) The low-pass filtering action of the pattern must be designed around the slowest-moving wavelet, since the 'cut-off frequency' of a pattern is directly proportional to the apparent wavelet velocity. This condition ensures that there is no cancellation of signals received from steeply-dipping beds. This apparent wavelet velocity can never be less than the lowest average velocity down to any of the reflectors and thus a limiting size for the pattern exists.

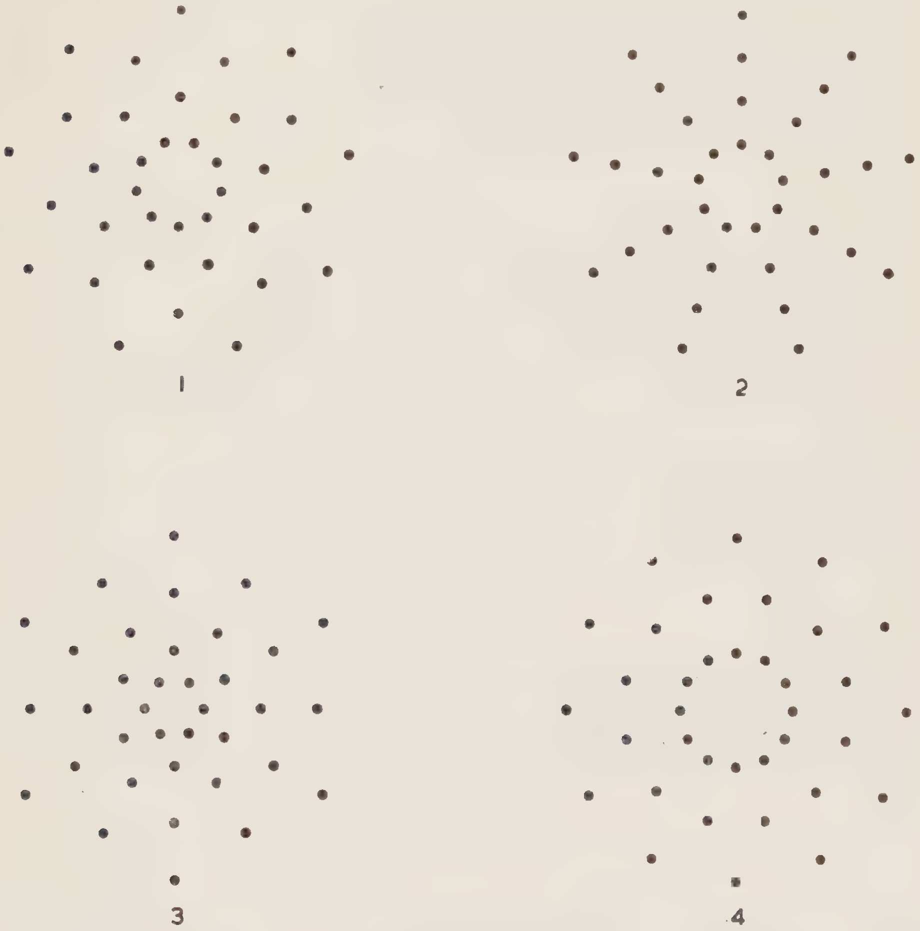

Fig. 4. Pattern comparison.

(3) The pattern must be symmetrical about its centre. This ensures that its response is independent of the direction of the horizontal travel path of the wavelet.

A pattern which fulfills all these conditions consists of a set of concentric circles of constantly increasing radii, each circle containing an equal number of elements and the outer-most having a diameter of $V/2f$, where V is the lowest average velocity to a reflector and f is the peak frequency of this reflection.

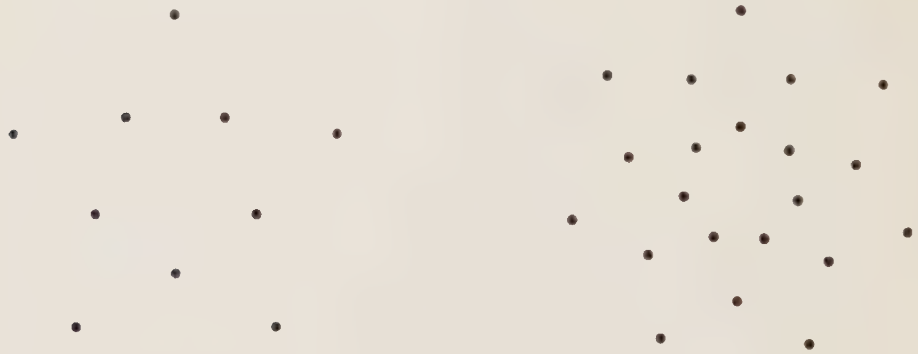

10 ELEMENTS 21 ELEMENTS

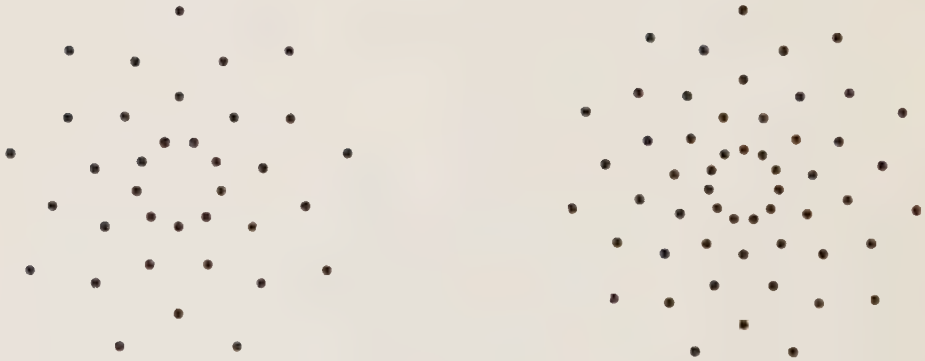

36 ELEMENTS 55 ELEMENTS

Fig. 5. Optimum patterns.

That this does not completely define the best pattern is illustrated in *Fig. 4*. Although these four patterns all contain 36 elements and have the same signal response, their noise response differs in that in patterns 2, 3 and 4 the elements are concentrated either radially or circumferentially with an increase in noise correlation. This concentration is minimized in an n-ringed pattern by having $2n + 1$ elements in each ring and by radially off-setting every other ring.

Patterns so designed are illustrated in *Fig. 5.* It is clear that shot-hole patterns must be similarly designed by virtue of the principle of reciprocal travel-paths.

Fig. 6. illustrates record improvement obtained by means of geophone and shot-hole patterns designed on the foregoing principles.

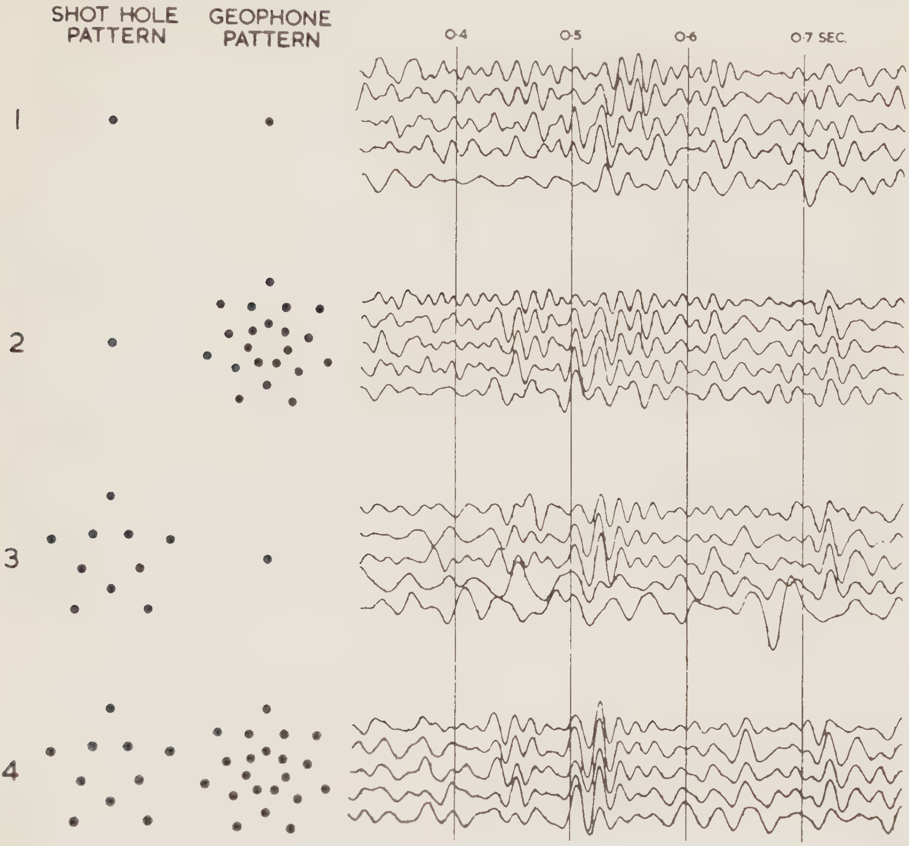

Fig. 6. Record comparison.

POINTS OF PRACTICAL IMPORTANCE

It should be noted that the seismic model used for the above treatment postulates velocity wavelets since the most commonly used geophones respond to earth particle velocities. The expressions used in Eqs. 1-4 would not, therefore, apply to an analysis involving displacement or acceleration-type geophones.

In practice, there may also be present unwanted regular pulses such as ground roll, but we believe that their treatment has been well discussed in the literature and that other methods exist for minimizing their effect.

For the experimental work illustrated in *Fig. 6,* the single shots of 1¼ lbs. of explosive were located at a depth of 120 ft. This had been found to be the minimum depth for which reflection indications were obtainable. The multiple shots were 10 ft. deep with a charge of 1 lb. in each hole and the diameter of the multiple patterns, both for geophones and shot-holes, was 80 ft.

Acknowledgments

The authors wish to express their indebtedness to the Directors of Seismograph Service Limited for their permission to publish this paper. Mrs. M. Whittle prepared the illustrations.

References

(1) Hales F. W. and Edwards T. E., 1955, Some Theoretical Considerations on the Use of Multiple Geophones Arranged Linearly along the Line of Traverse, Geoph. Prosp., 3, 65-73.

(2) Gaby Phil. P., 1947, Grading System for Seismic Reflexions and Correlations, Geophysics, 12, 590-617.

(3) Ricker N., 1951, The Form and Laws of Propagation of Seismic Wavelets, Proc. Third World Petroleum Congress, 514-536.

(4) Dwork B. M., 1950, Detection of a Pulse Superimposed on Fluctuation Noise, Proc. IRE., 38, 771-774.

(5) Wiener, 1949, Extrapolation, Interpolation and Smoothing of Stationary Time Series, MIT/McGraw-Hill.

(6) Guillemin E. A., 1949, Synthesis of RC Networks, Journ. Math. Phys., 28, 22-42.

(7) Orchard H. J., 1951, The synthesis of RC Networks, Proc. IRE., 39, 428-432.

Discussion

Mr. Koefoed: I do not think that the problem of groundroll has been solved yet. In view of this, the flat-response model of the back ground disturbance may be too simple. It is practically feasible to extend your theory to other models of the back ground disturbance?

Mr. Muir: I agree that the problem of groundroll has not been completely solved. We were concerned only with the problem of irregular or random noise. We are working on the groundroll problem.

ON SURFACE-WAVES IN LOOSE MATERIALS OF THE SOIL *

BY

A. KORSCHUNOW **

Abstract

For the first time a method of observing the effects of hammering and of small blasts has been applied in a series of experiments on various soils, using a three component set of small mechanical leaf spring seismographs. The seismograms have been subjected to a thorough harmonic analysis. By means of these experiments, the theoretical concept of Rayleigh waves generated in a layer overlying a semi infinite medium has been confirmed. The dispersion curves resulting from different experiments correspond well with theoretical dispersion curves.

It may be concluded that every seismic pulse generates a specific Rayleigh wave mechanism in loose layers. The depth of penetration of the Rayleigh wave mechanism and its frequency spectrum depend upon the delivery of energy and upon the consistence of the particular soil.

Most of the energy delivered is transformed into surface-waves, and it is obvious that the direct reading of pulses in seismograms effects mainly group velocities of the Rayleigh wave mechanism. Thus, all endeavours to procure information about near surface layers of loose soils by refraction seismic work, as the present investigations show, meet with far more difficulties than has been assumed in the past.

With regard to the determination of the critical frequencies of the generated surface waves, the method of harmonic analysis of seismograms is superior to the usual dynamic method of soil mechanics, since rotating weights do not give the characteristic phase velocities and transversal wave velocities necessary for judging the consistency of loose soils.

Finally, a method of determining the absorption of surface waves is discussed.

Introduction to the problem, abstract of theoretical backgrounds, presentation of theoretical model

Whenever seismic observations on loose soils are carried out, surface waves dominate the motion. In seismic prospecting for oil the so called "ground-roll" causes much difficulty since it tends to obscure valuable reflections. In engineering seismology computors are faced with the necessity of utilizing not only separate, distinct impulses on seismograms but also to include characteristics of seismograms over their whole length. It is evident that repeated registration of seismic pulses under equal conditions gives seismograms of extreme similarity, and seismograms from different loose soils seem to show a typical shape according to the soil's consistency. Such effects gave reason to investigate a number of different soils by means of hammering and small blasts.

---

* Presented at the Eighth Meeting of the European Association of Exploration Geophysicists, held in Paris, 18-20 May 1955.

** Institut für angewandte Geophysik der Universität München.

Every experimental investigation depends on a theoretical model. The mathematical treatment of surface waves is based on the introduction of single- or multilayered media into the theory. In earthquake as well as in exploration seismology observations showed that in any propagation of surface waves dispersion takes place. These observations, however, did not seem to be verified by the general theory of Rayleigh waves as established by Lord Rayleigh early in 1899. The general theory of Rayleigh waves propagated on the surface of a semi infinite medium, or half space, does not show dispersion. It was first shown by Sezawa (1927) that for the model: Rayleigh waves in a layer overlying a half space, dispersion does occur. (The dispersion of shear-waves was shown by Love as early as 1911). Further work on the theory of Rayleigh waves in a layer overlying a half space led to the publication of another paper (Sezawa and Kanai, 1935). In this paper the authors showed that there is a discontinuity in the slope of the resulting dispersion curve, which grows more distinct as the quotient (rigidity modulus of the layer rigidity modulus of the half space) decreases from 1/2 to 1/∞. The exact solution of the wave equations for the case of Rayleigh waves in a layer overlying a half space leads to a determinant of six columns and six rows. The calculation of the resulting dispersion curve requires therefore a great deal of work. Stoneley (1953) showed that the calculation of Rayleigh dispersion for a double-layer overlying a half space leads to a determinant of 10 columns and 10 rows. Haskell (1953) also demonstrated the extreme difficulties which rise from numerical solution of the dispersion problem of surface waves.

Based on former experiences of the school of the late Professor Angenheister (University of Göttingen), and the investigations of the former German Society for Soil Mechanics (DEGEBO), Berlin, Förtsch (1953) published theoretical dispersion curves, which promised to be adaptable to practical observations. Experimental data from other publications (Angenheister (1950), Förtsch (1950), Förtsch and Schulze (1948), Köhler (1936), Köhler and Ramspeck (1936), Ramspeck (1936), Ramspeck and Schulze (1936) caused Förtsch (1953) to modify the general dispersion-curve of Sezama and Kanai (1935) for the case:

$$\frac{\text{Rigidity modulus of the layer}}{\text{Rigidity modulus of the half space}} = 1/\infty .$$

This case expresses the condition that the half space should be rigid so far as surface wave energy is concerned, and the propagation of the elastic disturbance, as far as waves of the Rayleigh type are involved, is limited to the layer. The half space is no longer effected by the mathematical calculation. Thus the general Rayleigh dispersion curve given by Sezawa and Kanai

(1935) is simplified. The final view of the modified Rayleigh dispersion curve for the model: Rayleigh waves in a layer overlying a half space, is described by the equation

$$\begin{gathered} -4\,(2-v^2/V_{tr}^2) + [(2-v^2/V_{tr}^2)^2+4]\,.\cos\,(v^2/V_{1g}^2-1)^{1/2}.\,2\pi H/L \\ .\cos\,(v^2/V_{tr}^2-1)^{1/2}.\,2\pi H/L - [(2-v^2/V_{tr}^2)^2/(v^2/V_{1g}^2-1)^{1/2}.\,(v^2/V_{tr}^2-1)^{1/2} \\ +4\,(v^2/V_{1g}^2-1)^{1/2}.\,(v^2/V_{tr}^2-1)^{1/2}]\,.\sin\,(v^2/V_{1g}^2-1)^{1/2}.\,2\pi H/L \\ .\sin\,(v^2/V_{tr}^2-1)^{1/2}.\,2\pi H/L = 0 \quad \ldots\ldots\ldots\ldots \quad (1) \end{gathered}$$

in which
v = phase-velocity
V_{lg} = longitudinal wave velocity inside the layer
V_{tr} = transversal wave velocity inside the layer
L = wave length of phase
H = thickness of the layer.

According to theoretical dispersion-equation, experiments in the field should show a functional relation between the phase velocities and the wave length (or frequency). The present investigations by means of hammerings and small blasts on loose soils, carried out by means of mechanical seismographs of which the dynamical characteristics were well known, have been undertaken in order to verify the theoretical model: Rayleigh waves in a layer overlying a half space, providing phase velocities and frequencies by thorough harmonic analysis of seismograms over the whole length.

THEORETICAL DISPERSION CURVES, THEIR INTERPRETATION FOR PRACTICAL USE

Using the method of successive approximations, Förtsch (1953) succeeded in constructing dispersion curves from equation (1). These dispersion curves, as plotted in Fig. 1, give $v/V_{tr})$ (or C/V_{tr}) as function of $1/fH$ (or $L/2\pi H$). The two branches of the phase velocity (v) have been obtained by direct computation from equation (1). The two branches of the group velocity (C) have been obtained by graphic construction as indicated by Sommerfeld (1949) based on the formula:

$$C = v - L\,dv/dL \quad \ldots\ldots\ldots\ldots \quad (2)$$

As expression of the discontinuity first found by Sezawa and Kanai (1935), two distinct branches of the dispersion curves can be recognized. The statement of the discontinuity by Sezawa and Kanai (1935) was based on theoretical considerations. An experimental foundation was still lacking for it at that time. However, Förtsch (1953), on the basis of experiences in the past, indicated that the discontinuity of the dispersion curves of Rayleigh waves in a layer overlying a half space was due to the coupling, in the Rayleigh movement, of two component parts, one of longitudinal and one of transverse character. The branch O_a in Fig. 1 stands for the coupled wave of transverse character, the wing O_b for the coupled wave of longitudinal character.

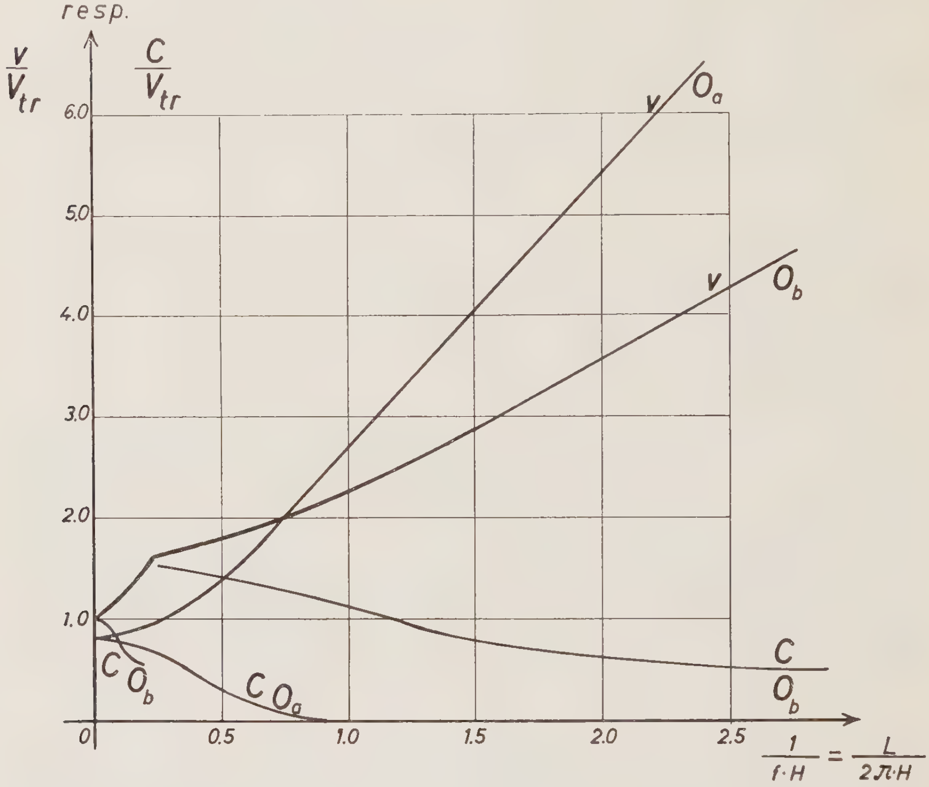

Fig. 1. Theoretical dispersion curves by O. Förtsch (1953) for the case: Poisson's ratio = 0,25.

Using the definition:

$$n_o = V_{tr}/H \quad . \ . \ . \ . \ . \ . \ . \ . \ . \ . \quad (3)$$

as reciprocal value of the half echo time of transverse waves inside the layer overlying a half space, Förtsch (1953) was able to transform the dispersion curves into a diagram on a double logarithmic scale (see Fig. 2). Fig. 2 gives v/V_{tr} (or C/V_{tr}) as a function of n/n_o. This special transformation yielded Rayleigh dispersion curves that could be fitted to observed values under any conditions of observation, since alteration of the conditions would go into the calculation only as proportionality factors which would merely cause translation without change of shape of the dispersion curves. By this curve fitting critical values of the field measurements can be obtained.

The coordinates of the point K in the diagram, where the two branches O_a

and O_b of the phase velocity function (v) meet, provide important values for practical calculation. (All values concerning the point K are indicated with the subscript k). The most important part of the dispersion curves has been

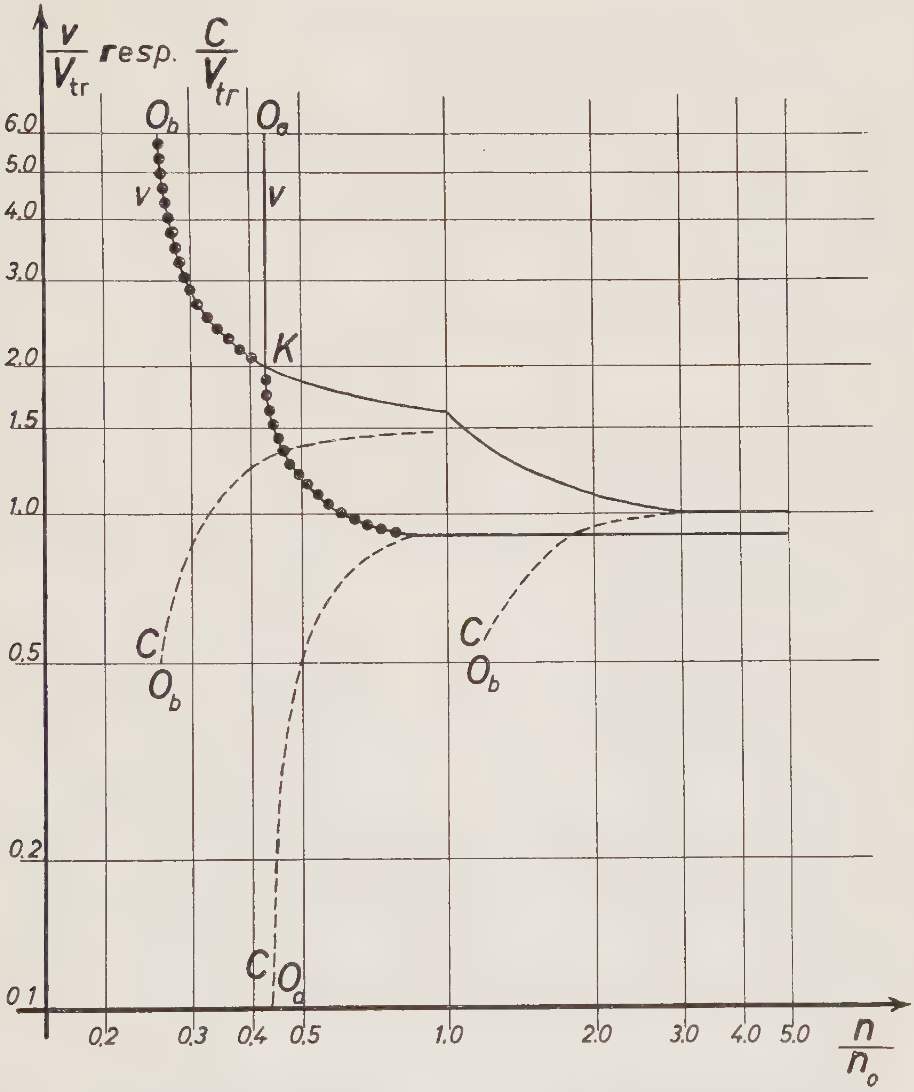

Fig. 2. Theoretical dispersion curves by O. Förtsch (1953), on double logarithmic scale.

indicated by a chain of black circles, which has the shape of a garland. In this part the point K figures as "break point" of the curves. The coordinates of the "break point" (K) are found to be

$$v_k/V_{tr} = 2{,}0 \qquad (4)$$

$$n_k/n_o = 0{,}43 \qquad (5)$$

and (with equations 3, 4, 5)

$$v_k/n_k = L_k = 4{,}65\ H \qquad (6)$$

where $L_k =$ wave length of phase at break point
$H =$ thickness of the layer.

Equation (6) indicates that for this theoretical model the critical wave length of phase belonging to the break point is 4,65 times the thickness of the layer.

Another value which is of importance for the characterization of the theoretical model of the Rayleigh dispersion is given by the branch C (O_b) (group velocity). The ordinate of the point of C (O_b) that has an abcissa $n/n_o = 0{,}43$, is

$$C_{theor.} = 1{,}3\ V_{tr} \qquad (7)$$

Equations (3) and (7) establish a theoretical group wave length

$$C_{theor.}/n_k = L_{theor.} = 3{,}0\ H, \qquad (8)$$

and the quotient

$$H/L_{theor.} = 0{,}33 = D_{theor.} \qquad (9)$$

Equation (9) establishes a theoretical value of penetration ($D_{theor.}$) for the model, Rayleigh waves in a layer overlying a half space, the theoretical penetration of the model with Rayleigh wave energy being determined by the dimensionless value 0,33.

It has already been said in the previous part of this paper that seismograms from measurements in the field have to be subjected to harmonic analysis in order to get the phase velocities of different frequencies. The practical use of the theoretical dispersion curves, as described, depends on equations (4), (6), and (9), which provide methods of determining the transverse velocity inside the effected layer, the thickness of the layer, and the penetration of Rayleigh wave energy respectively. Nevertheless it must be emphasized that the theoretical Rayleigh dispersion curves, as demonstrated in this paper, are idealized dispersion curves, valid for Poisson's ratio 0,25 only. Theoretical dispersion curves for other Poisson's ratios have not yet been calculated, as the calculation meets with extreme difficulties and requires much time. It may be assumed that the characteristic values, as fixed by equations (4), (6), and (9), will then be of different magnitude, since the relation

$$V_{lg}/V_{tr} = \sqrt{3} \qquad (10)$$

is then no longer valid. However, as the results of the measurements will show, the general shape of the dispersion curves, the typical garland of the two branches O_a and O_b and their junction at the "break point" (K) are maintained throughout the experiments. The following parts of this papers will show the practical results of measurements and analysis and will discuss special effects of various loose soils.

FIELD MEASUREMENTS, COMPUTATIONS, EXPERIMENTAL DISPERSION CURVES, AND TABLE OF NUMERICAL RESULTS

One of the most important aims of the present investigations was to examine various types of soils with respect to utilization of seismic energy. As there exist numerous types of soils, and it was impossible to carry out extensive experiments including all these soils, only some typical representatives could be chosen for practical measurements in the field.

In soil mechanics there are three main classifications of soils: bonding material, non-bonding material, and soils more or less mixed with organic matter. In the surroundings of Munich many typical representatives of each class were available, all of which had been well verified by bore-holes. At last six places were chosen. Special attention had been given to ensure that none of them was disturbed by foundation-walls and other engineering constructions that could possibly generate unwanted reflections and disturb the normal propagation of seismic waves.

A sample of bonding soil was chosen from a loam pit at Emmering. There were two cases available of non-bonding soils. At Lichtensee natural gravels of partly tertiary and diluvial character were included in the measurements, and at Schönbrunn clean quartzite sands of tertiary origin could be investigated. Soils mixed with greater or smaller amounts of organic matter were at hand in two cases, one of them a typical glacial bog at Staltach, and the other a marshy soil of alluvial character at Prittlbach. Another special type of non-bonding soil was chosen at Karlsfeld, consisting of excavated gravel, piled up by cranes and then rolled.

On all these soils measurements with a three component set of mechanical leaf-spring seismographs have been carried out. The seismographs were stationed in a tent, and the source of seismic energy (hammering, and, in three cases out of six, shooting) was moved along a profile. Hammering was done in increasing distances from the tent from 5 to 30 m, shooting took place in the range from 30 to about 200-250 m. Hammering was done in intervals of 5 m, blasting in intervals of 20 or 25 m.

The theoretical dispersion-curves already discussed show that any experiments should show a functional relation between the phase velocity and the frequency. The phase velocities and frequencies may be obtained from the Fourier- or harmonic analysis of seismograms obtained from a set of mechanical seismographs of which the dynamical characteristics (phase diagram and frequency response) are well known. This was the case with the mechanical leaf-spring seismographs used in the present investigations. They were of the type developed at the geophysical institute of the University of Göttingen under the late Professor G. Angenheister (a scholar of E. Wiechert). Rössiger (1932) and Förtsch (1952) gave details of the theory of such seismographs.

The numerous seismograms obtained from field investigations were subjected to thorough Fourier analysis. The analysis, as is well known, gives amplitudes and phase angles. The amplitudes as a function of frequency constitute the frequency spectrum. Figure 3 gives examples of such frequency spectra. In these examples the so-called "dispersion interval" ,the active part of each spectrum which is the basis for the construction of the experimental dispersion curves, has been specially marked. In practical calculation phase angles, calculated in milliseconds, give values for construction of the time-distance dia-

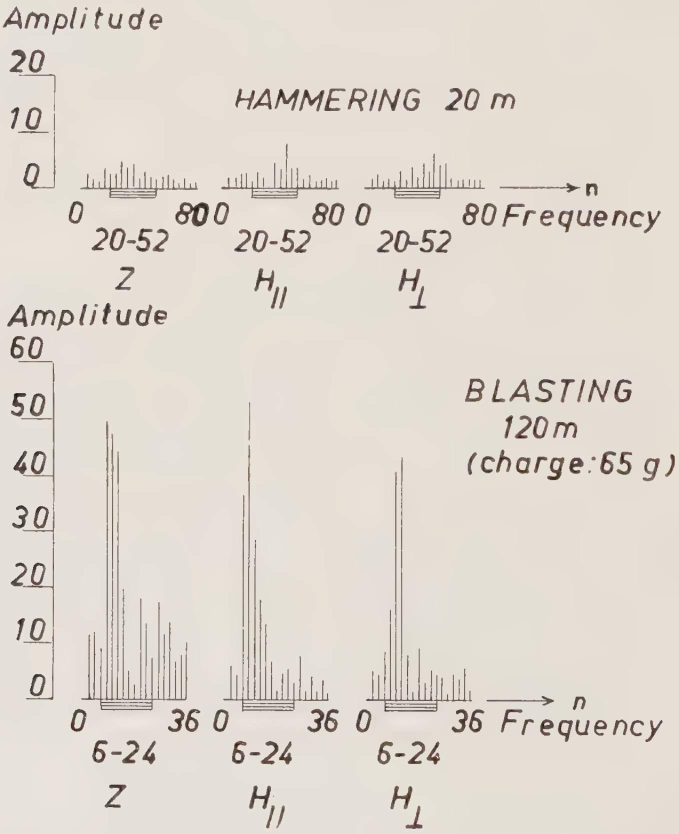

Fig. 3. Examples of frequency spectra from measurements at Emmering.

grams of the phase waves from which are derived the phase velocities needed for the plotting of experimental dispersion curves.

The calculation and construction of the experimental dispersion curves took much time. Observations with mechanical seismographs in the field also were very difficult. However, as will be shown later, such investigations allow conclusions to be drawn concerning the mechanism of propagation of surface waves in loose materials of the soil. Evidently, if such methods are to be used on an economical basis, measurements as well as computations will have to be modified.

The figures 4 to 7 show experimental dispersion curves. Attached to the dispersion curves are diagrams of the sequences of layers, for each case investigated, with the natural water level (if present) specially marked. The full drawn lines in the diagrams give the exact mean values from the computations of the three observed components, Z = vertical component, $H_{,,}$ =

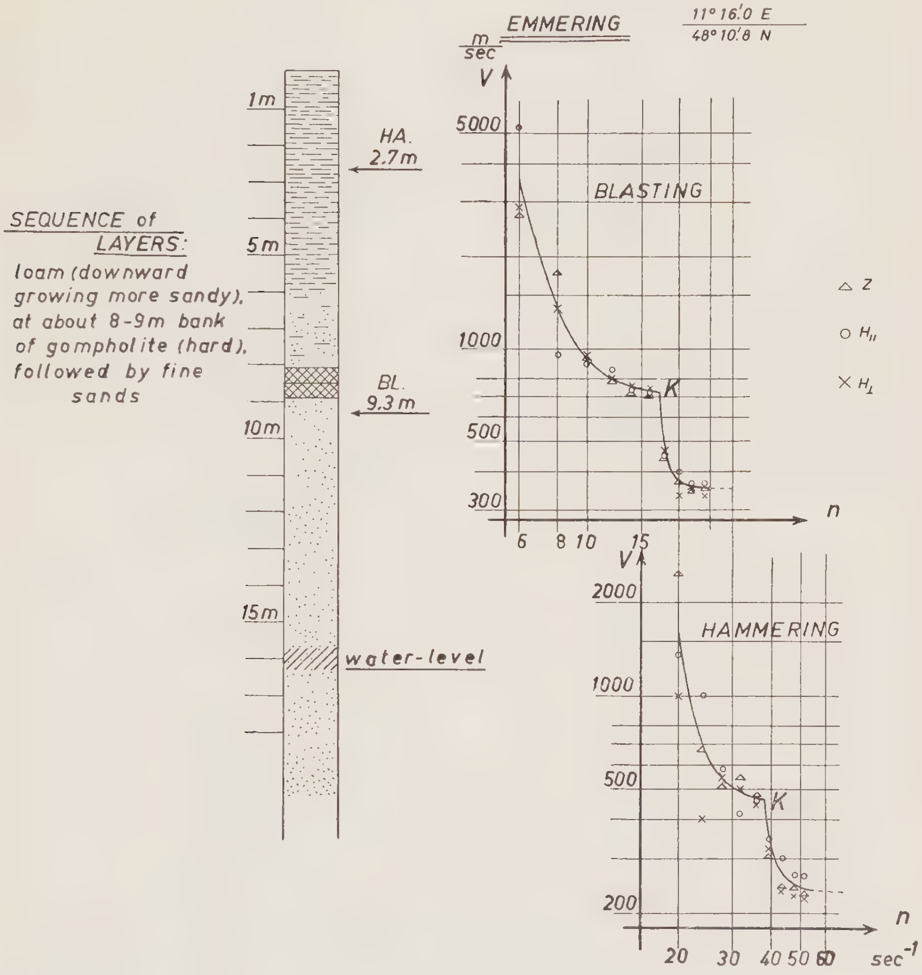

Fig. 4. Experimental dispersion curves from blasting and hammering at Emmering (with sequence of layers shown).

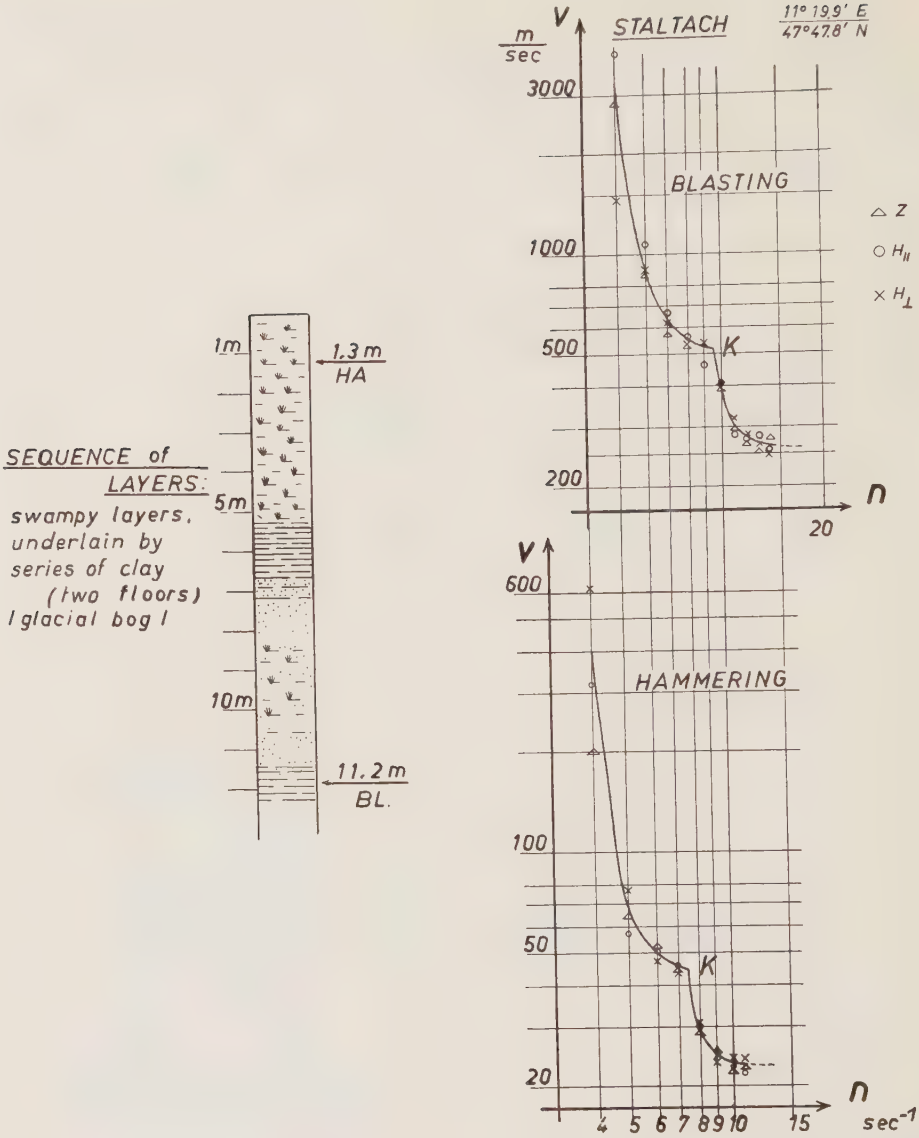

Fig. 5. Experimental dispersion curves from blasting and hammering at Staltach (with sequence of layers shown).

horizontal component parallel to wave direction, $H_{\perp} \rightarrow$ = horizontal component transverse to wave direction.

A comparison of the experimental dispersion curves with the theoretical dispersion curves (Fig. 2) shows astonishing similarity. The two branches of the special Rayleigh dispersion in a layer overlying a half space (o_b and o_a), meeting in the break point K, are developed quite distinctly. Apparently the theoretical model, Rayleigh waves propagated in a layer overlying a half space, seems to have support, as in all six cases the harmonic analysis of seismograms obtained from reliable seismographs led to the same character of experimental dispersion curves.

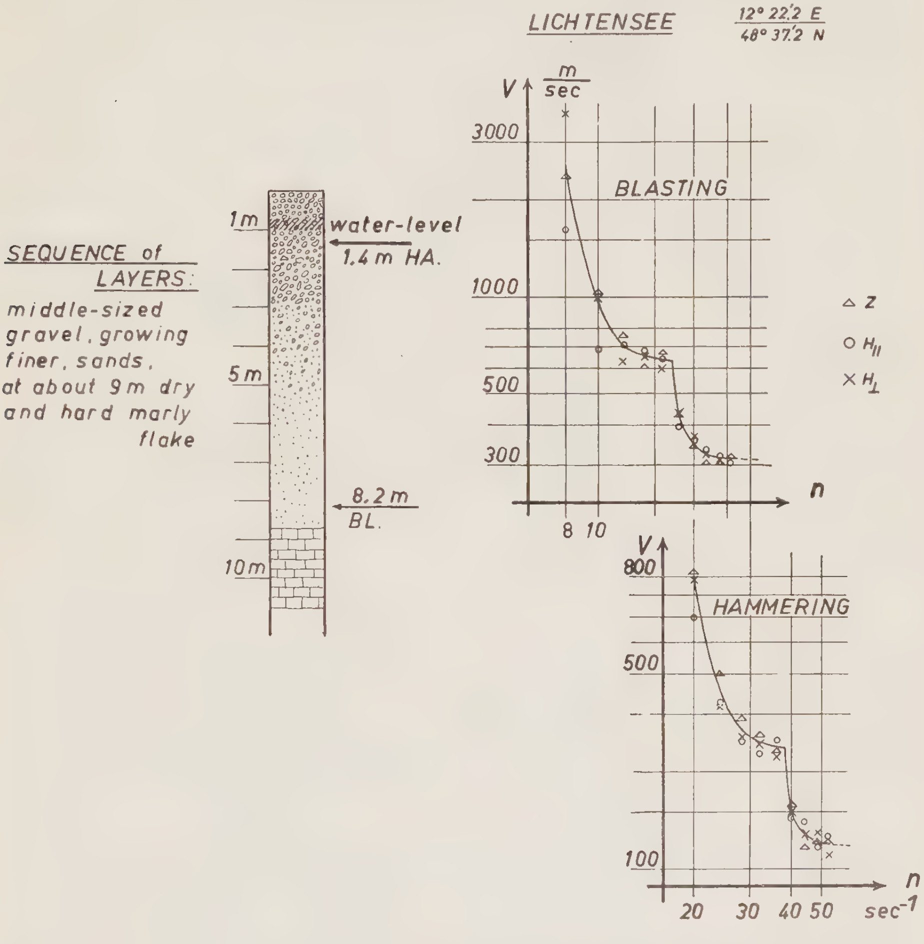

Fig. 6. Experimental dispersion curves from blasting and hammering at Lichtensee (with sequence of layers shown).

In each of the figures the coordinates of the break point, K, provide characteristic values which are shown in the table below. Obviously the frequency of the break point is typical for each experiment. After the presentation of experimental dispersion curves, the dispersion interval, formerly defined as the active part of the spectrum (see fig. 3), is more comprehensible. The

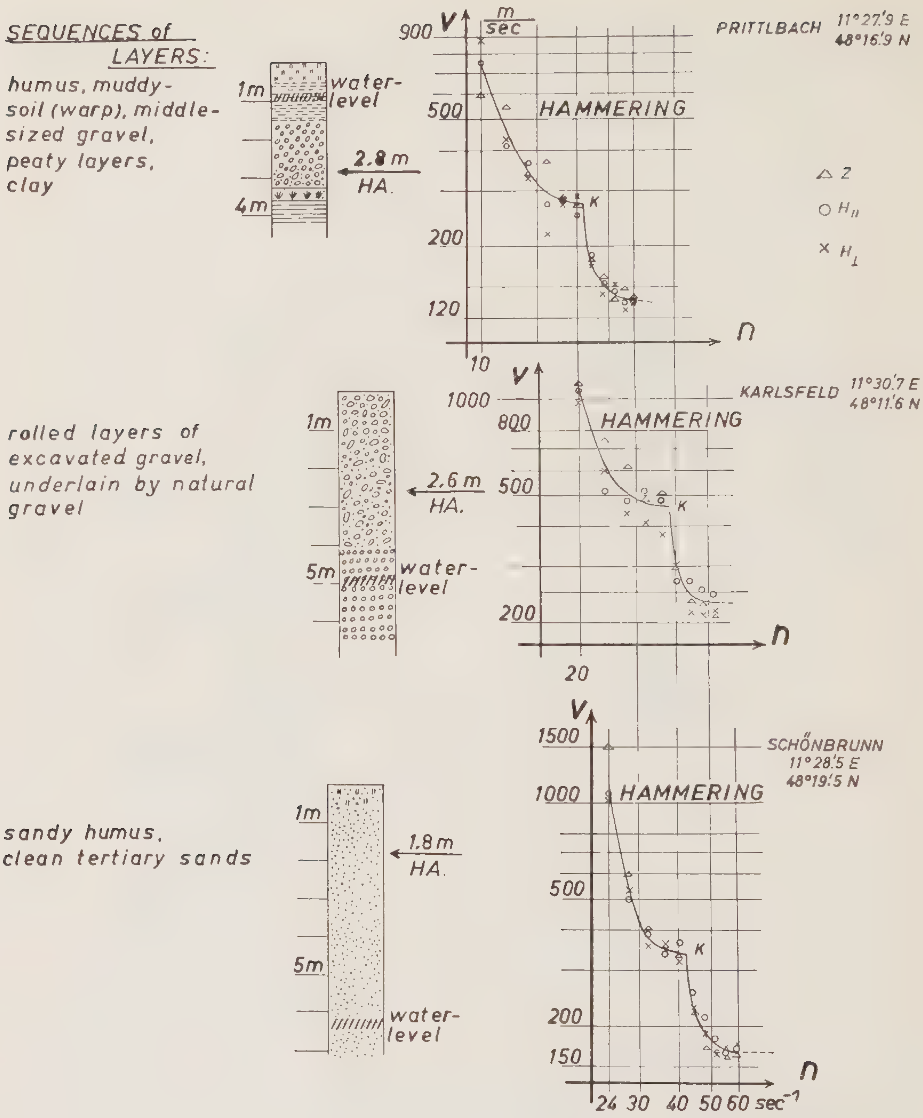

Fig. 7. Experimental dispersion curves from hammering at Prittlbach, Karlsfeld, and Schönbrunn (with sequences of layers shown).

dispersion interval contains the range of frequencies which covers the band from the beginning of the branch o_b of the experimental dispersion curves to the end of the branch o_a. Any frequencies lying outside the dispersion interval do not take part in the construction of the dispersion curves from the base elements of the harmonic analysis.

Figures 4 to 7 show very well the relative displacements of the dispersion interval of the various experiments. From shooting a low-frequency range results which is very nearly the same in the different types of soils. (How far such results apply to homogeneous soils will be discussel later). The dispersion interval from the observations of hammering, however, gives different ranges of frequencies, obviously depending on the typical consistency of the soils. From lowest frequencies on the bog the range of the dispersion interval rises up to highest frequencies on the sharp and clean quartzite sands.

All these frequency data, and other items derived from dispersion curves as well as from direct readings of impulses on seismograms allow the following statement: any seismic pulse is able to generate a Rayleigh wave mechanism. According to the energy delivered by the seismic pulse, and according to the consistency of the medium to which the seismic pulse is imparted, the Rayleigh wave mechanism has a greater or smaller vertical extension and gives special characteristics that may be found by thorough investigation.

In the following table the characteristics of the Rayleigh wave mechanism of those locations where investigations have been carried out, are presented.

The table shows the results of all measurements. Before discussing the results, it is necessary to explain the various characteristic quantities. There are quantities which entirely result from the harmonic analysis, others result from direct reading of impulses on the seismograms (similar to picking arrivals in the usual refraction and reflection method), and some of them are based on mixing the values that have been obtained by taking the harmonics and by direct reading.

1. *The dispersion interval,* as already defined, results from the harmonic analysis of seismograms.

2. *The frequency of the break point* can be directly read from the experimental dispersion curves, constructed from base values of the harmonic analysis.

3. *The transverse wave velocity* can be calculated from the coordinates of the break point with the aid of formula (4). So this quantity is also derived from the harmonic analysis.

4. *The group velocity* results from direct reading of impulses on the seismograms. The onset of the first strong motion in each of the seismograms has been chosen for computation. Theoretically the group velocity is connected with the transverse wave velocity by formula (7).

5. *The thickness of the layer* is obtained by calculation with formula (6) from the quotient of the coordinates of the break point of the experimental dispersion curves. So it is a quantity derived from harmonic analysis.

6. *The wave length (group).* This quantity is based on mixing of values from harmonic analysis and direct reading of seismograms. It is obtained as the quotient:

TABLE

Numerical results of measurements.

	Emmering (loam pit)		Lichtensee (dam-site, gravels)		Staltach (glacial bog)		Prittlbach (marshy soil)	Karlsfeld (excavated gravels)	Schönbrunn (clean sands)
Characteristics:									
Dispersion interval (sec^{-1})	6-24	20-52	8-26	20-52	5-14	4-11	10-30	20-52	24-60
Frequency of break point (sec^{-1})	17	38	17	38	9,5	7,5	21	38	41
transverse velocity (m/sec)	365	235	320	118	260	23	135	230	170
Group velocity (m/sec)	700	340	340	170	330	27	170	310	280
Thickness of layer (m)	9,3	2,7	8,2	1,4	11,9	1,3	2,8	2,6	1,8
Wave length (group) (m)	41,2	8,95	20,0	4,5	34,7	3,6	8,1	8,15	6,8
Refr. wave velocity (m/sec)	1900	(600)	1750	(650)	1150	—	(680)	(1000)	(590)
Penetration (—)	0,22	0,30	0,41	0,31	0,34	0,36	0,35	0,31	0,26
Coeff. of absorption (—) (from hammering interval 20-30 m)	—	0,407	—	0,048	—	0,309	0,239	0,238	0,068
	Bl.	Ha.	Bl.	Ha.	Bl.	Ha.	Ha.	Ha.	Ha.

(Bl. = blasting, Ha. = hammering)

(group-velocity as resulting from direct reading
of impulses on seismogram) / (frequency of
break point of experimental dispersion curves).

7. *The refracted wave velocity* is connected with the first onsets of seismograms, which in the case of hammering are very feeble. In the case of shooting as well as of hammering these motions in seismograms did not affect the harmonic analysis, amplitudes being too small and frequencies too high. The direct reading of the refracted wave velocity, however, extended the interpretation of the relations connected with the Rayleigh wave mechanism, as will be shown later.

8. *The penetration.* The theoretical penetration of a Rayleigh wave mechanism has been established in formula (9) as equal to 0,33. The value of penetration, as given in the characteristics of the Rayleigh wave mechanism (see table), concerns an actual value of penetration. Its definition is expressed by the quotient

(Thickness of layer) / (group wave length).

As far as the limited number of investigations allows, some remarks on this quantity will be made later.

9. *The coefficient of absorption (from hammering interval 20-30 m).* This quantity gives values which will be discussed in connection with the principal measurement of absorption. It is based on utilization of the frequency spectra.

Discussion of numerical results

The numerical results of the present measurements given in the preceeding table reveal a number of characteristics of the Rayleigh wave mechanism. The discussion of all characteristic quantities and conclusions concerning the propagation of waves in loose materials of the upper soil can be carried out in the following manner:

4.1. Remarks on the vertical extension of the Rayleigh wave mechanism with respect to the thickness of the layer and the penetration.

4.2. Notes on the significance of the dispersion interval and the transverse wave velocity.

4.3. Remarks on the refracted wave velocity.

4.4. Proposals on measurement of absorption.

4.1. As already mentioned, the measurements have been carried out with the intention of revealing seismic characteristics of various types of soil. A glance at the table of the numerical results shows that hammering and blasting gave different characteristic values. The sequences of layers shown with the experimental dispersion curves (figures 4 to 7) make it evident that the Rayleigh wave mechanism, in the case of hammering, was confined to the standard type of soil which had been chosen for the investigation. The Rayleigh wave mechanism of blasting, however, extended over a whole sequence of layers. In all three cases the boundary plane between the Rayleigh wave mechanism and the half space corresponded to a geologically and physically plausible discontinuity. At Emmering the Rayleigh wave mechanism was bounded by a hard bank of gompholite. At Lichtensee the boundary coincided with the beginning of a layer of dry and hard argillaceous marl. At Staltach the top of the second (lower) layer of clay underlying the bog formed the boundary plane of the Rayleigh wave mechanism.

Besides the thickness of the layer the value of the penetration, as shown in the table of numerical results, can well serve as a characterization of the vertical extension of the Rayleigh wave mechanism. Hammering at Staltach and Prittlbach (bog, muddy soil) showed a penetration value higher than the theoretical value (0,33, formula 9). Hammering at Emmering, Lichtensee, and Karlsfeld gave a penetration slightly lower than the theory. Hammering at Schönbrunn, with a penetration value of 0.26 had the smallest penetration of surface wave energy, as if the clean quartzite sands prevented the Rayleigh wave mechanism from attaining its full development. The penetration values of the blasting at Emmering and Lichtensee demonstrated that in both cases the situation of the geological and physical discontinuity (the bank of gompholite, and the argillaceous marl) influenced the characteristic extention of the Rayleigh wave mechanism. At Emmering vertical extension is prevented and at Lichtensee favoured, while at Staltach the situation of the discontinuity seems to allow normal penetration of surface wave energy.

Of course, on the strength of the limited number of observations it is not justified to conclude generally valid laws concerning the vertical extension of the Rayleigh wave mechanism corresponding to the theoretical model, Rayleigh waves in a layer overlying a half space; nevertheless they give hints as to the probable connection between the energy imparted to the soils by seismic impulses and the energy transformed into surface waves. In section 4.3 further remarks will be made upon this subject. As stated before in chapter 2 of this paper, the characteristic data of the Rayleigh wave mechanism have been derived from an idealized theoretical dispersion-curve, valid for Poisson's ratio 0.25. Whether or not the theoretical coordinates of the break point (K), see formulas (4) and (5), and consequently the standard factor of 4,65 for the determination of the thickness of the layer, see formula (6), are generally applicable to the interpretation of experimental dispersion curves, cannot yet be decided. The extreme similarity in shape of experimental dispersion curves to the theoretical dispersion curve, however, gave reason to discuss the different vertical extension of the Rayleigh wave mechanism in the case of hammering from that in the case of blasting.

4.2. This section is concerned with the method of dynamic investigation of soils, as developed by the former German Society of Soil Mechanics (DEGEBO), Berlin, in the thirties. The following authors referred to that method: Köhler (1936), Köhler and Ramspeck (1936), Ramspeck (1936), Ramspeck and Schulze (1938), Lorenz (1948), Schultze and Muhs (1950), and Schumann (1953). The dynamic investigation of soils leads to the construction of dispersion curves, and to the determination of transverse wave velocities for different types of soils. It is of the utmost importance in the application of the dynamic method to find the so-called limiting frequencies which define the highest and the lowest frequency which the medium under examination is capable of supporting. However, measurements have shown that low frequencies cannot be imparted to loose soils by rotating weights (that is the manner which is applied in the dynamic method) as readily as higher frequencies. The present investigations show that the range of frequencies for the blasting is very low. The dispersion interval runs from very low frequencies (5 c.p.s.) to values rarely in excess of 20 c.p.s. In section 4.1 the order of magnitude of the vertical extension of a Rayleigh wave mechanism has been discussed. Obviously only with small blasts does the surface wave energy penetrate into the loose soils to a depth of the order of magnitude that is needed to characterize a whole sequence of layers for engineering purposes. In order to establish a complete experimental dispersion curve, the soil must even be forced into frequencies of 3 or 4 c.p.s.; evidently that is not possible if rotating weights are used. Low frequency rotations do not deliver sufficient energy to generate the whole Rayleigh wave mechanism down to the first consolidated layers in alluvial and diluvial materials (or, as stated in section 4.1, the first geological and physical discontinuity).

The excitation of the soil by a small blast and the analysis of the seismograms generally gives the same effect as separate registration of frequencies produced by a set of rotating weights. A blast immediately generates a whole spectrum with a specific dispersion interval; rotation of weights, however, does not guarantee that the entire dispersion interval of a Rayleigh wave mechanism is completely reproduced. Consequently only a small blast can establish standard transverse wave velocities belonging to a specific Rayleigh wave mechanism. This transverse wave velocity corresponds to the consistency of the investigated soil, or that of the sequence of layers into which the surface wave energy penetrates.

4.3. This section is concerned with the method of seismic refraction shooting in loose materials of the upper soils of alluvial and diluvial character. Short distance seismic refraction investigations, as numerous examples in the literature show, gave relatively good results in the case of determination of depth of solid rocks in mountainous regions, where weathered layers of mechanically destructed material cover the rocks. In the wide plains of the alluvial and diluvial formations, however, short distance refraction shooting meets with difficulties, solutions of which have been attempted by various methods of observation and of interpretations of results.

The refraction shooting is mainly concerned with first arrivals on the seismogram; in particular the utility of second and even later pulses on the seismogram obtained from loose soils is very doubtful. The present investigations afforded a comparison between direct reading of seismograms and harmonic analysis of complete seismograms over their whole length. In other words: direct reading could be checked by the characteristics of the Rayleigh wave mechanism, and vice versa. Obviously, the main energy from a seismic pulse in loose soils is carried by wave groups of the Rayleigh wave mechanism. The same statement was made by Leet (1939). The refracted longitudinal waves which are continuously radiated from the boundary plane between the Rayleigh wave mechanism and the half space, always yield small, and, especially in the case of hammering, doubtful first impulses of the seismogram.

For the application of the refraction method two velocities are required: one velocity of longitudinal waves from inside the layer, and a second velocity from the underlying medium. The present investigations show that an exact velocity from inside the loose layer obviously cannot be obtained. Other authors have already found such difficulties which limit the application of short distance refraction shooting. Various methods have been developed to interpret the resulting time-distance diagrams by a continuous increase of longitudinal wave velocity with depth in the loose layer. The present investigations, however, show that inside the loose layer an independent longitudinal wave cannot exist and propagate. Longitudinal waves inside the layer are always coupled with the Rayleigh wave mechanism which is generated and propagates inside the layer. An independent longitudinal wave pulse is only observable as a refracted wave from the boundary plane between the Rayleigh wave mechanism and the half space.

Between hammering and blasting there is a large difference in energy. The result of this energy difference is manifested by a displacement of the dispersion interval, and, as the measurements show, the blasting generates a Rayleigh wave mechanism down to the first consolidated basement of the loose soils (see section 4.1). In all the three cases of blasting a high, refracted wave-velocity could be clearly distinguished. The same refracted longitudinal wave velocity was also exactly found and established by parallel observations with geophone equipment. All efforts to increase the depth of penetration of the seismic energy in the sequence of layers failed, even though the charges were increased from a few hundred grams of explosive to several kilograms. Likewise no higher refracted longitudinal wave velocity was registered by the geophone apparatus. It can be assumed that the lower boundary plane of the Rayleigh wave mechanism forms an energy threshold which can only be overcome by excessive energy increase of the seismic pulse. Such energy increase would never be considered in engineering seismology.

More generally it may be stated that seismic refraction shooting is only valid in the exact sense of the term for other orders of magnitude, where ten or twenty meters of upper loose materials do not play the decisive part, as is the case in near surface investigations. Indeed, the great successes of refraction shooting in the past have been obtained from observations in the range of several hundred meters depth. All present efforts to deal with engineering problems by means of seismic investigations are more or less modifications of the refraction shooting method. In some cases, such efforts lead to success, in others the results are far away from the facts the engineer wants to know. Therefore it is advisable not only to practice the various modifications of refraction shooting, but to turn more attentively to surface wave investigations which, as the present experiments show, bear every possibility of solving some of the pending problems.

This section cannot be closed without mentioning another characteristic of the Rayleigh wave mechanism which has been suggested by the author (1954). Very probably, the depth penetration of the Rayleigh wave mechanism, according to the energy delivered, shows a stepwise increase. From hammering to short distance refraction shooting, to long distance refraction observations, up to earthquakes of different orders of magnitude, the dispersion intervals of the possible dispersion curves might change, frequencies growing lower and lower. Keylis-Borok (1951) from another point of view came to an analogous conclusion concerning the gradual increase in dimensions of the crustal formations of the earth partaking in motions of global surface waves.

Returning to the present limited observations which only effectively include one energy step, from hammering to small blasts, and citing the results of numerous long distance refraction investigations well known from many publications (observations of large explosions, as for instance carried through by the institute for applied geophysics at Munich under the auspices of Prof. H. Reich, and seismic refraction work in prospecting for oil in the range of some 10 or 20 km), it may be stated that the independent refracted longitudinal wave velocity increases in the same way, step by step, according to the energy delivered. Any refracting horizon may possibly represent the above mentioned energy threshold for a Rayleigh wave mechanism. The group velocity of a Rayleigh wave mechanism is considerably lower than the velocity of body waves. So in long distance refraction shooting a number of independent longitudinal wave pulses from different refracting horizons can be registered before the seismogram is disturbed by the strong motions of the Rayleigh wave mechanism which is usually limited in its extension to the very first or second refracting horizon. Shor distance refraction investigations, as carried out in engineering seismology, are definitely limited to the loose upper layers. These layers overly the shallowest refracting horizon, which at the same time is the lower boundary of the Rayleigh wave mechanism. Thus, as already stated, the short distance refraction investigations meet with the difficulty of finding a reliable average longitudinal wave velocity v_1 that is needed for the computation of the depth of the first refracting horizon, of which the velocity v_2 is well known.

4.4. Since the first beginnings of earthquake and exploration seismic research, absorption of seismic energy has been the subject of numerous papers. Here it is not intended to go far into the problems. Merely one technical remark might be made.

Absorption measurements make use of the amplitudes from the seismograms. It is often difficult to find a representative amplitude on the whole length of the seismogram, and its determination depends mostly on the personal skill and opinion of the computor. The present method of harmonic analysis of recordings with mechanical seismographs, however, provides a much more objective type of amplitude. The frequency spectrum obtained by the Fourier analysis can give such an amplitude. There can be chosen an average amplitude from the three component dispersion volume (see figure 3). Exact measurements of absorption can only be carried out if there is an opportunity to register a single seismic pulse at different stations along the profile. This method has not been adopted in the present case, since it would require the use of several seismographs and a large number of skilled observers. However, there was a possibility of estimating the probable effect of absorption, using the method of hammering at a distance of 20 to 30 m, by assuming that the average intensity of hammering by one single person was constant throughout this range. The frequency spectra from hammering indeed showed a regular decrease in that range of distances.

The coefficients of absorption as indicated in the table of the numerical results have been calculated using a formula which has been given by Förtsch (1940) for the propagation of vibratory motions of engines:

$$y = y_o\,(x/x_o)\ 1/2\ \exp. - k(x - x_o)/L_c \qquad (11)$$

where:

y_o = amplitude at reference point
y = amplitude at point beyond reference point
x-x_o = reference distance along the profile
L_c = wave length of group of the surface-waves
k = coefficient of absorption to be determined.

The table of numerical results shows the different coefficients of absorption. The gravels of the dam site at Lichtensee and the clean sands at Schönbrunn give the lowest values of absorption. The highest values are given by the glacial bog at Staltach and the loam pit at Emmering. So even this small number of measurements with their gross approximation show somewhat reasonable results. Therefore, the utilization of the elements of the harmonic analysis of seismograms (such as the average amplitude from the three component dispersion volume, as defined before) leads to most encouraging results and will give another quantity for the seismic characterization of various soils.

FINAL REMARKS

This report on surface waves does not claim to solve the problem of seismic near surface investigations. On the contrary, with the application of surface waves analysis on loose soils still more difficulties are raised. Moreover, these few observations on some representative types of soil only give very limited results. Another difficulty in practical application of the method of harmonic analysis of seismograms is caused by the use of mechanical seismographs which are complicated in handling and can only be applied in special cases. The general application of the Fourier analysis requires seismograph systems of which the dynamic characteristics are well known and can be well controlled. Berson (1951) suggested a method of utilizing a seismic apparatus with multiple channels of registration for the solution of dynamical problems in seismic prospecting. Recently Zapolsky (1955) published results of near surface investigations that had been obtained by simultaneous registration on six channels of a seismograph system.

Specially designed damped coil seismographs with calibrated amplifiers will certainly produce seismograms suitable for harmonic analysis, so that the characteristics of the Rayleigh wave mechanism as developed in this paper could be established for more extensive observations. The present investigations with mechanical seismographs merely gave some new aspects, and perhaps they may show a way for further gradual development, both in geophysical research and in engineering seismology.

References

Angenheister G., 1950, Fortschreitende elastische Wellen in planparallelen Platten. Gerl. Beitr. z. Geophys., 61, 296-308.

Berson I. S., 1951, On revealing of dynamic characteristics of seismic registrations with different relations of sensibility in channels of registration. (in Russian). Izvest. Ak. Nauk SSSR, Sseriya geof., 6, 5-10.

Förtsch O., 1940, Ableitung des von der Frequenz unabhängigen Absorptionskoeffizienten aus Maschinenschwingungen. Zeitschr. f. Geophys., Heft 1/2, 57-84.

——, 1950, Untersuchungen von Biegewellen in Platten. Messungen ihrer Gruppen- und Phasengeschwindigkeit. Gerl. Beitr. z. Geophys., 61, 272-290.

——, 1952, Das Verhalten von Blattfederseismographen bei freier und erzwungener Schwingung. Annali di Geof., 5, 322-356.

——, 1953, Deutung von Dispersions- und Absorptions beobachtungen an Oberflächenwellen, I. Dispersion von Oberflächenwellen., Gerl. Beitr. z. Geophys., 63, 16-58.

——, und Schulze G. A., FIAT-Review of German science 1939-1946, Bd. 18., Geophysik, Teil II, edited by J. Bartels, Göttingen. Dieterich'sche Verlagsbuchhandl. Inh. W. Klemm, Wiesbaden.

Haskell N. A., 1953, The dispersion of surface-waves on multilayered media. Bull. of the Seism. Soc. of America, 43, 17-34.

Keylis-Borok V. I., 1951, On surface waves in a medium lying on an elastic halfsphere. (in Russian), Izvest. Ak. Nauk SSSR, Sseriya geof., 2, 17-39.

Köhler R., 1936, Eigenschwingungen im Boden. Veröffl. DEGEBO, 4, 3.

——, und Ramspeck A., 1936, Die Ausbreitungsgeschwindigkeit elastischer Wellen im Boden. Veröffl. DEGEBO, 4, 9.

Korschunow A., 1954, Ein Beitrag zur Seismik der Lockerböden und oberflächennahen Schichten (Dispersion von Oberflächenwellen aus Hammerschlägen und kleinen Sprenungen). Dissertation, Univ. München.

Leet L. D., 1939, Ground vibrations near dyamit blasts. Bull. of the Seism. Soc. of America, 29, 487-496.

Lorenz H. L., 1948. Stand des dynamischen Bodenuntersuchungsverfahrens. Abhandl. über Bodenmechanik und Grundbau; herausgegeben v.d. Forschungsgesellschaft f.d. Strassenwesen E.V., Bielefeld, 81.

Ramspeck A., 1936, Die Interferenz elastischer Wellen im Untergrund. Veröffl. DEGEBO, 4, 17.

Ramspeck A. und Schulze G. A., 1938, Die Dispersion elastischer Wellen im Boden. Veröffl. DEGEBO, 6.

Rössiger M., 1932, Beitrag zur Theorie des Blattfederseismographen. Zeitschr. f. Geophys., 8, 470-477.

Sezawa K., 1927, Dispersion of elastic waves propagated on the survace of stratified bodies and on curved surfaces. Bull. of the Earthquake-Inst. Imperial Univ. Tokyo, 3, 1.

Sezawa K. and Kanai K., 1935, Discontinuity in the disperision-curves of Rayleigh-waves. Bull. of the Earthquake-Inst. Imperial Univ. Tokyo, 8, 237-244.

Sommerfeld A., 1950, Vorlesungen über Theor. Physik, Bd. II., Mechanik d. deform. Medien, 163-199, Akad. Verl. Ges. Lpz.

Schultze E. und Muhs H., 1950, Bodenuntersuchungen für Ingenieurbauten., Springer-Verlag, Bln.-Göttingen-Heidelbg.

Schumann W., 1953, Über Entwicklungsarbeiten auf dem Gebiet geophys. Baugrunduntersuchungen. Physikal. Verhandl., 4, 242.

Stoneley R., 1953, The transmission of Rayleigh waves across Eurasia. Bull. of the Seism. Soc. of America, 43, 127-135.

Zapolsky K. K., 1955, On dynamic time-distance curves of seismic waves. (in Russian). Izvest. Ak. Nauk SSSR, Sseriya geof., 3, 198-206.

ON THE EFFECT OF POISSON'S RATIOS OF ROCK STRATA ON THE REFLECTION COEFFICIENTS OF PLANE WAVES *

BY

O. KOEFOED **

ABSTRACT

Calculations are presented of reflection coefficients of plane longitudinal waves incident at oblique angles on boundary planes between elastic media. It is shown that the manner in which these reflection coefficients vary with the angle of incidence is strongly affected by the values of the Poisson's ratios of the two media. It appears that, contrary to a conclusion arrived at by Muskat and Meres, the reflection coefficient may vary appreciably with the angle of incidence in the range between 0° and 30°. Possibilities of practical application of this phenomenon are discussed.

INTRODUCTION

By the term "reflection coefficient" as used in this paper, is meant the ratio of the amplitude of the reflected wave to that of the incident wave. C. G. Knott (1899) derived formulae for the reflection coefficients for plane waves incident on a boundary between two elastic media, permitting their values to be computed when the elastic constants of the media are known. Numerical values of reflection coefficients of plane waves have been published, in addition to those by Knott (1899), by Blut (1932a and 1932b), Dana (1944), Muskat and Meres (1940a and 1940b) and Schlichter and Gabriel (1933). Of these publications the most comprehensive is that by Muskat and Meres (1940a). By the results of their calculations these authors are led to the conclusion "that while the reflected energy from the various types of interface will decrease with increasing angle of incidence the magnitude of the effect of the angle of incidence is rather small." (Muskat and Meres 1940b).

This conclusion of Muskat and Meres is confirmed by the calculations of Blut (1932a and 1932b) and by those of Schlichter and Gabriel (1933). However, in a case calculated by Knott (1899) the reflection coefficient drops from a value of 20% at normal incidence to a value of 5% at an angle of incidence of 14°. An example computed by Dana (1944) shows a considerable increase of the reflection coefficient with increasing angle of incidence, but this example refers to a reflection at the boundary between an elastic solid and a fluid, and may therefore not be significant in seismic prospecting.

---

* Presented at the Eighth Meeting of the European Association of Exploration Geophysicists, held at Paris, 18-20 May 1955.

** N.V. De Bataafsche Petroleum Maatschappy, The Hague. (Royal Dutch Shell Group).

When investigating the possible cause of the discrepancy between the result obtained by Knott and the conclusion formulated by Muskat and Meres, one is struck by the fact that the different authors have made very different assumptions concerning the values of the Poisson's ratios of the media. In the calculations of Muskat and Meres (1940a) both media have been assumed to have a Poisson's ratio of 0.25. The same value has been used by Schlichter (1933). Blut (1932a and 1932b) used other values for the Poisson's ratio but, in all the cases computed by him, the incident medium had a Poisson's ratio very nearly equal to that of the underlying medium. In the case published by Knott, however, one of the media had a Poisson's ratio of 0.28 and the other medium had a Poisson's ratio of 0.16.

In view of the above it seemed desirable to investigate whether the discrepancy between the result of Knott and the conclusion of Muskat and Meres could be caused by their different assumptions concerning Poisson's ratios, and in general to establish the effect of Poisson's ratios of the media on the change of the reflection coefficient as a function of the angle of incidence.

As a first approach to this problem the author presents in this paper the results of calculations for 17 different cases. These calculations have been carried out using the formula that was derived by Knott (1899) in the form in which it is given by Muskat and Meres (1940a). Many more calculations will be required, but the results obtained so far point already towards important conclusions.

NOTATION

The following notation has been used in this paper.

V_l: longitudinal wave velocity.
ρ: density
σ: Poisson's ratio

The subscript 1 refers to the incident medium, the subscript 2 to the underlying medium.

DISCUSSION OF THE RESULTS

The results of the calculations have been plotted in figs. 1-7. One of the graphs in these figures, that for $V_{l2}/V_{l1} = 1.25$, $\sigma_1 = \sigma_2 = 0.25$ and $\rho_2/\rho_1 = 1$, has been plotted from the values published by Muskat and Meres (1940a).

Fig. 1 shows a set of curves for $V_{l2}/V_{l1} = 1.25$, $\rho_2/\rho_1 = 1$, $\sigma_1 = 0.25$, and varying values for σ_2. It is seen that the value of σ_2 has a very pronounced effect on the shape of the curve, high values of σ_2 causing an increase of the reflection coefficient with increasing angle of incidence, and low values of σ_2 causing a decrease of the reflection coefficient with increasing angle of incidence.

Fig. 2 shows two curves for $V_{l2}/V_{l1} = 1.15$, the same values for ρ_2/ρ_1 and σ_1 that were used in fig. 1, and again varying values for σ_2. These curves show the same general trend as those in figure 1. It is instructive, however, to compare these curves more closely with the curves in fig. 1 for which σ_2 has the same values. The two curves for which $\sigma_2 = 0.40$ are practically parallel to each other. Since, however, the absolute values of the reflection coefficients are much smaller in the case illustrated in fig. 2 it appears that the *relative* change in the reflection coefficient becomes greater as the velocity

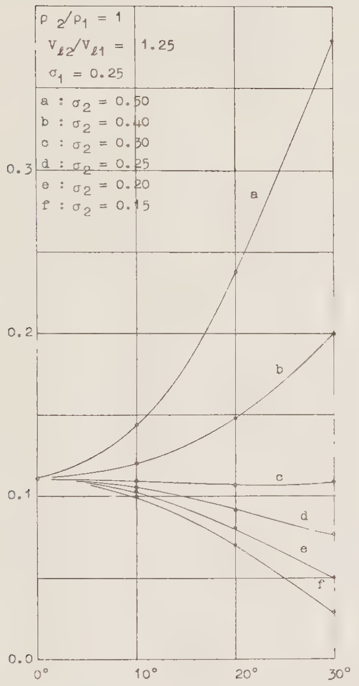

Fig. 1

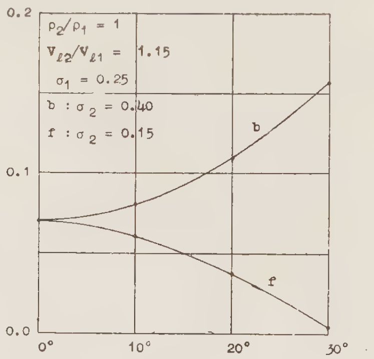

Fig. 2

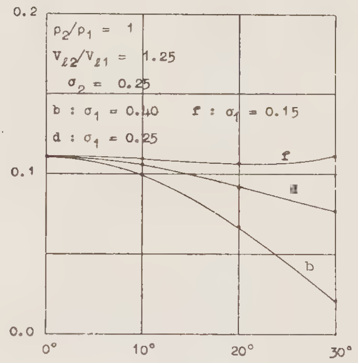

Fig. 3

Fig. 1. Reflection coefficient as a function of the angle of incidence, for varying values of σ_2.

Fig. 2. Reflection coefficient as a function of the angle of incidence, for varying values of σ_2.

Fig. 3. Reflection coefficient as a function of the angle of incidence, for varying values of σ_1.

contrast between the two layers becomes smaller. The two curves for which $\sigma_2 = 0.15$ converge as the angle of incidence increases, but still the *relative* change in the reflection coefficient is much greater in the case where the velocity contrast is smaller.

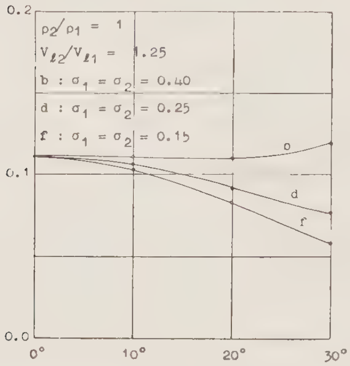

Fig. 4

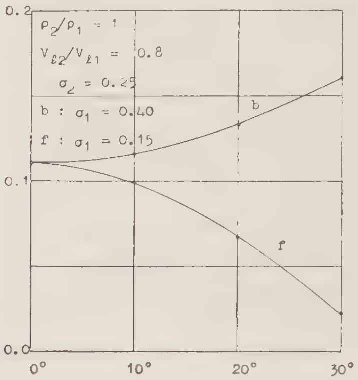

Fig. 5

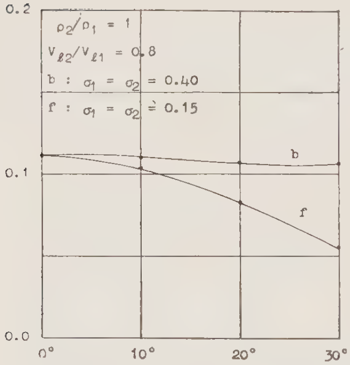

Fig. 6

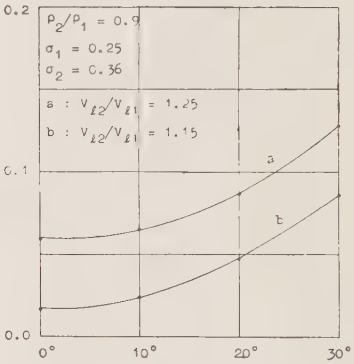

Fig. 7

Fig. 4. Reflection coefficient as a function of the angle of incidence, for varying values of $\sigma_1 = \sigma_2$.

Fig. 5. Reflection coefficient as a function of the angle of incidence, for varying values of σ_1.

Fig. 6. Reflection coefficient as a function of the angle of incidence, for varying values of $\sigma_1 = \sigma_2$.

Fig. 7. Reflection coefficient as a function of the angle of incidence, for varying values of the velocity contrast.

Fig. 3 shows three curves for $V_{l2}/V_{l1} = 1.25$, $\rho_2/\rho_1 = 1$ (the same values that were used in fig. 1), a constant value of 0.25 for σ_2 and varying values for σ_1. These curves show a trend opposite to that of fig. 1; a high value of

σ_1 causes a decrease of the reflection coefficient with increasing angle of incidence.

Fig. 4 shows three curves for $V_{l2}/V_{l1} = 1.25$, $\rho_2/\rho_1 = 1$ (the same values as in fig. 1), σ having in each case the same value for the two layers but different values for the different curves. In these conditions a high value of $\sigma_1 = \sigma_2$ causes an increase of the reflection coefficient with increasing angle of incidence, and a low value of $\sigma_1 = \sigma_2$ causes a decrease of the reflection coefficient with increasing angle of incidence. The effect, however, appears to be much less pronounced than in the conditions illustrated in fig. 1.

Fig. 5 shows two curves for $V_{l2}/V_{l1} = 0.80$, $\rho_2/\rho_1 = 1$, $\sigma_2 = 0.25$ and varying values for σ_1. These values refer to media that are identical to those in two of the cases illustrated in fig. 1, but with the incident and the underlying medium interchanged. A comparison between the curves of fig. 5 and the corresponding curves in fig. 1 brings out a rather remarkable similarity, which is particularly striking in the case where Poisson's ratios of the two media have values of 0.25 and 0.15.

Fig. 6 shows two curves for $V_{l2}/V_{l1} = 0.80$, $\rho_2/\rho_1 = 1$, and varying values of $\sigma_1 = \sigma_2$. These curves refer to media that are identical to those of the cases that are illustrated by the two outer curves of fig 4, but with the incident and the underlying medium interchanged. A comparison of these curves with the corresponding ones in fig. 4 indicates again a striking similarity.

Figures 5 and 6 seem to point towards the conclusion, that interchanging the incident and the underlying medium has only a slight effect on the shape of the curves—at least at the relatively small angles of incidence for which the calculations were carried out. It does not seem probable, however, that this conclusion would hold also for angles of incidence close to the critical angle.

Fig. 7 shows two curves in which a density contrast has been superimposed on the velocity contrast. For both curves $\rho_2/\rho_1 = 0.9$, $\sigma_1 = 0.25$, $\sigma_2 = 0.36$, and the longitudinal velocity ratio has different values for the two curves. It is seen again that the two curves are nearly parallel to each other. This implies that the *relative* change in the reflection coefficient is much greater in the case where the velocity contrast is smaller.

SUMMARY OF THE RESULTS

The calculations that have been carried out so far seem to point towards the following conclusions:

a) When the underlying medium has the greater longitudinal velocity and other relevant properties of the two strata are equal to each other, an increase of Poisson's ratio for the underlying medium causes an increase of the reflection coefficent at the larger angles of incidence.

b) When, in the above case, Poisson's ratio for the incident medium is increased, the reflection coefficient at the larger angles of incidence is thereby decreased.

c) When, in the above case, Poisson's ratios for both media are increased and kept equal to each other, the reflection coefficient at the larger angles of incidence is thereby increased.

d) The effect mentioned in a) becomes more pronounced as the velocity contrast becomes smaller.

e) Interchange of the incident and the underlying medium affects the shape of the curves only slightly, at least up to values of the angle of incidence of about 30°.

CONCLUSION AND PRACTICAL APPLICATIONS

The calculations presented in this paper cover only a small number of cases, and the author is perfectly aware that it would be premature to draw any *general* conclusions concerning the relation between the elastic properties of the rock strata and the change of the reflection coefficient as a function of the angle of incidence. Many more calculations will be required before a satisfactory understanding of this relation is reached. Work in this direction is being continued.

At the same time it is proved by the present calculations that the conclusion of Muskat and Meres, cited in the introduction of this paper, is not generally valid. The values for Poisson's ratios of rocks that have been published in the literature (Birch e.a. 1942) show a sufficiently wide variation to lead one to expect that the differences in Poisson's ratio of rock strata as they occur in nature, would affect the change of the reflection coefficient with the angle of incidence to an extent that would be of practical significance in seismic prospecting.

The possibilities of practical application of this phenomenon lie in three directions.

Firstly, the fact that the reflection coefficient may change as a function of the angle of incidence, emphasizes again the possibility of improving the quality of relections on a seismogram by a judicious choice of the distance from the shotpoint to the seismometers.

Secondly, the fact that the functional relation between the reflection coefficient and the angle of incidence may be different for different reflecting boundaries in a given area, provides a quantitative basis for the correlation of reflections across a fault *. At present correlation across a fault is based on the "character" of the reflections, a rather vaguely defined concept which is often poorly expressed on the seismograms or lacking altogether. In many cases such a correlation on the strength of the character is not possible; in other instances, where it does seem possible, this method has led to very considerable errors in the determination of the throw of the fault. However, by determining from field measurements the relative change of the reflection coefficient as a function of the angle of incidence, and by comparing the resulting curves on the two sides of the fault plane, a quantitative basis would be obtained for the correlation of the reflecting boundaries across the fault. Before this possibility can be realized, however, it will be necessary to improve our techniques for measuring the relative amplitudes of reflections and for deducing therefrom the relative change of the reflection coefficient as a function of the angle of incidence.

---

* Patent applied for.

Thirdly, in a more remote future it may become possible to draw conclusions concerning the lithological nature of rock strata from the shapes of the reflection coefficient curves of the interfaces by which they are bounded.

Acknowledgment

The author is indebted to the N.V. De Bataafsche Petroleum Maatschappij, The Hague, for permission to publish the results presented in this paper.

References

Birch F., Schairer J. F. and Spicer H. C., 1942, Handbook of Physical Constants, Geol. Soc. of America, Special Paper No. 36.

Blut, H., 1932a, Ein Beitrag zur Theorie der Reflexion und Brechung elastischer Wellen an Unstetigkeitsflächen, Zeitschr. f. Geophysik, VIII, 130-144.

——, H., 1932b, Ein Beitrag zur Theorie der Reflexion und Brechung elastischer Wellen an Unstetigkeitsflächen, Zeitschr. f. Geophysik, VIII, 305-322.

Dana, S. W., 1944, The Partition of Energy among Seismic Waves Reflected and Refracted at the Earth's Core, Bull. Seism. of America, 34, 189-197.

Knott, C. G., 1899, Reflexion and Refraction of Elastic Waves with Seismological Applications, Philos. Mag., XLVIII, 64-97.

Muskat, M. and Meres, M. W., 1940a, Reflection and Transmission Coefficients for Plane Waves in Elastic Media, Geophysics, V, 115-148.

——, —— 1940b, The Seismic Wave Energy Reflected from Various Types of Stratified Horizons, Geophysics, V, 149-155.

Schlichter, L. B. and Gabriel, V. G., 1933, Studies in Reflected Seismic Waves, Gerl. Beiträge z. Geophysik, 38, 228-238.

Discussion

Mr. Korschunow: Is it possible that the effects of the Poisson's ratio play a roll in the generation of surface waves in the loose layers? It appears that the problem perhaps is not only related to reflections at deeper discontinuities of rock-strata, but can be extended to near surface phenomena.

Mr. Koefoed: I agree.

SOME NOTES CONCERNING THE WENNER CONFIGURATION *

BY

E. W. CARPENTER **

Abstract

This paper deals with the four electrode method of electrical resistivity prospecting using direct current. It is shown that three resistances can be measured for any four electrode configuration, and a simple relation between them is derived. The particular case of the Wenner electrode configuration is discussed and a further relation derived between the three apparent resistivities corresponding to the three resistances. The practical value of the resistance relation as a means of avoiding experimental errors is indicated.

In general the three apparent resistivities are different in magnitude although there are certain particular cases where they are equal to one another. Their actual values are determined for a number of simple problems and the possibility of having a negative apparent resistivity is illustrated.

Finally, examples of field tests are given in which the three resistances were measured, and it is concluded that the method can often provide a simple way of distinguishing between the effects of lateral and vertical resistivity variations.

Introduction

The electrical resistivity method of geophysical prospecting essentially involves passing a current I through the earth by means of two current electrodes, C_1 and C_2, and measuring the resulting potential difference ΔV between two potential electrodes, P_1 and P_2. Mathematically the current electrodes may be treated as point sources of equal and opposite strength, and for the purpose of this paper C_1 will be considered to be the electrode of strength $+ I$ at which the current enters the earth. Since ΔV is defined as the potential difference between P_1 and P_2,

$$\text{i.e. } \Delta V = V(P_1) - V(P_2), \quad \ldots \ldots \quad (1)$$

it will be necessary, in the general case, to specify its sign as well as its magnitude.

Let x_{11}, x_{12}, x_{21}, and x_{22} be the distances between the electrodes C_1 and P_1, C_1 and P_2, C_2 and P_1, and C_2 and P_2. Then for the interpretation of experimental results a quantity ρ_a defined as the apparent resistivity is obtained by substituting the relevant values in the equation

$$\rho_a = 2\pi RG \quad \ldots \ldots \quad (2)$$

---

* Presented at the Eighth Meeting of the European Association of Exploration Geophysicists, held in Paris, May 18/20, 1955.

** Department of Mining, University of Leeds.

where R, the configuration resistance, equals $\Delta V/I$, and G, the configuration factor, is given by

$$G = [1/x_{11} + 1/x_{22} - 1/x_{12} - 1/x_{21}]^{-1} \quad . \quad . \quad . \quad . \quad (3)$$

The most commonly adopted electrode configuration has been that due to Wenner (1915) in which the four electrodes are placed at equal intervals s along a straight line on the surface of the earth, as shown in Fig. 1.

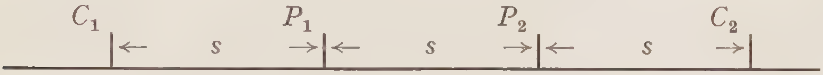

Fig. 1. The Wenner Electrode Configuration.

For this configuration the expression for the apparent resistivity becomes, from equations 2 and 3,

$$\rho_a = 2\pi s R \quad . \quad . \quad . \quad . \quad . \quad . \quad . \quad . \quad . \quad . \quad (4)$$

Two techniques for applying the Wenner electrode configuration can be distinguished, namely "traversing" and "probing". In the former system the electrode spacing s is held constant and the system as a whole is moved over the surface of the earth. The movement is usually made either along the line of the electrodes (longitudinal traversing) or perpendicular to it (transverse traversing). In the expanding electrode probe the line of the electrodes is fixed in direction and the spacing s varied, keeping the centre of the electrode line at the same point.

The purpose of the present paper is to indicate how additional information can be obtained from the Wenner configuration, and to give some results for certain simple cases. Although it is specifically the Wenner configuration which will be considered, the method is equally applicable to any other four electrode configuration.

The Three Characteristic Apparent Resistivities

Using the notation of the preceding section, there are twenty four ways in which C_1, C_2, P_1 and P_2 can be distributed amongst a four electrode configuration. For any particular arrangement interchanging the subscripts of either the potential or current electrodes separately will alter the sign but not the magnitude of both the resistance, R, and the configuration factor, G, (see equations 1 and 3). On the other hand, changing the subscripts of both the current and potential electrodes together does not affect either R or G. Therefore, since the apparent resistivity is given simply as a constant times the product of R and G (equation 2), its sign and magnitude are quite independent of the subscripts associated with the current and potential electrodes. Consequently, ignoring the subscripts for the time being, it is only necessary to consider the six ways in which two current and two potential electrodes can be distributed amongst a four electrode configuration. Now by a generalised form of Helmholtz's Reciprocal Relation (Searle 1910), interchange of current and potential electrodes has no effect on the measured resistance and therefore there can only be three basically different resistances for any four electrode configuration although, as described above, their signs will depend upon the way in which C_1, C_2, P_1 and P_2 are arranged. Also, from equation 3, an interchange of current and potential electrodes has no effect on the value of G, nor, therefore, on the corresponding apparent resistivity, and consequently there are only three apparent resistivities for any four electrode configuration.

Consider the Wenner configuration shown in Fig. 1, but let the electrodes be numbered 1 2 3 4 from left to right as shown in Fig. 2.

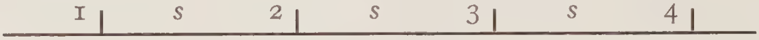

Fig. 2.

For the resistances and apparent resistivities the following nomenclature will be used:

(i) The α configuration, with either two current or two potential electrodes adjacent, i.e. *CPPC* or *PCCP* (reading from left to right in Fig. 2). For this configuration the resistance is termed $(\pm)R^{\alpha}$ and the corresponding apparent resistivity ρ_a^{α}.

(ii) The β configuration, with both current and both potential electrodes adjacent, i.e. *CCPP* or *PPCC*. For this configuration the resistance is termed $(\pm)R^{\beta}$ and the corresponding apparent resistivity ρ_a^{β}.

iii) The γ configuration, with neither potential nor current electrodes adjacent, i.e. *CPCP* or *PCPC*. For this configuration the resistance is termed $(\pm)R^{\gamma}$ and the corresponding apparent resistivity ρ_a^{γ}.

These definitions are summarised in Table I which also gives the relations between the resistances and apparent resistivities, obtained from equations 2 and 3 by substituting the relevant values of the inter-electrode spacings.

TABLE I.

	Electrode Arrangement				Resistance	Apparent Resistivity
	1	2	3	4		
i	*C*	*P*	*P*	*C*	$(\pm)R^{\alpha}$	$\rho_a^{\alpha} = 2\pi s R^{\alpha}$
ii	*P*	*C*	*C*	*P*		
iii	*C*	*C*	*P*	*P*	$(\pm)R^{\beta}$	$\rho_a^{\beta} = 6\pi s R^{\beta}$
iv	*P*	*P*	*C*	*C*		
v	*C*	*P*	*C*	*P*	$(\pm)R^{\gamma}$	$\rho_a^{\gamma} = 3\pi s R^{\gamma}$
vi	*P*	*C*	*P*	*C*		

Let φ_{jk} be the potential at an electrode j due to unit current entering the earth at an electrode k, and consider the following specific set of three electrode arrangements.

For the arrangement $C_1\ P_1\ P_2\ C_2$

$$R^{\alpha} = \varphi_{21} - \varphi_{24} - \varphi_{31} + \varphi_{34}, \quad . \quad . \quad . \quad . \quad . \quad . \quad . \quad . \quad (5)$$

for the arrangement $C_1\ C_2\ P_2\ P_1$

$$R^{\beta} = \varphi_{41} - \varphi_{42} - \varphi_{31} + \varphi_{32}, \quad . \quad . \quad . \quad . \quad . \quad . \quad . \quad . \quad (6)$$

and for the arrangement $C_1\ P_1\ C_2\ P_2$

$$R^{\gamma} = \varphi_{21} - \varphi_{23} - \varphi_{41} + \varphi_{43} \quad . \quad . \quad . \quad . \quad . \quad . \quad . \quad . \quad (7)$$

Since, as a corollary to the Reciprocal Relation, $\varphi_{jk} = \varphi_{kj}$, then from the above three equations

$$R^{\alpha} = R^{\beta} + R^{\gamma} \quad . \quad . \quad . \quad . \quad . \quad . \quad . \quad . \quad . \quad , \quad . \quad (8)$$

This relation has been derived specifically for the electrode arrangements $C_1\ P_1\ P_2\ C_2$, $C_1\ C_2\ P_2\ P_1$ and $C_1\ P_1\ C_2\ P_2$, but similar relations can readily be derived for any other set of three electrode arrangements and these can only differ from equation 8 by having the sign of one of the resistances changed. In practice it is quite convenient to measure the three resistances for these particular three arrangements, and for the sake of completeness it is proposed that, in the remainder of this paper, the three resistances will be defined by equations 5, 6 and 7.

Substituting the values for the apparent resistivities in equation 8,

$$3\,\rho_a^{\alpha} = \rho_a^{\beta} + 2\,\rho_a^{\gamma} \quad . \quad . \quad . \quad . \quad . \quad . \quad . \quad . \quad . \quad . \quad . \quad (9)$$

which is in fact a general relation for the Wenner configuration, quite independent of which specific electrode arrangements are employed. From equation 9 it will be seen that if ρ_a^{γ} differs from ρ_a^{α} by an amount y then ρ_a^{β} will differ from ρ_a^{α} by an amount $-2y$, with the important possibility of points at which the three apparent resistivities are equal. This is obviously true in the case of an homogeneous and isotropic earth bounded by a plane surface.

Although the three resistances are not independent and any two will enable the third to be determined by equation 8, by actually measuring all three separately a valuable check on instrumental and observational errors is available. It is therefore suggested that the technique of measuring three resistances for a four electrode configuration can be applied usefully in practice. The extra labour involved in measuring three resistances rather than the conventional single resistance is very small, since once the cables have been laid out all the terminal changes can be made at the instrument itself.

A number of theoretical problems will now be examined to investigate how the three apparent resistivities behave in certain ideal cases.

Constant Spacing Longitudinal Traverse Perpendicular To The Strike Of A Thin Vertical Insulating Sheet

Denoting the electrode spacing as s and the distance between the centre of the electrode system and the sheet as d, there are three cases to consider, viz.

i) $d > 3s/2$, (Fig. 3*a*), corresponding to all the electrodes on the same side of the sheet,

ii) $3s/2 > d > s/2$, (Fig. 3*b*), when three electrodes are on one side of the sheet and the fourth is on the opposite side,

and iii) $s/2 > d > 0$, (Fig. 3*c*), when two electrodes are located on each side of the sheet.

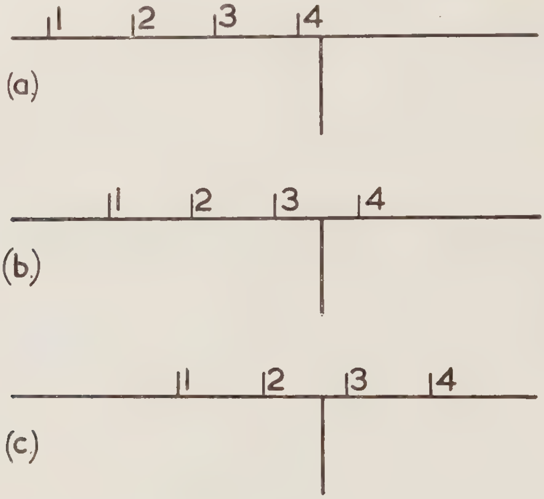

Fig. 3.

Applying image theory, the potential at any point on the surface due to a current source of strength I on the same side of the sheet is that due to the source of strength I and its image in the sheet, also of strength I. If the current source is on the opposite side of the sheet the potential is zero since no current can cross the sheet. Theoretically the sheet is considered to be semi-infinite in size, but in practice this will only be approximate, otherwise when the two current electrodes are on opposite sides of the sheet they would be electrically isolated and no current could flow.

In the following a current of strength I enters the earth at electrode 1, C_1 in each case, and the resistivity of the medium is ρ.

i) $d > 3s/2$.

For the electrode arrangement $C_1\ P_1\ P_2\ C_2$, the potential, V_2, of electrode

2 due to the current source I at 1, the current sink $-I$ at 4, and the images of both source and sink, is given by

$$V_2 = \rho I[1/s - 1/2s + 1/(2d + 2s) - 1/(2d - s)]/2\pi,$$

and similarly, for the potential at electrode 3,

$$V_3 = \rho I[-1/s + 1/2s + 1/(2d + s) - 1/(2d - 2s)]/2\pi,$$

so that

$$V_2 - V_3 = \rho I[1/s + 1/(2d + 2s) - 1/(2d + s) - 1/(2d - s) + 1/(2d - 2s)]/2\pi.$$

Thus, putting $t = d/s$,

$$\rho_a^\alpha = \rho\ [1 + 1/(2t + 2) + 1/(2t - 2) - 1/(2t + 1) - 1/(2t - 1)].$$

Similarly, for the electrode arrangement $C_1\ C_2\ P_2\ P_1$

$$\rho_a^\beta = \rho\ [1 + 3\{1/t - 1/(2t - 1) - 1/(2t + 1)\}],$$

and for the electrode arrangement $C_1\ P_1\ C_2\ P_2$

$$\rho_a^\gamma = \rho\ [1 + 3\{1/(2t + 2) + 1/(2t - 2) - 1/t\}/2].$$

ii) $3s/2 > d > s/2$

By a similar analysis it can be shown that, for the electrode arrangement $C_1\ P_1\ P_2\ C_2$

$$\rho_a^\alpha = \rho\ [1/2 + 1/(2t + 2) - 1/(2t + 1)],$$

for the electrode arrangement $C_1\ C_2\ P_2\ P_1$

$$\rho_a^\beta = \rho[3/2 + 3/2t - 3/(2t + 1)],$$

and for the electrode arrangement $C_1\ P_1\ C_2\ P_2$

$$\rho_a^\gamma = -3\ \rho\ [1/2t - 1/(2t + 2)]/2.$$

In the latter case it will be seen that the apparent resistivity ρ_a^γ is negative. This is because the potential of P_1 is less than the potential of P_2 so that the resistance for the electrode arrangement is negative whilst the configuration factor is still positive.

iii) $s/2 > d > 0$.

Again for the electrode arrangement $C_1\ P_1\ P_2\ C_2$

$$\rho_a^\alpha = \rho\ [2 + 1/(2t + 2) + 1/(2 - 2t)].$$

For the electrode arrangement $C_1\ C_2\ P_2\ P_1$ the current and potential electrodes are on opposite sides of the sheet and therefore $V_3 = V_4 = 0$ and $\rho_a^\beta = 0$. For the electrode arrangement $C_1\ P_1\ C_2\ P_2$

$$\begin{aligned}\rho_a^\gamma &= \rho\ [3 + 3\{1/(2t + 2) + 1/(2 - 2t)\}/2] \\ &= 3\ \rho_a^\alpha/2.\end{aligned}$$

Fig. 4*a* is a graph of ρ_a/ρ against *t* for the three different apparent resistivities, the outstanding feature being the abrupt changes of apparent resistivity which occur as each electrode crosses the sheet. Fig. 4*b* shows the results of a small scale model experiment designed to verify the above theoretical analysis. An ebonite sheet, 39 × 32 × 0.3 cms, was suspended in a brine filled tank with its long edge horizontal and just above the surface of the brine, and a system of four electrodes spaced at equal intervals of 4.0 cms traversed longitudinally over the centre of the sheet, the direction of the traverse being perpendicular to the plane of the sheet. A Geophysical Megger Earth Tester was used to measure the resistances, these being taken at intervals of 0.2 cms. When one electrode was on the opposite side of the sheet to the other three it was found necessary to interchange the potential leads in order to obtain a reading for the γ electrode arrangement, and the resistance R^γ was duly recorded as being negative. The experimental and theoretical results agree quite well, the differences between them being attributable to the finite area of the sheet, which enables electrical contact to be made between the two halves of the conducting medium, and also to its finite thickness.

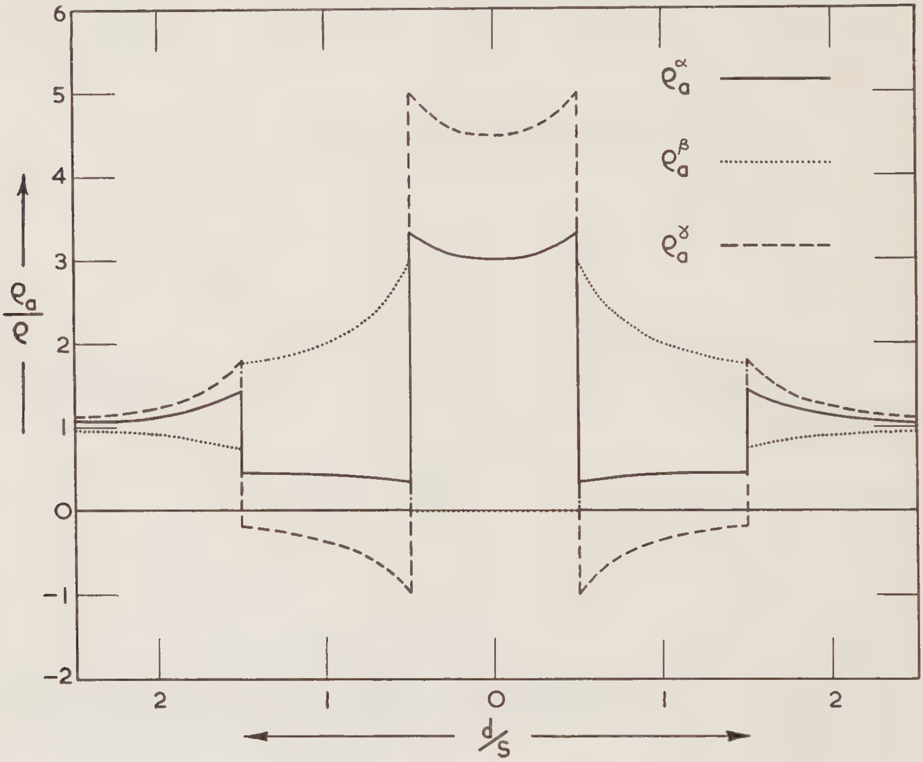

Fig. 4*a*. Longitudinal traverse over a thin vertical insulating sheet, theoretical curves.

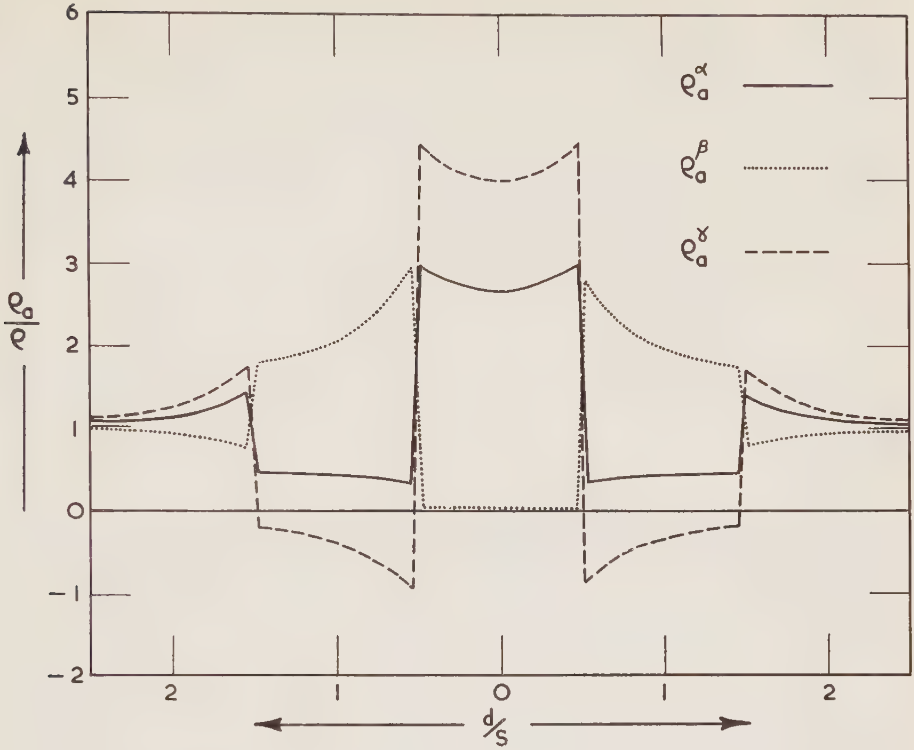

Fig. 4*b*. Longitudinal traverse over a thin vertical insulating sheet, experimental curves.

Constant Spacing Longitudinal Traverse Perpendicular To The Strike Of A Simple Vertical Fault

The case of a simple vertical fault separating media of resistivities ρ_1 and ρ_2 is well known for the normal Wenner electrode arrangement $C_1\ P_1\ P_2\ C_2$, and can again be treated readily by the method of images. Let d be the distance between the centre of the electrode system and the fault plane, and consider the problem where the centre of the electrode system is in the medium or resistivity ρ_1. As in the previous section there are three cases to consider. These three cases lead to the following equations in which, as before, $t = d/s$, and also $k = (\rho_2 - \rho_1) / (\rho_2 + \rho_1)$.

i) All the electrodes in the medium of resistivity ρ_1, $d > 3s/2$.

$$\rho_a^\alpha = \rho_1 \left[1 + 3kt/(t^2 - 1)(4t^2 - 1) \right],$$

$$\rho_a^\beta = \rho_1 \left[1 - 3k/t\,(4t^2 - 1) \right],$$

and

$$\rho_a^\gamma = \rho_1 \left[1 + 3k/2t\,(t^2 - 1) \right].$$

ii) Three electrodes in the medium of resistivity ρ_1, $3s/2 > d > s/2$.

$$\rho_a^\alpha = \rho_1[1 + k\{1/(2t+2) - 1/(2t+1) + 1/2\}],$$
$$\rho_a^\beta = \rho_1[1 + 3k\{1/2t - 1/(2t+1) - 1/6\}],$$
and
$$\rho_a^\gamma = \rho_1[1 + 3k\{1/(2t+2) - 1/2t + 2/3\}/2].$$

In this instance, for all values of k, there is a point at $t = 1/\sqrt{2}$ where $\rho_a^\alpha = \rho_a^\beta = \rho_a^\gamma$.

iii) Two electrodes in each medium, $s/2 > d > 0$.

$$\rho_a^\alpha = \rho_1[1 + k^2 + k(k+t)/(t^2 - 1)]/(1-k),$$
$$\rho_a^\beta = \rho_1[1 + k],$$
and
$$\rho_a^\gamma = \rho_1[1 + 2k^2 + 3k(k+t)/2(t^2 - 1)]/(1-k).$$

In this case there is a further point at which the three resistivities are equal if k is positive. The value of t at which it occurs is given as the admissable root of the equation

$$t^2 + t/2k - 1/2 = 0$$

The equivalent expressions for the apparent resistivities when the centre of the electrode system is in the medium of resistivity ρ_2 can readily be obtained from the above expressions simply by substituting ρ_2 for ρ_1 and $-k$ for k. Fig. 5 shows the values of the apparent resistivities plotted as a function of t for the fault problem defined by $k = (\pm)\ 0.3$.

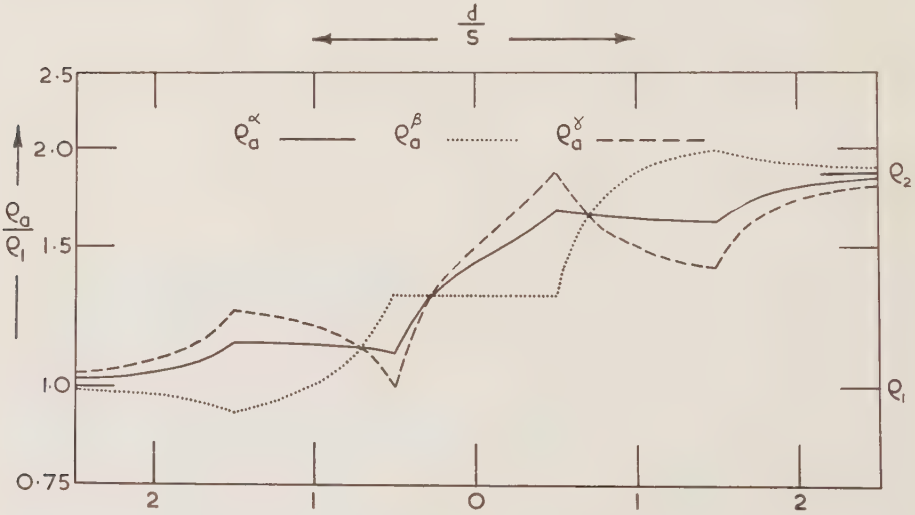

Fig. 5. Longitudinal traverse over a vertical fault, k = 0.3.

The Two Layer Case

The simplest type of depth variation of resistivity is the two layer case, where a homogeneous and isotropic overburden, of thickness h and resistivity

ρ_1, overlies a semi-infinite, homogeneous and isotropic medium of resistivity ρ_2, the interfaces being plane, parallel and infinite. If an expanding electrode probe is carried out on the surface the apparent resistivities will be a function of the uncontrollable constants ρ_1, ρ_2 and h, and the controllable variable s. In terms of image theory, the potential $\varphi(r)$ of a point on the surface at a distance r from a surface current source of strength I is given (e.g. Hummel 1932) by the equation

$$\varphi(r) = \rho_1 I\,[1/r + 2\sum_1^\infty k^n \{ r^2 + (2nh)^2 \}^{-\frac{1}{2}}]/2\pi,$$

where $k = (\rho_2 - \rho_1)/(\rho_2 + \rho_1)$.

Using Roman's W function (Roman, 1931) where

$$W(k, r/2h) = \sum_1^\infty k^n [\{n^2 + (r/2h)^2\}^{-\frac{1}{2}} - 1/n],$$

the expressions for the three apparent resistivities can be written as

$$\rho_a^\alpha = \rho_1[1 + 2s\,\{W(k, s/2h) - W(k, s/h)\}/h],$$
$$\rho_a^\beta = \rho_1[1 + 3s\,\{W(k, 3s/2h) + W(k, s/2h) - W(k, s/h)\}/h],$$
and
$$\rho_a^\gamma = \rho_1[1 + 3s\,\{W(k, s/2h) - W(k, 3s/2h)\}/2h].$$

The values of ρ_a^α / ρ_1, ρ_a^β / ρ_1 and ρ_a^γ / ρ_1 have been calculated for a number of different two layer problems, using Roman's Tables (1931) for ρ_a^α and ρ^γ and then using equation 9 to obtain ρ_a^β from them. Figs. 6 and 7 are curves of the three apparent resistivities plotted as a function of s/h for values of k equal to -0.5 and $+1.0$. The most interesting curve is that for ρ_a^β which shows that for values of s/h less than unity ρ_a^β can be greater than ρ_1 when k is negative, and less than ρ_1 when k is positive, thereby giving the curves an appearance more usually associated with three layer curves. This rather anomolous effect is quite small however, being greatest for $k = +1.0$ when the minimum value of ρ_a^β is $0.95\ \rho_1$

The Three Layer Case

Any problem where the resistivity of the earth is a function of depth only is characterized by the fact that $\varphi(r)$ (see the previous section) is independent of the position of the source on the earth's surface. Hence the apparent resistivities, $\rho_a(s)$, for a Wenner electrode configuration defined by the inter-electrode spacing s, can be written as

$$\rho_a^\alpha(s) = 2\pi s\,[2\varphi(s) - 2\varphi(2s)],$$
$$\rho_a^\beta(s) = 6\pi s\,[\varphi(s) + \varphi(3s) - 2\varphi(2s)],$$
and
$$\rho_a^\gamma(s) = 3\pi s\,[\varphi(s) - \varphi(3s)].$$

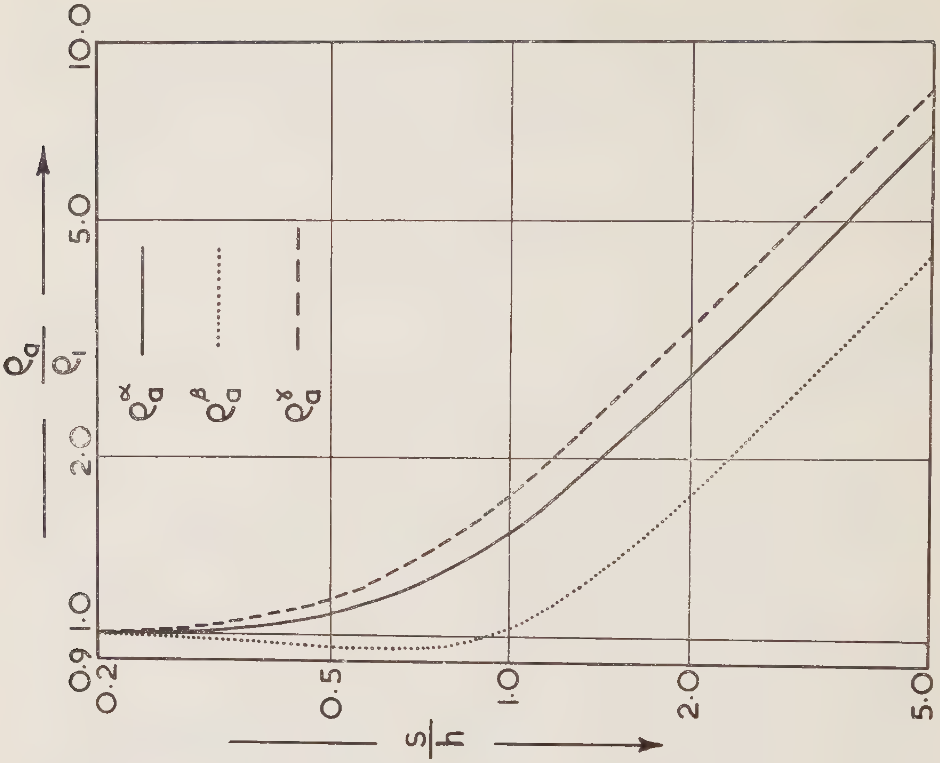

Fig. 7. Two layer curves, k = 1.0.

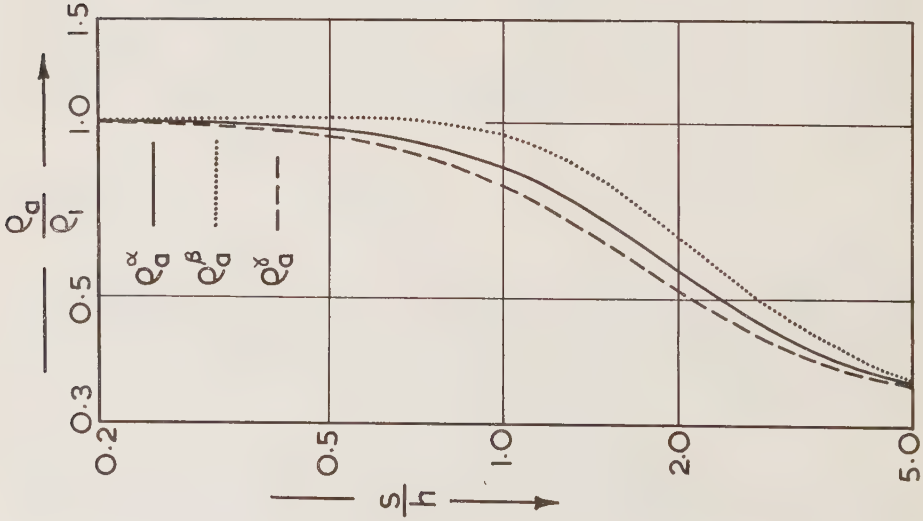

Fig. 6. Two layer curves, k = — 0.5.

Following West (1940), let

$$\rho_a^\alpha(s) = \xi_1,\ \rho_a^\alpha(ns) = \xi_n \text{ and } 4\pi s\varphi(ns) = \theta_n$$

Then $\xi_n = n\,[\theta_n - \theta_{2n}]$

giving

$$\theta_n = \xi_n/n + \xi_{2n}/2n + \xi_{4n}/4n + \xi_{8n}/8n + \xi_{16n}/16n + \text{etc.}$$

Since

$$\rho_a^\beta(s) \quad = 3\,[\theta_1 - 2\,\theta_2 + \theta_3]\,/2,$$

$$2\ \rho_a^\beta(s)/3 = \xi_1 - \sum_{n=1}^{\infty} \xi_{2^n}/2^n + \sum_{n=1}^{\infty} \xi_{3\,.\,2^{n-1}}/3\,.\,2^{n-1},$$

and

$$4\ \rho_a^\gamma(s)/3 = \xi_1 + \sum_{n=1}^{\infty} \xi_{2^n}/2^n - \sum_{n=1}^{\infty} \xi_{3\,.\,2^{n-1}}/3\,.\,2^{n-1}.$$

From the above equations it will be seen that ρ_a^β and ρ_a^γ can both be obtained from values of ρ_a^α. Unfortunately published data of ρ_a^α as a function of s are restricted to the two and three layer problems, and even then much of it is in a form which is unsuitable for computation, although a notable exception is that published by Wetzel and McMurray (1937) for a large number of three layer problems. Using the published data of Wetzel and McMurray (1937) and West (1940), an number of three layer curves have been computed and two of these are shown in Figs. 8 and 9. Both of these sets of curves show a point where the three apparent resistivities are equal, but there appears to be no simple relation between the electrode spacings at which they occur and the depths of the interfaces. The results show that the γ configuration is the most sensitive to depth changes of resistivity, i.e. the effects of the various layers are first noticeable on the ρ_a^γ curve, although it is the ρ_a^β curve which shows the maximum effect of the middle layer.

Application To Field Tests

From the preceding examples it will be seen that, in general, the three apparent resistivities differ from one another by measurable amounts, although there are particular instances when they are equal. From these and other examples, both theoretical and experimental, it would appear that when the electrode lines cross a lateral resistivity discontinuity the apparent resistivities ρ_a^α and ρ_a^γ often increase as ρ_a^β decreases, and vice versa. On the other hand, with a few minor exceptions, it appears that when the resistivity of the earth is a function of depth only the three apparent resistivity curves show the same general trend.

The results of two field tests are shown in Fig. 10, both sets of curves having been obtained in the same area. The effects of lateral resistivity variations are clearly shown, particularly in the case of Fig. 10*a*. Had only the

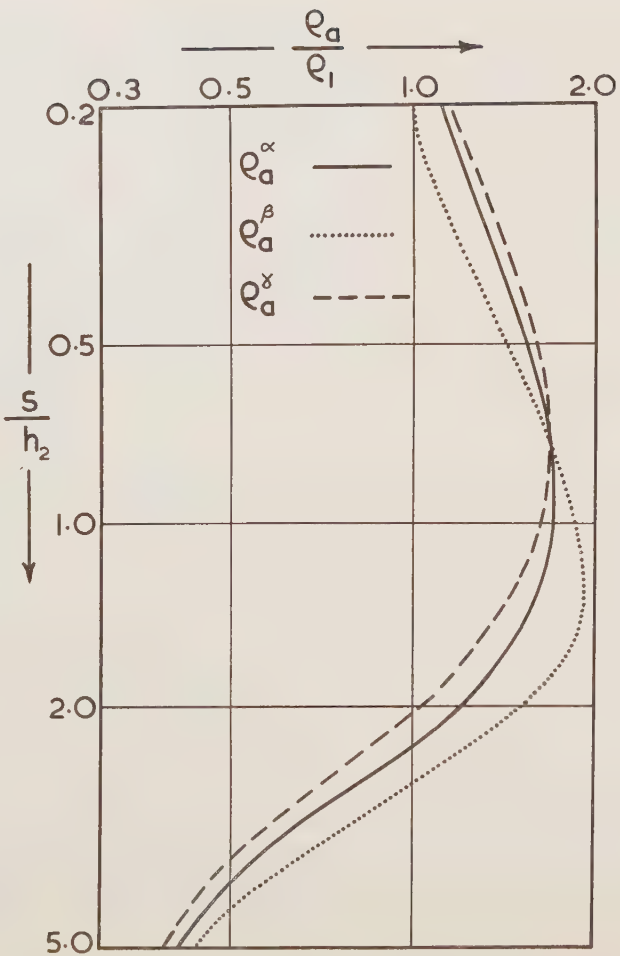

Fig. 8. Three layer curves, $\rho_1 : \rho_2 : \rho_3 = 1 : 3 : {}^1/_3$. $h_1 : h_2 = 1 : 4$

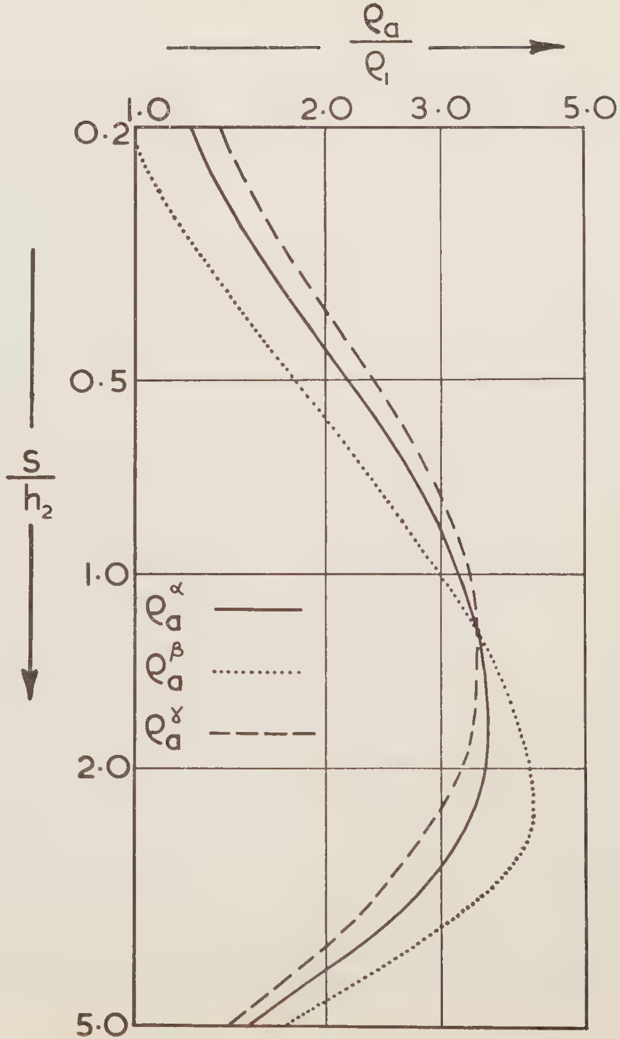

Fig. 9. Three layer curves, $\rho_1 : \rho_2 : \rho_3 = 1 : 10 : 1$. $h_1 : h_2 = 1 : 4$.

conventional ρ_a^α curve been obtained the effects of the lateral resistivity variations would have been much less obvious, and may have led to an erroneous interpretation.

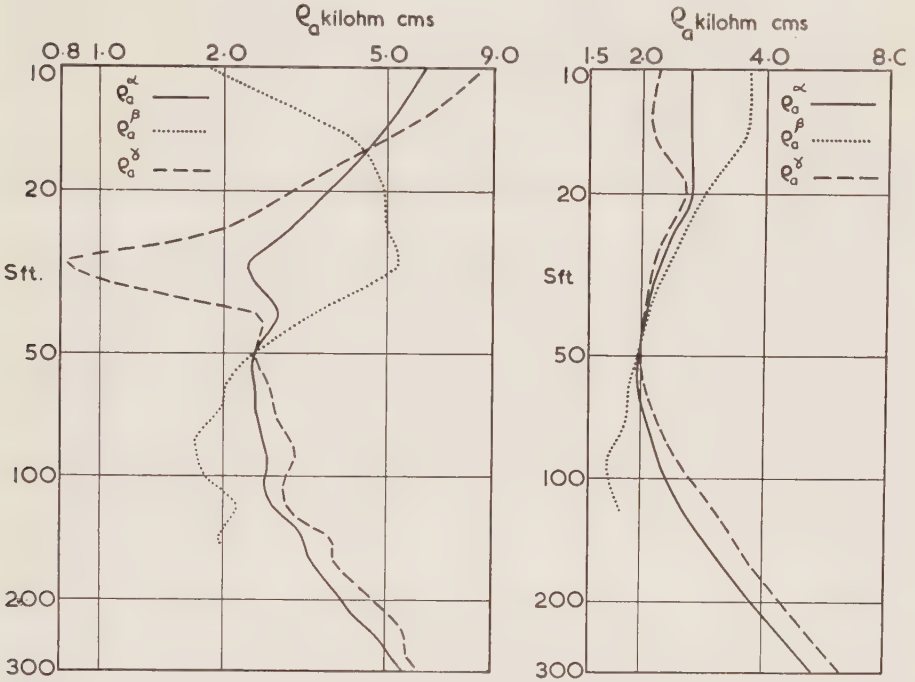

Fig. 10. Two Wenner Configuration probes.

Differentiating between the effects of lateral and vertical changes of resistivity is undoubtedly one of the major difficulties encountered in resistivity prospecting, and it is hoped that the above technique of measuring three resistances may help to resolve this difficulty, in addition to providing checks on observational and instrumental errors.

ACKNOWLEDGEMENTS

The author wishes to express his sincere thanks to Professor J. T. Whetton, Professor J. M. Bruckshaw and Dr. G. M. Habberjam for the keen interest they have taken in the work and for their valuable advice in the preparation of this paper.

Acknowledgment is made to the Department of Scientific and Industrial Research for a maintenance allowance, and also to the Scientific Department, National Coal Board, for a grant in aid of this research.

REFERENCES

HUMMEL J. N., 1932, A Theoretical Study Of Apparent Resistivity In Surface Potential Methods, A.I.M.E. Tech. Pub. 418, 1-32.

ROMAN I., 1931, How To Compute Tables For Determining Electrical Resistivity Of Underlying Beds, And Their Application To Geophysical Problems, U.S. Dept. of Commerce, Bureau of Mines Tech. Pub. 502, 1-44.

SEARLE G. F. C., 1910, On Resistances With Current And Potential Terminals, The Electrician, 66, 999-1002.

WENNER F., 1915, A Method Of Measuring Earth Resistivity, Bull. Bureau of Standards, 12, 469-478.

WEST S. S., 1940, Three Layer Resistivity Curves For The Eltran Configuration, Geophysics, 5, 1, 43-46.

WETZEL W. W. and MCMURRAY H. V., 1937, A Set of Curves To Assist In The Interpretation Of The Three-layer Resistivity Problem, Geophysics, 2, 4, 329-341.

GRAVITY VARIATIONS IN SURVEYS ACROSS GEOLOGICAL BOUNDARIES *

BY

G. C. COLLEY **

Abstract

The paper discusses the variations of Elevation Correction Factors (E.C.F.) across various stratigraphical and structural occurrences with particular reference to the dipping bed, fault and horst. Graphs are prepared giving E.C.F. variations for various angles of dip and a method is suggested for application in the field. Errors in the linear variation that is commonly used for small angles of dip are discussed.

The second part of the paper consists of the application to interpretation of (1) Change of gravity dip and (2) The gravity inversion. It is shown how from a gravity map the dip, position of outcrop and thickness of a dipping bed can be determined. The last part shows how anticlines can give rise to negative anomalies and that in the direction of dip similar structures can at one point have no surface expression and afterwards invert to positive anomalies. The danger of attempting to predict the size of structures in such areas is emphasised.

The study of geology has indicated that the rocks at the earth's surface are not of a homogeneous nature but consist of units varying in lithology, usually tilted or folded. This lateral variation in lithology naturally causes lateral variations in the density of the rocks, which again will lead to variations in the earth's gravitational field. It is of importance, therefore, that we know the effect of various structural and stratigraphical changes upon the earth's gravitational field so that any corrections to the observed values may be correctly applied and to aid in our interpretation of maps which may be produced from gravity surveys. In this paper, it is proposed to deal with two aspects of the effect of varying lithology on gravity surveys. Firstly the correction for elevation, and secondly the applications to interpretation of gravity maps. We will take each in turn.

A. Variations in the Elevation Correction Factor (E.C.F.)

The combined correction to be applied for elevation to reduce the reading at a given gravity station to datum for homogeneous beds is:—

$$F_a h - 2K\pi\sigma h$$
$$\text{or } h\{F_a - 2K\pi\sigma\} \qquad (1)$$

---

* Presented at the Seventh Meeting of the European Association of Exploration Geophysicists, held at The Hague, 8-10 December 1954.

** Iraq Petroleum Company Ltd., London.

where F_a is the Free Air Correction, h the elevation, K the gravitational constant and σ the rock density.

The factor $(F_a—2K\pi\sigma)$ is known as the Elevation Correction Factor, usually abbreviated to E.C.F. It will be seen that the E.C.F. depends on the density of the material between the station and sea level. Strictly speaking, the E.C.F. depends on the composite density of the rocks down to sea level. As long as density changes in a vertical sense only, the configuration of a gravity map will not be changed, but a constant amount will be added or subtracted. Lateral changes of density will, however, lead to vertical columns of material of different composite densities as we move laterally over the surface. These will lead to varying E.C.F.'s.

Various practical methods have been suggested to determine the E.C.F. without the necessity of determining the density, for example L. L. Nettleton (1939), A. J. F. Siegert (1942), et alia.

Gravity surveys in the past have often been what is described as 'local surveys': that is, they are unconnected to any national grid of surveys. In such surveys, the practice has been frequent of raising the datum as high as possible thus eliminating any lateral density changes below it. Nowadays the tendency is to connect up these surveys to the national, continental or even world network (J. W. de Bruyn, Woollard) which have as their datum, sea level. The supervisor of the local survey always has better knowledge of the local conditions than the national compiler and it is best, therefore, that even in local surveys the reduction for elevation is taken to sea level. The purpose of the first part of this paper is to reduce the work involved in such reductions.

Various cases occur in geology which can give rise to varying lithology. In some cases, the change is abrupt e.g. a fault; in others predictable e.g. a dipping bed; and in others gradual but unpredictable e.g. facies changes. Where the changes are predictable, it is usually better, knowing the E.C.F. from the practical method, to vary the E.C.F. on a theoretical basis. This avoids the necessity for carrying out a series of E.C.F. profiles to determine the E.C.F. by the practical method. Indeed, since the latter is dependent on there being present fairly abrupt changes of elevation, it is not always possible to run a series of E.C.F. profiles.

The various cases of lateral E.C.F. change that occur, can be divided, broadly speaking, into two main headings; variations due to structural conditions and variations arising from stratigraphical causes. We shall take each case in turn.

1. *E.C.F. Variations due to Structural Causes*

The Fault

The decrease or increase of the vertical component of gravity due to a fault has been determined by many writers. Here we require to find the total correction necessary, at various points on the surface, to reduce the gravity readings to the equivalent readings at sea level.

For the purposes of this discussion, we shall assume the fault to be vertical and that material of density σ_1 is thrown against rock of density σ_2, where σ_1 is the greater, and that E_1 and E_2 are the corresponding E.C.F's. In Fig. 1, *O* is the fault outcrop and *P* the point at which the E.C.F. is required to be known, at distance *p* from *O*.

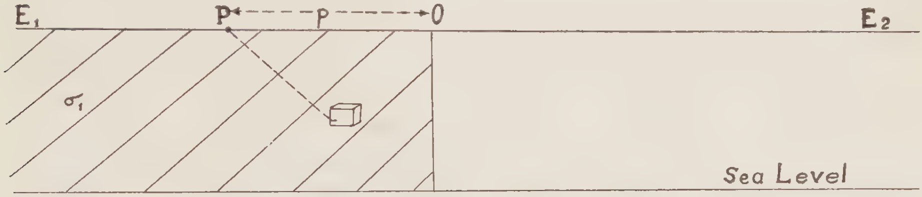

Fig. 1.

First we must determine the gravity fall due to the fault for the material above sea level. This is the gravity effect of the material of density $(\sigma_1 - \sigma_2)$ lying to the left of the outcrop, as it is the difference in densities only that produces the variation in gravity.

This gravity fall is (see Heiland's Exploration Geophysics P. 150):—

$$G_1 = 2K\,.\,(\sigma_1 - \sigma_2)\left[\frac{\pi}{2}\,.\,h + h\,.\,\tan^{-1}\frac{p}{h} + \frac{p}{2}\log.\frac{(h^2+p^2)}{p^2}\right]$$

The total gravity effect of the material between ground level and sea level, requires that to G_1 we must add the effect of an infinite slab of material of density σ_2. This has been shown by other writers to be $2K\,.\,\pi\,.\,\sigma_2\,.\,h$. Also the Free Air Effect must be allowed for.

The total correction G_3 to be applied at *P* is therefore:—

$$G_3 = F_a\,.\,h - 2\,K\,.\,\pi\,.\,\sigma_2\,.\,h\,. - 2K\,(\sigma_1 - \sigma_2)\left[\frac{\pi}{2}\,.\,h + h\,.\,\tan.^{-1}\frac{p}{h} + \frac{p}{2}\log.\frac{(h^2+p^2)}{p^2}\right]$$

But by definition of the E.C.F. the total correction at *P* is E.h. where *E* is the E.C.F. at *P*.

$$\text{Then}\quad E = F_a - 2K\,.\,\pi\,.\,\sigma_2\,. - 2K\,(\sigma_1 - \sigma_2)\left[\frac{\pi}{2} + \tan^{-1}\frac{p}{h} + \frac{p}{2h}\log.\frac{1+\left(\frac{p}{h}\right)^2}{\left(\frac{p}{h}\right)^2}\right]$$

But $(E_2 - E_1) = 2K\,.\,\pi\,.\,(\sigma_1 - \sigma_2)$ from (1)

$$\text{So}\quad E = E_2 - (E_2 - E_1)\left[\frac{1}{2} + \frac{1}{\pi}\tan^{-1}\frac{p}{h} + \frac{1}{2\pi}\,.\,\frac{p}{h}\log.\frac{1+\left(\frac{p}{h}\right)^2}{\left(\frac{p}{h}\right)^2}\right] \qquad (2)$$

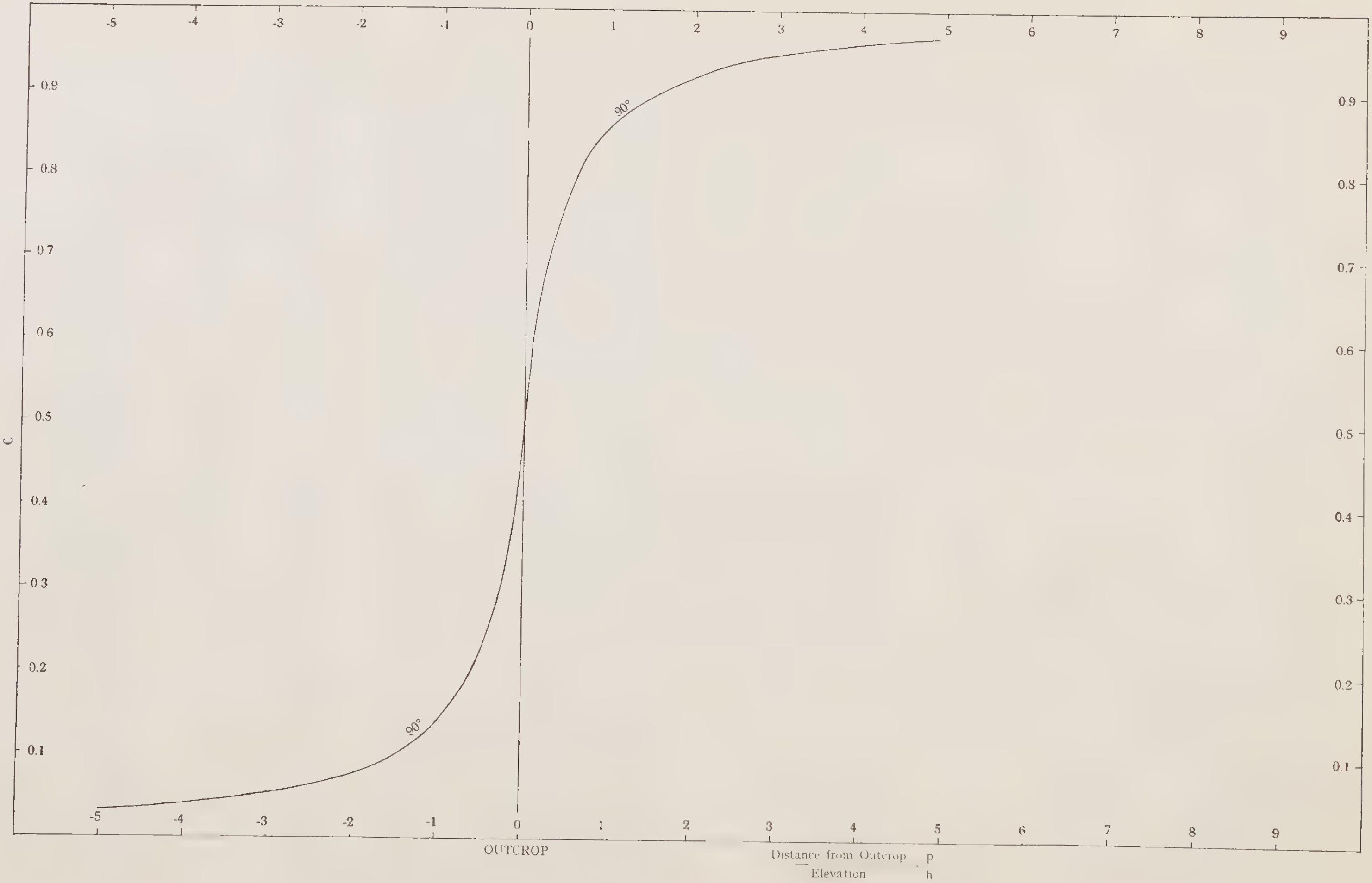

Fig. 2. Change of E.C.F. across a fault. $E = E_1 + (E_2 - E_1)\,C$.

$$\text{or}\qquad E = E_2 + (E_2 - E_1)\left[\frac{1}{2} - \frac{1}{\pi}\tan^{-1}\frac{p}{h} - \frac{1}{2\pi}\cdot\frac{p}{h}\log\cdot\frac{1+\left(\frac{p}{h}\right)^2}{\left(\frac{p}{h}\right)^2}\right] \qquad (3)$$

For the case where P lies to the right of O, that is, the integration for x is carried out between the limits $-\infty$ and $-p$, it can likewise be shown that:—

$$E = E_1 + (E_2 - E_1)\left[\frac{1}{2} + \frac{1}{\pi}\tan^{-1}\frac{[p]}{h} + \frac{1}{2\pi}\cdot\frac{[p]}{h}\log\cdot\frac{1+\left(\frac{[p]}{h}\right)^2}{\left(\frac{[p]}{h}\right)}\right] \qquad (4)$$

where $[p]$ is the numerical value of p, the negative sign having been allowed for.

At the limit $p = -\infty, E = E_1$
At $p = 0, E = E_1 + (E_2 - E_1)/2$
and at $p = +\infty, E = E_2$

We see, then, that the theoretical values E_1 and E_2 are only attained at $-\infty$ and $+\infty$ but in practice, at short distances from O these values are so nearly attained that differences from E_1 and E_2 cannot be measured by any modern gravity meters. In the field p and h are known so that the factor p/h is known, and as we see from (3) and (4) E is dependent only on E_1, E_2 and p/h. The limiting values E_1 and E_2 are normally determined in the field by Nettleton's or Siegert's method. Thus we can from formulae (3) and (4) determine the effective E.C.F. at any point in the vicinity of the fault, and so make the correct gravity reductions to sea level.

In Fig. 2, E is plotted against the factor p/h and $(E_2 - E_1)$ is assumed to be unity. For E.C.F. differences found in practice, the curve must be multiplied by that difference. For example, suppose that for a given value of p/h the E.C.F. difference is $(E_2 - E_1)\ C$ (say). Then if the field determined E.C.F. difference is t (say), the correct E.C.F. at P is:— $E = E_1 + tC$.

The Horst or Graben

In many cases, the Horst can be considered merely as an upthrown and downthrown fault. This occurs when the two bounding faults are sufficiently far apart that the centre block attains, within measurable limits, its own individual E.C.F. However, if the two faults are near enough together, the theoretical E.C.F. of the block (as computed from its density) is never reached. The rise (or fall) of E.C.F. due to the one fault, never reaches a maximum (or minimum) due to the influence of the other fault.

Let the width of the horst be $2a$ and the distance of a point P (at which we wish to determine the gravity effect) from the centre O of the horst be p. We are assuming here that the horst is a block of material of density σ_2 upthrown or downthrown into material (on both sides) of density σ_1 and E.C.F. E_1. Further, let σ_2 be greater than σ_1.

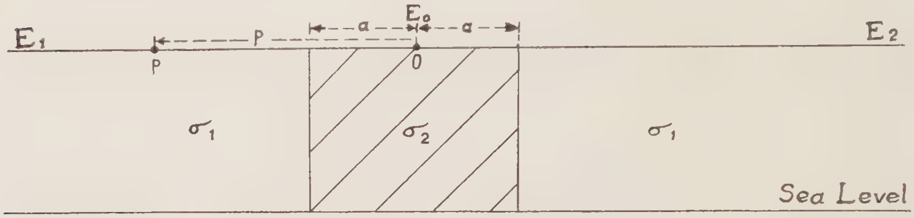

Fig. 3.

Proceeding as in the case of a fault we obtain a formula:—

$$E = E_1 - 2K(\sigma_2 - \sigma_1)\left[\tan^{-1}\frac{p+a}{h} - \tan^{-1}\frac{p-a}{h} + \frac{(p+a)}{2h}\log\left\{\frac{1+\left(\frac{p+a}{h}\right)^2}{\left(\frac{p+a}{h}\right)^2}\right\} - \frac{(p-a)}{2h}\log\left\{\frac{1+\left(\frac{p-a}{h}\right)^2}{\left(\frac{p-a}{h}\right)^2}\right\}\right]$$

The difficulty in this case is that we cannot determine in the field the E.C.F. corresponding to the density σ_2 as this E.C.F. value is never attained. The value of σ_2 will not normally be known. It is necessary, then, to determine the E.C.F. at some point between the two faults. Probably the best place is at the mid-point between the two faults where the graph of the E.C.F. is flat or where $p = 0$. If we suppose that this can be determined and is equal to E_o, then substituting in the above formula for $p = 0$

$$E_0 = E_1 - 2K(\sigma_2 - \sigma_1)\left[2\tan^{-1}\frac{a}{h} + \frac{a}{h}\log\left\{\frac{1+\left(\frac{a}{h}\right)^2}{\left(\frac{a}{h}\right)^2}\right\}\right]$$

or $(E_1 - E_0) = 2K(\sigma_2 - \sigma_1) \cdot f\left(\frac{a}{h}\right)$ (say)

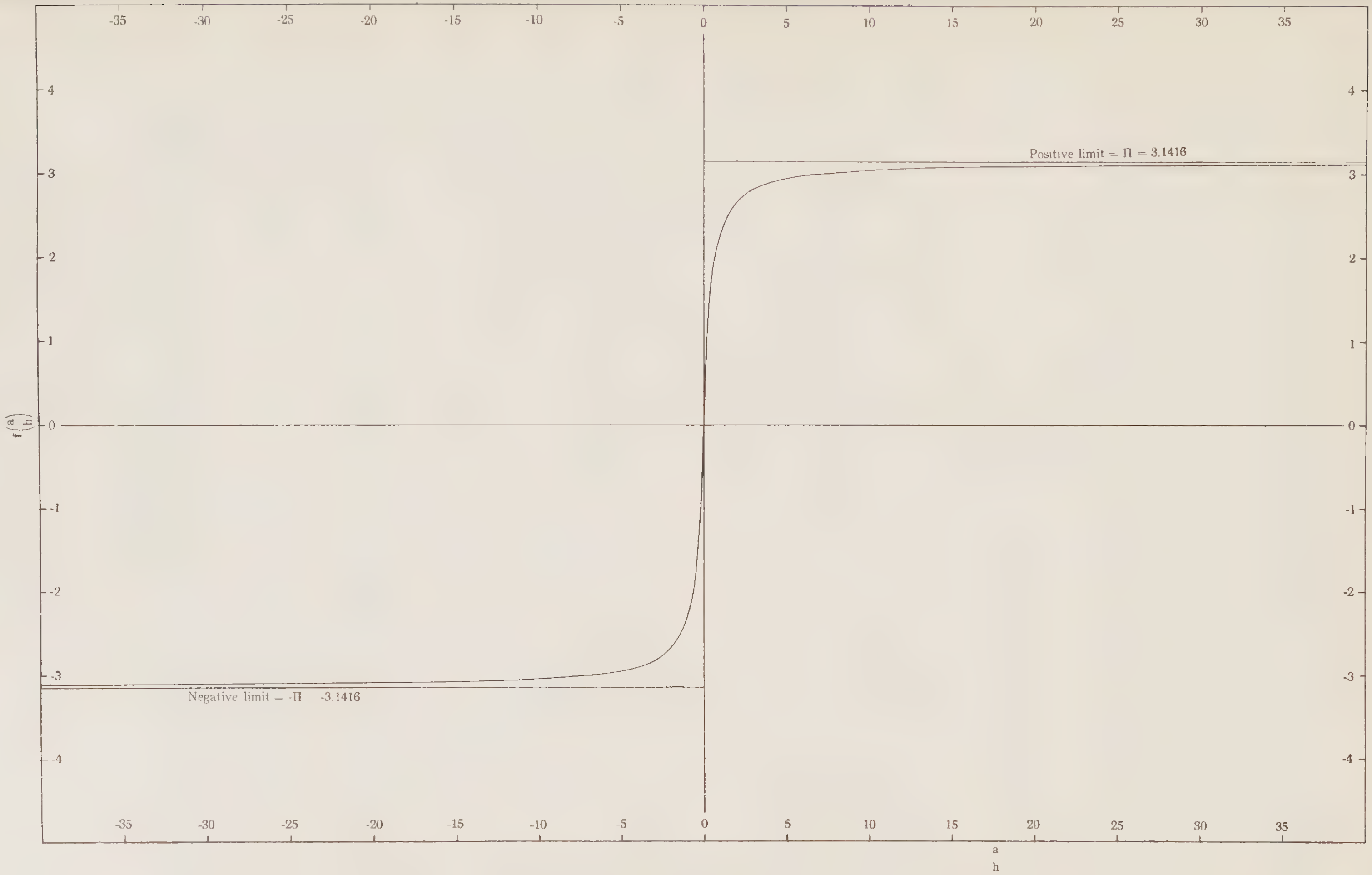

Fig. 4. Graph of $f\frac{a}{h} = 2\tan^{-1}\frac{a}{h} + \frac{a}{h}\log_e \frac{1+\left(\frac{a}{h}\right)^2}{\left(\frac{a}{h}\right)^2}$

$$\text{Then } E = E_1 - \frac{(E_1 - E_0)}{f\left(\frac{a}{h}\right)}\left[\tan^{-1}\left(\frac{p+a}{h}\right) - \tan^{-1}\left(\frac{p-a}{h}\right) + \left(\frac{p+a}{2h}\right)\log\left\{\frac{1+\left(\frac{p+a}{h}\right)^2}{\left(\frac{p+a}{h}\right)^2}\right\} - \frac{(p-a)}{2h}\log\left\{\frac{1+\left(\frac{p-a}{h}\right)^2}{\left(\frac{p-a}{h}\right)}\right\}\right] \quad . \quad . \quad (5)$$

$$\text{where } f\left(\frac{a}{h}\right) = 2\tan^{-1}\frac{a}{h} + \frac{a}{h}\log\left\{\frac{1+\left(\frac{a}{h}\right)^2}{\left(\frac{a}{h}\right)^2}\right\} \quad . \quad . \quad . \quad . \quad . \quad . \quad . \quad . \quad . \quad (6)$$

Here E is a function of E_1, E_0, p/h and a/h all of which will be known in the field.

For simplicity the value of

$$f(a/h) = 2\tan^{-1}(a/h) + (a/h)\log\left[\{1 + (a/h)^2\}/(a/h)^2\right]$$

has been graphed in Fig. 4. The term in the square brackets of formula 5 can be evaluated from Fig. 4, as it may be written

$$\tfrac{1}{2}\{f((p+a)/h) - f((p-a)/h)\}$$

Anticlines and Synclines

The E.C.F. over anticlines will be affected only when the density interface lies wholly or partly above the datum plane. The use of incorrect E.C.F's will have, in general, the effect of making anticlines too high and synclines too deep. This is frequently an advantage where the survey is conducted essentially for the determination of anticlines and synclines (for example those conducted by Oil Companies) for the structures are accentuated.

2. *E.C.F. Variations due to Stratigraphical Causes*

The Dipping Bed

The dipping bed is the most common of all sources of E.C.F. variations and occurs wherever dipping strata of different density overlie older rocks.

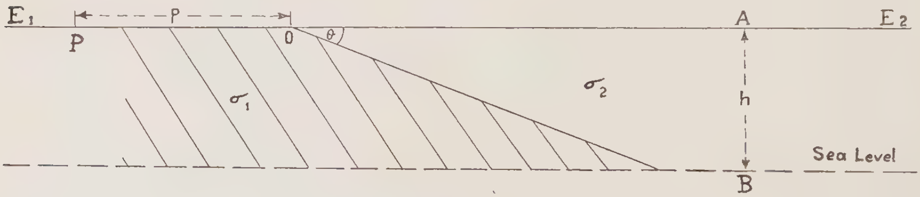

Fig. 5.

In Fig. 5, O is the outcrop of a bed dipping at an angle θ to the horizontal. Let the rock to the left have density σ_1 and corresponding E.C.F. E_1, and that to the right have density σ_2 and E.C.F. E_2. Suppose further that σ_1 is greater than σ_2, so that E_2 is greater than E_1.

The gravity effect of a slope is given by Heiland in Exploration Geophysics P. 153. Proceeding thereafter as for the fault we obtain the formula:—

$$E = E_1 + (E_2 - E_1)\left[\left\{\frac{1}{2} - \frac{1}{\pi}\tan^{-1}\left(\frac{p}{h} + \cot\theta\right)\right\}\left\{1 + \frac{p}{h}\frac{\sin.2\theta}{2}\right\} - \right.$$
$$\left. - \frac{p}{h}\frac{\sin^2.\theta}{2\pi}\log\left\{\frac{1 + \left(\frac{p}{h} + \cot\theta\right)^2}{\left(\frac{p}{h}\right)^2}\right\}\right] \quad . \quad . \quad . \quad . \quad (7)$$

For the case where the point P lies to the right of O, that is, when the upper limit in evaluating the integration for x becomes $(z.\ \cot\theta - p)$ the value of E likewise can be shown to be:—

$$E = E_1 + (E_2 - E_1)\left[1 - \left\{\frac{1}{2} - \frac{1}{\pi}\tan^{-1}\left(\cot\theta - \frac{[p]}{h}\right)\right\}\left\{1 - \frac{[p]}{h}\frac{\sin.2\theta}{2}\right\} + \right.$$
$$\left. + \frac{[p]}{h}\frac{\sin^2.\theta}{2\pi}\log\left\{\frac{1 + \left(\cot\theta - \frac{[p]}{h}\right)^2}{\left(\frac{[p]}{h}\right)^2}\right\}\right] \quad . \quad . \quad . \quad . \quad (8)$$

$[p]$, of course, being the numerical value of p, the negative sign having been allowed for.

At the outcrop, if we substitute the value $p = 0$ in (7) or (8) we obtain:—

$$E = E_1 + (E_2 - E_1)\ \theta/\pi\,. \quad . \quad . \quad . \quad . \quad . \quad . \quad . \quad (9)$$

At the other fixed point where the density interface between the two beds reaches datum level, i.e. where $p = h\cot\theta$, we obtain:—

$$E = E_1 + (E_2 - E_1)\left[1 - \frac{\sin^2.\theta}{2} - \frac{\sin.2\theta}{2\pi}\log.\cot\theta\right] \quad . \quad . \quad (10)$$

Both the above formulae are dependent on but independent of h.

By putting $\pi = \theta/2$ in formulae (7) and (8) we see that they reduce to formulae (3) and (4) respectively, so that the fault merely becomes a special case of the dipping bed, as we might expect.

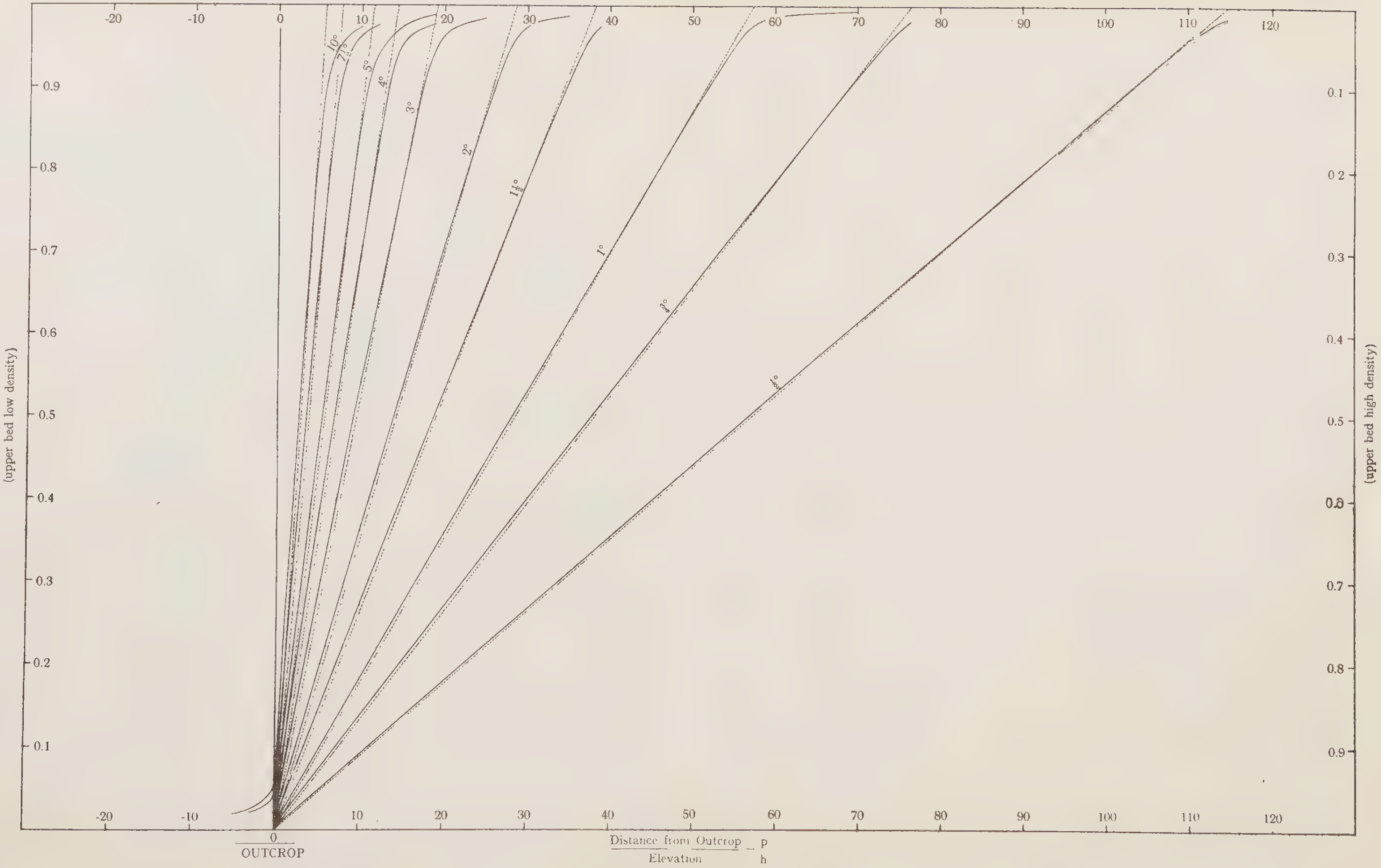

Fig. 6.5 E.C.F. variations of a Dipping Bed (angles up to 10°). $E = E_1 + (E_2 - E_1)\,t$

— = correct E.C.F.

= E.C.F. assuming $\frac{p}{h} = \cot\theta$

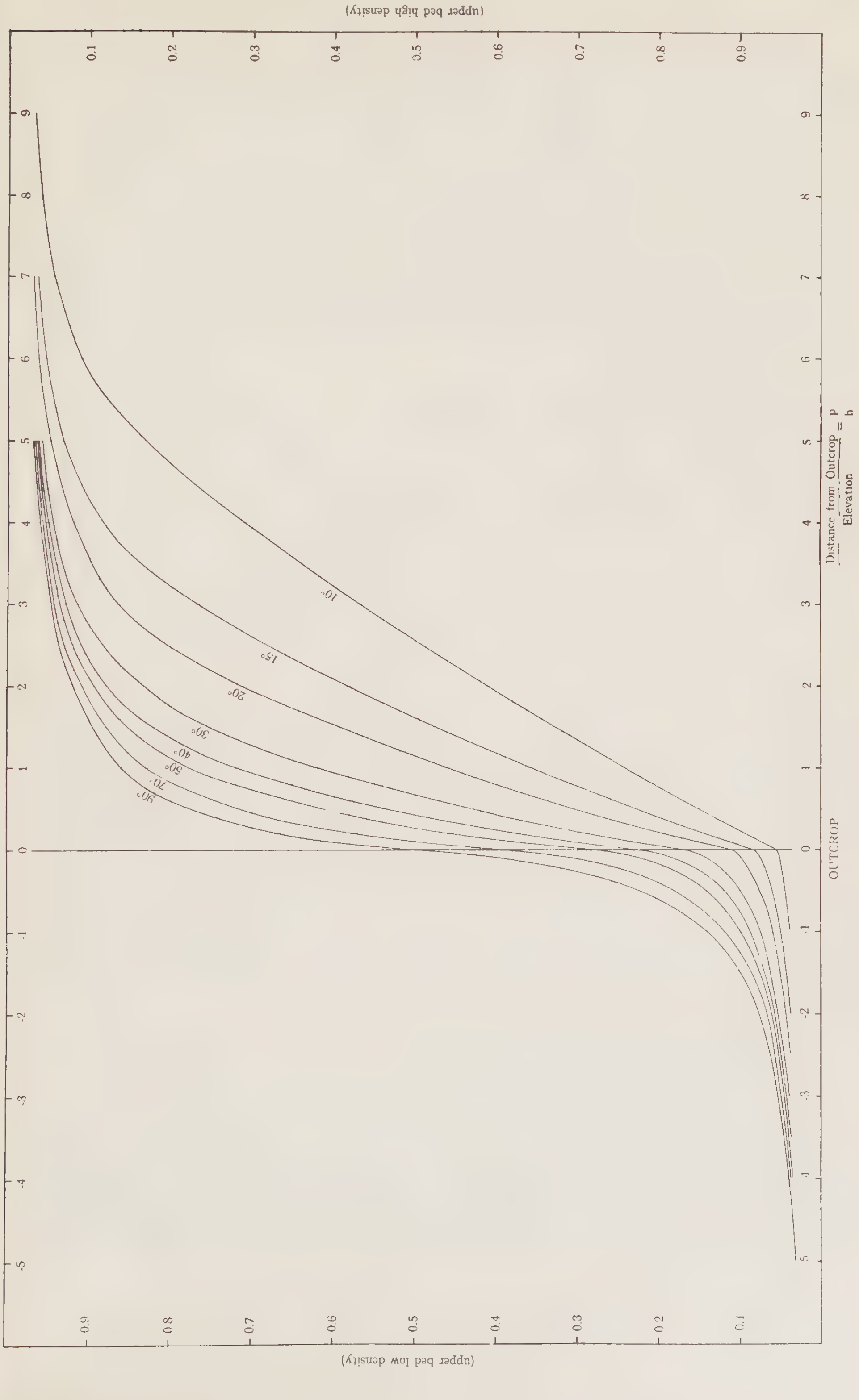

Fig. 7. E.C.F. variations of a Dipping Bed (10° — 90°). $E = E_1 + (E_2 - E_1)\,t$

Considering formulae (7) and (8), E_1, E_2, p/h and θ can all be determined in the field, so that E is uniquely determined. In a given set of field conditions, the only variables are p/h and θ, so that graphs can be prepared showing t (say) for various values of p/h and θ where:— $E = E_1 + (E_2 - E_1)t$. In figs 6 and 7, t is plotted against p/h for various values of θ. Fig. 6 covers small angles up to 10° and Fig. 7 angles from 10° to 90°. The decimal fractions of t plotted on the left side of the t axis should be used.

The usual assumption made for small angles of dip is that the fall in gravity is directly proportional to the thickness of the newer bed at a given point. The fall in gravity at a given point P is equated to the effect of an infinite horizontal sheet of thickness $p \tan\theta$, having as its density, the density difference of the two beds, or:—

$$\begin{aligned}\text{Fall in gravity} &= 2K\,.\,\pi\,(\sigma_1 - \sigma_2)\,p\tan\theta \\ &= (E_2 - E_1)\,p\tan\theta\end{aligned}$$

Then the total correction is:—

$$\begin{aligned}Eh &= E_1 h + (E_2 - E_1)\,p\tan\theta \\ \text{or } E &= E_1 + (E_2 - E_1)\,(p/h)\tan\theta \quad . \quad . \quad . \quad . \quad . \quad . \quad . \qquad (11)\end{aligned}$$

At the point where the density interface reaches datum

$$p = h\cot\theta \text{ so that } E = E_2$$
$$\text{At the outcrop } p = 0 \text{ or } E = E_1$$

This assumption, that the fall (or rise) of gravity is directly proportional to the thickness of the newer bed is plotted on Fig. 6 and shown by the dashed lines. It will be seen that the lines obtained, follow the correct curve fairly closely for small angles of dip except when E_2 and E_1 are approached, the main error occurring when E approaches E_2. If we assume that an average density difference is 0.3 gm/cm^3, this corresponds to an E.C.F. difference of 0.125 gravity units/metre, the gravity unit being 0.1 milligals. We rarely, if ever, require to know the E.C.F. to a greater accuracy than 0.005 gravity units/metre as our field determination of the E.C.F. is extremely doubtful beyond this accuracy.

$$\begin{aligned}\text{We have seen that } E &= E_1 + (E_2 - E_1)\,t \\ \text{or } E &= E_2 - (E_2 - E_1)\,(1 - t)\end{aligned}$$

At the limiting value $E_2 - 0.005$ we see that for $(E_2 - E_1)$ equal to 0.125 gravity units/metre, $t = 0.96$.

In the table below the percentage error in p/h is given for the assumption that the decrease in gravity is proportional to the thickness of the newer bed for the level $t = 0.96$.

Angle of Dip	*Percentage Error in p/h*
$\frac{1}{2}^\circ$	0.2%
$^3/_4{}^\circ$	0.8%
1°	1.2%
$1\frac{1}{2}^\circ$	2.1%
2°	4%
3°	7%
4°	12%
5°	18%
$7\frac{1}{2}^\circ$	25%
10°	34%

It will be seen that the error is inadmissible for angles over 5°, and even at 5° the error is about 18%.

Again assuming an average E.C.F. field difference of 0.125 gravity units/metre let us examine the conditions near the limit E_1 that is near the outcrop. Let us suppose we wish to know where the value $E_1 + 0.005$ lies relative to the outcrop.

Now at the outcrop $E = E_1 + (E_2 - E_1)\ \theta/\pi$

Thus for the point $E_1 + 0.005$

$$0.005 = 0.125\ \theta/\pi$$

so that $\theta = 7.2^\circ$.

That is, the value $E_1 + 0.005$ for an E.C.F. difference of 0.125 gravity units/metre lies at the outcrop for an angle of dip of 7.2°. Clearly for angles less than 7.2°, the value $E_1 + 0.005$ lies to the right of the outcrop. For greater angles it lies to the left.

If we differentiate E with respect to p/h in (7) we obtain

$$\frac{dE}{d\frac{p}{h}} = \frac{(E_2 - E_1)}{2\pi(1+\cot^2\theta)}\left[2\cot\theta\left\{\frac{\pi}{2} - \tan^{-1}\left(\frac{p}{h}+\cot\theta\right)\right\} - \log\left\{1 + \frac{\left(\frac{p}{h}+\cot\theta\right)^2}{\left(\frac{p}{h}\right)^2}\right\}\right] \quad (12)$$

At the outcrop, that is, where $p/h = 0$, $dE/d(p/h)$ becomes infinite.

Thus, at the outcrop, the tangents to the curves are at 90° and this is the maximum gradient. This fact will be discussed later in the paper.

Now let us consider the case where the newer rock has the higher density. In this case, we must determine the gravity effect of the wedge of material occupied by the newer rock, and the effective density difference will be $(\sigma_2 - \sigma_1)$ with corresponding E.C.F. difference of $(E_1 - E_2)$.

In this case we derive the formula:—

$$E = E_2 + (E_1 - E_2) \left[1 - \left\{ \frac{1}{2} - \frac{1}{\pi} \,.\, \tan^{-1}\left(\frac{p}{h} + \cot\theta \right) \right\} \left\{ 1 + \frac{p}{h} \frac{\sin.2\theta}{2} \right\} + \right.$$

$$\left. + \frac{p}{h} \frac{\sin^2.\theta}{2\pi} \log \left\{ \frac{1 + \left(\frac{p}{h} + \cot\theta \right)^2}{\left(\frac{p}{h} \right)^2} \right\} \right] \quad . \quad . \quad . \quad . \quad (13)$$

Similarly we obtain for positions of point P on the newer rock

$$E = E_2 + (E_1 - E_2) \left[\left\{ \frac{1}{2} + \frac{1}{\pi} \tan^{-1}\left(\cot\theta - \frac{[p]}{h} \right) \right\} \left\{ 1 - \frac{[p]}{h} \frac{\sin.^2\theta}{2} \right\} - \right.$$

$$\left. - \frac{[p]}{h} \frac{\sin^2.\theta}{2\pi} \log \left\{ \frac{1 + \left(\cot\theta - \frac{[p]}{h} \right)^2}{\left(\frac{[p]}{h} \right)^2} \right\} \right] \quad . \quad . \quad . \quad . \quad (14)$$

$[p]$ being the numerical value of p, the negative sign having been allowed for.

Figs 6 and 7 can be utilised for this case where the newer rocks have the higher density merely by inverting the curves. The percentage value of t is given on the right of the E.C.F. axis and this should be used for the case given above.

At the outcrop, where p/h is zero, we obtain from (13) or (14)

$$E = E_2 + (E_1 - E_2) \; [1 - (\theta/\pi)] \quad . \quad . \quad . \quad . \quad . \quad . \quad (15)$$

At the other fixed point, where the density interface between the two beds reaches datum level, i.e. where $p = h \cot \theta$, we obtain

$$E = E_2 + (E_1 - E_2) \left[\frac{\sin^2.\theta}{2} + \frac{\sin.2\theta}{2\pi} \log(\cot\theta) \right] \quad . \quad . \quad (16)$$

Lithological and Facies Changes

In cases where there is a gradual lithological change from older to newer beds, for example from a limestone to a sandstone, E.C.F. changes will also occur if the beds are dipping. Similarly, horizontal beds will lead to E.C.F. changes if facies changes are occurring, that is, where there are changes in lithology laterally in beds of similar age. In both cases, no estimate can be made of the E.C.F. at any point from knowledge of the E.C.F. at the end conditions. Changes will probably be gradual but irregular. If too close an accuracy of E.C.F. is not required, it is probably sufficient to vary the E.C.F. linearly between the point where, say, the rock is all limestone and the place where it is all sandstone. The only near accurate method of varying the E.C.F. in such cases, is to take frequent field determinations and vary the E.C.F's linearly between these values, so reducing the error in a direct linear variation between the limits.

3. *Field Applications of E.C.F. Changes*

Let us take the case of the dipping bed first, as this is the general case.

To all that has been written elsewhere on the determination of E.C.F.'s in the field, the foregoing discussion raises two points.

(i) As a precautionary measure, E.C.F's should always be measured parallel to the strike of the rocks. We can then be certain that the value obtained represents the true E.C.F. value at that point and not an average obtained along a profile over which there is varying E.C.F.

(ii) If the true or limiting E.C.F. of a given bed is required, it should be determined in the field as far as possible away from any outcrop of a bed of different lithology.

To apply the foregoing results in the field, two method are available. Firstly, the actual E.C.F. at each and every station which lies close enough to the outcrop to have a different E.C.F. from the limiting E.C.F's, can be read off the graphs by calculating its p/h value.

Secondly, the territory around the outcrop can be divided into zones, within each of which a constant E.C.F. can be assumed to apply. Although not as accurate as the first method, it is less laborious and its accuracy can be chosen to any desired limit.

Normally, the E.C.F. is required to be known within an accuracy of 0.01 gravity units/metre. The field determination of the limiting values can rarely be guaranteed to a closer value than this. Suppose we require to know the position of the zone $E_1 + 0.01$ relative to the outcrop. We can say that this zone lies between limits $E_1 + 0.005$ and $E_1 + 0.015$. The maximum error in the E.C.F. for stations within this zone is then 0.005 gravity units/metre. We can then mark off on our map a series of zones about the outcrop each representing an increase (or decrease) in E.C.F. of 0.01 units/metre. These zones would have values $E_1 + 0.01$, $E_1 + 0.02$, ... E_2. From the graphs on Figs 6 and 7 for the appropriate angle of dip, the limiting values of p/h for these zones can be read off for E.C.F. values of $E_1 + 0.005$, $E_1 + 0.015$, $E_1 + 0.025$ etc. However, it must be pointed out that the graphs are given for an E.C.F. difference of unity. The E.C.F. difference between the limiting values will never, in practice, attain this value. Suppose the determined difference is E_0.

Then $E = E_1 + E_0 m$ (say) where m is any value less than 1.

But we require to know $E_1 + 0.005$

Then $0.005 = E_0 m$

or $m = \frac{0.005}{E_0}$

The value we should read off from the graph then is m and *not* 0.005.

If, for example, the E.C.F. difference is 0.125 units/metre, the zone $E_1 + 0.01$ has limiting p/h values corresponding on the graphs to E.C.F. levels of $0.005/0.125 = 0.04$ and $0.015/0.125 = 0.12$.

Thus, for any E.C.F. differences, the width of zones, at a given point on the outcrop, in which a constant increase (or decrease) of E.C.F. of 0.01 units/metre is applicable, can be determined by reading off the appropriate p/h values and then determining the distance p from the outcrop as the elevation will be known. These zones can be plotted at various places along the outcrop and the points joined. The zones would normally be parallel to the outcrop, but will differ fractionally from parallelism as the elevation changes. Although roughly parallel with the outcrop, the width of the zones will expand as the elevation increases and diminish with decreasing elevation.

The E.C.F. changes over a fault, horst or graben, can be zoned in exactly the same way as for a dipping bed. In these cases, however, the zones will lie parallel to the outcrop of the fault and bear no relationship to the strike of the rocks.

The question of the accuracy to which the E.C.F. is required to be known is dependent mainly on the height of the topography. It has been suggested above that zones should have a width equivalent to 0.01 gravity units/metre change of E.C.F. Clearly the E.C.F. accuracy in this case is ± 0.005 units/metre. For an elevation of 100 metres, the Bouguer Anomaly of any station may then be in error by $0.005 \times 100 = 0.5$ units. This is usually of the order of accuracy that can be expected from the gravity meter, if the human error in reading is included. For elevations of 500 metres, however, the error is 2.5 units which is more serious. However, in the zone method suggested above, the actual E.C.F's can be read off by proration to a much greater degree of accuracy, if required. Knowing the zone limits, it should be possible to estimate the E.C.F. to within an accuracy of 0.002 units/metre leading to an error in Bouguer Anomaly for an elevation of 500 metres of 1 unit.

B. Applications to the Interpretation of Gravity Surveys

The foregoing discussion has considerable application to the interpretation of maps of gravity surveys. Two aspects are considered in the following pages.

1. *Interpretation of Change of Gravity Dip*

Wherever a change of dip of the isogals occurs on a gravity map, it must be borne in mind that it could be caused not only by a corresponding change in dip of the rocks or a change in the basement, but also by the advent of a dipping bed or fault which introduces rocks of different density. One criterion to assist in the choice of possibilities, is that a dipping bed giving rise to a fall (or rise) of gravity must be of considerable lateral extent, and occurs along a straight line. We have seen that in the case of a fault, the gravity curve so produced lies symmetrically about the outcrop whereas in the case of a dipping bed, the curve is asymmetrical, so that for small angles of dip, the outcrop lies near the commencement of the change in dip. Furthermore, that the gradient in each case is a maximum at the outcrop. It can be said, then, that if the maximum gradient occurs at the centre of the change of dip, the latter is caused by a fault. If it is asymmetrical and nearer the point where the change of dip first occurs, the latter is due to a dipping bed.

For small angles of dip, the gravity change will more or less follow a straight line. The greater the angle of dip the more the curve will diverge from linearity. For very small angles, the change in gravity is nearly proportional to the thickness of the new bed at any point. If p is the distance of any point from the outcrop then the thickness of the new bed below sea level will be $p \tan \theta - h$ where h is the elevation. So that the change in gravity g is given by:— $g = 2 K \sigma \pi \, (p \tan \theta - h)$ where σ is the density difference

$$\text{or } \tan \theta = \frac{\theta}{p(E_2 - E_1)} + \frac{h}{p} \qquad . \; . \; . \; . \; . \; . \; . \; . \; . \; . \; . \; . \; . \; . \qquad (17)$$

In the case where the rocks are covered by recent deposits of sand or soil so that no measurement of dip can be taken, the above formula gives a quick method of determining the dip.

The dip and depth which the newer bed reaches can be uniquely determined for any angle of dip. It can be shown that for a dipping bed the change in gravity is:— $G_1 = u(E_2 - E_1)d$ where $u = 1 - t$ (t is the function plotted in Figs 6 and 7). Suppose we have plotted the gravity curve over what is thought to be a dipping bed.

Clearly if a dipping bed is the cause of the distortion from a steady regional dip, the gravity curve will have a form as shown in Fig. 8 for an upper bed of lower density than that below. The effect of the dipping bed will be to displace the regional dip to a lower level. To determine the curve produced by the dipping bed, we must extrapolate the regional dip and plot the values A.B. at all points. We shall then have a curve similar to those on Figs 6 and 7 inverted except that the maximum value will not be unity. In the formula above u has a maximum value of unity. When this occurs, G_1 has its maximum value and $d = G_1 \text{ max}/(E_2 - E_1)$.

To determine the depth d to which the newer bed dips we have only to read off from the residual gravity curve the value of G_1 max. and divide it by $(E_2 - E_1)$ the E.C.F. difference. It should be noted that $(E_2 - E_1)$ is the E.C.F. difference for the rocks above the datum plane. If from the datum plane downwards the rocks are saturated with water, the density difference of the water filled rocks may not be the same as the density difference of the dry rocks. In this case, it is best to use $2K\pi(\sigma_1 - \sigma_2)$ instead of $(E_2 - E_1)$ if the density differences are known.

Clearly $u = G_1/G_1 \text{ max.} = 1 - t$

We see then that, if, at each point on the gravity residual curve over the dipping bed, we divide the gravity value by the maximum value of gravity attained we shall obtain the u curve for the dipping bed. By direct comparison with the curves on Figs 6 and 7 inverted, i.e. values on right ordinate axis, we can read off the angle of dip to what would normally be sufficient accuracy. Also determine the point of inflexion on the curve where the gradient is parallel to the u axis. Then this is the point where the density interface cuts the datum plane. If the dip is required to greater accuracy than can be obtained by comparison with the curves, determine the value of u at the point of inflexion. At this point

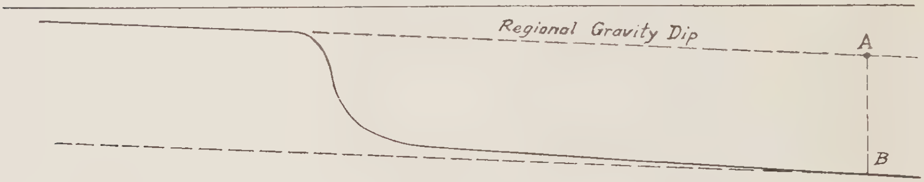

Fig. 8.

$$u = 1 - \theta/\pi$$

$$\text{or } \theta = \pi(1 - u) = \pi t \text{ where } \theta \text{ is the angle of dip.}$$

2. *The Gravity Inversion*

The normal case in geology is for density to increase downwards so that dipping beds cause a fall in gravity in the direction of dip. In the sense of density increasing downwards, the density difference is considered to be positive. Cases do occur where the density decreases with depth, for example limestones or anhydrites overlying low density sandstones. In these cases, the density difference may be considered to be negative and the upper beds will produce a gravity rise. The regional gravity picture is built up of a succession of positive and negative density differences but which in total effect is always equivalent to a positive density difference except in one case. That case occurs when the upper higher density bed is at the surface, when the effect of the gravity rise is greater, being near the surface, than the fall due to the net positive density difference at depth. Clearly, to produce such an effect, the main positive differential must be at some depth. If the base of the high density bed is folded, it will have the effect of bringing low density material nearer to the surface, and so a structural uplift will result in a gravity low. We have, then, a reversal of what is normally the case, so that structural uplifts are represented by gràvity lows and synclines by gravity highs.

Let us take a simple case of an infinite line mass to examine the effects that occur. Suppose the line mass is infinite in the y direction, that is at right angles to the dip and has density σ. Its maximum gravity effect is given by:—

$$G_{\max} = 2\,K\sigma/z$$

In Fig. 9 we have two density interfaces, the upper $= \sigma$ at depth z, the lower at depth cz where c is greater than 1. The upper one is negative and the lower one positive, the latter being numerically the greater. Let us suppose that this lower density differential $= b\,\sigma$ where b is greater than unity. Further imagine that a structure is reflected identically at each density interface and can be represented by a line mass. This is usually the case with most structures as the folding occurs at several or all density interfaces.

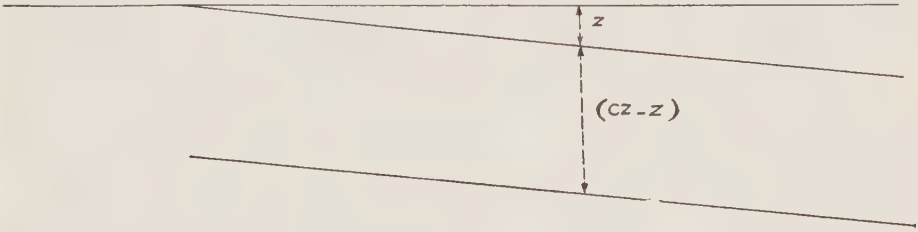

Fig. 9.

Then the maximum gravity effect of the line mass at the upper density interface is:— $G_1 = -2\,K\sigma/z$

The maximum gravity effect of the line mass at the lower density interface:— $G_2 = +2\,Kb\sigma/cz$

The condition that the net gravity result is negative is that

$2\,K\sigma/z$ is greater than $2\,Kb\sigma/cz$

For this to be true, c must be greater than b. The condition that a net negative anomaly should occur at the surface is that $c > b > 1$.

Now let us imagine that an identical structure exists down dip where the depth of each interface has increased by an amount t.

The effect of the line mass at the upper density interface is then:—

$$G_1 = -2\,K\sigma/(z+t)$$

and that of the lower:— $G_2 = +2\,Kb\sigma/(cz+t)$

The total gravity effect at the surface is:—

$$G = 2K\sigma\left\{-\frac{1}{z+t} + \frac{b}{cz+t}\right\} = 2K\sigma\,\frac{\left\{t - z\,\dfrac{(c-b)}{(b-1)}\right\}(b-1)}{(z+t)\quad(cz+t)} \quad . \qquad (18)$$

This will result in a net negative gravity effect at the surface as long as t is less than $z(c-b)/(b-1)$. The factor $(c-b)/(b-1)$ is always real and positive as we have seen that $c > b > 1$.

But clearly we can increase t to any value so that a point will be reached when $t = \{(c-b)/(b-1)\}z$ and here the net resultant will be zero.

If we further increase t, the net resultant gravity effect at the surface will be positive. This theory can be extended to structures of any form.

We can then put forward the general theorem that where two density interfaces exist, the upper being negative and the lower positive, the latter being numerically the greater, and if near the outcrop of the upper bed structures occur involving each interface equally and which produce net negative anomalies, a point will be reached on the surface in the direction of dip where similar structures will produce a zero resultant gravity effect. Beyond this point, in the direction of dip, the net resultant gravity effect will be positive.

The point at which the change from negative to positive anomalies occurs is entirely dependent on the values of c and b. Clearly if c is large, t will be large so that the distance p from the outcrop will be of considerable magnitude as $p = (z + t) \cot \theta$ where θ is the angle of dip. This, we might expect, for if the lower density interface is at considerable depth, its effect at the surface is small and with increasing depth, its effect further decreases. The effect of the upper interface is relatively large and though this is decreasing at a greater rate in the direction of dip than is that of the lower interface, a considerable distance will elapse before the net resultant is zero.

Similarly t will be large if $(b-1)$ is small. Thus if the density differences at each interface are nearly equal, we must proceed a considerable distance in the direction of dip before the change from negative to positive anomalies occurs.

The residual gravity anomaly produced by a structure at a negative density interface will always be less than that produced by a similar structure at a positive density interface, for whereas the latter is reinforced by the reflection of the structure at lower positive density interfaces, these lower density differentials tend to decrease the amplitude of the negative anomaly produced in the former case.

Wherever an interpretation is required of an area in which a gravity inversion exists, great care must be taken in subtracting the regional as very small residuals may represent considerable structures. Also, it is unwise to predict the amplitude of such structures unless very detailed information is available as to all the density differentials involved, und unless we have taken due note of the position of the anomaly relative to the outcrop of the density interface.

It is not necessary, of course, that this reversal of gravity anomalies should always exist over surface beds of high density. If the lower density differentials contribute a lesser positive contribution than the negative contribution of the upper interface, the anomalies will always be negative. This can occur either when the upper interface does not dip to sufficient depth, or if the upper density differential has larger magnitude than the effective positive differentials which are involved in the structural uplift. The surface bed may be for example anhydrite whose density is comparable with the density of the metamorphic rocks of the basement. Or again the structure may be reflected to no great depth so that few positive density differentials are involved to add their contribution.

To conclude, it must be remarked that the relationship of negative gravity anomalies to structural uplift occurs far more frequently than is usually considered to be the case. One has only to consider the rapid lithological changes from sandstone, limestone, clay etc. that has occurred throughout geological history to realise that gravity interpretation must have as many variations as there are changes in rocks and to point out that the gravity interpreter should always consult any surface geological information that may be available, before proceeding with the gravity interpretation.

REFERENCES

NETTLETON L. L., 1939, Determination of density for reduction of gravimeter observations, Geophysics, 4, 176-183.

SIEGERT A. J. F., 1942, Determination of the Bouguer correction constant, Geophysics, 7, 29-34.

DISCUSSIONS

Mr. BUTTERWELL: I wish to congratulate the author for tackling the very important problem of evaluating errors in E.C.F. corrections and showing how they may be adjusted. I should like, however, to enquire what is the type of survey for which they are designed. It seems to me that they can be used with advantage where regional surveys have been calculated on to a depth datum which lies well below the topography. In detailed surveys, however, the difficulty is that the formulae can only be accurately applied if the positions of the geological disturbances or boundaries are known. In these surveys it is usually preferable to take all steps to make the variations in the E.C.F. corrections as small as possible, e.g. by choosing a route across the structure which involves smallest changes in relief, and by computing from a datum at the mean of the topography.

Mr. COLLEY: The change of E.C.F.'s in "local" surveys must still be made. The effect of raising the datum is merely to make the E.C.F. change more abrupt. If changed linearly, spurious highs and lows will be about the outcrop, but if the elevation is kept small by careful choice of datum these anomalies will be small or negligeable. However, local surveys are constantly being tied into the regional picture of a country's national grid. Then the datum is sea-level and no choice is available and the correct E.C.F. changes must be made. It is better, then, that local surveys, choosing a high datum, should be avoided from the beginning, otherwise the later change of E.C.F.'s will be made by computors with less knowledge of the local structural conditions than the original interpreter.

As regards the positions of the boundaries, the E.C.F. changes over anticlines can only be done on a theoretical basis if the shape is known or when the density interface rises to the surface and we are reduced to the case of the dipping bed. If the interface lies between sea-level and the surface, wrong E.C.F.'s merely accentuate the structure. This is often an advantage as long as the interpreter does not try to correlate magnitude of anomalies with size of structures. As the last part of the paper shows, the position of the outcrop can be fairly accurately determined in the case of faults and dipping beds from the Bouguer Anomaly map. In this case the map must be adjusted by the interpreter before proceeding with his interpretation.

Mr. SCHLEUSENER: It seems to me very important to keep the datum level as close as possible to the surface. To a large extent this prevents the introduction of calculated disturbances into the isogam map. The final isogams then are not influenced by geological assumptions. All uncertainties remain for the final interpretations of the isogam map, as it normally should be.

But if the datum-level cannot be put near to the surface, then the careful investigation of Mr. Colley will be very helpful.

Mr. COLLEY: I agree, but as I remarked to Mr. Butterwell, the choice of datum depends on the survey being local, and which, sooner or later, becomes national as it is tied in. Raising the datum merely postpones the inevitable but is understandable if considerable computational labour is involved. It is to fill this gap in our literature and so reduce the work of the local interpretor or national computor, that the first part of this paper has been written.

E.A.E.G. ABSTRACT SERVICE

EXPLORATION — GENERAL

259. *What is Our Contribution?*

D. T. Germain-Jones, Geophysical Prospecting, Vol. 2, No. 3, pp. 177-184, September 1954.

The Presidential Address delivered at the Third Annual Meeting of the E.A.G., in Copenhagen, May, 1954.

Dr. Germain-Jones recalls the conception of the E.A.E.G. and reviews its progress to date. He then reviews geophysical activity in Europe during the latter half of 1953 and provides statistics that are compiled from data supplied by various organisations in the different countries. A total of 233 exploration parties were in operation: 117 Seismic, 42 Gravity, 19 Magnetic, and 55 Electric/Tellural. Personnel numbered about 710 geophysicists supported by approximately 1,100 technical men such as observers, computors and technical assistants.

260. *Geophysical Methods of Oil Prospecting — A Review. I. — Introduction.*

D. Taylor Smith, Petroleum, Vol. 17, No. 10, pp. 362-364, October, 1954.

A review of geophysical prospecting methods in current use. These include: seismic, gravitational, magnetic, and electrical.

The seismic method has so far proved to be the most applicable and successful in oil exploration. Gravitational and magnetic methods serve best to provide outlines of large areas which may be used as indicators for seismic work. Electrical methods employ either artificial or natural (Telluric) currents. The former technique can only be applied to shallow structures, whereas the Telluric method has deep penetration and provides reliable data cheaply.

261. *Geophysics for the Geologist in Mineral Exploration.*

S. J. Mayne, Pakistan J. Sci., Vol. 3, No. 4, pp. 145-155, 1951.

Having defined applied geophysics as the study of the problems of geology and mineral exploration by physical methods, Mayne then gives a brief description of the magnetic, electrical, gravitational, seismic and radioactive methods of prospecting. Many graphs illustrate typical anomalies observed in practice.

(From Geophysical Abstracts 156, U.S. Geol. Survey).

262. *Geology and its Application in Prospecting For Oil.* (In Slavonic).

F. Ozegovic, Nafta (Yugoslavia), Godina 4, Bro j 1, pp. 1-11, 1953.

The application of gravimetric, magnetic, electric and seismic methods in exploration for oil is briefly described. Results of surveys of several promising oil deposits in Yugoslavia are presented in the form of geologic profiles.

(From Geophysical Abstracts 156, U.S. Geol. Survey).

263. *Case History of Wild Goose Gas Field, Butte County, California.*

W. L. Matjasic, Geophysics, Vol. 19, pp. 509-516, July, 1954.

The discovery well of the Wild Goose gas field was drilled and completed in 1951 on a structure located by a reflection seismograph survey conducted in 1950. An additional seismograph survey was made subsequent to discovery to define the structure better for further development. The illustrations include two seismic cross sections, a contour map based on the original seismic reflection data, an aeromagnetic map, a structure contour map, and an electric log of the discovery well.

(Author's Abstract).

264. *Safety is Our Responsibility.*

B. W. Sorge, Geophysics, Vol. 19, No. 3, pp. 529-540, July, 1954.

The geophysical industry's safety record compares unfavourably with industry in general and the petroleum industry in particular. These safety problems represent a real challenge, as ways and means must be found to improve safety and accident prevention. We must accept this challenge in order to avoid possible future rules and regulations that may seriously interfere with the efficient conduct of exploration activities. It is just plain good bussiness to insist on safe operations of geophysical field parties.

(Author's Abstract).

265. *New Horizons.*

T. S. Peterson, Geophysics, Vol. 19, No. 3, pp. 541-548, July 1954.

Future petroleum discoveries in the U.S. depend on the scale and quality of prospecting. Oil seeps nowadays seldom provide clues to new fields. Instruments play a much larger part in this task and many more people are involved. Instruments have opened up new possibilities in vast new areas such as the Williston Basin and the continental shelf. The latter is outstanding in its possibilities. Offshore prospecting is very costly and needs to be carried out with extreme care to ensure a profit. The procedures for obtaining leases, equipping parties and carrying out surveys are described.

Examples of the operating costs of some of the companies engaged in this work are given. One company spent 7 million dollars before drilling commenced; the figure increased to 9 million dollars before oil was found.

266. *Using Geophysics in Vatican City.*

D. Linehan, Paper read at the Annual Meeting of the S.E.G., St. Louis, Missouri, April, 1954. (Not yet published)

This paper explains the employment of geophysical methods in directing archeologists where to excavate in their recent studies beneath Saint Peter's Basilica at Vatican City, Rome. For the most part the seismic refraction method was used, but this was also complemented with the electrical resistivity method. The paper is illustrated with Kodachrome slides taken during operations in Vatican City.

267. *The Geophysicist in Industry.*

R. L. Lay, Geophysics, Vol. 19, No. 3, pp. 383-387, July, 1954.

Present day scope of geophysics in industry is discussed. The geophysicist needs to be a business man as well as a scientist. Recruits with a broader scientific background are required in the industry. Favourable structures are becoming harder to find and new methods of exploration or interpretation have to be devised accordingly. A review section is recommended as an asset which should save much cost and time by devoting its efforts to extracting all available information from records.

SEISMIC —GENERAL

268. *Seismological Conditions in Southwest Hungary* (In Hungarian)

G. Szenas & O. Adam, Magyar Allami Eötvös Lorand Geofiz. Intezet Geofiz. Közlemenyek Kötet 2, Szam 9, pp. 73-89, 1953.

Great difficulties are always met with in seismic-reflection surveying in areas where karst basement is overlain by lenticular sediments. In an investigation designed to improve the technique of geophysical surveys of such areas and to find the limits of applicability of seismic-reflection methods in similar cases, numerous seismic profiles were made and the velocity of seismic waves determined at many points in southwest Hungary. Szenas and Adam conclude that, if the explosion of the charge is produced at some height above the ground, better results can be obtained, because of the more favourable frequency spectrum of the seismic waves.

(From Geophysical Abstracts 156, U.S. Geol. Survey).

269. *Seismic Measurements of Ice Thickness on the Formi Glacier* (In Italian)
R. Cassinis & E. Carabelli, Riv. Geofis. Appl., Vol. 14, No. 2, pp. 87-99, 1953.

A short experimental survey has been carried out by seismic reflection and refraction methods, on a branch of a glacier in a stage of very fast withdrawal. The methods employed are described and discussed, and the difficulties presented by the presence of a number of crevasses and by the low thickness of the ice, are pointed out.

270. *A Seismic Reflection Quality Map of North America.*
P. L. Lyons, Paper read at the Annual Meeting of the S.E.G., St. Louis, Missouri, April, 1954, (not yet published).

A reflection quality map of North America has been prepared by a subcommittee of the Programme and Arrangements Committee for 1953-54. The map brings to date the map of the United States prepared for the April meeting of the S.E.G. in 1951, and the remainder of the continent has been added. The map designates as good, fair, or poor to NG, all sedimentary areas of the continent in respect to reflection quality in conventional seismic explorations. A ready correlation is apparent between the areas of intensive oil and gas development and areas of fair to good reflection quality. The rapid oil and gas developments in recent years in western Canada may be directly ascribed to the unexpectedly good seismic data obtained. The committee notes the invasion of the poor to NG areas by the use of special techniques and the rewad to be gained by progress in this direction, for approximately half of the sedimentary area of North America yields poor to NG reflections.

SEISMIC — INSTRUMENTAL

271. *The Characteristics of Electromagnetic Seismographs* (In French).
G. Grenet, Ann. Geophys., Tome 8, No. 3, pp. 328-332, 1952.

It is shown how it is possible, using only two families of curves, to determine all the constants of the seismograph having a pendulum and a galvanometer, or, conversely, to construct a seismograph having specified properties. After presenting the necessary equations, Grenet generalizes the results partially in order to examine the case where several galvanometers are used, with two recorders mounted in cascade, only the last being used for registration.

(From Geophysical Abstracts 156, U.S. Geol. Survey).

272. *Low Frequency Electrodynamic Seismometer with Torsion-Blade Suspension.* (In Hungarian)
L. Stegena, Magyar Allami Eötvös Lorand Geofiz. Intezet Geofiz. Közlemenyek, Kötet 2, szam 5, pp. 34-44, 1953.

A description is given of a low-frequency electrodynamic seismometer constructed in the Hungarian geophysical institute. The oscillating system of this instrument is suspended on a torsionally-strained tape. This construction notably decreases the frictional resistance of the seismometer.

(From Geophysical Abstracts 156, U.S. Geol. Survey).

273. *Patents.* Abstracts in Geophysics, Vol. 19, No. 3, p. 554, July, 1954.

U.S. 2,660,716.	24 Nov., 1953.	A circuit for recording shot moment.
U.S. 2,667,531.	26 Jan., 1954.	A strain-carrying swivel for use where a marine seismic cable enters or leaves a geophone case.
U.S. 2,667,625.	26 Jan., 1954.	A system for transmitting seismometer signals by radio having a transmitter at each seismometer.
U.S. 2,667,812.	2 Feb., 1954.	A timing light control for oscillographs.
U.S. 2,668,282.	2 Feb., 1954.	A shot-moment transmitter where the blaster frequency reaches a discriminator via an audio oscillator and the r-f carrier.
U.S. 2,672,944.	23 March 1954.	A seismic filtering and recording system using playback magnetic recording tape.
U.S. 2,673,899.	30 March 1954.	An avc system having two circuits fed from the output, one operating on high amplitude first arrivals, the other on strong reflections.

SEISMIC — FIELD TECHNIQUE

274. *British Seismic Explosives — Their Storage and Use in the Field with Special Reference to Safety in Handling.*

S. H. Davidson, R. Westwater, & J. Hancock, Geophysical Prospecting, Vol. 2, No. 3, pp. 185-202, September, 1954.

The development of explosives for use in seismic prospecting is reviewed. Methods of handling, packing, storing and transporting are described, together with the various impact and friction tests that are carried out on explosives. A Shooter's full routine for loading the hole and firing the shot is given. Finally, the various types of explosive in present day use are discussed.

275. *Patents.* Abstracts in Geophysics, Vol. 19, No. 3, p. 555, July, 1954.

U.S. 2,670,926.	2 March, 1954.	A powered cable handling device.
U.S. 2,672,204.	16 March, 1954.	Shooting system, for areas where frequency of reflections varies with depth, in which shots are fired above ground in time sequence.

276. *Recording of Seismic Waves in Bore Holes.*

E. T. Howes, Paper read at the Annual Meeting of the S.E.G. at St. Louis, Missouri, April, 1954 (Not yet published).

Reflected and refracted seismic waves are normally detected by a „Horizontal Spread" of geophones placed at the surface of the ground. However, these same seismic waves can be detected by a "Vertical Spread" of geophones suspended in a fluid-filled borehole. Equipment specially designed for use as a vertical spread in shallow boreholes is described in this paper.

Sample records taken under various field conditions are shown. The relative advantages and operating problems are also discussed.

SEISMIC — INTERPRETATION

277. *Determination of the Reflecting Plane in Seismic Reflection Prospecting.* (In Hungarian with summaries in Russian and English).

I. B. Haaz, Magyar Allami Eötvös Lorand Geofiz. Intezet Geofiz. Közlemenyek, Kötet 1, Szam 6, pp. 50-55, 1952.

When the shot-detector spread is perpendicular to the strike of the reflecting plane, the vertical plane containing this spread is perpendicular to the reflecting plane and contains the straight line of its maximum dip. The reflecting plane is determined by this straight line, that is by its dip and angle γ, and its perpendicular distance n from the shot point, or by n, and by the horizontal distance d from the shot point to the point of intersection of the spread line and the dip line. The author shows that $1 : n^2$ and $1 : d$ satisfy a linear equation system containing as many equations as there are detectors in the spread. This system gives for $1 : n^2$ and $1 : d$ a normal equation system by the method of the least squares from which these quantities and also their mean errors may be calculated. (Author's Abstract).

(From Geophysical Abstracts 153, U.S. Geol. Survey).

278. *Determination of the Reflecting Plane and the Wave Velocity in Seismic Reflection Prospecting.* (In Hungarian).

I. B. Haaz, Magyar Allami Eötvös Lorand Geofiz. Intezet Geofiz. Közlemennyek, Kötet 2, Szam 6, pp. 53-56, 1953.

This is a continuation of the study of the determination of the position of the reflecting plane. In the present paper the problem is treated for the case when the velocity of the seismic wave is unknown and formulae are derived from which the position of the reflecting plane can be determined independently of the seismic velocity.

(From Geophysical Abstracts 156, U.S. Geol. Survey).

279. *Effect of the Inclination of Equal-Velocity Surfaces in the Calculation of Reflecting Surfaces in Seismic Reflection Surveys.* (In Italian).

C. Contini, Riv. Geofis. Appl., Vol. 14, No. 1, pp. 1-17, 1953.

In calculating reflecting surfaces from seismic-reflection survey data, it is usually assumed that the equal-velocity surfaces are plane and horizontal, whereas in reality they are complex and variable because of different tectonic conditions. In this paper Contini attempts to determine the errors resulting from this assumption and to devise a method to reduce these errors. Three configurations of the equal velocity and reflecting surfaces are considered: one in which the layers are plane and horizontal and then dip at a constant angle, and two in which layers of the previous case dip at increasing angles. Formulae are developed to take into account the effect of the tilted equal-velocity surfaces; correction charts, based on the structure of the middle Po plain are given.

(From Geophysical Abstracts 156, U.S. Geol. Survey).

SEISMIC — THEORY & RESEARCH

280. *Experimental Studies on the Mechanism of Generation of Elastic Waves II.*

K. Kasahara, Bull. Earthquake Research Inst., Tokyo Univ. XXXI, Part I, pp. 71-79, March, 1953.

Wave propagation in the vicinity of a point source with a vertical impulse, in contrast to the classical work of H. Lamb, is investigated mathematically.

The author confines himself to the phenomena on the free surface. The vertical displacements have been calculated for different velocities of propagation and graphically represented as functions of the distance from the source. The results of a provisional experimental investigation are compared with the theoretical values.

281. *Experimental Studies on the Mechanism of Generation of Elastic Waves.*

K. Kasahara, Bull. Earthquake Research Inst., Tokyo Univ. XXXI, Teil 3, pp. 235-243, Sept., 1953.

In this paper the formation and propagation of free surface waves are experimentally determined and examined mathematically together with the pressure distribution.

In the experiments the author used agar-agar for the elastic medium and a capacity receiver with a looposcillograph. In order to release the elastic impulse, a special wave-source was constructed. It consisted, in principle, of two eccentric discs which were driven by a synchronous motor. The motions of the eccentric discs were transmitted through two rods and two cables to the same oscillator which consisted of an aluminium bar lying immediately below the surface of the elastic medium.

The experiments indicate that complicated excitation shapes can lead to the forming of normal-shaped surface waves. The mathematical calculations which were made in connection with this experiment partly confirmed these results.

282. *On the Propagation of Seismic Waves in a Solid Body with Elastic Afterworking.*
H. Menzel, Geophysical Prospecting, Vol. 2, No. 2, pp. 139-150, June, 1954.

The different equations of elasticity concerning the departure of the behaviour of rocks from perfect elasticity are discussed. The theory of elastic afterworking and its significance for the propagation of elastic waves is studied in detail. It is found that this theory does not explain the observations on seismic waves in exploration geophysics so well as the theory of viscoelasticity suggested by Ricker.

(Author's Abstract).

283. *Comparative Study of Seismic Methods of Prospecting.* (In Spanish).
J. Garcia Sineriz, Rev. Geofis., Ano 10, No. 40, pp. 263-280, 1951.

The basic relations of two seismic methods, reflection and refraction, are derived, and formulae are given for the depth of reflecting layer, for the velocity of seismic waves, and the time of arrival at different geophones.

The advantages and drawbacks of both methods in particular cases are discussed. The treatment covers not only parallel horizontal layers but also inclined strata.

(From Geophysical Abstracts 156, U.S. Geol. Survey).

284. *Points for Seismic Prospecting in Areas where Reflections are Scarce or Insufficient.* (In Italian).
C. Contini, Ann. di Geofis., Vol. 6, No. 2, 213-227, April, 1953.

The paper discusses the precautions that must be taken in order to carry out seismic prospecting in areas where the reflections as obtained by ordinary methods are scarce or insufficient. In particular, methods are discussed for augmenting the energy of the wave sent into the ground and for diminishing the amplitude of the disturbances in comparison with the amplitude of the useful reflections. Finally, the system of registration with "Betrayal" of the waves, is discussed.

285. *Review of Pattern Shooting.*
A. E. McKay, Geophysics, Vol. 19, No. 3, pp. 420-437, July, 1954.

Patterns of shot holes and patterns of seismometers are now standard technique in many areas currently being surveyed by the seismograph. This paper reviews some of these pattern arrangements and shows comparison records in a number of areas such as New Mexico, West Texas, western Oklahoma, Mississippi, and Florida. Although pattern shooting is definitely proven as a useful technique, it is not to be construed as a cure-all for difficult shooting areas.

(Author's Abstract).

GRAVITY — GENERAL

286. *Geophysical Surveys, Oaklands-Coorabin Coal Field, New South Wales.*
R. R. Thyer & K. R. Vale, Australian Bur. Min. Resources Geol. & Geophys. Bull., 19, pp. 7-35, 1952.

During 1948-1950, extensive gravity surveys were made over an area of about 1,450 square miles around the Oakland-Coorabin coal field in the Riverina division of New South Wales to map the boundaries of the Coal Measures. Seismic surveys were made in addition to try to obtain thickness of sediments at several critical places and to provide a control for separating effect of sediments from the regional effect. The residual gravity map suggests the presence of a Permian basin approximately 600 square miles in area with a possible extension in northwesterly direction.

(From Geophysical Abstracts 156, U.S. Geol. Survey).

287. *Gravity and Magnetic Reconnaissance, Roma District, Queensland.*

J. C. Dooley, Austalian Bur. Min. Resources Geol. & Geophys. Bull., 18, p. 24, 1950.

Gravimetric and magnetic surveys were made during 1947 and 1948 in the Roma district of Qeensland, Australia, in search for oil. Altogether 750 stations were occupied. A Western gravimeter with a Watts vertical variometer were used. The results of the investigation are presented as gravity and magnetic contour maps of the areas.

(From Geophysical Abstracts 156, U.S. Geol. Survey).

288. *Gravity Surveys of Central Pennsylvania.*

L. O. Bacon, Trans. Am. Geophys. Un., Vol. 35, No. 3, pp. 495-502, June, 1954.

Gravity surveys were made in Central Pennsylvania in an attempt to obtain information which could be related to subsurface structures near the Allegheny Front. Results show no distinct relationship between gravity anomalies and major structural folding; however, they do indicate an intrusion or upthrust of the basement east of the Allegheny Front. It is believed that his basement feature was responsible for the forces causing the northwestward structural salient in the Appalachian Mountain of central Pennsylvania.

(Author's Abstract).

289. *Gravity Traverse in Northeastern Pennsylvania.*

J. C. Duecker, Trans. Am. Geophys. Un., Vol. 35, No. 3, pp. 503-507, June, 1954.

A gravity traverse was made in northeastern Pennsylvania. The data taken along the traverse revealed a gravity profile with two significant features: a local anomaly of about 15 mgals over a distance of 8 miles and a regional Bouguer gravity increase of 70 mgals over a distance of 65 miles.

290. *Diurnal Variations of Gravity in Europe.* (In Italian).

C. Morcelli, Ann. Geofis., Vol. 6, No. 2, 295-307, 1953.

This is a continuation of the previous study. A theoretical proof is presented that the curves of diurnal variation of gravity, calculated for northern Italy with $\varphi_0 = 45°$ and $\lambda_0 = 12°$ E from Greenwich, are also applicable for every other longitude, if times are corrected accordingly.

It can be seen, that difference $\triangle\varphi$ in latitude produces effects not exceeding 0.01 mgal for $\triangle\varphi < 2°$, where $\triangle\varphi = \varphi - \varphi_0$ and can be compensated up to the limit of $\triangle\varphi < 13°$ by a correction factor applied to amplitudes computed with the derived formulae.

In order to make possible the utilization of computed graphs for $\varphi < 32°$ or $\varphi > 57°$ curves can be readily constructed making easy interpolation possible. As an example such curves are computed for the second half of the year 1953 for $\varphi = 30°$ and $\varphi = 60°$.

(From Geophysical Abstracts 156, U.S. Geol. Survey).

291. *A Gravimeter Survey in the Bristol and Somerset Coalfields,*
A. H. Cook & H.I.S. Thirlaway, Geol. Soc. London Quart. J., Vol. 107, pt. 3, pp. 255-286, 1951.

The variations of gravity in the Bristol and Somerset coalfields are shown to correspond in a general way to the geologic structure, but discrepancies in detail indicate that the anomalies are partly due to structures underlying the coalfields that may have controlled the development of sedimentation and deformation in the region. Detailed studies were made in certain areas to assist the planning of a programme of exploratory boring.

(From Geophysical Abstracts 156, U.S. Geol. Survey).

292. *Geophysical Survey on the Plateau of Asiago.* (In Italian).
C. Morelli, Ann. di Geofis., Vol. 6, No. 2, pp. 239-250, April, 1953.

In order to study the geophysical behaviour of the calcareous plateau of Asiago, in the Venitian alpine border, in August 1952 magnetic observations at 215 stations and gravimetric observations at 206 stations were carried out on the plateau itself and in the surrounding zones. The instruments used were: variometer for the vertical component, and a Worden No. 50 gravimeter. The results show the behaviour of the volcanic instrusions underlying the calcareous layer and outcropping to the south and to the west of the plateau. The registration of the magnetic variation is undisturbed and comparison with two temporary registering stations on the Euganei confirms the normality of the conditions on the plateau of Asiago.

293. *Gravity Measurements on Malta and at Tunis.*
J. C. Harrison, Mon. Not. Roy. Astronom. Soc., Geophys. Suppl., Vol. 6, No. 9, pp. 604-609, April, 1954.

Free air and Bouguer anomalies are given for 22 stations on Malta. A density of 2.25 gm/cc is used for the Bouguer reductions on the basis of density measurements on five samples. In the second part of the paper discussion is made of the best Potsdam values for No. 3 dock Malta and at Tunis airport. The adopted values are shown to be consistent, within the rather low accuracy of the connections, with values accepted in Sicily.

GRAVITY — INTERPRETATION

294. *Methods of Modern Interpretation of Gravimeter Measurements.* (In Hungarian).
L. Facsinay, Magyar Allami Eötvös Lorand Geofiz. Intezet Geofiz. Közlemenyek, kötet 2, szam 11, pp. 95-120, 1953.

The interpretation of magnetic surveys was recently made easier by the introduction of the third partial differential coefficient of the potential function. The similarity of magnetic and gravitational fields suggests that the same procedure be used when interpreting gravitational surveys made both by gravimeters and by torsion balances. Facsinay shows how this method can be advantageously employed, using numerous ublished data of American surveys. The same procedure is applied to some recent surveys in Hungary in areas previously geologically investigated by drill holes.

(From Geophysical Abstracts 156, U.S. Geol. Survey).

295. *Density Determinations of Rocks Based on Subsurface Gravity Measurements at Different Depths.* (In Hungarian).
L. Facsinay, Magyar Allami Eötvös Lorand Geofiz. Intezet Geofiz. Közlemenyek, Kötet 2, szam 4, pp. 1-9, 1953.

Gravity measurements were made on different levels of a mine, the difference between extreme stations being 325.7 m. The densities of intermediate formations were computed from the measurements and were found to be in good agreement with the known geologic section, but higher than the densities found in laboratory measurements. It is therefore suggested that corresponding corrections be applied to densities when computing Bouguer anomalies. The accuracy of gravimetric measurements when these corrections are indicated is about 0.1 mgal.

(From Geophysical Abstracts 156, U.S. Geol. Survey).

296. *Regional Reduction and Second Derivative Methods of Gravity Interpretation.* (In Italian).

A. Marussi, Ann. di Geofis., Vol. 6, No. 2, pp. 155-160, April, 1953.

Some formulae given by Pizzetti are reviewed, which permit the derivation by practical procedures of divergence of the surface gradient of gravity (Beltrami's second differential parameter of surface gravity). Such researches are related to the methods of regional reduction and second derivatives, which have been recently proposed for practical applications by American authors.

297. *Significance of the Second Differential Parameter of Gravity in Geophysics.* (In Italian).

A. Marussi, Riv. Geofis. Appl., Vol. 14, No. 2, pp. 65-72, 1953.

Relations between differential characteristics of the gravimetric field, and the geometrical characteristics of the gravity field are sought. Amongst the former characteristics the divergence (space or surface) of the gravimetric gradient is of greatest importance; for its determination the method suggested by Pizzetti as early as 1909 may be used. Pizzetti's method, applied to the field of gravimetric anomalies, coincides with the method suggested in 1951 by Elkins; in this case the divergence of the surface gradient of the anomaly coincides, to a first approximation, with its second derivative along the vertical.

298. *Quantitative Studies Concerning the Vertical Gradient and Second Derivative Methods of Gravity Interpretation.*

O. Rosenbach, Geophysical Prospecting, Vol. 2, No. 2, pp. 128-138, June, 1954.

The first part of the paper investigates the possibility of localising highly situated inclined faults with the aid of the vertical gradient and the second derivative in the direction of the vertical. Since these quantities have been computed from gravity values by means of formulae of approximation, the question as to their applicability for possible quantitative interpretation arises. Particular caution should be exercised when making the usual comparison with theoretical test examples. For three effects have to be taken into account which result from the application of the formulae of approximation:

(1) The extreme values appear more or less smoothed out.
(2) Extremal abscissae are being displaced
(3) The results are influenced by the orientation of the grid which forms the basis of the calculation.

For a practical instance it was possible to locate a well under troublesome circumstances. This well is situated on the downthrow side of an inclined fault, the depth of the upthrow side being known as a result of another well.

The second part of the paper shows how small, deeply situated structures may be recognised in the diagrams of the vertical gradient and of the second derivative. In the case of two practical instances the effect of these structures is rendered unrecognisable in the isogam map in view of regional influences. The results according to the formulae of Baranov, Elkins and Rosenbach are contrasted with each other.

(Author's Abstract)

MAGNETIC — GENERAL

299. *Geophysical Survey on the Plateau of Asiago.* (In Italian).
C. Morelli, Ann. di Geofis., Vol. 6, No. 2, pp. 239-250, April, 1953.

In order to study the geophysical behaviour of the calcareous plateau of Asiago, in the Venitian alpine border, in August 1952 magnetic observations at 215 stations and gravimetric observations at 206 stations were carried out on the plateau itself and in the surrounding zones. The instruments used were: variometer for the vertical component, and a Worden No. 50 gravimeter. The results show the behaviour of the volcanic intrusions underlying the calcareous layer and outcropping to the south and to the west of the plateau. The registration of the magnetic variation is undisturbed and comparison with two temporary registering stations on the Euganei confirms the normality of the conditions on the plateau of Asiago.

300. *Gravity and Magnetic Reconnaissance, Roma District, Queensland.*
J. C. Dooley, Australian Bur. Min. Resources Geol. and Geophys. Bull., 18, p. 24, 1950.

Gravimetric and magnetic surveys were made during 1947 and 1948 in the Roma district of Queensland, Australia, in search for oil. Altogether 750 stations were occupied. A Western gravimeter and a Watts vertical variometer were used. The results of the investigation are presented as gravity and magnetic contour maps of the area.

(From Geophysical Abstracts 156, U.S. Geol. Survey).

MAGNETIC — THEORY & RESEARCH

301. *Rock Magnetism and Polar Wandering.*
J. Hospers, Nature, Vol. 173, No. 4416, pp. 1183-1184, June 19, 1954.

Lavas that have become permanently magnetized in the direction of the local geomagnetic field at the time of cooling, and ferriferrous sediments that have acquired a weak magnetic polarization during deposition, may be used with caution to indicate the direction of the geomagnetic field in the past. A brief description is given of a method of constructing a locus, for any given geological period, within which the geographic pole was situated (probability 95%) during that period.

302. *Natural Magnetization of Igneous and Sedimentary Rocks.*
Nature, Vol. 173, No. 4415, pp. 1114-1117, June 12, 1954.

A discussion on recent developments was held during January 8-9, 1954, at Birmingham University. Despite the large number of observation that have been collected, there are many important problems remaining to be solved; for example, the question of reversed magnetization, over which there is some conflict of opinion. There is also, as yet, no direct way of testing the stability of rock magnetization, and, as model experiments seem to show, there is still much to be learnt about the method by which magnetic moment is acquired.

303. *Rock Magnetism — Some Recent Developments.*
J. M. Bruckshaw, Science Progress, Vol. 42, No. 167, pp. 406-418, July, 1954.

The natural polarization of igneous rocks, their inverse magnetization, and the reverse remanent magnetism of sedimentary rocks are discussed as aspects of the permanent magnetism acquired by certain types of rocks, as distinct from their magnetic moment due to their existence in the earth's magnetic field.

304. *Anomalies of the Direction of Magnetism of the Rhön Basalt.* (In German).
R. Dixius, Geofis. Pura e Appl., Vol. 28, pp. 109-148, 1954.

The origin of reversed magnetism in igneous rocks is discussed. Results of measurements on various sorts of basalt and sediments from the Rhön mountains are presented. A method is given for measuring the Vertical-Gradient of the geomagnetic field. (Author's Abstract).

ELECTRICAL

305. *Fundamental Theory of Geoeltrans.* (In Italian).
A. Belluigi, Boll. Serv. Geol. Italia, Vol. 74, No. 1, pp. 245-263, 1953.

After a brief review of the development of electrical transient methods applied to oil prospecting, the "Eltrans" method is described and its fundamental theoretical features are discussed.

White's method, with collinear outer electrodes, is improved and developed. The time interval between the exciting transient voltage and the beginning of the ground response is calculated. This interval is a definite function of ground conductivity and of the electrode spacing; therefore by varying the spacing electrical sounding will be achieved. The new "Eltrans" method is more useful for geo-electrical investigations than the steady-state methods, especially so far as resistivity micro-differentiations are concerned. In addition, the effect of a non-homogeneous earth is considered in terms of previous work and the "Matrans" method.

306. *Theoretical Features of New Methods of Physical Logging: Matranslog and Phaselog.* (In Italian).
A. Belluigi, Geofis. Pura e Appl., Vol. 25, pp. 29-36, 1953.

The theory is developed for two new methods of drill-hole logging. In the first, called the Matranslog, changing patterns of an electromagnetic field around a drill-hole during the transient period are used. The pattern of the field changing with time differs from one point to another in the area under investigation even though the frequency of the electric impulses remains constant, and this differently varying behaviour of the electromagnetic field can be utilized as a characteristic of the subsurface.

In the second method, called the Phaselog, the frequency of the applied electric impulse is varied and consequently the pattern of the electromagnetic field produced during the building up period also changes, but still is influenced by the electric properties of the ground at a specific point. The parameters of the field in both of these methods are computed by a purely analytical procedure and can be used as characteristics of the subsurface.

(From Geophysical Abstracts 155, U.S. Geol. Survey).

307. *Theory of Electromagnetic Transient Logging.* (In Italia).
A. Belluigi, Riv. Geofis. Appl., Vol. 14, No. 1, pp. 19-29, 1953.

This paper is part of a study of logging of electromagnetic transients. The theory of the Matranslog is reviewed, a solution is given for measure of the voltage fall in the elementary Eltranslog, and some solution is given for the problem of mutual reception in the Matranslog. A new technique, the lateral electromagnetic transient log, is proposed.

(From Geophysical Abstracts 156, U.S. Geol. Survey).

308. *Spontaneous Potential Survey of a Copper Deposit at Sariyer, Turkey.*
S. Yüngül, Geophysics, Vol. 19, No. 3, pp. 455-458, July, 1954.

Several electrical methods were applied in the exploration for quartz-vein type chalcopyrite and auriferous pyrite deposits in the Sariyer area of Turkey. The spontaneous polarization method was found to be suitable for locating such deposits.

The anomalies found by this method were tested by drilling and all of them showed sulphide masses. One of these, the Nalbant Cesmesi anomaly, was partly developed afterwards and the geological section thus determined is in accord with the predictions based on the quantitative interpretation of the spontaneous polarization data. The sulphide mass here was found under a sterile cover of overthrusted schists. The topographic correction was of critical significance in locating this ore body.

(Author's Abstract).

309. *Geophysical Study of Circeo Mouna.* (In Italian).

A. Manfredini, Boll. Serv. Italia, Vol. 75, pp. 313-328, 1953.

The Circeo Mount, south of Rome, is an isolated calcareous hill of mesozoic age, surrounded by the sea and a marshy coastal plain. A geophysical survey has been carried out on the hill and the plain by means of vertical resistivity measurements. The electrode spacing extended to distances of 800-900 m. Low resistivities, of the same magnitude as that measured beneath the plain, appeared to exist beneath the Circeo Mounth's limestones. The author presents two profiles, based on his interpretation of the electrical results, in which the limestone is considered to be only a covering sheet, very thin in comparison with the hill's height.

310. *Hydrological Surveys in the Catania Area by Means of Electrical Soundings.*

J. J. Breusse & G. Huot, Geophysical Prospecting, Vol. 2, No. 3, pp. 227-231, September, 1954.

Exploration of the Catania region was carried out for over a year by means of electrical soundings. The thickness of the overburden (lava and alluvium) was thus computed and the contour map of the blue clays basement shows the existence of several buried channels where new wells were drilled, all of them successful.

(Author's Abstract).

311. *Note on Geoelectric Surface Measurements.*

N. Shalem, Research Council of Israel, Report for 1951-53 on Seismological Research, Jerusalem, 1954.

Recent developments of geoelectric surface measurements in Israel are briefly discussed. Hundreds of depth probes from 1,000 to 2,000 m. have been made. In this work the following main steps were taken.

(1) The use of powerful D.C. generators ensured that 30% of the current penetrated to the desired depths.

(2) Potentiometers (0.001 mV per scale div.) and galvanometers (0.0003 mA per scale div.) were used to measure the minute differences.

(3) Errors due to natural polarization, unequal contact resistances, near-surface inhomogeneities and anisotropy were eliminated or reduced.

(4) The organization allowed a 1500 m depth probe, with reading every 20m, to be completed within 4 hours.

Interpretations were obtained using a graphical-mathematical method.

Correlation with borehole data has shown that this method is the equal of seismic methods for the delineation of water horizons, whereas it is much more simple and far less costly.

312. *Theory of Electromagnetic Surfaces Waves over Geological Conductors.*

J. R. Wait, Geofis. Pura e Appl., Vol. 28, pp. 47-56, 1954.

The radiation fields of a vertical electric antenna on a horizontally-stratified ground are discussed. The attenuation and wave tilt of the surface wave and the height-gain factor are shown to be a function of the horizontal stratification in the ground. It is possible that the results have application to an airborne geophysical exploration scheme.

(Author's Abstract).

OTHER METHODS

313. *Geophysical Exploration Using Fields of High Frequencies.* (In Russian).
M. K. Krylov, Vestnik Moskov. Univ., No. 3, pp. 161-179, 1953.

When electromagnetic waves propagating through the ground from a transmitter on the surface of the earth meet a surface separating two layers of different electromagnetic properties, they are partly reflected back to the surface of the earth, producing interference with the initial waves. By observing on a separate receiver the returning combined wave, it is possible on the basis of known equations of electromagnetic field to comput the depth of the reflecting surface. The computations are based not on the relations controlling radio waves, but on those established for electric transmission lines with distributed electromagnetic constants, considering the ground as a wave guide. Established relations were used in several surveys made by the students of Moscow University, but have not yet been tested in practical field work.
(From Geophysical Abstracts 156, U.S. Geol. Survey).

314. *Propagation of Radio Frequency Energy through the Earth.*
F. M. McGehee, Jr., Geophysics, Vol. 19, No. 3, pp. 459-477, July, 1954.

Measurements have been made of some propagation characteristics in the earth of 1,614 and 1,700 kc radio frequency energy. The experiments were conducted at Carlsbad Caverns, New Mexico, and Mammoth Cave, Kentucky. Transmitters were set up at the surface 710 feet above an unwired tunnel in Carlsbad Caverns and the signal strength was measured at many points in the tunnels. A similar series of measurements was made in Mammoth Cave in a tunnel 270 feet below the surface. The data show that the attenuation constant is about 0.012 and 0.02 to 0.064 neper/meter at the two locations respectively. These values are in good agreement with theory.
(Author's Abstract).

315. *Patents.* Abstracts in Geophysics, Vol. 19, No. 3, p. 558, July, 1954.
U.S. 2,665,237. 5 Jan., 1954. A bacteriological method in which the hydrocarbon consumption of soil samples is measured.